

Lecture Notes in Networks and Systems 493

Vikrant Bhateja
Jnyana Ranjan Mohanty
Wendy Flores Fuentes
Koushik Maharatna *Editors*

Communication, Software and Networks

Proceedings of INDIA 2022

 Springer

Lecture Notes in Networks and Systems

Volume 493

Series Editor

Janusz Kacprzyk, Systems Research Institute, Polish Academy of Sciences,
Warsaw, Poland

Advisory Editors

Fernando Gomide, Department of Computer Engineering and Automation—DCA,
School of Electrical and Computer Engineering—FEEC, University of
Campinas—UNICAMP, São Paulo, Brazil

Okyay Kaynak, Department of Electrical and Electronic Engineering,
Bogazici University, Istanbul, Turkey

Derong Liu, Department of Electrical and Computer Engineering, University of
Illinois at Chicago, Chicago, USA

Institute of Automation, Chinese Academy of Sciences, Beijing, China

Witold Pedrycz, Department of Electrical and Computer Engineering, University of
Alberta, Alberta, Canada

Systems Research Institute, Polish Academy of Sciences, Warsaw, Poland

Marios M. Polycarpou, Department of Electrical and Computer Engineering,
KIOS Research Center for Intelligent Systems and Networks, University of Cyprus,
Nicosia, Cyprus

Imre J. Rudas, Óbuda University, Budapest, Hungary

Jun Wang, Department of Computer Science, City University of Hong Kong,
Kowloon, Hong Kong

The series “Lecture Notes in Networks and Systems” publishes the latest developments in Networks and Systems—quickly, informally and with high quality. Original research reported in proceedings and post-proceedings represents the core of LNNS.

Volumes published in LNNS embrace all aspects and subfields of, as well as new challenges in, Networks and Systems.

The series contains proceedings and edited volumes in systems and networks, spanning the areas of Cyber-Physical Systems, Autonomous Systems, Sensor Networks, Control Systems, Energy Systems, Automotive Systems, Biological Systems, Vehicular Networking and Connected Vehicles, Aerospace Systems, Automation, Manufacturing, Smart Grids, Nonlinear Systems, Power Systems, Robotics, Social Systems, Economic Systems and other. Of particular value to both the contributors and the readership are the short publication timeframe and the world-wide distribution and exposure which enable both a wide and rapid dissemination of research output.

The series covers the theory, applications, and perspectives on the state of the art and future developments relevant to systems and networks, decision making, control, complex processes and related areas, as embedded in the fields of interdisciplinary and applied sciences, engineering, computer science, physics, economics, social, and life sciences, as well as the paradigms and methodologies behind them.

Indexed by SCOPUS, INSPEC, WTI Frankfurt eG, zbMATH, SCImago.

All books published in the series are submitted for consideration in Web of Science.

For proposals from Asia please contact Aninda Bose (aninda.bose@springer.com).

Vikrant Bhateja · Jnyana Ranjan Mohanty ·
Wendy Flores Fuentes · Koushik Maharatna
Editors

Communication, Software and Networks

Proceedings of INDIA 2022

 Springer

Editors

Vikrant Bhateja
Department of Electronics
and Communication Engineering
Shri Ramswaroop Memorial College
of Engineering and Management
(SRMCEM)
Lucknow, Uttar Pradesh, India

Dr. A.P.J. Abdul Kalam Technical
University
Lucknow, Uttar Pradesh, India

Jnyana Ranjan Mohanty
School of Computer Applications
KIIT University
Bhubaneswar, Odisha, India

Koushik Maharatna
School of Electronics and Computer
Science
University of Southampton
Southampton, UK

Wendy Flores Fuentes
Facultad de Ingenieria
Autonomous University of Baja California
Mexicali, Baja California, Mexico

ISSN 2367-3370

ISSN 2367-3389 (electronic)

Lecture Notes in Networks and Systems

ISBN 978-981-19-4989-0

ISBN 978-981-19-4990-6 (eBook)

<https://doi.org/10.1007/978-981-19-4990-6>

© The Editor(s) (if applicable) and The Author(s), under exclusive license to Springer Nature Singapore Pte Ltd. 2023

This work is subject to copyright. All rights are solely and exclusively licensed by the Publisher, whether the whole or part of the material is concerned, specifically the rights of translation, reprinting, reuse of illustrations, recitation, broadcasting, reproduction on microfilms or in any other physical way, and transmission or information storage and retrieval, electronic adaptation, computer software, or by similar or dissimilar methodology now known or hereafter developed.

The use of general descriptive names, registered names, trademarks, service marks, etc. in this publication does not imply, even in the absence of a specific statement, that such names are exempt from the relevant protective laws and regulations and therefore free for general use.

The publisher, the authors, and the editors are safe to assume that the advice and information in this book are believed to be true and accurate at the date of publication. Neither the publisher nor the authors or the editors give a warranty, expressed or implied, with respect to the material contained herein or for any errors or omissions that may have been made. The publisher remains neutral with regard to jurisdictional claims in published maps and institutional affiliations.

This Springer imprint is published by the registered company Springer Nature Singapore Pte Ltd. The registered company address is: 152 Beach Road, #21-01/04 Gateway East, Singapore 189721, Singapore

Conference Organisation Committees

Chief Patron

Sri K. V. Vishnu Raju, Chairman, SVES

Patrons

Sri Ravichandran Rajagopal, Vice-Chairman, SVES

Sri K. Aditya Vissam, Secretary, SVES

Conference Chair

Dr. KVN Sunitha, Principal, BVRITH, Hyderabad, India

Dr. Suresh Chandra Satapathy, KIIT, Bhubaneswar, Odisha, India

Organizing Chair

Dr. J Naga Vishnu Vardhan, Professor, ECE & Professor-Incharge Academics, BVRITH, Hyderabad, India

Publication Chair

Dr. Vikrant Bhateja, Shri Ramswaroop Memorial College of Engineering and Management, Lucknow, U.P., India

Organizing Committee

Dr. Ch Sunil Kumar, Vice-Principal and HoD-EEE

Dr. K. Srinivasa Reddy, HoD-CSE

Dr. S. L. Aruna Rao, HoD-IT

Dr. Anwar Bhasha Pattan, HoD-ECE

Dr. L. Lakshmi, HoD-CSE (AI & ML)

Dr. M. Anita, HoD-BSH

Prof. Murali Nath, Prof. Incharge Accreditations

Dr. G. Naga Satish, Professor, CSE

Dr. K. Adinarayana Reddy, Professor, IT

Dr. J. Manoj Kumar, Prof. Incharge Admissions

Ms. M. Praveena, Associate Professor, ECE
 Mr. R. Guruswamy, Associate Professor, EEE

Website & Poster Committee

Ms. M. Shanmuga Sundari, Assistant Professor, CSE
 Ch. Anil Kumar, Assistant Professor, IT
 Mr. R. Priyakanth, Associate Professor, ECE

Publicity Committee

Dr. P. Kayal, Associate Professor, IT and R&D Incharge
 Dr. V. Rajeswari, Professor, EEE
 Dr. M. Parvathi, Professor, ECE
 Dr. V. Madhavi, Associate Professor, BSH
 Dr. M. Indrasena Reddy, Associate Professor, CSE
 Dr. P. Anji Reddy Polu, Assistant Professor, BSH
 Dr. A. Sudharshan Chakravarthy, Assistant Professor, CSE

Advisory Committee

- Aime' Lay-Ekuakille, University of Salento, Lecce, Italy
- Amira Ashour, Tanta University, Egypt
- Aynur Unal, Stanford University, USA
- Bansidhar Majhi, IIIT Kancheepuram, Tamil Nadu, India
- Dilip Kumar Sharma, Vice-Chairman, IEEE U.P. Section
- Yu-Dong Zhang, University of Leicester, UK
- Ganpati Panda, IIT Bhubaneswar, Odisha, India
- Govardhan, Professor in CSE & Rector, JNTUH, Hyderabad, India
- Wenxian Yang, Senior Lecturer, University of Newcastle
- Jagdish Chand Bansal, South Asian University, New Delhi, India
- Muruganandam, Lecturer, Department of Engineering (Electrical Engineering Section), University of Technology and Applied Sciences—Ibri, Sultanate of Oman
- João Manuel R. S. Tavares, Universidade do Porto (FEUP), Porto, Portugal
- Jyotsana Kumar Mandal, University of Kalyani, West Bengal, India
- K. C. Santosh, University of South Dakota, USA
- Le Hoang Son, Vietnam National University, Hanoi, Vietnam
- Naeem Hanoon, Multimedia University, Cyberjaya, Malaysia
- V. Vijaya Kumar, Dean, Department of CSE & IT, Anurag University, Hyderabad, India
- Nilanjan Dey, JIS University, Kolkatta, India
- Noor Zaman, Universiti Tecknologi, PETRONAS, Malaysia
- Roman Senkerik, Tomas Bata University, Zlin, Czech Republic
- C. Krishana Mohan, Professor, CSE, IIT, Hyderabad, India
- P. Radha Krishna, Professor, CSE, NIT Warangal, India
- Swagatam Das, Indian Statistical Institute, Kolkatta, India

- Vijayalakshmi Saravanan, University of South Dakota, Department of Computer Science, Buffalo, New York, United States
- Thanikanti Sudhakar Babu, Post Doctoral Fellow Institute of Power Engineering, Dept, of Electrical Power Engineering, Universiti Tenaga Nasional (UNITEN), Malaysia
- Siba K. Udgata, University of Hyderabad, Telangana, India
- K. M. Prasad, Senior R&D Engineer, ENGINIA RESEARCH Inc. Winnipeg, Canada
- Meenalosini Vimal Cruz, Assistant Professor, Computer Science, Georgia Southern University Port Wentworth, Georgia, United States
- Shri Nivas Singh, MMMUT, Gorakhpur, U.P., India
- Tai Kang, Nanyang Technological University, Singapore
- Valentina Balas, Aurel Vlaicu University of Arad, Romania
- Meenalosini Vimal Cruz, Assistant Professor, Computer Science, Assistant Professor at Georgia Southern University, Port Wentworth, Georgia, United States
- Anil Kumar V., Associate Professor, ECE, IIIT, Hyderabad, India

Technical Program Committee

- Abdul Rajak A. R., Department of Electronics and Communication Engineering Birla Institute of Dr. Nitika Vats Doohan, Indore, India
- Ahmad Al-Khasawneh, The Hashemite University, Jordan
- Alexander Christea, University of Warwick, London, UK
- Amioy Kumar, Biometrics Research Lab, Department of Electrical Engineering, IIT Delhi, India
- Anand Paul, The School of Computer Science and Engineering, South Korea
- Apurva A. Desai, Veer Narmad South Gujarat University, Surat, India
- Avdesh Sharma, Jodhpur, India
- A. K. Chaturvedi, Department of Electrical Engineering, IIT Kanpur, India
- Bharat Singh Deora, JRNRV University, India
- Bhavesh Joshi, Advent College, Udaipur, India
- Brent Waters, University of Texas, Austin, Texas, United States
- Chhaya Dalela, Associate Professor, JSSATE, Noida, Uttar Pradesh
- Dan Boneh, Computer Science Department, Stanford University, California, USA
- Feng Jiang, Harbin Institute of Technology, China
- Gengshen Zhong, Jinan, Shandong, China
- Harshal Arolkar, Immd. Past Chairman, CSI Ahmedabad Chapter, India
- Amlan Chakraborti, Head, Professor and Director, A. K. Choudhury School of IT, University of Calcutta
- H. R. Vishwakarma, Professor, VIT, Vellore, India
- Jayanti Dansana, KIIT University, Bhubaneswar, Odisha
- Jean Michel Bruel, Departement Informatique IUT de Blagnac, Blagnac, France
- Jeril Kuriakose, Manipal University, Jaipur, India
- Jitender Kumar Chhabr, NIT, Kurukshetra, Haryana, India
- Kalpana Jain, CTAE, Udaipur, India

- Komal Bhatia, YMCA University, Faridabad, Haryana, India
- Krishnamachar Prasad, Department of Electrical and Electronic Engineering, Auckland, New Zealand
- K. C. Roy, Principal, Kautaliya, Jaipur, India
- Lorne Olfman, Claremont, California, USA
- Martin Everett, University of Manchester, England
- Meenakshi Tripathi, MNIT, Jaipur, India
- Mukesh Shrimali, Pacific University, Udaipur, India
- Murali Bhaskaran, Dhirajlal Gandhi College of Technology, Salem, Tamil Nadu, India
- Nilay Mathur, Director, NIIT Udaipur, India
- Ngai-Man Cheung, Assistant Professor, University of Technology and Design, Singapore
- Philip Yang, Price water house Coopers, Beijing, China
- Pradeep Chouksey, Principal, TIT college, Bhopal, MP, India
- Prasun Sinha, Ohio State University Columbus, Columbus, OH, United States
- Rajendra Kumar Bharti, Assistant Prof. Kumaon Engg College, Dwarahat, Uttarakhand, India
- Pradeep Chowriappa, Assistant Professor at Louisiana Tech University Ruston, Louisiana, United States
- R. K. Bayal, Rajasthan Technical University, Kota, Rajasthan, India
- Sami Mnasri, IRT Laboratory Toulouse, France
- Savita Gandhi, Professor, Gujarat University, Ahmedabad, India
- Nishanth Dikkala, Research Engineer, MIT, Michigan, US
- Soura Dasgupta, Department of TCE, SRM University, Chennai, India
- Sushil Kumar, School of Computer & Systems Sciences, Jawaharlal Nehru University, New Delhi, India
- Prasad Mavuduri, CEO, University of Emerging Technologies University of Emerging Technologies, USA
- S. R. Biradar, Department of Information Science and Engineering, SDM College of Engineering & Technology, Dharwad, Karnataka
- Ting-Peng Liang, National Chengchi University Taipei, Taiwan
- Xiaoyi Yu, National Laboratory of Pattern Recognition, Institute of Automation, Chinese Academy of Sciences, Beijing, China
- Yun-Bae Kim, SungKyunKwan University, South Korea
- Karuppanan, Professor, Electronics and Communication Engineering, Motilal Nehru National Institute of Technology Allahabad
- Raghava Rao Mukkamala, Director of the Centre for Business Data Analytics, CBDA, CBS, Denmark
- Anil Kumar Vuppala, Assistant Professor, IIIT Hyderabad
- P. Bala Prasad, Technology Head, TCS Hyderabad M. Asha Rani, Professor, ECE, JNTUH Hyderabad
- M. Asha Rani, Professor, ECE, JNTUH Hyderabad
- P. Radha Krishna, Professor and Head, Computer Science and Engineering Department, National Institute of Technology, Warangal

- Narayana Prasad Padhy, Dean of Academic Affairs, Professor and Institute Chair, Department of Electrical Engineering, IIT Roorkee
- Sourav Mukhopadhyay, Professor, IIT Kharagpur
- Sukumar Mishra, Professor, Department of Electrical Engineering, IIT Delhi
- Siva Rama Krishna Vanjari, Associate Professor, Department of Electrical Engineering, IIT Hyderabad
- Durga Prasad Mohapatra, Professor, Department of Computer Science & Engineering, National Institute of Technology Rourkela

Preface

This book is a collection of high-quality peer-reviewed research papers presented at the “7th International Conference on Information System Design and Intelligent Applications (INDIA-2022)” held at BVRIT HYDERABAD College of Engineering for Women, Hyderabad, India during 25-26 February 2022.

After the success of past six editions of INDIA conferences which was initiated in the year 2012 and was first organized by Computer Society of India (CSI), Vizag Chapter. Its sequel, INDIA-2015 has been organized by Kalyani University, West Bengal followed by INDIA-2016, organized by ANITS, Vizag, INDIA-2017, organized by Duy Tan University, Da Nang, Vietnam, INDIA-2018, organized by Université des Mascareignes, Mauritius, and INDIA-2019, organized by LIET, Vizianagaram. All papers of past INDIA editions are published by Springer-Nature as publication partner. Presently, INDIA-2022 provided a platform for academicians, researchers, scientists, professionals and students to share their knowledge and expertise in the diverse domain of Intelligent Computing and Communication.

INDIA-2022 had received number of submissions from the field of Information system design, intelligent applications and its prospective applications in different spheres of engineering. The papers received have undergone a rigorous peer-review process with the help of the technical program committee members of the conference from the various parts of country as well as abroad. The review process has been crucial with minimum two reviews each along with due checks on similarity and content overlap. This conference has featured theme-based special sessions in the domain of Blockchain 4.0, AI in IoT, Bio-Inspired Computing, etc. along with main track.

The conference featured many distinguished keynote addresses by eminent speakers like: Prof. T. Bheemarjuna Reddy, Professor, CSE, IIT Hyderabad, India who addressed the gathering on V2X Technologies toward connected and autonomous navigation regulation, challenges and Research Opportunities. Prof. Amlan Chakrabarti, University of Calcutta delivered on IoT for Societal Applications. Prof. Sanjay Ranka, Distinguished Professor in the Department of Computer Information Science and Engineering at University of Florida delivered a talk on AIML for Smart Transportation.

These keynote lectures / talks embraced a huge toll of audience of students, faculties, budding researchers as well as delegates. The editors thank the General Chair, TPC Chair and the Organizing Chair of the conference for providing valuable guidelines and inspirations to overcome various difficulties in the process of organizing this conference. The editors also thank BVRIT HYDERABAD College of Engineering for Women for their whole-hearted support in organizing this edition of INDIA conference.

The editorial board take this opportunity to thank authors of all the submitted papers for their hard work, adherence to the deadlines and patience during the review process. The quality of a refereed volume depends mainly on the expertise and dedication of the reviewers. We are indebted to the TPC members who not only produced excellent reviews but also did these in short time frames.

Lucknow, India
Bhubaneswar, India
Mexicali, Mexico
Southampton, UK

Vikrant Bhateja
Jnyana Ranjan Mohanty
Wendy Flores Fuentes
Koushik Maharatna

Contents

A Novel Controller for Multiple-Input Bidirectional DC–DC Power Converter of HESS for DC Microgrid Applications	1
Punna Srinivas, Chava Sunil Kumar, M. Rupesh, and Battapothula Gurappa	
Model-Based Automatic Seizure Detection of EEG Signal Analysis by Frequency and Time Domain Methods	13
S. Sesha Sai Priya and N. J. Nalini	
Performance Assessment of FACTS Devices for Enhancing Stability and Control in Power Systems	25
T. S. Kishore and P. Upendra Kumar	
Filter Bank Multicarrier Modulation with OQAM-Based Sparse Channel Estimation	33
Nilofer Shaik and Praveen Kumar Malik	
A Cascaded H-Bridge MLI Fed Motor by Using Fuzzy-MPPT PV System	43
Kammari Rajesh, Y. Chintu Sagar, and K. C. Venkataiah	
EMG-Based Analysis of Rehabilitation Exercises for Diastasis Recti Abdominis	61
R. Menaka, R. Karthik, and P. Vinitha Joshy	
Secure Cloud Auditability for Virtual Machines by Adaptive Characterization Using Machine Learning Methods	71
Shesagiri Taminana and D. Lalitha Bhaskari	
Design of TPG BIST Using Various LFSR for Low Power and Low Area	85
Jugal Kishore Bhandari and Yogesh Kumar Verma	

Device-to-Device Data Transmission Over Sound Waves Using FSK/BPSK/QPSK	95
Gnaneshwara Chary, Charan Kumar, Shriram Ravindranathan, Suhruth Yambakam, and Janakiram Sunku	
Performance Evaluation of Radar Backscatter of S-Shaped Duct with Conventional Intake Duct	103
B. R. Sanjeeva Reddy, Sanjay Dubey, and J. Naga Vishnu Vardhan	
A Novel Flash-Type Time-To-Digital Converters (TDC) Using GDI Technique	115
Jakka Yeshwanth Reddy, Anthireddygari Sushma, Siripurapu Sravya, Sabavath Sai Kiran, and Puli Sai Sukitha	
A Symbiotic Model for Accurate Weather Forecasting	127
Vijay A. Kanade	
FPGA Design of Area Efficient and Superfast Motion Estimation Using JAYA Optimization-Based Block Matching Algorithm	137
Manne Praveena, N. Balaji, and C. D. Naidu	
Motor Vehicle Alert System in On-Campus Environments: Omniscient Vehicle Sensor	149
Phani Sridhar Addepalli, Tenneti Krishna Mohana, and G. Naga Satish	
Backup and Restore Strategies for Medical Image Database Using NoSQL	161
Jyoti Chaudhary, Vaibhav Vyas, and Monika Saxena	
Bandwidth Enhancement of Circular Wheel Slot Antenna for GPS, WLAN and C-Band Applications	173
Ramesh Deshpande, T. V. Ramakrishna, and B. Rama Sanjeeva Reddy	
Detection and Counting of Trees in Aerial Images Using Image Processing Techniques	181
Meda Lakshmi Hima Bindhu, Tejaswi Potluri, Chandana Bai Korra, and J. V. D. Prasad	
EGFR and HER2 Target-Based Molecular Docking Analysis—Computational Study of Metal Complexes	191
Ramaiah Konkanchi, Madhavi Vemula, and B. Anna Tanuja Safala	
A Comparative Study of Power Swing Blocking/Deblocking Techniques in Distance Relay Power System Protection	203
Cholleti Sriram and Jarupula Somlal	
Generation of Poly-Phase Frequency-Hopped Spread Spectrum Signal for LPI Radar Target Detection	213
Jayshree Das, S. Munnnavar Hussain, and I. A. Pasha	

Energy Efficient Memory Architecture for High Performance and Low Power Applications Under Sub-threshold Regime 225
 T. Vasudeva Reddy, K. Madhava Rao, V. Santhosh Kumar, and V. Hindumathi

Implementation and Performance Evaluation of Hybrid SRAM Architectures Using 6T and 7T for Low-Power Applications 235
 M. Parvathi and M. C. Chinnaiah

Survey of Identification of Alzheimer’s Disease Using MRI, Speech and MMSE 247
 Y. Bhanusree, Divya Bulusu, Divija Chinni, Akanksha Narahari, Suma Sree Simhadri, and Varshitha Bommareddy

Estimating the Low Cost Probability Error in QAM Using the SRRC Filter with Other Filter 259
 Preesat Biswas, Bharti Baghel, Shirin Khan, and M. R. Khan

Designing a Secure Physically Unclonable Function Using Light-weight LFSR 283
 B. V. D. N. Srilakshmi, Kiran Mannem, K. Jamal, and Manchalla O. V. P. Kumar

Empirical Evaluation of Local Model for Just in Time Defect Prediction 299
 Kavya Goel, Sonam Gupta, and Lipika Goel

Secured Messaging Using Image and Video Steganography 311
 Trupthi Mandhula, Blessy Kotrika, and Aditi Rayaprolu

OMSST Approach for Unit Selection from Speech Corpus for Telugu TTS 321
 K. V. N. Sunitha and P. Sunitha Devi

An IoT-Based Health Monitoring System for Elderly Patients 331
 Angelin Varghese and Senthil A. Muthukumaraswamy

Blockchain-Based Solution for Trusted Charity Donations 339
 A. N. Shwetha and C. P. Prabodh

Vedic Multiplier for High-Speed Applications 349
 J. V. R. Sudhamsu Preetham, Perli Nethra, D. Chandrasekhar, Mathangi Akhila, N. Arun Vignesh, and Asisa Kumar Panigrahy

Resolving Lexical Level Ambiguity: Word Sense Disambiguation for Telugu Language by Exploiting IndicBERT Embeddings 357
 Palanati Durgaprasad, K. V. N. Sunitha, and B. Padmajarani

Location-Based Bus Tracking Application Using Android 369
 Sourav Kumar, Shreyash Moundekar, Mansing Rathod, and Rupesh Parmar

Extended Informative Local Binary Patterns (EILBP): A Model for Image Feature Extraction 381
Sallauddin Mohmmad and B. Rama

Performance Analysis of 5G Micro-Cell Coverage with 3D Ray Tracing 393
Viswanadham Ravuri, M. Venkata Subbarao, Sudheer Kumar Terlapu, and T. Sairam Vamsi

A Novel Asymmetric Group Key Encryption Mechanism in MANETs 403
R. Rekha, M. Sandhya Rani, and K. V. N. Sunitha

EEG—Brainwaves Signal Based BCI Control Wheel Chair System 411
B. Ramesh and Phanikumar Polasi

Web Book Recommendation System Based on Collaborative Filtering and Association Mining 421
S. Prasanth Vaidya and G. Naga Satish

IOT-Based Smart Trash Collection with Swachh Survekshan 429
Nalla Siva Kumar, N. Akhila, S. Prasanth Vaidya, and G. Naga Satish

Particle Swarm Optimization-Based Energy-Aware Task Scheduling Algorithm in Heterogeneous Cloud 439
Roshni Pradhan and Suresh Chandra Satapathy

Deviation and Cluster Analysis Using Inductive Alpha Miner in Process Mining 451
M. Shanmuga Sundari and Rudra Kalyan Nayak

Image and Video Processing-Based Traffic Analysis Using OpenCV 459
Devineni Pooja Sri and K. Kiran Kumar

Energy Usage Data Extraction Methodology in Smart Building Using Micro Controller 467
K. Sai Himaja Chowdary, M. Neelakantappa, Ch. Ramsai Reddy, and M. Prameela

Designing a Secure Wide Area Network for Multiple Office Connectivity 477
Shaik Rehna Sulthana and Pasupuleti Sai Kiran

Polarity Identification from Micro Blogs Using Multimodal Sentiment Analysis 487
Haritha Akkineni, Myneni Madhubala, Madhuri Nallamothu, and Venkata Suneetha Takellapati

Software Defect Prediction: An ML Approach-Based Comprehensive Study 497
Kunal Anand and Ajay Kumar Jena

Stock Price Prediction Using Data Analysis and Visualization 513
K. Yashwanth Raj, B. S. Devpriyadharsan, and B. Sowmiya

A Comparative Study for Determining the Vehicle Routing Optimal Path 523
R. Aditi, R. Dhinakar, and B. Sowmiya

Tool-Based Prediction of SQL Injection Vulnerabilities and Attacks on Web Applications 535
B. Padmaja, G. Chandra Sekhar, Ch. V. Rama Padmaja, P. Chandana, and E. Krishna Rao Patro

Review on Load Balancing Techniques, Resource Scheduling, Sidechannel Attacks in Cloud Environment 545
C. Lakshminathreddy and Subbiah Swaminathan

Visual Heart Rate—A Key Biomarker to Diagnose Depressive Disorder 555
Purude Vaishali and P. Lalitha Surya Kumari

Predictive Analysis for Prognostication of Breast Cancer 565
Karuppiyah Santhi, Kandasamy Thinakaran, J. Jegan, and Perepi Rajarajeswari

Framework of Crop Yield Using pH Soil and Temperature Values 573
B. V. Ramana Murthy and B. N. S. M. Chandrika

A Blockchain-Based and IoT-Powered Smart Parking System for Smart Cities 583
A. R. Sathya

Proximity Coupled Antenna with Stable Performance and High Body Antenna Isolation for IoT-Based Devices 591
Anupma Gupta, Bhawna Goyal, Ayush Dogra, and Rohit Anand

Microscopic and Ultrasonic Super-Resolution for Accurate Diagnosis and Treatment Planning 601
Shivam Sharma, Ritika Rattan, Bhawna Goyal, Ayush Dogra, and Rohit Anand

Breast Cancer Detection Using Machine Learning 613
Somya Goyal, Mehul Sinha, Shashwat Nath, Sayan Mitra, and Charvi Arora

Current Trends in Methodology for Software Development Process 621
Somya Goyal, Ayush Gupta, and Harshit Jha

Author Index 631

Editors and Contributors

About the Editors

Vikrant Bhateja is an associate professor in Department of ECE, SRMGPC, Lucknow (Uttar Pradesh) and also the dean (Academics) in the same college. He has doctorate in ECE (Bio-Medical Imaging) with a total academic teaching experience of 18 years with around 180 publications in reputed international conferences, journals, and online chapter contributions; out of which 31 papers are published in SCIE indexed high impact factored journals. He has been instrumental in chairing/co-chairing around 30 international conferences in India and abroad as the publication/TPC chair and edited 45 book volumes from Springer Nature as a corresponding/co-editor/author on date. He has delivered nearly 20 keynotes, invited talks in international conferences, ATAL, TEQIP, and other AICTE sponsored FDPs and STTPs. He is the editor-in-chief of IGI Global—*International Journal of Natural Computing and Research* (IJNCR) an ACM and DBLP indexed journal since 2017. He has guest edited special issues in reputed SCIE indexed journals under Springer Nature and Elsevier.

Jnyana Ranjan Mohanty received his Ph.D. degree in Computer Science from Utkal University, Bhubaneswar, in the year 2008. He has more than 25 years of teaching experience (UG and PG levels). He joined KIIT Deemed to be University, Bhubaneswar, in July 1997 as a lecturer, and presently he is a professor. He has served KIIT in different administrative capacities too (as an associate dean and controller of examinations). Presently, he is the registrar of KIIT Deemed to be University. Prior to joining KIIT, he served as a lecturer at Institute of Business Administration and Training, Bhubaneswar. He is actively engaged in research work and has a number of Ph.D. scholars under his guidance. He has authored books and has to his credit innumerable publications in reputed international Scopus/ SCI indexed journals and in international conference proceedings. He has also edited books published

by Springer and IJCA Volumes. He has conducted several conferences and workshops as the organizing chair/program chair. His research interests include queuing theory, computational intelligence, and cloud computing.

Wendy Flores Fuentes received the master's degree in engineering from Technological Institute of Mexicali in 2006, and the Ph.D. degree in science, applied physics, with emphasis on Optoelectronic Scanning Systems for SHM, from Autonomous University of Baja California in June 2014. She has more than 115 publications which include journal articles in Elsevier, IEEE Emerald and Springer, chapters and books in Intech, IGI global and Springer, proceedings articles in IEEE. She has been Panel Reviewer of Taylor and Francis, IEEE, Elsevier, and EEMJ (Gheorghe Asachi Technical University of Iasi). Currently, she is a full-time professor-researcher at Universidad Autónoma de Baja California, at the Faculty of Engineering.

Koushik Maharatna received the Ph.D. degree from Jadavpur University, Kolkata, India, in 2002. From 2000 to 2003, he was a research scientist with Innovations for High Performance, Frankfurt (Oder), Germany. He joined the Department of Electrical and Electronic Engineering, University of Bristol, Bristol, UK, as a lecturer, in 2003. Since 2006, he has been with the School of Electronics and Computer Science, University of Southampton, Southampton, UK, where he is currently a professor. His current research interests include biomedical signal processing, next generation healthcare systems development, and very large-scale integration design for signal processing systems.

Contributors

Addepalli Phani Sridhar Aditya Engineering College (A), Surampalem, India; Jawaharlal Nehru Technological University Kakinada, East Godavari, Andhra Pradesh, India

Aditi R. Department of Computing Technologies, SRM Institute of Science and Technology, Chennai, India

Akhila Mathangi Department of ECE, Gokaraju Rangaraju Institute of Engineering and Technology, Hyderabad, Telangana, India

Akhila N. Aditya Engineering College, Surampalem, India; Jawaharlal Nehru Technological University, Kakinada, Andhra Pradesh, India

Akkineni Haritha PVP Siddhartha Institute of Technology, Vijayawada, Andhra Pradesh, India

Anand Kunal Kalinga Institute of Industrial Technology, Bhubaneswar, Odisha, India

Anand Rohit Department of ECE, DSEU, New Delhi, India

Arora Charvi Manipal University Jaipur, Jaipur, Rajasthan, India

Arun Vignesh N. Department of ECE, Gokaraju Rangaraju Institute of Engineering and Technology, Hyderabad, Telangana, India

Baghel Bharti Electronics and Telecommunication Engineering, Government Engineering College, CSVTU, CG, Jagdalpur, India

Balaji N. University College of Engineering, JNTU Vizianagaram, JNTUK, Kakinada, India

Bhandari Jugal Kishore SEEE, Lovely Professional University, Jalandhar, Punjab, India

Bhanusree Y. Department of CSE, VNRVJIET, Hyderabad, India

Bindhu Meda Lakshmi Hima Department of Computer Science and Engineering, Velagapudi Ramakrishna Siddhartha Engineering College, Kanuru, India

Biswas Preesat Electronics and Communication Engineering, Dr. C. V. Raman University, Bilaspur, India

Bommareddy Varshitha Department of CSE, VNRVJIET, Hyderabad, India

Bulusu Divya Department of CSE, VNRVJIET, Hyderabad, India

Chandana P. Department of Computer Science and Engineering (AI & ML), Institute of Aeronautical Engineering, Hyderabad, India

Chandrasekhar D. Department of ECE, Gokaraju Rangaraju Institute of Engineering and Technology, Hyderabad, Telangana, India

Chandrika B. N. S. M. Department of Math, Stanley College of Engineering and Technology for Women, Hyderabad, India

Chary Gnaneshwara Department of ECE, B V Raju Institute of Technology, Narsapur, Telangana, India

Chaudhary Jyoti Banasthali Vidyapith, Jaipur, India

Chinnaiah M. C. ECE Department, BVRIT Narsapur, Hyderabad, Telangana, India

Chinni Divija Department of CSE, VNRVJIET, Hyderabad, India

Chintu Sagar Y. Ashoka Women's Engineering College, Dupadu, India

Das Jayshree B V Raju Institute of Technology, Narsapur, Medak, Telangana, India

Deshpande Ramesh Department of ECE, Koneru Lakshmaiah Education Foundation, Vaddeshwaram Guntur, India;
Department of ECE, B V Raju Institute of Technology, Medak, India

Devpriyadharsan B. S. Department of Computing Technologies, SRM Institute of Science and Technology, Chennai, India

Dhinakar R. Department of Computing Technologies, SRM Institute of Science and Technology, Chennai, India

Dogra Ayush Ronin Institute, Montclair, NJ, USA

Dubey Sanjay Department of ECE, B V Raju Institute of Technology, Medak, India

Durgaprasad Palanati Department of Computer Science and Engineering, UCET, MGU, Nalgonda, Telangana, India

Goel Kavya Ajay Kumar Garg Engineering College, Ghaziabad, India

Goel Lipika Gokaraju Rangaraju Institute of Engineering and Technology, Hyderabad, India

Goyal Bhawna Department of Electronics and Communication Engineering, Chandigarh University, Mohali, India

Goyal Somya Manipal University Jaipur, Jaipur, Rajasthan, India

Gupta Anupma Department of ECE, Chandigarh University, Mohali, India

Gupta Ayush Manipal University Jaipur, Jaipur, Rajasthan, India

Gupta Sonam Ajay Kumar Garg Engineering College, Ghaziabad, India

Gurappa Battapothula B V Raju Institute of Technology Narasapur, Telangana, India

Hindumathi V. BVRIT Hyderabad College of Engineering for Women, Nizampet, Hyderabad, Telangana, India

Jamal K. Department of ECE, GRIET, Hyderabad, India

Jegan J. Aditya College of Engineering, Madanapalle, Andhra Pradesh, India

Jena Ajay Kumar Kalinga Institute of Industrial Technology, Bhubaneswar, Odisha, India

Jha Harshit Manipal University Jaipur, Jaipur, Rajasthan, India

Kanade Vijay A. Pune, India

Karthik R. Centre for Cyber Physical Systems, School of Electronics Engineering, Vellore Institute of Technology, Chennai, India

Khan M. R. Electronics and Telecommunication Engineering, Government Engineering College, CSVTU, CG, Jagdalpur, India

Khan Shirin Electronics and Telecommunication Engineering, Government Engineering College, CSVTU, CG, Jagdalpur, India

Kiran Kumar K. Koneru Lakshmaiah Education Foundation, Vaddeswaram, India

Kiran Pasupuleti Sai Koneru Lakshmaiah Education Foundation, Vaddeswaram, India;

Department of ECE, B V Raju Institute of Technology, Narsapur, TS, India

Kiran Sabavath Sai Department of ECE, B V Raju Institute of Technology, Narsapur, TS, India

Kishore T. S. GMR Institute of Technology, Rajam, Andhra Pradesh, India

Konkanchi Ramaiah Chemistry Division, H&S Department, BVRIT Hyderabad College of Engineering for Women, Hyderabad, India

Korra Chandana Bai Department of Computer Science and Engineering, Velagapudi Ramakrishna Siddhartha Engineering College, Kanuru, India

Kotrika Blessy Department of Information Technology, Chaitanya Bharathi Institute of Technology (CBIT-A), Hyderabad, Telangana State, India

Krishna Rao Patro E. Department of Computer Science and Engineering, Institute of Aeronautical Engineering, Hyderabad, India

Kumar Charan Department of ECE, B V Raju Institute of Technology, Narsapur, Telangana, India

Kumar Chava Sunil Electrical and Electronics Engineering Department, BVRIT HYDERABAD College of Engineering for Women, Hyderabad, Telangana, India

Kumar Manchalla O. V. P. Department of ECE, GRIET, Hyderabad, India

Kumar Nalla Siva Aditya Engineering College, Surampalem, India; Jawaharlal Nehru Technological University, Kakinada, AP, India

Kumar Sourav K.J. Somaiya Institute of Engineering and Information Technology, Mumbai, India

Lakshminathreddy C. Computer Science and Engineering, Saveetha School of Engineering, Chennai, India

Lalitha Bhaskari D. Department of Computer Science and Systems Engineering, Andhra University College of Engineering (A), Andhra University, Visakhapatnam, India

Lalitha Surya Kumari P. Department of CSE, Koneru Lakshmaiah Education Foundation, Aziznagar, Hyderabad, Telangana State, India

Madhava Rao K. B V Raju Institute of Technology, Narsapur, Medak, Telangana, India

Madhubala Myneni Institute of Aeronautical Engineering, Hyderabad, Telangana, India

Malik Praveen Kumar Lovely Professional University, Phagwara, Punjab, India

Mandhula Trupthi Department of Information Technology, Chaitanya Bharathi Institute of Technology (CBIT-A), Hyderabad, Telangana State, India

Mannem Kiran Department of ECE, GRIET, Hyderabad, India

Menaka R. Centre for Cyber Physical Systems, School of Electronics Engineering, Vellore Institute of Technology, Chennai, India

Mitra Sayan Manipal University Jaipur, Jaipur, Rajasthan, India

Mohana Tenneti Krishna Aditya College of Engineering, Surampalem, India

Mohammad Sallauddin Department of Computer Science and Artificial Intelligence, SR University, Warangal, Telangana, India

Moundekar Shreyash K.J. Somaiya Institute of Engineering and Information Technology, Mumbai, India

Munnavar Hussain S. B V Raju Institute of Technology, Narsapur, Medak, Telangana, India

Muthukumaraswamy Senthil A. School of Engineering and Physical Sciences, Heriot-Watt University, Dubai, United Arab Emirates

Naga Satish G. BVRIT Hyderabad College of Engineering for Women, Hyderabad, Telangana, India

Naidu C. D. VNR Vignana Jyothi Institute of Engineering and Technology, Hyderabad, Telangana, India

Nalini N. J. Department of Computer Science and Engineering, Annamalai University, Annamalai Nagar, Tamil Nadu, India

Nallamothe Madhuri Dhanekula Institute of Technology, Vijayawada, Andhra Pradesh, India

Narahari Akanksha Department of CSE, VNRVJIET, Hyderabad, India

Nath Shashwat Manipal University Jaipur, Jaipur, Rajasthan, India

Nayak Rudra Kalyan School of CSE, VIT Bhopal University, Sehore, India

Neelakantappa M. Department of Information Technology, B V Raju Institute of Technology, Narsapur, India

Nethra Perli Department of ECE, Gokaraju Rangaraju Institute of Engineering and Technology, Hyderabad, Telangana, India

Padmaja B. Department of Computer Science and Engineering (AI & ML), Institute of Aeronautical Engineering, Hyderabad, India

Padmajarani B. Department of Computer Science and Engineering, JNTUCEH, Hyderabad, Telangana, India

Panigrahy Asisa Kumar Department of ECE, Gokaraju Rangaraju Institute of Engineering and Technology, Hyderabad, Telangana, India

Parmar Rupesh K.J. Somaiya Institute of Engineering and Information Technology, Mumbai, India

Parvathi M. ECE Department, BVRIT HYDERABAD College of Engineering for Women, Hyderabad, Telangana, India

Pasha I. A. B V Raju Institute of Technology, Narsapur, Medak, Telangana, India

Polasi Phanikumar SRM Institute of Science and Technology, Chennai, India

Pooja Sri Devineni Koneru Lakshmaiah Education Foundation, Vaddeswaram, India

Potluri Tejaswi Department of Computer Science and Engineering, Velagapudi Ramakrishna Siddhartha Engineering College, Kanuru, India

Prabodh C. P. Siddaganga Institute of Technology, Tumkur, Karnataka, India

Pradhan Roshni School of Computer Engineering, KIIT Deemed to be University, Bhubaneswar, India

Prameela M. Department of Electrical and Electronics Engineering, B V Raju Institute of Technology, Narsapur, India

Prasad J. V. D. Department of Computer Science and Engineering, Velagapudi Ramakrishna Siddhartha Engineering College, Kanuru, India

Prasanth Vaidya S. Aditya Engineering College, Surampalem, India;
Jawaharlal Nehru Technological University Kakinada, East Godavari, Andhra Pradesh, India

Praveena Manne BVRIT HYDERABAD College of Engineering for Women, Hyderabad, Telangana, India

Rajarajeswari Perepi Vellore Institute of Technology, Vellore, Tamilnadu, India

Rajesh Kammari RGM College of Engineering and Technology, Nandyala, India

Rama Padmaja Ch. V. Department of Computer Science and Engineering (AI & ML), Institute of Aeronautical Engineering, Hyderabad, India

Rama Sanjeeva Reddy B. Department of ECE, B V Raju Institute of Technology, Medak, India

Rama B. Department of Computer Science, Kakatiya University, Warangal, Telangana, India

Ramakrishna T. V. Department of ECE, Sasi Institute of Technology and Engineering, Tadepalligudam, West Godavari, Andhra Pradesh, India

Ramana Murthy B. V. Department of CSE, Stanley College of Engineering and Technology for Women, Hyderabad, India

Ramesh B. SKR Engineering College, Chennai, India

Rathod Mansing K.J. Somaiya Institute of Engineering and Information Technology, Mumbai, India

Rattan Ritika Department of Electronics and Communication Engineering, Chandigarh University, Mohali, India

Ravindranathan Shriram Department of ECE, B V Raju Institute of Technology, Narsapur, Telangana, India

Ravuri Viswanadham Department of ECE, Shri Vishnu Engineering College for Women, Bhimavaram, A.P, India

Rayaprolu Aditi Department of Information Technology, Chaitanya Bharathi Institute of Technology (CBIT-A), Hyderabad, Telangana State, India

Reddy Ch. Ramsai Technology Leaders Program, Plaksha University, Punjab, India

Rekha R. University College of Engineering and Technology, MGU, Nalgonda, Telangana, India

Rupesh M. Electrical and Electronics Engineering Department, BVRIT HYDERABAD College of Engineering for Women, Hyderabad, Telangana, India

Safala B. Anna Tanuja Chemistry Division, H&S Department, BVRIT Hyderabad College of Engineering for Women, Hyderabad, India

Sai Himaja Chowdary K. Amazon Development Center India Private Ltd, Bangalore, India

Sairam Vamsi T. Department of ECE, Shri Vishnu Engineering College for Women, Bhimavaram, A.P, India

Sandhya Rani M. Bhoj Reddy Engineering College for Women, Hyderabad, Telangana, India

Sanjeeva Reddy B. R. Department of ECE, B V Raju Institute of Technology, Medak, India

Santhi Karuppiah Panimalar Engineering College, Chennai, Tamil Nadu, India

Santhosh Kumar V. BVRIT Hyderabad College of Engineering for Women, Nizampet, Hyderabad, Telangana, India

Satapathy Suresh Chandra School of Computer Engineering, KIIT Deemed to be University, Bhubaneswar, India

Sathya A. R. Department of Computer Science and Engineering, Faculty of Science and Technology, ICFAI Foundation for Higher Education, Hyderabad, Telangana, India

Saxena Monika Banasthali Vidyapith, Jaipur, India

Sekhar G. Chandra Department of Computer Science and Engineering, Institute of Aeronautical Engineering, Hyderabad, India

Sesha Sai Priya S. Department of Computer Science and Engineering, Annamalai University, Annamalai Nagar, Tamil Nadu, India

Shaik Nilofer Lovely Professional University, Phagwara, Punjab, India;
BVRIT HYDERABAD College of Engineering for Women, Hyderabad, Telangana, India

Shanmuga Sundari M. Department of Computer Science and Engineering, Koneru Lakshmaiah Education Foundation, Vaddeswaram, Andhra Pradesh, India;
Computer Science and Engineering, BVRIT Hyderabad College of Engineering for Women, Hyderabad, India

Sharma Shivam Department of Electronics and Communication Engineering, Chandigarh University, Mohali, India

Shwetha A. N. Siddaganga Institute of Technology, Tumkur, Karnataka, India

Simhadri Suma Sree Department of CSE, VNRVJIET, Hyderabad, India

Sinha Mehul Manipal University Jaipur, Jaipur, Rajasthan, India

Somlal Jarupula Department of Electrical and Electronics Engineering, Koneru Lakshmaiah Education Foundation, Vaddeswaram, AP, India

Sowmiya B. Department of Computing Technologies, SRM Institute of Science and Technology, Chennai, India

Sravya Siripurapu Department of ECE, B V Raju Institute of Technology, Narsapur, TS, India

Srilakshmi B. V. D. N. Department of ECE, GRIET, Hyderabad, India

Srinivas Punna Electrical and Electronics Engineering Department, BVRIT HYDERABAD College of Engineering for Women, Hyderabad, Telangana, India

Sriram Cholleti Department of Electrical and Electronics Engineering, Koneru Lakshmaiah Education Foundation, Vaddeswaram, AP, India

Sudhamsu Preetham J. V. R. Department of ECE, Gokaraju Rangaraju Institute of Engineering and Technology, Hyderabad, Telangana, India

Sukitha Puli Sai Department of ECE, B V Raju Institute of Technology, Narsapur, TS, India

Sulthana Shaik Rehna Koneru Lakshmaiah Education Foundation, Vaddeswaram, India

Sunitha Devi P. G.Narayanamma Institute of Technology and Science, Shaikpet, Hyderabad, Telangana, India

Sunitha K. V. N. Department of Computer Science and Engineering, BVRIT Hyderabad College of Engineering for Women, Bachupally, Hyderabad, Telangana, India

Sunku Janakiram Department of ECE, B V Raju Institute of Technology, Narsapur, Telangana, India

Sushma Anthireddygar Department of ECE, B V Raju Institute of Technology, Narsapur, TS, India

Swaminathan Subbiah Computer Science and Engineering, Saveetha School of Engineering, Chennai, India

Takellapati Venkata Suneetha Gokaraju Rangaraju Institute of Engineering and Technology, Hyderabad, Telangana, India

Taminana Shesagiri Computer Science and Systems Engineering, Andhra University College of Engineering (A), Andhra University, Visakhapatnam, India

Terlapu Sudheer Kumar Department of ECE, Shri Vishnu Engineering College for Women, Bhimavaram, A.P, India

Thinakaran Kandasamy Saveetha School of Engineering, Chennai, Tamil Nadu, India

Upendra Kumar P. GMR Institute of Technology, Rajam, Andhra Pradesh, India

Vaishali Purude Department of CSE, Koneru Lakshmaiah Education Foundation, Aziznagar, Hyderabad, Telangana State, India;
Neil Gogte Institute of Technology, Uppal, Hyderabad, Telangana, India

Varghese Angelin School of Engineering and Physical Sciences, Heriot-Watt University, Dubai, United Arab Emirates

Vasudeva Reddy T. B V Raju Institute of Technology, Narsapur, Medak, Telangana, India

Vemula Madhavi Chemistry Division, H&S Department, BVRIT Hyderabad College of Engineering for Women, Hyderabad, India

Venkata Subbarao M. Department of ECE, Shri Vishnu Engineering College for Women, Bhimavaram, A.P, India

Venkataiah K. C. Ashoka Women's Engineering College, Dupadu, India

Verma Yogesh Kumar SEEE, Lovely Professional University, Jalandhar, Punjab, India

Vinitha Joshy P. Centre for Cyber Physical Systems, School of Electronics Engineering, Vellore Institute of Technology, Chennai, India

Vishnu Vardhan J. Naga Department of ECE, BVRIT Hyderabad College of Engineering for Women, Hyderabad, India

Vyas Vaibhav Banasthali Vidyapith, Jaipur, India

Yambakam Suhruth Department of ECE, B V Raju Institute of Technology, Narsapur, Telangana, India

Yashwanth Raj K. Department of Computing Technologies, SRM Institute of Science and Technology, Chennai, India

Yeshwanth Reddy Jakka Department of ECE, B V Raju Institute of Technology, Narsapur, TS, India

A Novel Controller for Multiple-Input Bidirectional DC–DC Power Converter of HESS for DC Microgrid Applications



Punna Srinivas, Chava Sunil Kumar, M. Rupesh, and Battapothula Gurappa

Abstract Recently, the batteries deliver great discharging efficiency, but the capability extremely reduces the discharging effectiveness as the load current rises. This paper presented an advanced controller for multiple-input bidirectional DC–DC power converter (MIPC) in hybrid energy storage system (HESS). The supercapacitor (SC) association with battery is called as HESS. The projected system is utilized as an advanced controller for MIPC. The modeling of the proposed system is designed by MIPC, DC sources, HESS, and the controller. The controlling process is utilized with MIPC process, and the input is produced from the HESS. To achieve the optimal output load voltage maintained as constant output load voltage at any nonlinear condition is the novelty of the paper. The MATLAB/Simulink platform was utilized for simulating the proposed system. The simulation results are developed for proposed controller for two-input bidirectional converter for sudden change in photovoltaic (PV) generation and load demand.

Keywords DC link voltage · MIPC · HESS · Battery · SC and PI controllers

1 Introduction

Generally, the alternative energy origins are evaluated to employ a required portion in the world's power request based on the availability and not as much of impact [1]. As

P. Srinivas (✉) · C. S. Kumar · M. Rupesh
Electrical and Electronics Engineering Department, BVRIT HYDERABAD College of Engineering for Women, Hyderabad, Telangana, India
e-mail: srinivas.p@bvrithyderabad.edu.in

C. S. Kumar
e-mail: sunilkumar.ch@bvrithyderabad.edu.in

M. Rupesh
e-mail: rupesh.m@bvrithyderabad.edu.in

B. Gurappa
B V Raju Institute of Technology Narasapur, Telangana, India
e-mail: Gurappa.b@bvrithyderabad.edu.in

per the best renewable energy source (RES), the solar power generation stays recently conceived. The grouping of battery and SC can deliver an outstanding contest which shielded a broad collection of power and energy supplies in RESs, like wind and PV, individual power generators depend heavily on energy storage systems (ESSs) [2]. The important structures of ESSs comprise conservation, energy density, life span, power density, and cost [3].

The HESSs are classified by the procedure of power converters in the structures which are two types as passive or active [4]. For combining the storage device and DC link, the active technique uses one or more DC–DC converters [5]. A HESS must have a power conditioning component as well as an energy management strategy (EMS). If the DC–DC converters are utilized in HESS, the multi-input converters (MICs) can be situated for projecting the economical, simple for access also intelligent to stabilize the parameters of ESS [6]. These converters have demonstrated increased responsiveness when the circuit topology is simple, the storage component power flow is bidirectional controlled, there is high consistency, and the production cost and size are minimal. Managing the power flow of the SC with battery based on the controller approach stands necessary for HESS for improving the consumption and capability [7].

The SC-battery topology in the battery storage associated with the DC bus was the maximum useful and researched HESSs. To operate the power flow among the battery and SC, a bidirectional converter is applied [8–11].

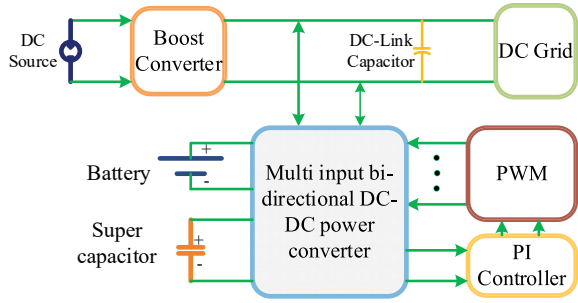
The organized paper is presented in the subsequent section. Section 2 describes the full study of the proposed method. The suggested structure's simulation findings are then evaluated in Sect. 3. The proposed approach in Sect. 4 is resolved in the concluding portion of this work.

2 Analysis of Proposed MIPC with Enhanced PI Controller

This section discussed the proposed MIPC and enhanced PI controller for improving the performance of the DC grid-integrated PV system. The MIPC is a cost-effective and flexible way to interface HESS like battery and SC. The proposed MIPC is employed to connect the various sources with dissimilar voltage levels, and also it decreases the system size, rate, and power losses outstanding to the less number of components used in the system. The purpose of MIPC is stabilizing the voltage level of the system with bidirectional power flow ability.

Figure 1 shows the control structures of proposed MIPC connected with PV integrated DC grid. The MIPC converter is used for power flow in sources to load as well as a load to sources. The brief explanation of the suggested control structure and the proposed converter is explained as follows.

Fig. 1 Block diagram of a proposed system with MIPC controller



2.1 Overview of MIPC

The MIPC is simple to design and control, and also it is highly flexible of interfacing multiple sources that are the purposes utilized in the proposed system. In this converter, it is possible to interconnect many DC origins of dissimilar voltage stages and to cover some amount of origins [12]. The MIPC transfers power in forward and reverse direction ability and potential toward manage power flow among some of the origins individually.

For each origin through an inductor, the proposed MIPC topology established in Fig. 2 could design by combining a switching leg. The following section has explained the modes of operation of the MIPC.

Mode A: Power Flow of Battery and DC Link:

Here, the battery has stored the energy and transmitted through DC link to the grid. The converter switching process is based on the sequence as given in Table 1. In the time period T_1 , the switches S_2 and S_3 are turned on by storing the energy of battery associated with DC link and inductor L_1 . The voltage across L_1 is measured as the battery voltage V_{bat} and the current with a slope of V_{bat}/L_1 . In the time period T_2 , the switches are in off condition, the diodes D_1 and D_4 are forward biased, and the inductor L_1 current i_{L_1} flows to the DC link capacitor. During the time T_1 , the storage of the energy in L_1 and the C_{dc} is being discharged with a negative slope of V_{dc}/L_1 .

Fig. 2 Control structure of MIPC

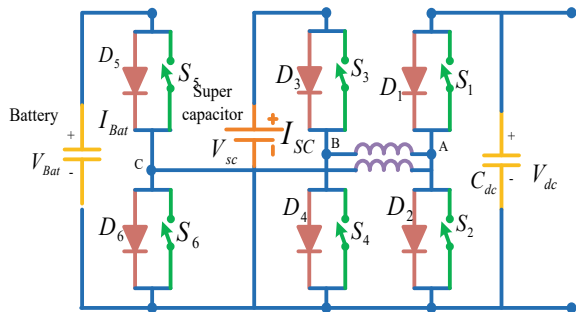


Table 1 Transmission of devices in some time periods of the modes

Modes of operation	T ₁	T ₂	T ₃
Mode A(i)	S ₂ and S ₃	D ₄ and D ₁	S ₁ and S ₄
Mode A(ii)	S ₁ and S ₄	D ₂ and D ₃	S ₂ and S ₃
Mode B(i)	S ₂ and S ₅	D ₆ and D ₁	S ₁ and S ₆
Mode B(ii)	S ₁ and S ₆	D ₂ and D ₅	S ₂ and S ₅
Mode C(i)	S ₃ and S ₆	D ₅ and D ₃	S ₅ and S ₃
Mode C(ii)	S ₅ and S ₃	D ₆ and D ₃	S ₃ and S ₆

The relation among the voltage of DC link and battery in steady-state operation is presented as Eq. (1),

$$V_{dc} = \frac{T_1}{T_2 + T_3} V_{bat} = \frac{D}{1 - D} V_{bat} \quad (1)$$

Here, the duty ratio D is determined by T_1/T_S . The switching cycle time period T_S is described in all three time periods. By controlling, the $D > 0.5$ converter boosts V_{bat} to V_{dc} when the voltage of the battery is not more than the DC link voltage V_{dc} . To control the DC link at $D > 0.5$, the converter charges the battery when the voltage of the battery is greater than the voltage of the DC link. Mode A (ii) switching sequence operation principle of transfer energy is similar, and the energy is stored in L_1 at the time period T_1 and applied to charge the battery at periods T_2 and T_3 . The relationship between the two voltages regarding duty ratio D to T_1/T_S is described in Eq. (2),

$$V_{bat} = \frac{T_1}{T_2 + T_3} V_{dc} = \frac{D}{1 - D} V_{dc} \quad (2)$$

Mode B: Power Flow of SC and DC Link:

This section explains about the energy transmitted from SC to DC link. The SC requires the voltage level that is boosted with the higher DC link voltage. The switching sequence of this mode of operation is presented in Table 1. During T_1 , the SC charges the inductor L_2 by turning on the switches S_2 and S_5 , while the other switches are turned off. With a slope of V_{SC}/L_1 , the inductor current i_{L2} rises. When the inductor L_2 is charged for a predetermined amount of time, the switches S_2 and S_5 are switched off, allowing diodes D_1 and D_6 to conduct. The SC saves energy in the inductor L_2 by charging the DC link capacitance and therefore supplying the load. The switches S_1 and S_6 are switched on during the time interval T_3 . This effectively forms a rectifier in the converter with a reduced voltage drop, resulting in lesser losses. By applying volt-sec balance, the voltages V_{dc} and V_{SC} are computed in Eq. (3),

$$V_{dc} = \frac{T_1}{T_2 + T_3} V_{sc} = \frac{D}{1 - D} V_{sc} \quad (3)$$

In the mode B (ii) as given in Table 1, the SC is charging through DC link, and the other devices are exchanged. The current flow of the inductor L_2 is in opposite direction of mode B (i), and the power flow is inverted. The relationship between two voltages based on the duty ratio D to be T_1/T_3 is given as Eq. (4),

$$V_{sc} = \frac{T_1}{T_2 + T_3} V_{dc} = \frac{D}{1 - D} V_{dc} \quad (4)$$

when the converter is controlled at $D > 0.5$, the SC from DC link has a higher voltage.

Mode C: Power Flow with Battery and SC:

The two energy sources voltage levels have a few changes conceivable by controlling four switches S_3 to S_6 . In mode C (i) while charging the SC from the battery, the converter could be controlled in boost, buck, or buck–boost mode. The voltage of the battery is utilized for charging the SC, and the switching states are presented in Table 1.

Here, the inductors L_1 and L_2 are saving energy in the interval T_1 as of the battery over S_3 and S_6 . Finally, the switch S_6 is closed and imposing the current of the inductor to flow by D_5 to charging the SC. The switch S_5 is gated on in the successive time interval T_3 controlling as a synchronous rectifier to decrease the voltage losses across D_5 . The relation among the two voltages is afforded as Eq. (5),

$$V_{sc} = \frac{T_1}{T_2 + T_3} V_{bat} = \frac{D}{1 - D} V_{bat} \quad (5)$$

Similarly, energy can be transported as of the SC to the battery using switching combination of switches S_3 , S_5 , and S_6 but with various reliable periods resulting in opposed current over the inductors as equated in mode C (i).

Energy transmitted to the battery from the SC was determined by the time interval T_1 for which S_5 is continued ON afforded by Eq. (6),

$$V_{bat} = \frac{T_1}{T_s} V_{sc} = D \cdot V_{sc} \quad (6)$$

From the equation, it is clearly explained about the energy transmitted only if V_{bat} is lesser than V_{sc} . If this condition is not satisfied, then the several operation modes are enforced to handle the switches without altering the structure of the circuit.

Mode D: Power Flow with Battery and SC to DC Link:

Table 2 lists the switching conditions for this operation mode, which divides the switching cycle T_s into five time periods. Switches S_1 and S_6 are given matching gate signals with a duty ratio of d_2 , while switches S_2 and S_5 are given signal balancing. The gate signal of the switch S_3 corresponds to that of a switch S_1 with a duty ratio

Table 2 Transmission of devices in different time periods

Modes	Time: T_1	Time: T_2	Time: T_3	Time: T_4	Time: T_5
Mode D	S_2, S_3, S_5	S_2, D_4, S_5	S_2, S_4, S_5	D_1, S_4, D_6	S_1, S_4, S_6
Mode E	S_1, S_3, S_5	D_2, S_3, S_5	S_2, S_3, S_5	S_2, S_4, S_5	S_1, S_3, S_5

of d_1 . With a dead time, the complimentary switched S_4 is to switch S_3 . Switches S_2, S_3 , and S_5 are allowed on charging both the inductors L_1 and L_2 by equivalent origins V_{bat} and V_{SC} during the interval T_1 , the current is raised with an angle of V_{bat}/L_1 and V_{SC}/L_2 correspondingly.

The switches S_2 and S_5 are in off states till the time period T_3 , imposing current to flow over series diodes of representing balancing switches. Stored energy in the inductor L_1 with L_2 is transmitted to the DC link over the diode D_1 subsequent in a voltage ripple of 1–1.2 V. An inaugurating the voltage–time stability for L_1 and L_2 , the association with the three voltages is afforded in Eqs. (7) and (8),

$$V_{\text{bat}} = \frac{T_4 + T_5}{T_1} V_{\text{dc}} = \frac{d_2 T_s}{d_1 T_s} V_{\text{dc}} = \frac{d_1}{d_2} V_{\text{dc}} \quad (7)$$

$$V_{\text{sc}} = \frac{T_4 + T_5}{T_1 + T_2 + T_3} V_{\text{dc}} = \frac{d_2 T_s}{T_s - d_2 T_s} V_{\text{dc}} = \frac{d_2}{1 - d_2} V_{\text{dc}} \quad (8)$$

Here, d_1 is the fraction of S_3 's on time compared to the whole switching period T_s , and d_2 is the fraction of S_2 's on time compared to the overall switching period T_s . For a required boost ratio of V_{SC} to V_{dc} , the d_2 may be calculated. Because the SC voltage is intended to be lower than V_{dc} , the voltage gain calculated, for example M_2 , operates the duty ratio d_2 every time it is less than 0.5. The variation of M_2 in d_2 lies between 0 and 0.5. Alternatively, the switch S_3 can control a duty fraction among 0 to $(1 - d_2)$ for enhancing the voltage of the battery to DC link. The gain M_1 connecting V_{bat} and V_{dc} is afforded in Eq. (9),

$$M_1 = \frac{V_{\text{bat}}}{V_{\text{dc}}} = \frac{d_2}{d_1}; \quad M_2 = \frac{V_{\text{sc}}}{V_{\text{dc}}} = \frac{d_2}{1 - d_2} \quad (9)$$

For a given value of d_2 , the minimum voltage gain M_1 can be calculated, and the maximum duty ratio d_1 can be imagined. The SC to DC link boost ratio is lower than the maximum value of the battery to DC link boost ratio. As a result, the switching sequence can only be used if V_{bat} is greater than V_{SC} .

Mode E: Power Flow of DC Link to Battery and SC:

The renewing power is extraordinarily enhanced than the battery which can engage in sudden braking condition. The additional energy that the battery is unable to capture is linked to the charging SC, which has a higher power density than the battery. Table 2 shows the switching sequence for this mode.

During the time period T_1 , switches S_1 , S_3 , and S_5 are active, transmitting energy from the DC link to both secondary sources. As V_{dc} arrives at point A, the inductor currents i_{L1} and i_{L2} increase. The switch S_1 is then switched off during the T_1 time period, and the inductor currents flow across the diode D_2 . The switch S_2 is turned on to serve as a synchronous rectifier in T_3 and reduce the voltage drop across the diode. The switch S_3 is turned off, and the switch S_4 is switched on to keep the current flowing through the inductor L_1 by controlling the charging of two sources separately. The inductor current i_{L1} continues to charge, while the switches S_2 and S_4 are turned off at the end of the time period T_4 . The inductor current flows from DC link to battery and SC over switches S_1 , S_5 and diode D_3 . The switch S_3 is turned on execution a way for i_{L1} by decreasing the voltage drop through it. The association among the three voltage sources can be derived by using voltage–time stability through the inductors. The SC voltage V_{sc} is controlled by varying d_1 which is related to Eqs. (10) and (11),

$$V_{bat} = \frac{T_1 + T_5}{T_1 + T_2 + T_3 + T_5} V_{dc} = \frac{T_1 + T_5}{T_s - T_4} V_{dc} = \frac{d_1}{d_2} V_{dc} \quad (10)$$

$$V_{sc} = \frac{T_1 + T_5}{T_s} V_{dc} = d_1 \cdot V_{dc} \quad (11)$$

By altering the variable d_2 for an afforded value of d_1 , the energy transported to the battery is aligned. Both voltage origins gain functions are determined as Eq. (12),

$$M_1 = \frac{V_{sc}}{V_{dc}} = d_1; \quad M_2 = \frac{V_{bat}}{V_{dc}} = \frac{d_1}{d_2} \quad (12)$$

The voltage gain variation M_1 is a linear function that is relevant to d_1 .

3 Results and Discussion

This section discussed the detailed results of the suggested system, which consists of the MIPC, PI controller, battery, and SC and DC source. The suggested system is simulated in MATLAB/Simulink. The proposed system maintains the DC link voltage constant at any variations. The proposed PI controller has controlled the MIPC for stabilizing the DC link voltages.

3.1 Case-I: Step Increase in PV Generation

Figure 3 shows the simulation results for a step increase in PV generation using an improved PI control system. Due to atmospheric fluctuations, the PV panel's power

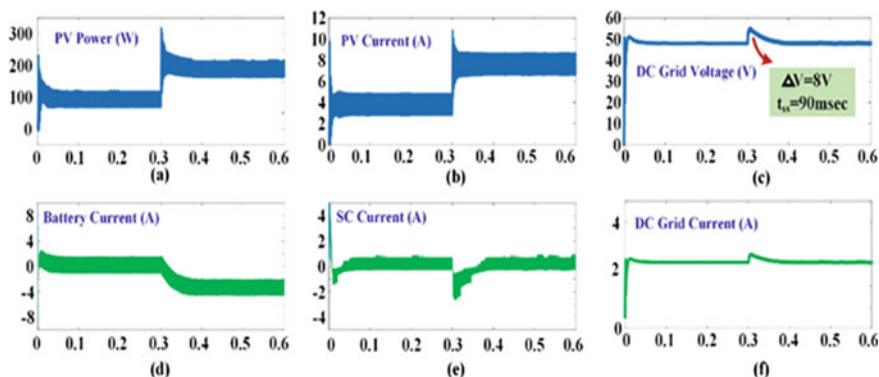


Fig. 3 Simulation results for increase in PV

output increases from 96 to 192 W at $t = 0.3$ s in the control scheme. PV current rises from 4 to 8 A at $t = 0.3$ s as a result of this. The load power requirement is constant at 96 W in this situation. When PV power exceeds the load power demand, DC grid voltage rises over 48 V. SC absorbs 96 W of surplus power in a short period of time until the battery can control the grid voltage to 48 V. As a result, the battery and SC charge in accordance with the energy management system to keep the grid voltage at 48 V constant. The simulation results show a settling time of 90 ms, and peak overshoot is 8 V for enhanced control scheme.

3.2 Case-II: Step Decrease in PV Generation

Figure 4 shows the simulation results for a step fall in PV generation with enhanced PI control systems. Due to atmospheric variations, the PV panel's power output varies from 192 to 96 W at $t = 0.3$ s under the enhanced control system. The reduction in PV generation produces a reduction in PV current from 8 to 4 A. The fall in PV generation results in reduction in DC grid voltage. The settling time and change in DC grid voltage for control schemes are 120 ms and 12 V, respectively.

3.3 Case-III: Step Increase in Load Demand

Figure 5 shows the simulation results for a step increase in load demand with an enhanced control strategy. The load demand increases from 96 to 192 W at $t = 0.3$ s. The load current is increased from 2 to 4 A as a result of this. PV current is constant at 4 A in this situation. The steady-state values are $V_{dc} = 48$ V, $i_{PV} = 4$ A, and $i_o = 2$ A before $t = 0.3$ s. The load demand rises to 192 W at $t = 0.3$ s, which is beyond the power range of PV production. This causes a power imbalance between the supply

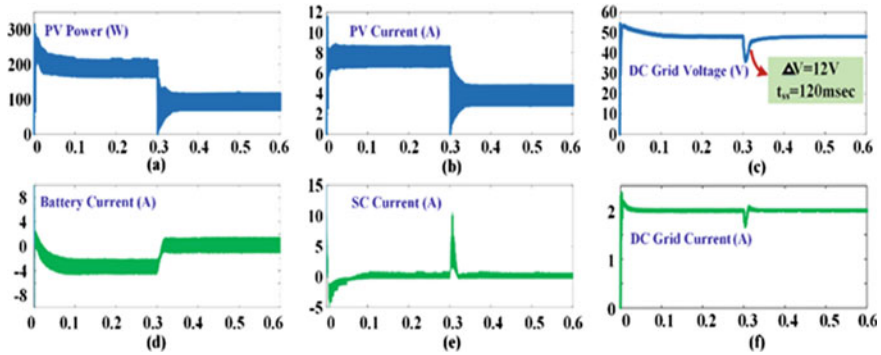


Fig. 4 Simulation results for decrease in PV

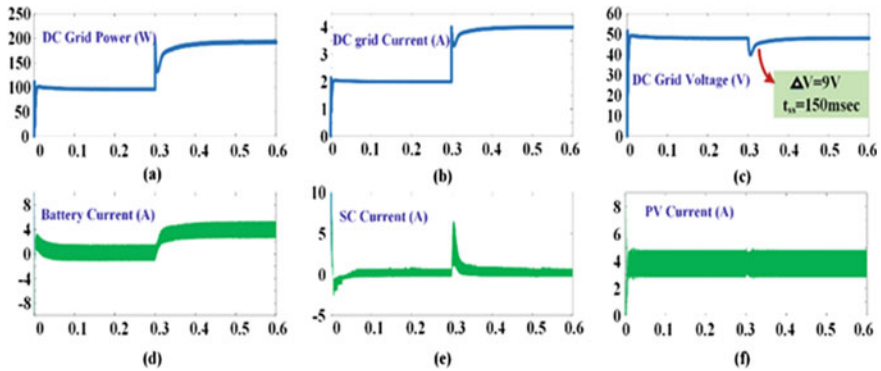


Fig. 5 Simulation results for increase in load

and the load. HESS responds quickly with the SC supplying the transient component of power demand and the battery supplying the steady-state component. The DC grid voltage is regulated in 150 ms, and DC grid voltage ripple is 9 V as shown in Fig. 5.

3.4 Case-IV: Step Decrease in Load Demand

Figure 6 shows the simulation results for a step decrease in load demand for enhanced control systems. The load power consumption drops from 192 to 96 W at $t = 0.3$ s. The load current drops from 4 to 2 A as a result of this. The DC grid voltage is affected by a quick change in load current. To handle the extra power in the DC microgrid, HESS reacts quickly to these variations. In an improved control system, the SC handles the transient component of power, while the battery handles the average or steady-state component. The voltage was restored in 120 ms with a DC grid ripple value of 5.5 V.

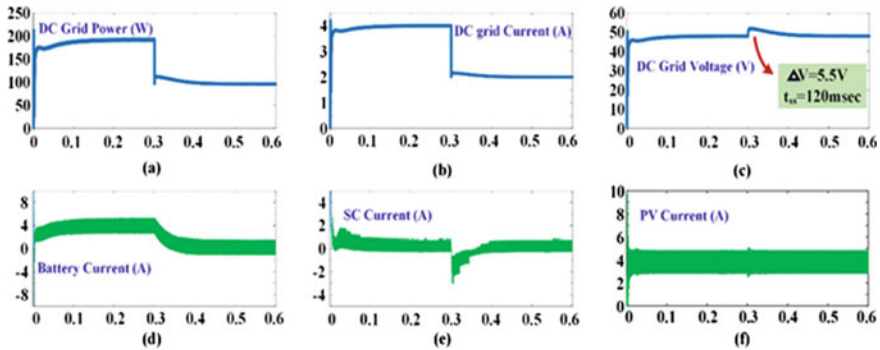


Fig. 6 Simulation results for decrease in load

4 Conclusion

A controller was designed for the two-input bidirectional converter for HESS control. The performance of designed controller is analyzed in various cases for the application of voltage regulation in DC microgrid. Controller could effectively stabilize DC microgrid against disturbances from source PV generation as well as load variations. It could utilize inherent fast dynamics of supercapacitor for absorbing incoming transients to the microgrid. This unified controller was found to be sufficient for both charging and discharging HESS. Decoupled, distinct, and independent control of supercapacitor and battery power, as well as power transfer between them, was also achieved. It may also be utilized in hybrid electric vehicle applications when power is supplied by two or more sources. Operation mode of HESS converter for maintaining SOC of supercapacitor always within desired limit was also demonstrated.

References

1. Hredzak B, Agelidis VG, Jang M (2014) A model predictive control system for a hybrid battery-ultracapacitor power source. *IEEE Trans Power Electronics* 29(3):1469–1479
2. Wee KW, Choi SS, Vilathgamuwa DM (2013) Design of a least-cost battery-supercapacitor energy storage system for realizing dispatchable wind power. *IEEE Trans Sustain Energy* 4(3):786–796
3. Onar OC, Khaligh A (2012) A novel integrated magnetic structure based DC/DC converter for hybrid battery/ultracapacitor energy storage systems. *IEEE Trans Smart Grid* 3(1):296–307
4. Shen J, Dusmez S, Khaligh A (2014) Optimization of sizing and battery cycle life in battery/ultracapacitor hybrid energy storage systems for electric vehicle applications. *IEEE Trans Ind Informatics* 10(4):2112–2121
5. Chia YY, Lee LH, Shafiabady N, Isa D (2015) A load predictive energy management system for supercapacitor-battery hybrid energy storage system in solar application using the support vector machine. *Int J Appl Energy* 137:588–602
6. Ma T, Yang H, Lu L (2015) Development of hybrid battery–supercapacitor energy storage for remote area renewable energy systems. *Int J Appl Energy* 153:56–62

7. Song Z, Hofmann H, Li J, Hou J, Han X, Ouya M (2014) Energy management strategies comparison for electric vehicles with hybrid energy storage system. *Int J Appl Energy* 134:321–331
8. Punna S, Manthati UB (2020) Optimum design and analysis of a dynamic energy management scheme for HESS in renewable power generation applications. *SN Appl Sci* 2(3):1–13
9. Kollimalla SK, Mishra MK, Narasamma NL (2014) Design and analysis of novel control strategy for battery and supercapacitor storage system. *IEEE Trans Sustain Energy* 5(4):1137–1144
10. Punna S, Manthati UB, Arunkumar CR (2021) Modelling, analysis and control of a two-input bidirectional DC-DC converter for HESS in DC microgrid applications. *Int Trans Electrical Energy Syst* 31(10):e1274
11. Rupesh M, Vishwanath Shivalingappa T (2019) Evaluation of optimum MPPT technique for PV system using MATLAB/Simulink. *Int J Eng Adv Technol (IJEAT)*. Blue Eyes Intelligence Engineering & Sciences Publication ISSN: 2249-8958
12. Rezkallah M, Hamadi A, Chandra A, Singh B (2015) Real-time HIL implementation of sliding mode control for standalone system based on PV array without using dumpload. *IEEE Trans Sustain Energy* 6(4):1389–1398

Model-Based Automatic Seizure Detection of EEG Signal Analysis by Frequency and Time Domain Methods



S. Sesha Sai Priya and N. J. Nalini

Abstract Model-based automatic seizure detection of EEG signals which detects seizures automatically in terms of electroencephalogram (EEG) signals. Hilbert marginal spectrum (HMS) is used to understand EEG signals as they are highly nonlinear and nonstationary signals, and hence, traditional Fourier analysis (TFA) method fails to represent amplitude of each frequency. The Hilbert spectrum works as a two-step process in which signal is separated into intrinsic mode functions, and then, Hilbert transform is applied to the result to obtain frequency spectrum (FS). The proposed methodologies useably developed an automatic seizure detection model in which frequency represented by HMS is fed into support vector machine (SVM), and hence, seizures are detected by comparing EEG signals with Fourier frequency analysis. In this paper, it is even proved that the developed method is more effective than the existent method by comparing the results obtained from both the methods on same database. MATLAB software is used for carrying out the results.

Keywords Frequency spectrum (FS) · Traditional Fourier analysis (TFA) · Support vector machine (SVM) · Fourier frequency analysis (FFA)

1 Introduction

First, EEG recordings of induced seizures by Cybulski (1914) and later first human EEG recordings invented the term electroencephalogram (EEG) which is formed in 1947 by American EEG Society [1].

Electrical signals that are generated by the brain as shown in Fig. 1. By using electrodes, the underlying mechanism in the generation of signals needs to know the neuronal activities and neurophysiologic properties of the brain together shown in Fig. 2. [2, 3] and their recordings, analysis, and treatment of various disorders in brain and the related diseases which is used to build the hybrid model.

S. Sesha Sai Priya (✉) · N. J. Nalini

Department of Computer Science and Engineering, Annamalai University, Annamalai Nagar, Tamil Nadu 608002, India

e-mail: saipriya.509@gmail.com



Fig. 1 EEG recordings of induced seizures by Cybulski



Fig. 2 EEG signal recordings in seizures by electrodes

2 Literature Survey

Table 1 describes the recent literature review stated which is relevant to classification of epileptic seizures. Electrical activity, recorded via electrodes on the scalp, denotes the potential fluctuations recorded from the brain by Table 1 [7].

3 Development of EEG Model

The brain starts neural activities between the generation of signals needs to know the neuronal activities and neurophysiologic properties of the brain. Electrical signals generated from the human brain represent not only functionality of the brain but also status of the whole body [4]. This assumption drives the motivation to process advanced signal processing approaches on modelling of the electroencephalogram

Table 1 Recent literature survey for classification of epileptic seizures

S. No	Author and Year	Application area	Datasets	Essential features extracted	Techniques applied	Accuracy yields (%)
1	Alickovic et al. (2018)	Epileptic seizure and prediction	CHB-MIT scalp EEG database	Mean, energy, entropy-time domain features	Multi-scale principal component analysis, Empirical mode decomposition, Random forest	96.90
2	Janjarasjitt (2017)	Classification of epileptic seizure	CHB-MIT scalp EEG database	Time & frequency domain features	Discrete wavelet transform, Radial basis Support vector machine	96.87
3	Acharya et al. (2018)	Diagnosis the epileptic seizure	Bonn University database	Raw EEG signals	Convolutional neural network	88.70
4	Li et al. (2018)	Epileptic seizure detection	Bonn University database	Fuzzy entropy and distance entropy-time domain features	Quadratic discriminant analysis	92.80

(EEG) signals measured from the brain of a human subject as shown in Fig. 3a, b [5–7].

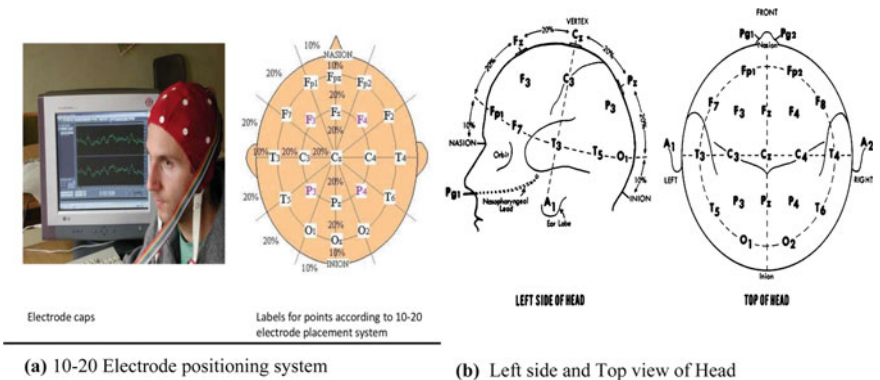


Fig. 3 a 10–20 electrode positioning system, b left side and top view of head

4 Proposed Methodology

Even when a human is in sleep state, the underlying mechanism in the generation of signals needs to know the neuronal activities [8]. This action shown as wavy lines on an EEG recording with proposed methodology overview as shown in Fig. 5.

Needle electrodes, the human brain represents not only functionality of the brain. The actual EEG signal may be even masked because of neuronal activities and neurophysiologic properties of the brain as shown in Fig. 4 [9] (Fig. 5).

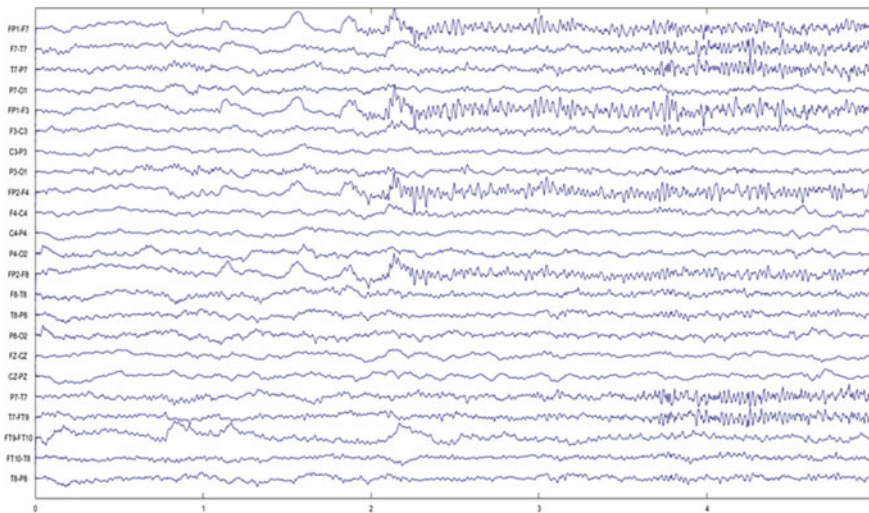


Fig. 4 Neuron membrane potential

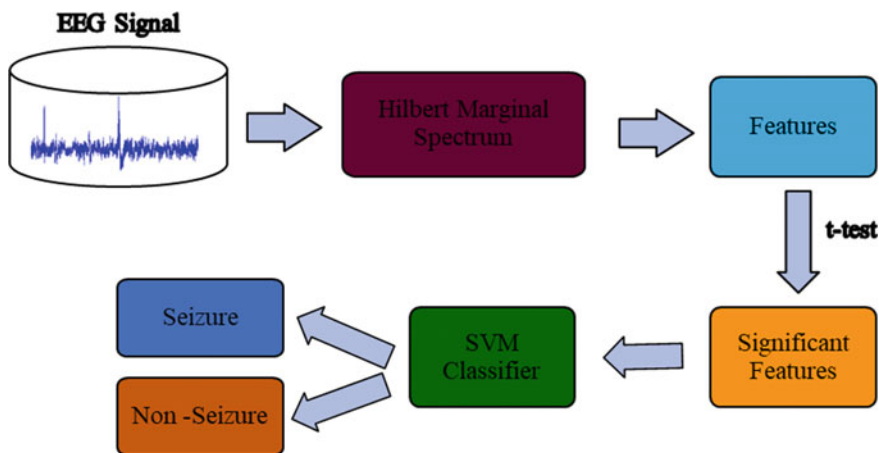


Fig. 5 Proposed methodology overview diagram

4.1 Empirical Model Decomposition (EMD)

The sampling rate is 128 Hz, which allows for frequency analysis up to 60 Hz which is most approximation from 14 probes places around the scalp. Empirical mode decomposition (EMD) and Hilbert spectral analysis, which are amplitude and frequency modulated signals as shown experimental results from Figs. 7, 8, 9, 10, 11 and 12. Measure of the brain’s electrical function, band energy features, and spectral entropies are extracted as features from the HMS. Therefore, the model obtained one as shown in Fig. 6 [10] and in a generalised distribution, maximal anteriorly, during drowsiness [11]. It is usually abnormal under other circumstances. Moreover, the significance of the EEG signals is tested by extraction as shown in Fig. 6.

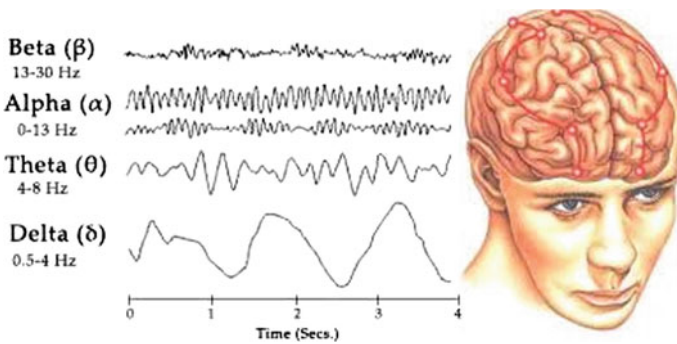


Fig. 6 Different brain rhythms

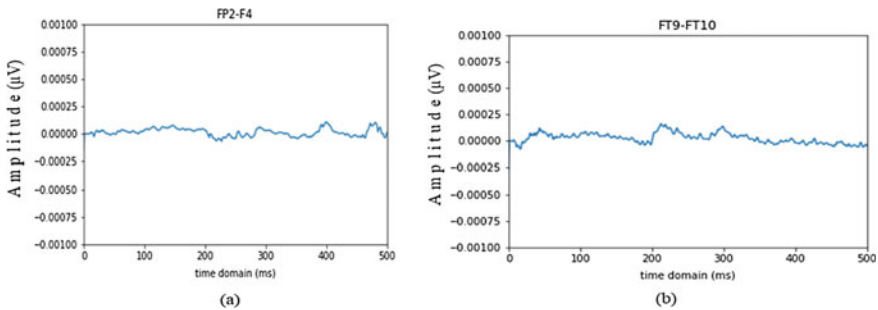


Fig. 7 Detect the seizure of EEG signal in time analysis at FP2-FP4 and FT9-FT10

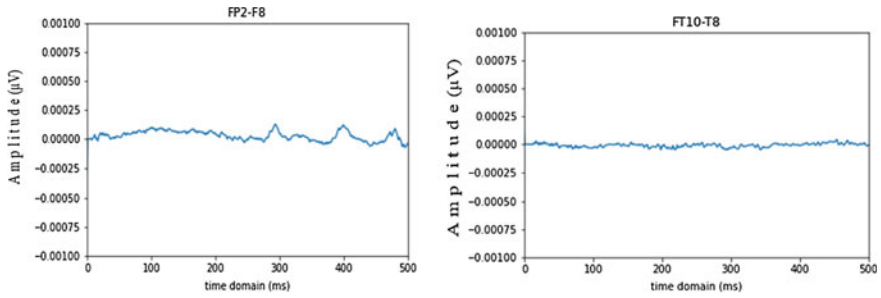


Fig. 8 Detect the seizure of EEG signal in time analysis at FP2-F8 and FT10-T8

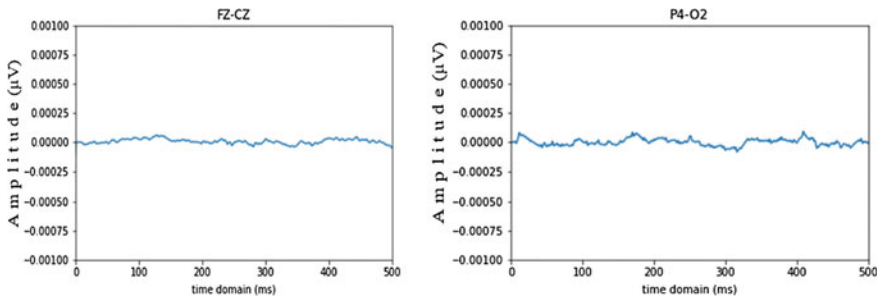


Fig. 9 Detect the seizure of EEG signal in time analysis at FZ-CZ and P4-O2

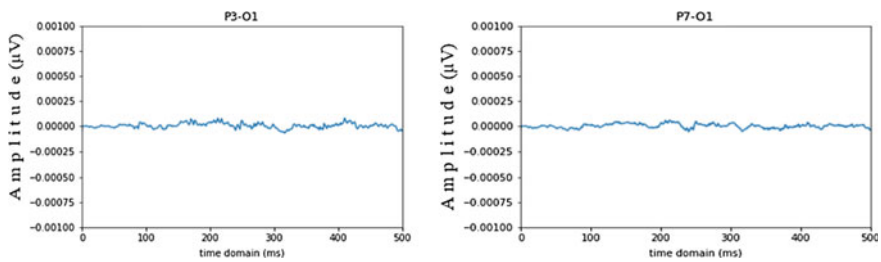


Fig. 10 Detect the seizure of EEG signal in time analysis at P3-O1 and P7-O1

4.2 Intrinsic Mode Functions (IMFs)

Electrode positioning system avoids the eyeball placement as the signals can be analysed to detect medical abnormalities, activation level based on the nonstationary of the different brain rhythms model wave forms as shown in Fig. 8 by HMS, recruitment order or to analyse of movements based on the emphatical model edf data. Therefore, those are analysed by using the HMS and SVM are two kinds of EEG in

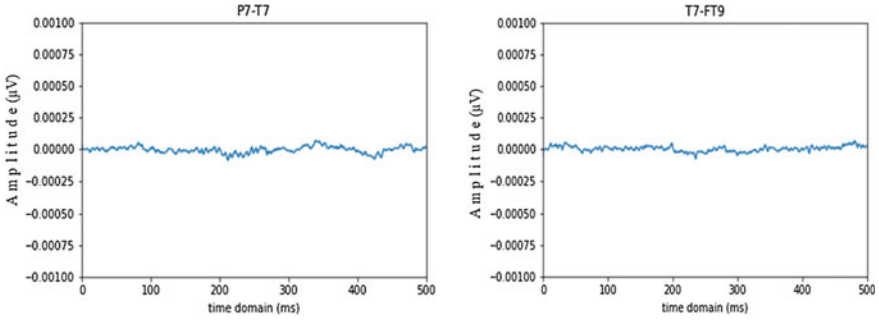


Fig. 11 Detect the seizure of EEG signal in time analysis at P7-T7 and T7-FT9

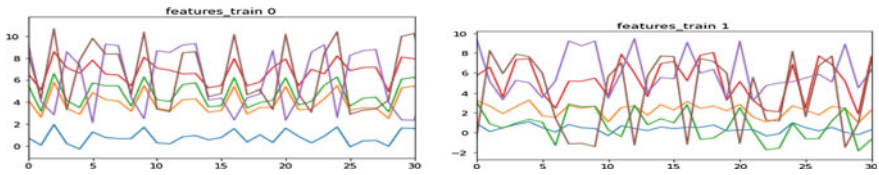


Fig. 12 Hypothesis testing is conducted at train 0 and train 1 for feature extraction

widespread uses to recognise to detect the automatic seizure detection of EEG signal analysis as show from Fig. 8.

The advantage of proposed methodology as shown in Fig. 5, because there are number of factors such neurophysiologic properties of the brain as shown Fig. 6, motor unit recruitment and the anatomy of the muscles are separated and surrounding tissues that contribute to the recording on individual frequency and time domain analysis from Figs. 7, 8, 9, 10 and 11 [12–14, 17].

4.3 Hilbert Marginal Spectrum (HMS)

The HMS analysis can be well applied to nonlinear and nonstationary processes. This work presents a new technique for automatic seizure detection in electroencephalogram (EEG) signals by using Hilbert marginal spectrum (HMS) analysis. A hypothesis testing is conducted for feature selection or extraction as shown in Figs. 12, 13 and 14.

The number of extreme points and the number of zero crossings must be the refuel or differ at most by one. At any hypothesis testing at each electrode point, which is defined by the average of the maximum and minimum envelopes from zero in this paper are shown from Figs. 12, 13 and 14 [15, 16]. The features with lower at hypothesis testing of activation function for classification of seizure and no seizure

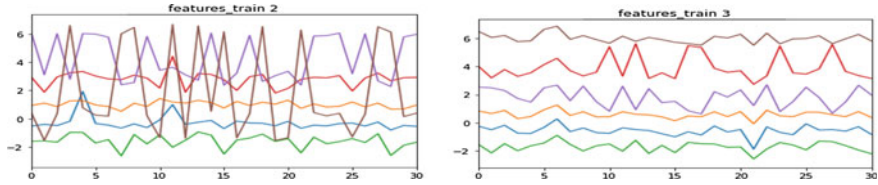


Fig. 13 Hypothesis testing is conducted at train 2 and train 3 for feature extraction

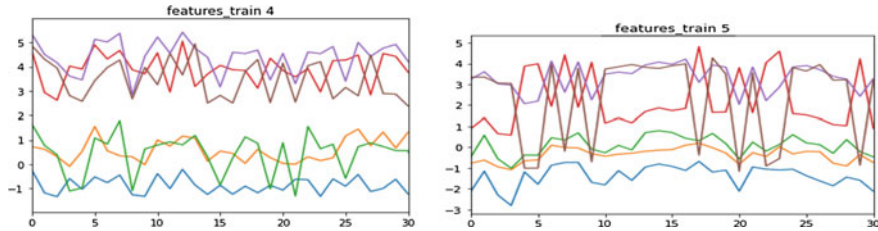


Fig. 14 Hypothesis testing is conducted at train 4 and train 5 for feature extraction

as shown in Table 2. The extended the proposed technique is to HMS as shown in Fig. 15.

5 Results and Discussion

The Fourier spectrum analysis of FFT method which was the HMS-based HHT method is applied to the EEG signals; Hilbert marginal spectrum (HMS) is used to understand EEG signals as they are highly nonlinear and nonstationary signals, and then, they can be obtained. Figures 9, 10, 11 and 12, and hence, traditional Fourier analysis (TFA) method fails to represent amplitude of each frequency. And Fig. 16 shows the relative entropy distribution of Shannon, Renyi and Tsallis of seizure and non-seizure on same database by MATLAB editor tool on feature extraction (Table 3).

6 Conclusion

The proposed methodologies useably developed an automatic seizure detection model in which frequency represented by HMS was fed into support vector machine (SVM), and hence, seizures are detected by comparing EEG signals with Fourier frequency analysis. Therefore, it is even proved that the developed method is more

Table 2 Classification accuracies for HMS and FFT-based feature extraction analysis

Brainwave Frequencies	Feature extraction				
Gamma (30 to 50) Hz	(7.604101253680111e-17, -	1.2418439763978288),	1.2361058792074007)	[(0.3365922112395738,	0.89574153504815945
Beta, (14 to 30) Hz	0.34374733394096496, -	1.0016415369557565),	(0.9157742224076064	0.8516700268390739)	0.31402302342118565)
Alpha, (8 to 14) Hz	(0.22667265410177617, -	(4.2303075026511913e-17,	0.693305669614743)	0.6908616436341476)	0.5870410514971045
Delta, (0.1 to 4) Hz	0.41916658263191064), (-	(2.5666550686485195e-17, -	0.2557240551721939	0.42833779241342484)	0.31402302342118565)
Theta, (4 to 8) Hz	4.08782435	5.10978044	6.13173653	7.15369261	0.89574153504815945
	4.34331337	5.36526945	6.38722555	7.40918164	
	4.5988024	5.62075848	6.64271457	7.66467066	
	4.85429142	5.87624751	6.89820359	7.92015968	

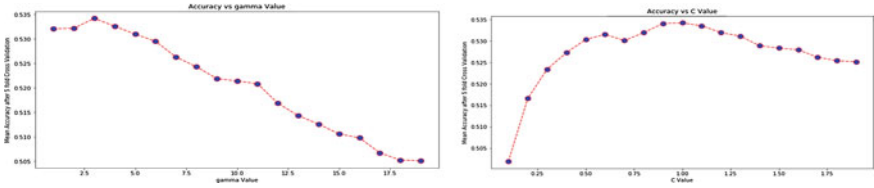


Fig. 15 SVM accuracy testing is conducted at micro average for feature extraction

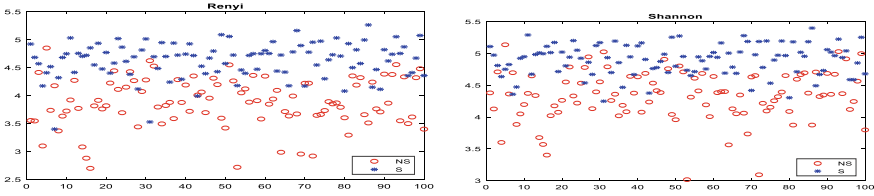


Fig. 16 Renyi, Shannon and Tsallis entropy features of seizure and non-seizure EEG signals

Table 3 Statistical values of Shannon, Renyi and Tsallis spectral entropy of seizure and non-seizure EEG signals

	Mean			Std		
	Shannon	Renyi	Tsallis	Shannon	Renyi	Tsallis
Seizure	5.2405	3.1803	0.9504	0.6337	0.5571	0.0361
Non-seizure	3.3424	1.6673	0.7646	0.9372	0.6087	0.1942

effective than the existent method by comparing the results obtained from both the methods are extended to compare with SVM in Figs.15 and 16.

References

1. Acharya UR, Sree SV, Swapna G, Martis RJ, Suri JS (2013) Automated EEG analysis of epilepsy: a review. *Knowl-Based Syst* 45:147–165
2. Ramgopal S, Thome-Souza S, Jackson M, Kadish NE, Fernández IS, Klehm J et al (2014) Seizure detection, seizure prediction, and closed-loop warning systems in epilepsy. *Epilepsy Behav* 37:291–307
3. Kovacevic N, Ritter P, Tays W, Moreno S, McIntosh AR (2015) ‘My Virtual Dream’: collective neurofeedback in an immersive art environment. *PLoS ONE* 10(7):e0130129
4. Menshaw ME, Benharref A, Serhani M (2015) An automatic mobile-health based approach for EEG epileptic seizures detection. *Expert Syst Appl* 42(20):7157–7174
5. Lushin I (2016) Detection of epilepsy with a commercial EEG headband
6. Subasi A (2007) EEG signal classification using wavelet feature extraction and a mixture of expert model. *Expert Syst Appl* 32(4):1084–1093
7. Lee S-H, Lim JS (2014) Minimum feature selection for epileptic seizure classification using wavelet-based feature extraction and a fuzzy neural network. *Appl Math Inf Sci* 8(3):1295

8. Guo L, Rivero D, Dorado J, Rabunal JR, Pazos A (2010) Automatic epileptic seizure detection in EEGs based on line length feature and artificial neural networks. *J Neurosci Methods* 191(1):101–109
9. Omerhodzic I, Avdakovic S, Nuhanovic A, Dizdarevic K (2013) Energy distribution of EEG signals: EEG signal wavelet-neural network classifier. arXiv preprint [arXiv:1307.7897](https://arxiv.org/abs/1307.7897)
10. Lima CA, Coelho AL, Eisencraft M (2010) Tackling EEG signal classification with least squares support vector machines: a sensitivity analysis study. *Comput Biol Med* 40(8):705–714
11. Chen D, Wan S, Bao FS (2015) Epileptic focus localization using EEG based on discrete wavelet transform through fulllevel decomposition. In: 2015 IEEE 25th international workshop on Machine Learning for Signal Processing (MLSP), pp 1–6
12. Li M, Chen W, Zhang T, Cortes, Vapnik V (1995) Support-vector networks. *Mach Learn* 20(3):273–297
13. Tsipouras MG (2019) Spectral Information of EEG signals with respect to epilepsy classification. 2019 EURASIP J Adv Signal Process
14. Ragavamsi D, Ragupathy R (2020) A survey of different machine learning models for Alzheimer disease prediction. *Int J Emerging Trends Eng Res* 8:3328–3337
15. Fasil OK, Rajesh R (2018) Time-domain exponential energy for epileptic EEG signal classification, Oct 2018
16. Usman SM, Khalida S et al (2019) Using scalp EEG and intracranial EEG signals for predicting epileptic seizures: review of available methodologies
17. Sessa Sai Priya S, Nalini NJ (2021) Epileptic seizure detection using EEG signals: a review. *J Cardiovascular Dis Res* 12(3). ISSN: 0975-3583, 0976-2833

Performance Assessment of FACTS Devices for Enhancing Stability and Control in Power Systems



T. S. Kishore and P. Upendra Kumar

Abstract With the electricity sector moving towards deregulation globally, the power system is being encountered with challenges which are technical, economic and environmental. The power system is enforced to operate under volatile conditions continuously to meet the demand without violating the operating constraints. In order to achieve this, the foremost system requirement is stability. From the congregation of all the stabilities, voltage stability has significant importance as it can jeopardise the system leading to complete or partial blackout without much information of system operators. It is high time to assess the voltage stability and control through rigorous simulations considering all the possible circumstances leading to voltage instability. This paper studies the efficacy of FACTS devices for ameliorating the voltage stability. IEEE 14 bus test system has been considered for implementing continuation power flow technique to assess the static voltage stability of the system for base and modified cases incorporating a range of FACTS devices, viz. STATCOM, SVC and UPFC. Results indicate that all the FACTS devices are capable of improving voltage stability limits, but STATCOM proves to be significant in improving the voltage stability margin.

Keywords Voltage stability · FACTS · STATCOM · Renewable energy · Power system

1 Introduction

Modern power systems continually encounter with increasing load demand, and the system is subjected to new challenges every single day. The interconnected system under deregulated environment is operating close to the limits of stability. Uninterrupted generation and transmission of power while maintaining all the operational

T. S. Kishore · P. Upendra Kumar (✉)
GMR Institute of Technology, Rajam, Andhra Pradesh 532127, India
e-mail: upendrakumar.p@gmrit.edu.in

T. S. Kishore
e-mail: kishore.ts@gmrit.edu.in

constraints is prominent for utilities to maintain system stability [1]. Voltage stability in the system is very paramount important as it leads to complete or partial black-outs. It is a local problem where insufficient reactive power support initiates the problem. If the system is overcompensated, then the voltages are deceptive and voltage instability occurs at the voltage levels above the nominal values. Voltage stability is defined as the “ability of a power system to maintain acceptable voltages at all buses under normal conditions and after being subjected to a disturbance [2]”. Voltage stability analysis is subdivided into two categories, long-term and short-term voltage stability. The short-term voltage stability is analysed from the dynamic analysis as this stability occurs due to dynamic loads like induction motor. The long-term voltage stability could be analysed from the power flow analysis, which is known as static analysis. In many instances in open literature, it has been found that static analysis is adequate for long-term voltage stability analysis. This technique is naïve enough to find the stability margin or distance to voltage collapse while considering all the constraints pertaining to the system. In view of the present scenario concerning stressed power system operation, this paper investigates the performance of FACTS devices for improving voltage stability and control limits of the power system. IEEE 14 bus system has been considered based on its robustness to conduct the present research. Static voltage stability analysis has been carried out for assessing the voltage stability limits by using continuation power flow technique. Further, a range of FACTS devices, viz. STATCOM, SVC and UPFC, have been incorporated, and the assessment was once again carried out to identify the best device for improvement of voltage stability margin. Results indicate that all FACTS devices are capable of improving voltage stability limits, but STATCOM proves to be significant in improving the voltage stability margin.

2 System Modelling

Power system stability is the capability of the system to remain intact or to reach acceptable equilibrium after been subjected to a disturbance [3]. Under stable condition, all the constraints should be satisfied and power demand should be met by the system. The renewable integrated grid is in close neighbourhood of various instabilities, especially voltage stability. The analysis of voltage stability in such grid is the main objective of this work, and it is implemented in IEEE 14 bus test system. The brief description of the system is available in [4, 5]. SVC is a FACTS device that regulates the terminal voltage by injecting or absorbing the reactive power in the system. It is a shunt device connected at a bus, and its reactive power is controlled to maintain the bus voltage close to nominal values. This is achieved by exchanging the capacitive or inductive currents at the node at which it is connected [6]. STATCOM is modelled as VSI for voltage stability improvement. It essentially converts the DC voltage into AC voltage and adjusts its real and reactive power as per the system requirement and eventually maintains power balance. As a whole, STATCOM is classified under the shunt device category and continually adjusts its internal voltage

and phase angle to support the load demand. The typical characteristics include a constant current behaviour when the system bus voltage is low or high and therefore behaves for dispatching reactive power within the acceptable bounds [7]. UPFC is a device which controls real and reactive power flows in transmission lines. UPFC can control simultaneously voltage, impedance and phase angle. However, selective control is also possible. UPFC should be placed between two nodes where real power and reactive power exchange should take place. It has two converters, series voltage source converter and shunt voltage source converter. The series converter is modelled as an ideal voltage source connected in series with line reactance X_s [8]. The shunt converter is modelled as ideal shunt current source.

3 Simulation and Results

Continuation power flow analysis is a powerful tool to assess the static voltage stability analysis of a power system network. It basically uses a modified power flow equations and then employs a predictor–corrector method to find the point of collapse or voltage stability margin as the loading parameter is increased. The loading parameter is usually the reactive power [9, 10]. This technique is adopted in the present study. Traditionally, voltage stability of a system is accessed from the PV and QV curves, obtained from increased loadings at all the buses, till the system reaches unstable state. The CPF method is used for obtaining these curves. All the operational limits of the system are monitored as well using CPF method. The CPF method is applied to IEEE 14 bus test system, and all the node voltages corresponding to nose point are identified. Then, the FACTS devices are incorporated at load buses making the test system into modified test system. The voltage stability analysis is performed on this modified test system to find the voltage magnitudes at nose point. This was done to identify which of the FACTS devices is capable of improving the voltage stability limit more significantly. The FACTS devices considered here are SVC, STATCOM and UPFC. It is to be noted that only shunt (SVC and STATCOM) and series-shunt (UPFC) devices are used as these are effective in providing reactive power support especially in transmission networks and hence improve voltage stability limits of the network. The results of these simulations along with performance evaluation of FACTS devices are presented in Tables 1, 2, 3 and 4.

From Table 3, it can be observed that the buses are arranged in the ascending order of voltage stability limits w.r.t base case. Out of the nine load buses, bus number 14 has the least voltage stability margin and is identified as the weakest bus in the network. The voltage stability margin of seven load buses has been significantly improved by STATCOM, whereas SVC and UPFC show improvement only in one load bus each as compared to STATCOM. Although the generators are intended to operate under stable limits irrespective of the loading condition, slight deviations in voltage magnitudes from the ideal operating value can be noticed in the base case loading condition. Generator bus voltage stability limits are also improved by STATCOM

Table 3 Performance evaluation of FACTS devices

Bus number	Bus type	Base case	Improvement of voltage magnitude by ^a		
			SVC	STATCOM	UPFC
14	Load	0.55	0.684	1.04	0.7
13	Load	0.807	0.928	1.041	0.93
12	Load	0.86	0.978	1.05	0.977
11	Load	0.76	0.961	0.955	0.88
10	Load	0.6	0.721	0.85	0.75
9	Load	0.6	0.696	0.851	0.72
8	Generator	0.98	1.09	1.09	1.09
7	Load	0.7	0.79	0.87	0.81
6	Generator	0.959	1.07	1.07	1.07
5	Load	0.65	0.676	0.72	0.885
4	Load	0.65	0.683	0.75	0.72
3	Generator	0.93	1.01	1.02	1.01
2	Generator	1	1.024	1.1	1.045
1	Generator	1.06	1.06	1.1	1.06

^aMaximum voltage margin increase considered irrespective of placement for load buses

significantly as compared to SVC and UPFC for three generator buses (1, 2 and 3) and for two generator buses (6 and 8), the improvement in voltage stability margin is same for all the FACTS devices. However, in voltage stability studies, load bus stability limits are of concern and are much affected by load variations and that of generators are neglected unless there is a serious concern. From this analysis, it can be deduced that STATCOM is best suitable for voltage stability margin improvement for the power system network under consideration (Fig. 1).

4 Conclusions

This paper attempts to analyse the performance of FACTS devices in enhancing the stability and control margins of power system networks. Such analysis is relevant for power system engineers to plan the future power systems and to devise means to shield against possible instabilities. The following are the conclusions deduced from the simulated results:

- (i) From the results of the base case simulation, it is observed that 14th bus is the weakest bus with a voltage collapse point corresponding to 0.55 magnitude.
- (ii) To improve this, three FACTS devices, viz. SVC, STATCOM and UPFC, have been considered for providing compensation, and the simulation results incorporating these devices have been presented in Tables 1, 2 and 3. It has been

Table 4 Voltage magnitudes of IEEE 14 bus test system with and without UPFC

Bus number	Base case	With UPFC placed between buses													
		1-2	2-3	3-4	4-5	5-6	6-7	7-8	8-9	9-10	10-11	11-12	12-13	13-14	14-1
1	1.060	1.060	1.060	1.060	1.060	1.060	1.060	1.060	1.060	1.060	1.060	1.060	1.060	1.060	1.060
2	1.000	1.045	1.045	0.996	1.045	1.045	1.045	1.045	1.045	1.045	1.045	1.045	1.045	1.045	1.045
3	0.930	1.010	1.010	0.927	1.010	1.010	1.010	1.010	1.010	1.010	1.010	1.010	1.010	1.010	1.010
4	0.650	0.690	0.690	0.680	0.662	0.690	0.690	0.690	0.700	0.700	0.700	0.700	0.700	0.700	0.720
5	0.650	0.690	0.885	0.660	0.658	0.670	0.680	0.670	0.690	0.690	0.690	0.700	0.700	0.700	0.700
6	0.959	1.070	1.070	0.957	1.070	1.070	1.070	1.070	1.070	1.070	1.070	1.070	1.070	1.070	1.070
7	0.700	0.780	0.790	0.790	0.704	0.790	0.790	0.800	0.800	0.800	0.800	0.800	0.800	0.810	0.800
8	0.980	1.090	1.090	0.981	1.090	1.090	1.090	1.090	1.090	1.090	1.090	1.090	1.090	1.090	1.090
9	0.600	0.690	0.700	0.690	0.604	0.690	0.700	0.700	0.710	0.710	0.710	0.710	0.710	0.720	0.720
10	0.600	0.680	0.720	0.710	0.608	0.750	0.720	0.720	0.730	0.730	0.730	0.730	0.740	0.740	0.740
11	0.760	0.870	0.870	0.870	0.771	0.870	0.870	0.870	0.880	0.880	0.880	0.880	0.880	0.880	0.880
12	0.860	0.970	0.970	0.970	0.864	0.970	0.976	0.976	0.977	0.970	0.970	0.970	0.970	0.970	0.970
13	0.807	0.920	0.920	0.920	0.812	0.920	0.925	0.920	0.920	0.920	0.920	0.920	0.930	0.930	0.930
14	0.550	0.670	0.670	0.680	0.565	0.680	0.680	0.680	0.680	0.690	0.690	0.690	0.700	0.700	0.700

IEEE 14 Bus test system results without STATCOM

IEEE 14 Bus test system results with STATCOM

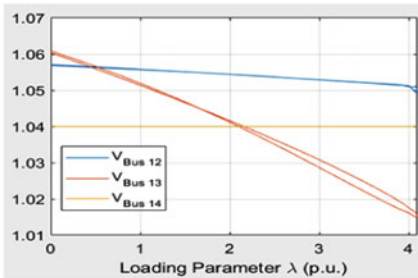
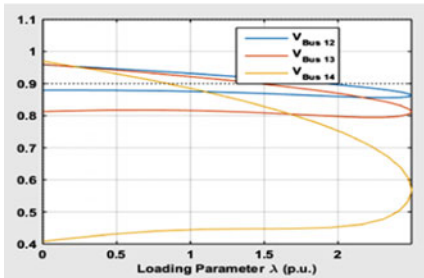
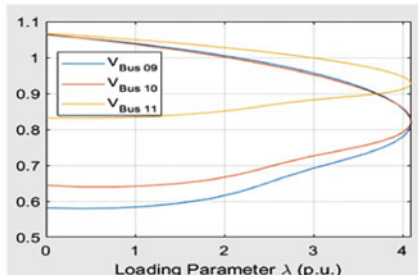
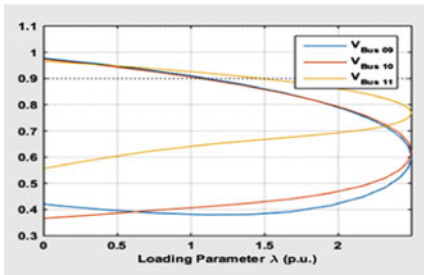
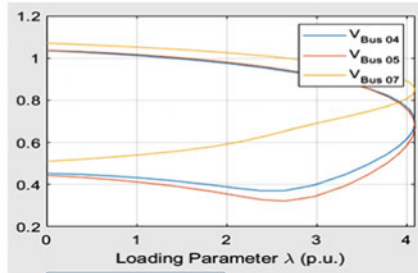
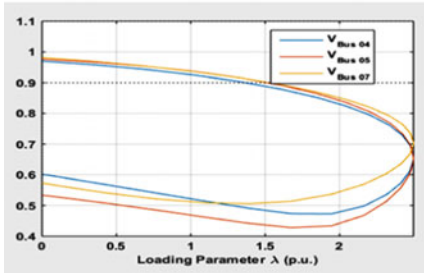
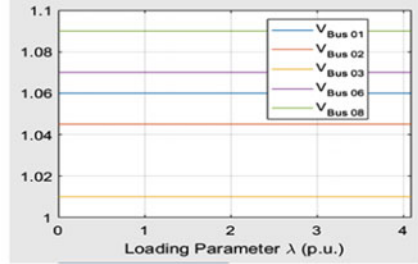
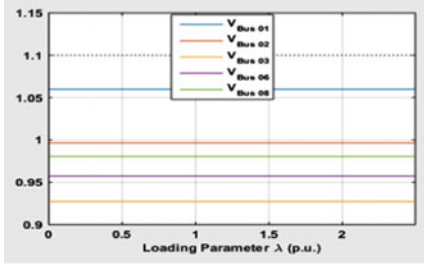


Fig. 1 PV curves for IEEE 14 bus test system

observed that all the devices are capable of increasing the voltage stability margin.

- (iii) A performance evaluation is carried out to select the best device for carrying out further work by taking the maximum voltage stability margin in maximum number of buses for the given system as criteria, and STATCOM has been found to be the candidate device. Table 4 shows the voltage stability margin improvements achieved by all the three devices justifying the above statement.

The simulation results show that voltage stability margin got improved using STATCOM and CPF is very powerful tool for PV curves, and it has the prowess to identify the nodes prone to instability.

References

1. Kishore TS, Singal SK (2014) Optimal economic planning of power transmission lines: a review. *Renew Sustain Energy Rev* 39:949–974
2. Chappa H, Thakur T (2020) Novel advancements in electrical power planning and performance. In: IGI Global, pp 283–299
3. IEEE/CIGRE Joint Task Force on Stability Terms and Definitions (2004) Definition and classification of power system stability. *IEEE Trans Power Syst* 19(2)
4. Milano F (2005) An open source power system analysis toolbox. *IEEE Trans Power Syst* 20(3):1199–1206
5. Karlsson D, Hill DJ (1994) Modeling and identification of nonlinear dynamic loads in power systems. *IEEE Trans Power Syst* 9(1):157–166
6. Tien DV, Hawliczek P, Gono R, Leonowicz Z (2017) Analysis and modeling of STATCOM for regulate the voltage in power systems. In: 2017 18th international scientific conference on Electric Power Engineering (EPE), Kouty nad Desnou, pp 1–4
7. Kishore TS, Kaushik SD, Venu Madhavi Y (2019) Modelling, simulation and analysis of PI and FL controlled microgrid system. In: 2019 IEEE International Conference on Electrical, Computer and Communication Technologies (ICECCT), Coimbatore, India, pp 1–8
8. Lin L, Zhou N, Zhu J (2010) Analysis of voltage stability in a practical power system with wind power. In: *Electric power components and systems*, vol 38
9. Canizares CA, Alvarado FL (1993) Point of collapse and continuation methods for large AC/DC systems. *IEEE Trans Power Syst* 8(1):1–8
10. Gan R, Luan Z, Yang Y, Liu W, Yang S (2015) Static voltage stability analysis based on improved continuous power flow. In: 2015 IEEE region 10 conference TENCON, Macao, pp 1–3

Filter Bank Multicarrier Modulation with OQAM-Based Sparse Channel Estimation



Nilofer Shaik and Praveen Kumar Malik

Abstract Fifth generation (5G) is anticipated to be the wireless communications technology in future applications. For a candidate transmission in 5G, filter bank multicarrier using offset quadrature amplitude modulation (FBMC-OQAM) technology is used. The commonly used channel estimation technique for FBMC-OQAM is based on preamble structure schemes, but because of intrinsic interference introduced the preamble-based channel estimation executes poor adaptation, especially in massive multiple-input multiple-output (mMIMO) systems. Leveraging the wireless channel with its nature of sparsity is used for developing an enhanced channel estimation technique for 5G FBMC-OQAM networks. In this paper, a sparse channel estimation (SCE) is implemented for mMIMO FBMC-OQAM systems. The executed results show that the sparse channel estimation (SCE) technique outperforms best athwart to conventional-based LS channel estimation (LSCE) technique. The proposed channel estimation spare channel estimation (SCE) approach is an effective channel estimation method for mMIMO wireless communication systems (WCS).

Keywords Filter bank multicarrier · Massive MIMO · Orthogonal quadrature amplitude modulation · Sparse channel estimation

1 Introduction

A rapid increase in wireless data traffic pushes for high spectral efficiency in mMIMO systems. This increase leads to increase of several number of antennas as well as the size of the alphabet. For example, the wireless LAN standard IEEE 802.11ac enables eight spatial streams through mMIMO channel and supports 256-ary QAM. The 5G probably be using carrier frequencies above 6 GHz allows a leverage in

N. Shaik (✉) · P. K. Malik
Lovely Professional University, Phagwara, Punjab, India
e-mail: nilofershaik@gmail.com

N. Shaik
BVRIT HYDERABAD College of Engineering for Women, Hyderabad, Telangana, India

half-wavelength spacing in amounts of small value and several number of antennas. Based on this, mMIMO systems will deploy several numbers of antennas at base station which are going to serve few ten to thousands of users simultaneously. In different (WCS) mainly in LTE and LTE-A systems, multicarrier modulation (MCM) technology is widely used [1]. FBMC with OQAM is a springing technology for 5G MCM which introduced filter banks to the basic orthogonal frequency division multiplexing (OFDM). FBMC castaways the requirement of cyclic prefix as used in OFDM. Instead of cyclic prefix, it uses filter for efficient modulation. FBMC has high spectrum efficacy, smaller sidebands and high verdure to narrow band interference. Because of well-localized time–frequency shaping filter, FBMC provides better spectral containment compared to OFDM [2, 3].

2 System Model

A $N \times M$ mMIMO system is considered, where N is number of transmitter antennas and M is number of receiver antennas [4]. The input symbols are considered as $N \times 1$ vector which are independent and identically distributed (i.i.d) symbols. Therefore, a received output is given as

$$\tilde{y} = \tilde{H}\tilde{x} + \tilde{n} \quad (1)$$

where

y = signal vector received

H = channel matrix

X = signal vector transmitted and

n = noise vector which is AWGN with zero mean and variance σ^2 (Fig. 1).

CE targets for equalization which is a main trouble in processing a signal and communications. The main problem of estimating the sparse channels (SC) is where the time domain impulse response has a greater number of zero taps in the standard uniform tapped delay line model. The prevailing approaches such as LS will consider the pilot information for the unknown channel which suffers poor performance over parameterization [5]. When the system has the long impulse response, the efficacy and the accuracy of the system reduce by estimating the channel as the error becomes high. If this same system is used with the OFDM MCM, the computational complexity also increases and the length of the guard interval is also high [6]. So, to overcome this limitation, a SCE using FBMC-OQAM is directed through this paper. The proposed SCE block diagram is shown in Fig. 2. The main goal of the sparseness is to enhance the performance of the system using FBMC-OQAM.

FBMC is designed same as the OFDM system. There is a slight modification in the FBMC system in contrast to OFDM System. In FBMC system, various number of subcarriers are filtered in reduction of side lobes. As the reduction of side lobes decreases the interference, the reduction of interference dwindles the OOB. So, to

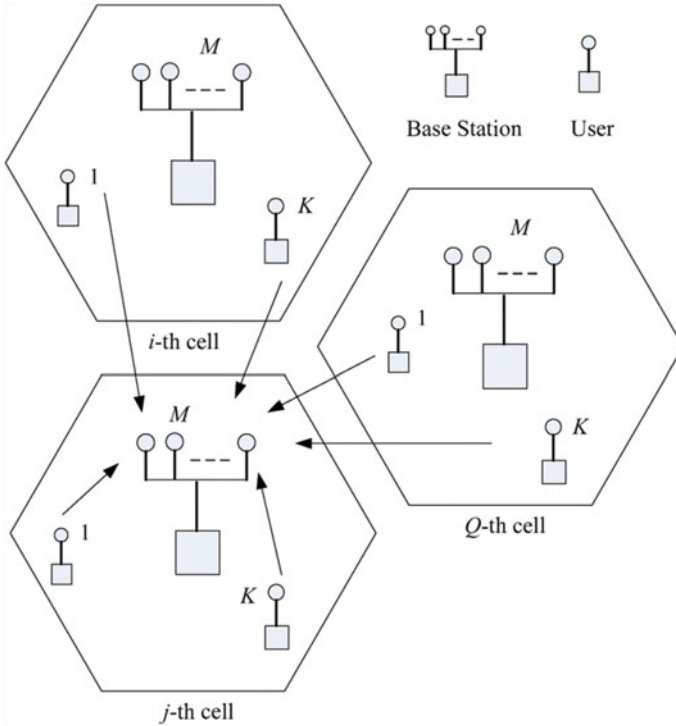
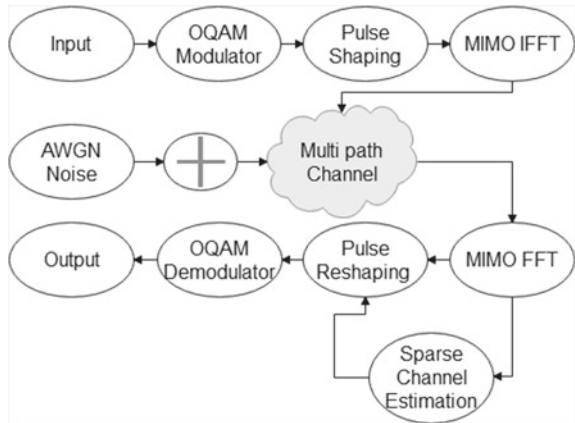


Fig. 1 Uplink transmission in massive MIMO system

Fig. 2 Block diagram of FBMC-OQAM sparse channel estimation



dwindle the OOB, the OFDM system uses CP instead FBMC system uses prototype filter (PF). The addition of CP has high PAPR. Addition of PFs can achieve higher data rates. The first design of PF is $p(t) = p(-t)$. The orthogonality is with the help of spacing by time and frequency.

where

$T = T_0$ (Time spacing)

$F = 2/T_0$ (Frequency spacing).

FBMC Hermite PF is written as

$$p(t) = \frac{1}{\sqrt{T_0}} e^{-2\pi\left(\frac{t}{T_0}\right)^2} \sum_{t = \{0, 4, 8, 12, 16, 20\}} \alpha_i H_i\left(2\sqrt{\pi} \frac{t}{T_0}\right) \quad (2)$$

Hermite polynomials $H_n(\cdot)$ are proposed. FBMC uses one more type of PF which is PHYDYAS PF and is written as

$$p(t) = \begin{cases} \frac{1+2\sum_{i=1}^{O-1} b_i \cos\left(\frac{2\pi t}{OT_0}\right)}{O\sqrt{T_0}} & \text{if } -\frac{OT_0}{2} < t < \frac{OT_0}{2} \\ 0 & \text{Otherwise} \end{cases} \quad (3)$$

Time spacing is $T = T_0/2$, and frequency spacing $F = 1/T_0$ is considered to maintain the orthogonality as a factor of two which is the second principle of FBMC. Moving the introduced interference to purely imaginary domain is the last principle of FBMC, and its phase shift is written as

$$\theta_{l,k} = \frac{\pi}{2}(l+k) \quad (4)$$

3 Channel Estimation

3.1 LS Channel Estimation

From the curve fitting, the mathematical statistics of the least square algorithm is developed. For the FBMC-OQAM WCS, the CE is considered using the known signal, and its estimate is given as

$$Y_k = X_k(l)H_k(l) + N_k(l) \quad (5)$$

where Y_k = Received pilot signal

X_k = Transmitted pilot signal
 H_k = Frequency domain response of a channel and
 N_k = AWGN added to the channel.

The LS estimate has less computational complexity, and the estimate is given as

$$\hat{h}_{ls}(l) = X(l)^{-1}Y(l) \quad (6)$$

3.2 Proposed Sparse Channel Estimation

The proposed sparse channel estimate procedure is as follows:

- i. Consider a sensing matrix of A , vector of measurement z with the initialization of signal vector $\hat{y} = 0$.
- ii. The residual value r_i is updated as $r_i = z - A\hat{y}_i$ as the initial value of r is z . The updating vector k is calculated from the residual and is given as $k_i = A^T r_{i-1}$.
- iii. By the use of updating vector k the column index in A is found v_{\max} , which maximizes the correlation with the residual r . The support vector A_i is updated using v_{\max} .
- iv. The shaping of A^+ is done using support vector, where $+$ is the notation considered for the pseudo-inverse operator.
- v. To minimize $z - A\hat{y}_2$ always \hat{y} is updated.
- vi. If the last update of \hat{y} is completed, iteration is stopped, and the estimate is completed and if the last update is not completed, then repeat the iteration is repeated by calculating the residual vector.

4 Simulation Result

The frequency and time domain spacing of PHYDYAS and Hermite PF [7] is observed in Fig. 3.

Hermite and PHYDYAS filter spectral efficacy is observed in Fig. 4. When subcarrier spacing is considered a low value, the Hermite filter spectral efficacy is better and if subcarrier spacing is taken an infinite value, the PHYDYAS filter spectral efficacy [8] is better in contrast to the Hermite filter (Fig. 5).

The proposed channel estimation and LSCE techniques are compared, and the results show that the proposed SCE-based FBMC MCM technique holds good compared to LSCE technique-based FBMC MCM technique (Table 1).

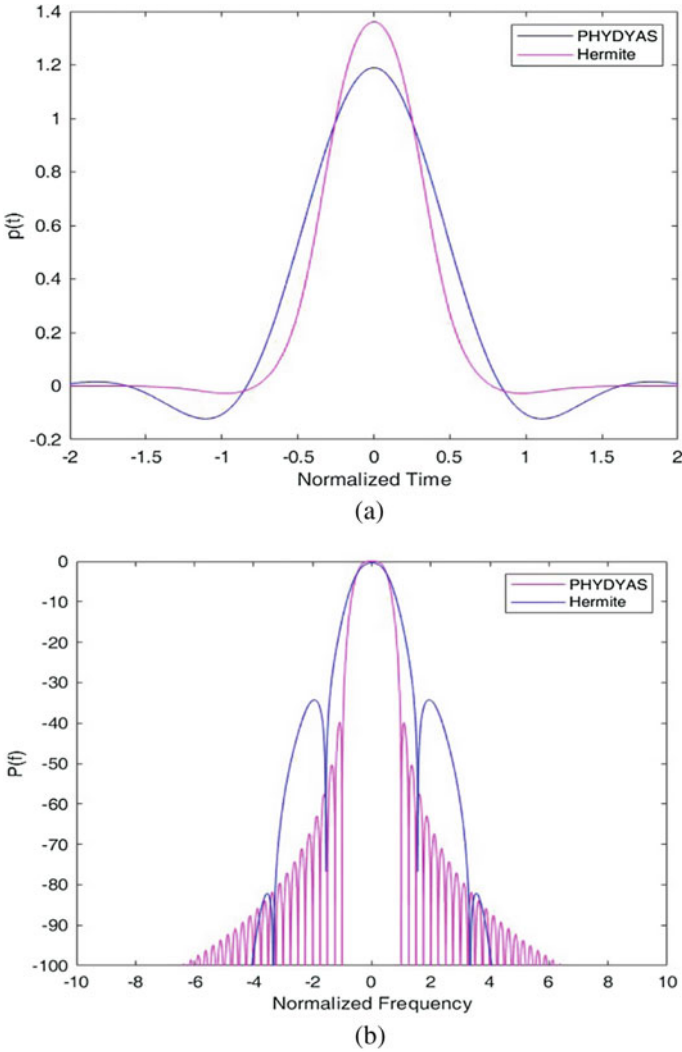


Fig. 3 FBMC prototype filter **a** spacing in time domain, **b** spacing in frequency domain

5 Conclusion

This research paper discusses the proposed channel estimation-based FBMC MCM techniques for 5G WCSs. This recommended channel estimation is implemented for sparse channels where the channel has many zero taps for estimating the channel. The results are implemented using MATLAB software and Monte Carlo simulation. The results are also implemented for the FBMC prototype filters which are best suitable instead of adding CP. The main results are implemented for sparse proposed channel

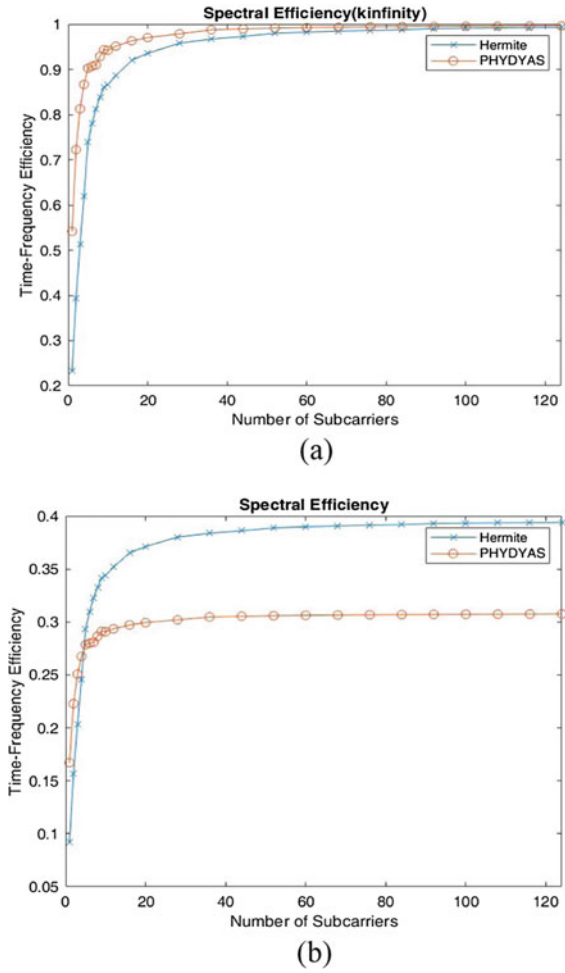


Fig. 4 Hermite and PHYDYAS spectral efficiency **a** $K = \text{infinite}$, **b** $K = \text{minimum}$

estimation-based FBMC multicarrier modulation and prove that BER reduces in contrast to conventional LSCE technique. The only limit of this method is as number of iterations increases, the computational complexity increases.

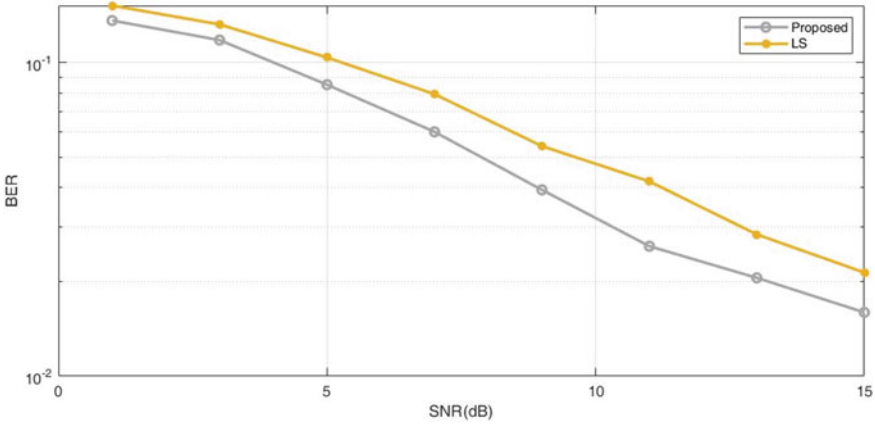


Fig. 5 Comparison of LS and proposed channel estimation

Table 1 Simulation parameters used for proposed and LS channel estimation techniques

S. No	Simulation parameters	Numbers
1	Subcarriers	1024
2	Bits per subcarrier	8
3	Modulation	OQAM
4	Modulation order	256
5	Number of taps	3
6	SNR (dB)	15
7	Number of iterations	25

References

1. Ali MS, Hossain E, Kim DI (2017) LTE/LTE-a random access for massive machine-type communications in smart cities. *IEEE Commun Mag* 55(1):76–83. <https://doi.org/10.1109/MCOM.2017.1600215CM>
2. Sahin A, Guvenc I, Arslan H (2014) A survey on multicarrier communications: prototype filters, lattice structures, and implementation aspects. *IEEE Commun Surv Tutor* 16(3):1312–1338. Third Quarter 2014. <https://doi.org/10.1109/SURV.2013.121213.00263>
3. He Q, Schmeink A (2015) Comparison and evaluation between FBMC and OFDM systems. WSA
4. Nilofer S (2020) A review of massive multiple input multiple output for 5G communication: benefits and challenges. *Int J Intelli Commun Comput Netw* 1(1):022–026. <https://doi.org/10.51735/ijiccn/001/09>
5. Shaik N, Malik PK (2020) A retrospection of channel estimation techniques for 5G wireless communications: opportunities and challenges. *Int J Adv Sci Technol* 29(05):8469–8479
6. Shaik N, Malik PK (2021) A comprehensive survey 5G wireless communication system: open issues, research challenges, channel estimation, multi carrier modulation and 5G applications. *Multimed Tools Appl*. <https://doi.org/10.1007/s11042-021-11128-z>

7. Bellanger M (2001) Specification and design of prototype filter for filter bank based multicarrier transmission. *IEEE Int Conf Acoustics Speech Signal Process* 4:2417–2420. <https://doi.org/10.1109/ICASSP.2001.940488>
8. Mirabbasi S (2002) Design of prototype filter for near-perfect-reconstruction overlapped complex-modulated transmultiplexers, I-821. <https://doi.org/10.1109/ISCAS.2002.1009967>

A Cascaded H-Bridge MLI Fed Motor by Using Fuzzy-MPPT PV System



Kammari Rajesh, Y. Chintu Sagar, and K. C. Venkataiah

Abstract Induction motor (IM) is utilized for variable speed control application in industries as these motors are reasonable, solid and straightforward. To get the desired speed and torque with irrelevant swells, this drive needs suitable converters for better performance. Nowadays, multilevel inverters (MLIs) are picking up prevalence and widely utilized for motor drive applications, and these inverters have emerged as vital option for more power and moderate voltage applications. In this topology, the speed of asynchronous motor (AM) is controlled by cascaded H-bridge multilevel inverter (CHBMLI), and multicarrier PWM method is utilized to deliver pulses for the inverter. The main purpose is to create control strategy for CHBMLI fed motor with PV utilizing a fuzzy logic-based maximum power point tracking (MPPT) technique and boost converter as separate source for CHBMLI. The performance of a 3- Φ CHBMLI fed motor by using PV source is verified by MATLAB simulation results and is represented in terms of PV curves, MPPT power, boost converter voltage, inverter voltage, speed, current and torque.

Keywords CHBMLI · PWM methods · PV cell · Boost converter · Fuzzy logic controller · Induction motor

1 Introduction

Generally, control electronic devices are a significant part in the transformation and control of electric power, mostly to extract power from photovoltaic cell and wind energy. DC to AC power control and transformation should be possible by the inverters. Ordinary inverter creates the alternating waveform, however having higher harmonics and also having more switching losses and furthermore there is an energy loss. In this way, the multilevel inverters were produced and these inverters are having

K. Rajesh (✉)

RGM College of Engineering and Technology, Nandyala, India

e-mail: k.rajesh.1165@gmail.com

Y. Chintu Sagar · K. C. Venkataiah

Ashoka Women's Engineering College, Dupadu, India

fewer harmonics. For the most part from recent couple of years, mechanical drives utilize the AC IM or asynchronous motor (AM) as that they are simple, solid and less maintenance. So AC IMs are the most commonly utilized in speed control applications and particularly polyphase IMs are utilized as a part of mechanical drives. Present days, MLIs are generally utilized for drive applications in light of the fact that these inverters are having lesser THD, less electromagnetic interference, less switching losses, great influence quality. For the most part, there are three multi-level inverters: They are (1) diode-clamped MLI (DCMLI), (2) flying capacitor MLI (FCMLI) and (3) cascaded H-bridge MLI (CHBMLI). In DCMLI, huge diodes are needed per phase. In FCMLI, huge capacitors are needed per phase. Contrasted with other two MLIs, CHBMLI needs a few number of parts and broadly favored for AC power supplies and high power applications and control of DC transport is direct. Conventional power generation causes the environmental problems, so nowadays renewable energy sources, particularly solar energy, have become preferable. For CHBMLI fed motor, every H-bridge cell has a separate DC source that is PV cell. In this paper, 3- Φ CHBMLI fed motor is outlined and simulated. The multicarrier PWM method is utilized to initiate pulses for the inverter. The performance of CHBMLI fed motor is examined, and the results are justified by utilizing MATLAB/Simulink software.

2 Photovoltaic (PV) Cell

A PV cell is a structure which utilizes one or more solar panels to change over solar energy into electricity. It comprised of at least two thin layers of semiconductor material most generally silicon when silicon uncovered to light electric charge is created. Ordinarily solar-oriented cell can be demonstrated by current source and diode associated in parallel to it. It has its own arrangement parallel resistance because of leakage current.

Modeling of PV cell:

The output current is acquired by Kirchhoff law

$$I_{\text{total}} = I_{\text{ph}} - I_{\text{dio}} \quad (1)$$

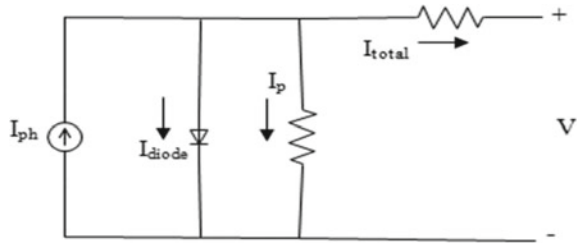
$$I_{\text{dio}} = I_{\text{rev dio}} \left[\exp\left(\frac{V}{V_T}\right) - 1 \right] \quad (2)$$

where I_{ph} is the photon current, I_{dio} is the current for the diode which is proportional to saturation current, V is the voltage of diode and I_{revdio} is reverse current of diode. V_T is the voltage coefficient of temperature and

$$V_T = kT/q \quad (3)$$

$$I_{\text{total}} = I_{\text{ph}} - I_{\text{rev dio}} \left\{ \exp\left(\frac{V + IR_s}{V_T}\right) - 1 \right\} - \frac{(V + IR_s)}{R_p} \quad (4)$$

Fig. 1 PV cell equivalent circuit



Photon current is based on irradiance and also on temperature.

$$I_{ph} = (G/G_{ref}) * (I_{phref} + \mu_{sc} \Delta T) \tag{5}$$

where G is the irradiance (w/m^2) and G_{ref} is the irradiance at standard test condition (STC) (Fig. 1).

$$\Delta T = T - T_{ref}. \tag{6}$$

$$I_{rev\ dio} = I_{rs}(T / T_{ref})^3 \exp [(q \varepsilon_G A k) * ((1/T_{ref}) - (1/T))] \tag{7}$$

where

T_{ref} = cell reference temperature

I_{rs} = reverse saturation at T_{ref}

A = Identity factor

ε_G = band gap energy.

Maximum Power Point Tracking (MPPT):

MPPT is a method utilized for extracting greatest accessible power from PV module under all conditions. The voltage at which PV module generates greatest power is called MPPT. In each H-bridge cell, a MPPT is added to create the DC-connect voltage reference. In this MPPT technique, fuzzy logic control (FLC)-based MPPT technique is developed. Mostly, fuzzy logic (FL)-based MPPT is utilized to make the system faster and more reliable. The proposed FLC is demonstrated as two inputs and one output. The two FLC input variables are E , CE, and output (U) is compared with sawtooth waveform to generate a PWM signal for duty cycle of converter where the inputs of FLC can be expressed as

$$E(k) = (P_{ph(k)} - P_{ph(k-1)}) / (V_{ph(k)} - V_{ph(k-1)}) \tag{8}$$

$$CE(k) = E(k) - E(k - 1) \tag{9}$$

The fuzzification procedure changes over real inputs E and CE into variables. Membership values are allotted as variables with fuzzy subsets: NB, NM and NS are considered as negative big, medium and small, and PB, PM and PS are considered as positive big, medium and small and ZE for zero. Fuzzy rule is accumulation of IF–THEN rules having every information for the parameters. Defuzzification assesses the rules based on a set of control activities for a given fuzzy inputs.

If E is NB and CE is ZE, then crisp U is PB; then if the operating point is far from the MPPT by right side, variation of the slope of curve is nearly zero.

Boost Converter:

A Boost converter is a change mode DC-to-DC converter in which the output voltage is more prominent than the input voltage. Figure 6 demonstrates a step-up or PWM help converter. It comprises a source voltage V , inductor L , switch S , diode D , capacitor C and the resistance R . At the point when the switch S is in the on mode, the current in the boost inductor increments directly and the diode D is off around then. At the point when the turn S is turned off, the vitality put away in the inductor is discharged through the diode to the output RC circuit.

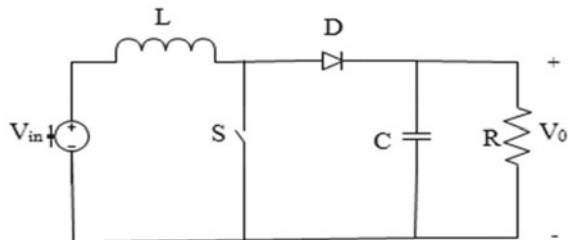
3 Multicarrier Modulation Techniques

By utilizing the multicarrier PWM methods, the proposed CHBMLI is examined. The modulation procedure depends on the examination of sinusoidal reference signal with the carrier signals (having the same frequency) which are normally chosen triangular signals. For m level inverter, all carriers utilize same frequency f_c and amplitude A_c , and they are arranged such that the bands they involved are contiguous to each other.

Multicarrier PWM is three sorts:

- (1) *Phase Disposition (PD)*: If all the carriers are chosen in phase as shown in Fig. 2, that is all are in phase, then the technique is PD strategy.
- (2) *Phase Opposition Disposition (POD)*: If the carriers over the zero reference are in phase, yet moved by 180° beneath the zero reference.

Fig. 2 Boost converter circuit



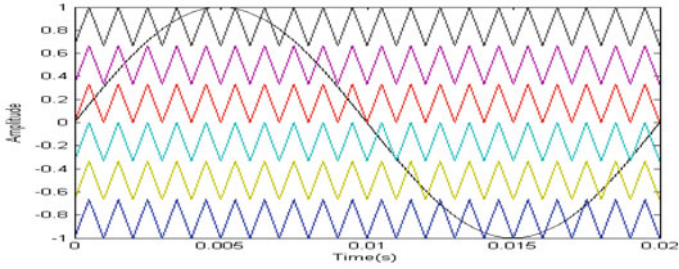


Fig. 3 Reference and carrier waveforms for PD PWM

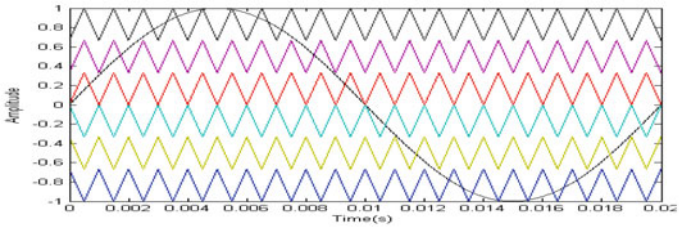


Fig. 4 Reference and carrier waveforms for POD PWM

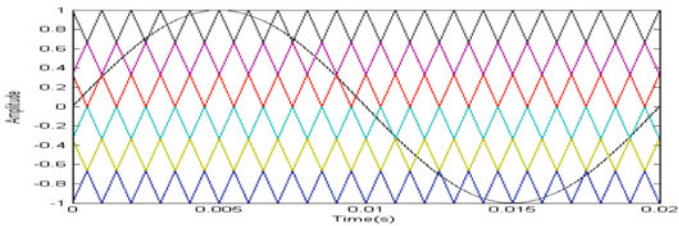


Fig. 5 Reference and carrier waveforms for APOD PWM

- (3) *Alternate Phase Opposition Disposition (APOD)*: In this technique, each triangular carrier is moved by 180° from its contiguous carrier (Figs. 3, 4 and 5).

4 Cascaded H-Bridge Multilevel Inverter

The CHBMLI circuit is illustrated in Fig. 1, and it comprised of separate, independent H-bridge cell; every cell is sustained by their own DC supply like full bridge inverter. Every cell comprises of four switches, and in this topology, IGBT is utilized as a switch, as a result of low switching losses. Three discrete voltage outputs ($+V_{dc}$, $-V_{dc}$, 0) are produced by every H-bridge cell. For seven-level inverter, every leg

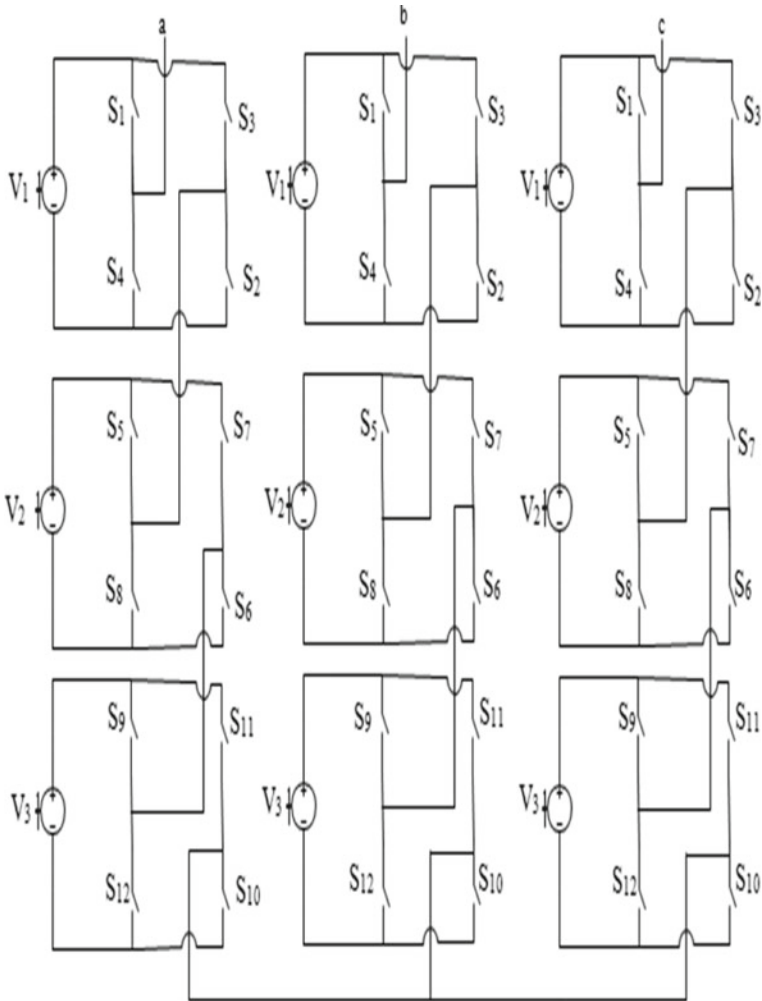


Fig. 6 3- Φ seven-level CHBMLI

comprises three H-bridge cells, and the AC output terminal voltages of every cell are coupled in series arrangement. By including the output voltage of every H-bridge cell, the output voltage is acquired as in condition (10).

$$V_0(t) = V_{01}(t) + V_{02}(t) + \dots + V_{0N} \tag{10}$$

The aggregate of every H-bridge cell AC voltage is the output AC voltage of CHBMLI. The achievable combination of switching sequence is illustrated in Table 1 where “1” demonstrates the on condition for a switch and “0” for off condition of the switch (Fig. 6; Table 2).

Table 1 Fuzzy rules

E/CE	NB	NM	NS	ZE	PS	PM	PB
NB	ZE	ZE	ZE	NB	NB	NB	NM
NM	ZE	ZE	ZE	NS	NM	NM	NM
NS	NS	ZE	ZE	ZE	NS	NS	NS
ZE	NM	NS	ZE	ZE	ZE	PS	PM
PS	PS	PM	PM	PS	ZE	ZE	ZE
PM	PM	PM	PM	ZE	ZE	ZE	ZE
PB	PB	PB	PB	ZE	ZE	ZE	ZE

Table 2 Switching sequence for one-leg seven-level CHBMLI

V_0	+V	+2 V	+3 V	0	-V	-2 V	-3 V
S_1	1	1	1	0	0	0	0
S_2	1	1	1	1	0	0	0
S_3	0	0	0	0	1	1	1
S_4	0	0	0	1	1	1	1
S_5	0	1	1	0	0	0	0
S_6	1	1	1	1	1	0	0
S_7	0	0	0	0	0	1	1
S_8	1	0	0	1	1	1	1
S_9	0	0	1	0	0	0	0
S_{10}	1	1	1	1	1	1	0
S_{11}	0	0	0	0	0	0	1
S_{12}	1	1	0	1	1	0	1

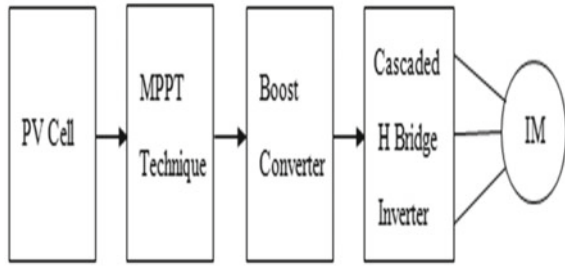
5 Proposed Topology

To demonstrate the execution of the proposed CHBMLI fed IM by using PV source, an adjustable speed IM drive is examined. The MATLAB/ Simulink is utilized to execute three-phase seven-level inverter fed IM drives by PV source. The block diagram of CHBMLI fed IM by using PV source is illustrated Fig. 7.

A 3- Φ CHBMLI has been created by utilizing an IGBT, in fact of that IGBT is a very preferable device among high-power switches. This three-phase seven-level inverter is given as source to the three-phase squirrel cage IM.

The multicarrier PWM strategy is utilized to create pulses for the inverter, and the THD is analyzed. In this topology, PV cell is utilized as DC source for CHBMLI and every PVcell has a separate boost converter with FL-based MPPT technique. The source voltage of every H-bridge cell is 133 V. In this topology, three-phase IM is treated as a load to the inverter.

Fig. 7 Block diagram for proposed topology



6 Simulation Results

In this paper, the simulation model of CHBMLI fed motor by using PV source is developed by MATLAB/Simulink software. The simulation circuit and results of the CHBMLI fed IM and converter with PV cell as a source for CHBMLI fed motor are designed and executed by utilizing a FLC-based MPPT technique in Simulink, and results are accompanied below (Figs. 8, 9, 10, 11, 12, 13, 14, 15 and 16).

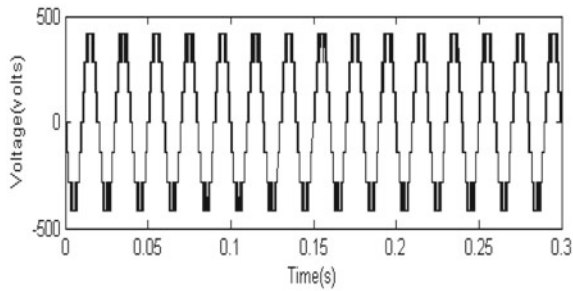


Fig. 8 Seven-level AC voltage under PD PWM

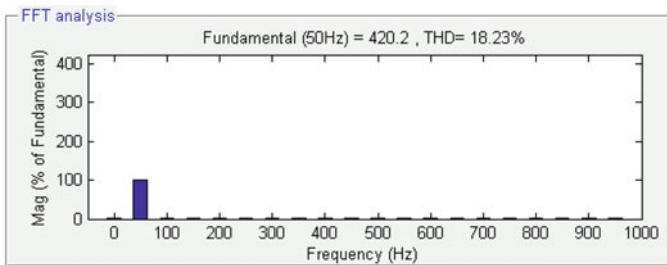


Fig. 9 Seven-level FFT analysis under PD PWM

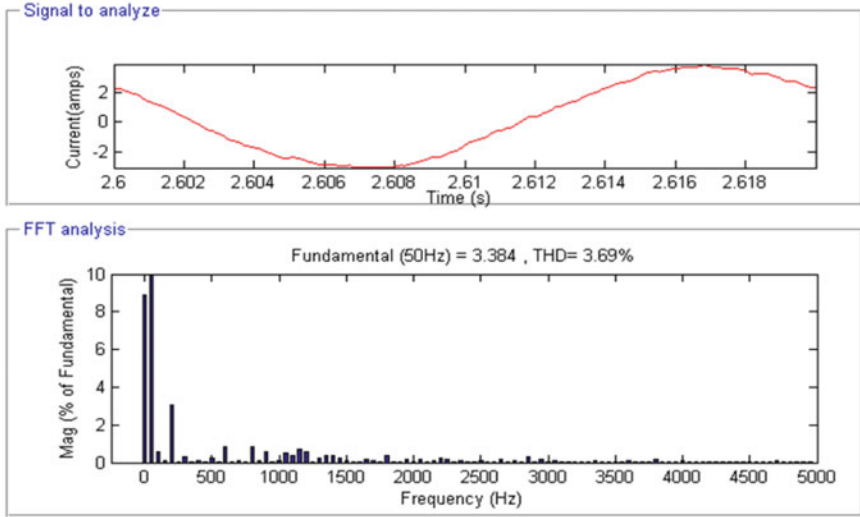


Fig. 10 FFT analysis for motor current under PD PWM

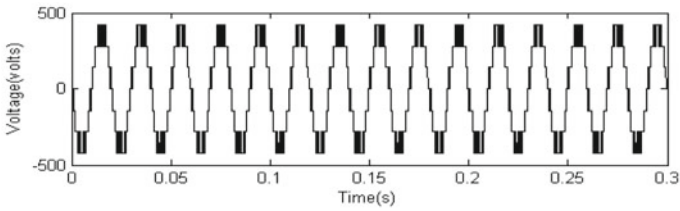


Fig. 11 Seven-level AC voltage under POD PWM

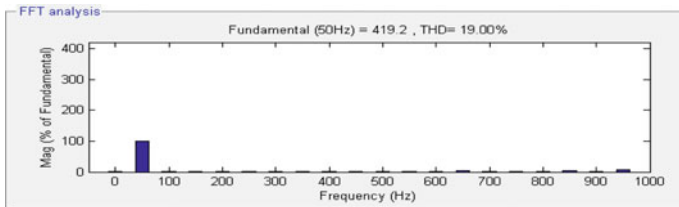


Fig. 12 Seven-level FFT analysis under POD PWM

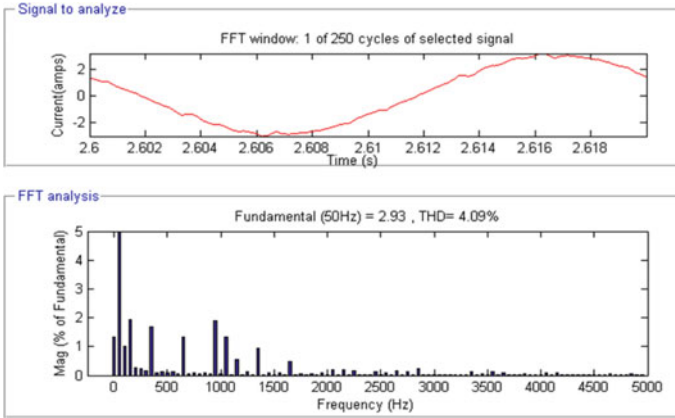


Fig. 13 FFT analysis for motor current under POD PWM

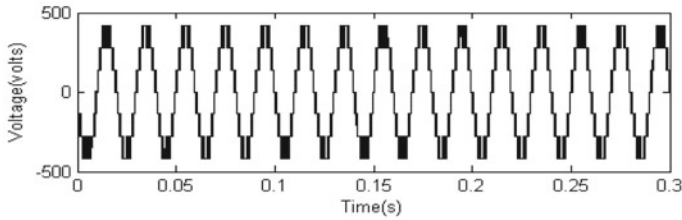


Fig. 14 Seven-level AC voltage under APOD PWM

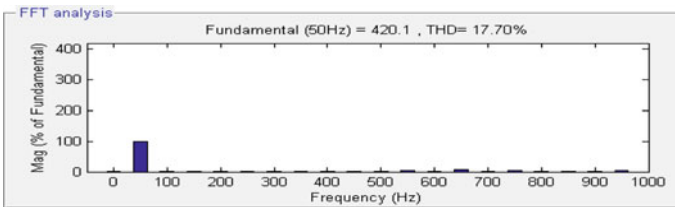


Fig. 15 Seven-level FFT analysis under APOD PWM

The current, speed and torque of the AC IM are examined by utilizing PV source with boost converter for seven-level H-bridge inverter fed motor and are illustrated in below figures under APOD technique (Figs. 17 and 18; Table 3).

Boost Converter Results:

During transient period, the boost converter and MPPT power is varied from 0 to 0.13 s and remains constant after 0.15 s as appeared in Fig. 19, and CHBMLI voltage is varied and remains constant after 0.15 s as in Fig. 23 (Fig. 20).

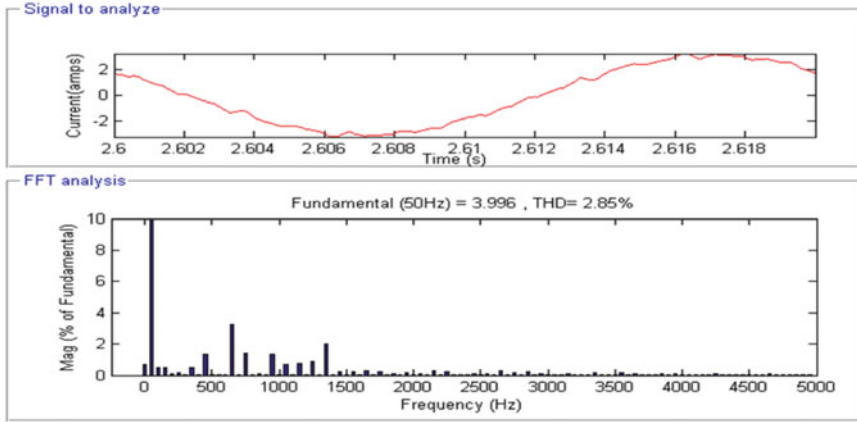


Fig. 16 FFT analysis for motor current under APOD PWM

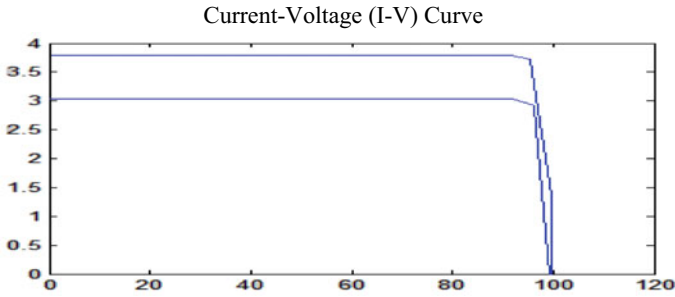


Fig. 17 I-V curve for PV cell

Fig. 18 P-V curve for PV cell

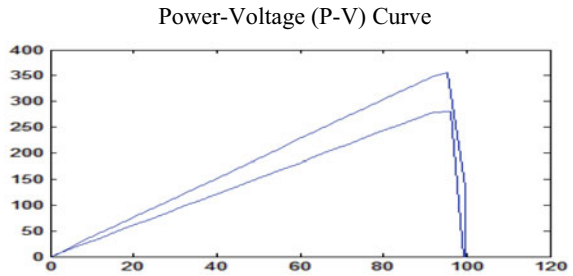


Table 3 Comparison of multicarrier PWM techniques for voltage and motor current THD%

PWM	PD	POD	APOD
Voltage THD%	18.23	19.00	17.70
Current THD%	3.69	4.09	2.85

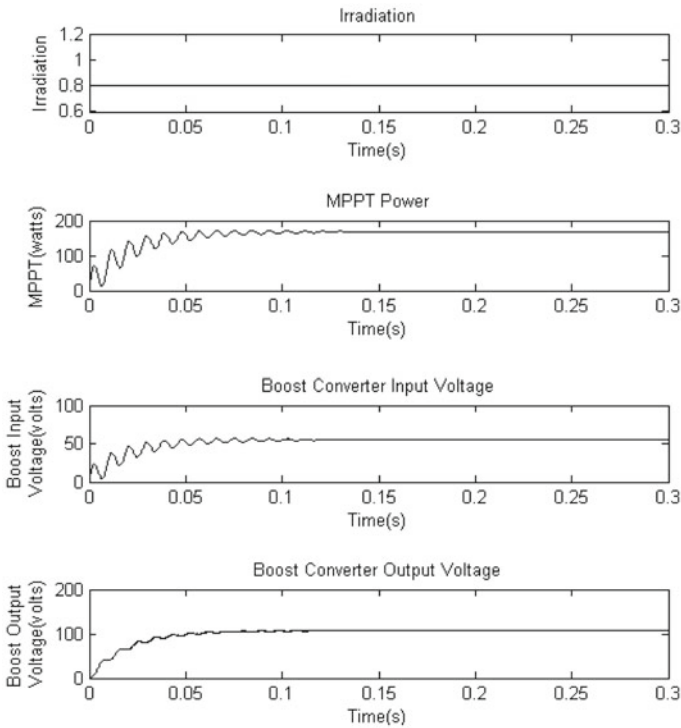


Fig. 19 Transient period of boost converter

During step response, the boost converter and MPPT power are constant from 0.3 s to 0.5 s and from 0.5 s boost converter, and MPPT power goes on rising as in Fig. 21 and CHBMLI voltage is constant from 0.3 to 0.5 s and from 0.5 s voltage goes on rising as in Fig. 24.

During steady-state period, the boost converter and MPPT power are constant from 1.4 to 1.6 s as appeared in Fig. 22, and CHBMLI voltage is also constant at 400 V from 1.4 to 1.6 s as in Fig. 25 (Figs. 23 and 24).

Cascaded H-Bridge Inverter Results:

Induction Motor Results:

During the transient period, torque and current will be varied and speed goes on rising from 0 to 1.9 s and remains constant. Torque and current remain steady after 1.9 s as in Fig. 25.

During step response, torque and current will be increased after 2.5 s and speed decreases after 2.5 s and remains constant. After 2.5 s, torque and current decrease and at that time speed increases as appeared in Fig. 26. During steady-state period speed, current and torque remain constant at 4.2–4.4 s as in Fig. 27.

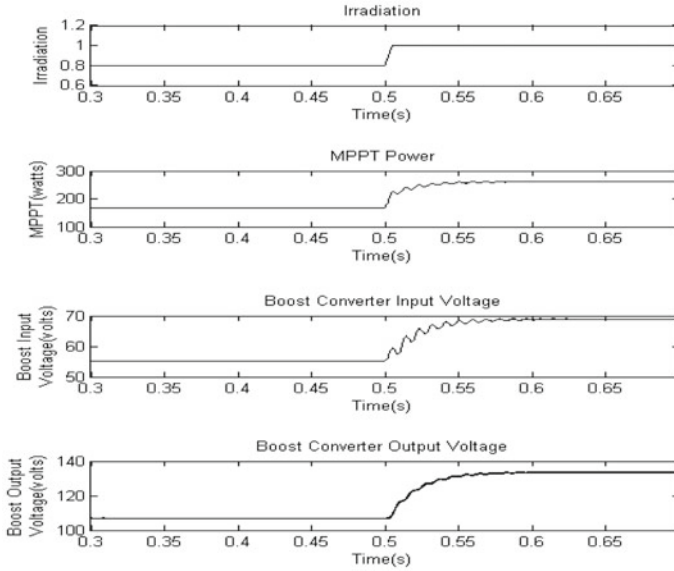
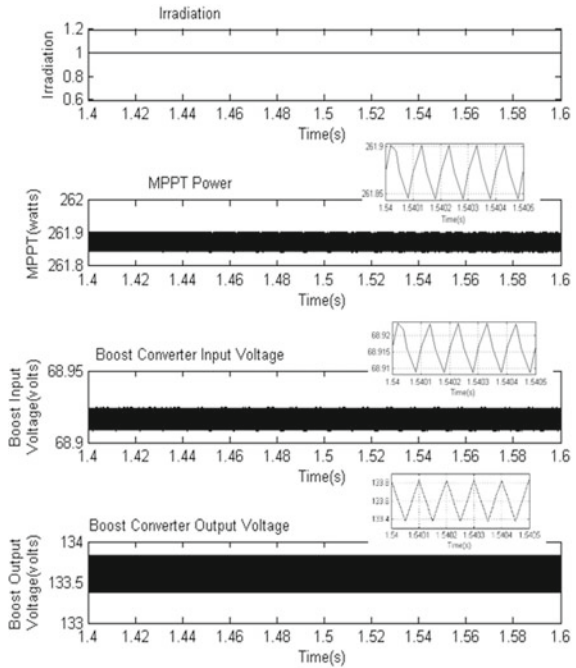


Fig. 20 Step response of boost converter

Fig. 21 Steady-state period of boost converter



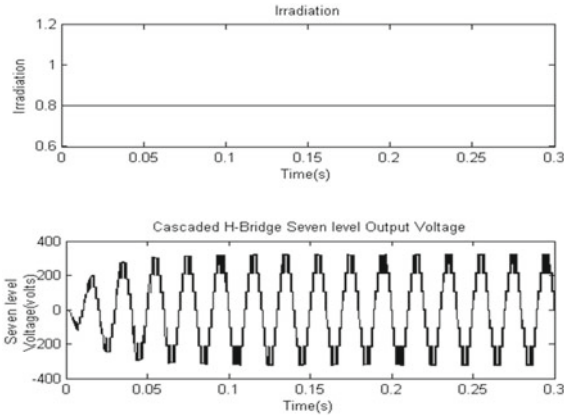


Fig. 22 Transient period of CHBMLI output voltage

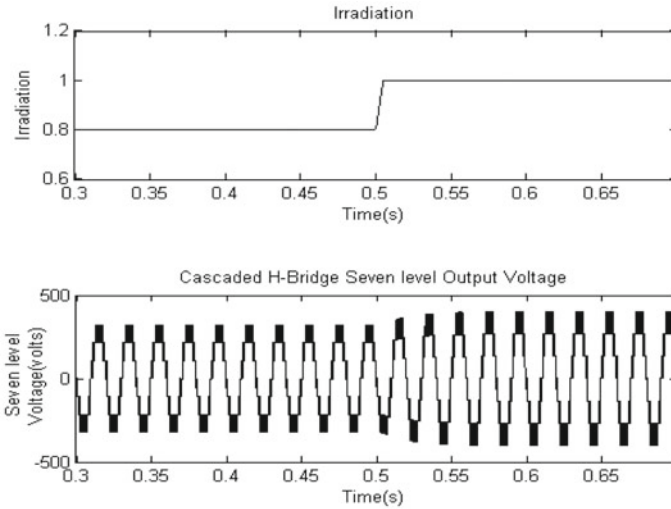


Fig. 23 Step response of CHBMLI output voltage

7 Conclusion

The inverter fed motor can be utilized in industries where adjustable speed drives are needed. The multicarrier PWM method for the 3- Φ CHBMLI has been developed by utilizing MATLAB/Simulink. Among the three PWM procedures, APOD PWM method has given better THD over other two strategies. So for the inverter fed motor, APOD PWM method is better under desired speed-torque. A MPPT-based FLC strategy is associated in a PV cell, and it concluded that the MPPT method modifies the duty cycle of the converter in varying irradiance to extract the MPPT from PV

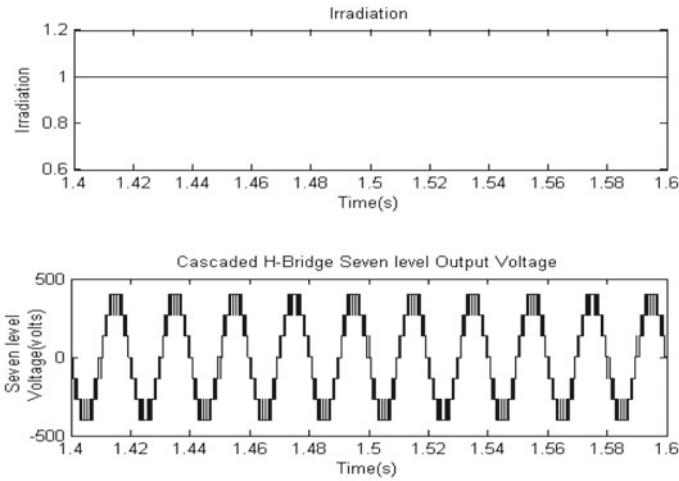


Fig. 24 Steady-state period of CHBMLI output voltage

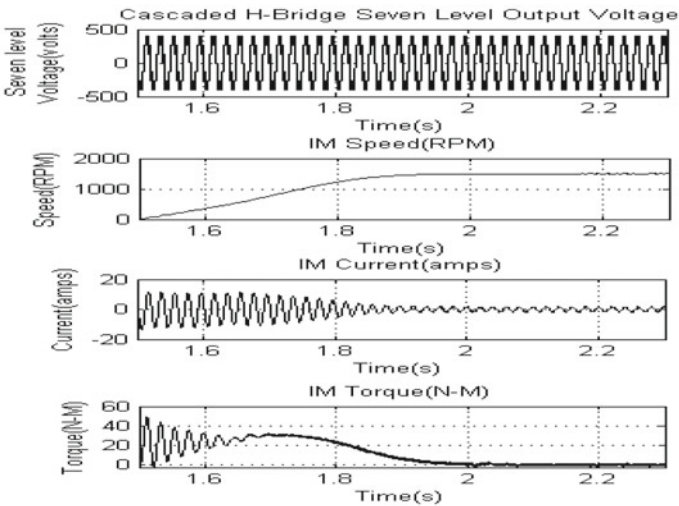


Fig. 25 Transient period of IM

and distributes it to load. The execution of PV with MPPT is approved with a boost converter for this cascaded inverter fed motor by utilizing APOD PWM procedure to initiate the pulses for the inverter, and these simulation results show that CHBMLI adequately controls the motor speed.

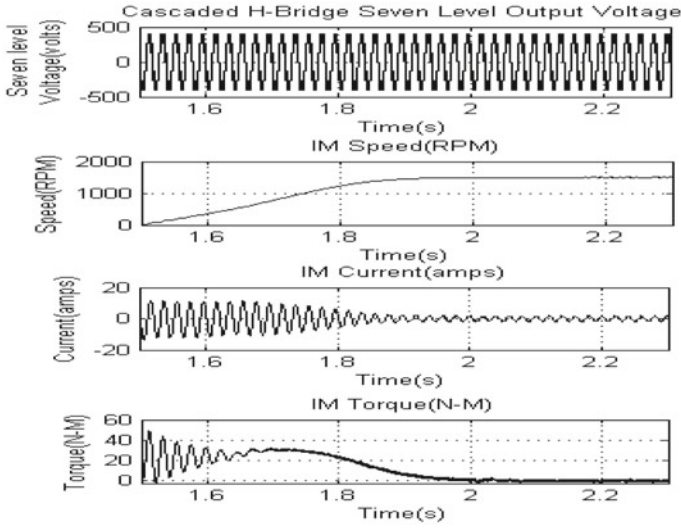


Fig. 26 Step response of IM

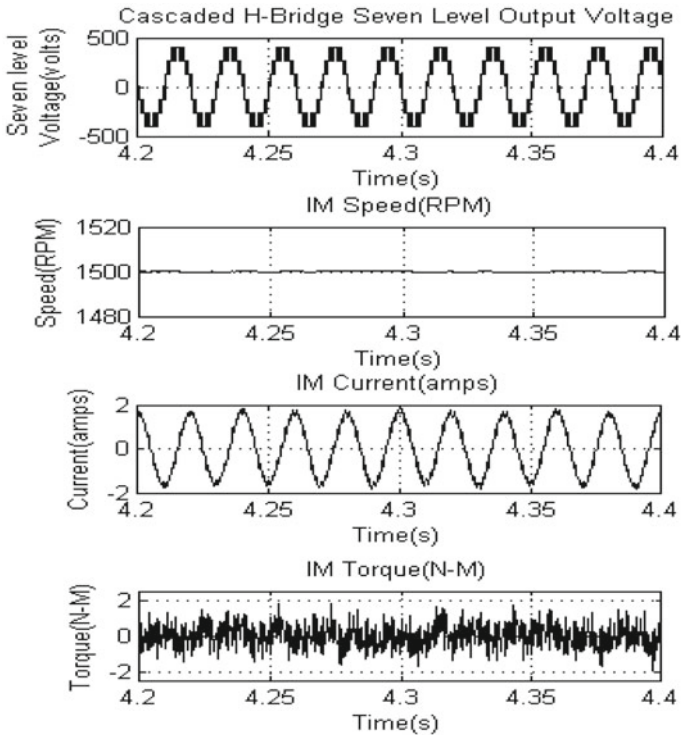


Fig. 27 Steady-state period of IM

References

1. Jih-Sheng L. Fang Zheng P (1996) Multilevel converters-a breed of power converters. IEEE Trans 32:1996
2. Bhuvanewari V, HariKumar ME. Analysis of asymmetrical and symmetrical 3- Φ CHBMLI using multicarrier techniques. IEEE Trans
3. Preeti, Gupta R (2015) Switching of 3- Φ CHBMLI fed IM drive. In: Advance Research in Electrical and Electronics Engineering (AREEE), vol 2, issue 5 April–June 2015, pp 36–40
4. Durga M, Lakshmi RV, Kumar P (2014) Analysis & comparison of APOD and PD PWM technique CHB inverter to 3- Φ IM. IJSR 3(11)
5. A. R. Shelar, S. M. Chaudhari, "Speed Control of 3- Φ IM by Using MLI," on IJIRAE -Vol 1 Issue 12 December 2014.
6. Venkadesan A, Panda P, Agarwal P, Puli V (2014) CHBMLI for IM drives. IJRET 03(05)
7. Venkadesan A, Panda P, Agarwal P, Puli V (2014) Performance of 3- Φ CHBMLI fed drive. IJRET 03(05)
8. Singh A, Jain M, Singh S (2015) Analysis of THD & output voltage for 7-level asymmetrical CHBMLI using LSCPWM method. IJCA 112
9. Xiao B, Hang L, Mei J, Riley CL, Burak TM (2015) Modular cascaded H-bridge PV inverter with MPPT for grid connected application. IEEE Trans 5

EMG-Based Analysis of Rehabilitation Exercises for Diastasis Recti Abdominis



R. Menaka, R. Karthik, and P. Vinitha Joshy

Abstract Diastasis recti abdominis (DRA) has been a concerning issue among researchers and women in recent years. The diagnosis of DRA is possible by measuring the inter-recti distance which is the separation of the abdominal muscle. Therapy for DRA includes various rehabilitation exercises, and surgery is done when this separation leads to other complications. Various rehabilitation procedures are identified with help of a medical practitioner and used for rehabilitation therapy. Hence, developing a biofeedback device helps in identifying the muscle signal for various positions and analysing the corresponding statistical parameters for better results in therapy. EMG sensors contribute a wide range of application in measuring the muscle signals. Here, we have used myoware muscle sensor integrated with Arduino to get the desired output EMG signal. Two groups each consisting of five subjects are evaluated for various exercises. The signal amplitudes for various rehabilitation positions are acquired, and the corresponding statistical measures are obtained for the analysis of them in the rehabilitation therapy.

Keywords Diastasis recti abdominis (DRA) · Electromyography (EMG) · Statistical features

1 Introduction

Diastasis recti abdominis (DRA) is the divarication of rectus abdominis muscle caused by the stretching and widening of the linea alba resulting in increased inter-recti distance [1–3]. DRA occurs due to the mechanical and functional disturbances

R. Menaka · R. Karthik (✉) · P. Vinitha Joshy
Centre for Cyber Physical Systems, School of Electronics Engineering, Vellore Institute of Technology, Chennai, India
e-mail: r.karthik@vit.ac.in

R. Menaka
e-mail: menaka.r@vit.ac.in

P. Vinitha Joshy
e-mail: vinitha.joshy@vit.ac.in

in the anterior abdominal wall. DRA is characterized by a protruding midline as a result of an increase in intra-abdominal pressure. A separation of the heads of the rectus abdominis muscle of more than 2 cm is considered pathological. DRA can affect both women and men of any age. However, it is most often diagnosed in pregnant and postpartum women, due to the changes occurring in a woman's body during pregnancy. DRA can occur in infants, people with abdominal obesity and those whose jobs involve heavy lifting [4]. Hence Caesarean section, pregnancy, maternal age, multiparity, foetal macrosomia, multiple gestations, age, obesity, greater abdominal circumference, the performance of full-excursion sit-ups, weight training, abdominal wall stress, weight gain, high birth weight, ethnicity, and childcare are the risk factors reported by the several studies in the literature. However, the risk factors for DRA appear to be not well-grounded, and the association of each risk factor with DRA requires further investigation [5, 6]. The most common symptom of DRA is bulging along the midline of the abdomen which becomes more prominent while abdominal muscles contract together with a visible depression in the linea alba.

Researchers have reported numerous findings regarding the consequences of DRA. Changes in abdominal muscle function, pelvic floor muscle dysfunction, and pain in the lower parts of the body are the physical symptoms in women at different stages after delivery. DRA at the lower level of the umbilicus may be negatively associated with the rectus abdominis and oblique muscles strength [7]. However, the experience of abdominal pain is positively associated with DRA in women during their early postpartum period. But its intensity seemed to be low and clinically irrelevant [8]. Pelvic floor dysfunctions include urinary incontinence, stress urinary incontinence, faecal incontinence, and pelvic organ prolapse. It is reasonable to be present in peri and post-menopausal women and urogynecological patients [9]. Low back pain and pelvic girdle pain are other consequences investigated in the literature. Women with increased IRD after childbirth are reported diminishing changes in their body image, function, and ability than before, and there was a lack of awareness on DRA among them [10]. The majority of the women undergo natural resolution of diastasis recti during the initial stage of their postpartum period. Although in some cases, DRA persists and tends to cause functional and cosmetic defects in women's bodies. Therefore, women with visible symptoms seek medical advice. Conservative therapy is the treatment prescribed in the initial stage. However, when conservative therapy seems inefficient in severe cases, women are directed towards surgical interventions. Both the treatments aim for improvements in the morphological, functional, and quality of life of patients.

Surgeons approach DRA in many ways like open, laparoscopic, endoscopic, and hybrid techniques. Each method has its benefits and drawbacks. In each method, different procedures are available that surgeons choose based on their experience in repairing DRA. The patients with symptomatic DRA without any cosmetic defects get appointed to the general surgeon, while the plastic surgeon treats DRA patients with cosmetic disabilities. DRA can occur even after the patient undergoes a surgical procedure. Few studies in the literature have reported an insignificant recurrence rate. Conservative treatment studies for DRA are scarce. It is considered the primary treatment for DRA. It involves physiotherapeutic exercises, training, and abdominal

binding. Studies on exercises for DRA are limited. While one group of researchers claims to reduce the IRD, another group of researchers claims to reduce the tension of the linea alba for effective rehabilitation. Hence, the exercise protocols that provide efficient results need to be investigated. Although there is a lack of evidence in exercise therapy, the main advantage is that it is a non-invasive treatment.

Today's technology has served rehabilitation medicine by bringing up various devices that help enhance the performance of the patients. One such device is the biofeedback device that helps track patient performance when required and provides continuous feedback. Rehabilitation for DRA must commence as early as possible. Therapists prescribe exercise protocols to the DRA patients during their visits to the clinic, and the patient's performance is being assessed manually. Once the patient leaves the clinic and continues their exercise regime at home, it is necessary to follow up with the patients to assess their performance. This leads to the requirement of a biofeedback device that analyses the patient's performance at their own home. Therefore, developing a biofeedback device for monitoring DRA patient's performance is required.

2 Proposed System

Recent advances in sensors have facilitated the investigation of muscle activities of the human body. The proposed system uses an EMG sensor to assess the seven therapeutic exercises performed by ten subjects with and without DRA.

2.1 Block Diagram

The block diagram of the proposed system is depicted in Fig. 1. The myoware muscle sensor is placed on the abdomen of the subjects. The sensor is connected to the Arduino UNO board. The code to obtain the EMG signal is uploaded onto the board through the USB cable. The digitized signal from the board can be seen using Arduino IDE. To store the obtained data, PLX-DAQ is used. PLX-DAQ stores the incoming data in a real time through the COM port. The stored data is then processed using MATLAB to obtain the features and to perform statistical analysis of the obtained data.

2.2 Data Acquisition

EMG muscle signals are acquired for various positions based on the rehabilitation exercises, and the corresponding statistical features are analysed.

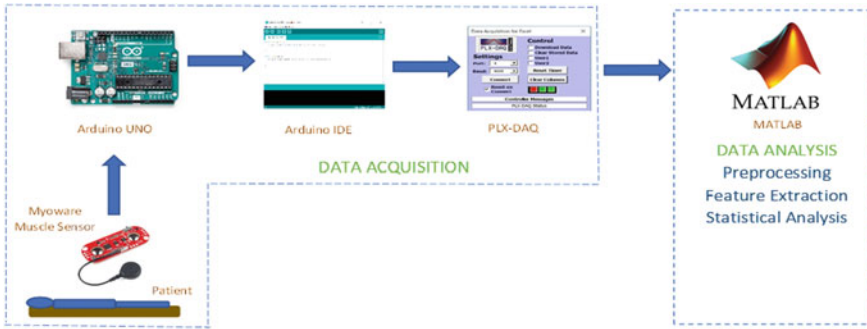


Fig. 1 Block diagram of the proposed system

2.2.1 Subjects and Exercises

This study included 10 subjects grouped into 2 groups with 5 subjects in each group. Group 1 consisted of 5 subjects without DRA, and group 2 consisted of 5 subjects with DRA. All the subjects were asked to perform 7 exercises with 3 repetitions in a supine position. The seven exercises are sit-up, curl-up, transverse abdominis (TA) muscle contraction with sit-up, TA muscle contraction with curl-up, TA muscle contraction with pelvic floor muscle along with curl-up, TA muscle contraction with straight leg raise, and reverse curl-up. The EMG signal was recorded during all the exercises using an EMG sensor. The active electrodes were placed at a distance from the left side of the umbilicus, and the reference electrode was placed at the anterior superior iliac spine (ASIS).

2.3 Feature Extraction

In processing a signal, the effective features are extracted from the modulated signals. Feature extraction reduces the dimensionality of modulated signals' raw data by selecting the effective features, which should capture the distinctive parameters of the modulation schemes [13]. Any redundant, noisy, unrelated features would be eliminated. As the number of features increases, this leads to more complicated system, as well as increasing the training time of the classifier.

2.3.1 Statistical Analysis

Mean

Mean is the measure of central tendency. It can be calculated for continuous or discrete data [11]. The mean (also known as average) is obtained by dividing the

sum of observed values by the number of observations. Mean \bar{X} can be calculated as shown in Eq. (1)

$$\bar{X} = \frac{1}{n} \sum_{i=1}^n x_i \quad (1)$$

where \bar{X} is the mean, x is the observed value, and n is the number of observations.

Median

Median is the central value of a data set in the distribution. The median is calculated by sorting all the observations from smallest to the largest and selecting the midpoint. The median is especially helpful when separating data into two equal sized bins. It can be calculated for continuous, discrete, or ranked data [12]. If the number of data points is even, then the average of the middle two data points is used as median.

Standard Deviation

The standard deviation gives an idea of how close the entire set of data is to the average value.

It is measured as the difference between any given value x_i and the mean \bar{X} . The variance is defined as the sum of the squared deviations of all the data points divided by the number of data points. Standard deviation is defined as the square root of variance. Standard deviation is at the same numeric scale as the data values [12]. Data sets with a small standard deviation have tightly grouped, precise data closer to the centre point. Data sets with high standard deviations have data spread out over a wide range of values around the centre. Standard deviation S can be calculated as shown in Eq. (2)

$$S = \sqrt{\frac{\sum_{i=0}^n (x_i - \bar{X})^2}{n}} \quad (2)$$

where S is the standard deviation, \bar{X} is the mean, x_i is the observed value, and n is the number of observations.

Kurtosis

Kurtosis is the measure of the peakedness of the data distribution. It shows how the distribution is related to a normal distribution. Thus, negative kurtosis indicates a flat

data distribution, positive kurtosis indicates a peaked distribution, and zero kurtosis indicates the normal distribution. Kurtosis K can be calculated shown in Eq. (3)

$$K = \frac{\sum_{i=0}^n (x_i - \bar{X})^4}{nS^4} \quad (3)$$

where K is kurtosis, S is the standard deviation, \bar{X} is the mean, x is the observed value, and n is the number of observations.

Skewness

Skewness is the measure of symmetry which is the statistical approach enabling computation of probability distribution of asymmetry of a signal about its mean. The data is considered positively skewed if there are extremely large values than extremely small ones. The data is considered negatively skewed if there are lot of extremely small values and not many extremely large values. When the data is negatively skewed, it indicates that the mean of the data values is less than the median and the distribution of data is left-skewed. Likewise, when the data is positive skewness, it indicates that the mean of the data values is larger than the median, and the distribution of data is rightness-skewed. Thus, skewness delivers information on whether a distribution is skewed to either the end of lower values or the end of higher values [13]. Skewness SK can be calculated shown in Eq. (4)

$$SK = \frac{\sum_{i=0}^n (x_i - \bar{X})^3}{nS^3} \quad (4)$$

where SK is skewness, S is the standard deviation, \bar{X} is the mean, x is the observed value, and n is the number of observations.

3 Results and Discussions

The rehabilitation exercises are suggested by the physiotherapists for the therapy of DRA. Hence, the rehabilitation positions chosen are sit-up, curl-up, TA with sit-up, TA with curl-up, TA PFM curl-up, TA SLR, and reverse curl-up. Subjects with DRA (abnormal controls) and non-DRA (normal controls) each consisting of 5 members are extracted with EMG signal for each corresponding exercises, respectively. The statistical features obtained for various rehabilitation positions are analysed for patients with normal and abnormal controls.

3.1 Analysis of Statistical Measures for Normal Controls

The table given as Table 1 shows the values of statistical parameters for various rehabilitation positions. The parameters are assessed for normal controls; those are subjects without DRA.

The figure given as Fig. 2 shows the plot of statistical features for normal controls. The corresponding values of mean, median, standard deviation, kurtosis, and skewness are calculated for various rehabilitation positions.

Here the plot shows the values are high for sit-up, TA with sit-up, TA with curl-up, TA PFM curl-up, and reverse curl-up, and the values are low for curl-up and TA SLR.

Table 1 Statistical measure for normal controls

Exercise name/parameters	Mean	Median	Standard deviation	Kurtosis	Skewness
Sit-up	391.0211	233.4	384.4945	1.9620	0.6359
Curl-up	243.1794	100.9	272.2202	6.9154	1.8250
TA with sit-up	420.9026	476	370.1482	2.1199	0.2682
TA with curl-up	383.3398	294.1	351.2549	2.9481	0.8134
TA PFM curl-up	368.3878	318.7	309.0774	4.2624	1.0626
TA SLR	169.0819	102.9	176.0762	6.9512	2.3778
Reverse curl-up	384.3054	395.9	340.6974	4.2283	0.9634

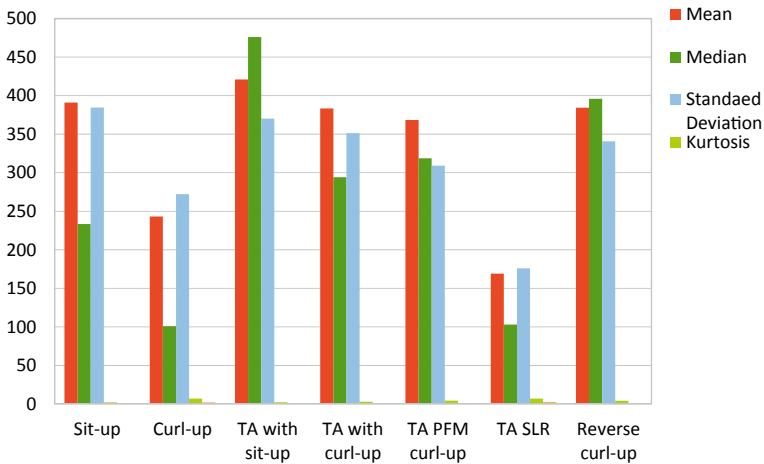


Fig. 2 Plot of statistical features for normal controls

3.2 Analysis of Statistical Measures for Abnormal Controls

The table given as Table 2 shows the values of statistical parameters for various rehabilitation positions. The parameters are assessed for abnormal control subjects with DRA.

The figure given as Fig. 3 shows the plot of statistical features for abnormal controls. The corresponding values of mean, median, standard deviation, kurtosis, and skewness are calculated for various rehabilitation positions.

Here the plot shows the values are lower for sit-up, TA with sit-up, TA with curl-up, TA PFM curl-up, and reverse curl-up compared to the ones we acquired for normal controls.

Table 2 Statistical measures for abnormal controls

Exercise name/parameters	Mean	Median	Standard deviation	Kurtosis	Skewness
Sit-up	315.8492	304.4	198.1872	28.6304	2.9311
Curl-up	218.0764	113.1	229.2284	6.6677	1.8348
TA with sit-up	278.2993	241.6	235.9601	12.3528	1.9846
TA with curl-up	247.7766	270.6	158.7900	48.1358	4.1007
TA PFM curl-up	181.1578	101.6	181.3933	17.5623	2.8975
TA SLR	221.9937	252.2	170.2477	12.9102	2.0666
Reverse curl-up	366.7701	397.8	297.8409	4.5091	1.0588

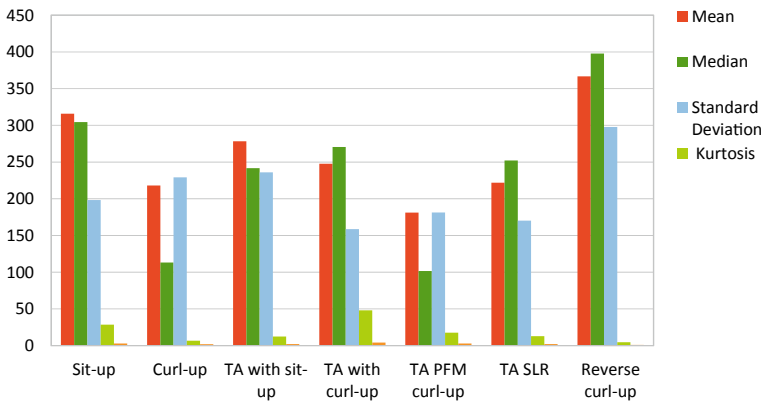


Fig. 3 Plot of statistical features for abnormal controls

4 Conclusion

The aim of this pilot study is to analyse the effect of rehabilitation exercises for diastasis recti abdominis. The surface EMG signals were extracted from the abdominal muscle by the myoware EMG sensor. With the plot of statistical features for DRA and normal subjects, we could infer that the statistical values obtained for sit-up, TA with sit-up, TA with curl-up, and TA PFM curl-up positions of abnormal controls (DRA subjects) are lower comparing to the statistical values obtained for sit-up, TA with sit-up, TA with curl-up, and TA PFM curl-up positions of normal controls. Hence by assessing the features of DRA and non-DRA subjects, we could be able to analyse the features of various rehabilitation positions. Future work involves extending this study to a larger population and generalize the findings effectively.

Acknowledgements This research was funded by the Department of Science and Technology DST under Biomedical Device and Technology Development (File No: TDP/BDTD/07/2021). We would like to render our sincere thanks to the Sri Ramachandra Institute of Higher Education and Research for their kind support and assistance in data acquisition.

References

1. Mota P, Pascoal AG, Vaz C, João F, Veloso A, Bø K (2018) Diastasis recti during pregnancy and postpartum. In: Women's health and biomechanics. Springer International Publishing, Heidelberg, pp 121–132. https://doi.org/10.1007/978-3-319-71574-2_10
2. Puri J, Sharma S, Samuel AJ, Chahal A (2021) Investigate correlation between diastasis of rectus abdominis muscle and low back pain in obese women. *J Lifestyle Med* 11(1):38–42. <https://doi.org/10.15280/jlm.2021.11.1.38>
3. Cardaillac C, Vieillefosse S, Oppenheimer A, Joueidi Y, Thubert T, Deffieux X (2020) Diastasis of the rectus abdominis muscles in postpartum: concordance of patient and clinician evaluations, prevalence, associated pelvic floor symptoms and quality of life. *Eur J Obstetrics Gynecol Reproductive Biol* 252:228–232. <https://doi.org/10.1016/j.ejogrb.2020.06.038>
4. Ptaszkowska L, Gorecka J, Paprocka-Borowicz M, Walewicz K, Jarzab S, Majewska-Pulsakowska M, Gorka-Dynsiewicz J, Jenczura A, Ptaszkowski K (2021) Immediate effects of kinesio taping on rectus abdominis diastasis in postpartum women—preliminary report. *J Clin Med* 10:5043. <https://doi.org/10.3390/jcm10215043>
5. Hills NF, Graham RB, McLean L (2018) Comparison of trunk muscle function between women with and without diastasis recti abdominis at 1 year postpartum. *Phys Ther* 98(10):891–901. <https://doi.org/10.1093/ptj/pzy083>
6. Parker MA, Millar LA, Dugan SA (2009) Diastasis rectus abdominis and lumbo-pelvic pain and dysfunction—are they related? *J Women's Health Phys Therapy* 33(2):15–22. <https://doi.org/10.1097/01274882-200933020-00003>
7. Sperstad JB, Tennfjord MK, Hilde G, Ellström-Ength M, Bø K (2016) Diastasis recti abdominis during pregnancy and 12 months after childbirth: prevalence, risk factors and report of lumbopelvic pain. *Br J Sports Med* 50(17):1092–1096. <https://doi.org/10.1136/bjsports-2016-096065>
8. Keshwani N, Mathur S, McLean L (2017) Relationship between interrectus distance and symptom severity in women with diastasis recti abdominis in the early postpartum period. *Phys Ther* 98(3):182–190. <https://doi.org/10.1093/ptj/pzx117>

9. Harada BS et al (2020) Diastasis recti abdominis and pelvic floor dysfunction in peri- and postmenopausal women: a cross-sectional study. *Physiotherapy Theor Pract* 1–7. <https://doi.org/10.1080/09593985.2020.1849476>
10. Eriksson Crommert M, Petrov Fieril K, Gustavsson C (2020) Women’s experiences of living with increased inter-recti distance after childbirth: an interview study. *BMC Women’s Health* 20(1). <https://doi.org/10.1186/s12905-020-01123-1>
11. Ross SM (2021) Descriptive statistics. *Introduction to probability and statistics for engineers and scientists*. Elsevier, pp 11–61. <https://doi.org/10.1016/b978-0-12-824346-6.00011-9>
12. Lee J (2020) Statistics, descriptive. *International encyclopedia of human geography*. Elsevier, pp 13–20. <https://doi.org/10.1016/b978-0-08-102295-5.10428-7>
13. Artemiadis PK, Kyriakopoulos KJ (2010) An EMG-based robot control scheme robust to time-varying EMG signal features. *IEEE Trans Inf Technol Biomed* 14(3):582–588

Secure Cloud Auditability for Virtual Machines by Adaptive Characterization Using Machine Learning Methods



Shesagiri Taminana and D. Lalitha Bhaskari

Abstract Cloud computing and cloud-based data centres are becoming more popular solutions for hosting applications as the need for better performance and availability grows. Several more studies, which are discussed later in this paper, have shown that a data centre's infrastructure must be audited in order to be secure. Third-party auditors will be hired by the data centres to verify the infrastructure, or more specifically, the virtual machines, during the auditing process. VMs, programmes, and data may be accessed by these auditors. A drawback of this auditing procedure is that the auditors may explicitly access any areas of the VMs, where the VMs' highly sensitive data is stored. It is difficult to allow access depending on the requests since this might increase the overall time required to conduct the audits. As a result, recent research calls for selective and adaptive auditing. Parallel researchers have proven a variety of ways to protect an auditing system. Although these results are more sophisticated in terms of both time and accuracy, they have been criticized for this. A unique prediction approach for analysing the features of the virtual machine applications and demand characteristics from auditors is proposed in this work, and eventually, the access to the virtual machine is granted using a predictive regression model. For making cloud-based application development safer and quicker, the suggested technique shows a 50% reduction in time complexity compared to existing parallel research results.

Keywords Adaptive · Coefficient-based regression · Selective auditing · Adaptive auditing

S. Taminana (✉)

Computer Science and Systems Engineering, Andhra University College of Engineering (A),
Andhra University, Visakhapatnam, India
e-mail: tsgiri32@gmail.com

D. Lalitha Bhaskari

Department of Computer Science and Systems Engineering, Andhra University College of
Engineering (A), Andhra University, Visakhapatnam, India

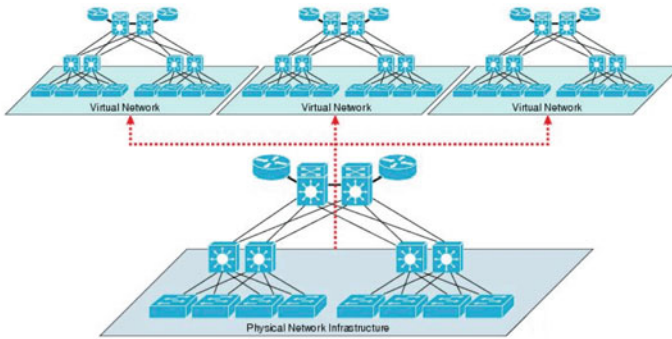


Fig. 1 Complex virtualized cloud-based data centre networks [2]

1 Introduction

In the application development market, performance is a primary concern, and the customer's need for better apps is continually growing. In order to get the most performance out of the software, developers often construct complicated architectures for the applications. The complexity of the designs will rise even more in cloud-based data centres as a result of these increasingly complex systems. As Dean et al. [1] have shown, network management and auditing may be very difficult when using dispersed data centre networks such as those in the cloud. In spite of this, the need for higher performance and zero downtime is compelling application developers and owners to move their applications to the sophisticated network topologies shown in Fig. 1.

As a result, there will be a growing need for auditing that is both selective and adaptable, using machine learning methodologies. According to Li et al. [3], utilizing machine learning-based solutions may save a lot of time. Parametric analysis or features study of cloud data centre resources may play an important role in accurately forecasting and assigning access for users and auditors, which is why this work is being done, as initially advocated by Li et al. [4]. Machine learning approaches will be used to forecast and analyses the auditing demand, which will then be mapped to the VM features for faster and more secure auditing.

2 Literature Study

In order to have a better knowledge of the current research topic, this section examines and discusses the results of related studies.

The typical data auditing approach is based only on requests. Owner requests are handled at the early stages of the data or apps that manage the data. In addition, the

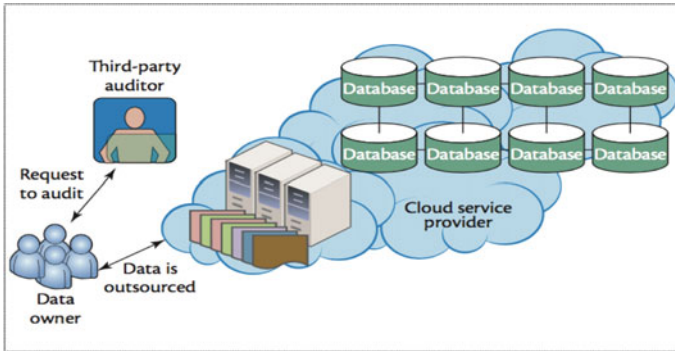


Fig. 2 Existing process of auditing [5]

auditing procedure gets underway. The auditing process begins when the data owner seeks access authorization, as shown in Fig. 2.

Wang et al. [6] go into the problems of cloud-based data centre audits in great depth. In the following phase of this study, the difficulties are re-examined. The first method offered by Yan et al. [7] for granting access rights to auditors, who already have access to the data, was based on the issues outlined by C. Wang. A method where data in motion cannot be assigned to any one auditor over the course of the audit is being criticized once again by a slew of parallel researchers.

When the applications are map-reduce apps and cannot be reduced for the datasets, the challenge of cloud data auditing grows. It was Sookhak et al. [8] who first noticed this issue, and it was solved using a map-reduce strategy known as divide and conquer. Everything worked out for a reason. As a result, it has also been criticized for being very time-consuming.

Zhao et al. [9] provide another path for the mobility cloud, and their study indicates that the auditing process issue exists even in the mobility cloud. This kind of mobility cloud scenario necessitates identity management, and Wang et al. [10] have proposed a solution to this issue. Many comparable research outputs have also criticized this study because of the difficulty in verifying the identity of a user when using a mobility cloud. Providing a one-step proxy-oriented authentication technique is the answer to this issue, as stated by Hussain et al. [11].

Contrarily, as Zhang et al. [12] suggest, numerous parallel studies have shown that auditors may get access to data and the associated ID of the data or application by using this method. Yu et al. [13] provided a strategy for verifying the data after the auditing procedure in order to ensure the integrity of the data to support this proposed scheme. Again, this technique is often criticized for being a reactive approach rather than a proactive approach to auditing for data security. Shen et al. [14] have presented a solution to this issue based on the notion that sensitive information may be hidden from auditors. In the auditing process, this method might generate major trust concerns, and therefore cannot be utilized in data centres.

In the light of this development, it is clear that the auditing scheme's applicability is expanding beyond cloud data centres, as proposed by Zhu et al. [15] and He et al. [16] for IoT-based devices and storage solutions.

That's why this issue is addressed utilizing a mathematical modelling technique, in order to make the suggested solution clearer and more comprehensible in the following parts.

3 Problem Formulation

Cloud auditing process basics and parallel research findings are examined in this phase of the study, before a mathematical model is used to identify and report an issue with generic auditing.

For simplicity, we will use the assumption that each data centre server is designated as I_X and that each server or instance is a collection of compute C , memory M , storage S , and network bandwidth N in Fig. 3.

The following is a formulation of this relationship:

$$I_X = \langle C_X, M_X, S_X, N_X \rangle \quad (1)$$

Every instance is also virtualized in cloud data centres with “ n ” virtual machines and may be expressed as

$$I_X = \sum_{i=1}^n VM_i \quad (2)$$

If you have a large number of machines, each one consumes a portion of the available hardware

$$VM_i = \langle C_i, M_i, S_i, N_i \rangle \quad (3)$$

$A[]$ may have several A_X and A_Y components, where A_X is the application's general functional component, and A_Y is the application's business logic component. Because of this, it should be obvious that D_X and D_Y may be used in various ways during operation or service delivery. This relationship may be expressed as follows

$$D_X \Rightarrow A_X \quad (4)$$

And

$$D_Y \Rightarrow A_Y \quad (5)$$

where

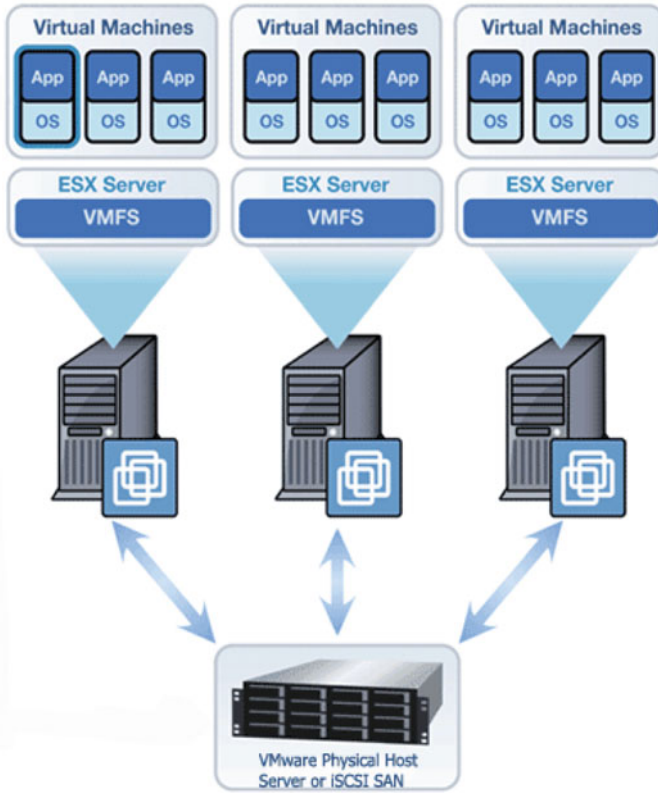


Fig. 3 Data centre structure for virtualization [17]

$$A = \langle A_X, A_Y \rangle \tag{6}$$

And

$$D = \langle D_X, D_Y \rangle \tag{7}$$

Cloud data centres may also divide a big application into many virtual machines (VM_X and VM_Y) so that they may distribute the application’s load more evenly across the virtual machines,

$$D_X \Rightarrow A_X \Rightarrow VM_X \tag{8}$$

And

$$D_Y \Rightarrow A_Y \Rightarrow VM_Y \tag{9}$$

where

$$VM = \langle VM_X, VM_Y \rangle \quad (10)$$

Auditor access to the whole VM set (VM_X and VM_Y) is required throughout the auditing process, with the second virtual machine hosting business-critical and secure data that should not be available to any third party,

$$Au \Rightarrow VM_X \quad (11)$$

And

$$Au \Rightarrow VM_Y \quad (12)$$

A general auditing methodology has this difficulty.

As a result, the highlighted issues must be addressed, and the suggested solution is reformulated in the next portion of the paper.

4 Proposed Solution—Mathematical Modelling

Every physical server in the data centre is labelled as I_X , and a physical server or an instance is a collection of compute C , memory M , storage S , and network bandwidth N , as suggested by H_P et al. [18]. The following is a formulation of this relationship:

$$I_X = \langle C_X, M_X, S_X, N_X \rangle \quad (13)$$

Every instance is also virtualized in cloud data centres with “ n ” virtual machines and may be expressed as

$$I_X = \sum_{i=1}^n VM_i \quad (14)$$

If you have a large number of machines, each one consumes a portion of the available hardware

$$VM_i = \langle C_i, M_i, S_i, N_i \rangle \quad (15)$$

In order to find the correlation factors of each element for VM characteristics, the next step is to determine the initial adjustment factors (0) and the correlation coefficients (1, 2, and 3) for each of the VM characteristics, as follows: The coefficients are a way to quantify the degree of correlation between two different facets of a virtual machine. This is how these parameters are expressed

$$\beta_1 = \text{Mean}(C_i) / \text{Mean}(M_i) \quad (16)$$

$$\beta_2 = \text{Mean}(M_i) / \text{Mean}(S_i) \quad (17)$$

$$\beta_3 = \text{Mean}(S_i) / \text{Mean}(N_i) \quad (18)$$

In addition, the CH_i correlation formula may be expressed as follows

$$CH_i = \beta_0 + \beta_1.C_i + \beta_2.M_i + \beta_3.S_i + N_i \quad (19)$$

where β_0 can be represented as

$$\beta_0 = CH_i - (\beta_1.C_i + \beta_2.M_i + \beta_3.S_i + N_i) \quad (20)$$

Similarly, Au may be expressed as a set of “Rules” describing auditor qualities

$$Au = [\text{Rules}] \quad (21)$$

For a total of n rules, this may be further developed as follows

$$Au = \sum_{i=1}^n \text{Rule}_i \quad (22)$$

Regression may be used to determine the features, CH_j , and it can be expressed as follows

$$CH_j = \sum_{i=1}^n \beta_i . \text{Rule}_i \quad (23)$$

It is also possible to match the characteristics of the auditor to the features of the virtual machine throughout the auditing process, so allowing the license to be granted in less time and without any security problems

$$CH_i \Leftrightarrow CH_j \quad (24)$$

Thus, in the next portion of the work, the suggested method will be described in further detail.

5 Proposed Algorithms

In this portion of the paper, the suggested method is presented and discussed after the problem's mathematical definition and solution proposal.

Algorithm: Adaptive Coefficient-Based Regression Method for Selective Auditing (ACB-RM-SA)

- Step-1. Assume that the VMs are listed as VM[]
 Step-2. It is acceptable to accept the auditors' list as a valid audit
 Step-3. To identify each virtual machine, we will refer to it as VM[i]
 a. C is the average amount of processing power
 b. Calculate the average amount of memory you have by multiplying your total memory by M
 c. S is the arithmetic medium storage capacity
 d. N is the average capacity of the network
 Step-4. $X1 = C/M$, $X2 = M/S$, $X3 = S/N$ are the regression coefficients
 Step-5. Each $Au[]$ as $Au[i]$ is calculated as $CH(VM) - X0 = CH(VM) - X1.C + X2.M + X3.S + N$
 Step-6. Rules[j] one by one As per Rule[j-1], Xn is equal to $1/Rule[j]$
 a. Take $CH(Au[i])$ and multiply it by Xn
 b. Rule[]
 c. If $CH(Au[i]) = CH(VM)$, then audit access should be granted
 d. As an alternative, refuse the request
-

Further, in the next section of the work, the obtained results are analysed and discussed.

6 Results and Discussion

When the research topic has been well understood, a formulation has been offered, and an algorithm has been provided, the findings are presented here. The simulation is based on the dataset from Planet Lab [19] with the following settings Table 1.

As the generated results are high in volume, in this work, only few sample results are produced. Firstly, the VM characteristics are identified below in following Table 2.

New frameworks of memory over commitment may be used to supervise memory sharing across distinct virtual machines on a single PC working framework when innovation advances virtual memory for reasons for virtualization. Memory pages with indistinguishable content may be shared over several VMs, which may lead to

Table 1 Experimental setup

Parameters	Descriptions
"Number of virtual machine"	"300"
"Number of audit request"	"255 * 255 * 255 * 255"
"Initial load on the server"	"100 MB read and write"

Table 2 VM characteristics identification—sample results

VM ID	Access type	Access Freq	Access volume (MB)
534	Shared access	0	74,350
896	Exclusive access	0	27,779
662	Shared access	2	87,419
350	Shared access	0	6928
762	Exclusive access	3	28,592
512	Shared access	3	91,974
692	Exclusive access	5	28,578
52	Shared access	0	70,938
394	Exclusive access	1	56,066
928	Exclusive access	5	59,119
674	Shared access	1	19,397
157	Shared access	1	44,576
690	Shared access	4	38,179
120	Shared access	1	73,639
525	Exclusive access	4	75,201
326	Shared access	5	96,833
10	Exclusive access	2	86,018
70	Shared access	4	38,313
317	Exclusive access	5	51,853
677	Shared access	4	77,317

mapping them to a physical page via a mechanism called part same page combining. The data is shown and analysed Figs. 4 and 5.

Further, the auditor characteristics analysis is carried out here Table 3 (Figs. 6 and 7).

Finally, the time complexity of the proposed algorithm is analysed here in Table 4.

The result is visualized graphically here in Fig. 8.

In the next portion of the paper, when the findings are realized, the suggested approach is compared to the other results of parallel study.

7 Comparative Analysis

There is a significant likelihood that a comparison study would show that the suggested approach outperforms competing research findings. This portion of the paper compares the proposed method with results from related research Table 5.

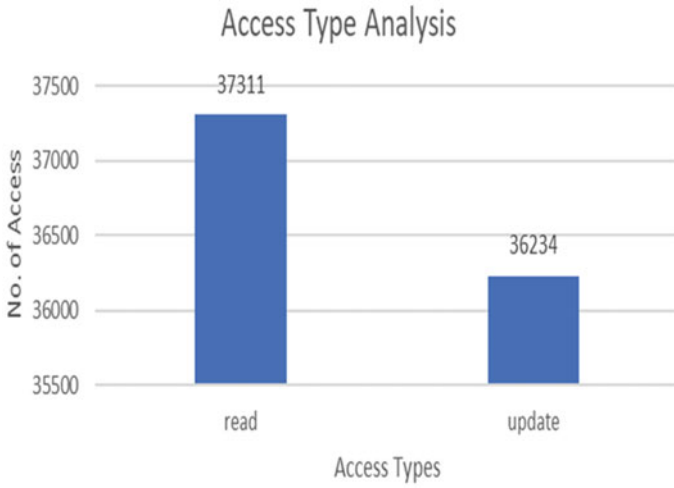


Fig. 4 “Access type analysis—VM”

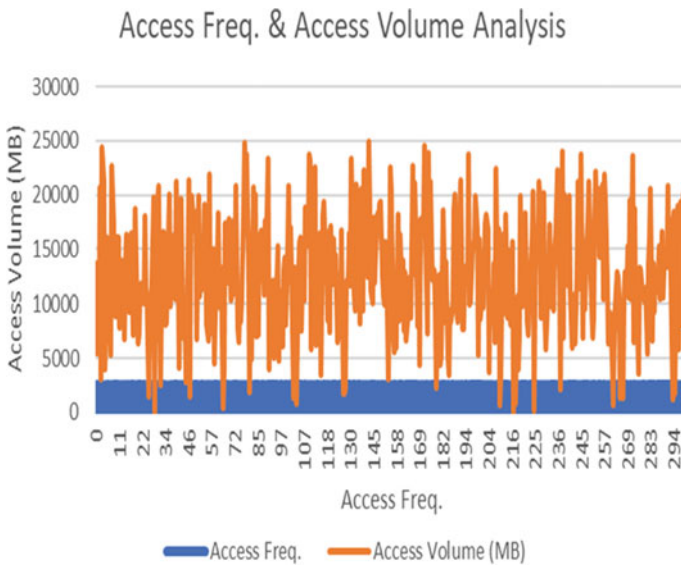


Fig. 5 “Access volume analysis—VM”

It is natural to realize that, the proposed algorithm has outperformed the other parallel research works as the proposed work demonstrates nearly 50% reduction in time.

Table 3 Auditor characteristics identification—sample results

User ID	Access type	Access Freq	Access volume (MB)
534	Shared access	0	74,350
896	Exclusive access	0	27,779
662	Exclusive access	2	87,419
350	Shared access	0	6928
762	Exclusive access	3	28,592
512	Shared access	3	91,974
692	Exclusive access	5	28,578
52	Shared access	0	70,938
394	Exclusive access	1	56,066
928	shared access	5	59,119
674	Exclusive access	1	19,397
157	Shared access	1	44,576
690	Exclusive access	4	38,179
120	Shared access	1	73,639
525	Exclusive access	4	75,201
326	Exclusive access	5	96,833
10	Shared access	2	86,018
70	Exclusive access	4	38,313

8 Conclusion

Cloud-based data centres have become the preferred hosting option for most application developers because of the rising need for high-performance apps. The business-critical data, or secure data, must not be accessible to a third party in addition to the performance criteria expected by programme owners and users. While several polls have shown that auditors' access cannot be controlled throughout the auditing process, our study using mathematical modelling shows that this cannot be done. As a result, this research provides a new approach to selective and adaptive auditing of cloud-based data centres. A coefficient-based regression model is used to map the two qualities of auditors onto a VM and then to choose the best auditors based on these two characteristics being mapped into the best auditors. The auditing process has improved by about 50%, which means that cloud-based data centres are now a safer, better, and quicker choice for application hosting.

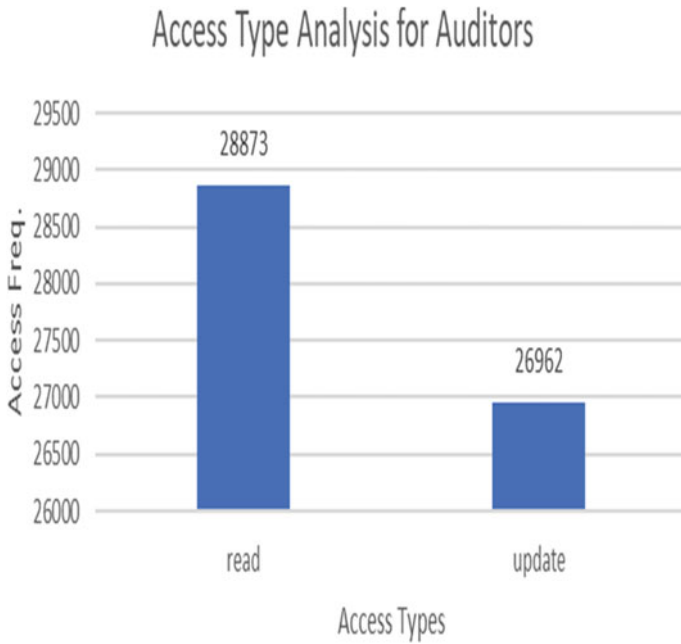


Fig. 6 Access type analysis—auditors

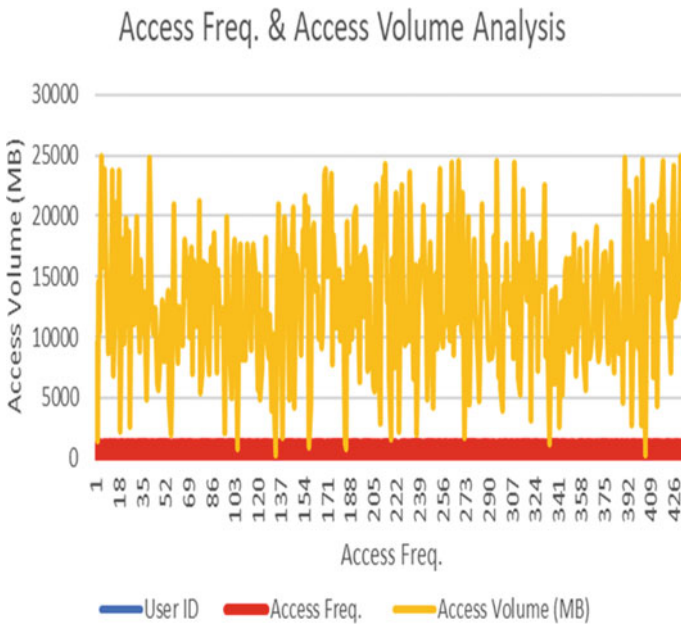


Fig. 7 Access volume analysis—auditors

Table 4 Time complexity analysis

“VM characteristics analysis time (ms)”	577
“Auditor characteristics analysis time (ms)”	170
“Selective auditing selection time (ms)”	178
“Total process time (ms)”	925

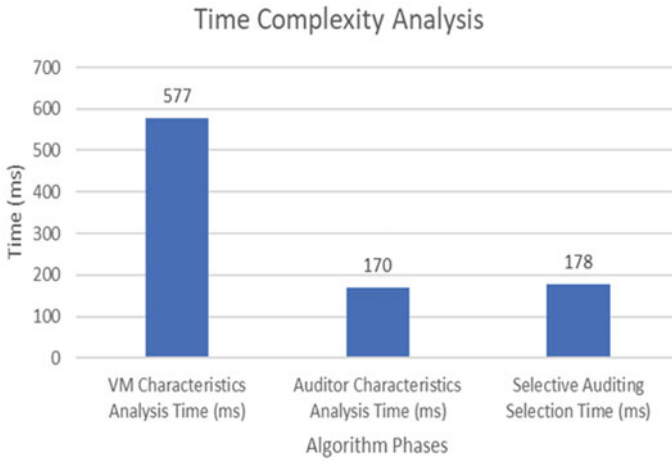


Fig. 8 Time complexity analysis

Table 5 Comparative analysis

Proposed method, author, and year	Fundamental methodology	Model complexity	Mean time complexity (ms)
Identify-based auditor selection, Hussain [11], 2019	Proxy-based user validation	$O(nm)$	1955
Data hiding, Shen et al. [14], 2019	Selective data hiding	$O(n)$	1831
Data integrity verification, Zhu et al. [15], 2019	Identification of data breaches	$O(n \cdot \log nm)$	1820
Proposed ACB-RM-SA algorithm, 2020	Adaptive coefficient-based Regression method for selective auditing	$O(n^2)$	925

References

1. Dean J, Corrado GS, Monga R (2013) Large scale distributed deep networks. In: Proceeding international conference neural information process System, pp 1223–1231
2. <https://i2.wp.com/www.mycloudwiki.com/wp-content/uploads/2016/06/2.png?fit=699%2C354&ssl=1>
3. Li M (2014) Scaling distributed machine learning with the parameter server. In: Proceeding International Conference Big Data Science Computer (BigDataSci), pp 583–598
4. Li Z, Smola A (2013) Parameter server for distributed machine learning. In: Proceeding big learning NIPS workshop, pp 1–10
5. <https://res.infoq.com/articles/cloud-data-auditing/en/resources/1Screen%20Shot%202017-07-19%20at%2013.05.54.png>
6. Wang C, Chow SSM, Wang Q (2013) Privacy-preserving public auditing for secure cloud storage. *IEEE Trans Comput* 62(2):362–375
7. Yan H, Li J, Han J, Zhang Y (2017) A novel efficient remote data possession checking protocol in cloud storage. *IEEE Trans Inf Forens Secur* 12(1):78–88
8. Sookhak M, Yu FR, Zomaya AY (2018) Auditing big data storage in cloud computing using divide and conquer tables. *IEEE Trans Parallel Distrib Syst* 29(5):999–1012
9. Zhao H, Yao X, Zheng X, Qiu T, Ning H (2019) User stateless privacy-preserving TPA auditing scheme for cloud storage. *J Netw Comput Appl* 129:62–70
10. Wang H (2015) Identity-based distributed provable data possession in multicloud storage. *IEEE Trans. Services Comput* 8(2):328–340
11. Hussain R (2019) Subashini, “Identity-based proxy-oriented data uploading and remote data integrity checking in public cloud.” *IEEE Trans Inf Forens Secur* 11(6):1165–1176
12. Zhang J, Dong Q (2016) Efficient ID-based public auditing for the outsourced data in cloud storage. *Inf Sci* 343:1–14
13. Yu Y, Au MH, Ateniese G, Huang X, Susilo W, Dai Y, Min G (2017) Identity-based remote data integrity checking with perfect data privacy preserving for cloud storage. *IEEE Trans Inf Forens Secur* 12(4):767–778
14. Shen W, Qin J, Yu J, Hao R, Hu J (2019) Enabling identity-based integrity auditing and data sharing with sensitive information hiding for secure cloud storage. *IEEE Trans Inf Forens Secur* 14(2):331–346
15. Zhu H, Yuan Y, Chen Y, Zha Y, Xi W, Jia B, Xin Y (2019) A secure and efficient data integrity verification scheme for cloud-IoT based on short signature. *IEEE Access* 7:90036–90044
16. He K, Huang C, Shi J, Wang J (2016) Public integrity auditing for dynamic regenerating code-based cloud storage. In: Proceeding IEEE symposium on computers and communications (ISCC), pp 581–588
17. Research Report from VM Ware. <http://aspiresignaturetechnology.com/VMWare-installation-support.html>
18. HP Integrity Virtual Machines Version 4.0 Installation, Configuration, and Administration. <https://docstore.mik.ua/manuals/hp-ux/en/T2767-90141/ch03.html>
19. SonerSevinc, PlanetLab Data Sets. <https://www.planet-lab.org/datasets>

Design of TPG BIST Using Various LFSR for Low Power and Low Area



Jugal Kishore Bhandari and Yogesh Kumar Verma

Abstract In Built-In Self-Test (BIST) schemes to generate different test patterns a Test Pattern Generator (TPG) is used, for testing of VLSI circuits. Standard TPGs generate a program independent test which is customizable to any explicit Automatic Test Equipment (ATE). Generating various test patterns which will cover maximum testing of the logic is a crucial task. To generate a variety of exhaustive and/or pseudo random pattern sequences—Linear Feedback Shift Register is used (LFSR) which is also used as compactor. In this paper different LFSR structures such as Modular LFSR, cellular Automation pattern generator, LT-LFSR are designed and compared with standard LFSR for parameters such as area, power, bit transitions and delay. The proposed schemes are evaluated on a synchronous 8×8 array multiplier. Verilog HDL code is written for the simulation and synthesis (tsmc90) results, it is verified for the proposed methods, the power and bit transitions are reduced by a significant percentage. These study gives an overall view and showcases the advantages of all different LFSR structures.

Keywords BIST · Low power · LFSR · TPG · Multiplier · DFT · ATE

1 Introduction

Engineering economy plays major role in satisfying clients. This is the study showing how engineers can choose designs and construct methods for those designs to produce systems and objects that could optimize their efficiency. The concepts dealing with benefits of production analysis and operational costs versus cost analysis applied to test of electronic, lead to design for testability [1]. DFT Engineers are majorly concerned with optimizing the technological efficiency. 30% of the total costs of large electronic systems accounts for testing and still it is crucial yet tough to justify

J. K. Bhandari (✉) · Y. K. Verma
SEEE, Lovely Professional University, Jalandhar, Punjab, India
e-mail: bhandari.jugal@gmail.com

Y. K. Verma
e-mail: yogesh.25263@lpu.co.in

the cost applied on DFT at the component level. Of all the critical factors testing is the most important criteria of VLSI circuits quality. To obtain the quality level which is required at low cost several trade-offs are often necessary to be considered. Total cost of DFT includes the test development cost (CAD tools to generate test vectors and for test programming), the cost of automatic test equipment (ATE). Therefore, DFT techniques should be incorporated in the device specification and the test plan.

Most challenging problem for design and testing of System-on-Chips (SOCs) is power dissipation. There are two different modes in which system works, test mode and normal mode. When system is in test mode the power dissipation is more in comparing to that of the normal mode [2]. There are four major reasons for more power dissipation during test [3].

There is High switching activity due to patterns of test vectors.

Internal cores Parallely activated during test.

Power consumption due to extra circuit under test or design for test circuitry.

Less or no correlation among present and next test vectors.

Some major issues due to extra peak and average power consumption are instant power rise that could cause racing circuit damage, development of strong spots, complexity in verification of performance, and the most important—decrease of the product line of work and lifetime [4]. Therefore, extra care would be required to guarantee that the power evaluation of circuits does not exceed during test mode. There are many practices offered in the works to reduce the power utilization, these techniques mainly include procedures for test organizing consuming least power, methods to reduce peak power and average power, methods to reduce power consumption and dissipation during scan test and standard BIST techniques. We know that on-chip communication on FPGA with a processor unit is faster than off-chip communication, to reduce and optimize the time requisite for setting the constraints, the BIST design with testability technique approach is proposed as per suitability.

To reduce power dissipation and consumption in test mode, we have several techniques resulting in reducing the switching activities between and in test patterns, which results in reducing the power in test mode. One best technique to understand this scheme is design proposed by Giard. A modified clock scheme is proposed for linear feedback shift register in which half of all D flip-flops are actively working, resulting to switching of only half of the test pattern [4]. There are different hardware pattern generation approaches such as ROM, LFSR, Binary counters, modified counters, LFSR and ROM, Cellular automation, To gain maximum fault coverage, LFSR uses a pseudo random test pattern generator that requires tests of around one million or more than that, but this requires less hardware than other schemes. This is the most used method for pattern generations in BIST [1] with LSFR as a pseudo random pattern generator. These patterns are generated algorithmically using hardware generator which has all the desirable properties of random numbers and may also generate repeatable patterns, which is essential for BIST [5].

A BIST scheme has been projected by Bo Ye and Tian [6] which is efficient low power technique. This is a generator with single change in input and produces seeds. It also has an Exclusive-OR array, which results in generating pseudo random signal with less variation in present and next input seeds. This has a minimized switching

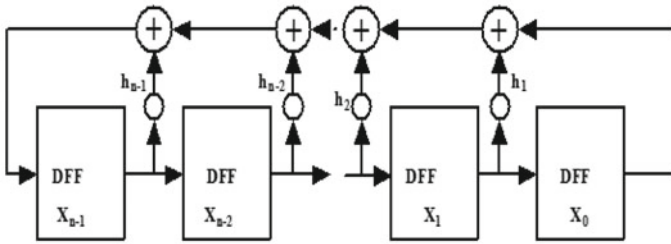


Fig. 1 Standard LFSR

activity in circuit. Selvan and Mohan [7] built a MISC test pattern generator with fixed seed which reduces static power and avoids clock distribution. Mukesh [8] has proposed a selective BIST-based testing with end-to-end framework for enabling along with diagnosis for 3D stacked ICs. This could help in reducing test time with negligible overhead of area and power with insertion of BIST in design. Design of complete linear feedback shift register [9] for memory and logic circuits testing was proposed. This can be used for the generation of test pattern sequences for BIST applications and memory address. BIST architecture with different MARCH algorithms [10] has been discussed for memory BIST, MARCH Y occupies less area, least power consumption with a smaller number of states.

2 Types of LFSRS

2.1 Standard LFSR

Standard LFSR with external exclusive-OR is shown in Fig. 1, consisting of flip-flops in chain of D type along with linear gates of exclusive-OR. It is called an external XOR LFSR, since the feedback network composes XOR gates feed outwardly from X_0 to $X_{(n-1)}$. It is also called an n -stage LFSR depending on n number of flip-flops. A best constructed LFSR know how to operate as optimized exhaustive test sequence generator, where the distinct states are of $2(n-1)$ cycles. The only emitted pattern is all zeros generated by the flip-flops, which is known as maximal length LFSR shown in Fig. 1.

2.2 Modular LFSR

The modular, internal exclusive-OR is defined by a fellow matrix $TM = TST$ that is the transpose of TS . Since the feedback logic has XOR gates located adjacent to each flip-flop, it is known as an internal XOR LFSR. In comparison to the standard

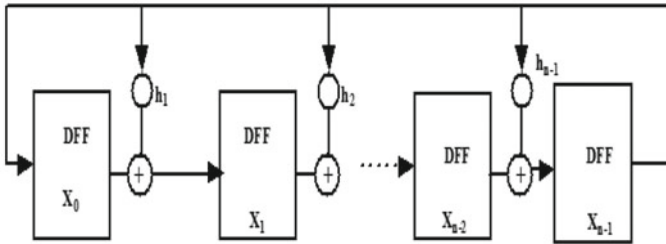


Fig. 2 Modular LFSR

LFSR modular LFSR can run faster. At most there is a delay of only one XOR gate in the middle of the adjacent flip-flops. Yet, this is not a severe contemplation in assessment, because there will be more logic between the flip-flop stages. XOR gates as the feedback network of the external XOR LFSR is shown in Fig. 2.

2.3 Primitive Polynomial Modular LFSR

The most desirable LFSR is expected to generate all possible pattern sequences. To have a primitive polynomial-based LFSR, following conditions are mandatory to be satisfied.

- It should have a monic characteristic polynomial
- That means the coefficient of the highest order x -term of the polynomial must be '1'.
- The polynomial be required to divide the characteristic polynomial by $1 + x^k$ times for $k = 2n - 1$, only for lesser value of k .

2.4 Cellular Automaton Pattern Generation

For pattern generator Cellular Automata (CA) is exceptional. It gives a LFSR with better uncertainty distribution (randomness). A cellular automaton is a cell collection with each cell connected only to its local neighbors. All connections are expressed as rules and should follow the protocol. This protocol determines the next state. The next state is centered on the state of the neighbor cells. Cell 'c' be able to communicate only with 'c-1' & 'c + 1' which are the neighbor cells, this gives us rule-90 (it has many other rules like rule-150), Rule-90 creation is explained with an example sequence below.

$X_{c-1}(t) X_c(t) X_{c+1}(t)$	111	110	101	100
	011	010	001	000

(continued)

(continued)

$X_c(t + 1)$	0	1	0	1
	1	0	1	0
Rule 90: $2^6 + 2^4 + 2^3 + 2^1 = 90$				
$X_{c-1}(t) X_{c(t)} X_{c+1}(t)$	111	110	101	000
	011	010	001	000
$X_c(t + 1)$	1	0	0	1
	0	1	1	0
Rule 150: $27 + 24 + 22 + 21 = 150$				

2.5 Low Transition LFSR

The less toggling pattern is generated by using transition controller. The transition controller decreases the switching of sequent test pattern. The test pattern is formed by re-alignment of the second half of the test pattern according with respect to the next test pattern. Interpolation of interceder pattern reduces the switching activity.

1	0	0	1	0	1	0	0	1	0	1	0	0	0	1	0
										↓		↓			
1	0	0	1	0	1	0	0	1	1	1	1	0	0	1	1
									↓		↓				
1	0	0	1	0	1	0	0	0	1	0	1	0	0	0	1
	↓					↓									
1	1	0	1	1	1	1	0	0	1	0	1	0	0	0	1
↓			↓		↓										
0	1	0	0	1	0	1	0	0	1	0	1	0	0	0	1

3 BIST, TPG and Its Operation

The BIST standard architecture is shown in Fig. 3. It consists of three major hardware components that is test vector/pattern generator, a test module controller and a response analyzer. A ROM which has sequences stored (patterns), a LFSR or a bit counter used as a pattern generator, A analyzer can be an LFSR called as a signature analyzer, or a compactor called as response analyzer with stored responses. A control signal is provided to trigger all the blocks from a control unit. BIST has a simple operation where the generated test patterns are applied to the CUT or design under

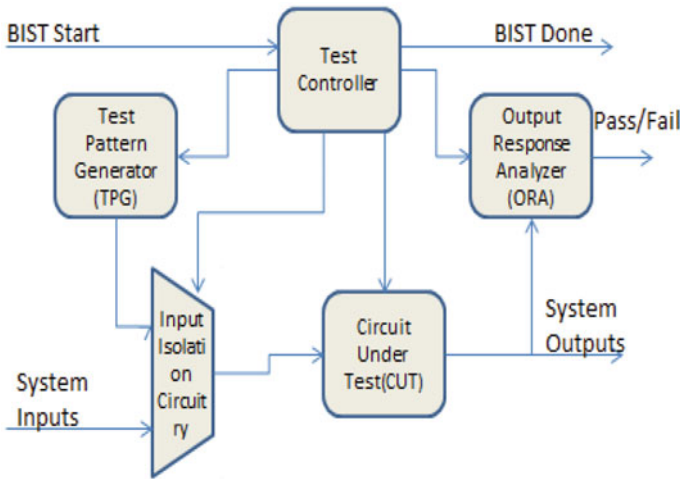


Fig. 3 BIST Architectural Block Diagram

test (DUT), which internally will give the respective logical outputs. These outputs are sent to the response analyzer to verify whether the generated output is true or false. The product of response analyzer is the count of CUT pass/fail.

All these major blocks will work on digital logics {1, 0}, but the transitions from 1 to 0 and 0 to 1 counts on more power consumption. The use of best TPG leads to reduce the power consumption. Figure 4 shows the TPG architecture in consideration of switching activities and better randomness.

Linear feedback shift register [LFSR] has simple hardware circuit with less area employment, which benefits in generating maximum varying test sequence patterns. Inside the proposed architecture the test sequence patterns are generated with benefit of short switching or shifting activities. This TPG structure comprises of low power linear feedback shift register (LP-LFSR), NOR-gate and array structures, counter with m -bit length and gray counter.

All zeros pattern is initialized to the m -bit counter this generates $2 \times m$ (m -bit counter) test patterns in sequence. Clock signal -CLK is used to trigger and operate the gray-code generator and ' m ' bit sequence counter. The gray-code counter is fed input from m -bit counter and to the input of NOR-gate structure. The NOR-gate output is set to one (bit '1') when all the bits of counter gives zeros (bits all '0') as output. When the output of NOR-gate is set to one (bit '1') only then the Clock signal (CLK) is utilized to trigger LFSR which activates it and generates the next seed. Then the gray-code data is Exclusive-ORed with this generated seed from LFSR. The pattern finally generated due to the Exclusive-OR array is the ultimate sequence pattern.

By using different LFSR architectures in the above TPG circuit, we can verify the best LFSR in terms of low power, less switching activities, and better randomness. Here we have verified the TPG circuit by applying various LFSRs such as Standard

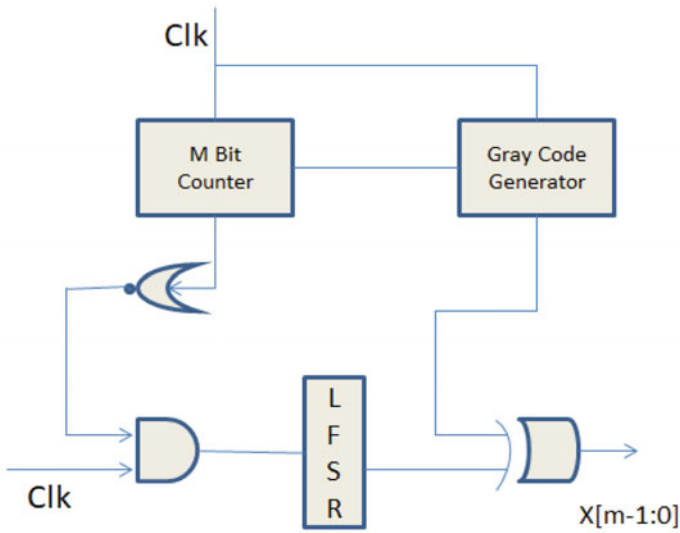


Fig. 4 LFSR and GRAY-Code-based TPG

LFSR, Modular LFSR, primitive polynomial modular LFSR, Cellular automaton-based pattern generator and Low transition LFSR.

4 Implementation

The proposed method is validated by using TPG first with conventional LFSR and comparing it with other LFSRs. Tables 1 and 2 displays the list of all LFSRs designed and validated. Table 1 shows the assessment of power consumption among various LFSRs such as—TPG Standard LFSR, Modular LFSR, primitive polynomial modular LFSR, Cellular automaton-based pattern generator and Low Power LFSR (LP-LFSR). The evaluation is carried out by applying the generated test vectors on standard 8*8 Braun array multiplier.

Simulation Analysis is carried out using Xilinx ISE 14.2 version. Synthesis is done using Cadence nc simulator tool. For power analysis rc compiler is used. In test mode average power consumption achieved from power analysis is compared with the power consumption using test pattern generator (TPG) with conventional

Table 1 Results pertaining to various LFSR architectures in 90 nm technology

	TPG stand	TPG-LT	TPG-CA	TPG-ModPr	TPG-Mod
Area (μm^2)	1649	1675	1667	1542	1599
Power (μW)	63.62	62.93	63.14	58.49	57.99

Table 2 Results pertaining to various LFSR-based BIST architectures in 90 nm technology

	BIST stand	BIST-LT	BIST-CA	BIST-ModPr	BIST-Mod
Area (μm^2)	3141	3167	3159	3034	3091
Power (μW)	112.15	92.17	113.02	99.55	119.87

LFSR. Table 1 presents the area and power consumption for the TPG using various LFSR including standard conventional LFSR. The test patterns generated from these LFSR's are tested on 8×8 Braun array synchronous multiplier. Table 2 presents the area and power consumption for the Braun array multiplier after applying the generated test sequences from conventional and proposed LFSRs.

5 Conclusion and Future Workspace

For a low power test pattern generator, we have analyzed available LFSR structures such as Modular LFSR, primitive polynomial modular LFSR, Cellular automaton-based pattern generator and Low transition LFSR and compared the results with standard LFSR. Thus, from the analysis we can predict that Modular LFSR method considerably cuts the power consumption in test mode. It also results in low transition activities using Modular LFSR with respect to conventional LFSR or standard LFSR (circuit used for test sequence generator). Future work will be on Modular LFSR for Memory BIST, which could result in less area and less power consumption. We can implement the design on standard FPGA boards and understand the utilization of LUTs on fabric, as this would be important as BIST will be the part of fabric in FPGA.

References

1. Bushgnell ML, Agrawal VD (2004) Essentials of electronic testing for digital, memory and mixed-signal VLSI circuits
2. Zorian Y (1993) A distributed BIST control scheme for complex VLSI devices. In: Proceeding VLSI test symposium, pp 4–9
3. Girard P (2002) Survey of low-power testing of VLSI circuits. *IEEE Des Test Comput* 19(3):80–90
4. Girard P, Guiller L, Landrault C, Pravossoudovitch S, Wunderlich HJ (2001) A modified clock scheme for a low power BIST test pattern generator. In: 19th IEEE Proceeding VLSI test symposium, CA, pp 306–311
5. Design of Low Power TPG BIST Technique using LP-LFSR, Kavitha A, Seetharaman G, Prabakar TN, Shrinithi S (2013) A 2013 third international conference in intelligent systems modelling and simulation
6. Ye B, Li T (2010) A novel BIST scheme for power testing. In: 3rd international conference on computer science and information technology IEEE, vol 1. <https://doi.org/10.1109/ICCSIT.2010.5563904>

7. Selva Kumar V, Mohan J (2014) Multiple single input change test vector for BIST schemes. In: International conference on green computing communication and electrical engineering (ICGCCEE) IEEE, Oct 2014. <https://doi.org/10.1109/ICGCCEE.2014.6922320>
8. Agrawal M, Chakrabarty K, Eklow B (2016) A distributed, reconfigurable, and reusable BIST infrastructure for test and diagnosis of 3-D-Stacked ICs. IEEE 35(2). <https://doi.org/10.1109/TCAD.2015.2459044>
9. John PK, Antony PR (2018) Optimized BIST architecture for memory cores and logic circuits using CLFSR. In: International conference on intelligent computing, instrumentation and control technologies (ICICT), IEEE 2018. <https://doi.org/10.1109/ICICT1.2017.8342751>
10. Singh A, Mahanth Kumar G, Aasti A (2020) Controller architecture for memory BIST algorithms. In: International students' conference on electrical, electronics and computer science, IEEE 2020. <https://doi.org/10.1109/SCEECS48394.2020.43>

Device-to-Device Data Transmission Over Sound Waves Using FSK/BPSK/QPSK



Gnaneshwara Chary, Charan Kumar, Shriram Ravindranathan, Suhruth Yambakam, and Janakiram Sunku

Abstract There are many-a-ways to transfer data wirelessly between two devices. There are many technologies which are ubiquitous now, such as Wi-Fi and Bluetooth which make use of electromagnetic waves as a means to send and receive data. One of the more unconventional ways that data is transmitted wirelessly is by encoding and sending the data over the air via sound waves using the speaker and microphone pair of the devices. The object of this study is to observe the performance of audio frequency modulation as a means of data transmission and to understand its drawbacks.

Keywords Data transmission · Encoding · Frequency modulation · Wireless

1 Introduction

Sending data over audio is not a new concept. All of the digital modes existing in ham radio are audio-based; the only difference is that operator just chooses to send the audio over a radio link. The audio goes into the microphone jack and comes out of the headset jack. This study however, attempts to understand why transmission of data over sound waves is unreliable and what data rate can be achieved using this medium of communication.

The main and one of the only advantages of using sound waves as a medium of transmission is that it is easy to set up and almost all modern devices have the

G. Chary (✉) · C. Kumar · S. Ravindranathan · S. Yambakam · J. Sunku
Department of ECE, B.V. Raju Institute of Technology, Narsapur, Telangana 502313, India
e-mail: gnaneshwara.chary@bvrit.ac.in

C. Kumar
e-mail: charankumar.k@bvrit.ac.in

S. Ravindranathan
e-mail: 18211a0412@bvrit.ac.in

S. Yambakam
e-mail: 18211a04p7@bvrit.ac.in

J. Sunku
e-mail: 18211a0419@bvrit.ac.in

infrastructure already in place to facilitate a data transfer via sonic means. Many IoT devices come with microphones and speakers as do all mobile phone units. Thus, it may be extremely viable to use sound as a means to transfer data and facilitating interaction between these devices.

Fundamentally, the system described here is very similar to the first digital telephone modems in which encoded digital data was modulated and sent through a wire. Here, the idea of using sound in air as a transmission medium instead is explored. The microphone acts as the receiver and the received signal is decoded in software hence.

The methods used in this research operate on the physical layer, which is the bottom-most layer of the OSI model. Here, only the raw data transmission performance is considered. Although in a real-world application of this technology, error correction and channel coding would be absolutely immaterial, those aspects are not explored as they would be beyond the scope of this paper.

2 Literature Survey

2.1 *Historical Approaches to Data Transmission*

The early methods of signalling certain states in rudimentary telephone systems often represented some form of encoding that is now mimicked in digital systems. In 1908 the dial tone was invented and by 1919 there was a system in place which used different pulses to indicate what digit was being dialled. However, it would not be until 1963 when the first true touch-tone dial was introduced.

According to one research [1], it was not until 1962 that the first commercial modem, the Bell 103, was released by AT&T which could conduct full-duplex communication through frequency shift keying (FSK) at 300 bps (baud). Certainly, this technology still holds good today as the mobile phone, which has become ubiquitous in the modern society has all the infrastructure it needs to transmit data in this manner and the necessity of a dedicated cable is now alleviated.

In a book [2] published in the infancy of Usenet groups, the various modulation schemes and baud rates which were hence used in the creation of the Internet are described. For this study the Audio Frequency Shift Keying scheme which was used in one of the pioneering modems of the Internet, the bell 202, is used, along with more complicated techniques such as BPSK and QPSK with differential encoding.

These modes of modulation used to be very common as documented in a paper [3] published towards the end of the era of internet over telephone lines. Moreover, it is straightforward and will satisfactorily serve the purposes of this study.

2.2 Data Transmission Protocols

The various protocols used in the infancy of the dial-up modems all were composed keeping the limitations of audio frequency modulation in mind. Many of these protocols as described in a reference guide [4] such as the V.21, V.23, have various advantages over the other. Using one of these protocols, it is possible to connect to the internet even over a sonic link. A protocol which was designed for wireless systems, the AX.25 protocol which is a data-link layer protocol for ham radio can be used along with this technology in order to transmit data using IP - packets which are the standard form of data transfer on the Internet as well as on LTE networks.

3 Methodology

3.1 Frequency Shift Keying

The entirety of this research is conducted on the open source SDR platform, Gnuradio. The flowgraph used for implementing the FSK transmitter and receiver is shown in Figs. 1 and 2. The transmitting section as displayed in Fig. 1, consists of a pseudo-random source sending an 8-bit number periodically. This data is encoded into the mark and space frequencies of 1200 and 2200 Hz. These frequencies were chosen in order to mimic the Bell-202 standard and also because these frequencies are audible quite conspicuously to the human ear. This data which has now been encoded as symbols is fed into a VCO and transmitted out into the air via a computer speaker to be received by a nearby computer microphone.

Demodulating FSK synchronically is called coherent demodulation. Demodulating FSK coherently requires incoming carrier phase locking (phase synchronisation), which is normally done with Phase lock Loops (PLL) which does not work well unless the Signal to Noise Ratio (SNR) is at least 10 dB.

Normally a sound broadcast does not have such a high SNR, so coherent demodulation is not possible. Besides in practise with electromagnetic signals the non-coherent FSK requires, at-most, only 1 dB more Eb/No than that for coherent FSK for a Bit Error Probability $P_b = 10^{-4}$. Thus it can be inferred that for obtaining the same Bit Error Probability, transmitting an extra dB of power in each bit shall suffice.

The non-coherent FSK demodulator is considerably easier to build since coherent reference signals need not be generated. Therefore in practical systems almost all of

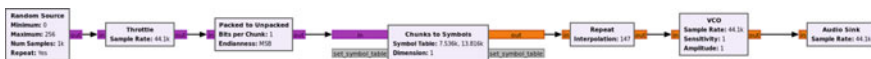


Fig. 1 The transmitter section of the AFSK modem. The audio sink here is a computer speaker

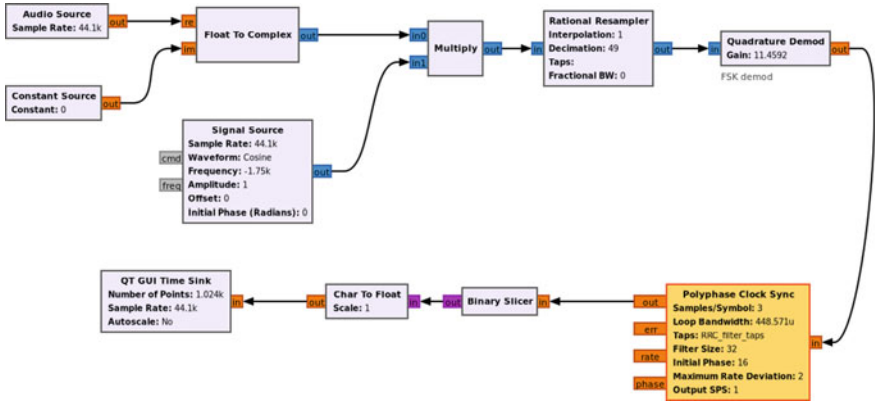


Fig. 2 The Receiver section of the AFSK Modem, The audio source here is an ordinary computer microphone. The Binary Slicer is a decision block which converts the demodulated signal into digital bits

the FSK receivers use non-coherent demodulation because everyone prefers transmitting an extra dB of power instead of tackling the synchronisation problems that arise with coherent demodulation. Some of its salient benefits are:

- It is resilient to noise upto a certain level if a BCH error correcting code is used, with the ability to repair up to 8 error per data block. BCH codes have their biggest coding gains when there is a 25–50% redundancy added.
- Preferably 16–20 kHz carrier wave with 44.1 kHz sampling is used (default in pc and mobile sound cards).

For this study, distance is taken to be less than 1 m for neglecting doppler shift and multi-path fading.

This AFSK will encode digital binary data at a data rate of 880 bits/s. It uses the frequencies 1200 and 2200 Hz to encode the 0’s and 1’s (space and mark) bits.

Generally, for demodulation of BFSK an FM demodulator is not required, two bandpass filters may be used to separate the two symbols and then get the space and mark signals, however, here we use the inbuilt demodulation block in Gnuradio.

3.2 Binary Phase Shift Keying

Similar to the method employed for FSK, a pseudo-random vector source is modulated into a BPSK constellation at 50 samples per symbol and transmitted through the computer speaker as shown in Fig. 3.

For the demodulation section, the modulated signal is picked up by the microphone and heterodyned with a local oscillator as shown in Fig. 4. This received baseband signal is sent through a low-pass filter before carrier recovery is performed at the

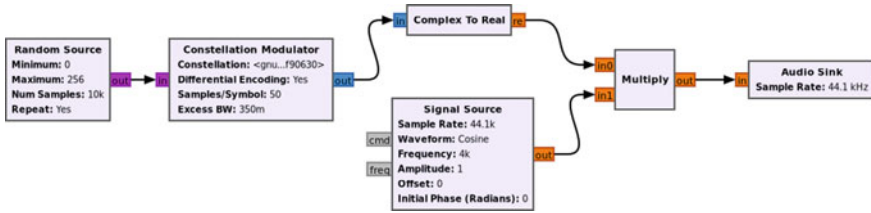


Fig. 3 The transmitter section of the BPSK modem

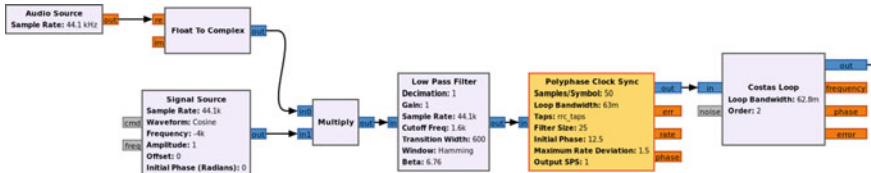


Fig. 4 The receiver section of the BPSK modem

Costas PLL. The subsequent decoding and BER calculation along with the received baseband’s SNR calculation is common for all modulation methods used here, it is demonstrated in the next section.

3.3 Quadrature Phase Shift Keying

The *I* and *Q* signals generated during the transmission section are in quadrature with each other. Hence, they have to be multiplied with cosine and sine signals before being combined to get a real signal. The transmitter and receiver sections are shown in Figs. 5 and 6, respectively.

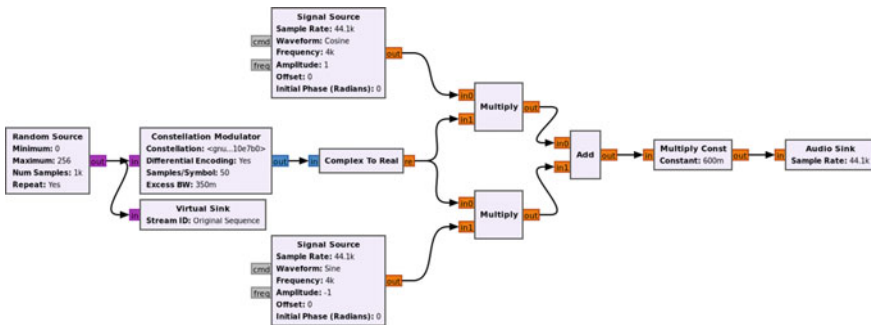


Fig. 5 The transmitter section of the QPSK modem

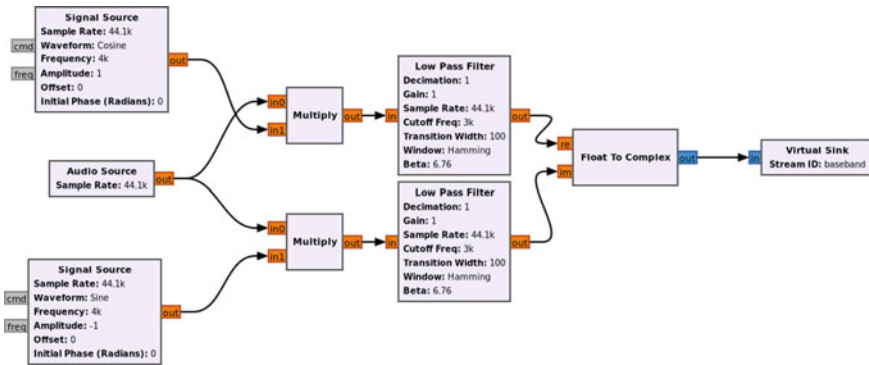


Fig. 6 The receiver section of the QPSK modem without the PLL and demodulation sections

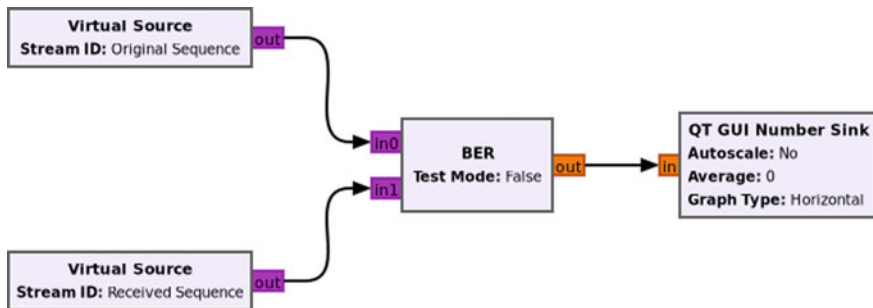


Fig. 7 The BER block which calculates the log of it bit error rate

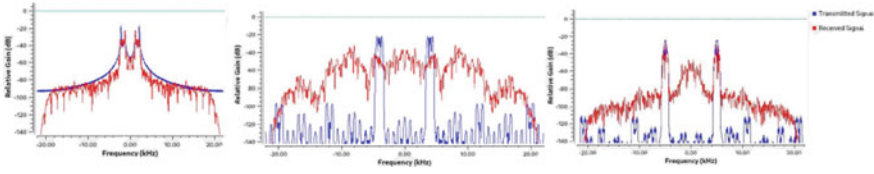
The demodulation process is more or less the same as the one used with BPSK. Once demodulated, the symbols are decoded into pairs of bits, as is expected from a QPSK modulated signal. These bits once unpacked give the raw bitstream of data which can be compared with the transmitted bitstream and analysed.

The two bitstreams (Original and Received Sequences) are compared at the BER block as shown in Fig. 7. This BER reading is recorded at various distances and the corresponding SNR's of those distances.

4 Observations

Figure 8 shows the frequency spectra of the transmitted and received signals at the computer speaker and microphone, respectively.

There are 50 samples per symbol in the BPSK and QPSK experiments and 147 samples per symbol (Bell-202 Standard) in the FSK experiment. The sampling rate for all the experiments is the standard 44.1 kHz which is ubiquitous now. Thus the



Figs. 8. Frequency spectra of the FSK, BPSK and QPSK signals Transmitted (Blue) and Received (Red), respectively. The light blue line indicates 0 dBFS

bitrates for the BPSK, QPSK and FSK transmissions works out to be 884, 1764 and 300 bits per second, respectively.

5 Results

In order to evaluate the properties of a digital modulation scheme the bit error rate (BER) curves are computed as a function of signal to noise ratio (SNR). The BER is the number of bit errors (received bits that have been altered due to decoding error) divided by the total number of transmitted bits. The observed values are given hence. The BER values are taken here as the logarithm of the actual Bit Error Rate (Fig. 9, Table 1).

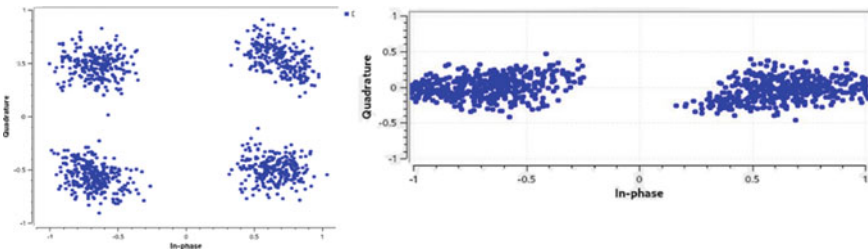


Fig. 9 The constellation plots of QPSK and BPSK signals, respectively, after carrier recovery

Table 1 The average log of the BER readings vs the distance of mic. from the speaker

Distance (cm)	Average SNR (dB)	QPSK BER log	BPSK BER	FSK BER
1	15 dB	-3.833105	-2.486754	-4.201321
10	6 dB	-2.789761	-1.275346	-2.132962
100	4 dB	-2.074042	-1.234892	-1.562394
500	1 dB	-1.206634	-1.232030	-0.301847
1000	NaN	-1.256361	-1.237340	-0.302989

6 Conclusion

In this study, we have compared the performance of the various modulation schemes viz. FSK, BPSK and QPSK over a sonic channel. The experimental results show that it is certainly a viable method of transmitting data over very short distances.

Acknowledgements The authors would like to thank Dr. Sanjay Dubey, HOD of the Dept of ECE for his help and guidance. The work was also supported and made possible by the management of B.V. Raju Institute of Technology.

References

1. Oxford T (2009) Getting connected: a history of modems. Internet
2. Jennings F (1986) Practical data communications: modems, networks and protocols
3. Stanton W, Spencer T (2001) A primer on asynchronous modem communication
4. Ritter F, Krempel S, Tietze S, Backer A, Wolfschmitt A, Drese KS (2018) Data transmission by guided acoustic waves. In: Sensors and measuring systems; 19th ITG/GMA-symposium, pp 1–4

Performance Evaluation of Radar Backscatter of S-Shaped Duct with Conventional Intake Duct



B. R. Sanjeeva Reddy, Sanjay Dubey, and J. Naga Vishnu Vardhan

Abstract Stealth technology or low observability is rapidly being adopted by world militaries due to the immense warfare related advantages. It is essentially the reduction of the radar cross section of a fighter jet or any other military vehicle almost down to an insect's or a bird's radar cross section in order to evade the enemy and gain an upper hand. Stealth can be incorporated in several ways. The present study takes into account the shaping configurations of intake ducts of a fighter jet and the implications of using an S-shaped or bent duct rather than a straight duct. Comparison between radar backscatters of the two kinds of intake ducts is the focus of this study. The results are obtained by simulating 3D models of a straight intake duct and a bent intake duct at X band frequencies without an external source of RF illumination. An S-shaped duct is found to give lower radar backscatter than the straight duct. The study demonstrates that incorporation of a bent or an S-shaped intake duct can significantly contribute to lower radar cross section of a fighter jet.

Keywords Stealth technology · S-shaped intake duct · Radar backscatter · Radar cross section

1 Introduction

The adoption of radar technology started being extensively used in the 1930s and the 1940s, especially in World War II where superpowers such as Great Britain, Germany, France and the United States of America were using radars to navigate ships and

B. R. Sanjeeva Reddy (✉) · S. Dubey
Department of ECE, B V Raju Institute of Technology, Medak 502313, India
e-mail: sanjeev.reddy@bvrit.ac.in

S. Dubey
e-mail: sanjay.dubey@bvrit.ac.in

J. N. Vishnu Vardhan
Department of ECE, BVRIT Hyderabad College of Engineering for Women, Hyderabad 500090, India
e-mail: vishnu.j@bvrithyderabad.edu.in

aircrafts, and a newer use—to detect incoming enemy aircrafts and warships. It was only in the late 1970s that two prototype planes were built to study and test low observability, better known as stealth technology in today's times. The project was kept top secret, and several billions of dollars were spent into developing the prototypes. Advancements in the projects lead to the introduction of the F-117A which became fully operational in 1983 and was used in Operation Just Cause at Panama in 1989. This was the first ever use of a stealth aircraft in warfare which changed the course of evasion and low observability techniques. The F-117A gave way to expansion in the fleet of the United States Air Force, and new stealth fighters like the B-1 and B-2 Bombers were introduced, along with the F-22 and F-35 Raptor, presently leading in the stealth technology development race. John Cashen of Northrop Grumman was the first to employ blending of edges and transitions between surfaces to reduce radar cross-section sidelobes [1]. Stealth aircrafts also have significant operational limitations due to shape impositions and materials used, limited fuel-carrying capacity and the constraint that most payload should be carried inside the fuselage. Incorporation of stealth technology decreases the maneuverability of a fighter aircraft, which is one of its most important features. Any pylon, tank, missile or pod carried outside the jet increases the radar signature. But with stealth technology, operations can be carried out with almost no casualties every time without even getting noticed by the enemy radar.

There are four basic methods of incorporation of stealth technology: shaping configurations, radar absorbent materials (RAM), passive cancelation and active cancelation. In order to reduce RCS or radar cross section, surfaces and edges of the fuselage should be oriented in such a way that they reflect the radar energy away from the radar antenna that caused the incidence rather than back to it. Overall, all bumps and curves should be avoided, any external payload such as missiles should be kept within armament bays, and the doors of landing gear bay and armament bay should be tightly closed with no gaps in between. Conventional aircrafts have rounded shapes and noses making them highly aerodynamic but making highly efficient radar reflectors. This is the reason most stealth aircrafts are designed with sharp geometric shapes, and all payload is mounted inside the plane [2]. The aforementioned shaping configurations provide about 60% or stealth or low observability [3]. Radar absorbent materials or RAM are also very common incorporations for stealth technology which contribute about 30% low observability. They are mostly placed on the skin of the aircraft as plates or coated as paint to absorb most of the RF energy incident on the aircraft's body. Active and passive cancelations are similar techniques which use the concept of destructive interference and plasma screens respectively to contribute to stealth [4].

Since changes in shape provide the highest camouflage or stealth features, this study takes into account, a prominent part of a fighter aircraft which contributes very highly to radar signature—the intake ducts. After extensive research, Lockheed Martin, a very well-known aerospace technology development company based in United States of America, which is credited the creation of stealth aircrafts, introduced S-shaped intake ducts instead of the conventionally used straight intake ducts.

The hypothesis behind the change was to investigate the effect of multiple reflections inside the curvature of an S-shaped intake duct which results in lower radar backscatter. The present study aims to validate the hypothesis at the lower most level possible—a simulation of 3D models at military uses frequencies to show that bent ducts are more efficient than straight ducts in terms of radar cross-section reduction.

2 Geometry and Method

2.1 Configuration of the Geometry

The 3D models for the straight intake duct and S-shaped intake duct were made using SolidWorks. The geometry of the S-shaped intake duct consists of three major parts: inlet, outlet and curvature. It is advisable to have unequal inlet and outlet lengths. This ensures that there is no influence of duct length on upstream flow from the outlet end, and that there are uniform inlet conditions which are essential for proper air flow through the duct. Two of the major techniques to deduce the parameters of ducts are—computational fluid dynamics (CFD), a technique widely used in the mechanical engineering field for design and simulation of vehicles, and free form deformation (FFD), a very highly used geometric modeling technique [5, 8]. The available literature on the aforementioned modeling techniques contributed to easier design of the 3D models of the ducts as shown in Fig. 1a, b.

Table 1 shows the measurements used in the modeling of the S-duct pipes as well as the straight pipes. It also shows the measurements of the segments used to conduct the test. The angles in the curvature of the S-shaped duct can be varied to be tested iteratively, but larger bend angles contribute to impaired aerial maneuverability. Ideally, angles between 22.5° and 30° could be suitable for an S-shaped intake duct [6]. Geometrical models and baseline geometries are defined in a large number of academic research papers, and the main governing equation was found as below:

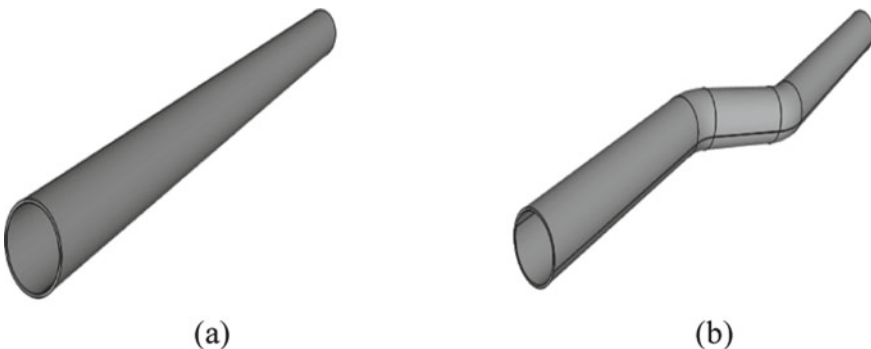


Fig. 1 a Straight intake duct 3D configured model. b Straight intake duct 3D configured model

Table 1 Measurements for 3D modeling of ducts

Type of duct	Angle (degrees)	Diameter (m)	L_{inlet} (m)	L_{outlet} (m)	L_{duct} (m)	Offset (m)	Total length (m)
Straight	30°	0.75	–				12
S-duct	30°	0.75	5.6	4.2	2.2	2.2	12

$$\frac{r}{r_1} = 1 + 3\left(\frac{r_2}{r_1} - 1\right)\left(\frac{\theta}{\theta_{max}}\right)^2 - 2\left(\frac{r_2}{r_1} - 1\right)\left(\frac{\theta}{\theta_{max}}\right)^3 \quad (1)$$

where

r_1 radius of inlet

r_2 radius of outlet

θ_{max} maximum curvature angle for S-shaped duct.

2.2 Methodology

Since the models used were 3D, the files were saved with an IGES extension which allows the investigator to use a wide range of simulation software since IGES is a universally accepted 3D model extension.

Simulation for this particular experiment was done in HFSS which is a simulation software for electromagnetic structures by Ansys. The process was conducted within an 8 GHz region around the segments of the ducts taken. These models were assigned aluminum as their material since that is the most commonly used aircraft body material. Although, practically, alloys of several metals are used to give strength to aircraft bodies, particularly in fighter jets. The usage of an external source antenna was avoided in this particular approach, but the former is still a valid way of carrying out the investigation. The 3D models with the high-frequency regions around them were subjected to a plane wave excitation incident from the $Y-Z$ plane direction implemented with an infinite sphere radiation.

Other alternatives for software could be CST, in which the asymptotic solver gives a very accurate measure of radar backscatter from electrically large objects. Focus of this study is primarily on the effect of the curvature as shown in Fig. 2; hence, some aspects such as the duct thickness and cross-sectional diameter have not been taken into consideration as primary constraints. More detailed parameters such as pressure loss have also not been discussed in this study. The smallest possible pressure loss is preferred for a uniform flow in the duct which is key in military aircrafts for high-speed take-offs and beyond usual maneuvering [7]. The main principle to be considered here is the number of internal reflections that takes place due to the bent structure of the pipe causing phase cancelations of the incident RF wave. This eventually decreases the duct's contribution in the total radar cross section or radar backscatter which is the main aim of stealth.

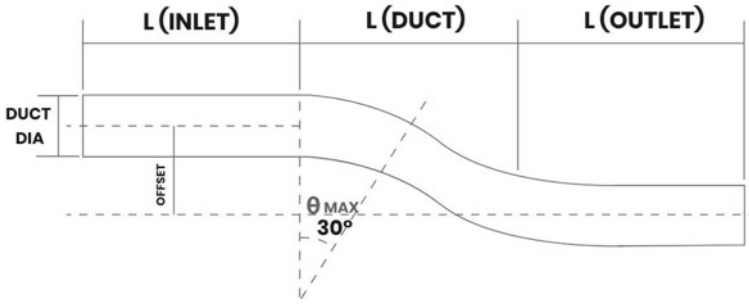


Fig. 2 S-shaped duct basic geometrical diagram

2.3 Governing Equations

The amount of publicly declassified information is also very less since the study is directly related to military applications. But attenuation for any part of the stealth fighter jet can be deduced by the following equation [9].

$$\text{Attenuation} = R + M + A \tag{2}$$

where R is the attenuation by reflection from the object as is in the case of the S-shaped duct, M is the attenuation caused by multiplied reflections, which is the primary principle on which the present investigation is being done, and A is the absorbent attenuation which is a result of the radar absorbent materials discussed in Sect. 1. Individual attenuation for R , M and A is explained below:

$$R = 20. \log \left| \frac{Z_0 + Z_M}{2Z_M} \cdot \frac{Z_0 + Z_M}{2Z_0} \right| \tag{3}$$

where Z_0 = impedance of environment and Z_M = impedance of material

$$M = 20. \log \left| 1 - \left(\frac{Z_0 - Z_M}{Z_0 + Z_M} \right)^2 \cdot e^{-\frac{2t}{\delta}} \cdot e^{-j\frac{2t}{\delta}} \right| \tag{4}$$

Individual characters indicate:

- Z_0 impedance of environment (dielectric)
- Z_M impedance of material
- δ δ intrusion depth.

$$A = 20. \log e^{\frac{t}{\delta}} \tag{5}$$

$$\delta = \sqrt{\frac{2}{\omega\mu\sigma}} \quad (6)$$

Individual characters indicate:

- t material thickness
- δ intrusion depth
- σ conductivity
- μ permeability
- ω wave frequency.

The above calculations are valid only for academic purposes since in practical conditions, many more parameters such as temperature, pressure, et al. come into the picture making the equations much more complex.

In theoretical terms, radar cross section of an object/target can be calculated by the following equation:

$$\sigma = \left(4\pi r^2 * S_r / S_t\right) \quad (7)$$

where

- S_r is power scattered by target and
- S_t is power transmitted by radar.

3 Results and Discussion

3.1 Simulation Methodology

For the aforementioned simulations of the 3D models of the ducts, HFSS was used. HFSS is simulation software provided by Ansys which makes use of finite element method (FEM) as a solution methodology. Finite element method is one of the most widely used solution methods for engineering and mathematical models/problems related to electromagnetics. Basic principle behind FEM is that the system divides the larger equation consisting of partial differential equations into several smaller finite elements and then solves them. This is also referred to as finite element analysis (FEA).

Principle of minimization of energy forms the backbone of FEM, which means that when a particular boundary condition is applied to a body, this can lead to several configurations, but yet only one particular configuration is practical, and the results remain the same even after iteratively simulating the model several times. Another important aspect to understand is that FEM also takes into account discretization, which means the entire model is converted into a mesh. Each cell of the mesh acts as a discrete point in a matrix of finite elements.

3.2 Simulation Results

Figures 3 and 4 indicate the generated radiation patterns of the conventional and modified ducts. As discussed in Sect. 2.2, the simulation should ideally produce lesser RCS for an S-shaped intake duct than a straight duct due to phase cancellations caused in the curvature of the S-shaped duct arising from multiple reflections and scattering.

The results show that RCS (in dB) for the conventional intake duct is quite high. Since exact military specifications are not publicly declassified, the results may be further refined. The results also show that the RCS (in dB) for the S-shaped intake duct is lower than that of the conventional straight duct. Results have been arranged in two forms—radiation pattern which is a polar plot and a 3D visualization of the radar backscatter from both the models. Figures 5 and 6 display the radiation backscatter 3D plot for conventional and S-shaped duct configuration. In a radiation pattern polar plot, all aspect angles or theta (θ) are plotted representing the area illuminated by the phase array of radar antenna. A polar plot is the best way to visualize spherical radiation, which is exactly what has been used for this study. It is a plot of magnitude versus phase angle in a complex plane which can capture the system behavior over an entire range of frequencies in a single plot. The 3D polar plot or 3D visualization of radar backscatter gives the observer a much better understanding of how the radar return from S-shaped intake ducts is lower than that of straight ducts. It is essentially a contour of the reflected RF waves from the ducts back to the source. The observer can clearly see the different measurements for as many parameters as needed, each

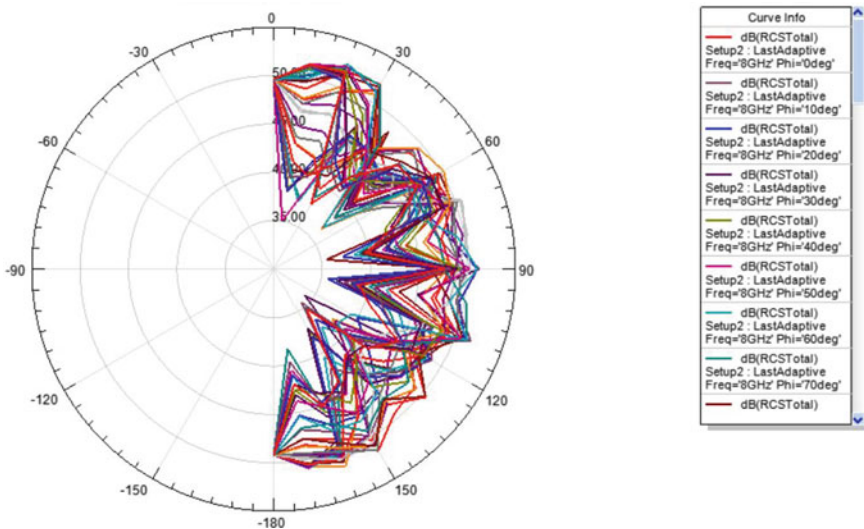


Fig. 3 Radiation pattern for conventional straight duct at 8GHz

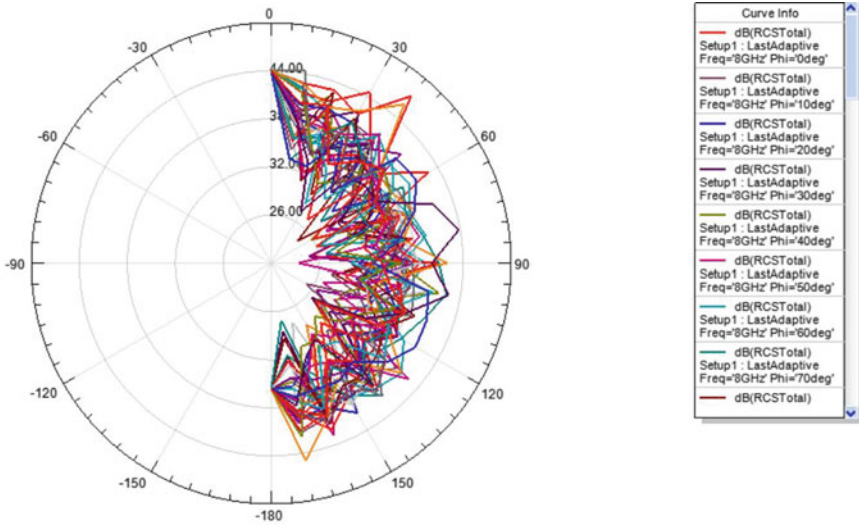


Fig. 4 Radiation pattern for S-shaped duct at 8 GHz

associated to a color. This particular study will take into account bistatic RCS in terms of dB, both in the 3D plot and the 2D radiation plot.

The two major kinds of radar systems based on the antenna arrangement are monostatic radars and bistatic radars. Conventionally, most radars initially used were monostatic, since the concept of illuminating and entire sphere of the airfield was not put to practical use. Contemporary radars are mostly bistatic, which means that the transmitting antenna and the receiving antenna are physically separated by some

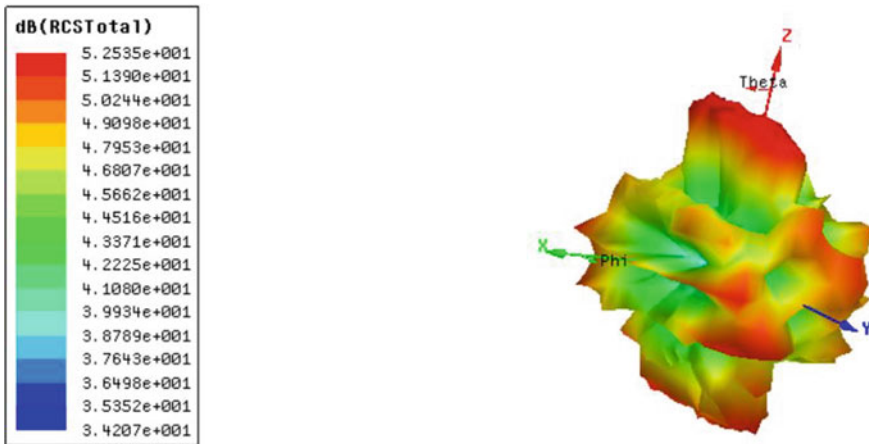


Fig. 5 Radiation backscatter 3D plot for straight duct at 8 GHz

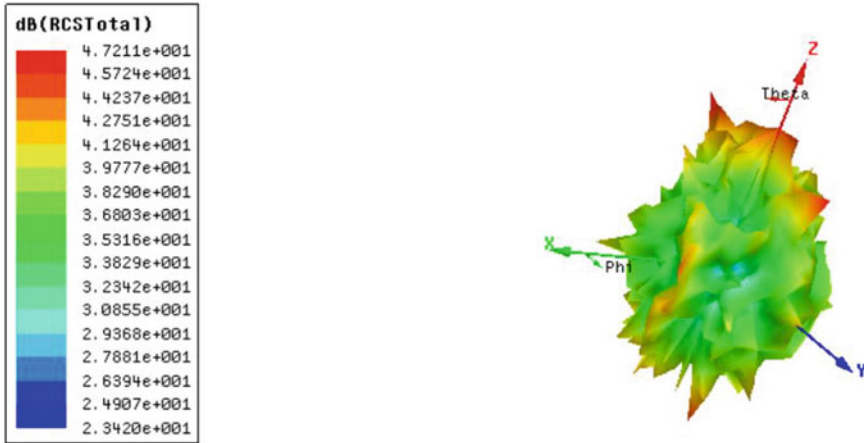


Fig. 6 Radiation backscatter 3D plot for S-shaped duct at 8 GHz

distance. Most militaries of the world use bistatic radars, since it has several practical advantages—it has shown some resistance against stealth aircrafts as the targets that are designed with minimized monostatic RCS still may present a very high bistatic RCS. Even in the presence of large amount of clutter, the target detection capabilities of a bistatic radar are much higher. Since the transmitter and receiver are physically distant apart, the receiver can be kept covert so as to decrease the effect of electronic countermeasures and also reduce detectability. Some bistatic radars use Babinet’s principle which implies resilience to stealth coatings and shaping since the radar cross section may be solely determined by the silhouette of the aircraft seen by the transmitter. Many long-range air-to-air and surface-to-air missile systems use semi-active radar homing, which is a form of bistatic radar.

Due to the above-stated reasons, it is crucial to consider bistatic radar instead of monostatic, in order to develop better stealth vehicles and equipment. The physical separation between the two antennas of the bistatic radar is comparable to the expected target distance, which helps in expanding the illumination region.

Another aspect to consider is that the radiation was set to be far-field. Consideration of the weakest of signals is taken in case of far-field radiation which is very useful in target detection. In practical radars, the distance of the target from the antenna is higher than the size of the antenna itself and its operating wavelength. This is a necessary condition for far-field radiation, which is fulfilled in the simulation conducted for this investigation.

3.3 *Computing Requirements to Carry Out Simulation*

The above-discussed simulations have been carried out on a desktop computer with version 15 of HFSS by Ansys. Higher versions of the software may provide upgraded simulating options for better results.

4 Real-Time Applications

If we carefully look at the under-wing fuselage of an F-15 Eagle, it can be observed that the world-class combat fighter jet uses a pair of straight intake ducts. Although excellent in combat with maneuverability like no other of its class, F-15 has quite the radar cross section, which is the reason why it depends on its speed for combat advantages. A counter-observation can be made about the F-22 Raptor and F-35 Lightning II. Manufactured by Lockheed Martin, both fighter jets are known to be the best stealth fighter jets in today's time. These two jets use an S-shaped intake duct system contributing to lower RCS and lower radar backscatter. F-22 and F-35 weigh in with more stealth features due to the highly aerodynamic size, better wing placement, smooth body shape and S-shaped duct systems. In addition, both of these world-class fighter jets make use of infrared and acoustic muffling, electronic countermeasures.

5 Conclusions

The simulation of 3D models of a conventionally used straight intake duct and a stealth feature S-shaped intake duct has been conducted at 8 GHz in order to compare the radar backscatter from both models. The major findings of the present study include reduction in radar cross section of intake ducts can contribute significantly to overall reduction of radar cross section of the stealth fighter jet. The 3D models of intake ducts—both S-shaped and straight—can be made using CFD or FFD modeling techniques, resulting in three major parts of the duct pipe: inlet, outlet and curvature. Simulation of the two 3D models of conventional straight duct and modern S-shaped duct was conducted in HFSS at 8 GHz. For further investigation, segments were taken and simulated to study the effect of curvature on radar backscatter/radar cross section.

Simulation results show that at 8 GHz, straight duct has an RCS of 49.61 dB and S-shaped duct has an RCS of 44.07 dB. From the simulation, it was found that the S-shaped intake duct gives about 4–5 dB decrease in the radar backscatter from that of the conventionally used ducts. Although, results can be further refined with the use of actual measurements and taking overhead parameters such as heat flow, pressure into account. It is suggested that S-shaped intake ducts can be used to contribute to

shaping configurations for stealth incorporation in a fighter jet. Similar techniques can be used for warship vessels and even private airplanes which need security or covertness. Compared to existing designs in most fighter jets, which use conventional straight ducts, S-shaped ducts can prove much more efficient due to reduction in overall RCS of the vehicle. A large number of American fighter jets now use the S-shaped duct and have a lower RCS than the aforementioned conventional ones.

References

1. Lynch D (2004) Introduction to RF stealth, vol 573. Scitech Publishing Inc, Raleigh, NC
2. JPRS-CEA V (1985) FBIS foreign broadcast information service
3. Zikidis K, Skondras A, Tokas C (2014) Low observable principles, stealth aircraft and anti-stealth technologies. *J Comput Model* 4:129–165
4. Zhao B, Xing S, Li C (1998) Simulation of effect of anti-radar stealth principle. JPRS report: science and technology, China
5. D'Ambros A, Kipouros T, Zachos P, Savill M, Benini E (2018) Computational design optimization for S-ducts. *Designs* 2(36)
6. Papadopoulos F, Valakos I, Nikolos I (2012) Design of an S-duct intake for UAV applications. *Aircraft Eng Aerospace Technol* 84:439–456
7. Bansod P, Bradshaw P (1972) The flow in S-shaped ducts. *Aeronaut Q* 23(2):131–140
8. Chiereghin N, Guglielmi L, Savill M, Kipouros T, Manca E, Rigobello A, Barison M, Benini E (2017) Shape optimization of a curved duct with free form deformations
9. Stanislav K, Jan V, Hana U (2017) Calculation of shielding effectiveness of materials for security devices. *MATEC Web Conf* 125:02036

A Novel Flash-Type Time-To-Digital Converters (TDC) Using GDI Technique



Jakka Yeshwanth Reddy, Anthireddygari Sushma, Siripurapu Sravya, Sabavath Sai Kiran, and Puli Sai Sukitha

Abstract A proficient flash-type time-to-digital converter is designed by using D flip-flop which is internally designed by using NAND and NOR gates. The internal architecture of flash-type TDC also consists of buffer, inverter, XOR, NAND and NOR gates, respectively. This flash-type TDC is executed by using gate diffusion input (GDI) technique which prompts the decrease of the power usage, intricacy likewise the space of the circuit and increment the productivity of the carried-out item. The exhibition and examination are finished with outstanding methods dependent on number of transistors, which additionally analyze the power consumption. The circuit which has low power utilization can be used for designing of the flash-type TDC. The flash-type TDC is designed by utilizing 90 nm technology. The different circuits are designed by various advancements which are contrasted and proposed GDI structure. The simulation and synthesis of flash-type TDC can be implemented using Custom Compiler tool, and reproduction results are accounted.

Keywords Time-to-digital converters · Gate diffusion input · Flash-type TDC · D flip-flop

1 Introduction

1.1 Time-To-Digital Converter

Time-to-digital converter is similar to analog to digital converter which does quantization on voltage and current, whereas the time-to-digital converters use the quantization method for time intervals between the two given input signals [1]. TDC is used to determine the time interval between two signal pulses (known as start and stop pulses). Measurement is started and stopped when the rising or falling edge of a signal pulse crosses a set threshold. There are four types of time-to-digital converters: flash-type TDC, Vernier-type TDC, replica Vernier-type TDC and ring-type TDC [2].

J. Yeshwanth Reddy (✉) · A. Sushma · S. Sravya · S. S. Kiran · P. S. Sukitha
Department of ECE, B V Raju Institute of Technology, Narsapur, TS, India
e-mail: yeshwanthreddy.j@bvrit.ac.in

2 Flash-Type TDC

Flash-type TDC is the most essential kind of TDC. Its name comes from the similarity with the flash ADC, which typically utilizes a resistor ladder to create uniformly distributed levels in voltage domain, whereas flash-type TDC utilizes a delay line to accomplish the same in time domain [2].

Flash-type TDC consists of buffer elements, D flip-flops and XOR gates. These gates are designed by using GDI technique. As demonstrated in Fig. 1, the leading edge of the start signal is fed into the delay line. During this propagation, the lagging edge of the stop signal which shows up after T is fed to the D flip-flop, and here, the D flip-flop is latched by the rising edge of the stop signal. The time difference between these two signals is noted in the thermometer code; lastly, all these thermometer coded bits are added together to get the final output (Fig. 2).

A GDI method is a low-power circuit design technique; this procedure is predominantly used to design quick, low-power circuits utilizing only few transistors when contrasted with different techniques like CMOS and PTL. GDI cell is similar to that of the CMOS inverter structure. In CMOS inverter, PMOS is associated with Vdd and NMOS is grounded. But in GDI cell, there are three sources, namely G, P and N, and distribution of these input terminals to supply or ground is not fixed. Any of the input terminal could be given an inventory of Vdd or can be grounded or can be provided with input signal contingent on the circuit to be planned. The primary benefit of utilizing this GDI method is on the grounds that it utilizes less number of transistors which bring about low power dissipation and lesser delay utilizing less number of transistors which additionally bring about smaller area and less interconnect impact [3] (Table 1).

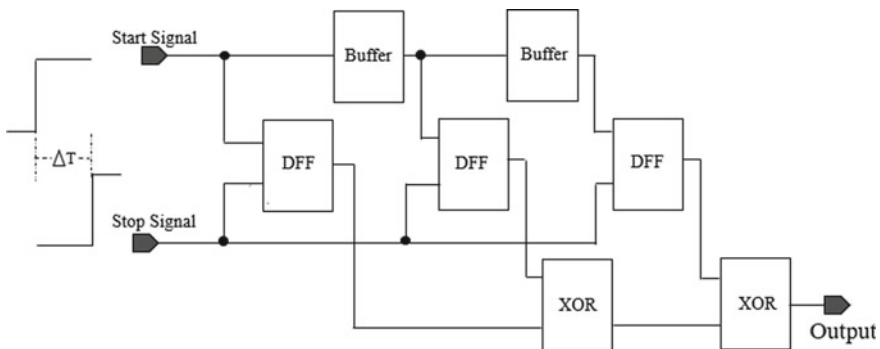


Fig. 1 Block diagram for flash-type TDC

Fig. 2 GDI basic cell

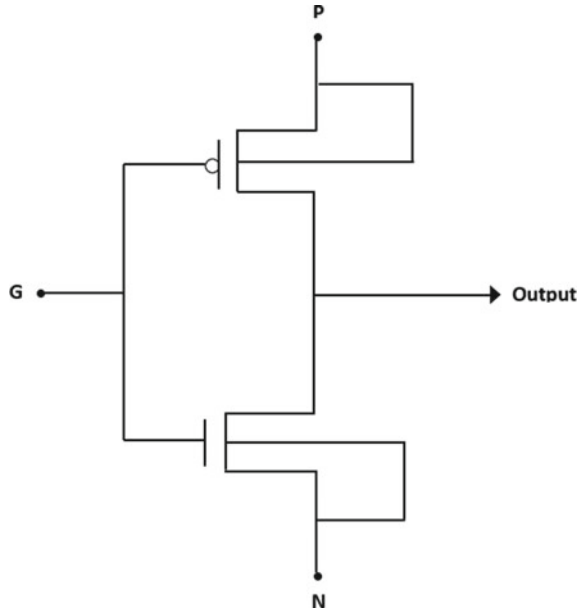


Table 1 Some of the logic functions which can be designed using GDI cell

G	N	P	Function
X	Y	Vss (0)	AND (X. Y)
X	Vdd (1)	Y	OR (X + Y)
X	Vdd (1)	Vss (0)	Buffer (X)
X	Vss (0)	Vdd (1)	Not (X')

3 XOR Gate

In flash-Type TDC, XOR gate can be designed by utilizing two PMOS and two NMOS gates; though in CMOS technique, XOR gate can be designed by utilizing eight PMOS and eight NMOS gates (Fig. 3).

Fig. 3 XOR gate using GDI technique

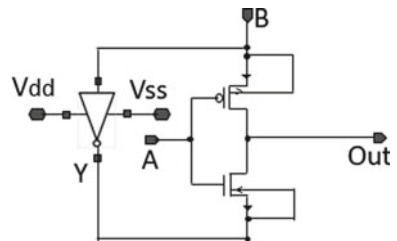
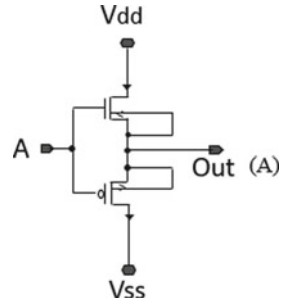


Fig. 4 Buffer using GDI technique



Operation:

- Case 1 If the A is 0 and B is 0.
Then $Y = 1$ and the final output is 0.
- Case 2 If the A is 0 and B is 1.
Then $Y = 0$ and the final output is 1.
- Case 3 If the A is 1 and B is 0.
Then $Y = 1$ and the final output is 1.
- Case 4 If the A is 1 and B is 1.
Then $Y = 0$ and the final output is 0.

4 Buffer

In flash-type TDC, buffer gate can be designed by utilizing one PMOS and one NMOS gate (Fig. 4).

Operation:

- Case 1 If $A = 0$.
Then Output is 0.
- Case 2 If $A = 1$.
Then Output is 1.

5 Working

The designed flash-type time-to-digital converter is a single-delay chain flash-type one which is shown in Fig. 1. In Fig. 3, we can clearly observe that the delay produced by the buffer is T . It is necessary to resolve the difference between the rising edges of pulse start and stop signals. The flip-flop present in the structure observes that the delay time (or) displacement in the time of the retarded start to the stop T is indicated by the thermometer—encoded output by considering each and every flip-flops that are having enough time to solve.

The output of flash-type time-to-digital converter depends on internal architecture which is designed by using D flip-flop using NAND and NOR gates, buffer and XOR gates. The start signal acts as an input signal and stop signal as clock signal as rising edge of the clock signal. Internally, the D flip-flop works when the clock signal is high, then the output will be same as input signal of flip-flop. Even the buffer which is given with some input and the output consists of with some delay in time (i.e., T).

6 Flash-Type TDC Using D Flip-Flop NAND Gates

The output of the two consecutive D flip-flop of NAND gate is given as input to the XOR gate. If both the inputs are same, then the output of XOR gate is low. Another successive D flip-flop output and first XOR gate output are given as input to another XOR gate which is also a finalized output of the flash-type time-to-digital converter using D flip-flop NAND gates (Fig. 5).

Operation:

- Case 1 If the start signal is 0 and stop signal is 0.
The final output is 0.
- Case 2 If the start signal is 1 and stop signal is 0.
The final output is 0.
- Case 3 If the start signal is 0 and stop signal is 1.
The final output is 0.

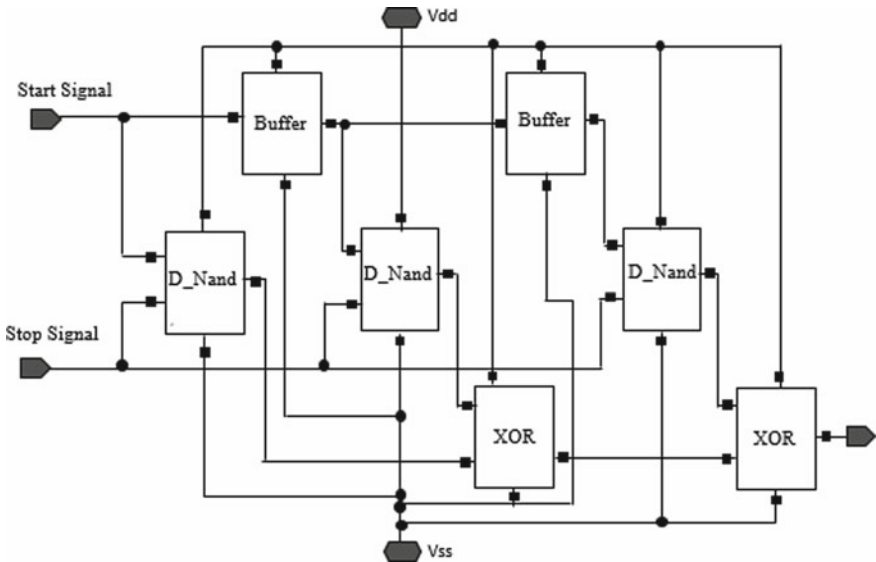


Fig. 5 Circuit diagram of flash-type TDC using D flip-flop NAND gate

Case 4 If the start signal is 1 and stop signal is 1.
The final output is 1.

From Case 4, we can clearly observe that the output is high when the stop signal and stop signal are high.

7 Flash-Type TDC Using D Flip-Flop NOR Gates

The output of the two consecutive D flip-flop of NOR gate is given as input to the XOR gate. If both the inputs are same, then the output of XOR gate is low. Another successive D flip-flop output and first XOR gate output are given as input to another XOR gate which is also a finalized output of the flash-type time-to-digital converter using D flip-flop of NOR gates (Fig. 6).

Operation:

- Case 1 If the start signal is 0 and stop signal is 0.
The final output is 0.
- Case 2 If the start signal is 1 and stop signal is 0.
The final output is 0.
- Case 3 If the start signal is 0 and stop signal is 1.
The final output is 0.
- Case 4 If the start signal is 1 and stop signal is 1.
The final output is 1.

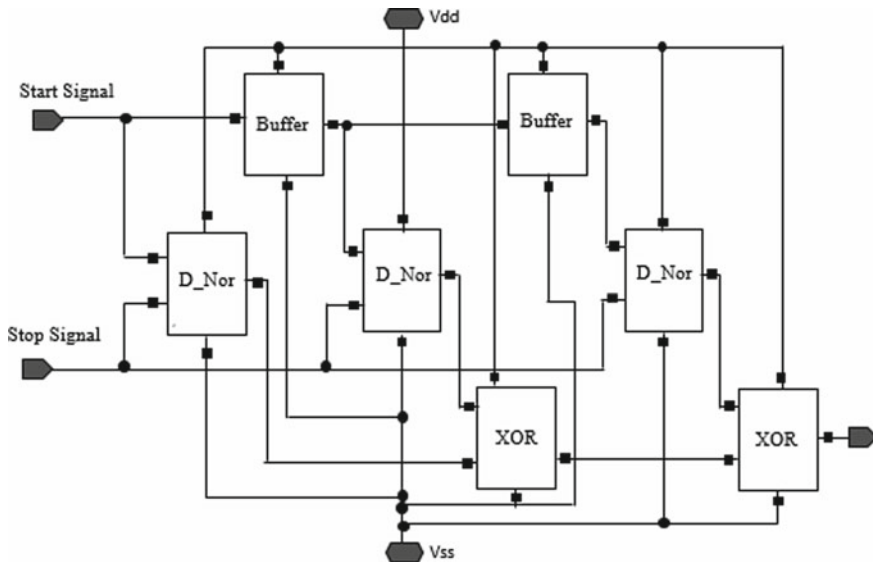


Fig. 6 Circuit diagram for flash-type using D flip-flop

From Case 4, we can clearly observe that the output is high when the stop signal and stop signal are high.

The main disadvantage of the flash-type time-to-digital converter using gate diffusion input technique is which cannot get the strong 0 or strong 1 as the output at the end of the operation.

8 Simulation Result

In general, the power is defined as the product of the voltage and the current flow in the circuit (Figs. 7, 8 and 9).

$$P = VI \text{ (in watts).}$$

The above-mentioned graph clearly gives the information about the power consumption of flash-type time-to-digital converter using D flip-flop NAND and NOR gates. Generally, the power consumption is high if the circuit consists of more number of transistors in its circuitry. These circuits are designed with less number of transistors and also calculated the power consumption using Custom Compiler tool itself (Table 2).

The first plot of the graphs shows the dynamic power of the TDC in which the NAND gate consumes less power compared to NOR gate. The second plot shows the static power of the TDC in which the NOR consumes less power compared to NAND gate.

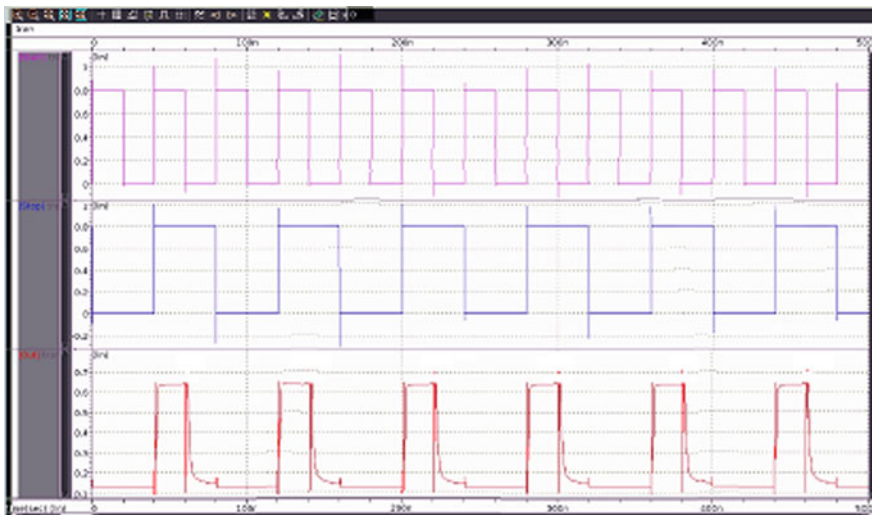


Fig. 7 Output waveform for flash-type TDC using D flip-flop NAND gate

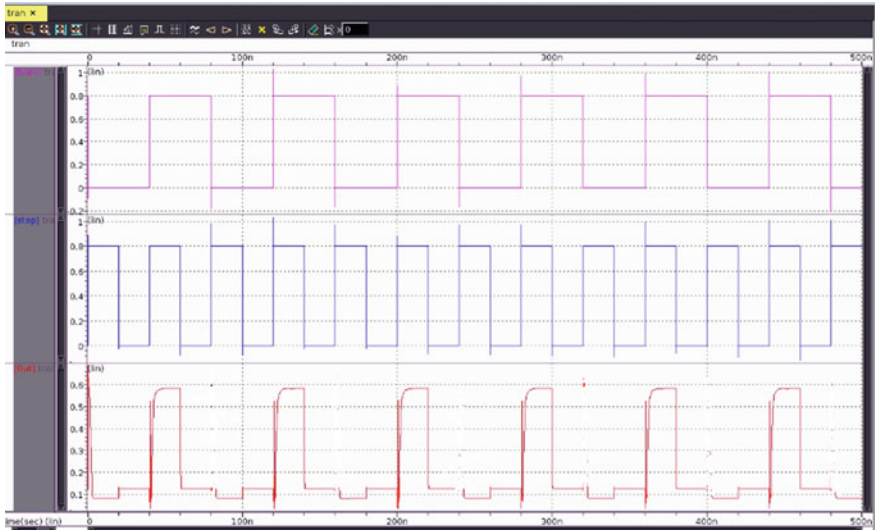


Fig. 8 Output waveform for flash-type TDC using D flip-flop NOR gate

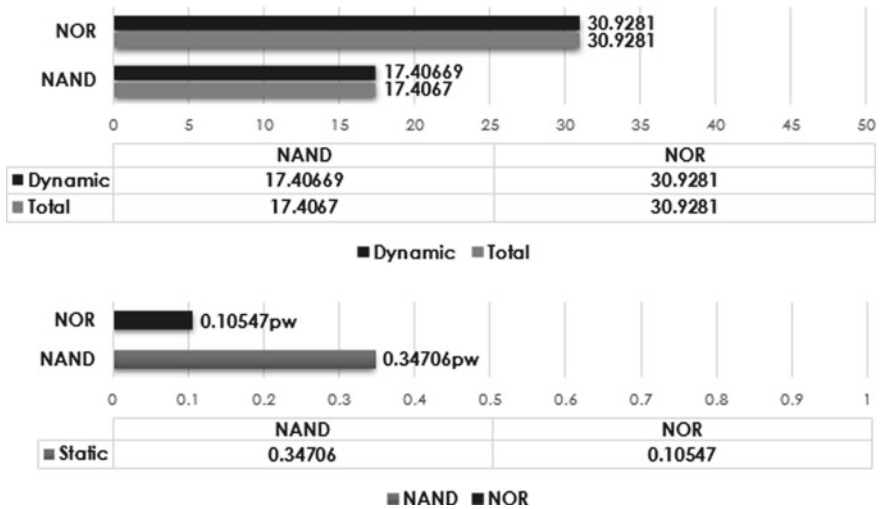


Fig. 9 Power consumption of flash-type TDC using NAND and NOR gates

Table 2 Comparison table of flash-type TDC using D flip-flop by NAND and NOR gates

Flash-type TDC	Total power	Static power	Dynamic power
D_NAND	17.4067UW	0.34706PW	17.4067UW
D_NOR	30.9281UW	0.10547PW	30.9281UW

Table 3 Comparison table of D flip-flop using NAND and NOR

D flip-flop	Total power	Static power	Dynamic power
NAND	9.56702UW	57.1338AW	9.56702UW
NOR	4.07214UW	91.3397AW	4.07214UW

To find out the total power, we used an equation.
 i.e., $Dynamic\ power = Total\ power - Static\ power$
 which is modified as $Total\ power = Dynamic + Static\ power$.

From the above equation, the total power of the TDC is calculated and shown in Table 3.

The below-mentioned graph also shows the power consumption of internal architecture, i.e., D flip-flop using NAND and NOR gates.

In the internal architecture, we can clearly see that the NAND gates consume more dynamic power compared to NOR gate. Whereas from the second plot, the static power is less for NAND gate when compared with NOR gate and is also calculated the total power consumption of D flip-flop using NAND and NOR gates by using previously mentioned equation (Fig. 10).

So, from the above two graphs, we can declare that flash-type TDC consumes less power depending upon the number of D flip-flop used and by ignoring the delay elements in the architecture.

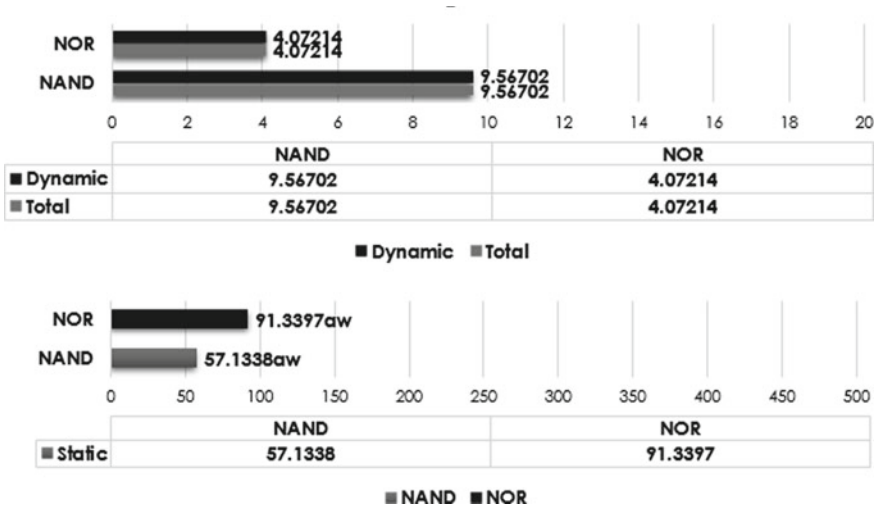


Fig.10 Power consumption of D flip-flop using NAND and NOR gates

9 Conclusion

The flash-type time-to-digital converter is implemented by high-performance D flip-flop using gate diffusion input technique which is presented here. A simple structure is implemented by using universal gates called NAND and NOR gates. An enhancement method was implemented for designing D flip-flop using gate diffusion input. This optimized flash-type time-to-digital converter consumes low power with lower number of transistors in its design, which targets the higher efficiency. The complexity of the circuit is lesser to gain the better efficiency. We implemented this flash-type TDC by using sequential circuit called D flip-flop under 90 nm technology. We used the Custom Compiler for designing the internal structure and reported the simulation results clearly which may also help in the future research on gate diffusion input technique.

10 Future Scope

The same idea can be extended to high-resolution modulators and also to higher order digital modulators, where the reduction in area, delay and power dissipation can be even greater by using modified gate diffusion input (MGDI).

References

1. Roberts GW, Ali-Bakhshian M (2010) A brief introduction to time-to-digital and digital-to-time converters. *IEEE Trans Circ Syst—II: Express Briefs* 57(3)
2. Priyanka C, Latha P (2015) Design and implementation of time to digital converters. In: IEEE sponsored 2nd international conference on innovations in information embedded and communication systems ICIECS' 15
3. Morgenshtein A, Fish A, Wagner IA (2002) Gate-diffusion input (GDI)—a technique for low power design of digital circuits: analysis and characterization. In: 2002 IEEE International symposium on circuits and systems. Proceedings (Cat. No. 02CH37353), vol 1
4. Bhardwaj A, Chauhan V, Kumar M (2019) Design of CMOS based D flip-flop with different low power techniques. In: 2019 6th International conference on signal processing and integrated networks (SPIN)
5. Hiremath S, Mathad A, Hosur A, Koppad D (2017) Design of low power standard cells using full swing gate diffusion input. In: IEEE international conference on smart technology for smart nation, pp 940–945. 948-1-5386-0569-1
6. Lu P, Liscidini A, Andreani P (2012) A 3.6 mW, 90 nm CMOS gated-vernier time-to-digital converter with an equivalent resolution of 3.2 ps. *IEEE J Solid-state Circ* 47(7)
7. Levine PM, Roberts G (2004) A high-resolution flash time-to-digital converter and calibration. In: 2004 international conference on test
8. Morgenshtein A, Fish A, Wagner IA (2004) An efficient implementation of D-flip-flop using the GDI technique. In 2004 IEEE international symposium on circuits and systems (IEEE Cat. No. 04CH37512), vol 2
9. Dudek P, Szczepanski S, Hatfield JV (2000) A high resolution CMOS time-to-digital converter utilizing a vernier delay line. *IEEE Trans Solid-State Circ* 35:2

10. Morgenshtein A, Fish A, Wagner A (2002) Gate-diffusion input (GDI): a power-efficient method for digital combinatorial circuits. *IEEE Transactions on very large-scale integration (VLSI) systems* October 2002
11. Input (GDI)—A novel power efficient method for digital circuits: a design methodology. In: 14th ASIC/SOC conference, Washington D.C., USA, September 2001
12. Dudek P, Szczepanski S, Hatfield JV (2000) A high-resolution CMOS time-to-digital converter utilizing a Vernier delay line. *IEEE J. SolidState Circ* 35(2):240–247
13. Input (GDI)—A power efficient method for digital combinatorial. *IEEE transactions on VLSI systems*. In: Weste N, Eshraghian K (eds) *Principles of CMOS digital design* (1985). Addison-Wesley, pp 304–307

A Symbiotic Model for Accurate Weather Forecasting



Vijay A. Kanade

Abstract With the advent and evolution of AI, ML and predictive analytics, weather forecasting has become an important area of research in the last few years. As the non-linearity in the nature of weather data is widely known, emphasis has been on non-linear prediction of the weather. However, despite the technological sophistication, weather prediction has lacked precision. The paper proposes a symbiotic model that harnesses the collaborative intelligence of all species and integrates it with modern forecasting systems to predict weather with pin-point accuracy. The developed system decodes the variables processed by various bio-indicators—plants, insects, birds and animals that are currently not a part of any weather forecasting system. Hence, the developed model shows multi-fold increase in the accuracy of weather prediction as it blends the intelligence of biomarkers and modern systems to forecast weather better.

Keywords Weather forecasting · Bio-indicators · Symbiotic model · Collaborative intelligence · Traditional knowledge

1 Introduction

Weather is a highly dynamic component of nature. Today, the scientific community is investing substantial time and resources to develop systems that forecast weather accurately. These efforts come to fore due to the importance of weather prediction in our lives. Right from farming, manufacturing to traveling, precise forecasts are crucial [1]. Moreover, with the ongoing environmental changes, it has become even more vital to anticipate the weather so that our daily activities are not hampered.

Fundamentally, weather forecasts are made by collecting current atmospheric data (such as temperature, pressure, humidity, wind and unknown variables) and employing numerical or statistical models to learn and determine how the atmosphere may evolve in the future. However, with the non-linear nature of the weather data

V. A. Kanade (✉)
Pune, India
e-mail: kanade.science@gmail.com

and lack of clarity on underlying atmospheric processes the forecast becomes less accurate as we go from short-range to long range forecasting.

Consider a simple analogy of an air filled balloon. The task here is to predict the path of the balloon on untying its knot. Although one is able to determine various parameters such as the size, surface area or even volume of the balloon, it is highly improbable to predict the path it may traverse. This is because we are not aware of the status of each atom or molecule in that balloon which directs its motion. We do not have much clue of the quantum properties of all the quantum particles in the balloon which makes it difficult to predict the exact trajectory of the balloon with certainty.

Modern weather forecasting systems face the similar uncertainty issue, due to which it is difficult to predict weather accurately. This implies that there are certain unknown variables in nature that predictive systems cannot fathom due to their hidden nature. Hence, there seems to be a long standing need to understand, study and consider such parameters that are alien to humans and incorporate them in the weather forecasting systems to improve weather prediction accuracy. Moreover, considering the inaccuracy and unreliability of current weather systems, there's also a need to develop a framework that integrates traditional knowledge into modern weather forecasting systems to achieve greater precision in weather forecasting [2].

In this paper, we propose a symbiotic model to forecast weather. The model tracks the behavior of various bio-indicators—plants, insects, birds and animals in different weather conditions to better understand the mysterious variables in atmospheric data. The response of bio-indicators is noted and further combined with the modern system's weather data to make the final weather prediction.

2 Literature Survey

Weather forecasts are extensively used by city dwellers and the rural groups such as tribes, farmers, fishers and hunters. Local city community relies on modern weather forecasting systems, while rural people rely on traditional knowledge of weather forecasting which is devoid of any electronic device. Let's look at each system in greater detail.

2.1 *Modern Weather Forecasting Systems*

Modern weather forecasting models employ methods and techniques such as persistence forecast, trend forecast, analog forecast, barometric forecast, nowcasting and statistical forecast to predict weather [3].

Today, weather data is collected from various sources including ground centers, observations from ships, aircraft observations, radio sounds, balloons, doppler radar and satellites [4]. These weather stations use devices such as anemometer, barometer,

wind vane, thermometer, hygrometer and others to sense weather changes [5]. The obtained data is then sent to meteorological centers for study and analysis where modern high-speed computers assimilate the thousands of observations. The conclusions on weather are then made through a variety of charts, maps and graphs and made available to weather broadcasters.

2.2 Traditional Knowledge

Rural groups, especially farmers, fishermen, hunters and tribes are keen weather watchers. They are quick to recognize the dynamic weather conditions and decide upon whether they are favorable to their plans.

These groups practice local forecasting that considers the phonological patterns of plants and the behavior of birds, animals and insects [6, 7]. They tend to make local forecasts as it is derived from the close interaction between biotic components and the rhythmic cycles of seasonal variations. This indigenous knowledge is helpful as it indicates whether it will be a wet or dry year, the onset of the rainy season or any other adverse weather conditions [8].

Farmers often use these plant and animal indicators to plan their cropping or agricultural activities. It has been identified that plants and certain fungi are accurate forecasters of wet and dry weather. For example, dandelions and tulips tend to fold their petals just before the rain. Similarly, an edible mushroom (fungus) that grows on stumps and tree trunks tends to expand prior to a rain and shrinks or closes in dry weather [6].

On the other hand, there is a distinct pattern in the behavior of birds and animals for a weather change. On an upcoming rain there is unusual chirping of birds and bathing with sand, croaking of frogs near swampy areas and hiding their eggs and low flying pattern of dragon-flies. Similarly, some groups of animals tend to seek shelter when they sense potentially violent weather. For example, storms and hurricanes tend to decrease the air and water pressure considerably. Birds and bees are experts in sensing such barometric changes. Thus, they instinctively make a move toward their nests or hives. Some bird types also decide upon the migration time by sensing the atmospheric air pressure [9].

Thus, the traditional indicators are helpful for rural people as it overcomes uncertainty and gives them time to prepare for adverse or favorable events.

3 Observations for Different Bio-indicators

During drastic atmospheric changes, it has been observed that certain plants regenerate a number of defensive chemicals, hormones and enzymes along with production of anti-nutrients. Similarly in animals, the nervous system of certain vertebrates and invertebrates becomes more active during such chaotic climatic conditions. Various literature sources cite substantial evidence and possible explanations for such biological events. The observations and evidences are noted in Tables 1, 2 and 3.

Notation: X—Onset of rainy season; Y—Upcoming rain; Z—Abnormal weather condition (storm or flood).

3.1 Bio-indicator: Plants

See Table 1.

Table 1 Plant response [6]

S. No.	Bio-indicator	Plant name	Region	Forecast type
1	Ripening and early rotting of fruits	<i>Abroma angusta</i>	Dry field and basin	Y
2	Early unusual flowering of plants	<i>Abutilon indicum</i>	Basin area	Y
3	Increased length of leaves	<i>Ceratopteris thalictroides</i>	Marshy area	Y
4	Dark color of leaves and stem	<i>Psidium guineense</i>	Upper dry land	Z
5	Early unusual flowering of plants and wide open blooms indicating fine weather	<i>Naravelia zeylanica</i>	Dense moist forest	Z

3.2 Bio-indicator: Birds

See Table 2.

Table 2 Behavioral pattern of birds [6]

S. No.	Bio-indicator	Bird name	Forecast type
1	Unusual chirping	Black-throated sunbird	X
2	Unusual chirping and bathing with sand	White-throated bulbul	Y
3	Unusual movement to take shelter in shadow of leaves	Mountain imperial pigeon	Z
4	Unusual activity with rotation around the tree	Gray-headed woodpecker	Y
5	Unusual chirping and flying in fleet	Vernal hanging parrot	Y

3.3 Bio-indicator: Animals

See Table 3.

Table 3 Animal behavior [6]

S. No.	Bio-indicator	Forecast type
1	Biting nature of mosquitoes	X, Y
2	Incessant chirping of insects	Z
3	Loose dogs excreting waste in the middle of road or at higher elevation	Y
4	Chicken staying under shade at noontime and also taking a bath with dust	Y
5	Earthworm coming out of ground	Z

4 Symbiotic Model: A Hybrid Framework

The proposed symbiotic model tracks the behavior and response of all bio-indicators simultaneously as seasonal weather changes. This is achieved by deploying data chips on these bio-indicators that record the behavioral data of various bio-indicators living in separate habitats. The recorded response is then sent to a computing device that analyzes it further to derive useful insights.

The system concurrently collects weather data from modern forecasting systems. This creates a hybrid framework that provides holistic view of weather change as it processes data from biotic species and integrates it with the knowledge of modern systems to further optimize the weather prediction.

The red highlight in the Table 4 represents the proposed synergistic model where we blend symbiotic intelligence with modern systems to predict weather accurately.

Table 4 Accuracy for the symbiotic model (in %)

Hybrid framework	Bio-indicator			Modern weather forecasting systems	Accuracy for symbiotic model (in %)
	Plants	Birds	Animals		
Use case – I	✓	✓	✓	✓	≈ 96-100
Use case – II	✓	✓	✗	✓	≈ 75
Use case – III	✓	✗	✓	✗	≈ 50
Use case – IV	✗	✓	✗	✗	≈ 25

This implies, when both bio-indicators (plants, birds and animals) and modern forecasting systems predict a related or similar weather, then the probability of its occurrence is expected to be very high (i.e., approx. 96–100%). However, the failure of any single participating component can affect the weather prediction accuracy significantly as seen in the use cases-II, III and IV shown above.

For example, consider the use cases below where both bio-indicators and modern systems forecast weather in response to weather changes.

Notation: *X*—Onset of rainy season; *Y*—Upcoming rain; *Z*—Abnormal weather condition (storm or flood).

Description: Referring to Table 5, it is observed that for case-I, most bio-indicators generate a response that hints toward the forecast *Y* but one plant indicator indicates forecast *Z*. Modern weather systems predict *Y* or *Z* type forecasts. Now, as in the proposed hybrid system we integrate both these approaches, the forecast type *Y* can be fixated with certainty due to its high probability as the response pattern of both bio-indicators and modern systems point at forecast *Y*. Forecast type *Z* can be taken into consideration at a later stage as it seems like a consequence of forecast *Y*, but immediate weather prediction shows an inclination toward forecast type *Y*.

Similarly, for the case-II, all bio-indicators along with modern systems generate a response that hints toward the forecast *Z*, hence there's a high probability for its occurrence. Although there's an animal bio-indicator response that predicts *X* or *Y* forecast, it can be considered as an anomaly as the majority indicators fall for *Z* type weather.

5 Deployed Bio-indicators

The proposed hybrid framework offers a concept for better local weather forecasting as local parameters specific to a geography are considered to anticipate weather in the area. Following are the images of various bio-indicators with attached 'data chips' that are used in our approach to determine the change in their behavior due to weather changes (Fig. 1).

Table 5 Weather forecasts using the symbiotic model

Hybrid framework	Bio-indicator			Weather prediction by modern systems	Symbiotic model for weather forecasts
	Plants	Birds	Animals		
Case-I	Ripening and early rotting of fruits [Y]	Unusual chirping and bathing with sand [Y]	Loose dogs excreting waste in the middle of road or at higher elevation [Y]	[Y, Z]	Y
	Early unusual flowering of plants and wide open blooms indicating fine weather [Z]	Unusual activity with rotation around the tree [Y]	Chicken staying under shade at noontime and seem like taking a bath with dust [Y]		
Case-II	Dark color of leaves and stem [Z]	Unusual movement to take shelter in shadow of leaves [Z]	Biting nature of mosquitoes [X, Y]	[Y, Z]	Z
			Earthworm coming out of ground [Z]		

Note: The experiments are currently in the preliminary stage and the task of data collection from above bio-indicators is underway. Therefore, the acquired results have not been highlighted in the paper.

6 Advantages

The research proposal monitors and considers the sequence of activities of species at moments when they look to take precautionary measures to safeguard themselves from upcoming natural dangers. The hybrid model further integrates data from weather forecasting systems with the data from bio-indicators. At this stage of rapid climate change, the traditional knowledge and awareness helps in better local weather prediction at specific times and in specific regions. The proposed model is especially suitable for weather reliant countries like India, which are dependent largely on seasonal rainfall for agriculture and associated activities. The countries can benefit immensely from the proposal as it is tailor made for short, medium and long range weather forecasting.

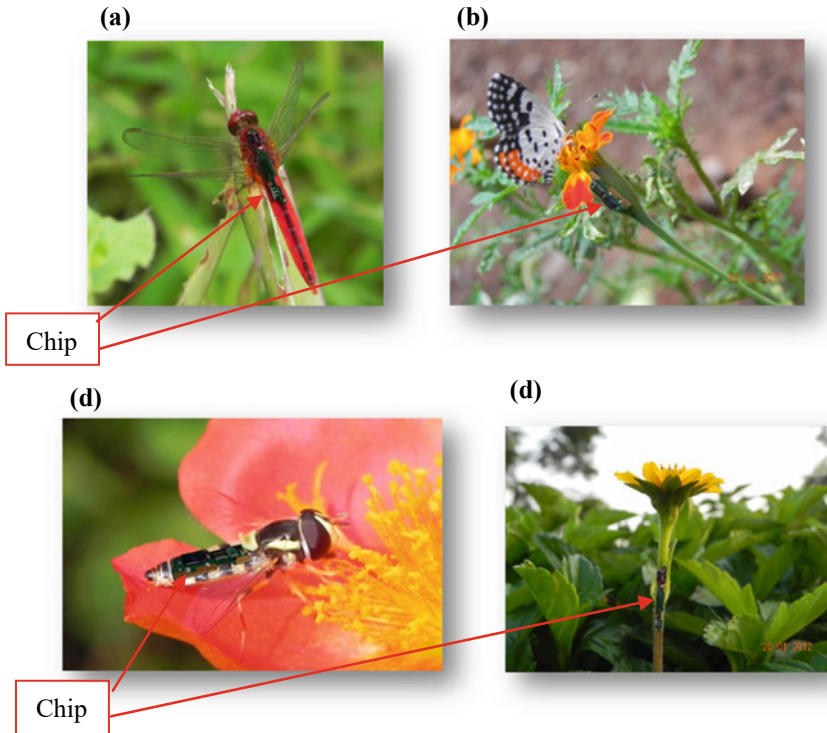


Fig. 1 a Dragonfly, b Marigold flower c Long hoverfly, d Singapore daisy

7 Conclusion

The proposed symbiotic model combines the intelligence of biotic species and modern systems to predict weather accurately. The response of bio-indicators will inevitably pick up the unknown variables or signals that modern systems miss out on which can introduce possible errors in prediction. It could very well be the missing piece in the 'precise weather prediction' puzzle.

The hybrid framework provides an opportunity to utilize nature's mind and combine it with factors that human intellect can think of to develop an even smarter system for weather tracking.

Acknowledgements I would like to extend my sincere gratitude to Dr. A. S. Kanade for his relentless support during my research work.

Conflict of Interest The authors declare that they have no conflict of interest.

References

1. Patel A, Kumar Singh P, Tandon S (2021) Weather prediction using machine learning, 5 May 2021
2. Irumva O, Twagirayezu G, Nizeyimana JC (2021) The need of incorporating indigenous knowledge systems into modern weather forecasting methods. *J Geosci Environ Protect* 09(02),16 pages. Article ID:107144. <https://doi.org/10.4236/gep.2021.92004>
3. Jaseena KU, Kovoov BC (2020) Deterministic weather forecasting models based on intelligent predictors: a survey. *J King Saud University—Comput Inf Sci* 4
4. Brookes V, How's the weather out there? forecasting the chaos of weather. *The pages of national geographic magazine*
5. McFadden C (2020) 15+ Weather forecast instruments and inventions that helped define how we predict the weather, Mar 23, 2020
6. Acharya S, Biology P (2011) Lessons from nature in weather forecasting. *Ind J Tradit Knowl* 10(1):114–124
7. Schlanger V (2003) Short range forecasting using plant and animal behavior. *Environmental Science Published for Everybody Round the Earth*, 12 Dec 2003
8. Nyadzi E, Werners SE, Biesbroek R, Ludwig F (2020) Techniques and skills of indigenous weather and seasonal climate forecast in Northern Ghana. *Clim Dev* 13(6):551–562. <https://doi.org/10.1080/17565529.2020.1831429>
9. <http://science.howstuffworks.com/nature/climate-weather/storms/animals-predict-weather2.htm>

FPGA Design of Area Efficient and Superfast Motion Estimation Using JAYA Optimization-Based Block Matching Algorithm



Manne Praveena, N. Balaji, and C. D. Naidu

Abstract We are in modern world and preferred to use modern services such as high-definition television, video-on-demand, video email, and video conferencing. The modern communication system exchanges information via audio, image, video, and graphics formats for long distance. The different video coding formats are MPEG-1, MPEG-2, MPEG-4, H.261, H.263, H.264, Theora, Real video RV40, VP9, and AVI, used for those services. Due to the temporal and spatial redundant problem, codes required a motion estimation algorithm. This paper proposes an area efficient motion estimator using JAYA optimization-based block matching (JAYA-BM), without compromising searching speed. The JAYA-BM algorithm strives to search the motion vector by superfast manner. The field programmable gate array (FPGA) design of proposed motion estimator performed using Verilog language and synthesized with different FPGA device families in Xilinx tool. The simulation result shows that our motion estimator is able to enhance the hardware usage and searching speed with better quality.

Keywords FPGA · Superfast motion estimator · JAYA optimization · Block matching

1 Introduction

Reliably, digital videos are in every way that really immune to noise, easier to transmit, and can give a shrewder interface to users [1]. Additionally, the measure of video substance can be made more noteworthy through enhanced video weight in

M. Praveena (✉)

BVRIT HYDERABAD College of Engineering for Women, Hyderabad, Telangana, India
e-mail: atluri.praveena@gmail.com

N. Balaji

University College of Engineering, JNTU Vizianagaram, JNTUK, Kakinada, India

C. D. Naidu

VNR Vignana Jyothi Institute of Engineering and Technology, Hyderabad, Telangana, India
e-mail: cdnaidu@vnrvjiet.in

light of the way that the data transmission required for clear transport can be utilized for more channels [2–4]. The video compression systems end users can stream video, change video and offer video to associates by strategies for the web or IP systems [5]. The sound and video weight are required for changing video pennants and arrangements to hold unprecedented quality. In a video format, information emphasis ascends out of spatial, transient, and quantifiable relationship between edges [6]. Motion estimation and compensation are used to reduce temporal and spatial redundancy between successive frames [7]. The demand for communication with moving video and images are quickly developing. It is required in different remote video conferencing frameworks, and it is customary in not too evacuated future remote structures which will send and get constant video [8]. The multimedia terminal contains video encoder and decoder facilitates for pack the video stream to be transmitted over a communication medium.

Motion estimation computes the displacement between the current frame and a stored past frame that is used as the reference. The reference frames are assumed as an immediate past frame from current frame. The computational complexity of motion estimation poses great challenge for real-time codec implementation. Recently, block matching (BM) algorithms [9–14] used for those operation and minimize the computation cost of total design. Other than software design, hardware implementation also very complicated one. In this paper, we propose a new motion estimator using JAYA optimization-based block matching (JAYA-BM) for area and speed efficiency. The hardware implementation of proposed motion estimator performed with the different FPGA families in Xilinx tool.

2 Motion Estimation

The enormous amount of temporal information redundancy affects the sequencing of time-oriented frame of pixels in video coding. It can be removed by proper motion estimator. Our proposed superfast motion estimator will address that problem. The loss of temporal redundancy can have a big impact on video quality and bitrate. Motion estimation is a technique for extracting the motion of a block of pixels between the current and prior frames, commonly known as the reference frames. A motion vector difference (MVD), which is the displacement of a block of pixels from its current location, is used to indicate motion. The position difference between a template block in the current frame and the best matched block in the reference frame is the motion vector. The most widely applied criterion for BM algorithm is the sum of absolute difference (SAD), and it is between two frames with R —the reference frame and C —the current frame, (x, y) were coordinates of search position, and were macro block dimensions and were coordinates of the evaluated offset between frames. The SAD function defined as follows:

$$\text{SAD}(\tilde{m}, \tilde{n}) = \sum_{i=0}^{N-1} \sum_{j=0}^{N-1} |C_t(x+i, y+j) - R_{t-1}(x+\tilde{m}+i, y+\tilde{n}+j)| \quad (1)$$

Other than SAD, we include extra two matching criteria, which are pixel difference classification (PDC) and binary level matching criterion (BPROP). PDC is the simple counts matching pixel between two macro blocks. The function is defined as follows:

$$\text{PDC}(\tilde{m}, \tilde{n}) = \sum_{i=0}^{m-1} \sum_{j=0}^{n-1} T_{i,j}(\tilde{m}, \tilde{n}) \quad (2)$$

where $T_{i,j}(\tilde{m}, \tilde{n}) = \begin{cases} 1; & \text{if } \text{SAD}(\tilde{m}, \tilde{n}) \leq t \\ 0; & \text{otherwise} \end{cases}$.

The difference between two pixels can be expressed not only by an arithmetical difference, but also by exclusive disjunction of corresponding bits. It is computed by the BPROP function and defined as follows:

$$\text{BPROP}(\tilde{m}, \tilde{n}) = \sum_{i=0}^{m-1} \sum_{j=0}^{n-1} [C_t(x+i, y+j) \oplus R_{t-1}(x+\tilde{m}+i, y+\tilde{n}+j)] \quad (3)$$

Finally, the motion vector (MV) defined as follows:

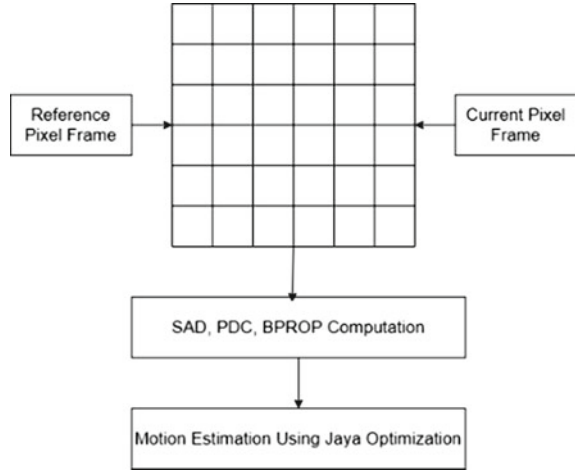
$$\text{MV} = \arg \min_{S=(\tilde{m}, \tilde{n})} (\text{SAD}(\tilde{m}, \tilde{n}) \&\& \text{PDC}(\tilde{m}, \tilde{n}) \&\& \text{BPROP}(\tilde{m}, \tilde{n})) \quad (4)$$

A fast block motion estimation using hybrid search algorithm [15] computes the accurate MV, considering all locations within the search space S . The process consumes high computational cost. To overcome such a problem, by JAYA optimization algorithm, it reduces the redundant in searching space.

3 Proposed Model

The proposed design's system model is shown in Fig. 1. The main modules are matching criteria's computation module and proposed motion estimation module. The key benefit of the suggested architecture is that it may reuse the results of previously calculated matching criterion searches (SAD, PDC, and BPROP). By comparing neighbor macro blocks with saved block size values, the matching criteria will be calculated in parallel.

Fig. 1 System model of proposed design



3.1 JAYA-BM Algorithm

Venkata Rao [16] presented JAYA, a new population-based optimization technique, that generates the best solutions for confined and unrestrained optimization problems. JAYA algorithm doesn't have a count-specific regulating parameter, instead relying on the two standard controlling factors of mass size and number of times. This methodology's upgrade strategy is triggered by the possibility that the plan devised to address a specific problem must progress toward the ideal strategy while avoiding the trivial strategy. The essential JAYA algorithm has only a solitary stage as shown by the beforehand specified thought, making it a fundamental streamlining procedure.

The basic JAYA algorithm applied for the block matching in motion estimation for optimize the matching criteria. As a result, given the limited search space, the optimum penetration delivers the best match values. The formula of the objective problem is shown as:

$$\text{Minimize } F(s); \quad s = 1, 2, 3 \quad (5)$$

Subject to SAD ($R(1)$), PDC ($R(2)$), and BPROP ($R(3)$), the problem is solved using the BM algorithm. The initial procedure is where we describe the algorithm's size of the population, design parameters, and termination requirements. Then, for the initial status, compute the values of the objective functions SAD, PDC, and BPROP using Eqs. (1), (2), and (3), respectively. Then, within the specified design variable bounds, generate an initial random population using the defined controlling parameters. The population (P) is formulated as follows:

$$P = \begin{bmatrix} R_1(1) & R_1(2) & \cdots & R_1(n) \\ R_2(1) & R_2(2) & \cdots & R_2(n) \\ \vdots & \vdots & \vdots & \vdots \\ R_m(1) & R_m(2) & \cdots & R_m(n) \end{bmatrix} \quad (6)$$

where “ n ” is the number of control variables, and “ m ” is the number of candidate solutions of any iteration. Let the finest candidate has the best $R(1)_{\text{best}}$ value and the worst candidate get the worst $R(1)_{\text{worst}}$ value in the complete candidate solutions. If $R_{m,n,p}$ is the value of n th variable for the m th candidate during p th iteration can be written as follows:

$$R'_{m,n,p} = R_{m,n,p} + r_{m,1,p}(R_{m,\text{best},p} - |R_{m,n,p}|) - r_{m,2,p}(R_{m,\text{worst},p} - |R_{m,n,p}|) \quad (7)$$

where $r_{m,1,p}$ and $r_{m,2,p}$ are random numbers between 0 and 1. For details, let assume the 16×16 frame pixels as input and three matching criteria. This results in total population size of $m = 256$ and design parameters as $n = 3$. The physical elements can be described as follows:

$$P = \begin{bmatrix} R_1(1) & R_1(2) & R_1(3) \\ R_2(1) & R_2(2) & R_2(3) \\ \vdots & \vdots & \vdots \\ R_{256}(1) & R_{256}(2) & R_{256}(3) \end{bmatrix} \quad (8)$$

Run the control stream software for each candidate approach to determine the target cutoff estimate for each philosophy. See which of the contending storylines has the finest and most easily detectable cursed game-plans. Change each approach without hesitation considering the finest and most definitely spectacular diagrams. If any design parameter upper/segregate down most cleared point is damaged for any restored plan, replace the assessed a focal reason with anything beyond what many would assume possible. Examine the target work values for the previous and upheld approach for each iteration. Examine the current arrangement to see if it is superior to the previous method. Something else, stick to the previous strategy. If the final presentation is refined, come to a halt and report the optimal system. Something else, push the structure from see finest and most exceedingly wretched approach among the contender outlines.

In this work, Rastrigin’s function is used for fitness computation as given below:

$$F_{\min} = \sum_{s=1}^n [f_s^2 - 10 \cos(2\pi f_s) + 10] \quad (9)$$

Rastrigin’s function is based on cosine modulation to produce many local minima. The algorithm is always attempting to get nearer to victory (i.e., evaluate ideal candidate) while attempting to avoid collapse (i.e., maximum searching).

3.2 FPGA Design of JAYA-BM Algorithm

The FPGA design of JAYA-BM algorithm consists of different sub-modules that include memory module, modifier module, fitness module, and comparator module. The complete architecture of JAYA-BM is shown in Fig. 2, which composed of the registers, such as i, j for address generator module, 3 registers for storing the initial estimates of matching criterion— $I_1, I_2,$ and I_3 ; 3 registers for storing the matching criterion estimates $X_1, X_2,$ and X_3 with respect to the fitness values.

3.2.1 Memory Module

The motion estimate is done on a 16×16 pixel block with a horizontal search range of $(16 \text{ and } + 32)$ pixels and a vertical search range of $(16, + 32)$ pixels. Processor modules and two sets of comparators make up the memory module. To store the values and to store the current block, a distribution unit and two memories are used. The memory storing the search values is split into three partitions managed by the distribution unit, each partition containing 16 pixels that is then loaded into the matching criteria. At each clock cycle, the MMs are used to generate $n \times 41$ matching criteria. The best matched value is computed using these $n \times 41$ values. The memory size will depend on the frame pixel size and decision variables. In our

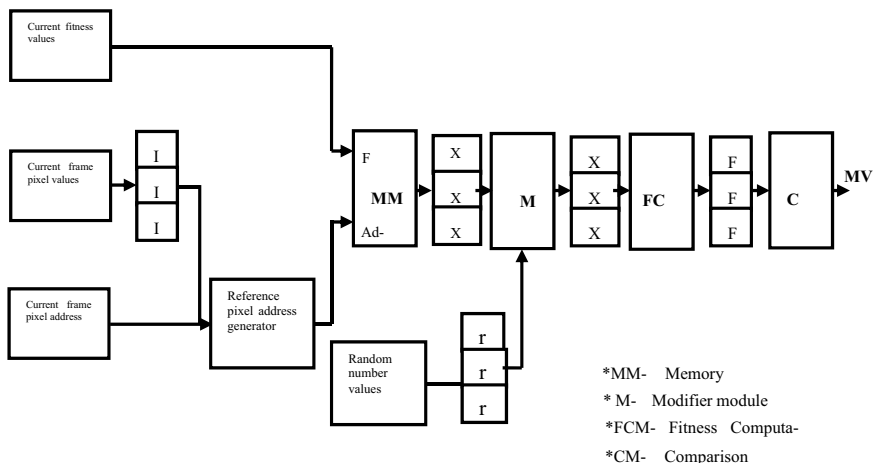


Fig. 2 FPGA design of proposed JAYA-BM algorithm

work, we consider m populations (frame pixel size) and three decision variables as SAD, PDC, and BPROP.

3.2.2 Modifier Module

Modifier is the main module of proposed JAYA-BM algorithm, which is used to compute the new values for all frames respected to decisions variables. From initial frame pixel values and their fitness values, we determine the finest and worst solution in the initial iteration. Let's consider the best value as $F(1)_{\text{best}}$ and the worst value as $F(1)_{\text{worst}}$ in the entire candidate solutions. In our work, three different design parameters are used, so we derive the three modifiers from Eq. (7) as follows: If $F_{m,n,p}$ is the value of n th variable for the m th candidate during p th iteration can be written as follows:

$$R'_{m,1,p} = R_{m,1,p} + r_{m,1,p}(R_{m,\text{best},p} - |R_{m,1,p}|) - r_{m,2,p}(R_{m,\text{worst},p} - |R_{m,1,p}|) \quad (10)$$

$$R'_{m,2,p} = R_{m,2,p} + r_{m,3,p}(R_{m,\text{best},p} - |R_{m,2,p}|) - r_{m,4,p}(R_{m,\text{worst},p} - |R_{m,2,p}|) \quad (11)$$

$$R'_{m,3,p} = R_{m,3,p} + r_{m,5,p}(R_{m,\text{best},p} - |R_{m,3,p}|) - r_{m,6,p}(R_{m,\text{worst},p} - |R_{m,3,p}|) \quad (12)$$

where $R'_{m,1,p}$, $R'_{m,2,p}$, and $R'_{m,3,p}$ represent the new solution for m number frame pixels; first, second, third control variables, and p th iteration, respectively, in the subsection. The $R_{m,1,p}$, $R_{m,2,p}$, and $R_{m,3,p}$ represent the previous solution for m number frame pixels; first, second, third control variables, and p th iteration, respectively, in the subsection. The $r_{m,1,p}$, $r_{m,2,p}$, $r_{m,3,p}$, $r_{m,4,p}$, $r_{m,5,p}$, and $r_{m,6,p}$ represent the random numbers, for every candidates, which requires two random numbers to generate the new solution. The hardware design of three modifiers is very similar to each other.

3.2.3 Fitness Computation Module

The output of modifier module is the new candidate solutions. Then it is forwarded to fitness computation module (FCM) for fitness computation. FCM depends on specific application, and we can change the benchmark functions which depend on the type of application. Rastrigin's function is based on De Jong's function, but with cosine modulation added to produce many local minima. As a result, the test function is strongly multimodal, and the minima are evenly distributed. The Rastrigin's function is given in Eq. (9). The output of FCM is the new fitness value.

3.2.4 Controller Module

The computed fitness values, corresponding matching constraints are maintained in the registers. Then the values are compared with the initial or previous fitness values. Based on our rule formation, the computed fitness value is better than previous fitness means; we accept and update the fitness value as new one. Otherwise, we retain the old fitness value. The condition is written as follows:

if borrow is high (i.e. new fitness is less than old)

$$|\text{new fitness} - \text{old fitness}| = \text{old fitness} - \text{new fitness}$$

Output = Sub2 output

else (i.e. old fitness is less than new)

$$|\text{new fitness} - \text{old fitness}| = \text{new fitness} - \text{old fitness}$$

Output = Sub1 output

4 Simulation Result

The proposed motion estimator is efficient than existing techniques. Our proposed motion estimator implemented on FPGA technologies such as Virtex7 (XC7VX330t-2Lffg1157), Virtex6 (XC6vhx250t-2ff1154), Kintex7 (XC7K480t-3ffg901), Zynq (XC7Z045-2fbg676), and Artix7 (XC7a100t-3csg324) device using Xilinx tools versions 14.5. The performance metrics considered are hardware utilization, maximum frequency, and power consumption used to analyze the performance of proposed motion estimator. Table 1 gives the performance comparison of proposed superfast motion estimator with different devices.

From Table 1, performance metrics of proposed superfast JAYA-BM algorithm with Artix7 (XC7a100t-3csg324) FPGA device utilize very less devices in terms of 687 slice registers, 1262 slice LUTs, 497 occupied slices, 1437 LUT, and FF pairs,

Table 1 Performance of proposed superfast JAYA-BM

Performance metrics	FPGA devices				
	Virtex7	Virtex6	Kintex7	Zynq	Artix7
No. of slice registers	687	691	687	687	687
No. of slice LUT	1266	1267	1268	1256	1262
No. of occupied slices	590	672	548	602	497
No. of LUT and FF pairs	1519	1603	1535	1524	1437
Max. frequency (MHz)	346.518	312.906	392.665	46.518	297.734
Power consumption (mW)	143	5793	182	176	42

and the power consumption is also very low as 42 mW, but not achieved the maximum clock frequency. Maximum frequency achieved in the Kintex7 (XC7K480t-3ffg901) device as 392.906 MHz, and it is very high compared to other FPGA devices.

4.1 Performance Comparison

The performance of proposed superfast JAYA-BM algorithm compared with existing algorithms such as FFT-based motion estimator [17], adaptive computationally-scalable motion estimator [18], ETSS [19], ARPS [20], integer motion estimator for H.264/AVC encoder [21], motion estimator using modified XOR function [22], MFSBME [23], integer motion estimator for HEVC encoder [24], fractional motion estimator [25], variable block size motion estimator [26], and cross-diagonal hexagon search-based motion estimator [15]. Table 2 gives the proposed and existing routing designs’ performance parameters, such as device utilization and maximum frequency. Table 2 gives that the proposed algorithm device consumption and maximum frequency outperforms other motion estimator techniques.

The proposed superfast JAYA-BM algorithm with Virtex7 device consumes the number of slice register of 687, and it is 96.8% lower than existing algorithm in

Table 2 Performance comparison of proposed superfast JAYA-BM and existing algorithms

References	FPGA device	Device utilization	Maximum clock frequency (MHz)	Power consumption (mW)
[17]	Spartan3 (XC3S20)	No. of LUTs—241	68.95	NA
[18]	Arria II Gx	No. of LUTs—19,106	200	NA
[27]	Virtex 4 (XC4VFX14)	No. of slice reg.—129 No. of LUTs—238 No. of slice FFs—154	222.875	6
[19]	Virtex5 (VLX110ff676-2)	No. of slice reg.—112 No. of LUTs—256 No. of LUT-FF pairs—94	NA	NA
[20]	Virtex6 (XC6VLX757-3)	No. of slice reg.—165 No. of LUTs—237 No. of LUT-FF pairs—118	320	NA

(continued)

Table 2 (continued)

References	FPGA device	Device utilization	Maximum clock frequency (MHz)	Power consumption (mW)
[21]	Virtex7 (XC7VX550T)	No. of slice reg.— 21,487 No. of LUTs— 30845	443	NA
[22]	Cyclone IV	Gate count—6157 LUTs	293	190
[23]	Altera	Gate count—21K	43	130
[24]	Virtex7	No. of FFs—144,302 No. of LUTs— 188,664	NA	NA
[25]	Virtex5	No. of slice reg.—7246 No. of logic cells—7089	100	NA
[26]	NA	NA	90	NA
[15]	Cyclone4 (EP4CE115F29C7)	No. of logic cells—9532	295	NA
Proposed	Virtex7 (XC7VX330t-2Lffg1157)	No. of slice reg.— 687 No. of LUTs— 1266 No. of LUT-FF pairs—1519	346.518	143
	Virtex6 (XC6VHX250t-2ff1154)	No. of slice reg.—691 No. of LUTs—1267 No. of LUT-FF pairs—1603	312.906	5793
	Kintex7 (XC7K480t-3ffg901)	No. of slice reg.—687 No. of LUTs—1268 No. of LUT-FF pairs—1535	392.665	182
	Zynq	No. of slice reg.—687 No. of LUTs—1256 No. of LUT-FF pairs—1524	346.518	176
	Artix7	No. of slice reg.—687 No. of LUTs—1262 No. of LUT-FF pairs—1437	297.734	42

[21]. The proposed superfast JAYA-BM algorithm with Virtex7 device consumes the number of slice LUTs of 687, and it is 95.89% and 99.33% lower than existing algorithm in [21, 24], respectively. Table 2 gives the maximum operating frequency of our proposed superfast JAYA-BM algorithm achieves maximum of 392.665 MHz; it is higher than existing algorithms in [15, 17, 18, 20, 22, 23, 25, 26]. The power consumption of proposed superfast JAYA-BM algorithm achieves minimum as 41 mW in Artix7 FPGA device; it is very lower than existing algorithms in [22, 23].

5 Conclusion

In this work, we have proposed a superfast motion estimator using block matching (JAYA-BM), without compromising searching speed. The JAYA-BM algorithm strives to search the motion vector by superfast manner. The proposed motion estimator have been implemented and synthesized using Xilinx ISE 14.5 with different FPGA families such as Virtex7 (XC7VX330t-2Lffg1157), Virtex6 (XC6vhx250t-2ff1154), Kintex7 (XC7K480t-3ffg901), Zynq (XC7Z045-2fbg676), and Artix7 (XC7a100t-3csg324). Our faster JAYA-BM outperformed previous algorithms in terms of device utilization, maximum frequency, and power consumption, according to simulation results.

References

1. Kibeya H, Belghith F, Ben Ayed M, Masmoudi N (2016) Fast coding unit selection and motion estimation algorithm based on early detection of zero block quantified transform coefficients for high-efficiency video coding standard. *IET Image Process* 10(5):371–380
2. Singh N, Mishra A (2016) Block matching algorithm for motion estimation using previous motion vector pattern. *Int J Comput Appl* 150(8):1–5
3. Radicke S, Hahn J, Wang Q, Grecos C (2014) Bi-predictive motion estimation for HEVC on a graphics processing unit (GPU). *IEEE Trans Consum Electron* 60(4):728–736
4. Chen P (2002) A fuzzy search block-matching chip for motion estimation. *Integr VLSI J* 32(1–2):133–147
5. Chen P, Chen H, Hung K, Fang W, Shie M, Lai F (2006) Markov model fuzzy-reasoning based algorithm for fast block motion estimation. *J Vis Commun Image Represent* 17(1):131–142
6. Cai J, David Pan W (2012) On fast and accurate block-based motion estimation algorithms using particle swarm optimization. *Inf Sci* 197:53–64
7. Alex Pandian S, Bala G, Anitha J (2013) A pattern based PSO approach for block matching in motion estimation. *Eng Appl Artif Intell* 26(8):1811–1817
8. Cuevas E (2012) Block-matching algorithm based on harmony search optimization for motion estimation. *Appl Intell* 39(1):165–183
9. Nie Y, Ma K-K (2005) Adaptive irregular pattern search with matching prejudgment for fast block-matching motion estimation. *IEEE Trans Circuits Syst Video Technol* 15(6):789–794
10. So H, Kim J, Cho W, Kim Y (2005) Fast motion estimation using modified diamond search patterns. *Electron Lett* 41(2):62
11. Cheung C-H, Po L-M (2005) Novel cross-diamond-hexagonal search algorithms for fast block motion estimation. *IEEE Trans Multimedia* 7(1):16–22

12. Tsai T, Pan Y (2006) A novel 3-D predict hexagon search algorithm for fast block motion estimation on H.264 video coding. *IEEE Trans Circuits Syst Video Technol* 16(12):1542–1549
13. Jing X, Chau L (2007) Partial distortion search algorithm using predictive search area for fast full-search motion estimation. *IEEE Signal Process Lett* 14(11):840–843
14. Chen H, Chen P, Lin C, Liu C (2012) Content-adaptive thresholding early termination scheme on directional gradient descent searches for fast block motion estimation. *Opt Eng* 51(11):117401
15. Vani R, Sangeetha M (2015) A new hybrid search algorithm with novel cross-diagonal-hexagon search video coding algorithm for block motion estimation. *Wireless Pers Commun* 88(2):211–222
16. Venkata Rao R (2016) Jaya: a simple and new optimization algorithm for solving constrained and unconstrained optimization problems. *Int J Ind Eng Comput* 19–34
17. Meyer-Baese U, Meyer-Baese A, González D, Botella G, García C, Prieto-Matías M (2014) Code obfuscation using very long identifiers for FFT motion estimation models in embedded processors. *J Real-Time Image Proc* 11(4):817–827
18. Pastuszak G, Jakubowski M (2015) Optimization of the adaptive computationally-scalable motion estimation and compensation for the hardware H.264/AVC encoder. *J Signal Process Syst* 82(3):391–402
19. Biswas B, Mukherjee R, Saha P, Chakrabarti I (2015) An efficient VLSI architecture of the enhanced three step search algorithm. *J Inst Eng (India) Ser B* 97(3):303–309
20. Biswas B, Mukherjee R, Chakrabarti I (2015) Efficient architecture of adaptive rood pattern search technique for fast motion estimation. *Microprocess Microsyst* 39(3):200–209
21. Yahi A, Toumi S, Bourennane E, Messaoudi K (2015) A speed FPGA hardware accelerator based FSBMA-VBSME used in H.264/AVC. *Evol Syst* 7(4):233–241
22. AlQaralleh E, Abu-Sharkh O (2015) Low-complexity motion estimation design using modified XOR function. *Multimedia Tools Appl*
23. Basha S, Kannan M (2016) Design and implementation of low-power motion estimation based on modified full-search block motion estimation. *J Comput Sci*
24. Alcocer E, Gutierrez R, Lopez-Granado O, Malumbres M (2016) Design and implementation of an efficient hardware integer motion estimator for an HEVC video encoder. *J Real-Time Image Process*
25. Lung C, Shen C (2016) Design and implementation of a highly efficient fractional motion estimation for the HEVC encoder. *J Real-Time Image Process*
26. Lee J (2017) Energy efficient processing of motion estimation for embedded multimedia systems. *Multimedia Tools Appl*
27. Praveena M, Balaji N, Naidu CD (2019) Hardware efficient block matching algorithm based on modified differential evolution optimization for fast motion estimation. *Analog Integrated Circuits and Signal Processing* 100(2):389–404. <https://doi.org/10.1007/s10470-018-1348-5>

Motor Vehicle Alert System in On-Campus Environments: Omniscient Vehicle Sensor



Phani Sridhar Addepalli, Tenneti Krishna Mohana, and G. Naga Satish

Abstract Nowadays, huge building infrastructure is the rock bottom must- has contrivance across the globe in every walk of life, especially in Educational Institutes and corporate buildings. This leads to inter-conveyance facility in celebutante moving and in general flexibility. In this view, motor vehicles are not the option as they produce noise and release pollutants. The battery-powered vehicles are chosen as their purpose is more strictly inside the campus or among the approach roads of various buildings inside the colleges or corporate buildings. But, this frequent movement of vehicles may cause hindrance to the pedestrians as well to the self in some instances. To get the better of, this paper suggests battery-powered vehicle alert mechanism. This will adopt omniscient vehicle sensors that is controlled and programmed by Arduino (or Raspberry Pi) through recognition of vehicles by magnetic field traced from the battery of the vehicles. This will activate the alarm or buzzer that alerts pedestrians and other battery-powered vehicles passing nearby. This may also help to overcome blowing the horn, intermittent unusual movement of vehicles creating difficulty to pedestrians, and vice versa. The buzzer/alarm mechanism or LED alerts are employed for better output and immediate responsive action. Solutions provided are merely for internal approach, but can be apprehended to real-time scenario if better throughput is observed.

Keywords Hall Effect sensor · Omniscient vehicle sensor · Magnetic field · Raspberry Pi · Arduino

P. S. Addepalli (✉)

Aditya Engineering College (A), Surampalem, India

e-mail: phani.addepalli@aec.edu.in

Jawaharlal Nehru Technological University Kakinada, East Godavari, Andhra Pradesh, India

T. K. Mohana

Aditya College of Engineering, Surampalem, India

e-mail: krishnamohana_ece@acoee.edu.in

G. Naga Satish

BVRIT Hyderabad College of Engineering for Women, Hyderabad, Telangana, India

e-mail: nagasatish.g@bvrithyderabad.edu.in

1 Introduction

Sensors are participatory in all process and development ecosystems as they operate on remote parameter sensing, capturing, observation, action mechanisms. Real-time usage, adoption in versatile applications imparting ecological appearance in daily life of human beings by making better decisions in all aspects especially safety and security, ease of access and independent behavior of instruments, appliances and mechanical equipment. In this deem, field of application is commute so as to uphold various characteristic architectural styles REST, RESTful, etc. In any of the feeling, prime need of developing a solution is not to be deviated for a wrong choice of sensor.

There are many road accidents [1] happening in the world creating disturbance in lives of people. This is happening because precautions are seriously not considered; detection and avoidance mechanisms are very poor even in metro cities. Better decisions will always make life happier, so in four junctions, busy roads, industrial areas adoption of vehicle prediction are much safer to reduce loss of life and improving technological uplift. According to World Health Organization, latest studies speak around 1.8 million people are suffering in road crashes due to various reasons, viz., unusual driving skills, abnormal mechanical failures, intermittent automobile interruptions, motor ridges etc. In all these aspects, best countries are losing approximately 3% of their gross domestic product. More accidents occur to road users like pedestrians, cyclists, walkers, motor cyclists as they are the vulnerable users. All these users are approximately in the age of nine to 29 years and from low and middle class income families in most of the identified countries as shown in Fig. 1. To overcome pitfalls facing, better solutions are proposed in different technologies with the help of various tools available in Internet of Things, machine learning, deep learning, and far more [2–4]. Perceptions in choosing sensor are more prominent rather than disseminating the prototype design. Collaborative references or external connections are taken much care, especially in outward designs to withstand wear and tear. So, sensor selection along with its inclusion in module by reserving all external factors like climatic conditions is more necessary. Especially, in huge campus, the sensors are planted in methodical locations that are approachable to all stakeholders and working people. This could be little disturbing in such a way that unknowingly, people might be the reason for damage of prototype or causation effects will arise. In this regard, the point of understanding always falls with the best chance for sensors, installation location, clear resilience to extreme conditions is prime addressable in multifaceted works by researchers. Also, more stress is made on geographical characteristics of employing a specific design methodology by majority of the researchers [5–7].

A broad view of characteristics, technical support, achievability in terms of design and methodological aspects are shown in Fig. 2.

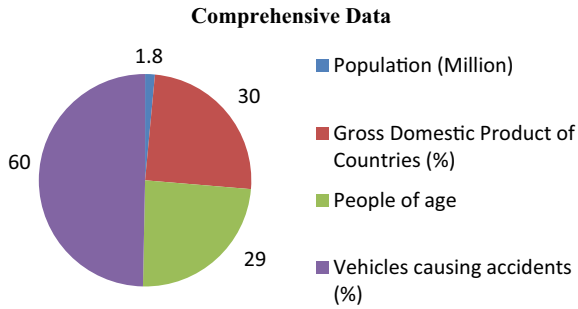


Fig. 1 Comprehensive study on effect of vehicles in various countries

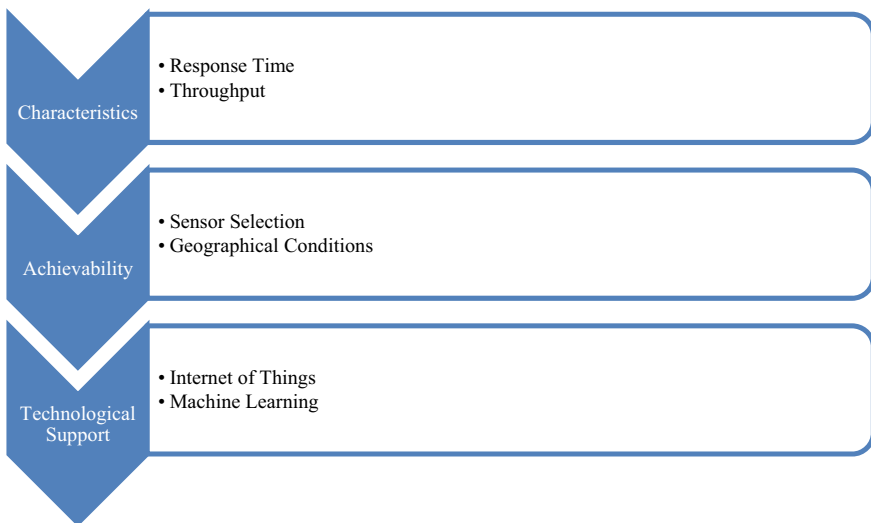


Fig. 2 Flow diagram for parameters in technology

2 Related Work

Most of the authors have made a clear identity in employing the best way of choosing sensors in design methodology like magnetometer used for vehicle detection as the sensor is suitable for either the bright side or the dark side, but in this aspect, a demerit falls in difficulty of mounting sensor on chip. Some works propose the use of ultrasonic sensor in cases of earning accuracy for soft materials attached to it, alongside the disallowance in farther distances is also an inevitable situation. Also, radar sensors [8] are applicable for some instances of vehicle detection even withstanding adverse conditions, but its range is short beside termed as a disadvantage. In some ambient requirements, optical sensors are chosen in applications like wearable technologies where no direct contact is needed, interference of direct operation is

observed as a disadvantage. Automotive sensor technologies are upheld with driving factors like detecting weight [9], observation of reducing bottom thrust, collision avoidance delivery systems, air bags lifting assurance are clear throat discussions made in some of the works. An accident alerting system and detection mechanism by dividing road side IoT clusters, providing security, and MAC layers involvement in greatest infrastructure details in turn relative adverse effects are reduced. Influx and outflux in human body are such a parameter indicating the abnormal behavior indicating the regular intervention of multiple process involving regular entities [10]. Adverse affects in heart conditions lead to prediction of accidents to overcome huge losses [11].

Especially, in automobile industry, ease of applications made Hall Effect sensor applicable as alternate of temperature control valve for balancing the cool engine parameters [12]. In land vehicle transporting mechanisms, the sensors employed for design of alert mechanism are achieving better solution set up for creating responses in a well effective manner in order to overcome percipitous entry of pedestrians and vehicles. Aggressions of mechanical perceptivity could be handled by inverting clear accelerometer in this design methodology. In another corner the behavioral analysis, design and integration of Hall Effect sensors [13] are assessed in veracity for Hall voltage, sensitivity, offset [14–17], temperature, and residual drift. At the end of this work, the concluding remarks are referred with behavioral and prediction in different Hall cell types. Some other studies Hall Effect sensors are experimented in four directions like single Hall Effect sensor, 5-array Hall Effect sensor, 4-crossing Hall Effect sensor, 4-array Hall Effect sensors. These results in understanding the influences in direction and position of Hall Effect sensors. Concluding remarks in these four direction experiments were given in obtaining optimum results by selecting the position of placement of Hall Effect sensor in various applications. Some prototype designs convey methodologies to overcome the road accidents while inconvenience of reading or understanding the sign boards. Here too, Hall Effect sensors will try to adopt the detection of vehicles in vicinity of magnetic fields. Unattended magnetization in order to approve and assess the performance measurement of sensors, performance observation, and performance identification to detect and prevent the vehicle crashes. Closest point approach is calculated as an identification point in order to verse the fixation and overcoming the clear regulation and care of the land vehicles. Magnetoresistive sensors are attaining much interest in order to consume less power toward unmanned vehicles. Here too, Hall Effect sensors are applicable in clear thought of investigation for UAVs [18–20], and comparative results were given in terms of accuracy, energy, and temperature variation. Many researchers worked in identifying, detecting, and alerting vehicles in busy areas to avoid mishap and cause of accidents. This is best enactment using various sensors in versatile design methods employing classes of sensors. For instance, vehicle detection is possible with magnetometer that really helps in getting better through put, but mounting on chip is difficult. This includes the smart foot wear, smart watch; household accessories, ovens, smart vehicles and every non-living thing/accessory interacted with the cloud, and analyzing and evaluating thereafter. The pin diagram and functional diagram of Hall Effect sensor is shown in Figs. 3 and 4.

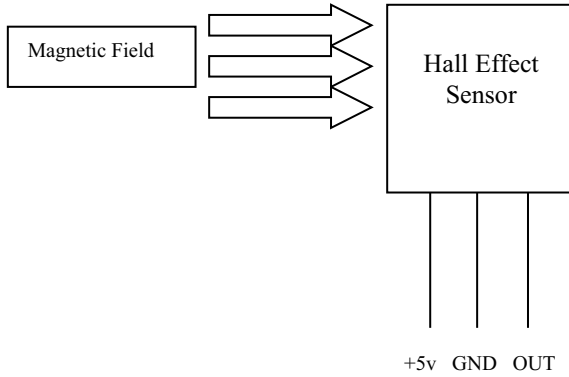


Fig. 3 Pin diagram of Hall Effect sensor

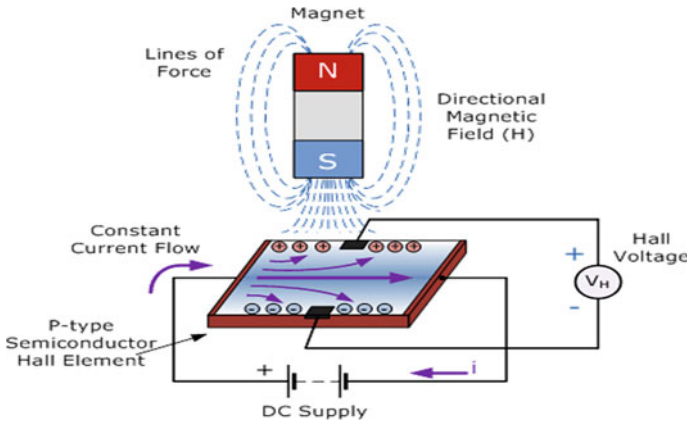


Fig. 4 Functional diagram of Hall Effect sensor

3 Design Methodology

In general, the design methodology for on-campus vehicle movement makes use of sensor for vehicle presence along with the LED/buzzer/alarm to show the near approach of vehicles. In this view, the pedestrians will be able to know the nearby arrival and can make sure of the unwanted ruptures. The working model for real-time implementation is shown in Fig. 6 that includes the sensor to recognize the magnetic field induced, and its resemblance is shown through the LED. Figure 7 depicts the block diagram of vehicle detection of Hall Effect sensor, Arduino board, and LED. The similar real-time usage is shown in Fig. 5 that recognizes the road vehicles in turn applies the enabling of lights attached to the circuit. The physical model shown in Fig. 8 takes a view of a junction in the connected campus where two sensors are embedded on a sheet for identifying the vehicle approachability. Here, it is necessary

to understand the need of multiple sensors that is the because of the less range of sensors used in the design. As we can see, the top layer is implanted with sensors, and black sheet is termed as roads, and the connections are made in such a way the Arduino board is communicating with the sensors in parallel.

Once the vehicles are identified upon detection of induced magnetic field beyond a threshold value, then the control action can be immersed upon requirement. The magnetic field impulse is generally acted upon the pressure applied on the accelerator blade of the four wheelers as shown in Fig. 6. So, the main opportunity is to apply the complete process on the four-wheeler vehicles on the approach roads between the buildings inside the campus. The similar deployment is possible in real time by implanting the sensors under the ground at certain distances. The distance measured marked for multiple sensor installation is based on the threshold values of the sensors. In industrial applications, high-end sensors with better response time, threshold, and efficiency are used to achieve best results because of the frequent



Fig. 5 Snapshot of lights responding to sensor

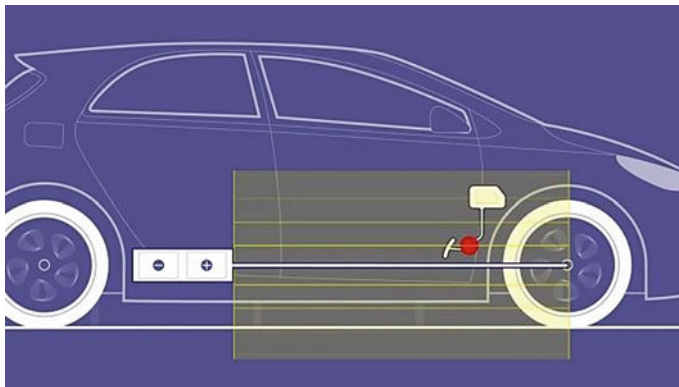


Fig. 6 Opaque view of magnetic induction in a motor vehicle

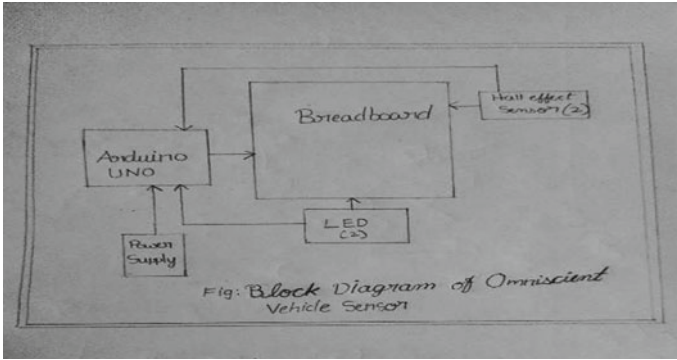
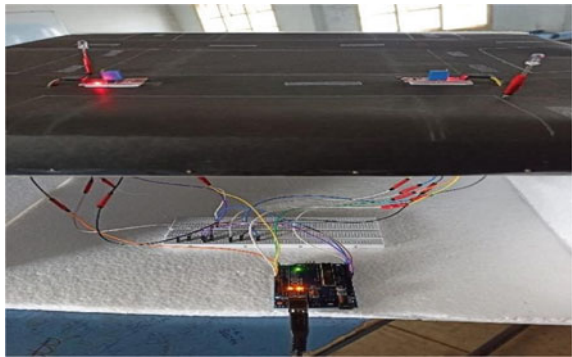


Fig. 7 Block diagram of omniscient vehicle sensor

Fig. 8 Design model of omniscient vehicle sensor



movement of vehicles due to integrated processes among the multiple production units. More certainly, threshold values are much more critical so as to enact the responsive measures between the sensors, in turn integrating resultant activities in order to gather the creation alerts.

4 Results

In the design methodology, couple of Magnetometers have been installed as shown in Fig. 9: Sensor is shown with LED's shown opposite of the sensors, and it is remarkable to share the glowing of Magnetometer 1 (MM1) or Magnetometer 2 (MM2). Similarly, in the other Fig. 10, if the magnetic field is induced near to Magnetometer 1 (MM1) or magnetometer 2 (MM2), the LEDs connected in respect to the sensors are activated, and indication is made for presence or approaching of vehicles.

Fig. 9 Design model for MM–MM2 of omniscient vehicle sensor

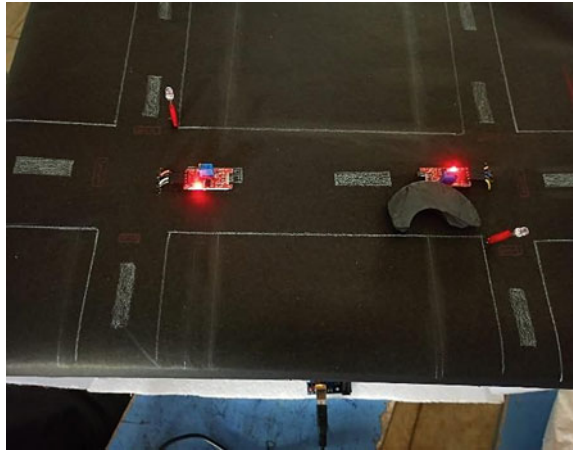


Fig. 10 Design model for MM1–MM2 LED resemblance



4.1 Finding 1

The output graph for the proper balancing of sensors working in reference of vehicles with active magnetic field shown in Fig. 11. It is also observed that the same kind of results is obtained in respective areas of implementation, viz., four road junctions, building cross-over, zebra crossings across the parking areas.

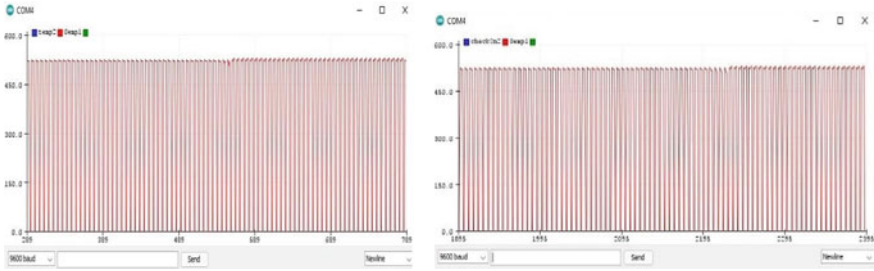
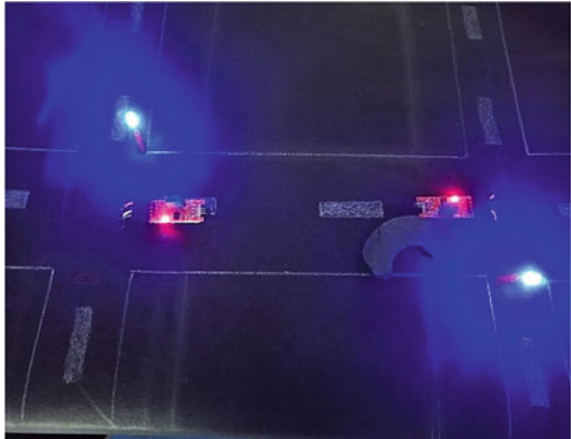


Fig. 11 MM1-graph with respect to MM2-graph

Fig. 12 Design model for MM2-MM1 of omniscient vehicle sensor



4.2 Finding 2

Figures 12 and 13 depict the influence of magnetic field induced across the lanes and its effect in LEDs. Figure shows the identification nearer to the field of magnetism whereas the figure shows the far detection and resemblance of magnetic field induced and its unchanged closure on the Hall Effect sensors.

The output graph in Fig. 14 gives results the effect of Magnetometer 1 toward Magnetometer 2, whereas graph in figure shows the significance of Magnetometer 2 to Magnetometer 1.

4.3 Finding 3

Among all the discussed and detailed results and findings, even though many sensors are applicable for addressing the problem in much better and simpler way, Hall Effect sensors are employed in this work due to its approachability and better results.

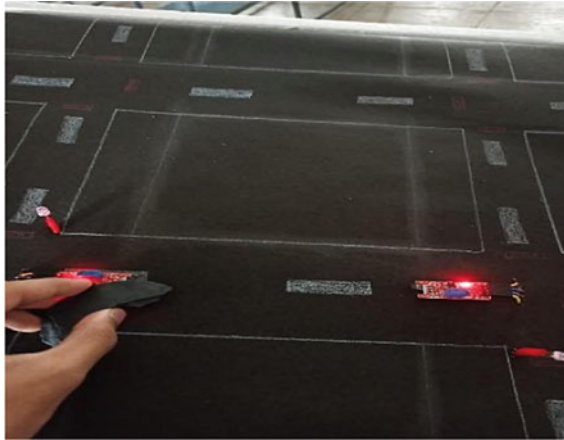


Fig. 13 Design model for MM2–MM1 LED resemblance

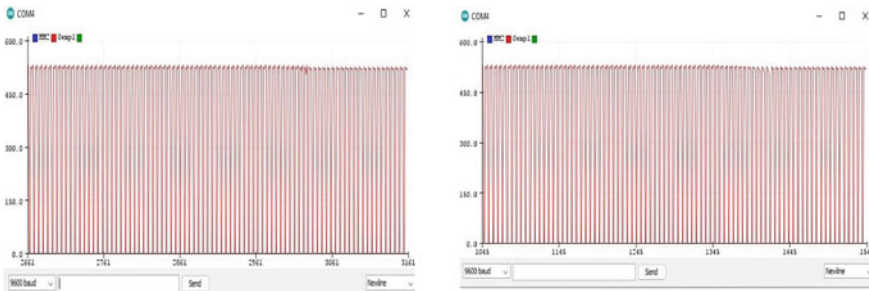


Fig. 14 MM2-graph with respect to MM1-graph

This is exactly true and the differential understanding could be mentioned clearly in Table 1 under various situations and scenarios. Also, the alert mechanism can be distinguished in order to approve better results, reliability, and usage.

Table 1 Epitome of sensor selection and its comparison

Type(s) of sensor	Reliability	Applicability	Results	No. of sensors used
Hall Effect sensor	H	Suitable	Accurate	As required
Proximity sensor	L	Only for local boundaries	Unpredictable	Massive
Ultrasonic distance sensor	M	Shorter range	Unpredictable	NA
Motion sensor	L	NA	Unpredictable	NA
Pressure sensor	L	NA	Unpredictable	NA

H—high, L—low, M—moderate, NA—not applicable

5 Conclusion

As the transport conveyance is a mandate need in large spread campus of educational institutes, software firms and other sector domains, this paper shows an economical and fruitful solution that overcomes the problems raised. The Hall Effect sensors used will predict the magnetic field induced from the motor/battery vehicles and raise an alarm or buzzer that alerts the pedestrians to give a safe passage without creating any disturbance. Also, comparative statement and study is made at the end of the paper to show case the differentiation among various sensors, its implementation, reliability, applicability, and some other factors.

6 Future Scope

In future, the working prototype can be properly replicated in huge campus environments by installing the sensors under the ground. The sensors are connected either wired/wireless for transfer of information, i.e., communication is through various wired/wireless technologies. Besides the data collection, analysis and prediction can also be done with sound technologies and tools. Much more data analysis is applicable with collection tools along with versatile cloud storage mechanisms.

References

1. Keerthika R, Atchaya S, Bharathi M, Hamsaleka K, Monika C (2018) Road vehicle alerting and accident detection system using IoT. *Int J Pure Appl Math* 118(11)
2. (2014) Vehicle detection and tracking techniques: a concise review. *Signal Image Process Int J* 5(1)
3. Hu J, Sun Y, Xiong S (2021) Research on the cascade vehicle detection method based on CNN. *Electronics* 10:481. <https://doi.org/10.3390/electronics10040481>
4. Tak S, Lee J-D, Song J, Kim S (2021) Development of AI-based vehicle detection and tracking system for C-ITS application. *J Adv Transp* 2021:15, Article ID 4438861
5. Chikaka TP, Longe OM (2021) An automatic vehicle accident detection and rescue system. In: 2021 IEEE 6th International forum on research and technology for society and industry (RTSI), pp 418–423. <https://doi.org/10.1109/RTSI50628.2021.9597212>
6. Lopes PC, da Silva JCS, Guarieiro LLN et al (2021) Study of environmental data from vehicle's sensors and its applicability to complement climate mapping from automatic meteorological stations and assess covid-19 impact. *AI Perspect* 3:5
7. Taheri Tajar A, Ramazani A, Mansoorizadeh M (2021) A lightweight Tiny-YOLOv3 vehicle detection approach. *J Real-Time Image Proc* 18:2389–2401
8. Fleming WJ (2008) New automotive sensors—a review. *IEEE*
9. Mandal NK et al (2018) Accident detection and alerting system with continuous heart rate monitoring using Arduino for two wheeler
10. Paun M-A (2013) Hall effect sensors design, integration and behavior analysis. *J Sens Actuator Networks*
11. Sriratana W (2012) Application of Hall effect sensor: a study on the influences of sensor placement

12. Mario A. GN (2018) Alert system for high speed and acceleration in land vehicles. *Indian J Sci Technol*
13. Bressan P (2019) Application of Hall effect sensor in temperature control valve of automotive internal combustion engine. *Int J Adv Eng Res Sci (IJAERS)* 6(12)
14. Mounika J, Charanjit N, Saitharun B, Vashista B (2021) Accident alert and vehicle tracking system using GPS and GSM (17 Apr 2021). *Asian J Appl Sci Technol (AJAST)* 5(2):81–89
15. Wang B, Han Y, Tian D, Guan T (2021) Sensor-based environmental perception technology for intelligent vehicles. *J Sens* 2021:14, Article ID 8199361. <https://doi.org/10.1155/2021/8199361>
16. Sanguesa JA, Torres-Sanz V, Garrido P, Martinez FJ, Marquez-Barja JM (2021) A review on electric vehicles: technologies and challenges. *Smart Cities* 4:372–404. <https://doi.org/10.3390/smartcities4010022>
17. Herrero R (2022) Ultrasonic physical layers as building blocks of IoT stacks. *Internet Things* 18, 100489. ISSN 2542-6605
18. Prabhakar P (2020) Traffic control management system and collision avoidance system. *IOP Ser*
19. Christou CT (2014) Vehicle detection and localization using unattended ground magnetometer sensors
20. Zhu K (2018) Performance study on commercial magnetic sensors for measuring current of unmanned aerial vehicles. *IEEE*

Backup and Restore Strategies for Medical Image Database Using NoSQL



Jyoti Chaudhary, Vaibhav Vyas, and Monika Saxena

Abstract Health care is one of the fast-growing industries. It is among the foremost well-known divisions within the world where the information created from such industries is extremely huge in volume. It generates relevant healthcare data, including medical images, as part of the healthcare information system (HIS). This data can be used for current and future decision-making of some clinical aspects; it can be sometimes real time too. Moreover, presenting an image in real time can be very challenging. In this way, a legitimate reinforcement is required to preserve for such valuable information so that it can be reestablish at the time of prerequisite. This huge data of medical industry are hard to store and recover at the time of requirement. Keeping the earlier research in observation, few strategies are presented in this paper which centers on the diverse strategies that can be utilized to store the medical images utilizing NoSQL database which are considered the leading to store expansive volume of information.

Keywords Backup · Large datasets · Medical images · DICOM · MongoDB · NoSQL database · Recovery · Storage

1 Introduction

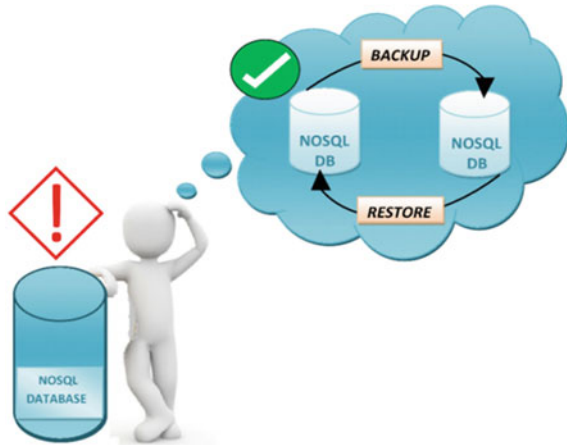
The billions of medical images are assessed to be produced each year with a huge increase. It is indeed evaluated that the healthcare industry information will develop around 30% from year 2020. And this gigantic sum of information requires a best reasonable database which can handle it productively. NoSQL databases are considered as best databases as they are able to store the organized, semi-structured, and

J. Chaudhary (✉) · V. Vyas · M. Saxena
Banasthali Vidyapith, Jaipur, India
e-mail: [jyotichaudhary1410@gmail.com](mailto: jyotichaudhary1410@gmail.com)

V. Vyas
e-mail: [vvaibhav@banasthali.in](mailto: vvaibhav@banasthali.in)

M. Saxena
e-mail: [smonika@banasthali.in](mailto: smonika@banasthali.in)

Fig. 1 Backup and restore using NoSQL



unstructured information viably [1]. But, reestablishing the information after a few disappointments or catastrophe is presently another challenge that is confronted within the industry. Since information is the center prerequisite of any industry, the organizations spend a part to ensure the information from any undesirable disappointment or destruction. The data can be lost or impassable due to various reasons. When it comes to software, the data misfortune can be done due to two reasons, these can be catastrophic failure and human error (Fig. 1).

Catastrophic failure is a kind of natural disaster in which all the data from the roots of production system is deleted including every node. When data are stored in the same data centers, disasters are more likely to destroy it. So, the servers should be kept at different data centers, which should a thought when provoking a backup strategy [2, 3]. Human error includes the bugs, hacking of the system, or accidentally deleting of the data. This data can be fixed by replicas of the data automatically within seconds [2, 3]. Therefore, to protect data from such instantaneous conditions, backup and recovery are a perfect suite. The backup and recovery strategies can be used to ensure the safety of data even in the case of any kind of data loss. Through this, business operations can be restored easily without any economic harm to the organization.

2 Literature Review

Rebecca and Shanthi [2, 3] suggest that the huge amount of data has given rise to the concept of NoSQL databases. This is necessary due to the fact that such schema-less data must be stored. As a result, NoSQL databases are particularly effective and acceptable databases for storing and retrieving heterogeneous data. The IT industry is undergoing a paradigm shift that entirely disrupts the reality of

storing and accessing data via NoSQL databases. The healthcare business is increasingly becoming a component of organizations that deal with large amounts of data, necessitating the use of effective database models for storing and retrieving data, particularly medical pictures. Medical images must be kept in good condition, which can be harmed if they are not stored appropriately. Furthermore, the results of how different databases are reviewed and compared to deal with medical data will be presented in this study.

Gotseva et al. [4] found a database should enable for the recovery of lost data that may have been missing or lost due to a dispute such as system failure, user error, or any other unwelcome tragedy. Before enhancing a software installation, backups are recommended as a precautionary measure to protect data, and they can also be utilized to transfer the installation to another system. As a result, the focus of this study is on possible backup and recovery methods for huge databases. When transactions are required to backup hourly, a backup might be measured on a weekly, daily, or monthly basis. As a result, this paper will outline all related solutions for dealing with databases containing large amounts of data.

Kaur [5] stated that NoSQL databases are highly effective and optimized to perform retrieval and adjoining operations of huge amount of data. Thus, this paper demonstrates various NoSQL databases among which highly scalable database are MongoDB, which is a document-oriented database. Therefore, these databases can be considered for huge amount of data which needs to be scalable and perform effective such as real-time data and medical data like images.

Zaman and Butt [6] say it is not a matter of any century which requires the backup; it is a focal attribute which should be associated with every database management system to provide a security toward data loss. Every business is using different approaches of database systems to manage all the functioning of the organizations that are interconnected through Internet which requires finding an appropriate strategy of attaining backup and restoring of data. Yet, few technologies like ORACLE have their backup and recovery tools, but these tools cannot be used with every DBMS. These can be contributed with heavy price set depending on the licenses acquired by an enterprise. Thus, this paper targets on the solutions required to keep in spotlight before designing or subscribing a backup and recovery tool for the current architecture used. This further will introduce the quick fixes to provoke the efficient recovery during any cause. This has reshaped the simplest ways to enforce, and these can be employed to any category of database, i.e., single or multiple database systems.

Karanjkar et al. [7] explain how MongoDB is a big data innovation, and its capacity to accommodate numerous data types and improve efficiency can help it broaden its reach across the data sector. Considering the importance of RDBMS, author agrees that they are useful, but the storage requirements for new applications are vastly different from those for older applications. Further, MongoDB has been chosen over MySQL because of ease of use and performance. MongoDB GridFS is a high-performance storage specification for images and huge files in MongoDB. It ensures that the file is broken down into manageable bits and saved in a database. MongoDB is the future of data storage, posing a threat to established relational database systems.

Thus, MongoDB is proven here the best NoSQL database to deal with unstructured data in effective way.

3 Backup Deliberations

The backup systems used to take screenshots of the work that had been done in the system at the time. One of the most powerful features of these systems is that when data are lost, the clock reverts to normal operation and rolls back the data from the unexpected event. Before establishing a backup strategy, an organization assesses recovery point objective (RPO) and recovery time objective (RTO). RPO refers to the maximum quantity of data that can be lost, whereas RTO refers to the time it takes to recover the data. These two elements aid in determining the backup maintenance costs. Despite this, a few other factors are taken into account when determining the optimum backup and recovery method, including isolation, performance, restore procedure, sharding, and deployment complexity [8].

After all of the criteria have been determined, a better plan must be examined. Why do we need a backup or the ability to travel back in time? Sundry is one of the reasons behind this. Operational failures might result in a slew of issues. An operator error, for example, can result in data loss, which is fairly common. It is also tough to revert to a previous version after making such a mistake [9]. If all goes well, the next step is to consider the recovery. The best backup system in the world won't save you [10], but a competent recovery system can. One effective suggestion for recovering data after a loss is to list the criteria before moving on to the next phase. The following are a few topics to think about:

- Amount of data that can be loose without concern? Is it fine to loss data worked after the last backup?
- How much time is required to recover data and how fast it can be done?
- Which data are actually required to recover like tables and databases?

4 MongoDB and Its Possible Backup Strategies

The NoSQL movement is a modern approach to data persistence that uses novel storage mechanisms [11]. These databases were created to accommodate the large amounts of data that are being generated on a daily basis. The latency and scalability that is more suitable for picking an appropriate document-oriented database to deal with huge images and voluminous data [12]. As a result, the MongoDB NoSQL database is used in this work to offer backup and recovery for massive amounts of medical data. MongoDB is a schema-free document-oriented NoSQL database that stores documents that are divided into collections. It is written in C++, Python, Go, and Javascript, among other languages. It provides indexing of document fields, making them quickly available through the entire collection. It is also a smart database

as it only supports indexing if number of reads is much greater than number of writes. It supports map reducing which helps in managing the large-sized files. Though it is a combination of great features, it also provides some backup and restoring mechanisms which can be used to protect the data from any unexpected event.

Since the medical industries are facing challenges in managing different types of image patterns which includes DICOM and raw image data. As we are aware with the fact that MongoDB is capable of holding binary data as well as immense data by using JSON data swapping composition. MongoDB has great features like BSON format and grid file system [2, 3]. Researchers have demonstrated that the MongoDB NoSQL database can be used to store medical images. The author suggests document-oriented databases as the best for DICOM format files. Thus, let us review few backup strategies provided by MongoDB. These include:

- 4.1 Mongodump
- 4.2 File system snapshot
- 4.3 MongoDB management service (MMS)

External backup strategies:

- 4.4 OPS manager software
- 4.5 Cluster control backup.

4.1 Mongodump

It is a utility tool bundled with MongoDB which performs backup of MongoDB data. It can dump an entire database, collection or result of a query. It constantly captures the screenshot of the data by dumping the oplog [8]. The archive mode in mongodump allows several collections to be packed non-contiguously within the archive. As a result, multiple collections can be restored in simultaneously in mongorestore (as is already feasible in directory mode). Goroutines are used in mongodump as it is initially written in GO language. Mongodump archive architecture is shown below to take a look how it works (Fig. 2).

Later on, the mongorestore utility can be used to restore the data to new or existing database. Mongorestore imports the data from BSON database dump that was produced by mongodump and restores the oplog. Mongorestore imports the data from BSON database dump that are produced by mongodump and rerun the oplog.

4.2 Copying the Underlying Files

It is applicable to file which database processes to store the data. It captures the screenshots of the respective files. These snapshots are portable and can be relocated to any datacenter. As a result, you have complete control over the file snapshots. These snapshots are also referred to as diff snapshots because they simply record



Fig. 2 Mongodump archive architecture [13]

the differences between the snapshots taken previously. These snapshots can be used to construct a new volume. To restore the database, you do not need to download the snapshots. But, to capture a consistent screenshot of the database, all the write operations must be stop and use either snapshot copy tools like cp and resync or capture the screenshot of entire file system if the volume manager supports. Stopping all the writes is also required to ensure the consistency of the data. If these two requirements are satisfied, then no more preparation is required for this process. The command used to stop all write operations in MongoDB is `db.fslock()` [14]. Snapshots can be captured at two levels [15]:

- Cloud—Level snapshots
- OS—Level snapshots

If the snapshot has been captured at cloud level and the cloud service providers like AWS are used to store database, then AWS EBS snapshots will be taken for the backup. If the database is stored in OS level, like LINUX, then LVM snapshots have to be taken. But, these snapshots, i.e., LVM snapshots are not portable that means they are not comfortable to run at any device. Thus, the cloud-based snapshots are preferred better (Fig. 3).

Snapshot of data is like copying modified data to original volume of snapshot whenever any write operation is performed as shown in the figure [15]. To restore, mongod must not be in running state. The command varies to restore depending on the file system [14].

4.3 MongoDB Cloud Manager

It is a cloud-based backup solution which provides point in time restore. It stores backup in MongoDB cloud for which a backup agent is installed that manages an

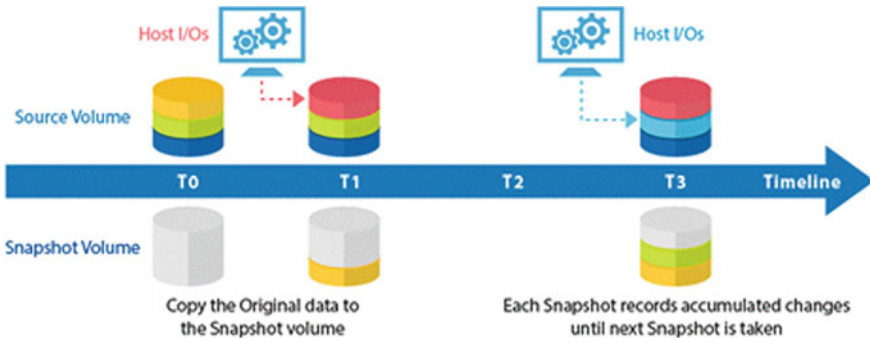


Fig. 3 Snapshot process [15]

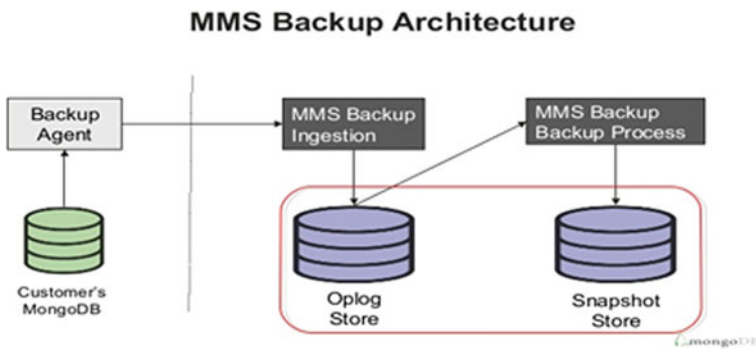


Fig. 4 MMS backup architecture

initial sync to secure MongoDB and replicas at different centers. After that initial sync, MMS supports encryption and compression of oplog data to have a continuous backup of data (Fig. 4).

By default, snapshots captured by this service are after every 6 h; oplog data keep it for 24 h [8]. The backup for sharded systems is also maintained by reading the oplog data which is hardly supported by any other backup strategy.

4.4 OPS Manager

It ensures the point in time by default. It captures the screenshots as the backup starts for the database, or it can be said the screenshots captured at the end of the mongodump process. And the backup for sharded systems, each shard's primary member is been synced such that the initial sync and oplog data are back to ops manager from https. The ops manager maintains the one-head database for every replica set further the backup executes the initial sync and the tailing of oplog by using

mongo queries. The snapshot capturing process for sharded systems temporarily stops the balancer to insert marker token for all the shards and config servers. The snapshots by ops manager are captured when the marker token comes into the view. The space required to store the snapshot can be reduced on the location of its storage like MongoDB block store, Aws S3 bucket, and file system store. This is something like which can be incorporated to overcome the drawback of mongodump which takes long span for large-sized inputs [15].

4.5 Cluster Control Backup

It is a database management system that allows monitoring, deploying, and managing and scaling of the database. This automates some operations like deploying a cluster, adding or removing of node from a cluster, continuous backups, and scaling the cluster.

The abovementioned tasks can be done using GUI provided by cluster control. There are two backup approaches braced [16] are mongodump and MongoDB consistent backup.

Both the methods can be selected according to the need and requirement. These tools sign a unique id to all the backups and store this under path: CLUSTER CONTROL > SETTINGS > BACKUP > BACKUPID. When the specified node is not live during backup, then this backup technology automatically finds the node from the cluster and then processes it for backup. It also provides scheduling job for backup. Figure 5 shows the architecture for cluster control [17].

5 Comparison Between MongoDB In-Built Backup Strategies

Parameters	Mongodump	File system	MMS cloud backup
Initial complexity	Medium	High	Low
System overload	High	Low	Low
Point in time recovery	Yes	No	Yes
Consistent snapshot of sharded system	Yes	Yes	Yes
Scalable	No	Yes	Yes
Restore time	Slow	Fast	Medium

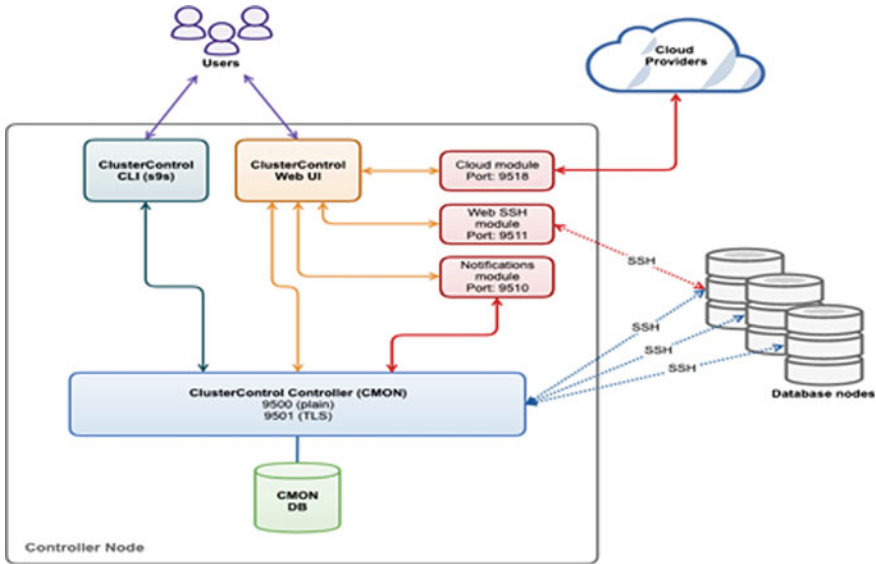


Fig. 5 Cluster control architecture [17]

6 Comparison Between Cluster Control and Ops Manager

Parameters	Cluster control	OPS manager
Deploy replica set, sharded cluster	Yes	Yes
Metrics monitored	Host metrics, MongoDB metrics	Host metrics, MongoDB metrics
Custom dashboards	Yes, plus advisors	Yes
Cloud/IaaS provider integration	AWS S3 (for backups)	AWS S3 (for backups)
Consistent backups (sharded)	Yes	Yes
User and group management	Yes	Yes
Secure installation	Default	Supported
Auto-recovery	Explicit	No
Scriptable command line	Yes	No

7 Future Scope and Conclusion

NoSQL document store-based approach is cost-effective, highly scalable, and provides superior data loading performance, with scarification of real-time data

consistency [18]. Since NoSQL is center of properties required to work on medical images or unstructured data, then one can too utilize their reinforcement and recuperation components to improve the complexity of structure required at the time of reinforcement. All the conceivable backup techniques with MongoDB NoSQL database have been talked about over which guarantees that the significance of backup and recovery. On the off chance that the disappointment happens with the database must be recuperate accurately and conveniently. NoSQL databases give them possess backup strategies and a few outside strategies which can be utilized to optimize the database without affecting the execution. In spite of the fact that MongoDB can be a total structure to bargain with enormous amount of data, this doubtlessly can offer assistance analysts to upgrade the compatibility required at the time of restoring data at whatever point required. Thus, this study in future can help the researchers in implementation of the strategies to contribute a system which provides everything at one place which further results to benefit medical industries.

References

1. Rebecca DR, Shanthi IE (2017) Medical image handling in the cloud based on document databases. *Int J Comput Appl* 169(7):46–49
2. Rebecca DR, Shanthi IE (2016) A NoSQL solution to efficient storage and retrieval of medical images. *Int J Sci Eng Res* 7(2)
3. Rebecca DR, Shanthi IE (2016) Analysing the suitability of storing medical images in NoSQL databases. *Int J Sci Eng Res* 7(8)
4. Gotseva D, Gancheva V, Georgiev I (2011) Database backup strategies and recovery models. In: *Challenges in higher education & research*
5. Kaur H (2021) Analysis of NoSQL database state-of-the-art techniques and their security issues. *Turk J Comput Math Educ* 12(2):467–471
6. Zaman M, Butt MA (2013) Enterprise data backup & recovery: a generic approach. *IOSR J Eng (IOSRJEN)* 3(5):40–42
7. Karanjkar D, Barve K, Metri M (2019) NOSQL over RDBMS in image storing using MongoDB. *NCRD's Tech Rev e-J* 4(1):1–10
8. Backup and its role in disaster recovery (n.d.). MongoDB. Retrieved 15 Dec 2021, from <https://www.mongodb.com/backup-and-its-role-disaster-recovery>
9. Carvalho N, Kim H, Lu M, Sarkar P, Shekhar R, Thakur T, Zhou P, Arpaci-Dusseau RH (2016) Finding consistency in an inconsistent world: towards deep semantic understanding of scale-out distributed databases. *Hot Storage*
10. Schwartz B, Zaitsev P, Tkachenko V, Zawodny JD, Lentz A, Balling DJ (2008) High performance MYSQL: optimization, backups, replication, load balancing & more, p 472
11. Mackin H, Perez G, Tappert CC (2016) Adopting NoSQL databases using a quality attribute framework and risks analysis. In: *Proceedings of the fifth international conference on telecommunications and remote sensing*, pp 97–104
12. Băzăr C, Iosif CS (2014) The transition from RDBMS to NoSQL. A comparative analysis of three popular non-relational solutions: Cassandra, MongoDB and Couchbase. *Database Syst J* 5(2):49–59
13. Mongodump archive principles (2016, Aug 30). Alibaba cloud. Retrieved 21 Dec 2021, from <https://www.alibabacloud.com/forum/read-370>
14. Chodorow K (2013) MongoDB: the definitive guide, p 357
15. Point-in-time, space-saving copies (n.d.). Infortrend. Retrieved 27 Nov 2021, from <https://www.infortrend.com/us/solutions/snapshot>

16. A review of MongoDB backup options (2018, Aug 08). Severalnines. Retrieved 20 Dec 2021, from <https://severalnines.com/database-blog/review-mongodb-backup-options>
17. Cluster control components (n.d.). Severalnines. Retrieved 15 Nov 2021, from <https://severalnines.com/docs/intro.html>
18. Teng D, Kong J, Wang F (2019) Scalable and flexible management of medical image big data. *Distrib Parallel Databases* 37(2):235–250. <https://doi.org/10.1007/s10619-018-7230-8>

Bandwidth Enhancement of Circular Wheel Slot Antenna for GPS, WLAN and C-Band Applications



Ramesh Deshpande, T. V. Ramakrishna, and B. Rama Sanjeeva Reddy

Abstract This work proposes is for a single line—feed, tri-frequency hexagonal Substrate circular Micro-strip Patch Antenna (SMPA) with a wheel shape five slots covering different wireless applications. With a bandwidth of 1630 MHz, 930 MHz and 890 MHz, the novel antenna resonates at 1.31 GHz (GPS L-band), 3.72 GHz and 5.14 GHz (C-band), respectively. To produce circular polarization at lower resonant modes for GPS applications, a wheel shaped slots are carved inside the radiating patch. The circular micro-strip patch antenna has a radial dimension of 18.36 mm.

Keywords Tri band · CP · Wheel slot · HFSS · FR4

1 Introduction

With the developing demand for wireless communications, more users are searching for antennas that satisfy the 1.31 (1.22–1.557 GHz)/5.14 (5.1–5.35 GHz) standards in L-Band, Wireless Local Area Network (WLAN) and Satellite communications. Patch antennas with slots have excellent performance because to its low profile, compact size, light weight and ease of construction [1, 2]. The most basic version of a patch antenna, which consists of a conducting patch and ground plane printed on substrate and radiates exclusively at one resonant frequency band [3, 4]. However, the increasing demand for wireless telecommunication services necessitates the usage of multi band antennas that resonate at several frequencies and can be utilized for a variety of functions in current wireless communication systems. So, in recent years,

R. Deshpande (✉)

Department of ECE, Koneru Lakshmaiah Education Foundation, Vaddeshwaram Guntur, India
e-mail: ramesh.23211@gmail.com; ramesh.deshpande@bvrit.ac.in

T. V. Ramakrishna

Department of ECE, Sasi Institute of Technology and Engineering, Tadepalligudam, West Godavari, Andhra Pradesh, India
e-mail: tvrk@sasi.ac.in

R. Deshpande · B. Rama Sanjeeva Reddy

Department of ECE, B V Raju Institute of Technology, Medak, India

a number of approaches for overcoming the aforementioned challenge have been developed, one of which is the creation of an antenna employing slot structures [5]. Some unique slots, including as the rhombus and cross slot, are introduced in [6–9] to expand the flexibility and generality of antennas. Antenna resonant modes and impedance matching are greatly influenced by slots variation in shapes of. Moreover, various novel patch shapes are used to improve the antennas' faults in terms of the boundary condition and cavity model. It is constructed with a circularly polarized antenna based on a rectangular patch antenna surrounded by a circle ground.

A wheel shaped slot antenna is implemented to generate tri bands for WLAN applications. After optimization, the developed wheel shaped slot antenna achieves tri band features and excellent impedance matching to meet WLAN requirements. The antenna is simulated on FR4 substrate with side of 28.5 mm. The analysis and implementation outcomes are thoroughly explored in this work.

2 Design and Analysis of Wheel Slot Antenna

Figure 2 depicts the proposed antenna's configurations and a detail view. The wheel slot antenna is made up of an annulus ground (the outer radius is R_1 and the inside radius is R_2) and a circle patch (R_3) that is divided into five symmetrical sector sections by five slots intersecting at the patch's centre. The five slots are coupled with the spacing between the centre patch and the ground. In this proposed design, the ground plane and the patch are made up of conductor (copper) with thickness of 35μ .

The antenna is simulated over Ansoft HFSS software Designed using FR4 substrate with a dielectric constant of 4.4 and a thickness of 1.57 mm, as shown in Fig. 1, as a part of Antenna 1 and it represents the Conventional Hexagonal substrated circular patch antenna with Dimensions of side 28.5 mm. This Hexagonal Patch antenna is modified as shown in Fig. 2 by making five slots inside the circular patch with equal angle of 72° with a dimensions of $18.36 \times 2 \text{ mm}^2$. Performance of the patch is observed by changing the dimensions of the slots as part of Antenna 2.

3 Implementation

The optimized antenna design has a VSWR (≤ 1.5) in different modes by modifying the structure of the printed antenna, as illustrated in Fig. 2. Circular patch having a radius show it in figure designed on a regular Hexagonal FR-4 substrate side of 28.5 mm with a relative permittivity of 4.4 and a thickness of 1.57 mm. In the Ansoft HFSS simulator, a line feed of $2.4 \times 7 \text{ mm}^2$ is used to simulate these dimensions. When compared to previous iterative designs, simulation is used to acquire the optimum outcomes with impressed bandwidth, gain and VSWR, as well as the requisite tri band frequencies.

Fig. 1 Design of antenna iterations **a** Antenna 1 **b** Antenna 2 **c** Antenna 3

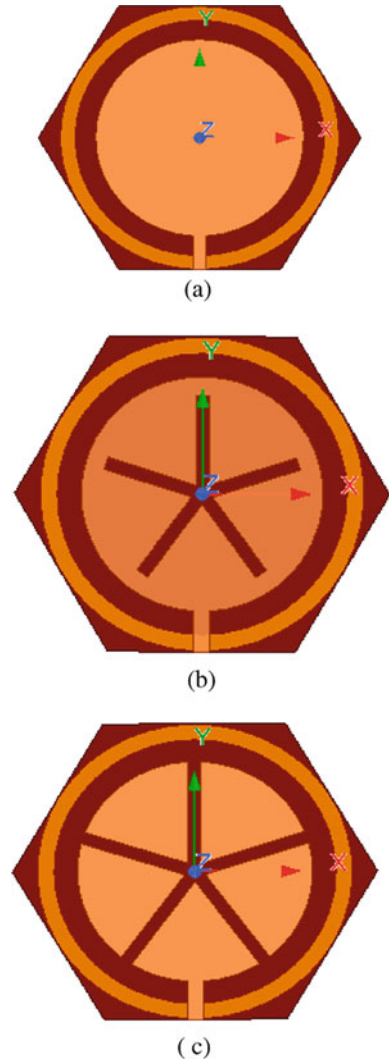


Table 1 shows the dimension of the optimum final desired shape of the high performance antenna design with line feed.

4 Results and Discussion

Figure 3 shows return loss curve, while numerous iterations on the conventional patch can result in more resonant bands, it is critical to extract the best gain and impedance bandwidth for all of the resonant bands generated by the final iterative

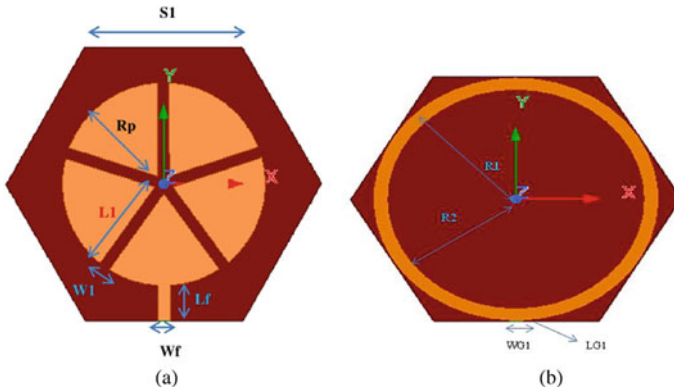


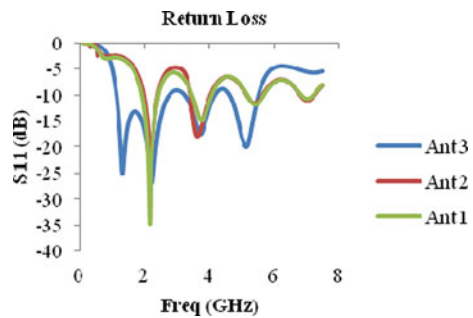
Fig. 2 Optimized proposed antenna structure

Table 1 Dimensions of the optimized antenna structure

Parameter	mm	Parameter	mm
S1	28.5	W1	2
Rg1	24.6	L1	18.36
Rg2	22	Wf	2.4
Rp	18.36	Lf	6.35
WG1	2.4	LG1	0.082

design. Figures 4 and 5 shows when compared to the performance metrics of the other design iterations, the response of the return loss curve shows that an impedance bandwidth of 1630 MHz is attained at 1.31 GHz resonant band with a high gain value of 9.57 dBi, and 930 MHz is attained at 5.14 GHz resonant band with a high gain value of 9.53 dBi which gives the best performance characteristics. Figure 6 shows the radiation pattern of different resonant frequency and Table 2 shows the all parameters of three different iterations.

Fig. 3 Simulated return loss characteristics curve for Antenna 1, Antenna 2 and Antenna 3



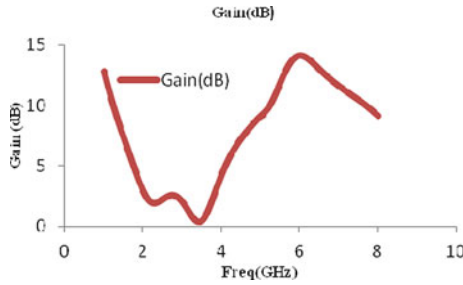


Fig. 4 Gain versus frequency response curve for the Antenna 3

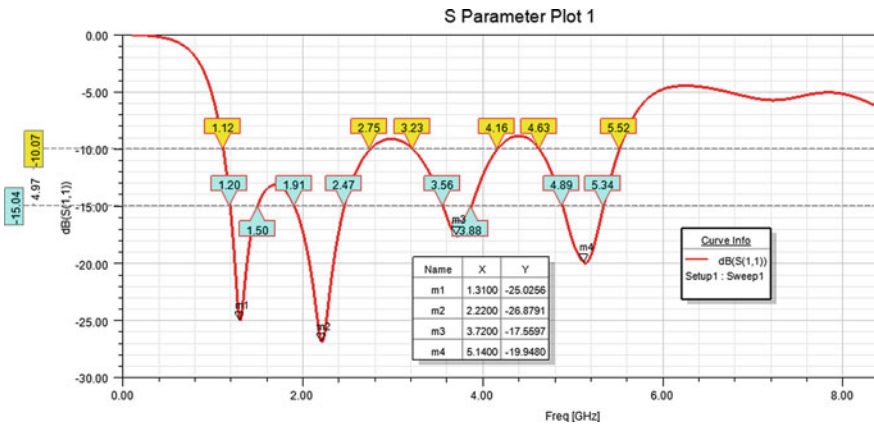


Fig. 5 Return loss versus frequency response for Antenna 3

5 Conclusions

The design and simulation of a hexagonal substrated circular patch antenna with wheel slot is presented in this study. When compared to existing structures in the literature, the results indicate superior impedance bandwidth and gain. The circular patch and wheel slot shaped are used throughout this work to improve prototype performance. The constructed prototype and the simulated circular wheel slot patch antenna are found to be in good agreement. This technique produces a linear polarization with high gain in two bands 3.72 and 5.14 GHz (C-band) and a circular polarization with high gain in one band 1.31 GHz (GPS L-band). It is also suggested that a wheel slot shaped method with a high impedance bandwidth be designed and simulated. Both of the approaches used in this research are simulated using the HFSS 2015 software simulator and will be built on a FR4 substrate. Further the proposal work is extended to use anechoic chamber and Vector Network analyzer will be used to undertake experimental validation and testing, which will be compared to simulated results at a later study.

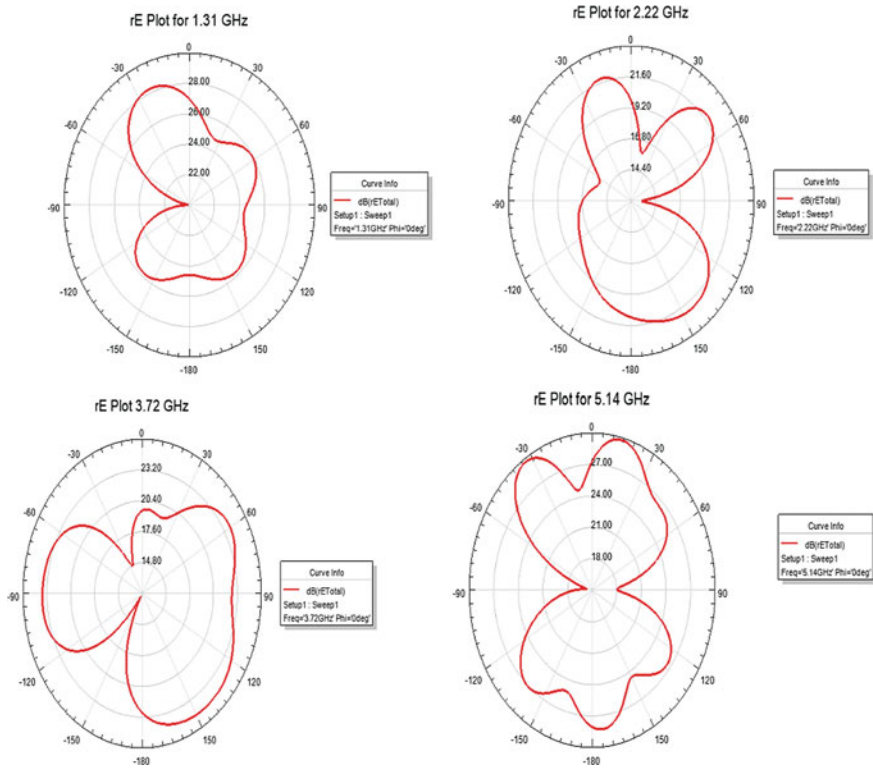


Fig. 6 Radiation pattern of proposed antenna at 1.31 GHz, 2.22 GHz, 3.72 GHz and 5.14 GHz, respectively

Table 2 Comparison of performance metrics of iterative antennas with the proposed antenna

Antenna design	f_r (GHz)	Return loss (dB)	Impedance bandwidth (MHz)	Gain (dBi)	VSWR	Efficiency (%)
Conventional patch (Antenna 1)	2.15	-34.82	500	-0.48	1.03	28.6
	3.76	-15.06	610	2.0	1.42	7.2
	5.42	-11.94	530	4.85	1.67	11.3
Modified patch with half wheel slot (Antenna 2)	2.18	-22.20	440	1.64	1.16	21.1
	3.63	-17.9	630	2.72	1.28	7.02
	5.41	-11.63	500	5.32	1.71	3.01
Modified patch with wheel slot (Antenna 3) proposed antenna	1.31	-25.02	1630	9.21	1.11	57.1
	2.22	-26.87	1630	1.97	1.09	44.1
	3.72	-17.56	930	1.83	1.30	9.1
	5.14	19.95	890	9.57	1.22	53.2

References

1. He X, Jiao Y (2014) Dual-band wheel slot antenna fed by CPW for WLAN applications. In: Proceedings of 2014 3rd Asia-Pacific conference on antennas and propagation, pp 273–276. <https://doi.org/10.1109/APCAP.2014.6992472>
2. Norra SR, Azremi AAH, Soh PJ, Saidatul NA, Ibrahim MI (2007) Small rectangular parasitic plane as patch antenna ground plane for broadband WLAN application. In: Asia Pacific conference on applied electromagnetics, Melaka, Dec 2007, pp 1–5
3. Patel RH, Upadhyaya TK (2017) Compact planar dual band antenna for WLAN application. *Progr Electromagnet Res* 70:89–97
4. Patel RH, Desai A, Upadhyaya T (2015) A discussion on electrically small antenna property. *Microw Opt Technol Lett* 57:2386–2388
5. Rama Sanjeeva Reddy B, Akula V, Deshpande R (2019) Bandwidth enhancement feature of Koch fractal shaped patch antenna for tri-band applications. In: 2019 IEEE Indian conference on antennas and propagation (InCAP), pp 1–4. <https://doi.org/10.1109/InCAP47789.2019.9134615>
6. Lin C-C, Yu E-Z, Huang C-Y (2012) Dual-band rhombus slot antenna fed by CPW for WLAN applications. *IEEE Antenna Wirel Propag Lett* 11:362–364
7. Wu CM (2007) Dual-band CPW-fed cross-slot monopole antenna for WLAN operation. *IET Microwave Antenna Propag* 2(1):542–546
8. Madhav BTP, Anilkumar T, Kotamraju SK (2018) Transparent and conformal wheel-shaped fractal antenna for vehicular communication applications. *AEU Int J Electron Commun* 91:1–10. ISSN 1434-8411
9. Kumawat B, Yadav S, Sharma M, Deegwal JK, Dadhich A (2019) Tri-band rectangular patch antenna with C slot. In: 2019 IEEE Indian conference on antennas and propagation (InCAP), pp 1–3. <https://doi.org/10.1109/InCAP47789.2019.9134584>

Detection and Counting of Trees in Aerial Images Using Image Processing Techniques



Meda Lakshmi Hima Bindhu, Tejaswi Potluri, Chandana Bai Korra, and J. V. D. Prasad

Abstract Pixel classifier is required for assigning a class label. Morphological counting with limited success so far. However, in case of dense areas, the trees are more densely packed as differences in their structure of crown and openness of crowns. This makes more challenging. Therefore, the trees counting algorithm has to be more robust and intelligent. The image segmentation deep learning comes into play. The pixel level classification is used as a partitioning algorithm to separate tree and non-tree regions in an image. We are making kernel for tree and finding the matches for our input image the programme uses pixel by pixel classification to draw boundaries around tree crowns. In this we are detecting and counting the no of trees in an image.

Keywords Tree crown detection · Template matching · Deep learning

1 Introduction

Forests have an important responsibility in the ecosystem. They might, for example, aid in the maintenance of the water cycle, the conservation of soils, the sequestration of carbon, and the protection of human and animal habitats. Many programmes have been implemented to strengthen environmental governance and ensure sustainable ecological growth as a result of the aforementioned roles of forests. It is critical that we develop a model for automatically detecting and counting trees. The number of trees may be used to monitor and analyse forest health, as well as offer a baseline data reference for forest management decision-making by relevant agencies and regulatory bodies. This is critical for improving forest management and exploitation

M. L. H. Bindhu (✉) · T. Potluri · C. B. Korra · J. V. D. Prasad
Department of Computer Science and Engineering, Velagapudi Ramakrishna Siddhartha
Engineering College, Kanuru, India
e-mail: medalakshmihimabindu@gmail.com

J. V. D. Prasad
e-mail: prasadj@vrsiddhartha.ac.in

in the face of climate change, as well as accomplishing forest-related sustainable development goals.

Individual tree inventories in the field are a time-consuming and costly operation. Although Lidar may be used to automatically recognize trees, its expensive cost prevents it from being extensively used. For recognizing and counting trees, satellite photos are more feasible. For example, collecting 429,775 datasets from more than 50 nations took more than two years, and they were calculated using various statistical approaches. To obtain better results, we use morphological processing, and photos are transformed to hsv images to obtain colour differences. Traditional approaches, on the other hand, are extensively employed to process remote sensing data with a coarser spatial resolution. Filtration is used to minimize picture noise and provide accurate findings.

1.1 Template Matching

It is method used for finding the areas which are similar to the patch. We will take two images as input one is source image and the other one is template image. The template image process over the source image and we will compare our images and find the matched area and the result image will be compared with the threshold. If it is greater than threshold it will be marked as detected.

1.2 Image Processing

It is used to get clarified image and extract the information which is required and removes noise. It mainly includes three steps:

- Importing the image via image acquisition tools
- Analysing and manipulating the image
- Report which is based on analysing that image.

Phases of image processing:

- Acquisition
- Image Enhancement
- Image Restoration
- Colour image Processing
- Resolution Processing
- Image Compression
- Morphological Processing
- Segmentation Procedure
- Representation and Description
- Object Detection and Recognition.

1.3 Problem Statement

We will detect and count the number of trees individually. It will be useful for forest management to track the information about forests and control the cutting down trees. However, this requires tools and technology that would give reliable information on forest communities is very difficult because it is time-consuming, and unsuited for large areas.

1.4 Scope

The scope of this system is to count the number of trees using aerial images, firstly this project can be implemented in small regions like parks, gardens and later on it can be implemented on agricultural lands, forests and in an uncontrolled environment.

1.5 Objectives

The main objective of the project is to convert the image into binary image adopting template matching to detect the trees individually and count them and thresholding the image and giving pixel value 0 for background and 1 for trees and use filtration for binary image to reduce noise in the image.

1.6 Organization

This paper is organized as follows: Section 2 describes Literature Survey on different feature extraction methods for detection and counting of trees. Section 3 describes the proposed framework. Section 4 describes the Results and Analysis. Section 5 describes Conclusion and Future Work.

2 Literature Survey

The literature survey describes [1] about the studies that make use of references. Using convolutional neural networks, the methodology proposed an innovative deep learning framework for the automated counting and geolocation of palm trees from aerial photos. Distance adjustments are used to automatically locate the location of palm trees using geo-tagged metadata from aerial pictures and photogrammetry concepts. Some of the models have been used for automated counting and geolocation

they are Efficient Det CNN model, Faster R-CNN, YOLOv3 and YOLOv4 were used. Palm trees are uniquely identified and counted from a series of images using GOS tagging, even the image overlapping are also correctly dealt. MADAN is used for counting of trees.

The methodology provides an approach to count the number of trees in urban environment. A multi rotor with RGB camera was used to get images which are areal and by using this we will count number of trees. Image segmentation technique was used for implementation. Colour threshold technique is used to get count of trees. Because this is an approximation algorithm some of the results may be false negative. The errors and the accuracy of the model can be increased by machine learning techniques.

This paper proposed a method [2] for recognizing and counting oil-palm trees from elevated airborne photography data. Comprises six major parts: (1) spectral analysis to differentiate oil-palms from non-oil-palms, (2) roughness examination, (3) edge augmentation, (4) segmentation process, (5) morphological analysis and (6) blob analysis. This process was carried out by using Eco system 4.0 and Matlab 7.5.0. The MNF technique was used to enhance the isolation of image noise that could appear in one or more of the original bands. This approach works well if the palm oil plantations crowns are not linked to one another.

This article proposed a method [3] that successfully explored deep learning based on CNNs, the probabilistic combination of classifiers outputs, and traditional post-processing with non-maxima suppression. The detection procedure is implemented using a sliding window approach. Combining CNN's will improve the accuracy in detection of oil-palm trees. Non-maxima suppression removes weak detections. Detections in commercial plantations can be made accurate using orthomosaics derived from RGB imagery collected by unmanned aerial vehicles (UAVs). This can provide a way for non-experts to obtain estimates of oil-palm tree counting for large areas and also an estimate confidence for each oil-palm tree detected.

This article proposed a method [4] that successfully explored deep learning based on CNNs, the probabilistic combination of classifiers outputs, and traditional post-processing with non-maxima suppression. The detection technique is adopted to use a sliding window method. Combining CNNs will enhance the accuracy of spotting oil-palm plants. Non-maxima suppression removes weak detections. Detections in commercial plantations can be made accurate using derived from RGB imagery collected by unmanned aerial vehicles. This can provide a way for non-experts to obtain estimates of oil-palm tree counting for large areas and also an estimate confidence for each oil-palm tree detected.

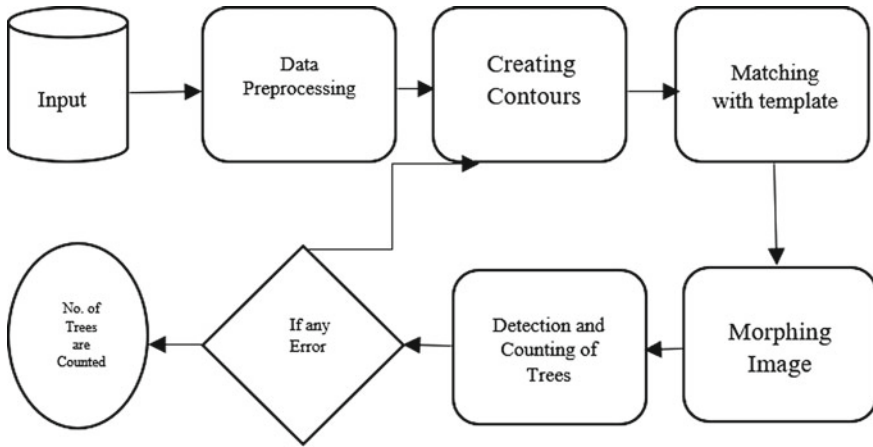


Fig. 1 Architecture of proposed framework

3 Proposed System

3.1 Architecture

The proposed system’s architecture is shown in Fig. 1. The proposed system consists of three main modules. Module I—Filtration, Module II—kernel creation, Module III—Template matching. The detailed information about each module is mentioned in Sect. 3.2.

3.2 Methodology

The proposed system is divided into three main modules. They are filtration, kernel creation, template matching. The model is fed data from the “Counting Trees Using Aerial Images” from Github, which has 6252 images in the training dataset and 2680 images in the test data. The aerial images are converted as binary images and then to prediction and finally number of trees are counted.

3.3 Filtration

First we have to load our image using imread function and now we have to highlight our tree tips by converting image into HSV colour channel using cv2.cvtColor method. Now we have to threshold the image in range 120–210 with OSTU for HSV image. Range was found by searching different values. OSTU performed better than

other methods. The output image consists of pixel value 0 for the trees and 1 for background. Normally noise will be generated in our input to reduce the noise we have to do filtering on the binary image by using filters. We are applying filters to our data. The output after filtration will be better than the previous one.

3.4 Kernel Creation

Now we have to perform distance transform and it will calculate the distance to the closest zero pixel for each pixel of the source image. Now apply some padding to the image so that further kernel operations will be easy. Now perform template matching by extracting an image of the single tree chosen at random from the image.

3.5 Template Matching

The template file is loaded and it is converted to HSV channel and the same thresholding that is done to the original image is done to get the template that we can use for matching with the actual image. Also, applied some denoising with median filter for the opencv to consider the kernel template we made it must be a binary image with 0 and 1. Convert the pixel values to 0's and 1's and there are better methods performed better than without filtering. Apply distance transform on the template. Finally, now we can try to match our template not on the actual image but on the outputs of distance transforms. The operation was able to find contours. To avoid problems with contours we are sharpening the images. Even though some of the trees are getting considered in a good way, we can see some connected contours. These could be dealt with by some sharpening to the image.

4 Results and Analysis

Figure 2 explains about importing the required libraries. The required libraries are opencv library for recognizing the images, numpy and matplotlib.pyplot libraries are used for plotting of the tree images. Load the dataset into our python file. Trees.jpg contains the areal images of some areas where the number of trees are to be detected and counted. Reading of the file and then display the images that has been read. By using imread function the file is read and by using imshow function the image will be shown as output. The conversion of areal image to the hsv colour channel so that the trees will be darkened and will be easy to identify the trees. The tree crowns will be highlighted here. For this conversion cvtcolor function is used and imshow function with parameters hsv_image and cmap are used to output the result as hsv images. Thresholding the range of image between 120 and 210 with OTSU.

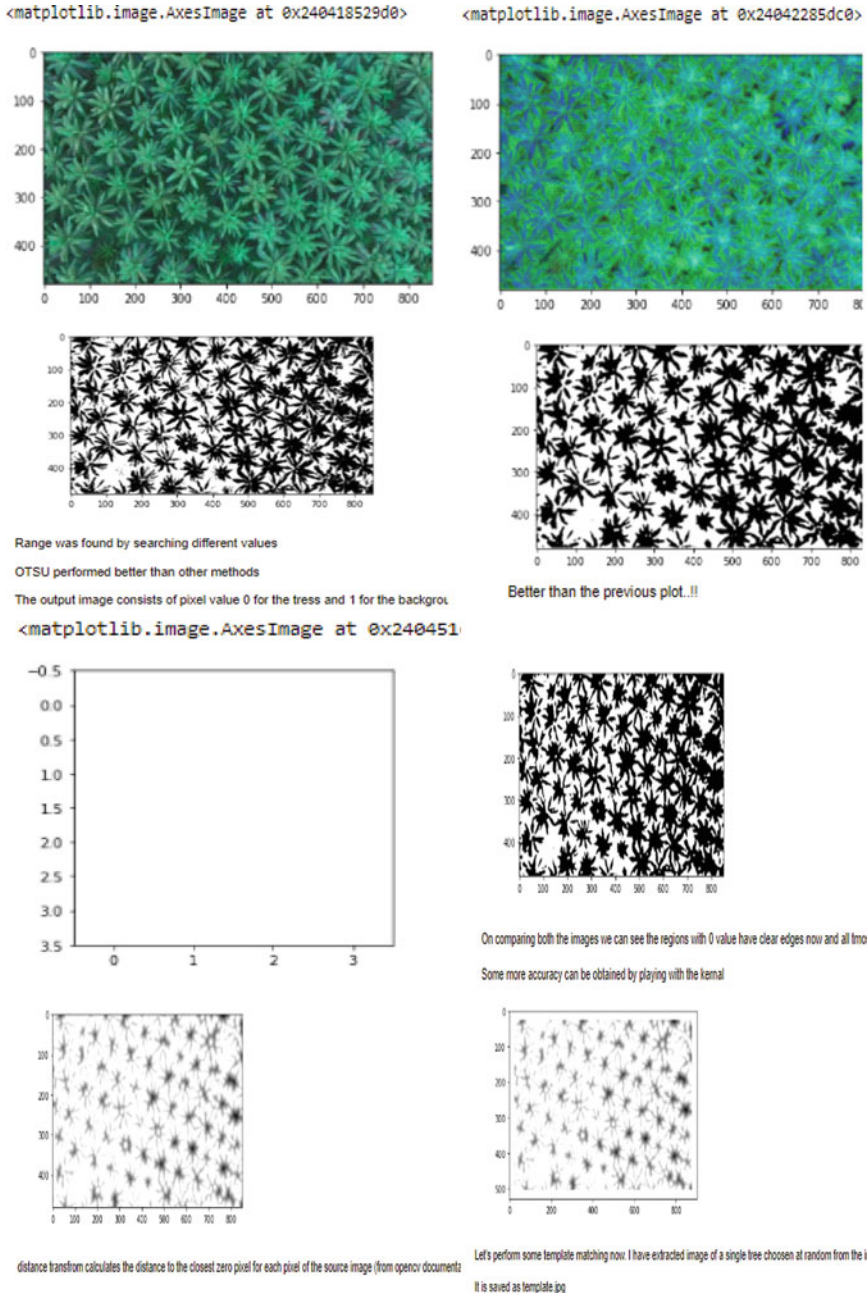


Fig. 2 Results at each step of the process

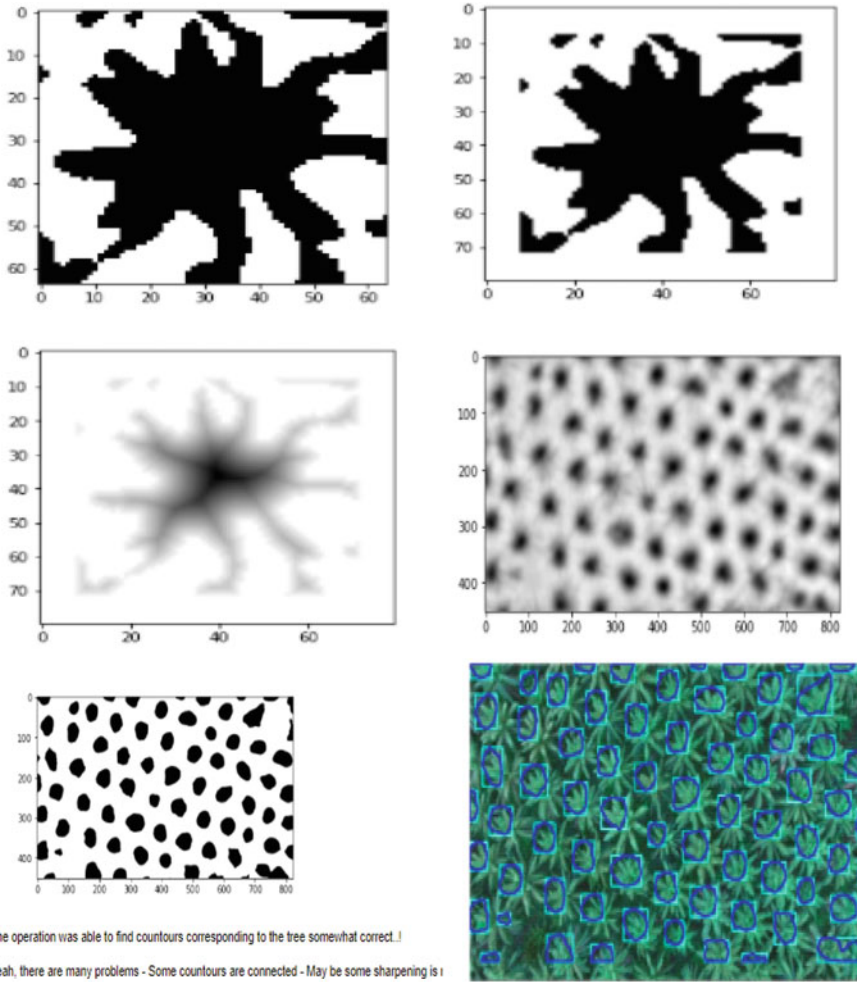


Fig. 2 (continued)

Threshold function is applied to set the range and the hsv colour channel images are also converted to binary images using the thresh_binary. Some filtering on the binary images are applied to reduce the noise. To apply the filters import filters from the skimage module and also import numpy. Now the filters.median function is applied on the binary images to remove noise. The application of template matching not on the actual images but it is done on the outputs of distance transformed images to make it easy.

5 Conclusion and Future Work

In this study we have illustrated an approach to the automatic detection of tree tops that gives detailed tree crown outlines and accurate tree top counts. This approach consists of contour creation, creating a kernel to fit our images and by using template matching and morphological processing this will detect the number of trees present in an image. Though the approach is very encouraging, the automatic tree top detection and counting potential precise towards the VHR areal images of semi-automatic forestry has not been completely analysed. The test that is reported here has benefited from two favourable conditions, they (1) the conical shape of the exclusively deciduous tree crowns, and (2) a low sun angle late fall image providing magnified shade-related tree top separation. It has been proved that the images that are having more sun angle are more difficult for analysing and the tree crown images of forests are even more difficult to separate and analyse. The above two aspects will be the subject for future research endeavours.

References

1. Bazi Y, Malek S, Alajlan N, AlHichri H (2014) An automatic approach for palm tree counting in UAV images. IGARSS, IEEE
2. May P, Ehrlich HC, Steinke T (2006) ZIB structure prediction pipeline: composing a complex biological workflow through web services. In: Nagel WE, Walter WV, Lehner W (eds) Euro-Par 2006. LNNS, vol 4128. Springer, Heidelberg, pp 1148–1158
3. Foster I, Kesselman C (1999) The grid: blueprint for a new computing infrastructure. Morgan Kaufmann, San Francisco
4. Czajkowski K, Fitzgerald S, Foster I, Kesselman C (2001) Grid information services for distributed resource sharing. In: 10th IEEE International symposium on high performance distributed computing. IEEE Press, New York, pp 181–184

EGFR and HER2 Target-Based Molecular Docking Analysis—Computational Study of Metal Complexes



Ramaiah Konkanchi, Madhavi Vemula, and B. Anna Tanuja Safala

Abstract The semicarbazone ligand with metal(II) complexes are synthesized. Various methods such as NMR, ESR, FTIR, UV-Visible, elemental analysis and molar conductance are used for the characterization of the ligand and its metal complexes. The new compounds were optimized by using Gaussian 09W program package and by using 6-311++G (d, p)/SDD basis set. In addition, the antimicrobial activity of the semicarbazone ligand and its metal complexes are evaluated for their different organisms such as gram positive and gram negative bacterial strains. The compounds Zn(II) and Cd(II) are exhibited potent activity against the tested organisms. In addition, the docking studies was performed against epidermal growth factor receptor and HER2 protein receptors and also compared to the standards of EGFR and HER2. The zinc and nickel complexes were showed least binding energy values of -10.23 and -8.70 kcal/mol.

Keywords EGFR · HER2 · DFT calculations · Molecular docking · Scavenging activity · Antimicrobial activity

1 Introduction

Schiff bases are the products of reaction between ketones or aldehydes with amine [1]. Schiff base ligands are supposed to be suitable chelating agents and the $-OH$ functional group close to the azomethine includes them in a unique class of ligands [2]. Additionally, it is also documented in the literature that heteroatom increases the Schiff base activity [3]. Schiff base ligands transition metal complexes bared O and N donor atoms are very significant because of their variety of biological applications such as antioxidant [4], anti-diabetic [5], anticancer [6], anti-inflammatory [7], antibacterial [8], antifungal agents [9], in addition, Schiff base metal complexes are also used as catalysts in multi-component reaction [10], fluorescent materials [11], organic photovoltaic materials [12] and also as a sensor [13]. Literature survey

R. Konkanchi (✉) · M. Vemula · B. A. T. Safala
Chemistry Division, H&S Department, BVRIT Hyderabad College of Engineering for Women,
Hyderabad 500090, India
e-mail: ramaiah.k@bvrithyderabad.edu.in

reveals that a number of metal complexes of Schiff bases composed of 3-indole aldehyde [14], 2-benzoylpyridine [15] and 2-hydroxy-1-naphthaldehyde/5-methoxy salicylaldehyde with semicarbazide or thiosemicarbazide, etc., have been reported to possess different pharmacological properties and exhibit antimicrobial, antiviral and anticancer activities. Semicarbazones belongs to a special class of compounds because of the fact that these compounds are endowed with various analytical and biological applications and that they show diverse ligating behavior toward metal ions and in complexation with them exhibit a wide range of stereo chemistries. Therefore, in view of above mention literature, this work aims to synthesize the new compounds. Moreover, the biological applications and theoretical results (DFT and docking) are discussed.

2 Experimental

2.1 Materials and Methods

Analytical grade organic solvents and metal salts were obtained from the Merck and Sigma Aldrich. Buchi–Electrothermal melting point apparatus was used for Melting point, Vario MICRO CHNS/15082029 analyzer was used calculate elemental analysis. ^1H NMR, 400 MHz using tetramethylsilane is an internal standard, chemical changes in ppm are expressed on the δ scale. For conductance measurement, Systronic Conductivity meter 304-cell type CD-10 was used. IR spectra were recorded on Perkin Elmer spectrophotometer in the range $4000\text{--}400\text{ cm}^{-1}$. UV–VIS spectroscopic data was recorded on Hewlett-Packard 8452 diode-array spectrophotometer.

2.1.1 Synthesis of 2-Aminonicotinaldehyde (ANA)

The starting material ANA was synthesized by a well-known method [13].

2.1.2 Synthesis of 2-Aminonicotinaldehyde Semicarbazone

A mixture of 2-aminonaldehyde (0.122 g, 1 mmol) and semicarbazide hydrochloride (0.072 g, 1 mmol) were dissolved in methanol containing 0.082 g of sodium acetate was added. The contents of the flask were refluxed for 1 h. The yellow compound that separated out on cooling in an ice bath was filtered washed with methanol and recrystallized from aqueous alcohol to get a very light yellow compound.

2.1.3 Synthesis of Metal Complexes

The complexes are synthesized by direct reaction between the freshly purified ligand dissolved in methanol and the corresponding metal chlorides salt dissolved in minimum quantity of aqueous/methanolic solution in 2:1 ratio, by stirring followed by refluxing for 3 h to form new compounds and filtered to acquire 70–80% yield.

2.2 Computational Consideration

The new compounds were optimized by using Gaussian 09 program [16]. Structural benchmarking of compounds were using B3LYP functionals with 6-311++G (d, p) basis set. In all further computations, the initial data consisted of the reference geometry and corresponding force constants. With the help of MOLVIB 7.0 program [17, 18].

2.2.1 Molecular Docking

In addition to the biological activity, silico studies were carried out to explain the interactive mechanism of ligand and its complexes with target EGFR and HER2 protein receptor and to examine the possible binding modes in between them by using molecular docking simulations. One of the main targets of cancer inhibitors-EGFR was majorly responsible for the cancer disease. The mutations of the EGFR is the main cause for the several cancer diseases like c, squamous-cell carcinoma of the lung, epithelial tumors and anal cancers of the head and neck. Chem Draw Ultra 12.0 are used to draw the 2D structures of ligands and its metal complexes and optimized with Gaussian 09. The docking studies were carried out by using AutoDock Tools 1.5.6 version and 4.2.5.1.

2.3 Biological Evaluation

2.3.1 Antimicrobial Activity

The antimicrobial activity of the new compounds was assessed by using agar diffusion method against one gram +ve (*Bacillus subtilis*), and one gram –ve (*Escherichia coli*) bacteria and also against fungi such as *Alternaria* and *Aspergillus flavus*.

2.3.2 Antibacterial Screening

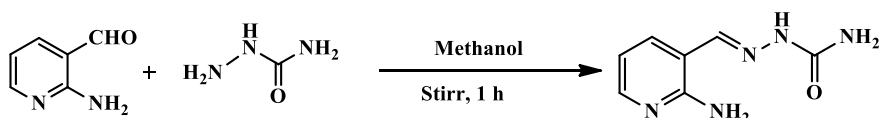
The protocol of the antibacterial activity is seen in the Ref. [4].

2.3.3 Antifungal Screening

Stock culture maintenance: Sub-culturing of test organism was carried out every week using Asthana-Hakers medium with the following composition. Glucose: 500 mg, KNO_3 : 0.175 mg, KH_2PO_4 : 0.075 mg, $\text{MgSO}_4 \cdot 7\text{H}_2\text{O}$: 0.0075 mg, Agar-Agar: 1.5 g and Distilled water: 1000 mL. The detailed procedure is seen in the Ref. [4].

3 Results and Discussion

A mixture of 2-aminonaldehyde (0.122 g, 1 mmol) and semicarbazide hydrochloride (0.072 g, 1 mmol) was dissolved in methanol containing sodium acetate was added. The contents of the flask were refluxed for 1 h. The yellow compound that separated out on cooling in an ice bath and it is filtered and recrystallized to get a very light yellow compound. Yield: 95%. M.p.: 155 °C. Anal. Calcd. for $\text{C}_7\text{H}_9\text{N}_5\text{O}$ (%): C, 46.92; H, 5.03; N, 39.10. Found: C, 46.81; H, 5.00; N, 38.96. After preparation of the ligand, take 1:2 ratio metal salts and ligand. After that reflux for 3 h, filtered that compound and dried it (Schemes 1 and 2).



Scheme 1 Synthesis of ligand

Scheme 2 Proposed structures of complexes

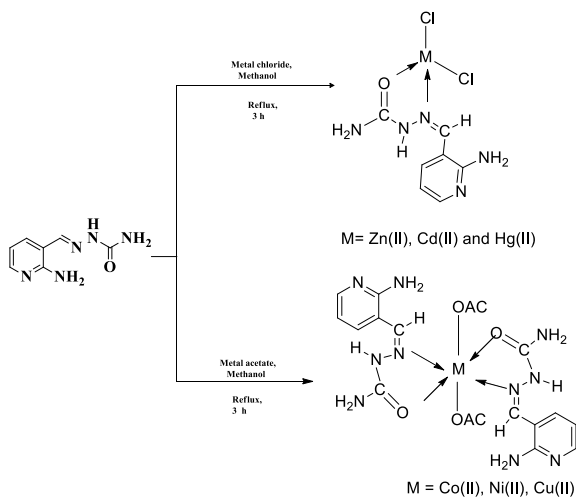


Table 1

Complexes	Assignments	μ_{eff} (BM.)	Geometry
Co(II)	${}^4T_{1g}(F) \rightarrow {}^4T_{2g}(F) (\nu_1)$ ${}^4T_{1g}(F) \rightarrow {}^4A_{2g}(F) (\nu_2)$ ${}^4T_{1g}(F) \rightarrow {}^4T_{1g}(P) (\nu_3)$	4.66	Octahedral
Ni(II)	${}^3A_{2g}(F) \rightarrow {}^3T_{2g}(F) (\nu_1)$ ${}^3A_{2g}(F) \rightarrow {}^3T_{1g}(F) (\nu_2)$ ${}^3A_{2g}(F) \rightarrow {}^3T_{1g}(P) (\nu_3)$	3.51	Octahedral
Cu(II)	${}^2B_{1g} \rightarrow {}^2B_{2g}$ ${}^2B_{1g} \rightarrow {}^2E_g$	1.92	Distorted octahedral
Zn(II)	–	Diamagnetic	Tetrahedral

3.1 Characterization

To investigate major functional groups composition in substances IR spectroscopy is a technique used widely. The ligand C=N and C=O stretching frequencies were occurred at 1562 and 1244 cm^{-1} . After binding with metal ions, these both bands were shifted to lower frequency (1510–1525 and 1245–1230 cm^{-1}). The above information clearly observed that ligand bind with metal ion via C=N nitrogen and C=O, oxygen, respectively. The electronic spectral frequencies are given in Table 1. The spectral characteristics of the Co(II) complex frequencies observed at 21,000, 16,244 and 8791 cm^{-1} indicating referring to octahedral geometry. The transitions of the Ni(II) complexes are observed at 24,571, 17,390 and 8500 cm^{-1} are evidence that the transitions indicating octahedral geometry. The Cu(II) complex observe the transition 17,000 cm^{-1} evidence that transitions referred to distorted octahedral geometry. The detailed transitions for the above peaks are represented in Table 1. The zinc, cadmium and mercury complexes refers to most favored tetrahedral geometry are observed. The detailed magnetic momentum values are represented in Table 1, reference to the geometry of the complexes (Fig. 1).

3.2 EPR Spectra

The copper complex ESR spectrum has been obtained in a solid state. The ESR spectrum is reproduced in Fig. 2. ESR parameters such as g_{\parallel} , g_{\perp} , g_{ave} , A_{\parallel} , A_{\perp} , α^2 , β^2 , Γ^2 and λ are given in Table 2. The present complex is anisotropic and shows two peaks. Following the Kneubuhl's method, g values: g_{\parallel} , g_{\perp} , the former from the small intensity peak(s) and the later from the large intensity peak(s) have been calculated. From these values, the g_{ave} has been calculated using the equation.

$$g_{\text{ave}} = 1/3(g_{\parallel} + g_{\perp})$$

Fig. 1 UV spectrum of cobalt metal complex

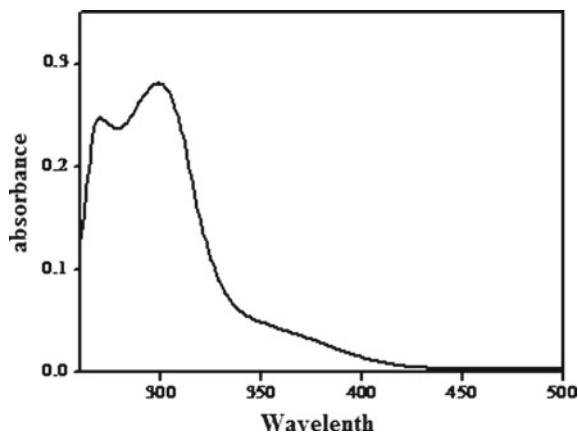


Fig. 2 ESR spectrum

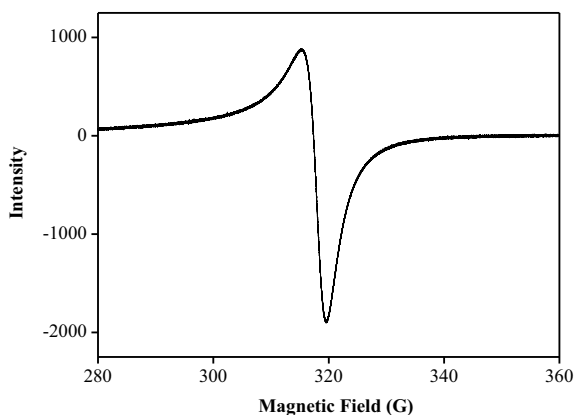


Table 2 ESR spectral data

Complex	g_{\perp}	g_{\parallel}	$ g $	G	$A_{\parallel} \times 10^5 \text{ (cm}^{-1}\text{)}$	K_{\parallel}^2	K_{\perp}^2	$-\lambda$
Copper complex	2.04	2.25	2.13	4.43	481	0.524	0.455	452

In a tetragonally elongated octahedral complexes, the $g_{\parallel} > g_{\perp} > 2$ with $d_{x^2-y^2}$ orbital have unpaired electron. In a tetragonally compressed octahedron, the other one is the d_{z^2} orbital with $g_{\perp} > g_{\parallel} = 2$. The results (Table 2) indicate that $g_{\parallel} > g_{\perp} > 2$ suggesting elongated octahedral or square planar geometry and unpaired electron lies in $d_{x^2-y^2}$ orbital.

The α^2 , β^2 and γ^2 of the complexes have been calculated by using the equation [19]. The results obtained for the present complex is given in Table 2. If A value of $\alpha^2 = 0.5$ or 1 refers to 100% covalent nature or complete ionic character. The β^2 and γ^2 parameters are similarly a measure of covalency in the in-plane and out-of-plane

π -bonding, respectively. β^2 or $\gamma^2 = 1$ indicates total ionic character and β^2 and $\gamma^2 = 0.5$ corresponds to a total covalent character.

$$g_{\parallel} = 2.0023 - \frac{8\lambda_0\alpha^2\beta^2}{\Delta E(2B1g)} + \dots$$

where $\lambda_0 = -828 \text{ cm}^{-1}$ for free Cu(II) ion. Under investigation (Table 2), the observed α^2 value is 0.69 indicative of strong/appreciable in-plane σ -bonding. The β^2 and γ^2 values of present Cu(II) complex is 0.61 and 0.77, respectively, which suggest appreciable/moderate in-plane and out-of-plane π -bonding in the present complex. Further, λ (spin-orbit coupling constant) is calculated using this below equation

$$g_{\parallel} = [2 - (8\lambda/10Dq)]$$

The investigated complex λ value (452 cm^{-1}) less than $\lambda_0 = -828 \text{ cm}^{-1}$ referring to considerable mixing of ground and excited terms.

3.3 Molecular Geometry

The geometric optimized structures of the compounds were optimized by DFT/B3LYP with 6-311G++(d, p) basis set with -2015.46335 , -2656.988047 and -3533.703372 Hartree, respectively, and minimum optimization energies of resulting C_1 point group symmetry. The geometrical parameters of metal complexes under investigation, it was in good concord to experimental counter parts.

3.4 Antioxidant Activity

DPPH method is used for determination of scavenging activity of the new compounds. The reference compound ascorbic acid was chosen. The antioxidant activity results are expressed in terms of IC_{50} . The complete IC_{50} values are represented in Table 3.

3.5 Antimicrobial Activity

In the oxygen carriage mechanism of hemoglobin in respiration, formation and deformation of hydrogen bonds among the groups in the protein chain of a single heme unit on oxygenation of Fe(II) ion leads to cooperative effect as a result of which other three heme units are also oxygenated. The compounds were tested for their

Table 3 Antioxidant activity of compounds

Compounds	IC ₅₀ (μM)
Co(II)	29.03 ± 0.24
Ni(II)	45.30 ± 0.25
Cu(II)	9.11 ± 0.14
Zn(II)	55.02 ± 0.35
Cd(II)	91.56 ± 0.57
Hg(II)	68.66 ± 0.61
Ascorbic acid	2.15 ± 0.11

antimicrobial activity. The results are summarized in Tables 4, 5 and 6. From the interesting results, they observed that the metal complexes are greater activity than the ligand. The value of percentage activity index in any concentration of solutions < 60% has been considered marginal and that of > 60% as significant activity. Zinc and mercury complexes show significant activity whereas cadmium, cobalt and nickel complexes exerts moderate activity against *B. subtilis* gram (+ve) bacteria. Mercury complex shows significant activity, and zinc and cadmium complexes exert moderate activity against *E. coli* gram (–ve) bacteria. Against fungi, cadmium complex shows moderate activity, and mercury and zinc complexes show significant activity.

Table 4 Antibacterial activity of the compounds

Compound	<i>Bacillus subtilis</i> G(+ve)						<i>Escherichia coli</i> G(–ve)					
	Zone of inhibition (mm)			Activity index (%)			Zone of inhibition (mm)			Activity index (%)		
	A*	B*	C*	A*	B*	C*	A*	B*	C*	A*	B*	C*
Ligand (ANA)	–	–	–	–	–	–	–	–	–	–	–	–
Zn(II) complex	04	07	12	40	58	86	–	03	05	–	30	38
Cd(II) complex	03	06	08	30	50	57	03	04	06	37	40	46
Hg(II) complex	07	09	11	70	75	79	05	07	10	62	70	77
Streptomycin sulfate	10	12	14	100	100	100	08	10	13	100	100	100

Test solution and standard solution: A* = 200 μg/ml, B* = 400 μg/ml, C* = 600 μg/ml, – = no activity

Zone of inhibition excludes bore size and zone of inhibition of control. Error $-2 \leq 0 \leq +2$

Table 5 Antifungal activity of the compounds

Compound	<i>Alternaria</i>					
	Zone of inhibition (mm)			Activity index (%)		
	A*	B*	C*	A*	B*	C*
Ligand	–	–	–	–	–	–
Co(II) complex	06	07	08	49	59	75
Ni(II) complex	10	08	16	71	83	66
Zn(II) complex	04	06	08	57	75	80
Cd(II) complex	03	04	06	43	50	60
Hg(II) complex	03	06	08	43	75	80
Streptomycin sulfate	07	08	10	100	100	100

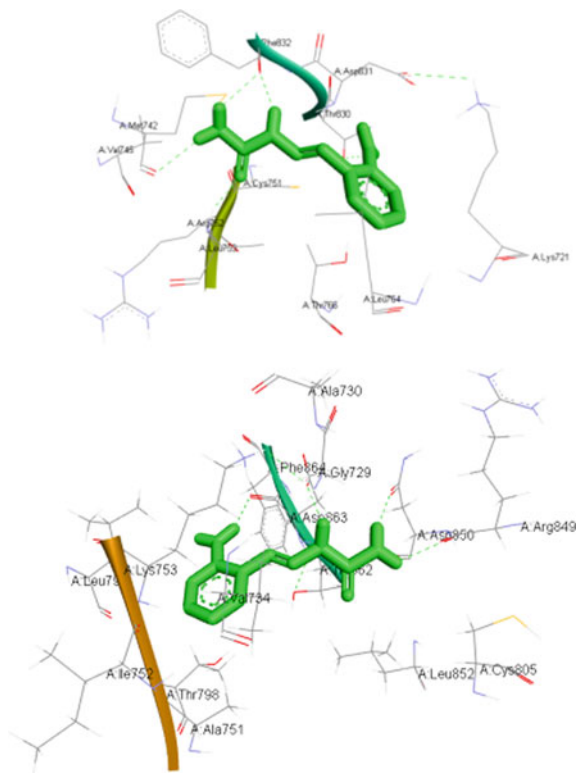
Table 6 Zone of inhibition values of compounds

Compound	<i>Aspergillus flavus</i>					
	Zone of inhibition (mm)			Activity index (%)		
	A*	B*	C*	A*	B*	C*
Ligand	–	–	–	–	–	–
Co(II) complex	8	10	19	88	91	64
Ni(II) complex	44	19	18	84	90	57
Zn(II) complex	10	12	15	83	86	100
Cd(II) complex	03	07	09	25	50	60
Hg(II) complex	10	12	14	83	86	93
Streptomycin sulfate	12	14	15	100	100	100

3.6 *In Silico* Molecular Docking

The docking activity was performed by EGFR protein with PDB ID: 4JHO. By the results, we have to observe the binding energy values and interactions of molecule. The results are reported in and shown in Fig. 3. *In silico* molecular docking, results reveals that the molecule under investigation ligand exhibits good binding energy of -6.77 kcal/mol, containing 5 H bonds with amino acid residues GLY255(3), ASN375, HIS266 and VAL228. The titled molecule exhibits four hydrogen bonding interactions with GLY255(3) amino acid by a distance 2.1817 Å, 2.1309 Å and 2.3309 Å; ASN375 amino acid by a distance 2.1523 Å; HIS226 amino acid by a distance 2.0961 Å and VAL228 amino acid by a distance 2.2211 Å, respectively.

Fig. 3 EGFR (top, PDB ID: 4HJ0) and HER2 (bottom, PDB ID: 3PP0) target-based ligand interactions



4 Conclusion

In the present paper, a new semicarbazone ligand and its metal complexes were synthesized and characterized by analytical and spectral (mass, NMR, FTIR and UV–Vis) techniques. The theoretical parameters are well agreement with experimental counter parts in the molecules under investigation. HOMO-LUMO energy gap and MEP calculations predicted reactivity, nucleophilic and electrophilic attacks within the molecules. Antioxidant activity of the complexes has shown higher activity compared to ligand. Antimicrobial activity of the compounds was exhibited moderate to poor activity observed against the strains. Molecular docking studies are shown least binding energies are strongly supports the experimental results.

Acknowledgement The author Ramaiah Konkanchi, thank BVRIT Hyderabad College of Engineering for Women, for the constant support and encouragement during this research work.

References

1. Shi L, Ge HM, Tan SH, Li HQ, Song YC, Zhu HL, Tan RX (2007) Synthesis and antimicrobial activities of Schiff bases derived from 5-chloro-salicylaldehyde. *Eur J Med Chem* 42:558–564
2. Booyesen IN, Maikoo S, Piers Akerman M, Xulu B, Munro O (2013) Ruthenium (II/IV) complexes with potentially tridentate Schiff base chelates containing the uracil moiety. *J Coord Chem* 66:3673–3685
3. Rajput S, Gardner CR, Failes GM, Arndt DSC, Black NK (2014) Synthesis and anticancer evaluation of 3-substituted quinalin-4-ones and 2,3-dihydroquinolin-4-ones. *Bioorg Med Chem* 22:105–115
4. Konakanchi R, Pamidimalla GS, Prashanth J, Naveen T, Kotha LR (2021) Structural elucidation, theoretical investigation, biological screening and molecular docking studies of metal(II) complexes of NN donor ligand derived from 4-(2-aminopyridin-3-methylene)aminobenzoic acid. *BioMetals* 34:529–556
5. Konakanchi R, Haribabu J, Prashanth J, Nishtala VB, Mallela R, Manchala S, Gandamalla D, Karvembu R, Reddy BV, Kotha LR (2018) Synthesis, structural, biological evaluation, molecular docking and DFT studies of Co(II), Ni(II), Cu(II), Zn(II), Cd(II) and Hg(II) complexes bearing heterocyclic thiosemicarbazone ligand. *Appl Organomet Chem* 32:e4415
6. Srishailam K, Ramaiah K, Reddy KL, Venkatram Reddy B, Ramana Rao G (2021) Synthesis and evaluation of molecular structure from torsional scans, study of molecular characteristics using spectroscopic and DFT methods of some thiosemicarbazones and investigation of their anticancer activity. *Chem Pap* 75:3635–3647
7. Rahis-ud-din K, Saleem HY (2011) Social aspects of cancer genesis. *Cancer Ther* 8:6–14
8. Moideen M, Ramaiah K, Rakesh G, Perumal P, Anandaram S (2020) Synthesis, characterization, in silico and in vitro biological activity studies of Ru(II) (η^6 -p-cymene) complexes with novel N-dibenzosuberene substituted aroyl selenourea exhibiting Se type coordination. *Res Chem Intermed* 46:3853–3877
9. Gandhaveeti R, Konakanchi R, Aneesrahman KN, Mohana CA, Bhuvanesh NSP, Reddy KL, Anandaram S (2018) Biological evaluation, DNA/protein-binding aptitude of novel dibenzosuberene appended palladium (II)-thiourea complexes. 32:e4567
10. Ramaiah K, Shravankumar K, Laxma RK (2018) Zinc-catalyzed multicomponent reactions: facile synthesis of fully substituted pyridines. *Synth Commun* 48:1777–1785
11. Sun H, Sun SS, Han FF, Ni ZH, Zhang R (2019) A new tetraphenylethene-based Schiff base: two crystalline polymorphs exhibiting totally different photochromic and fluorescence properties. *J Mater Chem C* 7:7053–7060
12. Huang J, Wang X, Xiang Y, Guo L, Chen G (2021) B \leftarrow N coordination: from chemistry to organic photovoltaic materials. *Adv Energy Sustain Res* 2:2100016
13. Ramaiah K, Ramachary M, Ramu G, Reddy KL (2018) Synthesis, characterization, biological screening and molecular docking studies of 2-aminonicotinaldehyde and its metal complexes. *Res Chem Intermed* 44:27–53
14. Aneesrahman KN, Ramaiah K, Rohini G, Stefy GP, Buvanesh NSP, Srikanth A (2019) Synthesis and characterisations of copper(II) complexes of 5-methoxyisatin thiosemicarbazones: effect of N-terminal substitution on DNA/protein binding and biological activities. *Inorg Chim Acta* 492:131–141
15. Moideen M, Ramaiah K, Rakesh G, Anandaram S (2020) Novel dibenzosuberene substituted aroyl selenoureas: synthesis, crystal structure, DFT, molecular docking and biological studies. *Phosphorus Sulfur Silicon Relat Elem* 195:331–338
16. Frisch MJ et al (2010) Gaussian 09, Revision B.01. Gaussian, Inc., Wallingford CT
17. Jyothi P, Ramaiah K, Byru Venkatram R (2019) Barrier potentials, molecular structure, force field calculations and quantum chemical studies of some bipyridine di-carboxylic acids using the experimental and theoretical using (DFT, IVP) approach. *Mol Simul* 45:1353–1383

18. Ramaiah K, Prashanth J, Haribabu J, Srikanth E, Venkatram Reddy B, Karvembu R, Reddy KL (2019) Vibrational spectroscopic (FT-IR, FT-Raman), anti-inflammatory, docking and molecular characteristic studies of Ni(II) complex of 2-aminonicotinaldehyde using theoretical and experimental methods. *J Mol Struct* 1175:769–781
19. Kavitha P, Laxma Reddy K (2012) Synthesis, spectral characterisation, morphology, biological activity and DNA cleavage studies of metal complexes with chromone Schiff base. *Arab J Chem* 9:596–605

A Comparative Study of Power Swing Blocking/Deblocking Techniques in Distance Relay Power System Protection



Cholleti Sriram and Jarupula Somlal

Abstract Distance relays are the most important type of protective equipment which is to be used to protect the transmission lines against faults. Mainly, to protect long transmission lines, mho type of relays is used. These relays usually operate against faults. Due to power fluctuations, the measured impedance seen by mho relay will enter into respective R-X characteristics, and the relay maloperates considering it as a fault. To make the relay blocked during power swing, number of blocking techniques introduced by the researchers. This paper discusses about the power swing blocking techniques which helps for better understanding of the blocking of power swing.

Keywords Power swing · Lissajous figure · First zero crossing · Differential voltage · SVM

1 Introduction

Power system is facing blackouts from years. But, there is no exact or accurate solution to any problem, or identifying a problem is also not much accurate which bringing the power system as so weak. It is not only required to figure out the problem, whenever the blackout took place but also require to give an accurate solution to the problem which the blackout should not took place again with the same problem.

The most developed countries also facing the blackout problems which makes the whole country in dark. So, it is required to bring the solutions to the problems which recently blackouts took place. The main reason for the blackouts is due to maloperation of a distance relay. This maloperation of relay is mainly due to the power swing. So, if required to block the power swing accurately, then there are

C. Sriram (✉) · J. Somlal

Department of Electrical and Electronics Engineering, Koneru Lakshmaiah Education Foundation, Vaddeswaram, AP 522502, India

e-mail: cholletisriram6@gmail.com

J. Somlal

e-mail: jarupulasomu@kluniversity.in

less chances for power system blackouts [1]. There are many blocking techniques. This paper discusses about the different power swing blocking techniques which are introduced by the researchers.

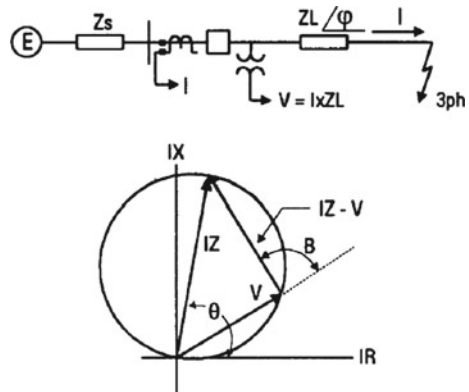
The outline of the review paper is as follows: Section 2 discusses about the problem of power swing detection; Sect. 3 discusses about different methods of power swing blocking techniques introduced by researchers; Sect. 4 discusses about the comparison of different PSB techniques, and Sect. 5 concludes the paper.

2 Power Swing Detection

Power system network will face several short-circuit faults, continuous switching of transmission lines, synchronous generator connection or disconnection, and the application or loss of heavy load result in abrupt variations in generated electrical output power, whereas the input mechanical power of a generator remains almost constant. This will lead stresses in the network, will cause severe oscillations in synchronous machine rotor angles. This will result in changes in current flowing through the system, will causes changes in power delivered called as power swings. These swings are momentary changes in active power flow that usually occur when the internal voltages of generators slip with respect to each other which are placed at individual locations of the system. Severe system disturbances will lead to wide separation of generator rotor angles between number of generators and cause eventual loss of synchronism between groups of generators. When two areas of a power system losing synchronism, the affected areas should be separated from one another rapidly and automatically by mho-type distance relays as shown in Fig. 1, in order to keep away from equipment damage and power system blackouts.

The synchronism lost between generator and the power system network affects the protective relays and systems in different ways. The essential settings for power swing

Fig. 1 Mho relay function



blocking (PSB) elements will be very difficult to determine in many applications [1, 2].

3 PSB Techniques

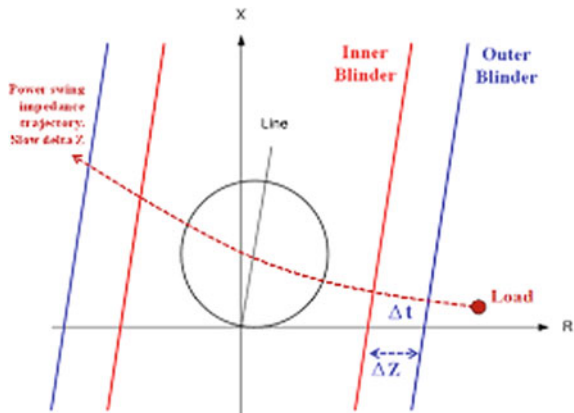
3.1 Blinder Scheme

The rate of change of relay measured impedance is very fast during the fault conditions and too slow during the power swing conditions. Based on this concept, blinders technique is used. In two blinders scheme, there will be an outer blinder and inner blinder. Time setting is provided to be done between the blinders. Two blinders scheme is shown in Fig. 2. Either the change in the impedance is due to fault or power swing, the relay measured impedance will enter into the outer and inner blinders, which can be able to calculate the time taken by the measured impedance locus to cross from outer blinder to inner blinder. If this calculated time is less than the time setting, then the rate of change in relay impedance is fast and is due to the fault, and the relay gets unblocked which will be tripped. But, if the calculated time is greater than the time setting, then the rate of change in relay impedance is slow due to power flow swing, and relay gets blocked where there will be no tripping [2].

Based on this blinders scheme, it is possible to detect as well as distinguish power swing and fault. Nowadays, latest distance relays are using this technique recently. Single blinder scheme is only used to control the relay tripping for loads outside of the blinders. Two blinders method is possible to discriminate power swing and fault which is not possible by single blinder scheme.

There are two major disadvantages of this scheme. First one, when power swing is in blocking, it will not give response to the faults. Second one, time delay setting

Fig. 2 Two blinders scheme



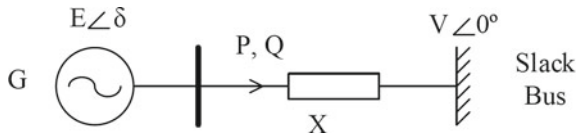


Fig. 3 Equivalent single machine system

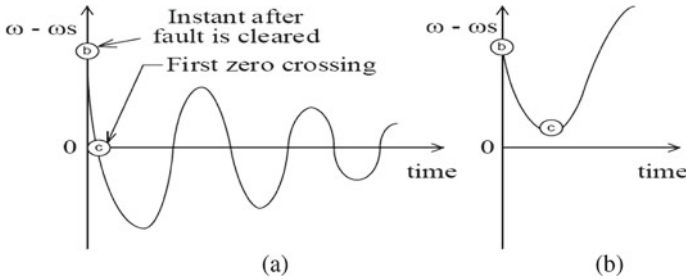


Fig. 4 Relative angular velocity of the equivalent single machine during **a** stable and **b** unstable power swing

is becoming too difficult, when the power swing frequency is as high as 4–7 Hz or as low as 1–3 Hz.

3.2 First Zero Crossing (FZC)

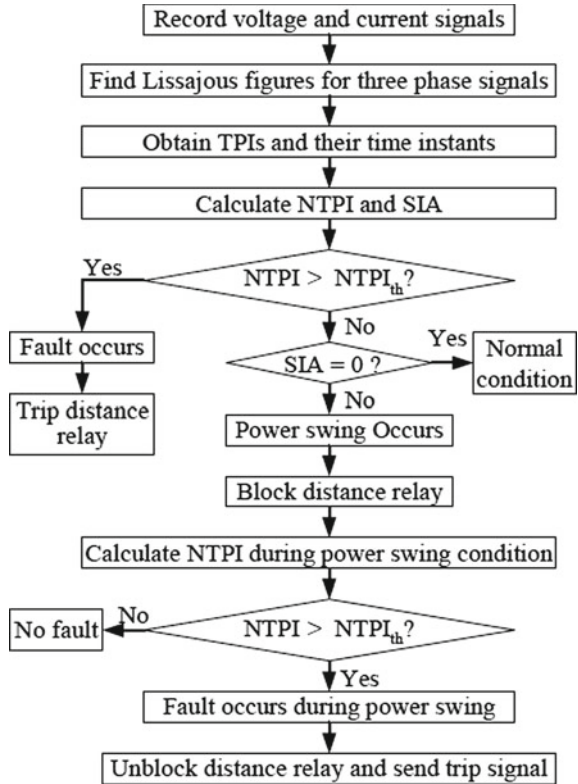
This is a novel blocking method of mho relay during power swings. This method represents converting n -bus system into an equivalent single machine system connected to infinite bus as shown in Fig. 3 [3].

Collecting measurement data from the distance relay of equivalent network at the respective bus, it is required to calculate the speed/angular velocity of the synchronous generator. The plot of relative angular velocity versus time for stable and unstable power swing shown in Fig. 4. If the curve crosses the zero axis called as first zero crossing (FZC), it can be observed as stable power swing, and if the curve not crosses the zero axis, it can be observed as an unstable power swing or fault.

3.3 Lissajous Figure

Detecting and blocking of power swing of a distance relay can be accurately done by using Lissajous figure, which is drawn between voltage and current signals considering a hybrid transmission line. Hybrid transmission lines usually used in off-shore power transmission, consisting of an underground cable and an overhead line [4].

Fig. 5 Flowchart of Lissajous figure method



During the conditions of normal, fault, and power swing, the Lissajous figures of current and voltage will have distinct natures which help to develop a power swing blocking function for deblocking and blocking of relay due to power swing. To distinguish power swing and faults, two indices should be continuously monitored: average sample points of time interval (SIA) and number of tangents perpendicular to current signal (NTPI). The proposed method flowchart is shown in Fig. 5.

The performance of this method is verified in different fault resistances, fault conditions, fault locations, load angles, swing frequencies, fault inception times.

3.4 Differential Voltage

This method proposes a novel technique to distinguish power swing and faults using derivative of voltage signals. Sample interval of differential voltage (SIPD) between two successive peaks will decrease gradually during the fault, while its value during power swing always remains above a minimum value. This distinguishing feature

of voltage differentiation is established mathematically in order to recognize faults during power swing [5, 6].

During the condition of power swing, the frequency of signal voltage deviates from the power frequency. The voltage signal can be represented by the below equation

$$v = V_{m1} \sin(\omega_1 t + \theta_1) + V_{m2} \sin(\omega_2 t + \theta_2) \tag{1}$$

where V_{m1} and V_{m2} are the voltage magnitudes of the two sinusoidal signals and θ_1, θ_2 are the respective voltage angles. Differentiating the above equation, the time interval (Δt) can be calculated. Based on this time interval, if f_s is the sampling frequency, the SIPD is determined by using:

$$\text{SIPD} = \frac{\Delta t}{1/f_s} \tag{2}$$

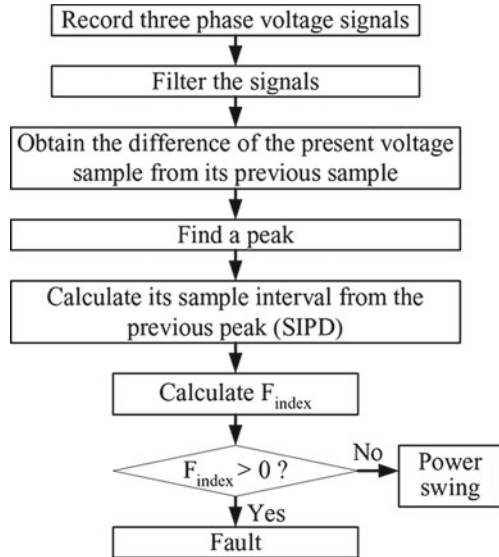
Fault index (F_{index}) is calculated based on SIPD value.

$$F_{\text{index}} = \begin{cases} \text{SIPD} & \text{for SIPD} \leq 50 \\ 0 & \text{Otherwise} \end{cases} \tag{3}$$

Based on the calculated value of SIPD, distinguishing between a fault and power swing is detected. Threshold value chosen for SIPD is 50. Whenever its value is greater than 0, a fault will be detected as shown in Fig. 6.

This method also tested under noisy conditions, different swing frequencies, different power angles, different fault resistances, different types of faults.

Fig. 6 Flowchart of differential voltage scheme



3.5 Differential Power Co-efficient (DPC)

Calculation of differential power co-efficient (DPC) is established on cumulative differences in active power flow due to power swing. This method is to forecast the current and voltage samples at $t + 1$ which helps to calculate the differential power [7].

To predict the next sample, auto-regression technique is used. The voltage and current n th samples are given by:

$$V_n = a_0 + a_1 V_{n-1} + a_2 V_{n-2} + \dots + a_q V_{n-q} \quad (4)$$

$$I_n = a_0 + a_1 I_{n-1} + a_2 I_{n-2} + \dots + a_q I_{n-q} \quad (5)$$

where $a_0, a_1, a_2, \dots, a_q$ are the co-efficients of regression.

Then, find out the differential rms voltages and currents based on equations given by:

$$\Delta V_{\text{rms}} = \sqrt{\frac{1}{r} \sum_{l=1}^r \Delta V_l^2} \quad (6)$$

$$\Delta I_{\text{rms}} = \sqrt{\frac{1}{r} \sum_{l=1}^r \Delta I_l^2} \quad (7)$$

where r indicates the number of samples per cycle.

The differential power is calculated by:

$$\Delta P = \Delta V_{\text{rms}} \times \Delta I_{\text{rms}} \quad (8)$$

After including the effect of power swing, the differential power co-efficient is calculated by using:

$$\text{DPC} = \Delta P \times \sin \delta \quad (9)$$

3.6 Support Vector Machine (SVM)

This scheme identifies power swing along with impedance measuring unit. It is used to distinguish between the power swings and faults. Generally, power swings are phase symmetric in nature, which helps to distinguishing power swings from symmetrical faults [8].

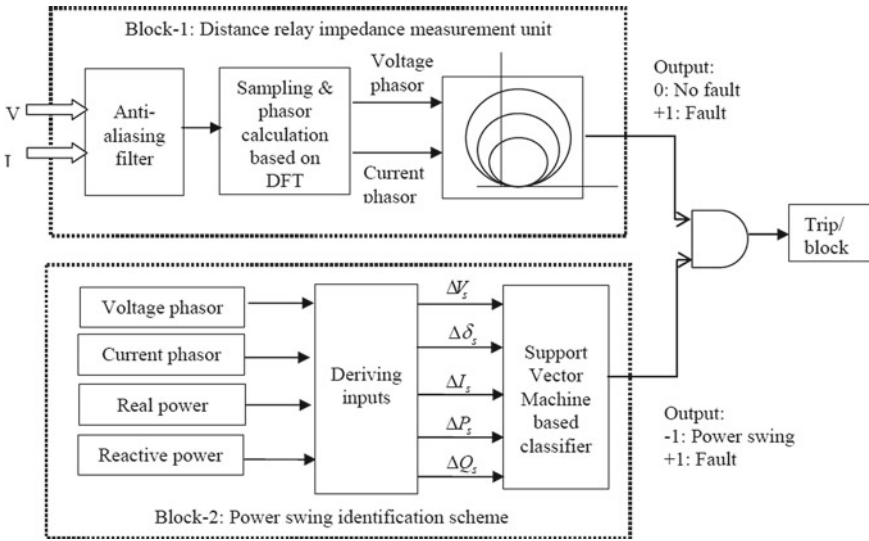


Fig. 7 Block diagram of the SVM scheme

This scheme makes use of the local signals of rate of change of relay input quantities such as real power, reactive power, current, voltage, and its angles. The proposed scheme will have two blocks. Block 1 represents relay measuring unit. This unit will take a decision on whether fault took place or not such as 0 indicates No fault and 1 indicates fault. Block 2 represents scheme of power swing identification which will classify the fault as +1 and power swing as -1 as shown in Fig. 7. This classifier output decides to block or to trip the relay.

Many researchers [9–15] had introduced blocking and deblocking techniques for the distance relay and is shown in Fig. 8, elaboratively based on the criteria of the technique.

4 Comparison of PSB Schemes

Comparison of different power swing blocking/deblocking techniques is shown in Table 1.

5 Conclusion

Protective distance relays are mis-operating during power swings. It is necessary to block the relays due to power swings. Also, deblock of relays are required when

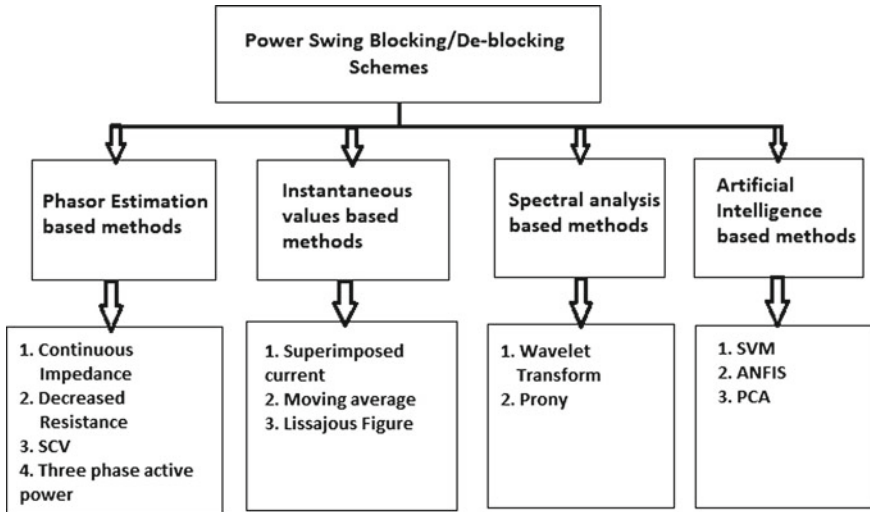


Fig. 8 Classification of PSB schemes

Table 1 Comparison of different PSB techniques

S. No.	Methods	Settings	Measurements required	Fault detection time	Computational burden
1	Continuous impedance	Change in impedance < threshold	All phase V, I	2 cycles	Moderate
2	Swing center voltage (SCV)	Rate of change of SCV ≈ 0	All phase V, I	2 cycles	Moderate
3	Superimposed current	5% of nominal current	All phase V, I	>2 cycles	Less
4	Moving average (MA)	MA of all phase current ≈ 0	All phase V, I	1-3 cycles	Less
5	Lissajous figure	TPI with half-cycle spacing	All phase V, I	<0.5 cycle	Less
6	Wavelet transform	Numerical	All phase V, I	<1 cycle	High
7	ANFIS	Numerical	All phase V, I	>1 cycle	High
8	Support vector machine (SVM)	Numerical	All phase V, I	<1 cycle	High

a symmetrical fault has taken place during the blocking of distance relays. Many researchers had proposed blocking and deblocking techniques. These methods have advantages as well as disadvantages. This paper discusses mainly about few methods of techniques and its respective operation also discussed. Comparison of parameters also made between few blocking and deblocking techniques. This paper helps new researchers to understand thoroughly the techniques and its proposed method usage.

References

1. Fischer N, Benmouyal G, Hou D, Tziouvaras D, Byrne Finley J, Smyth B (2012) Tutorial on power swing blocking and out-of-step tripping. In: Proceedings of 39th annual western protective relay conference, Oct 2012
2. IEEE Power System Relaying Committee (2005) Power swing and out-of-step considerations on transmission lines. Baltimore, PSRC WG D6, June 2005
3. Kang D, Gokaraju R (2016) A new method for blocking third-zone distance relays during stable power swings. *IEEE Trans Power Delivery* 31(4):1836–1843, Aug 2016
4. Patel B, Bera P (2018) Detection of power swing and fault during power swing using Lissajous figure. *IEEE Trans Power Delivery* 33(6):3019–3027, Dec 2018
5. Patel B, Bera P, Dey SHN (2020) Differential voltage-based fault detection during power swing. *IET Gener Transm Distrib* 14(1)
6. Sriram C, Kishore MNR (2020) Teaching distance relay protection and circuit breaker co-ordination of an IEEE 9 bus system using MATLAB/SIMULINK". In: Lecture notes in electrical engineering, Springer, 2020
7. Hari V, Kumar DS, Savier JS (2018) Phasor measurement based fault detection and blocking/deblocking of distance relay under power swing. In: 2018 international CET conference on control, communication, and computing (IC4), pp 134–139
8. Seethalekshmi K, Singh SN, Srivastava SC (2010) SVM based power swing identification scheme for distance relays. In: IEEE PES general meeting, 2010
9. Sriram C, Ravi Kumar D, Suryanarayana Raju G (2014) Blocking the distance relay operation in third zone during power swing using polynomial curve fitting (PCF) method. In: International conference on SEG, IEEE digital library, pp 1–7
10. Hida S, Pradhan V, Naidu OD, Cheriyan EP (2019) A critical review of distance relaying techniques under power swing condition. In: IEEE PES GTD grand international conference and exposition Asia (GTD Asia), pp 500–505
11. Esmacilian A, Astinfeshan S (2011) A novel power swing detection algorithm using adaptive neuro fuzzy technique. In: International conference on electrical engineering and informatics (ICEEI), pp 1–6
12. Zadeh HK, Li Z (2008) A novel power swing blocking scheme using adaptive neuro fuzzy inference system. *Electr Power Syst Res* 78:1138–1146
13. Lin X, Gao Y, Liu P (2008) A novel scheme to identify symmetrical faults occurring during power swings. *IEEE Trans Power Del* 23(1):73–78, Jan 2008
14. Brahma SM (2007) Distance relay with out-of-step blocking function using wavelet transform. *IEEE Trans Power Del* 22(3):1360–1366, July 2007
15. Sriram C, Kusumalatha Y (2019) A review on power swing blocking schemes of distance relay during stable power swings. *Int J Eng Adv Technol* 8(4)

Generation of Poly-Phase Frequency-Hopped Spread Spectrum Signal for LPI Radar Target Detection



Jayshree Das, S. Munnnavvar Hussain, and I. A. Pasha

Abstract Signal design problem is a challenge in a Low Probability of Intercept (LPI) radar system. The novelty of the work is to design LPI waveform to minimize the probability of intercept by an enemy receiver and improve the detection performance. The focus of the present work is to improve the detection performance of LPI radar system which can be achieved by additional interpretation and signal processing at the receiver. Novel poly-phase frequency-hopped spread signal is transmitted and on reception additionally decoded into various interpretations using poly-gram readings. This work is also focused to address the optimization problem using correlated filter technique to improve the detection performance of the LPI radar. Discrimination Factor (DF) and Peak Sidelobe Level (PSL) are taken into account to analyze single and multiple targets in presence of noise and Doppler shift environment.

Keywords Discrimination factor · Doppler shift · Low probability of intercept · Poly-phase

1 Introduction

Today, many users of radar are specifying the Low Probability of Intercept (LPI) as a tactical requirement. The term LPI is that property of radar, because of its low power, wide BW, frequency variability, makes it difficult to be detected by an intercept receiver. LPI design focuses on the ability to defeat the threats such as security of matched filters, minimized signal power spectral density, randomized radar parameters, and wide power density and operations. These requirements can be achieved by specially designed emitted waveforms. Binary and poly-phase codes are popular

J. Das (✉) · S. Munnnavvar Hussain · I. A. Pasha
B V Raju Institute of Technology, Narsapur, Medak 502313, Telangana, India
e-mail: jayshree.das@bvrit.ac.in

S. Munnnavvar Hussain
e-mail: hussain.m@bvrit.ac.in

I. A. Pasha
e-mail: pasha.ia@bvrit.ac.in

for designing of the LPI waveforms. These codes should have the low sidelobes and Doppler tolerance. Poly-phase codes have better sidelobe suppression and Doppler tolerance than the binary codes and hence most useful for LPI designers [1]. Obtaining phase-coded pulse compression sequences with peaky aperiodic autocorrelation has long been an important problem in the LPI waveform design. A high sidelobe level of 22.7 dB is obtained by the Barker sequence with the length of 13 [2]. Several codes such as P1, P2, P3, and P4 are used for designing of radar waveforms [3]. To minimize the peak-to-mean envelope power ratio of the radio communication waveform, first method is implemented using different subcarrier complex weights [4], and the second method is implemented using phase code technique [5]. These two methods are take-on to improve the peak sidelobe level ratio. Lower peak-to-mean envelope power ratio and higher peak sidelobe level ratio of radio communication waveform cannot be achieved simultaneously by using both of these two methods [6, 7].

In order to obtain the sequences of bigger lengths with good merit factor and discrimination values, global optimization techniques such as genetic algorithm, Eugenic algorithm, and Simon–Kronecker–Hamming (SKH) algorithm have been used [8–10]. This paper is motivated by an idea that only poly-phase frequency-hopped spread (PP FHSS) signal is transmitted as a waveform, and everything else is taken care of by additional signal processing at the receiver. In this work, the problem of improving the detection performance of LPI radar system is attempted through the signal design problem and optimization algorithm. This is solved by the notation of PP FHSS for single and multiple targets through coincidence detection strategy. This paper also discusses the design of LPI radar signal processing for detection of single and multiple targets in presence of noise and noise-free environment.

1.1 Poly-Phase Frequency-Hopped Spread Signal

This section explains the generation of PP FHSS. The PP FHSS signal comprises of poly-phase signal and frequency-hopped spread signals.

Step 1: To set up notations and to design an algorithm for interpretations of signals, let

$S = [S_1, S_2, S_3, \dots, S_N]$ be an input binary code of length ' N '.

Step 2: The carrier is exponential signal and given as.

$C = \exp(j * \theta_i)$, where $\theta_i = [\varphi_1, \varphi_2, \varphi_3, \varphi_4, \varphi_5, \varphi_6]$ are phases used in sub-carrier pulse width.

Here, θ_i ($w = 6$) is considered.

Step 3: Generation of poly-phase-coded (PP) signal

$$PP = \sqrt{\frac{2Es}{T}} \cos 2\pi f_c t + \frac{2\pi i}{M} \quad (1)$$

where $i = 1, 2, 3, \dots, M - 1$.

Quadrature phase shift keying-coded (Q-PSK) signal, 8-PSK-coded signal, and 16-PSK-coded signals are generated and given by Eqs. 2, 3, and 4.

$$\text{Q-PSK} = \sqrt{\frac{2Es}{T}} \cos(2\pi f_c t) + \frac{2\pi_i}{M} \quad (2)$$

where $i = 0, 1, 2, 3$.

$$\text{8-PSK} = \sqrt{\frac{2Es}{T}} \cos(2\pi f_c t) + \frac{2\pi_i}{M} \quad (3)$$

where $i = 0, 1, 2, 3, 4, 5, 6, 7$.

$$\text{16-PSK} = \sqrt{\frac{2Es}{T}} \cos(2\pi f_c t) + \frac{2\pi_i}{M} \quad (4)$$

where $i = 0, 1, 2, 3, 4, 5, 6, 7, 8, 9, 10, 11, 12, 13, 14, 15$.

Equations 2–4 are used to generate Q-PSK, 8-PSK, and 16-PSK-modulated signals which have the symbol length of $2WN$, $3WN$, and $4WN$, respectively, is the first level of modulation in waveform generation.

1.2 Frequency-Hopped Spread Spectrum (FHSS) Signal Generation

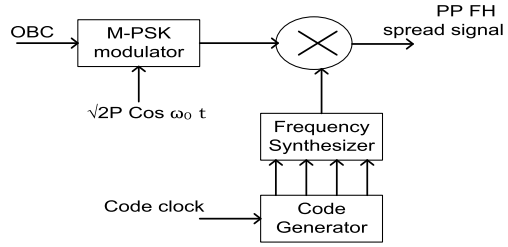
Spread spectrum (SS) is a modulation technique that makes use of the transmission bandwidth much more than the modulating signal bandwidth. One of the reasons to employ the SS modulation is to supply a signal with modulating low spectral level so that it is covered with background noise, i.e., to supply low probability of range and detection resolution measurement. In order to get the frequency spectrum of the transmitted signal wider than what is required to carry the information of the signal, wideband modulation spreads the energy of the signal in frequency. The signal strength per information is reduced by spreading the signal energy. To spread the signal in frequency, the signal frequency to be swept at high rate or chirping is frequency-hopped (FH) modulation and incorporates in the LPI. The steps for generation of the FHSS signal are given:

1. Random spreading sequence $C_i(t)$ is exponential signal given by

$$C_i(t) = \exp(j * \theta_i), \quad \text{where } i = 1, 2, 3, \dots, n \quad (5)$$

2. There is a change in carrier frequency of a pulse over a preselected set of sub-carrier frequencies in a FH modulation.

Fig. 1 PP FHSS signal generation



$$FH = \sum_{k=-\infty}^{\infty} A(t) \sin(2\pi(f_o + C_i B_c)t + \theta(t)) P \frac{t - k\tau_c}{\tau_c} \tag{6}$$

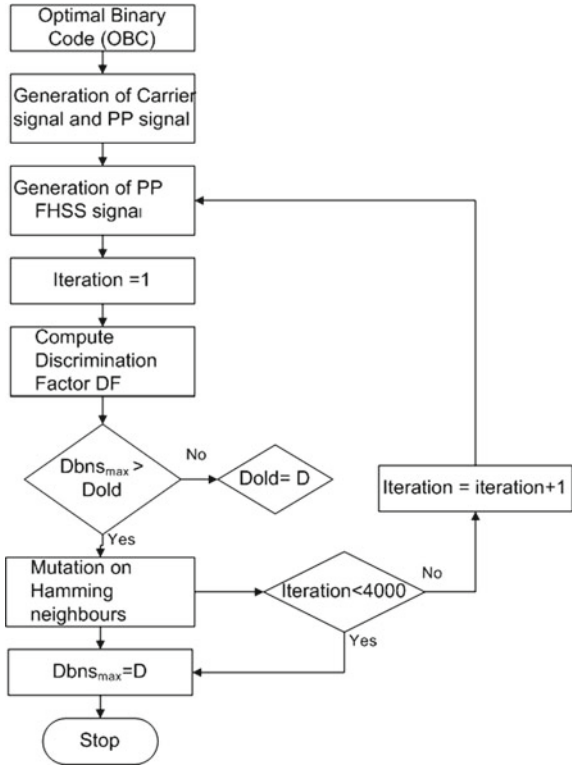
The last step in PP FHSS signal generation is to multiply the FH-modulated signal by PP-modulated signal, and this process is brought about in two level of modulation (Fig. 1).

$$PP\ FHSS = \sqrt{\frac{2Es}{T}} \cos(2\pi f_c t) + \frac{2\pi}{M} * \sum_{k=-\infty}^{\infty} A(t) \sin(2\pi f_o + C_i B_c)t + \theta(t) P \left(\frac{t - K\tau_c}{\tau_c} \right) \tag{7}$$

1.3 Hamming Scan Algorithm

Though the Hamming scan is suboptimal, it is an optimization algorithm which is more efficient. In case of binary sequence, binary elements mutation implies $+1 \rightarrow -1$ or $-1 \rightarrow +1$. A hamming distance of one from original sequence is the resultant of the single mutation in a sequence [11]. Hamming scan performs a recursive local search among all the Hamming neighbors and picks the one with the maximum objective function. The algorithm is repetitively extended there from, taken into account the sequence which has enhanced value of DF which is better than the original sequence. Thus, the complete local search is the replacement of entirely probabilistic mechanism of mutation. The Hamming scan (HS) can be accelerated and hence made applicable at longer length [12] (Fig. 2).

Fig. 2 PP FHSS sequence generation and optimization of sequence using Hamming scan algorithm



2 Poly-Phase Frequency-Hopped Spread Spectrum Signal with Additional Gray Binary Interpretation

Making the signal harder to detect and analyze by non-cooperative intercept receiver, there is a requirement to have complicated signal structure in LPI radar system. Specially designed Poly-Phase Frequency Hopped Spread Spectrum (PP FHSS) signals are transmitted so that there is no change in transmission technology. Before further processing, these signals are decoded on reception. The change in current practice is required to obtain an additional advantage of signal processing at the receiver. After the received signals are decoded, they are subjected to additional interpretations: (1) Received signal from the target and (2) Additional Gray binary interpretation. To set up the coincidence detection at the receiver, even though the PP FHSS signal is transmitted here, it could be interpreted on reception as additional Gray binary signal through poly-gram reading. Thereafter, they can process separately through the multiple matched filters at the receiver. In generation of poly-alphabetic LPI sequences, bigram reading is viewed as quaternary element; a trigram is being viewed as octal element, and quad gram is used as Hexa element; this is to some extent a constraint concept [13]. Gray-code technology is used here to improve

the DF of the designed waveform and simultaneously choose the optimization algorithm to improve the performance of the PP FHSS signal [14]. The quaternary, octal and Hexa elements as independent structure would have 3, 7, and 15 order Hamming neighbors, but when it under goes HS, the bi-gram, tri-gram, and quad-gram are the layers of binary monogram which have only two, three, and four first-order Hamming neighbors. At higher lengths, the enlarged alphabets deteriorate the noise and Doppler performance. In order to address this drawback and to overcome it, we have restricted the enlarged alphabet of the PP FHSS sequences to Gray binary sequences at the receiver.

2.1 Signal Design Problem and Optimization Problem

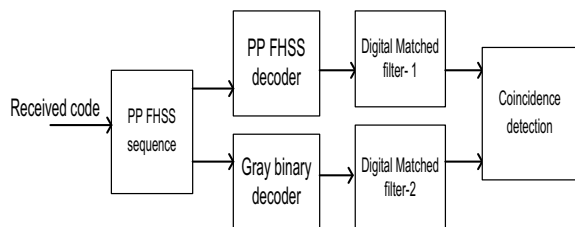
Signal design problem and optimization problem at the receiver are the center point of the work.

Signal Design Problem: In case of LPI radar, PP FHSS sequence of length L ($M * W * N$) is transmitted here M (4, 8 and 16) in case of LPI radar, and upon reception, the decoded PP FHSS sequence can be additionally interpreted as Gray decoded binary sequence of length $2L$. This facilitates an efficient implementation of coincidence detection strategy as the central peak of the autocorrelation function of two matched filters is aligned, while their time sidelobes may not.

Optimization Problem: The transmitted PP FHSS signal is optimized such that the sum of the discrimination of the PP FHSS sequence ($D1$) and Gray binary decoded sequence ($D2$) is optimum (Fig. 3).

Figures 4, 5, and 6 show the coincidence detection plots and ambiguity function plots for Q-PSK FHSS, 8-PSK FHSS, and 16-PSK FHSS signals. The Q-PSK FHSS signal of length 288 and Gray binary signal of length 576 are processed through two matched filters. Similarly, 8-PSK FHSS signal of length 288 and Gray binary signal of length 864 where as 16-PSK FHSS signal of length 288 and Gray binary signal of length of 1152 are processed through the two digital matched filters. In all the three case, the main peaks of the two channels of the matched filters are aligned, whereas the sidelobes do not. This results in efficient detection of the target. From the ambiguity plots of Q-PSK, 8-PSK, and 16-PSK FHSS signals, it is observed that the main peak in all the three cases has maximum amplitude, whereas more sidelobes are

Fig. 3 PP FHSS with Gray binary decoded signal processing in LPI radar



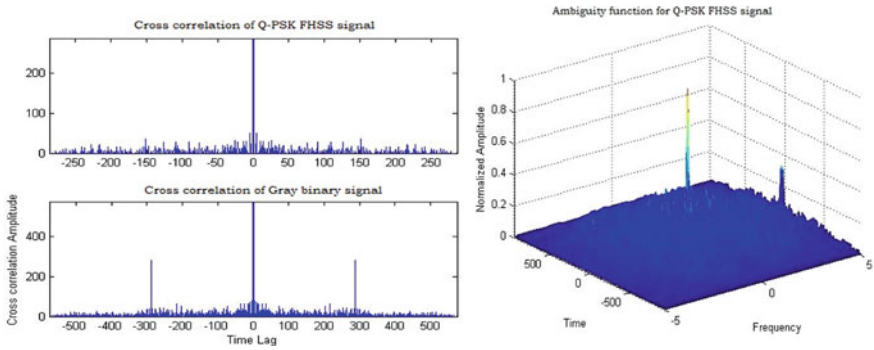


Fig. 4 Coincidence detection and ambiguity plot of Q-PSK FHSS signal length L (288) and Gray binary signal length L (576)

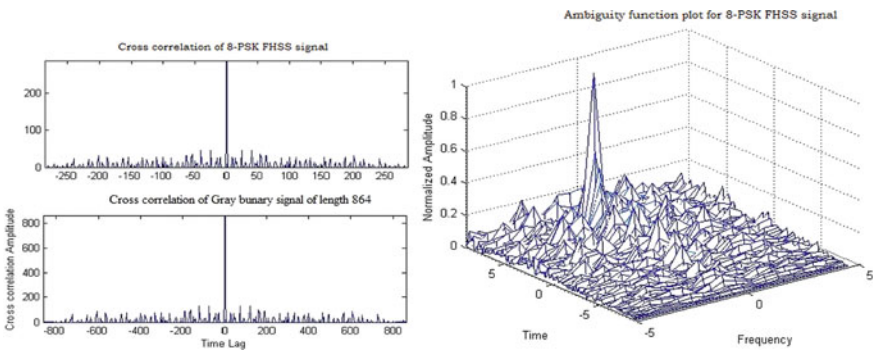


Fig. 5 Coincidence detection and ambiguity plot of 8-PSK FHSS signal length L (288) and Gray binary signal length L (864)

results in case of 16-PSK FHSS signal compared with the Q-PSK FHSS and 8-PSK FHSS signals.

2.2 Noise Robustness in PP FHSS with Additional Gray Binary Signal

By applying the noise echo pulse at the input of the matched filter, the noise performance of the proposed PP FHSS signal and Gray binary interpreted signal is analyzed in case of single target and multiple targets.

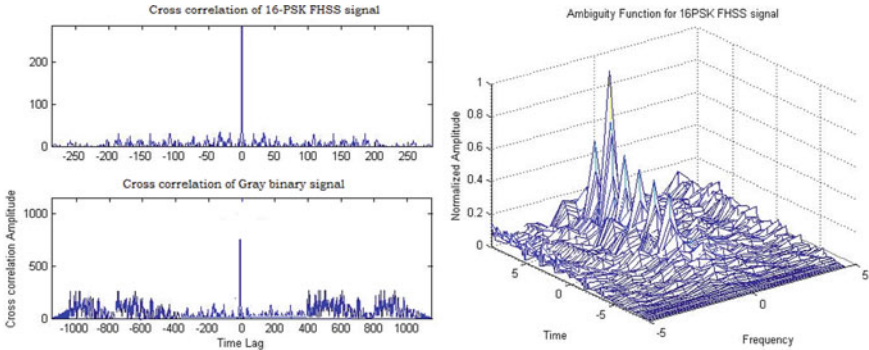


Fig. 6 Coincidence detection and ambiguity plot of Q-PSK FHSS signal length L (288) and Gray binary signal length L (1152)

2.2.1 Single Target

The joint objective function (DF) is sum of $D1$ and $D2$ where $D1$ is DF for Gray binary interpreted signal and $D2$ is DF for PP FHSS signal. In noise-free environment, the DF for Gray binary sequence ($D1$) is slightly more (1 dB) than PP FHSS sequence ($D2$). At 0 dB, SNR with standard deviation Sd ($=0.3, 0.5$ and 0.9) is being considered to evaluate the noise performance of the PP FHSS with additional Gray binary interpreted signal. The variations of DF with OBC 13–48 along with noise for Q-PSK FHSS, 8-PSK FHSS, and 16-PSK FHSS sequences are given in Fig. 7.

From Fig. 7, it is observed that the DF decreases with increase in the noise strength. At $Sd = 0.3$, the DF has the maximum value, whereas at $Sd = 0.9$ the values of DF is minimum (Fig. 8).

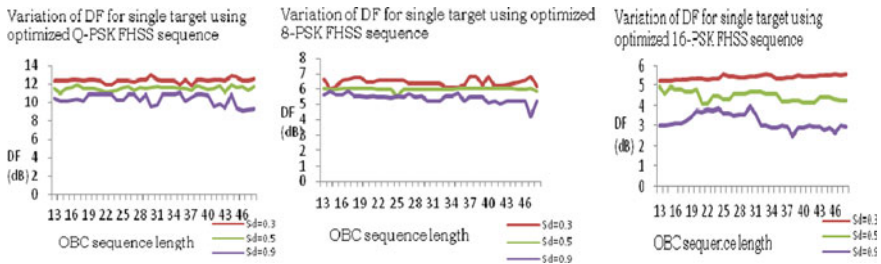


Fig. 7 Variation of DF (dB) for single target using optimized PP FHSS sequences at 0 dB SNR in noisy environment ($Sd = 0.3, 0.5$ and 0.9)

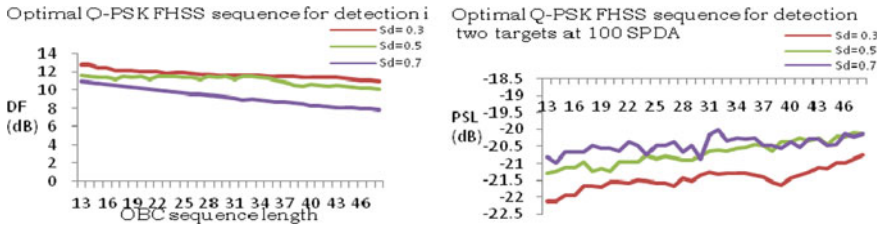


Fig. 8 Variation of DF (dB) and PSL (dB) for optimal Q-PSK FHSS sequences when two targets at 100 SPDA in presence of noise strength S_d ($=0.3, 0.5,$ and 0.7) at 0 dB SNR

2.2.2 Multiple Targets

In noisy environment, when two targets are separated at 100 SPDA and noise strength is varying from 0.3 to 0.7 at 0 dB SNR, the corresponding change in the DF and PSL values varying in between 2 and 3 dB in case of Q-PSK FHSS and 8-PSK FHSS sequences where as in case of 16-PSK FHSS sequence 1 dB variation is observed in DF and PSL value. Figures 9 and 10 show the variation of DF and PSL values for optimal PP FHSS sequences in presence of noise.

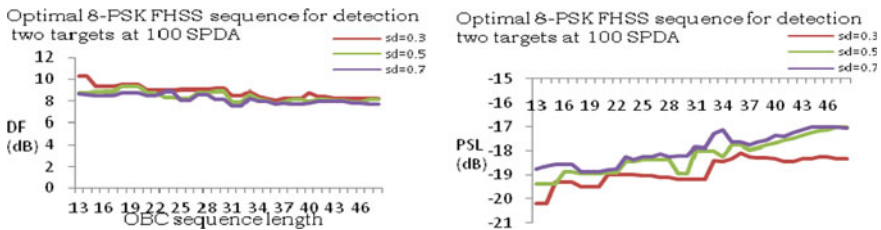


Fig. 9 Variation of DF (dB) and PSL (dB) for optimal 8-PSK FHSS sequences when two targets at 100 SPDA in presence of noise strength S_d ($=0.3, 0.5$ and 0.7) at 0 dB SNR

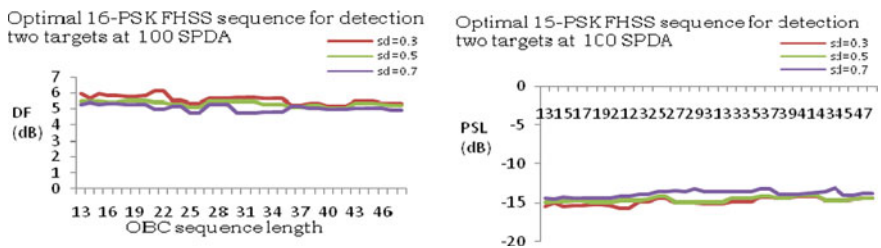


Fig. 10 Variation of DF (dB) and PSL (dB) for optimal 16-PSK FHSS sequences when two targets at 100 SPDA in presence of noise strength S_d ($=0.3, 0.5$ and 0.7) at 0 dB SNR

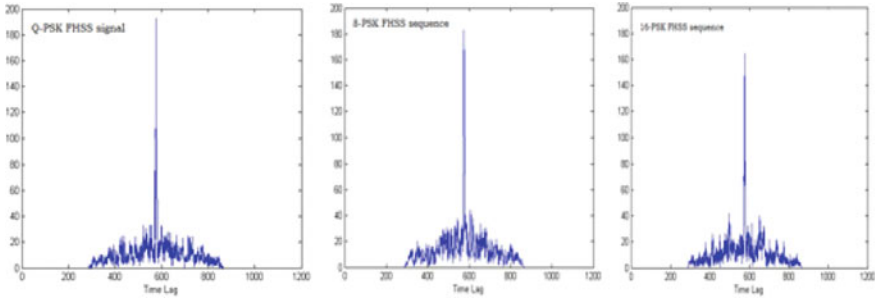


Fig. 11 Detection of single target in absence of noise using Q-PSK FHSS sequences

3 Doppler Tolerance in PP FHSS with Additional Gray Binary Signal

The detection of single and multiple targets is analyzed considering Doppler-phased shift (f_d) of 10 Hz. This is accomplished by transmitting PP FHSS sequences in absence and presence of additive noise.

3.1 Single Target

By considering PP FHSS signals, the Doppler Effect is observed for single target in absence of noise. The variation of amplitude of the main peak at Doppler frequency f_d (10 Hz) in noise-free environment is shown in Fig. 11. The effect of the Doppler shift is negligible if single target is considered. In case of Q-PSK FHSS signal, 8-PSK FHSS signal, and 16-PSK FHSS with additional Gray binary signal, the marginal variation in sidelobe amplitude is observed.

3.2 Multiple Targets

By considering PP FHSS signals, the Doppler Effect is considered for two targets when they are at 100 sub-pulse delay apart (SPDA). Figure 12 shows the Doppler performance in case of Q-PSK FHSS, 8-PSK FHSS, and 16-PSK FHSS with additional Gray binary interpretation when two targets are considered in presence of noise. When SNR of 0 dB and standard deviation S_d ($=0.3$) considered, the amplitude of the sidelobe levels is less than the amplitude of the main peak of the two targets.

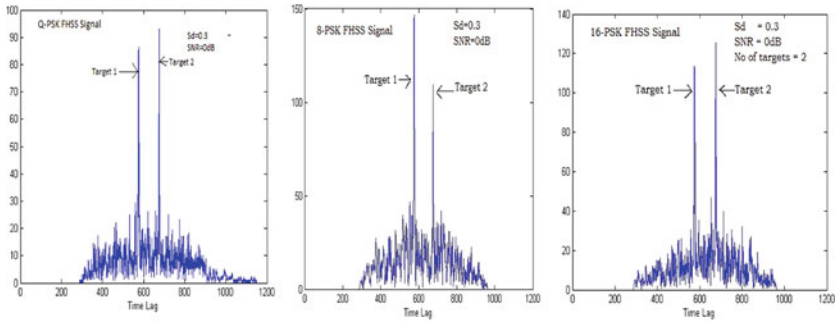


Fig. 12 Output waveform of Q-PSK FHSS with additional Gray binary sequence when two targets are at 100 SPDA in noisy environment at SNR 0 dB

4 Discussion and Conclusion

In this work, the PP FHSS LPI radar signals design and the problem of target detection are studied. If part of the burden of obtaining good results can be shared by additional signal processing at the receiver, the signal design problem can be solved more satisfactorily. This is a scheme where the advantages of cooperation are available when only one, i.e., PP FHSS sequence is transmitted. To exploit the coincidence detection characteristics of matched filter, a LPI radar waveform is designed. To generate PP LPI radar signals and achieve target detection with an objective, the signal design algorithms are developed using PSK scheme, specifically Q-PSK, 8-PSK, and 16-PSK; the first step is to design PP-coded signals. The PP signals here are put through the FHSS technique. The second step is to develop optimization algorithm using Hamming Scan (HS) for generation of PP FHSS sequences which in turn result into joint coincidence detection using multiple matched filters.

Subjected to Gray binary interpretation scheme, the PP FHSS sequence is being decoded as the two-bit binary in case of Q-PSK scheme. In case of 8-PSK FHSS and 16-PSK FHSS sequences are decoded as three-bit binary and four-bit binary sequence. In terms of DF and PSL, the detection performance of the proposed PP PSK schemes is analyzed. The OBC signal of length L (N) results in the PP FHSS sequence of length L ($L * W$), where W is the number of sub-carrier samples (6). By considering PP FHSS signals with AWGN of noise strength, the isolated return signals from the target are modeled to evaluate the noise performance, when S_d ($=0.3, 0.5$ and 0.9) at SNR 0 dB. Q-PSK FHSS signal of length L ($=288$), S_d 0.3 and SNR 10 dB has DF ($=11.33$ dB). Increase in values of DF observed when S_d varies from 0.3 to 0.9. Compared with the 8-PSK FHSS and 16-PSK FHSS with additional Gray binary sequences, Q-PSK FHSS with additional Gray binary sequence has high DF/PSL values when only one target is present in noise-free environment. DF = 18.7 dB in case of Q-PSK FHSS signal with Gray binary interpretation, whereas 10.22 dB and 7.63 dB in case of 8-PSK FHSS signal with Gray binary interpretation and 16-PSK FHSS signal with Gray binary interpretation, respectively. Since signal

becomes noisier with increase in phase constellations, therefore, 16-PSK FHSS signal with Gray binary interpretation results less DF compared with the other two. To analyze the Doppler tolerance, the ratio of f_d/bw is taken as performance evaluation parameter. The dispersed echo signals are subjected to Doppler frequency of 10 Hz by keeping bandwidth constant for a given code in noisy and noise-free environment. The effect of Doppler on single target in noise-free environment is analyzed using Q-PSK FHSS, 8-PSK FHSS, and 16-PSK FHSS sequences. Improved DF is observed when the target is stationary. Noise and Doppler performance compared in presence of single target and multiple targets. Multiple targets are more sensitive to Doppler tolerance and noise compared with the single target.

References

1. Pace PE (2008) Detection and classifying low probability of intercept radar, 2nd edn. Artech House, Boston, London
2. Sklonik M (2008) Radar handbook, 3rd edn. Mc-Graw Hill Publication
3. Griep KR, Ritcey JA, Burlingame JJ (1995) Poly-phase codes and optimal filters for multiple user ranging. *IEEE Trans Aerosp Electron Syst* 31(2):752–767
4. Hu L, Du Z, Xue G (2014) Radar-communication integration based on OFDM signal. In: proceedings of the 2014 IEEE international conference on signal processing, communications and computing, ICSPCC 2014, pp 442–445
5. Zhao J, Huo K, Li X (2014) A chaos-based phase coded OFDM signal for joint radar-communications systems. In: Proceedings of 2014 12th IEEE international conference on signal processing, ICSP 2014, pp 1997–2002
6. Huang SCH, Wu HC, Chang S, Liu X (2010) Novel sequence design for low-PMEPR and high code rate OFDM system. *IEEE Trans Commun* 58(2):405–410
7. Mozeson E, Levanon N (2003) Multicarrier radar signals with low peak-to-mean envelope power ratio. *IEEE Proc Radar Sonar Navig* 150(2):71–77
8. Singh R, Moharir PS, Maru VM (1996) S-K-H algorithm for signal design. *J Inst Eng Technol Electron Lett* 32(18):1648
9. Hu H, Liu B (2008) Genetic algorithm for designing polyphase orthogonal code. In: International conference on wireless communications, networking and mobile computing
10. De Wurtz GC, Hoffman KH (2007) Low autocorrelation binary sequences: exact enumeration and optimization by evolutionary strategies. *J Math Program Oper Res* 23(4):369–438
11. Eiben AE, Michalewicz Z, Schoenauer M, Smith JE (2007) Parameter control in evolutionary algorithms. In: Studies in computational intelligence, vol 54. Springer, Berlin, Heidelberg, pp 19–46
12. Pasha IA, Moharir PS, Pandaripande VM (2003) Equi-length polyalphabetic sequence design. *IRSI-Bangalore* 24:237–243
13. Simon HA (1981) The sciences of the artificial, 3rd edn. MTI Press, Cambridge. ISBN: 9780262190510
14. Zli C, Bao W, Xu L, Zahang H, Huang Z (2017) Radar communication integrated waveform design based on OFDM and circular shift sequence. *Hindawi Math Prob Eng* 2017:1–11

Energy Efficient Memory Architecture for High Performance and Low Power Applications Under Sub-threshold Regime



T. Vasudeva Reddy, K. Madhava Rao, V. Santhosh Kumar,
and V. Hindumathi

Abstract In recent years, digital VLSI circuits operating under sub-threshold operation have gained a lot of attention due to the rapid growth in technology from low to high performance applications. In addition to that, performance is improved by device dimensions and circuit operations under threshold regime. This leads to promising technology for future memory designs for ultra-low power applications. On the other hand, there is an issue of static or leakage current that leads to a reduction of performance. Novelty of research in the paper described the design and implementation of energy efficient SRAM designs such as Saturated NMOS SRAM, Schmitt trigger-based SRAM's working under sub-threshold for ultra-low power applications by measuring leakage power. Both logic, circuit and architecture level designs have extensively analyzed to evaluate the performance and functionality of SRAM designs. Comparative analysis is made on the basis of read, write performance, SNM, along with the functionality of static, dynamic characteristics.

Keywords Saturated NMOS · Schmitt trigger SRAM · Sub-threshold · Static current · Low power

T. Vasudeva Reddy (✉) · K. Madhava Rao
B V Raju Institute of Technology, Narsapur, Medak, Telangana 502313, India
e-mail: vasu.tatiparthi@bvrit.ac.in

K. Madhava Rao
e-mail: madhavarao.k@bvrit.ac.in

V. Santhosh Kumar · V. Hindumathi
BVRIT Hyderabad College of Engineering for Women, Nizampet, Hyderabad, Telangana 500090, India
e-mail: santhosh.v@bvrithyderabad.edu.in

V. Hindumathi
e-mail: hindumathi.v@bvrithyderabad.edu.in

1 Abstract

In digital VLSI design significant amount of space is given to high performance, low power applications due to the increasing the portable and battery operated devices and consumer applications. Though number of sub-threshold techniques and designs are available, still there is demand for power minimization techniques such as logic optimization, interconnects, device sizing, voltage reduction, switching function, pipe line and parallelism and so on. Still there is demand of less power hungry designs that functions under sub-threshold region leads to high performance but due to aggressive scaling of transistors, reverse biased leakage current (RBL) and drain induced barrier lowering (DIBL) increasing exponentially.

2 Literature Survey

Researchers and engineers have introduced various design techniques to minimize delay and power optimization. But still there is a necessity of reduction especially designing a biomedical and health care applications. The proposed designs illustrates the techniques of memory designs functions under low power sub-threshold regimes.

3 Proposed Saturated NMOS SRAM Design

In this technique, the dynamic power can be reduced by inserting one extra saturated NMOS in conventional CMOS inverter. Due to this short circuit current will be reduced, therefore overall power consumption is reduced. The saturated NMOS inverter, shown in Fig. 1, has the NMOS NM1 connected between NM0 and PM0. The drain of NM0 is connected to NM1's source. PM0's drain is connected to both the gate and the drain of the NM1 [1–3]. Because NM1's gate and drain are shorted, it can be in either saturation or cutoff mode only if V_{gs1} is greater than NM1's threshold voltage will NM1 begin to conduct. So, at least the output should be V_{th} times V_{ds0} for NM1 to begin conduction. PM0 turns on during the falling transition indicated in Fig. 1 when input falls below $V_{dd} - |V_{tpl}|$ point. The charging current begins to flow from V_{dd} through PM0, charging the output node. NM1 is initially in the off state since the output node is not charged. As a result, the entire current flowing from V_{dd} is used to charge the output node [4, 5].

CMOS inverters are replaced with the saturated NMOS based inverters to reduce the power consumption. The read and write operations identical to those of the conventional 8T SRAM cell shown in Fig. 2, transient and DC analysis are represented in Figs. 3 and 4.

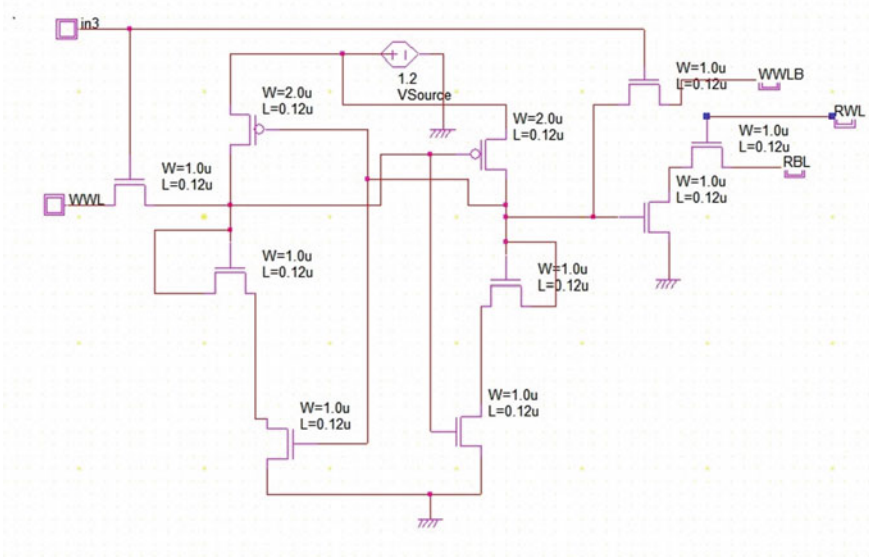


Fig. 1 Saturated NMOS inverter based 8T SRAM cell

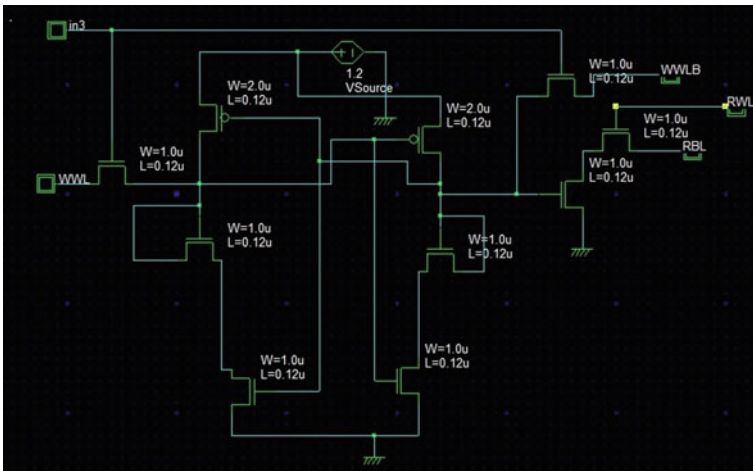


Fig. 2 Schematic of saturated NMOS-based 8T SRAM

SRAM is consists of two back to back connected inverters to store the one bit of data. Therefore CMOS inverters are replaced with saturated NMOS inverter to reduce the short circuit power.

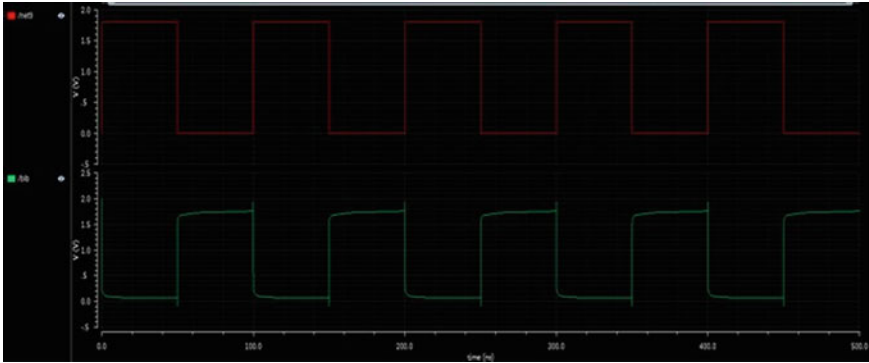
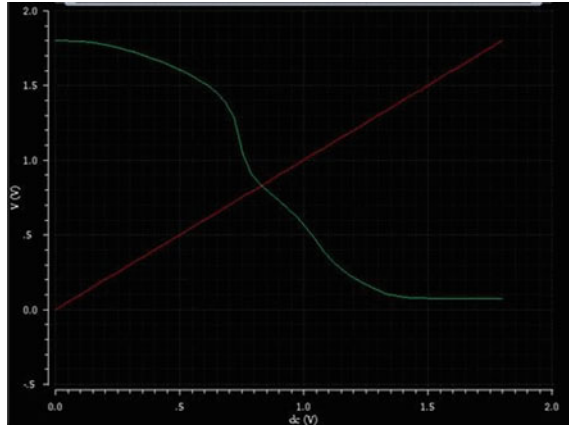


Fig. 3 Transient analysis of saturated 8T SRAM

Fig. 4 DC analysis of saturated NMOS 8T SRAM



3.1 Transient Analysis

Transient analysis is taken into consideration with the characteristics of input and the output relation in view of the voltage response.

3.2 DC Analysis of Saturated NMOS

DC analysis of the design is used to analyze the exact q point of the transistor and also to view the functional performance of the design in terms of voltage.

4 Proposed Schmitt Trigger SRAM Design

At very low voltages, the cross coupled inverter pair stability is a key concern. To improve inverter properties, the Schmitt arrangement is utilized. Depending on the direction of the input transition, a Schmitt trigger raises or lowers an inverter’s switching threshold. The proposed Schmitt trigger-based 8T SRAM cell design focuses on making the SRAM cell’s basic CMOS inverter pair efficient for low voltage applications [6–9]. As shown in Fig. 5 PMOS transistors forms the inverter pair and NMOS transistor acts as an access transistors. 8T Schmitt trigger SRAM is used to improve the read stability and it is having the better noise immunity and having better power consumption. These are achieved with the help of feedback mechanism. The Schmitt trigger-based inverter is having the property of altering the threshold voltages of the inverter those are present in the SRAM circuit, so that it can improve the noise margin in the design.

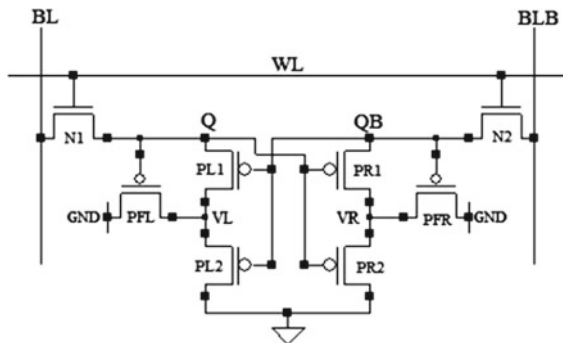
4.1 Write Operation

In the write process, bitline BL is pulled high and bitline bar BLB is pulled low to write logic 1, and vice versa for writing logic 0. The word line is then enabled, causing the NMOS access transistors to switch on, allowing the values to be written into the cell at the appropriate nodes.

4.2 Read Operation

First, the logic values must be present at the nodes Q and QB, i.e., $Q = V_{DD}$ and $QB = 0$, in order to read the logic 1. The QB voltage is applied to the PL1 and PL2 transistors’ gates, causing both transistors to flip on. To switch on access transistors

Fig. 5 Schmitt trigger-based 8T SRAM cell



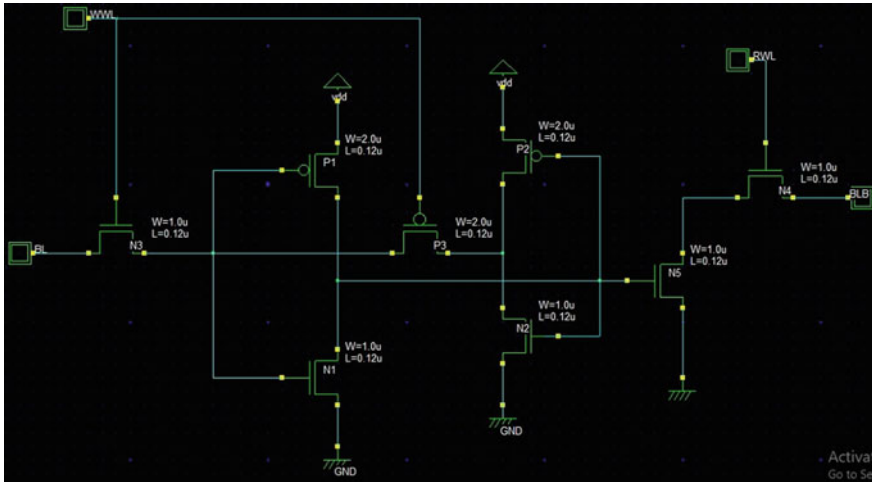


Fig. 6 Proposed Schmitt trigger-based 8T SRAM

the wordline is asserted, the bitlines are precharged to ground for read operation [10]. Because the voltage at node Q discharges through N1, the charges in the bitlines will cause the data at nodes Q and QB to be disrupted. As a result of the unintentional modification, the read failure occurs.

The feedback technique is utilized to solve this problem by increasing the inverter pair's threshold. PR2 transistor will turn on when the voltage at Q reaches V_{tp} , while PR1 will remain off because PFR is on. Because the PR1 is directly linked to ground when the PFR is turned on, its source voltage is zero. As a result, the feedback mechanism increases stability by adjusting VL and VR voltages to improve threshold voltages. So, the read is successfully done due to this feedback in Schmitt trigger 8T SRAM cell indicated in Fig. 5.

In Schmitt trigger-based 8T SRAM, the PMOS inverter pair is replaced with the saturated NMOS based Inverter pair. So that we can reduce the power dissipation even more when compared with the basic Schmitt trigger-based 8T SRAM cell [10–13]. The proposed Schmitt trigger-based 8T SRAM cell is shown Fig. 6 also transient and DC analysis are indicated in Figs. 7 and 8. Rise time delay, fall time delay, propagation delay and also total delay is indicated in Figs. 9 and 10. A comparative analysis of power and delay for novel techniques are summarized in Tables 1 and 2.

5 Conclusion

The reports are collected from the various models once they have been analyzed. Here, I have analyzed the transient and DC response of various models those are implemented by using the 90 nm technology in the cadence virtuoso tool. When all

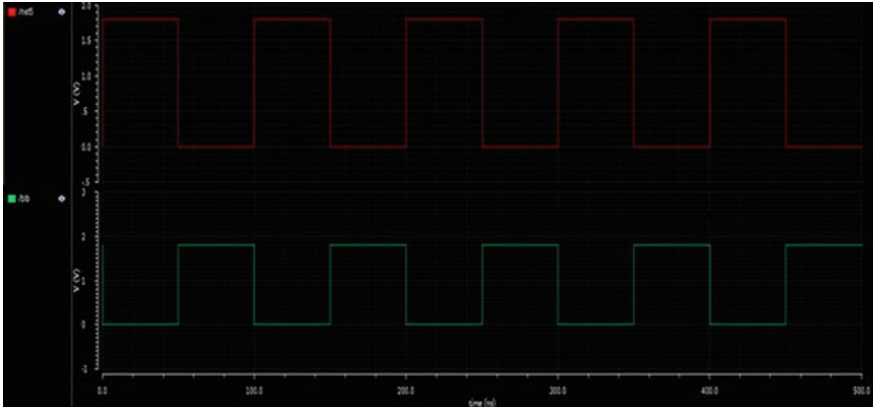


Fig. 7 Transient analysis of Schmitt trigger 8T SRAM

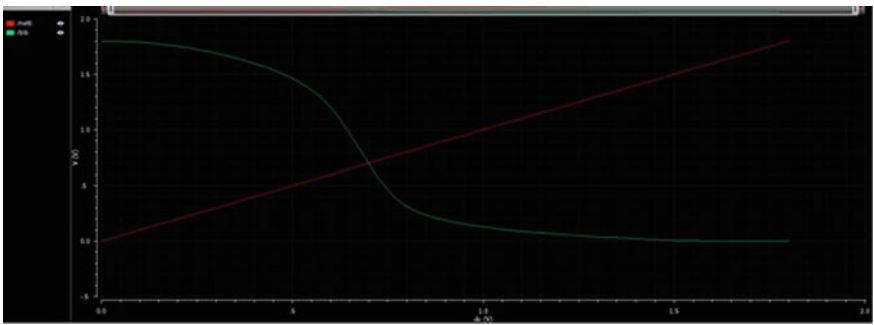


Fig. 8 DC analysis of Schmitt trigger 8T SRAM

Fig. 9 Comparative analysis of delay in SRAM designs

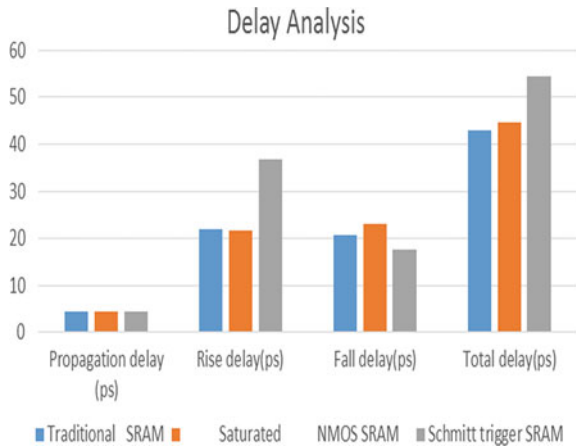


Fig. 10 Comparative analysis of power in SRAM designs

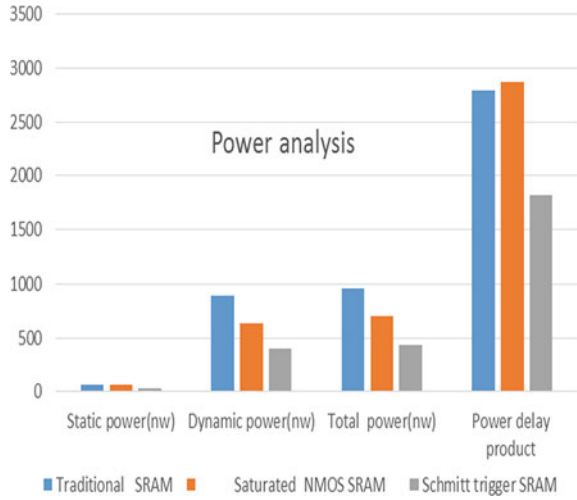


Table 1 Comparative analysis of delay analysis different SRAM designs

Parameter	Traditional SRAM	Saturated NMOS SRAM	Schmitt trigger SRAM
Propagation delay (ps)	4.588	4.515	4.379
Rise delay (ps)	21.99	21.55	36.79
Fall delay (ps)	20.89	23.02	17.73
Total delay (ps)	42.88	44.57	54.52

Table 2 Comparative analysis of power results for different SRAM designs

Parameter	Traditional SRAM	Saturated NMOS SRAM	Schmitt trigger SRAM
Static power (nw)	64.2	63.76	32.91
Dynamic power (nw)	895.2	636.1	405.1
Total power (nw)	959.4	699.86	438.01
Power delay product	2791.0952	2869.8623	1816.6064

of these models are evaluated in terms of propagation delay, rising delay and fall delay, dynamic power and static power. Schmitt trigger 8T SRAM has less power dissipation (16%) compared to other SRAM model. So, the design can be applicable for Low power applications such as Wrist watches, Pacemakers and so on. Saturated NMOS design can be preferable for high speed applications such as modems, routers, embedded processor and so on.

References

1. Kulkarni JP, Roy K (2012) Ultra low voltage process variation tolerant Schmitt trigger based design. *IEEE Trans Very Large Scale Integr* 20, Feb 2012
2. Suzuki T, Yamauchi H, Yamagami Y, Satomi K, Akamatsu H (2008) A stable 2-port SRAM cell design against simultaneously read/write disturbed access. *IEEE J Solid State Circuits* 43(9), Sept 2008
3. Grossar M, Stucchi M, Maex K, Dehaene W (2006) Read stability and write ability analysis of SRAM cells for nanometer technologies. *IEEE J Solid State Circuits* 1(11), Nov 2006
4. Chakraborty S, Chaudhuri AR, Bhattacharya TK (2009) Design and analysis MEMS cantilever based binary logic inverter. In: *IEEE international conference on advances in computing, control, and telecommunication technologies*, pp 184–188
5. Weste NHE, Harris D, Banerjee A (2006) *CMOS VLSI design*, 3rd edn. Pearson Education, pp 129–130
6. Roy K, Prasad SC (2000) *Low power CMOS VLSI circuit design*, 1st edn. Wiley India, pp 29–32
7. Weste NHE, Harris D, Banerjee A (2006) *CMOS VLSI design*, 3rd edn. Pearson Education, pp 132–133
8. Khellah MM, Keshavarzi A, Somasekhar D, Karnik T, De V (2008) Read and write circuit assist techniques for improving V_{ccmin} of dense 6T SRAM cell. In: *Proceedings of IEEE international conference on integrated circuit design and technology and tutorial*, pp 185–189
9. Noda K, Matsui K, Takeda K, Nakamura N (2001) A loadless CMOS four-transistor SRAM Cell in a 0.18- μm logic technology. *IEEE Trans Electron Devices* 12(12):2851–2855
10. Yeknami AF (2008) Design and evaluation of a low-voltage, process variation-tolerant SRAM cache in 90 nm CMOS technology. Master's thesis, Department of Electrical and Electronics Engineering, Linköping Universitet, Linköping, Sweden [Online]. Available: <http://urn.kb.se/resolve?urn=urn:nbn:se:liu:diva-12260>
11. Carlson I, Andersson S, Natarajan S, Alvandpour A (2004) A high density, low leakage, 5T SRAM for embedded caches. In: *Proceedings of 30th European solid state circuits conference*, pp 215–218
12. Kutila M, Paasio A, Lehtonen T (2014) Simulations on 130 nm technology 6T SRAM cell for near-threshold operation. In: *Proceedings of ISCAS*, June 2014
13. Mandal S, Sarpeshkar R (2017) A simple model for the thermal noise of saturated MOSFETs at all inversion levels. *IEEE J Electron Devices Soc* 5(6):458–465, Nov 2017. <https://doi.org/10.1109/JEDS.2017.2751421>

Implementation and Performance Evaluation of Hybrid SRAM Architectures Using 6T and 7T for Low-Power Applications



M. Parvathi and M. C. Chinnaiah

Abstract Static random access memory (SRAM) is one of the key components in the growing embedded systems with a demand in its increased capacity. It is necessary to do power analysis at the early stages of the design process for such large sized SRAMs to avoid further complexities that degrade system performance to worst. SRAMs are greatly delved from 6T to 10T with its size against to the read and write stability issues. However, use of 10T alone in the large sized memories is not feasible for the low-power system architectures. In this paper, a unique style of dual-port hybrid SRAM memory architectures is proposed using different combinations of 6T and 7T. The hybrid model using 6T-7T SRAM cell is performing well over traditional 6T-6T and 7T-7T architectures with power reduction improvement of 27.2% and 30.5%, respectively, and with area reduction improvement of 26.1% and 8.15%, respectively.

Keywords SRAM · Low-power designs · Hybrid memories · Embedded systems · 6T to 10T

1 Introduction

The ever growing demand in portable electronic device applications leads to technology evolution in the VLSI design architectures. One of the critical empirical parameters that needs control over the microelectronic technology is power dissipation, especially required in low-power VLSI circuit designs. The trending submicron meter technologies designs for high speed results in increased circuit complexity in addition to power consumption. In the lower technology nodes, one of the traditional methods for power reduction technique follows supply voltage scaling [1]. However, for the circuits like SRAM with large capacity building blocks, the so called power

M. Parvathi (✉)
ECE Department, BVRIT HYDERABAD College of Engineering for Women, Hyderabad,
Telangana, India
e-mail: parvathi.m@bvrithyderabad.edu.in

M. C. Chinnaiah
ECE Department, BVRIT Narsapur, Hyderabad, Telangana, India

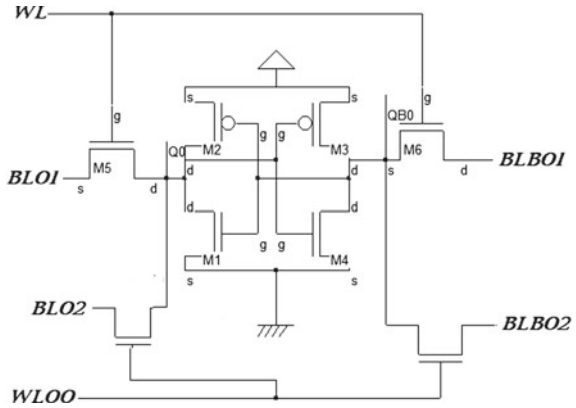
reduction techniques always cause stability issues. Hence, circuit and system level techniques are needed since the device and voltage level scaling are not feasible methods in providing good results while achieving for low power. Most of the literature suggests supply voltage reduction technique [2] to use as effective and efficient way for leakage power reduction. SRAMs are in general used as primary memory or caches in portable devices due to their inherent faster response. Also, SRAMs are free from periodical refreshing in contrast to its counter memories. However, the predominant limitation of use of SRAM is subthreshold and gate leakage current [3], which are dominant in the large high capacity memory structures.

In multi-core or multiprocessor environment such as high speed computers or and digital signal processors, the use of multiport SRAMs is essential [2, 4–6]. The multiport SRAMs are essential building blocks used as multiport register files in high range modern FPGAs or in multi-core system-on-a-chip (SoC) devices. The advantage multiport over traditional single-port SRAMs is, the multiport memories allow simultaneous access to multiple devices that results in increased throughput. More research is happening in the recent years in the development of various high density, fast multiport memories due to the increased demand for high performance multi-core processors. Few are hybrid memories [7] uses combination of SRAM and DRAM that allow to store multiple bits in each cell. However, to perform read and write operations using this type of hybrid memory, more context switching operations are required, that leads to degradation of system speed. Other hybrid model can be observed using combination of SRAM and CAM [8] for the low-power applications, but its use is specific to applications due to its uniqueness in the design. In this paper, the various dual-port hybrid SRAMs are proposed using the combinations from 6T to 7T. Section 2 presents contemporary design approaches of the SRAM cells using conventional techniques. Design of proposed SRAM cell using hybrid techniques is discussed in Sect. 3. Section 4 presents simulation results and comparative analysis followed by conclusions in Sect. 5.

2 SRAM Cell—Contemporary Design Approaches

Due to poor write stability and read disturbances, the 6T SRAM cell has been reformed to 7T to 10T in the due course of its development for the betterment of signal to noise stability. However, for the present multi-core embedded system, environment needs multiport SRAMs rather than single port. Simple dual-port SRAM cell is shown in Fig. 1. In contrast to single port in which only one port will be used for reading and writing the data, dual-port will have two ports operated as address inputs. In single-port memories, the data lines separated to be used as output and input connections, in addition single address input. This causes either a read or write operation only can be performed as it can be accessed at a time for any operation. This drawback can be overcome using multiports, which consists of many address inputs with corresponding data inputs and outputs. It allows read and write operations in parallel depends on the number of input address line. The minimum sized

Fig. 1 Dual-port SRAM cell



multiport memory is dual-port memory itself. Though the bit capacity is same, one drawback with multiport memories to its counterpart single-port memory is that, it needs more area due to separate address decoder and data multiplexers to access each port. Hence, it is necessary to identify suitable multiport memory architectures that suits low-power design systems.

When it comes to multi-cell array designs, two types of architectures can be followed such as two cell bit line model and two cell word line model. Two cell bit line model is mere similar to the single-cell model with the additional memory bit cell stacked on the bit lines, whereas a two cell word line model includes two horizontally nested bit cells with two pre-charge and bit line circuits. However, the two cells belong to the same word line, hence, only one word line driver is desirable. The proposed work is based on two cell word line models only due to its importance over single-cell structures.

3 Design of Proposed Dual-Port Hybrid SRAM Cell

This section discusses about various hybrid designs of dual-port memories that uses combination of SRAM circuits with 6T and 7T.

3.1 Two Cell Dual-Port SRAM Architectures

The work on dual-port hybrid SRAM architectures is divided into two sections, one is two cell architecture and other is four cell architecture. In the two cell architecture model, we have considered 6T-6T and 7T-7T SRAM models using traditional CMOS design, then designed the proposed hybrid SRAM using 6T-7T and 7T-6T combination.

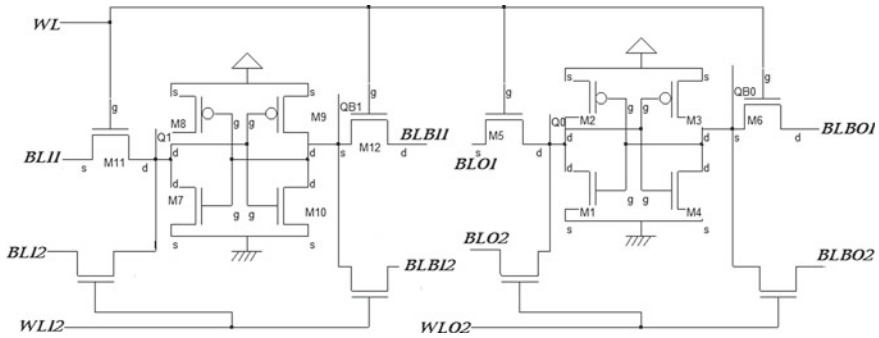


Fig. 2 Dual-port two cell 6T-6T SRAM word line model

3.1.1 Dual-Port 6T-6T SRAM Two Cell Model

At the initial stage, the dual-port SRAM using 6T-6T two cell model is implemented using two cell word line model, as shown in Fig. 2. Write operation can be performed by selecting bit line with data and assert either of the word lines. For write '1' in port 1 operation, assert BL_{11} to logic '1', and then assert WL_{12} line. Similarly, for write '0,' assert BLB_{11} to '1' (indicates BL_{11} to '0'), then assert WL_{12} . In the same for port 0, but write operation happens through WL_{02} line. For read operation to perform, pre-charge both the bit lines BL_{11} and BLB_{11} to high, then assert corresponding port word line (WL_{11} in this case). As a result, one can observe that the pre-charge value at BLB_{11} gets discharge to '0' through the corresponding nMOS transistor connected to that bit line, while retaining charge on BL_{11} to indicate read '1' operation. If 'WL' is used to write or read operations, then two-port SRAM operation is similar to single-port cell operation. Corresponding simulation results indicates the minimum read delay of 24 ps, with 0.311 mw power consumption by the architecture.

3.1.2 Dual-Port 7T-7T SRAM Two Cell Model

The dual-port 7T-7T SRAM two cell model is implemented to observe the performance variation in terms of minimum read delay, power dissipation along with critical path delay compared to its counter models 6T-6T and hybrid model 6T-7T. The corresponding 7T-7T SRAM cell simulation results indicate 38 ps of minimum read delay with 0.622 mw power dissipation by the architecture.

3.1.3 Hybrid 6T-7T and 7T-6T Dual-Port SRAM Two Cell Model

The dual-port SRAM using 6T-7T two cell model is implemented using two cell word line model, as shown in Fig. 3.

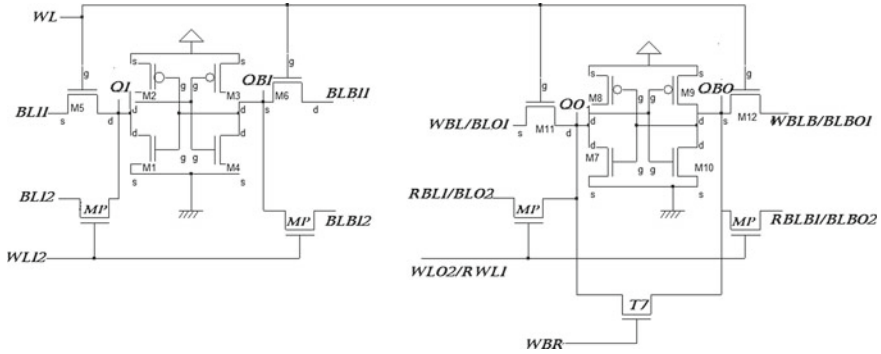


Fig. 3 Two bit dual-port hybrid memory using 6T-7T combination

It uses additional control for write operation in 7T structure with the name WBR using additional 7th transistor compared to its 6T counterpart. Transistors with name ‘MP’ are used to perform write or read operations in dual-port mode. Using WL line, both 6T and 7T cells get activated simultaneously to write through BL₁₁ and WBL (or BL₀₁) into their cells, respectively, for port1. Similarly, for port2, the write operation can be performed using BL₁₂ and RBL1 (or BL₀₂). The data will be read by the two cells by the same bit lines in the read mode using prior pre-charge requirement. Additional transistor T7 in 7T is to be maintained in the state 1/0 as per read/write operation.

The simulation results of 6T-7T dual-port hybrid SRAM model are shown in Fig. 4, in which the minimum read delay of 1058 ps, and 0.407 mw of power dissipation are observed. In the similar way, hybrid model using 7T-6T two cell SRAM is designed in which the first cell is taken as 7T followed by 6T. The worth note point in this model is, raise in power dissipation by 16% compared to 6T-7T architecture.

3.2 Four Cell Dual-Port SRAM Architectures

The dual-port SRAM architectures are further studied taking four cell models into consideration. For this, the initial 6T-6T dual-port cell is used twice for obtaining four cell model, then, extended to 7T four cell model. Further, the hybrid four cell models are designed using the combination of 6T and 7T dual-port cells. The four cells can be drawn either column wise or row wise by taking their corresponding read lines or write lines common.

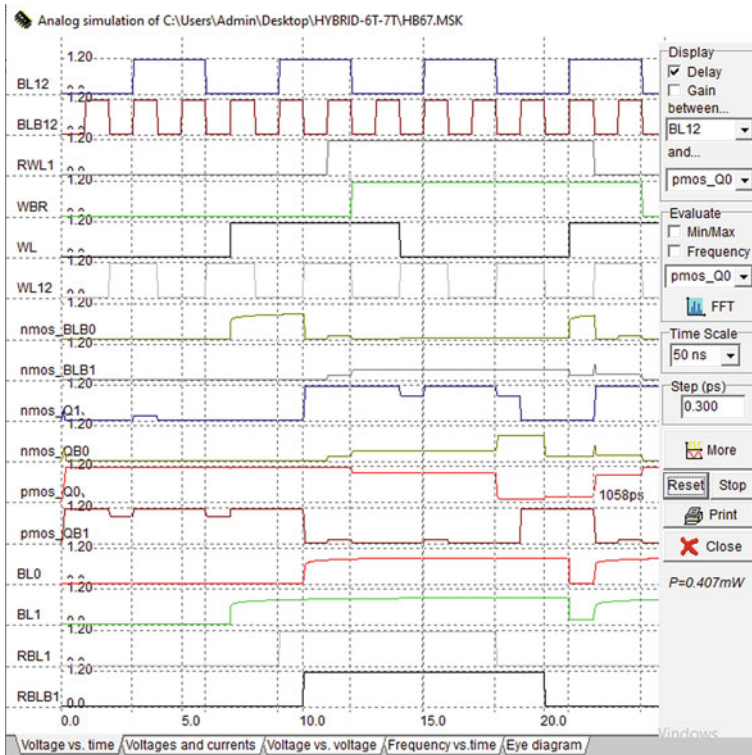


Fig. 4 Simulation results for 6T-7T dual-port hybrid SRAM model

3.2.1 Four Cell Model Using Two 6T-6T Dual-Port SRAM Cells

The dual-port SRAM using 6T-6T four cell model is implemented using four cell—two word line model, as shown in Fig. 5. The two word lines are brought from each pair of 6T-6T dual-port combination and are connected to output of multiplexer. The role of mux is to select the particular word line through which the corresponding dual-port two bit memory will be accessed to perform any operation like write into or to read from it. When the select line given a ‘0,’ the upper two cell combination of memory is ready for the write/read operation. Similarly, when the select line is ‘1,’ the lower two cell combination of memory will get ready for write/read operation.

On every write or read operation, the cell is need to reset to its initial start state. While in the write 1/0 operation, place the value on the corresponding bit lines then access the WL through mux. For example, to write ‘1’ in the upper two cell memory, place the value ‘1’ on bit lines BL₁₁, then assert write line WL₁₀, keeping select line low. On the other hands, to write into lower two cell memory, choose the corresponding lower bit lines BL₀₁, assert corresponding write line WL₀₁, keeping select line high. In the similar way, both the upper and lower memory cells can be

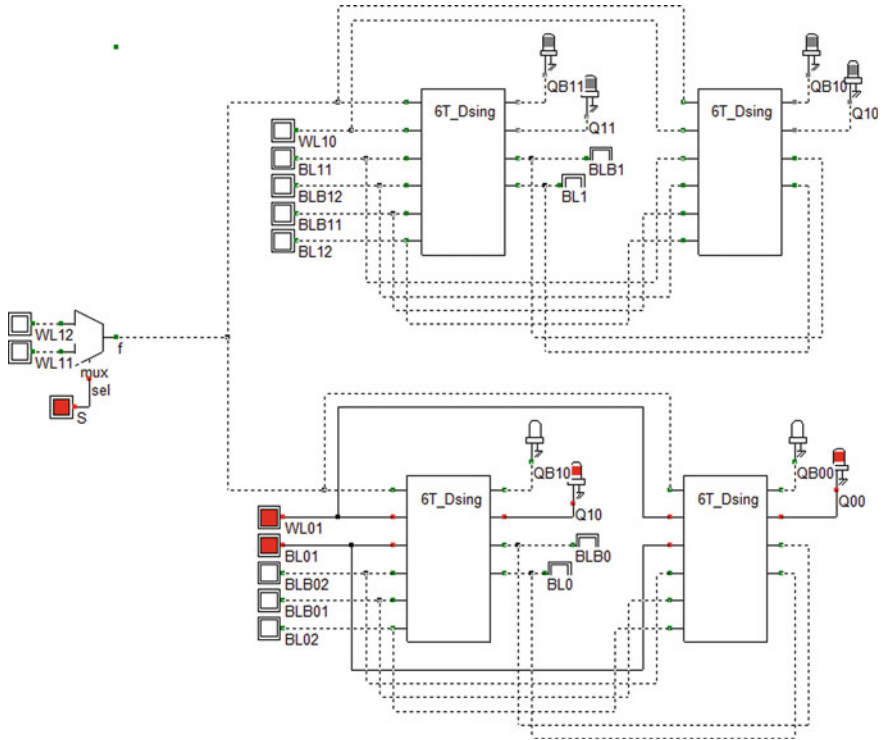


Fig. 5 Two bit four cell dual-port memory using 6T-6T (2×2) combination, write '1' in lower two cell memory

accessed for write/read using external write lines through mux. In the similar way, row-based four cell model is also implemented using double the two cell model.

3.2.2 Four Cell Model Using Two 7T-7T Dual-Port SRAM Cells

The dual-port SRAM using 7T-7T four cell model is implemented using both ways, one is in four cell—two word line model (2×2), and the other is in row-based model using double the two cell model. The simulation results indicate the 2×2 7T-7T model have minimum power dissipation of 0.688 mw compared to its row-based 7T-7T with 1.151 mw. Hence, the power dissipation is reduced by 71.8% in the case of 2×2 7T-7T model.

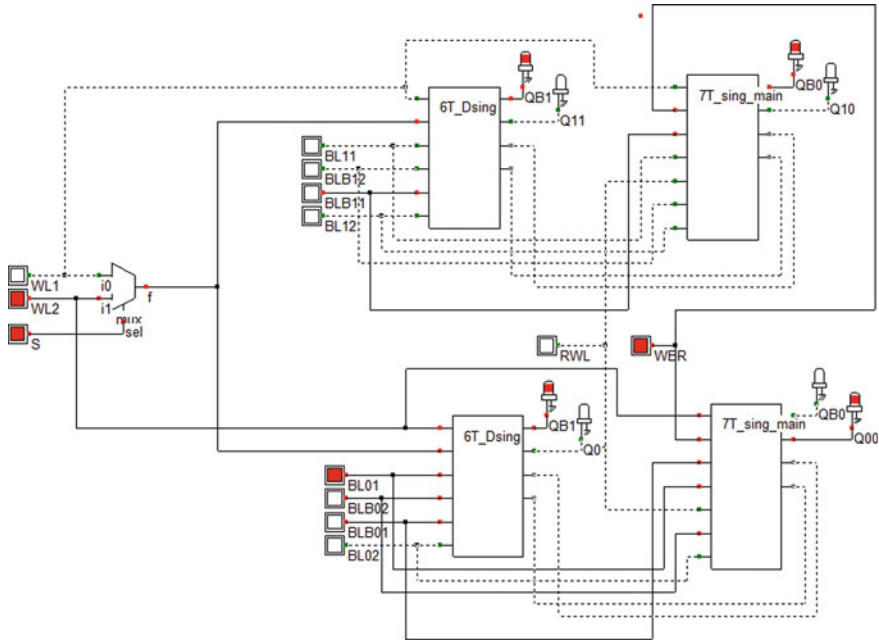


Fig. 6 Two bit four cell dual-port hybrid memory using 6T-7T combination, read ‘0’ in upper memory cell, write ‘1’ in lower memory cell

3.2.3 Dual-Port 6T-7T Hybrid SRAM Four Cell Model (2 × 2 Memory)

The dual-port hybrid SRAM using 6T-7T four cell model is implemented using two cascaded—two cell models as shown in Fig. 6. Due to involvement of 7T SRAM cell, the write or read operations are little different compared to 6T-6T two cell model. Using mux, the cells are activated individually through the select line. When the select line is ‘0,’ upper two cells will be activated to perform data operation. Similarly, when select line is ‘1,’ the lower cell will get activated. While performing write operation the active signal on WBR line causes the two 7T cells to act in dual to each other. Hence, the cell write ability increases using 6T-7T by providing more combinations in writing/reading the data.

4 Results and Comparative Analysis of Hybrid SRAMs

The simulation results for each hybrid model were carried out using microwind tool using 120 nm technology. Each 6T-6T and 7T-6T hybrid model is drawn in dsch tool, observed corresponding critical path delays. The same are extracted into automatic layouts in microwind environment to observe corresponding power consumptions.

The overall comparisons among the proposed hybrid dual-port SRAMs over its traditional counter parts are given in Table 1. One can understand the hybrid model using 7T-6T SRAM cell is performing well over 7T-7T architecture with power reduction improvement of 21.54%, and area reduction improvement of 8.15%.

In the similar way, four cell architectures are compared in Table. 2. For 6T-6T four cell model, the performance is poor in terms of high rage in area, delay and power dissipation including I_{max} compared to other proposed models in this paper. However, row-based four cell model using 6T resulting improved low-power dissipation. While comparing the hybrid models 6T-7T with other architectures under consideration, it results in features like marginal critical path delay of 5.9 ns, with minimum read delay of 16 ps, with low power of 0.799 mw and with low area of 831 μm^2 as observed in Figs. 7, 8, 9, 10 and 11.

Table 1 Comparative analysis of hybrid SRAMs (two cell models)

Type of circuit	# Tr	CPD (ns)	Min. read delay (ps)	Pd (mw)	I_{max} (mA)	Area (μm^2)
6T-6T	16	2.42	24	0.311	1.32	337
7T-7T	18	3.29	38	0.622	1.64	401
6T-7T-H	17	3.29	1058	0.407	1.66	368.3
<i>7T-6T-H</i>	<i>17</i>	<i>3.12</i>	<i>1023</i>	<i>0.488</i>	<i>1.357</i>	<i>368.3</i>

Table 2 Comparative analysis of hybrid SRAMs (four cell models)

Type of circuit	CPD (ns)	Min. read delay	Pd (mw)	I_{max} (mA)	Area (μm^2)
6T-6T (2 × 2)	11.78	14 ns	1.098	2.639	1126
6T-6T-row based	1.35	956 ps	0.619	1.994	859
7T-7T-row based	1.77	39 ps	1.151	2.461	943.4
7T-7T (2 × 2)	6.79	1030 ps	0.688	1.87	873
<i>6T-7T-H</i>	<i>5.955</i>	<i>16 ps</i>	<i>0.799</i>	<i>1.789</i>	<i>831</i>

Fig. 7 Comparison of maximum current variation in dual-port four cell models

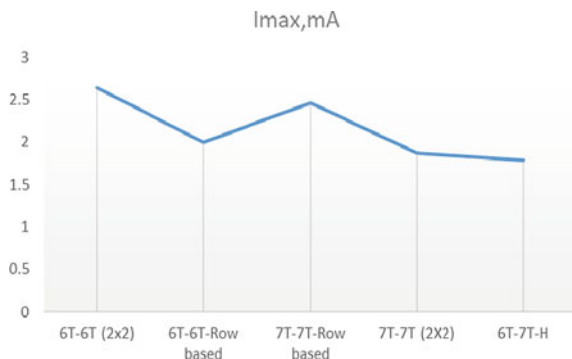


Fig. 8 Comparison of critical path delay in the chosen models

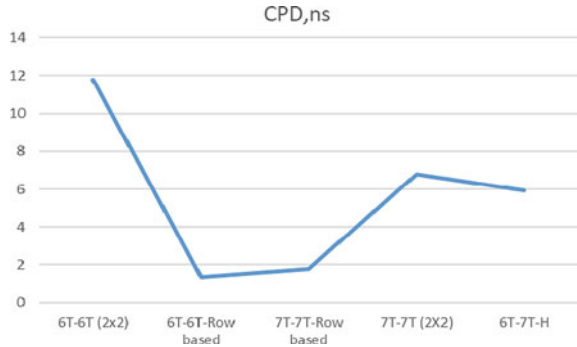


Fig. 9 Comparison of power dissipation variation in dual-port four cell models

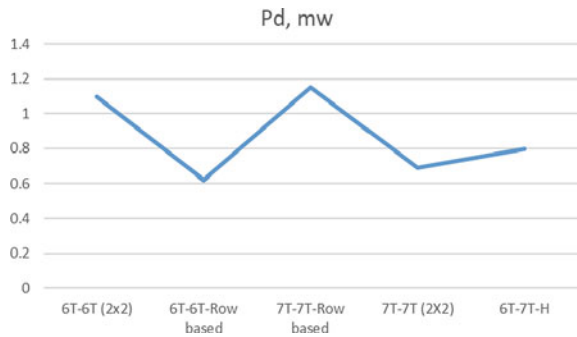
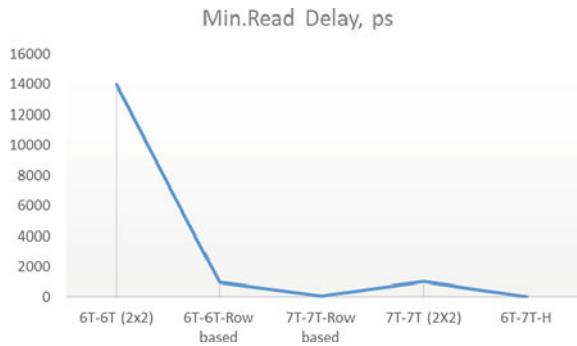


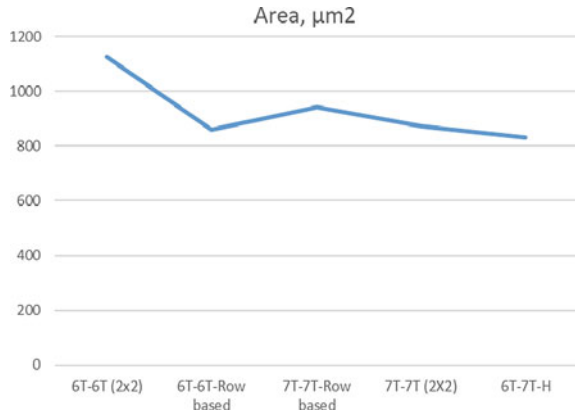
Fig. 10 Comparison of minimum read delay in the chosen models



5 Conclusions

The proposed dual-port hybrid model is implemented using 6T-7T and 7T-6T SRAM cell models observed that 6T-7T is greatly predominant in reducing power consumptions over other models using higher cell architectures under consideration. The power reduction improvement in proposed 6T-7T hybrid four cell is observed with 27.2% and 30.5% over 6T-6T (2 × 2), and 7T-7T (2 × 2) four cell traditional models.

Fig. 11 Comparison of area requirement in chosen dual-port four cell models



Similarly, area reduction improvement in 6T-7T hybrid model observed with 26.1% and 8.15%, respectively, when compared with 6T-6T (2×2) and 7T-7T (2×2) four cell traditional models. Since this proposed model is novel and new, the comparisons are made among the self-dual combinations. This kind of hybrid models is essential under low-power multi-core processor applications.

References

1. Kankanala B, Srinivasulu A, Musala S (2013) 7-T single end and 8-T differential dual-port SRAM memory cells. In: Proceedings of 2013 IEEE conference on information and communication technologies (ICT 2013). IEEE, pp 1243–1246. 978-1-4673-5758-6/13
2. Sil A, Bakkamanthala S, Karlapudi S, Bayoumi M (2012) Highly stable, dual-port, sub-threshold 7T SRAM cell for ultra-low power application. In: IEEE 10th international new circuits and systems conference (NEWCAS), Montreal, QC, Canada. IEEE, pp 493–496. 978-1-4673-0859-5/12/\$31.00©2012
3. Gavaskar K, Ragupathy US, Malini V (2019) Design of novel SRAM cell using hybrid VLSI techniques for low leakage and high speed in embedded memories. *Wirel Pers Commun* 1–29. Springer. <https://doi.org/10.1007/s11277-019-06523-7>
4. Pasandi G, Pedram M (2018) Internal write-back and read-before-write schemes to eliminate the disturbance to the half-selected cells in SRAM. *IET Circuits Devices Syst* 12(4):460–466
5. Nii K et al (2009) Synchronous ultra-high-density 2RW dual-port 8T-SRAM with circumvention of simultaneous common-row-access. *IEEE J Solid-State Circuits* 44(3):977–986. Digital Object Identifier, Mar 2009. <https://doi.org/10.1109/JSSC.2009.2013766>
6. Ataei S, Gaalswyk M, Stine JE (2017) A high performance multi-port SRAM for low voltage shared memory systems in 32 nm CMOS. *IEEE*, pp 1236–1239. 978-1-5090-6389-5/17
7. Yu WS, Huang R, Xu SQ, Wang S, Kan E, Suh GE (2011) SRAM-DRAM hybrid memory with applications to efficient register files in fine-grained multi-threading. In: 2011 38th annual international symposium on computer architecture (ISCA), pp 247–258
8. Liang X, Turgay K, Brooks D (2007) Architectural power models for SRAM and CAM structures based on hybrid analytical/empirical techniques. *IEEE*, pp 824–830. 1-4244-1382-6/07

Survey of Identification of Alzheimer's Disease Using MRI, Speech and MMSE



Y. Bhanusree, Divya Bulusu, Divija Chinni, Akanksha Narahari, Suma Sree Simhadri, and Varshitha Bommareddy

Abstract Alzheimer's disease [AD] is the commonest form of neurodegenerative disorder. It's a progressive illness starting with a gentle state of mind and presumably resulting in loss of the flexibility to hold on to voice communication and reply to the surroundings. Alzheimer's disease involves elements of the brain that manage thought, memory and language. Within the later stages, people lose their ability to speak or reply to the surroundings and need constant care. AD is commonest in people over the age of sixty-five. This illness is a difficult one as there's no treatment for it. MRI is the most common method used to detect AD in patients. But in early stages, AD can't be determined by MRI as changes in the brain can't be detected in early stages. Speech and MMSE are new fields of research to detect AD. Various ML and deep learning techniques are used in detecting AD using speech, MRI and MMSE. This paper is going to provide five detailed information about previous research done in the field of AD Identification using speech, MRI and MMSE.

Keywords CNN · Alzheimer's disease · Deep learning · Neural networks · Speech · MRI · MMSE

1 Introduction

Alzheimer's disease is the most typical variety of neurodegenerative disorder. It's a progressive malady starting with gentle amnesia and presumably resulting in loss of the flexibility to hold on to voice communication and answer the surroundings. Presenile dementia involves components of the brain that manage thought, memory and language.

In the late stages of Alzheimer's, people lose their ability to speak or answer the surroundings and need constant care. Presenile dementia is most typical in individuals over the age of sixty-five. The chance of Alzheimer's and different styles of dementia will increase with age. This malady is a difficult one as a result of there's no treatment

Y. Bhanusree (✉) · D. Bulusu · D. Chinni · A. Narahari · S. S. Simhadri · V. Bommareddy
Department of CSE, VNRVJiet, Hyderabad, India
e-mail: bhanusree_y@vnrvjiet.in

for it. If the malady is foreseen earlier, the progression or the symptoms of the malady are often bogged down.

Machine learning techniques will immensely improve the method for correct identification of Alzheimer's malady. In recent days deep learning techniques have achieved major success in medical image analysis. Speech process is proving to be another relevant and innovative field of investigation because it may be an inexpensive analysis which may be of growing importance within the close to future for identification of Alzheimer's just in case of psychological feature impairment because the analysis is non-invasive in nature.

The difficulties to appropriately identify those who suffer from mild cognitive impairment (MCI) who would proceed on to develop AD from those with MCI symptoms owing to other causes has been suggested as one of the reasons for the lack of success in developing disease-modifying drugs [1].

Brain scans that have not been processed are considerably too huge and noisy to be used for diagnosis. The MR brain picture is partitioned into distinct anatomical regions, i.e. regions of interest (ROIs), to help morphological analysis, by grouping voxels using a labelled atlas, and then regional measurements are created as image classification features [2]. In 2019, 5.8 million persons of all ages were diagnosed with Alzheimer's disease; by 2050, it is projected that the number would climb to 14 million people. One out of every ten adults over the age of 65 has Alzheimer's disease, with females having a higher risk than males [3]. Both Alzheimer's disease and non-Alzheimer dementia have been demonstrated to impact human speech and language. Furthermore, dementia causes considerable alterations in speech and language use early in the disease's course [4]. Using the MMSE unified cognitive scale in automatic and non-invasive screening procedures would be tremendously advantageous to clinicians in terms of efficiency and enabling consistent diagnosis by non-experts [5]. Voice analysis and speech processing, which aim to discover traits linked to the aforementioned problems, could be useful tools in the early detection of AD. For this aim, language analysis may be directly concerned, but other relevant variables in the patient's voice may also be explored [6]. Patients are asked a series of questions in five separate domains (orientation, registration, attention, memory and language) by clinicians giving the MMSE; their responses are graded on a scale of 0–30 [7].

2 Background

Alzheimer's is the commonest cause of dementia in older people. Dementia causes loss of cognitive functioning like thought, memorizing and ability of reasoning and behavioural abilities. It affects to an extent such that the affected person's daily life is disturbed. The person who is affected with AD completely depends on others for any help in mild to severe stages. Mini-mental state examination [8, 9] is a thirty point questionnaire in which reasoning and behavioural abilities are tested. Based on these points, whether a person is affected with AD is predicted. The most commonly used prediction method is MR imaging [1–7, 10, 11]. Based on the structure of the

brain and damage caused to neurons AD is predicted and the extent to which the disease has affected the person is also known. Existing literature has suggested three techniques for the identification of AD. They are:

1. MRI
2. Speech
3. MMSE.

2.1 MRI

Amongst all the survey articles reviewed, the model developed from EMR data containing the person's MRI data had the best accuracy of 98.2%. The data is converted to observational medical outcomes partnership (OMOP) format. The OMOP common data model (CDM) permits the collection of information from many institutions in a consistent manner and provides a single data standard for analysing several data sources at the same time. A dataset known as the selected clinically relevant positive (SCRCP) dataset was established using this data from patients who visited at least four times. For each of the criteria, one SCRCP positive dataset was created. This was fed into a recurrent neural network (RNN) model with long-short-term memory (LSTM).

2.2 Speech

The data gathered from AP HP Broca Hospital, which employs audio recordings of patients, was utilized to construct a model to predict Alzheimer's disease in its early stages. The feature selection process is divided into two steps. KNN, support vector machine and binary decision tree were used as classifiers. The KNN classifier with $k = 1$ achieved the greatest accuracy of 94% [12]. Amongst all the survey articles considered, this model generated the best accuracy.

2.3 MMSE

One of the most recent studies used the ADNI dataset to predict Alzheimer's disease in a person using the MMSE approach [9]. The Alzheimer's disease assessment score (ADAS) and the mini-mental state examination (MMSE) are the two most regularly used cognitive evaluations to predict the course of Alzheimer's disease. On the TensorFlow backend, a deep learning model was built using the Keras Python package. With 340 features, the model obtained an accuracy of 90.6%, with accuracy increasing as additional hidden layers were included, and an ADAS root-mean square

error of 3.59. Amongst all the papers considered for MMSE, this model had the highest accuracy.

CNN is one of the best methods used to predict AD using MRI data. Acoustic data can also be used to predict the disease but very little research has been done in this field [1]. A person with Alzheimer’s loses the ability to memorize names, words and sentences which can be observed through acoustic features such as shimmer, pause duration and speech rate [12–17]. Highest accuracy is obtained using KNN on optimal speech features [12]. The three MMSE, MRI and acoustic data are equally important at different stages in AD prediction.

3 Related Work

See Fig. 1 and Table 1.

3.1 MRI

Basaia et al. [1] in 2018 proposed a model to determine AD using CNN taking MRI images as input. MRI scans of the structural brain of the ADNI database are used in the proposed model. The model architecture that uses 3D convolutional network which takes MR images as input was used in this model. The network architecture consists of twelve repeated blocks of convolutional layers. The CNN model was trained using an augmented dataset, and each classification was validated using ten-fold cross validation. The CNN weights used to categorise ADNI AD versus HC were transferred to the other CNNs and utilized as beginning weights to increase the classifier’s performance. Finally, the raw images from the testing set were classified using CNN. Sensitivity, specificity and accuracy are performance measures on which

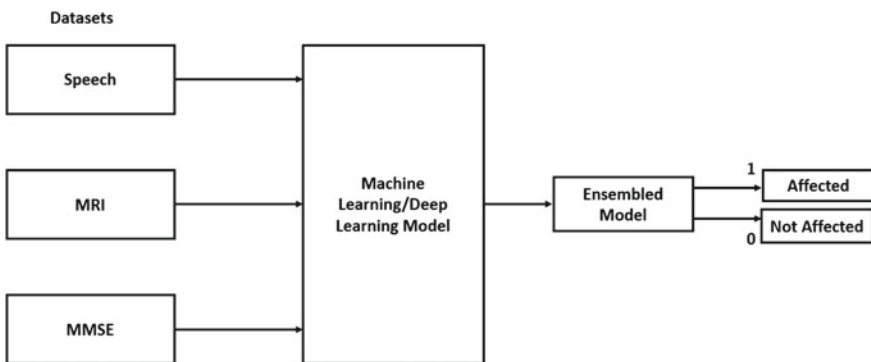


Fig. 1 Model architecture

Table 1 The table gives brief description about few papers using three models MRI, speech and MMSE

Model	Title	Methodology	Database
MRI	Multi-scale deep neural network-based analysis of FDG-PET images for the early diagnosis of Alzheimer’s disease	Multi-scale deep neural network (MDNN) was used for classification	ADNI
	RNN-based longitudinal analysis for diagnosis of Alzheimer’s disease	Deep CNN was used to extract spatial features. RNN was used for classification	ADNI
	Classification of Alzheimer’s disease with and without imagery using gradient boosted machines and ResNet-50	MMSE data was also considered and ResNet-50 was used for classification	OASIS-1
Speech	Speech-based detection of Alzheimer’s disease in conversational German	Acoustic features were extracted from audio samples. Linear discriminant analysis classifier was used for classification	ILSE
	Detecting and predicting Alzheimer’s disease severity in longitudinal acoustic data	SVM and LOOCV were used for classification	Dementia Bank
	Two-stage feature selection of voice parameters for early Alzheimer’s disease prediction	Two stages of the feature selection process were undergone. KNN, SVM and binary DT were used for classification	AP-HP Broca Hospital Data
MMSE	Exploring MMSE score prediction using verbal and non-verbal cues	A variety of verbal and non-verbal signals were employed in the model	ADReSS
	Early prediction of Alzheimer’s disease with a multi-modal multitask deep learning model	To predict AD diagnosis, a deep learning model that leverages multi-modal input data and conducts multitask categorization was deployed	ADNI

CNN’s performance was measured. Using AD versus HC classification performance obtained is higher than 98%.

Lu et al. [2] in the year 2018 proposed a model with two steps: one is image processing and the other is classification using multi scale DNN. In the first step, T1 MR images are segmented in a coarse-to-fine manner, and metabolic characteristics in these localized areas are retrieved using FDG-PET images and T1 MR images

co-registered. In the classification stage, a DNN-based model is trained on multi-scale data to understand the patterns of AD pathology and categorise mild cognitive impairment patients. To assess the proposed model, experiments were conducted on binary classifications NC versus AD, sMCI versus pMCI and sMCI versus pMCI, with accuracy of 93.58%, 81.55% and 82.51%, respectively.

Lin et al. [3] in 2018 presented a model which uses an ADNI database. In the proposed framework, MRI data processing was done in two steps to extract image features. In the CNN based feature extraction, the CNN is trained on the AD/NC image patches before extracting CNN-based features from MRI images. In the FreeSurfer-based feature extraction, the structural information from MR images was mined using FreeSurfer. Further, for classification, a feature vector derived from the combination of these features was sent to a feed-forward neural network with a single layer of hidden nodes. The suggested model's performance is measured via cross validation. When CNN was trained using AD/NC patches, it achieved an accuracy of 73.04%.

Cui et al. [10] in 2019 used the ADNI dataset to build a deep learning model. Their proposed framework consists of both convolutional as well as recurrent neural networks for longitudinal analysis of AD prevalent MRI for accurate diagnosis. Deep CNN has been used to understand spatial features from Grey matter density map and RNN with three cascaded bidirectional gated recurrent units layers present on output of CNN for extraction of longitudinal features. This model obtained 91.33% accuracy.

Hong et al. [4] proposed a model in which the ADNI dataset is used. An LSTM network consisting of fully connected activation layers is constructed to understand the temporal relation between features and the successive stage of AD. LSTM was chosen as the algorithm for this study as it is very useful to understand long short-term dependencies. For understanding the progression of the AD in patients, the LSTM network can be helpful to correlate prior diagnoses to current state. The model has obtained up to 90% accuracy.

Fulton et al. [5] suggested a model to predict AD using MRI data. The OASIS-1 cross-sectional MRI dataset was used in this study. The purpose of this study is to predict the presence of AD using MRI, clinical as well as socio-demographic data. A gradient boosted machine (GBM) was used to predict the presence of AD with establishing correlation with features like gender, age, education, socioeconomic status and a mini-mental state exam (MMSE). A residual network with 50 layers consisting of 48 convolution layers, 1 Max Pool Layer and 1 Average Pool Layer, (ResNet-50) achieved a mean 91.3% prediction accuracy.

Feng et al. [6] in the year 2019 put forward a methodology that uses the ADNI dataset. 3D-CNN was used to extract the primary features of both MRI and PET inputs. Then, FSBi-LSTM is used to extract high level semantic and spatial information from the output of 3D-CNN instead of traditional FC layer to further improve the model's performance. Their method achieved accuracies of 94.82%, 86.36% and 65.35% for differentiating AD from normal control (NC), pMCI from NC, and sMCI from NC, respectively.

Lee et al. [11] in 2019 suggested a mechanism for identification of the conversion from MCI to AD. ADNI Dataset was used for the purpose. The suggested

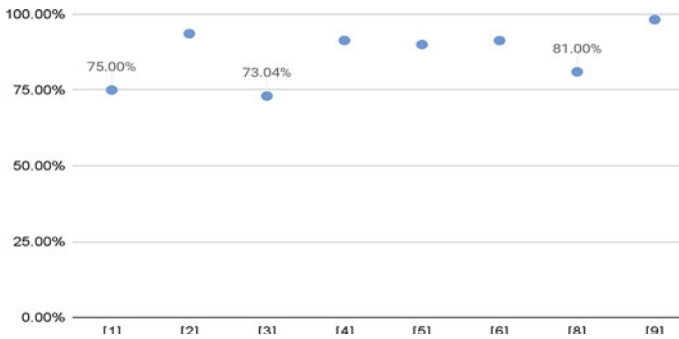


Fig. 2 Accuracies of MRI models

system included longitudinal CSF biomarkers, demographic data, cross-sectional neuroimaging biomarkers and longitudinal cognitive performance derived from the ADNI. The method they used is a multi-modal RNN. This method makes use of the data’s multi-modal and longitudinal character to uncover nonlinear patterns. They compared the results of three different tests. “Baseline” is the name of the first experiment. At the baseline visit, four types of data were combined: CSF, cognitive performance, MRI and demographic information. In the following technique, called “single modal,” just longitudinal cognitive performance data was used as the predictor. They tried every other modality and discovered that cognitive scores were the most effective. Finally, the four modalities of longitudinal data were pooled and used to train the classifier in the “proposed” experiment. The model had an accuracy of 81% when using longitudinal multi-domain data.

Ljubic et al. [7] in 2020 presented a model in which data was gathered from a heterogeneous ambulatory EMR data store. The participants’ electronic medical records are referred to as EMRs. It is the computerized data of the person that contains information about the medications, number of surgeries, etc. The data is formatted in observational medical outcomes partnership, abbreviated as OMOP. The OMOP CDM (common data model) permits equivalent data collection from diverse institutions and provides a single data standard for analysing many data sources at the same time. Conditions, measurements and medicines were used in the research. A dataset known as selected clinically relevant positive (SCRCP) dataset was constructed using data from patients who attended at least four times. For each of the parameters, a single SCRCP positive dataset was created. This was the input to a RNN with LSTM. They achieved an accuracy of 98.2% (Fig. 2).

3.2 Speech

Weiner et al. [13] in the year 2016 proposed a methodology that uses speech recordings as inputs to determine if a person has AD or not. The dataset chosen is from

ILSE corpus. This contains speech recordings of individuals from an interview. The interview consisted of general questions that any member of any age group can easily answer. Ten features were retrieved from the audio recordings to detect AD, six of which are acoustic. Linear discriminant analysis was performed to determine whether a person belongs in one of the three groups: control, AACD or AD. With an F -score of 0.8, this study had an accuracy of 85.7%. The flaw in this paper cannot be overstated. The longitudinal data research was not included in this study. Data obtained consecutively from the same respondents across time is referred to as longitudinal data. This paper did not investigate the change and effects of AD in an individual over time.

Al-Hameed et al. [14] in the year 2017 utilized the dataset from Dementia Bank, which is open to the public and free to use. The audio recordings utilized in the study were of people who were given a visual to describe. They were given a cookie picture and told to describe all of the tasks. Here, two different ML models are built. The first machine learning model was used to determine whether a person falls into one of three kinds: AD, HC or MCI. SVM and LOOCV were employed in this model. The second model was used to look at how Alzheimer's disease affects a person over time. In this paper, the prior paper's flaw is addressed. This model examines the change in AD using the mini-mental state examination score. The accuracy obtained ranges from 89.2 to 92.4%.

Mirzaei et al. [12] in the year 2018 put forward a model in which data samples of healthy patients, early-stage AD patients and MCI patients are gathered from AP HP Broca Hospital which is located in Paris. The feature set of each audio sample comprises 39 elements, MFCCs and FBEs. Feature selection was done in two stages. In the first stage, optimal features from every feature set are extracted. Backward feature elimination approach is used for MFCCs, FBEs and 39 elements. After extracting the best features from each feature set, the best features are combined to create a new feature vector. The optimal features obtained in the first stage are used as input to second backward feature elimination to pick the final set of optimal features in the second stage of feature selection. Three classifiers are employed for classification. KNN with Euclidean distance, where k is 1, support vector machine and binary decision tree are the three. The accuracy rates were 94%, 68% and 67%, respectively. The most significant flaw in this paper is that better accuracy is acquired after the first stage of feature selection rather than the second.

Chien et al. [15] in 2019 suggested a model in which Mandarin_Lu Corpus and NTU dataset were utilized. The collected speech samples were given as input to the feature sequence generator. There were two methods to generate the feature sequence. They are manually labelling and another was to be automatically by CRNN trained by CTC loss. The feature sequence is sent into the AD disease engine, and the result is a score that indicates whether or not you have Alzheimer's. A single-layered bidirectional RNN with 128 GRU cells in each direction is used to model the AD illness. The evaluation score is a positive numerical number ranging from 0 to 1, with the higher the score, the higher the risk of Alzheimer's disease. The obtained score is 0.838. The quality of the feature sequence generator is substandard, which is a disadvantage.

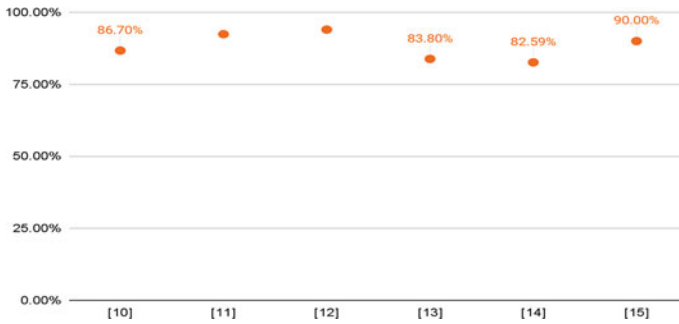


Fig. 3 Accuracies of speech models

In 2021, Liu et al. [16] created a model using a photo description task from the dementia Bank Pitt Corpus as a dataset. This strategy uses bottleneck features collected from audio clips using an automatic speech recognition model, rather than relying entirely on hand transcriptions and annotations of a patient’s speech. For classification, the neural network uses CNN layers for local and BiLSTM layers for global context modelling, and an attention pooling layer. To address the data shortage problem, a masking-based data augmentation technology was developed. Experiments on the Dementia Bank dataset revealed that their proposed methodology’s accuracy in detecting AD was 82.59%, which is higher than the base model, which is based on manually-designed acoustic features and SVM.

In the year 2021, Nasreen et al. [17] proposed an approach based on the Carolinas Conversation Collection data set (CCC). To be extracted, there are two sorts of features. Interactional and acoustic features are the two types. Interactional features include pausing behaviour and floor control. Amplitude, cepstral coefficients, pitch and energy are all acoustic characteristics. For feature selection, the iterative recursive feature elimination (RFE) method is used. It removes a certain amount of features and examines the impact on classification accuracy. Recursively, the features that contribute the least to improving accuracy are deleted until just the appropriate number of features remain. Combining these two features with feature selection has obtained promising results. Standard models like SVM, LR and RF are used for classification. SVM has obtained 90% accuracy. Interactional features alone obtained 87% accuracy (Fig. 3).

3.3 MMSE

Farzana et al. [8] in 2020 put forward a model which aims to predict clinical MMSE scores using verbal and non-verbal features extracted from the transcripts of 108 speech samples from the ADReSS challenge dataset. This dataset contains spontaneous speech to recognize AD and is balanced in terms of age and gender. It contains

speech recordings and transcripts of the participants where they describe a simple picture with no time limit. They worked on different machine learning techniques to determine the relationship between the obtained results and clinical results. They experimented with two statistical regression algorithms, support vector regression (SVR) and gaussian process regression (GPR). A root mean squared error (RMSE) of 4.34, 29.3% percentage decrease was achieved. The performance impacts of acoustic versus linguistic, text-based features were analysed. The model demonstrated that MMSE score prediction is best addressed using input from multiple perspectives, by using a selection of verbal and non-verbal cues.

Seshadri et al. [9] in 2021 suggested a model that used the ADNI Dataset to predict AD in an individual. The proposed approach comprises of a deep learning model that predicts AD diagnosis and ADAS and MMSE scores using multi-modal input data and multitask categorization. Alzheimer’s disease assessment score (ADAS) and mini-mental state examination (MMSE) are the two most commonly used cognitive assessments to predict progression of AD. Based on the criteria specified by The Alzheimer’s Disease Prediction of Longitudinal Evolution (TADPOLE) Challenge, the dataset was analysed using the Python packages NumPy, pandas and scikit-learn. A deep learning model was constructed with the Keras Python library on the TensorFlow backend. The model produced a 90.6% accuracy with 340 features, with accuracy increasing as more hidden layers were added, and RMSE of 3.59 and 3.82 for ADAS and MMSE, respectively, with errors reducing as more hidden layers were added. The disadvantage is that it does not use CNN to directly interpret data from clinical images or to train and validate the model (Fig. 4).

GENERAL

Lopez-de-Ipina et al. [15] in the year 2018 presented a non-technical general paper that examines how speech can aid in the detection of AD. It proposed three methods: verbal fluency, image description and spontaneous speech. People were asked to identify the names of animals they remembered in one minute as part of a verbal fluency test. People with Alzheimer’s disease were shown to be unable to recall more than 5–6 animal names. People were asked to describe a picture that was displayed

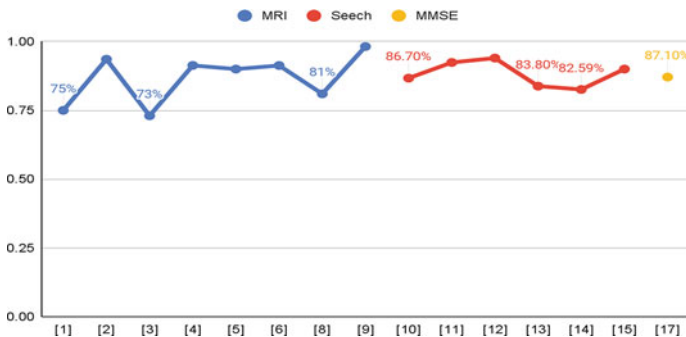


Fig. 4 Histogram depicting comparison of accuracies of MRI, speech and MMSE models

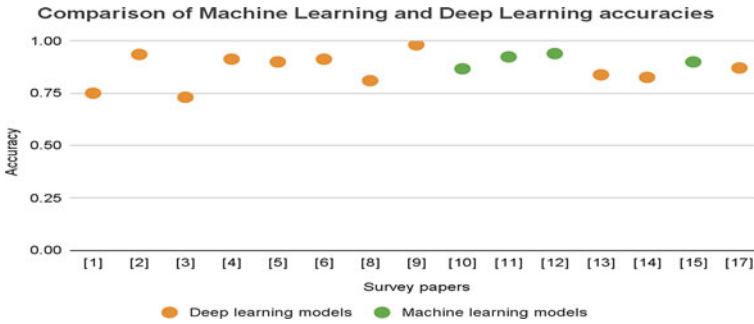


Fig. 5 Scatter plot depicting accuracies of ML and DL models

in front of them in the second way picture description. People were given a random topic to talk about in the third method. People with Alzheimer’s disease exhibited little interest in talking, and a few even dropped out of the task (Fig. 5).

4 Conclusion

Early detection of AD helps in early diagnosis and gives a higher chance of getting better results from the treatment. Predicting AD using MRI, speech and MMSE data is worth the investment. The conclusion drawn from this survey is that various techniques such as CNN, deep learning and neural networks can be used to detect Alzheimer’s disease at an earlier stage. In the survey, various models such as MRI, acoustic and speech are used in AD prediction. It is observed that prediction of AD are of a good deal using MRI and MMSE methods. Few models were in combination of MRI and MMSE for better classification of healthy and AD patients. Though acoustic is a prominent feature in AD prediction, not much research has been done on this model. The highest accuracy of 94% is obtained using machine learning algorithms on acoustic features which concludes that speech plays a prominent role in AD prediction.

References

1. Al-Hameed S, Benaissa M, Christensen H (2017) Detecting and predicting Alzheimer’s disease severity in longitudinal acoustic data. In: ACM international conference proceeding series. Association for Computing Machinery, pp 57–61
2. Basaia S, Agosta F, Wagner L, Canu E, Magnani G, Santangelo R, Filippi M (2019) Automated classification of Alzheimer’s disease and mild cognitive impairment using a single MRI and deep neural networks. *NeuroImage Clin* 21. <https://doi.org/10.1016/j.nicl.2018.101645>

3. Chien YW, Hong SY, Cheah WT, Yao LH, Chang YL, Fu LC (2019) An automatic assessment system for Alzheimer's disease based on speech using feature sequence generator and recurrent neural network. *Sci Rep* 9. <https://doi.org/10.1038/s41598-019-56020-x>
4. Farzana S, Parde N (2020) Exploring MMSE score prediction using verbal and non-verbal cues. In: Proceedings of the annual conference of the international speech communication association, INTERSPEECH. International Speech Communication Association, pp 2207–2211
5. Feng C, Elazab A, Yang P, Wang T, Zhou F, Hu H, Xiao X, Lei B (2019) Deep learning framework for Alzheimer's disease diagnosis via 3D-CNN and FSBi-LSTM. *IEEE Access* 7:63605–63618. <https://doi.org/10.1109/ACCESS.2019.2913847>
6. Fulton LV, Dolezel D, Harrop J, Yan Y, Fulton CP (2019) Classification of Alzheimer's disease with and without imagery using gradient boosted machines and resnet-50. *Brain Sci* 9. <https://doi.org/10.3390/brainsci9090212>
7. Lee G et al (2019) Predicting Alzheimer's disease progression using multi-modal deep learning approach. *Sci Rep* 9. <https://doi.org/10.1038/s41598-018-37769-z>
8. Nasreen S, Hough J, Purver M (2021) Detecting Alzheimer's disease using interactional and acoustic features from spontaneous speech
9. Seshadri N, Shah R, McCalla S Early prediction of Alzheimer's disease with a multimodal multitask deep learning model
10. Cui R, Liu M (2019) RNN-based longitudinal analysis for diagnosis of Alzheimer's disease. *Comput Med Imaging Graph* 73:1–10. <https://doi.org/10.1016/j.compmedimag.2019.01.005>
11. Hong X, Lin R, Yang C, Zeng N, Cai C, Gou J, Yang J (2019) Predicting Alzheimer's disease using LSTM. *IEEE Access* 7:80893–80901. <https://doi.org/10.1109/ACCESS.2019.2919385>
12. Ljubic B, Roychoudhury S, Cao XH, Pavlovski M, Obradovic S, Nair R, Glass L, Obradovic Z (2020) Influence of medical domain knowledge on deep learning for Alzheimer's disease prediction. *Comput Methods Programs Biomed* 197. <https://doi.org/10.1016/j.cmpb.2020.105765>
13. Lin W, Tong T, Gao Q, Guo D, Du X, Yang Y, Guo G, Xiao M, Du M, Qu X (2018) Convolutional neural networks-based MRI image analysis for the Alzheimer's disease prediction from mild cognitive impairment. *Front Neurosci* 12. <https://doi.org/10.3389/fnins.2018.00777>
14. Liu Z, Guo Z, Ling Z, Li Y (2021) Detecting Alzheimer's disease from speech using neural networks with bottleneck features and data augmentation. In: ICASSP, IEEE international conference on acoustics, speech and signal processing—proceedings. Institute of Electrical and Electronics Engineers Inc., pp 7323–7327
15. Lopez-de-Ipina K, Martinez-de-Lizarduy U, Calvo PM, Mekyska J, Beitia B, Barroso N, Estanga A, Tainta M, Ecay-Torres M (2017) Advances on automatic speech analysis for early detection of Alzheimer disease: a non-linear multi-task approach. *Curr Alzheimer Res* 15:139–148. <https://doi.org/10.2174/1567205014666171120143800>
16. Lu D, Popuri K, Ding GW, Balachandar R, Beg MF (2018) Multiscale deep neural network based analysis of FDG-PET images for the early diagnosis of Alzheimer's disease. *Med Image Anal* 46:26–34. <https://doi.org/10.1016/j.media.2018.02.002>
17. Mirzaei S, el Yacoubi M, Garcia-Salicetti S, Boudy J, Kahindo C, Cristancho-Lacroix V, Kerhervé H, Rigaud AS (2018) Two-stage feature selection of voice parameters for early Alzheimer's disease prediction. *IRBM* 39:430–435. <https://doi.org/10.1016/j.irbm.2018.10.016>
18. Weiner J, Herff C, Schultz T (2016) Speech-based detection of Alzheimer's disease in conversational German. In: Proceedings of the annual conference of the international speech

Estimating the Low Cost Probability Error in QAM Using the SRRC Filter with Other Filter



Preesat Biswas, Bharti Baghel, Shirin Khan, and M. R. Khan

Abstract Nowadays, mobile communication is a part of our life and it is essential for us. On the transmission and receiver side using quadrature amplitude modulation (QAM) with square root raise cosine (SRRC) filter using transmission and receiver side. In a transmission system, four signals pass through at a time in multiplication and addition system in one bandwidth, the incoming signal in receiver side which reduce in cost per time, less error rate bit error rate (BER), signal-to-noise ratio (SNR) with low power. On the receiver side, we pass through the multistage filter, Nyquist filter, and SRRC filter. As a result, the best filter which is QAM with SRRC filter shown in this paper using “ESTIMATING THE LOW-COST PROBABILITY ERROR IN QAM USING THE SRRC FILTER WITH OTHER FILTER” simulated MATLAB 2019a.

Keywords SRRC · QAM · BER · RoF · ISI

1 Introduction

As this is the era of modern communication. Our technology becomes so significant that it must progress in parallel with the growth of mankind and modern society [1]. The process of “sending or transmitting” and “receiving” a message from a source point to a destination point across a communication channel is known as communication. Only when the receiver can decode the exact message sent by the transmitter is communication said to be conclusive [2]. It is now critical to adopt the required procedures for each system in order to construct multipath communication networks. During data transmission, the phase and frequency are reassembled using quadrature amplitude modulation (QAM) to reduce bandwidth and then pass through

P. Biswas (✉)

Electronics and Communication Engineering, Dr. C. V. Raman University, Bilaspur, India
e-mail: preesat.eipl@gmail.com

B. Baghel · S. Khan · M. R. Khan

Electronics and Telecommunication Engineering, Government Engineering College, CSVTU, CG, Jagdalpur, India
e-mail: mrkhan@gecdp.ac.in

the AWGN channel check comparator, error count, and calculate bit error rate (BER) with signal-to-noise ratio (SNR) in the received signal) [1, 2].

1.1 QAM Process

The signal must travel a long distance and must reach a large number of destinations, modulation is preferred. The method of altering the carrier signal properties in accordance with the modulating signal is known as modulation. In QAM, there are four carrier signals separated by $\pm 45^\circ$ (00, 01, 10, and 11). As a result, two phases “I” and quadrature or “Q” are created. These are normally located within the baseband area supplied. The four follow-on signals are added together, and the result is used to forward the required RF signal. Frequency amplification is required to convert this frequency to the final frequency. Demodulation is the reversal of the QAM process. The discriminator receives the QAM output here. It separates QAM output into four quadrants and feeds them into a mixer. A local oscillator signal is received by the mixer and the local carrier, one in-phase and the other with phase shift. The ‘I’ output and the “ $\pm O$ ” output are the mixer’s four outputs. When a $\pm 45^\circ$ phase-shifted carrier is applied to the mixer, the “ $\pm O$ ” output is produced; otherwise, the “ $\pm I$ ” output is produced. 256-QAM contains eight “I” and eight “Q” values, implying high proficiency and production [1, 3, 4] (Fig. 1).

Generally, a baseband channel, modulator, and demodulator are used to process a binary data stream via a communications network. A stem plot to depict a part of the random data, constellation diagrams to show the broadcast and received signals, and a bit error rate calculator (BER).

In this model Process, the input signal converts from serial to Parallel, where the signal passes through the SRRC filter to the QAM processor then pass through SRRC with the FIR filter and modulates the signal for broadcasting. In receiver side the incoming signal those are pass through the Channel Modulating with AWGN

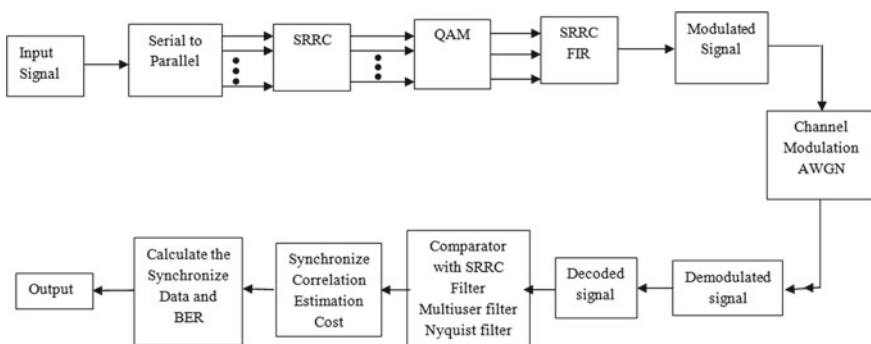


Fig. 1 Block diagram of QAM with SRRC filter

and Demodulate the signal. After demodulation system signal are decoded and comparator check with SRRC filter, Multiuser filter and Nyquist filter. All the process synchronize correlation estimation cost those are adder and multiply the signal and calculated it. Then it was synchronize data and BER calculate and signal goes to output data.

1.2 Generate Random Binary Data Stream

A vector or matrix is the most common way to represent a signal in MATLAB. A binary data stream which is converted to radiant function generates a column vector. By default, set binary data stream's length to 240,000.

To make the sample repeatable, rearrange the radiant function into its default state or any static seed value. After that, the radiant function can be used to create a random binary data stream [5]. To depict the first 40 bits [5] into binary values from the random binary data stream, use a stem plot. Use the colon (:) operator in the stem function call to select a part of the binary vector.

1.3 Convert Integer from Signal Binary Signal to Integer Value and Us 16 QAM, 64 QAM, 128 QAM, and 256 QAM

By default, the QAM modulation function expects integer-valued data for modulation input symbols. Before using the QAM modulation function, the binary input stream is preprocessed into integer values. The binary to decimal function converts each four-tuple into an integer in the range $[0, (M - 1)]$. The modulation order, M , is 16, 64, 128, and 256.

Transform the data into binary k -tuples, where k equals the amount of bits per symbol ($k = (\log 2). (M)$). After that, each four-tuple is converted to an integer number using the binary function.

The modulation process produces complex column vectors with values that are 16 QAM, 64 QAM, 128 QAM, and 256 QAM signal constellation elements. The natural and gray binary symbol mapping is shown later in this example constellation diagram.

More information on modulation functions can be found at digital modulation. Gray coding using phase-shift keying (PSK) modulation is a form of gray coding.

1.4 *Converted Integer_Valued Signal to Binary Signal*

The data symbols from the QAM demodulator are converted. Data Symbols Out, to a binary matrix, data Out Matrix, with “**d**” dimensions of sym by N number bits/symbol, use the decimal to binary function.

Nbits/sym means the number of bits per symbol and the total number of QAM symbols in the matrix is Nsym. Nbits/sym = 4 in 256-QAM, converting the matrix to a column vector with a length equal to the number of input bits, which is 240,000. As a result the process for the Gray-encoded data symbols, data Symbols Out G.

1.5 *Compute BER System*

Bit error statistics are generated by the bit error function using the original binary data stream data In and the receiving data streams data Out and data Out Gray code-wise. The BER lowers considerably when gray coding is utilized. Error statistics can be computed using the error rate function [5].

2 Math

1. Raised Cosine Filter

In broadcasting system, individual pulses are typically used to convey the bits. In order to keep power emissions below the legal limit, it is necessary to regulate them. A significant lobe exists in the signal. The minor lobe is prone to showing up in the adjacent ISI spectral region. The minor lobe has a proclivity for appearing in adjacent spectral bands, ISI. To avoid ISI implementation in the transmission system, and stopband filter use for the high attenuated stop-band filter. In the case of time domain pulse shaping, RCF is the optimum option. The RRC is given by (5) and (6).

$$h_{RC}(f) = \begin{cases} 1 & \text{for } |f| < 2W_0 - W \\ \cos^2 \cdot \left[\frac{\pi}{4} \cdot \frac{|f| + W - 2W_0}{W - W_0} \right] & \text{for } 2W_0 - W < |f| < W. \\ 0 & \text{For } |f| > W. \end{cases} \quad (1)$$

where $W - W_0$ is surplus bandwidth and form this signal raised cosine falls above bandwidth W_0 . As a result, “Nyquist” pulse filters are pulses that have no ISI when sampled. The Nyquist pulse shaping metric is satisfied with zero ISI [2]. The following relation

$$x(k.T_c) = \delta.(k.) \quad (2)$$

where

$$\delta.(k) = \begin{cases} 1. & k. = 0 \\ 0. & k. \neq 0 \end{cases} \tag{3}$$

It was simplified as

$$\sum_{m=-\infty}^{\infty} X.\left(f + \frac{m.}{T_C.}\right) = T_C. \tag{4}$$

where $X.(f.)$ is representing the Fourier transform signal $X.(t.)$ and $T_C.$ the time period of the pulse [2]

$$h_{RC.}(t) = 2W_0. \sin c.(2W_0.t) \frac{\cos.[2\pi(W - W_0.)t]}{1 - [4.(W - W_0.)t]^2} \tag{5}$$

Another α is the ROF, it is determines the sharpness of the frequency response [2].

$$\alpha = \frac{W - W_0.}{W_0.} \tag{6}$$

The ROF shows how much power is used in RC emitters across a certain bandwidth $W_0.$ Therefore $0. \leq \alpha. \leq 1$ When we use an RC pulse in conjunction with an equalization at the receiver, we can determine the sampling time.

$$h_{RC.}(f) = h_{Tx.}(f).h_{\tau.}(f).h_{Rx.}(f).h_E.(f) \tag{7}$$

where the transmission filter $h_{Tx.}(f)$ is the channel frequency response is $h_{\tau.}(f)$ receiver filter is $h_{Rx.}(f)$, the equalizer is $h_E.(f)$. Before they can be used, the transmitter and receiver filters need to be constructed.

$$h_{RC.}(f) = h_{Tx.}(f).h_{Rx.}(f) \tag{8}$$

and

$$h_E.(f) = \frac{1}{h_{\tau.}(f)} \tag{9}$$

2. Square Root Raised Cosine Filter

The SRRC (12) filter, a more advanced RCF technique, is used here. The frequency response of the SRRC filter is unity gain at low frequencies and full gain at high frequencies. It's very frequent in communication networks, whereas the SRRC channel is applied first, and then a matching filter is applied in the receiver portion [2].

The SRRC is given by (7) and (8)

$$h_{Tx}(f) = h_{Rx}(f) = \sqrt{h_{Rx}(f)} = h_{SRRC}(f) \tag{10}$$

3. Additive White Gaussian Noise (AWGN)

AWGN is created by thermally dissipative electrical components emitting electrons. It can be represented as a Gaussian, zero-mean process. And, a random signal is a combination of random noise variables and a signal that is distinct from the current one as show in (9), (6), (7) and (14).

$$Z = \alpha + v \tag{11}$$

The noise is Gaussian in nature. Has the following probability distribution function:

$$p(z) = \frac{1}{\sigma \cdot \sqrt{2\pi}} \exp \left[-\frac{1}{2} \left(\frac{z - a}{\sigma} \right)^2 \right] \tag{12}$$

The noise model is Gaussian, with a PSD $G_n(f)$ that is flat for all frequencies denoted as;

$$G_n(f) = \frac{N_0}{2} \tag{13}$$

SRC pulses, according to (9) are extremely similar to Nyquist pulses, which have a finite bandwidth with PSD.

$$G_{SRRC}(\alpha., f) = \begin{cases} \frac{T_c}{2} \cdot \left\{ 1 + \cos \cdot \left[\frac{\pi T_c}{\alpha} (\|f\|) - \frac{1-\alpha}{T_c} \right] \right\} & \frac{1-\alpha}{T_c} \leq \|f\| \leq \frac{1+\alpha}{2T_c} \\ 0 & \|f\| > \frac{1-\alpha}{2T_c} \end{cases} \tag{14}$$

$$\int_{-\infty}^{\infty} G_{SRRC}(\alpha., f) \cdot df = 1 \tag{15}$$

The problem suggests that the PSD may be a bilateral spectrum. Such version noise is common in all digital communication systems, and it is the primary source of noise in many systems with an AWGN physical appearance. AWGN is utilized in practically every communication system to create a noise model, which we have simulated here to attain a suitable performance [2].

$$S.(t) = \frac{4 \cdot \alpha}{\pi \cdot \sqrt{T_c}} \cdot \frac{\cos \cdot \left[\left(\frac{1-\alpha}{T_c} \right) \cdot \pi t \right] + \frac{T}{4 \cdot \alpha \cdot t} \cdot \sin \cdot \left[\left(\frac{1-\alpha}{T_c} \right) \cdot \pi t \right]}{1 - \left(\frac{4 \cdot \alpha \cdot t}{T} \right)^2} \tag{16}$$

4. Multistage Filter

Filters with a cut-off frequency of [5] one quarter of the [5] sampling frequency f_s are low pass FIR filters. and odd symmetry around $\frac{f_s}{2}$ are known as half-band filters. As it happens, over half of the coefficients are “O”. These filters are quite useful. As it happens, over half of the coefficients are “I”. These filters are quite useful. Almost half of the coefficients are zero, as it occurs. Because the pass band and stop band bandwidths are equivalent, these filters are suitable for decimation-by-2 and interpolation-by-2. These filters are common in signal systems because their zero coefficients make them computationally efficient by $\pm \frac{1+\alpha}{2T}$.

The window method can be used to compute half-band coefficients. While the window technique may not always offer the smallest number of taps for a given performance, it is beneficial in understanding half-band filters. The MATLAB 2019a function FIR half-band can be used to create efficient equiripple half-band filters.

3 Result and Discussion

3.1 Error Rate Calculation

The help of this block to compute the error rate by making a comparison between receiver data with the cost of multi filter, Nyquist filter, and SRRC filter [2], which is after filtering and scatted signal arrange one place and error-free data in this system.

3.2 Transmit Pulse Shaping in Raised Cosine Filter

Through transmit filtering using a Nyquist pulse, the formation symbol α_m with a symbol period T can be transmitted without inter symbol interference (ISI) by using Nyquist pulse [2].

$$g(t) = \frac{\text{Sin}(\pi.t/T)}{\pi.t/T}., t = -\infty. \text{ to } .\infty \tag{17}$$

With the help of higher cosine filtering for pulses, we acquire results in a narrow range limited to frequencies between [2] $-\frac{1}{2T}$ Hz and $+\frac{1}{2T}$ Hz.

Using MATLAB 2019a, I plotted the time domain and frequency domain illustrations of the RCF for various values of, i.e., $\alpha = 0.27, \alpha = 0.35, \alpha = 0.42,$ and $= 1$. We found that the filter tail of the RCFr with a value larger than 0 fades off quicker in time domain samples. As can be observed from the frequency response, the filter response is band limited only until for values larger than 0. When compared to Nyquist bandwidth, we require a bigger bandwidth to transport the wave from.

Time domain waveform of RC pulse shaping shown in Fig. 2 and frequency domain waveform of RC pulse filter shown in Fig. 3.

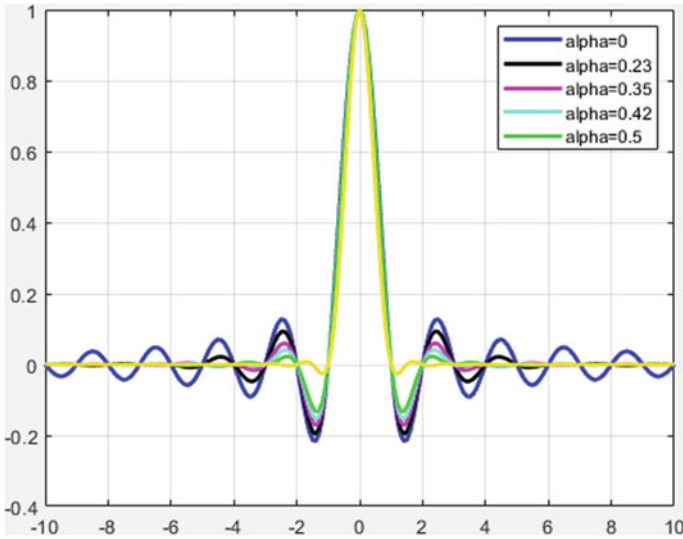


Fig. 2 Time domain pulse shaping filter

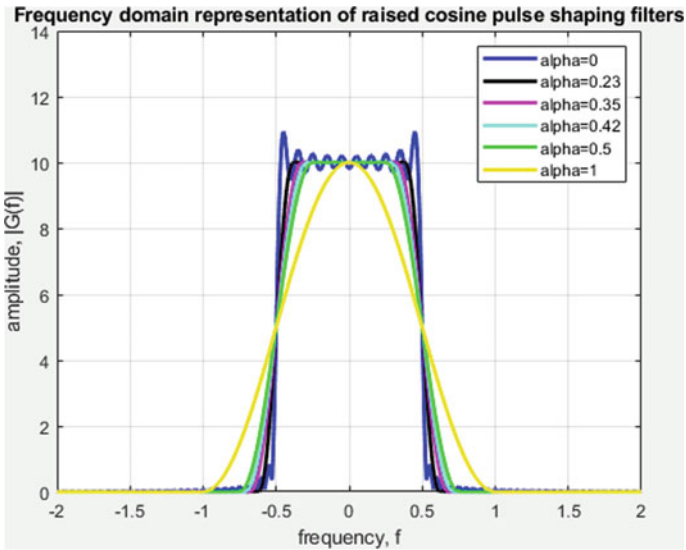


Fig. 3 Alpha 0.23, 0.35, 0.42, and 0.5 using frequency domain waveform of RC pulse shaping filter

3.3 Comparison Between RRC and SRRC Filters Impulse Response

A standard RCF and a SRRCF are compared in this case. In a cascade setup, an ideal normal RC pulse shaping filter is comparable to twice the number of an ideal SRRCF [2]. As a result, when a FIR filter is convolved with itself, the impulse response should be comparable to that of an RCF.

Creating a standard RCF with a roll of factors 0.23, 0.35, 0.42, and 0.5 means this filter spans four symbols and contains three samples for each symbol. It cut short the impulse response outward from the largest after converting the square-root filter with itself.

3.4 Specification of Raised Cosine Filter

The most significant limitation of an RCF is its RoF, which in a roundabout manner reveals the filters transmission capacity. The number of taps on a perfect RC channel is infinite. Following that, all valid RC channels are windowed. The window length property of the channel span in symbols property is used to regulate the window length. The window length is expressed in terms of six symbol lengths, i.e., the channel ranges six picture terms. A bunch delay of three symbol terms is also included in this sort of channel. RCF is a pulse shaping technique in which the signal is upsampled. As a result, we need also provide the upsampling factor. To obtain the desired channel characteristics, we use the cosine transmit filter framework object and specify its attributes. This item is a straightforward depiction of a standard polyphase FIR filter with a unity energy. The Nyquist system samples PerSymbol, or Nyquist system samples PerSymbol + 1 taps are arranged on the channel. The gain property was used to normalize the filter coefficients such that the filtered and unfiltered data matched when compared [2].

3.5 Roll-off Factor with Square Root Raised Cosines Filter

The filtered output signal is received by changing the roll-off factor from input sampled signal 0.5 (blue curve) to 0.23 (red curve [3]), 0.35 (yellow curve), and 0.42 (gray curve). The turning point of 0.5 (blue curve) filtered signal has greater than for 0.23 (red curve), 0.35 (yellow curve), and 0.42 (gray curve).

The raised cosine filtering is used to divide into the filter for transmitting and receiver signal, and this transmitting and receiving signal used to be square root raised cosine filter [6] which output is minimum ISI.

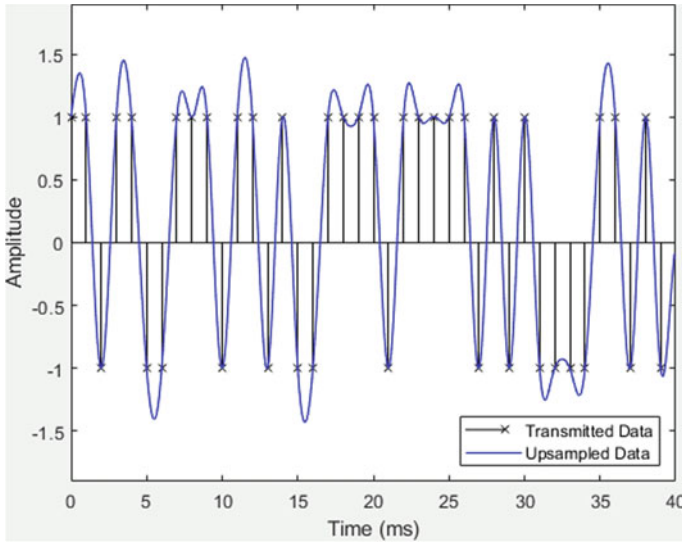


Fig. 4 Transmitted data and unsampled data

This plotting figure shows the up-sampled and filtered transmitting signal where square-root raised cosine filters are used. And [6], we have not destroyed the filter output of transmitted signal (magenta curve).

The default unit of energy for arranging data in a database to ensure that the gain of a normalized raised cosine filter and the [6] gain of a mixer of transmit and other side raise cosine filter arrange again and convert to normalized signal from receiver. The receiving filter signal is almost similar to the single raised cosine filter signal on which curve is blue signal [6] (Figs. 4, 5, 6, and 7).

Table 1 Shown Implementation cost comparison between C1, C2, C3, and C4. Where C4 Number of coefficient is 97, Number of State is 96, Multiplication Per 97 and Additions per input 96. When we pass through 100 symbols in each state.

3.6 Pulse Shaping with Raised Cosine Filter

Now, bipolar information structure is created. As a result we profile the waveform using the RCF rather than providing ISI. In this graph, the digitized data and the injected signal are compared. The channel's bunch delay ($Nyquist\ symbol/(2R)$) delays the channel's top reaction, making comparison of the two signals difficult.

By inserting ($Nyquist\ symbol/2$) zeroes after input x we level all the beneficial tests out of the channel. We may compare the RCF group delay by delaying the input signal. At the present determining how the raised-cosine-filter up-samples and channels the signal at the input test timings is simple. The RCF's ability to band

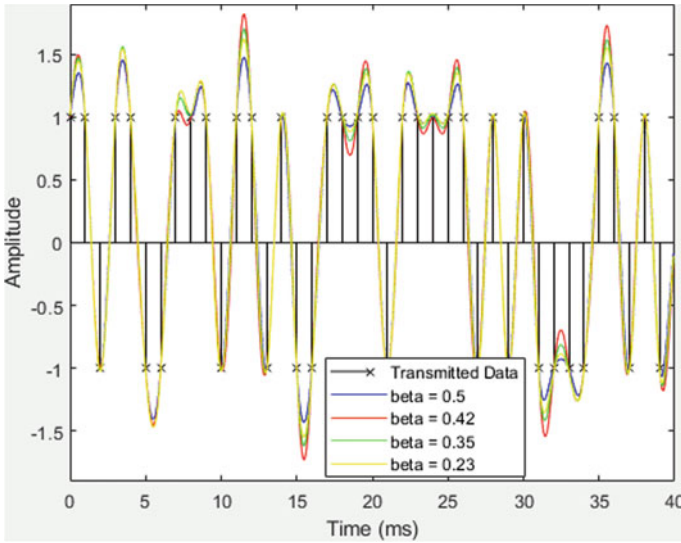


Fig. 5 Transmitted data with angle alpha 0.23, 0.35, 0.42 and 0.5

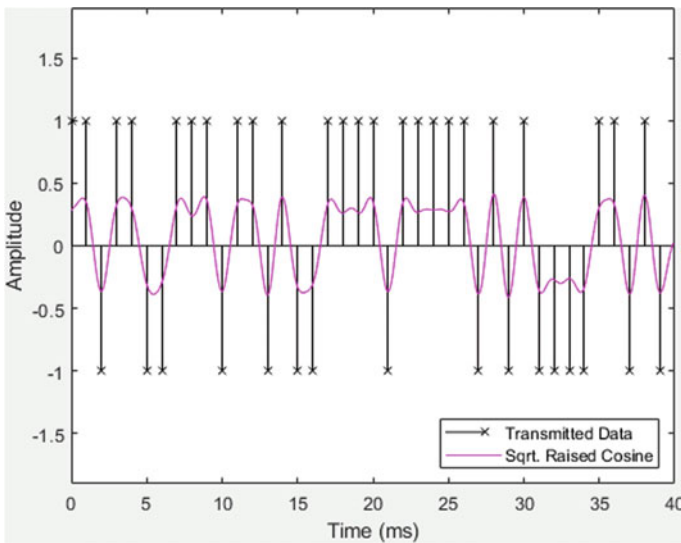


Fig. 6 Transmitted data and square raised cosine

restricts the signal while avoiding ISI is the reason behind this. Shape in ordinary with RoF 0.23, 0.35, 0.42, and 0.5 filter span in symbols 6 output sample per symbol 8 and gain is 1 means the sum of the total sample not more than 1.

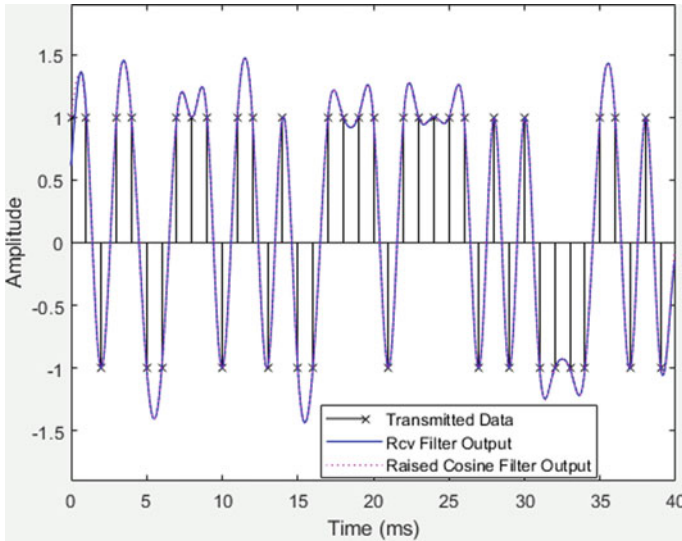


Fig. 7 Transmitted data, receiver filter output

Table 1 Implementation cost comparison

Cost	Num coefficients	Num states	Multiplications per	Additions per input
C1	97	8	97	85
C2	97	96	97	96
C3	97	96	97	96
C4	97	96	97	96

3.7 Square Root Cosine Filter (SRRCF)

Filtering is separated between the transmitter and receiver portions. The RCF was utilized. We used SRRC channels in both portions. It’s possible that the RCF with the lowest ISI will emerge from a combination of transmitter and receiver channels. To partition the filtering across the transmitter and receiver sections, the RCF was used. SRRC channels were used in both portions. It’s possible that the mix of transmitter and receiver channels will result in an RCF, which will have the lowest ISI.

To illustrate the SRRC filter, change the form to square root. At that point, the receiver sorts the sent signal (maroon bend). Standard unit energy normalization guarantees that the transmit and receive channel configurations are detected. Data that has been submitted as well as upsampled data. Data with betas of 0.23, 0.35, 0.42 and 0.5 was supplied. The square as well as the transmitted data cosine have been increased. Transmitted Data Receiver Filter Output and output of a raised cosine filter using a normalized RCF pick-up of alpha 39 and alpha 26 data were sent. The

sifted acquired flag is represented by the blue bend at the receiver section shown, which is nearly indistinguishable from the signal $\pm 45^\circ$ sifted with a single RCF [2].

3.8 Use Pulse Shaping of on Various QAM Signal

On a wide range of QAM signals, pulse shaping several variants of QAM are utilized in the execution of pulse shaping with the help of the matched filtering technique and a combination of SRRC filters. In addition to the forward error correction (FEC) method to the communication line, the increase cosine function provides filters, and the results may be regarded as an improvement in BER performance. Adding SRRC to the communication connection to the pulse-shape filtering in various kinds of QAM. That is a 16 QAM, 64 QAM, 128 QAM AND 256 QAM [2].

A binary data stream is used in a communication link that includes a baseband modulator, channel demodulator, pulse shaping, and match filters. This exhibition shows the transmission of random data in a specific stem plot. In received side constellation diagrams, incoming signals are formed with a bit error rate (BER) [2]. Applying the RRC filter with 256 QAM in 0 dB power after upsampling the signal by the oversampling factor to clean the filter, do the following: the up fir function adds zeros to the end of the upsampled signal. The channel is then applied by the function. We transformed the ratio of energy per bit to noise E_b/N_0 to an SNR value using the number of k and the sample space system [2, 4].

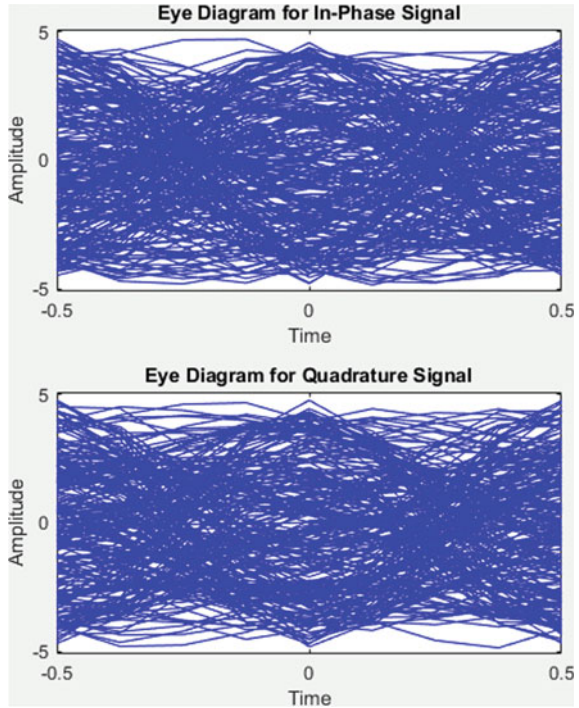
3.9 Eye Pattern the Filter Effect

We first reduced the E_b/N_0 value, then used 16-QAM and 256-QAM filter effects to reconstruct the received data in an eye pattern. In a cascade, an RCF is employed as a same pair of filters, such as 256-QAM and 512-QAM. Due to a high SNR of the signal and no kind of multipath effects, the ISI reduction output data in a matched pair of pulse shaping RRC filters [2] is not zero—ISI until the second RRC filter is attached in this system. The noisy eye pattern signal reveals ISI as a narrowing after matched receive filtering and pulse shaping.

When filtering is used, the constellation diagram of the received signal is shown, as well as when filtering is not used. Multiply the received signal by the square root of the number of samples per symbol to equalize the transmit and receive power levels [2]. Here we show the scatter plotting diagram of the data mode modulated signal and also show the receiving noisy signal after the channel.

The filter effects on the eye pattern We initially reduced the E_b/N_0 value setting and regenerated the received data in an eye pattern Fig. 8 the filter effects of 256-QAM and cascade as a matched pair of 256-QAM. ISI reduction output data in matched pair of pulse shaping RRC filters is not zero—ISI until the second RRC filter is connected in this system due to a high SNR of the signal without any form

Fig. 8 Eye diagram for in-phase signal and 256-QAM



of multipath effects. After matched receive filtering and pulse shaping, the noise eye pattern signal shows ISI as a narrowing [7]. Again rearranging the scattered signal as shown in Fig. 9.

The result shown of different QAM in receiver side before and after filtering 8-QAM in Fig. 10, 16-QAM in Fig. 11, 128-QAM in Fig. 12, and 512-QAM in Fig. 13.

In this, Table 2 shown different QAM with roll-off factor 0.23, 0.42 which is error estimation with binary code, gray code, and bit error rate. The best result is 256-QAM with binary 4.03e-02 and error detect 9638.

3.10 Pulse Shaping Different Between Multistage, Nyquist, and Raised Cosine Filter

Now, we used a raised cosine filter, multistage filter and Nyquist filter for shaping the waveform without ISI and generating bipolar data sequences. The plot is difficult to compare three digital signals and interpolated signals because the group delay of the filter delayed the response of peak point.

Fig. 9 Receiver signal, before and after in 256-QAM

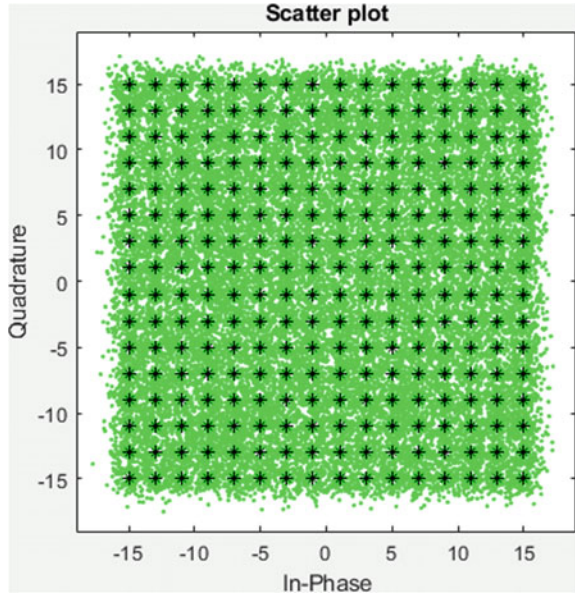


Fig. 10 Received signal. Before after filtering 8-QAM

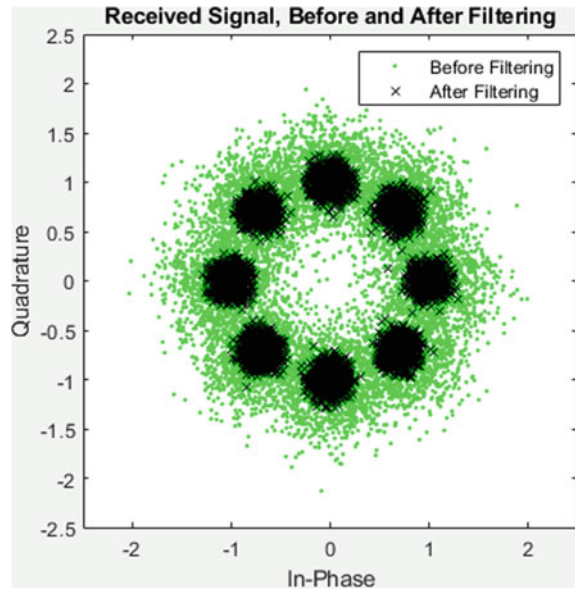


Fig. 11 Received signal.
Before after filtering
16-QAM

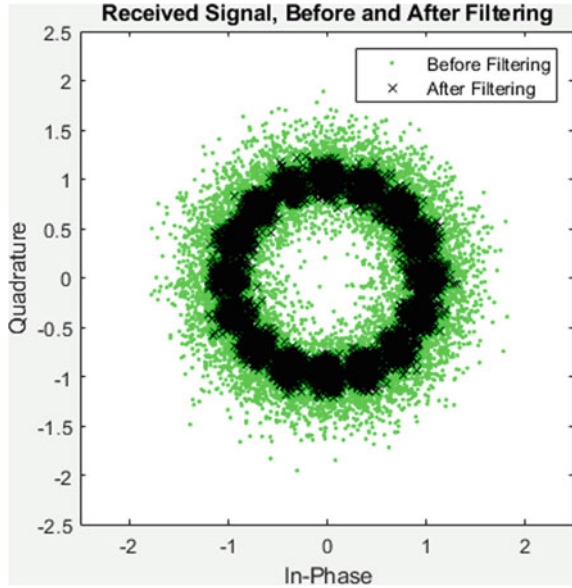


Fig. 12 Received signal.
Before after filtering
128-QAM

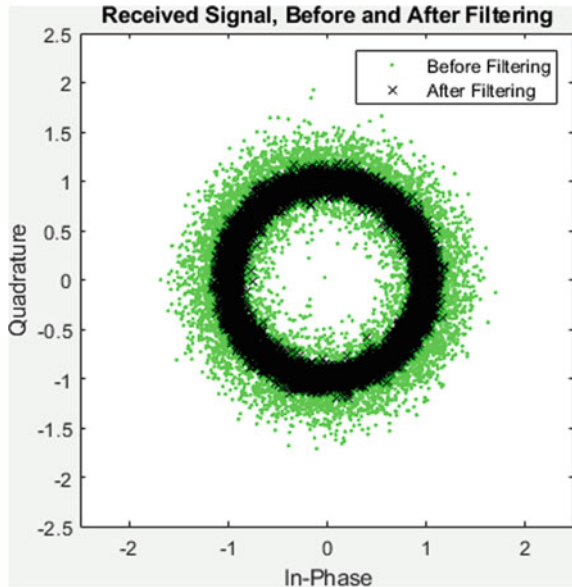


Fig. 13 Received signal.
Before after filtering
512-QAM

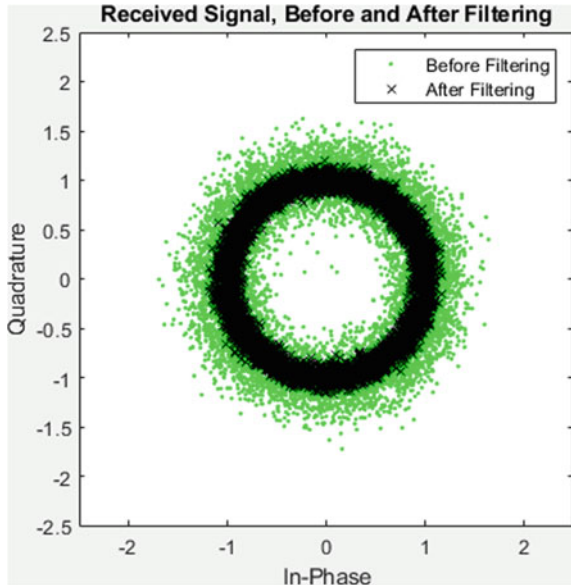


Table 2 Different QAM with Roll_off factor, Binary error, Gray errorError, & Bit error.

S. No.	QAM	Roll_off factor	Binary error	Error	Gray error	Error	Bit error	Error
1	16_QAM	0.23	4.17e-05	10	2.92e-05	7	2.50e-05	6
2	16_QAM	0.35	4.17e-05	10	2.92e-05	7	1.67e-05	4
3	16_QAM	0.42	4.17e-05	10	2.92e-05	7	1.25e-05	3
4	64_QAM	0.23	7.81e-03	1874	4.84e-03	1162	5.19e-03	1245
5	64_QAM	0.35	7.81e-03	1874	4.84e-03	1162	5.11e-03	1227
6	64_QAM	0.42	7.81e-03	1874	4.84e-03	1162	5.00e-03	1200
7	256_QAM	0.23	6.87e-02	16,495	3.95e-02	9487	4.03e-02	9678
8	256_QAM	0.35	6.87e-02	16,495	3.95e-02	9487	4.02e-02	9640
9	256_QAM	0.42	6.87e-02	16,495	3.95e-02	9487	4.03e-02	9638

The sampled input signal is with input sample time and this shows a raised cosine filter to band-limit signal without ISI (Fig. 14).

3.11 Using Multistage Filter with Magnitude

Using the multistage filter applied in the signal process, which is create low pass, high pass, band pass, in default system, which created with limitation conditions.

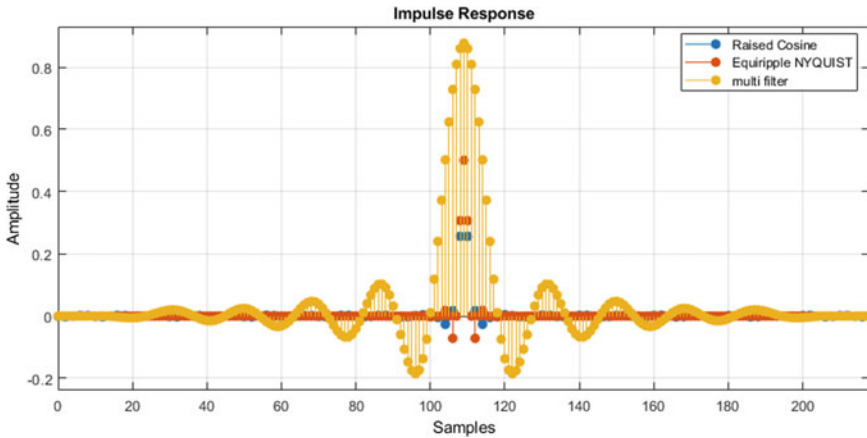


Fig. 14 Impulse response between raise cosine, Nyquist, multistage

Generally, it is designed for a special purpose which is to specify the number of stags to be used in this design and automatically generate it for filtering the signal. Then it allows the optimal number of stages while minimizing the cost of using the resulting filter. It also specifies an integer for the design algorithm that minimizes the cost for the number of stages we want.

It compares all filters with raised cosine and square root raised cosine filters. It is used for digital transmission systems in pulse shaping and also used under interpolation, decimation and filter banks.

3.12 *Using Nyquist, Raised Cosine Filtering and Multistage Filter*

The output response of the equiripple Nyquist filter, multistage filter and increased cosine filter is shown in the plotting Fig. 15. An ideal equiripple stopband filter with a bigger stopband attenuation filter and transition width is an equiripple Nyquist filter. The roll-off factor for all filter orders is 0.23. This raised cosine filter is made by cutting off the analytical impulse response at the end.

In this Nyquist filter we can use square-root raised cosine spectral factor filters with the filtering application. A square-root filter fixed on both transmitter and receiver of the end.

The decrease of different roll-off factor ($RoF = 0.23$, and $Rof = 0.42$) shown in Figs. 16 and 17 improves the response of raised-cosine filters and this is caused by containing the direction of the maximum radiation frequency response rectangular window which is used in cutting off the end of the impulse response.

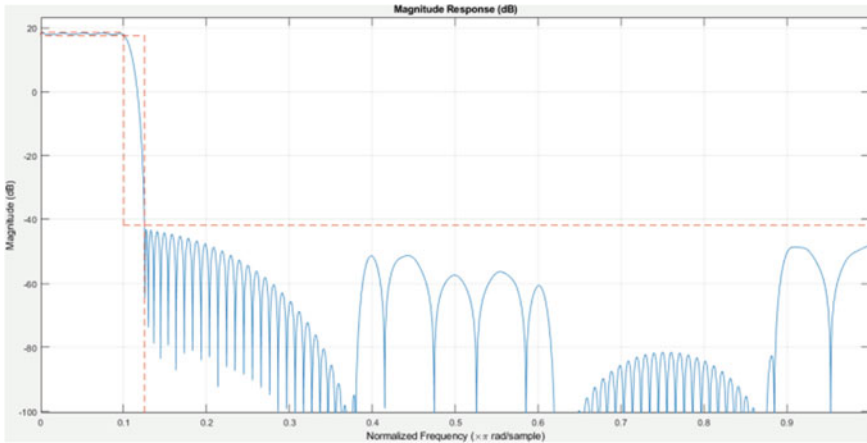


Fig.15 Magnitude response in dB normalize frequency

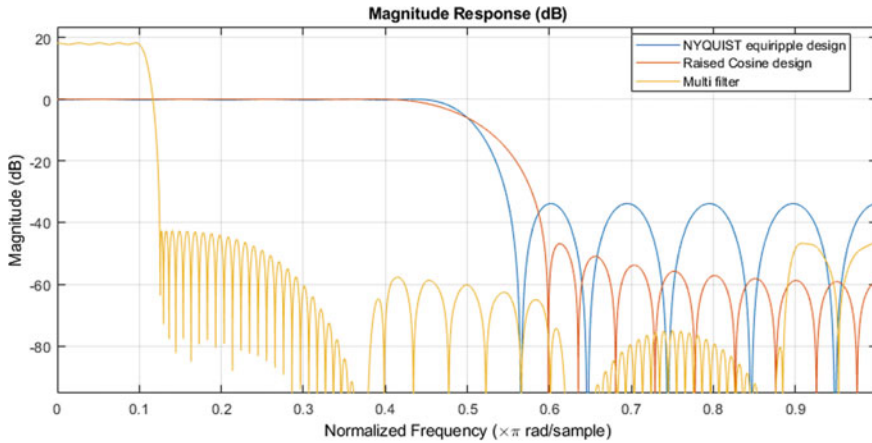


Fig. 16 Roll-off factor 0.42 using magnitude response in normalized frequency-(13 dB) by Nyquist, raised cosine and multi filter

Now we can design a windowed impulse response method and cut off frequency response with a multi filter. Due to side lobe increase more than multi filter, raised-cosine design and also requires order raised-cosine filter and equiripple to meet the stopband specs.

The polyphase all pass filters have multipliers, which allows for an efficient implementation of that polyphase branch. The input is delivered directly to the interpolation filter but raised cosine filter is more better then multi filter and Nyquist filter shown in Fig. 16. The capability of rejection system is inter symbol interference and splitting the raised cosine filter between transmitter and receiver with filter system object (comm. Raised Cosine Transmit Filter and comm. Raised Cosine Receive

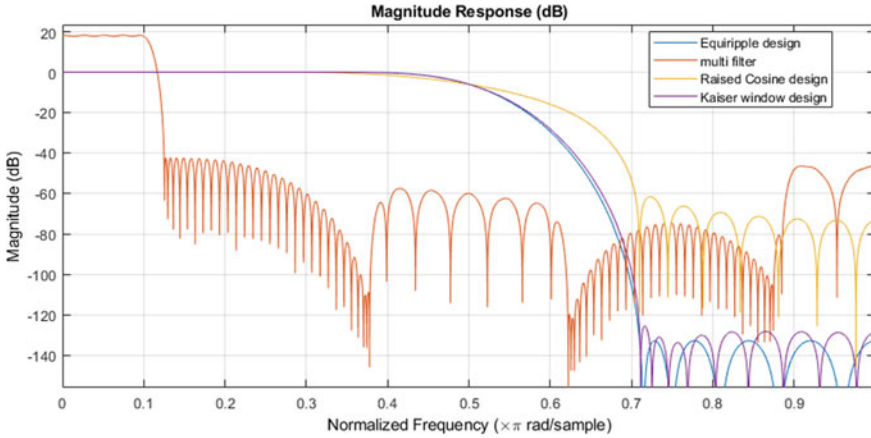


Fig. 17 Roll-off factor 0.42 using magnitude response in normalized frequency-(39 dB) by Nyquist, raised cosine and multi filter

Filter). The roll-off factor of raised cosine filter parameters indirectly specifies bandwidth filter [8]. An ideal raised cosine filter has an infinite number of taps. Raised cosine filter used for pulse shaping on which upsample signals are used for specification. The object designs a polyphase FIR filter through the energy order of $N_{sym} * \text{sampsPERSym}$ or $N_{sym} * \text{PerSym} + 1$ taps. In an overlaid situation we can apply the gain property to normalize the coefficient filter and unfiltered data. In this situation, we use filtered down sampling from the receiving signal to upsample the broadcast signal. Now that the SRRC filter is in use, half of the symbol's filter length is added to the delay. The filter length is equal to the receiving signal. $16_QAM = 39$ dB, $64_QAM = 39$ dB, $128_QAM = 39$ dB, and $256_QAM = 39$ dB, impulse response.

3.13 Kaiser Window Design with Equiripple Filter, Multi Filter and Raise Cosine Filter

Kaiser window design for modified discrete cosine transform which length $N + 1$ the formula apply when $2N$ and Constructi “ d_n ” satisfies with equiripple filter, multi filter and raise cosine filter as shown in Fig. 17 in roll of factor 0.42 and 39 dB power of normalized frequency.

Comparing magnitude response in 13 dB with Kaiser window filter, Nyquist filter, multi filter and raised cosine filter in normalized frequency as shown in Fig. 18.

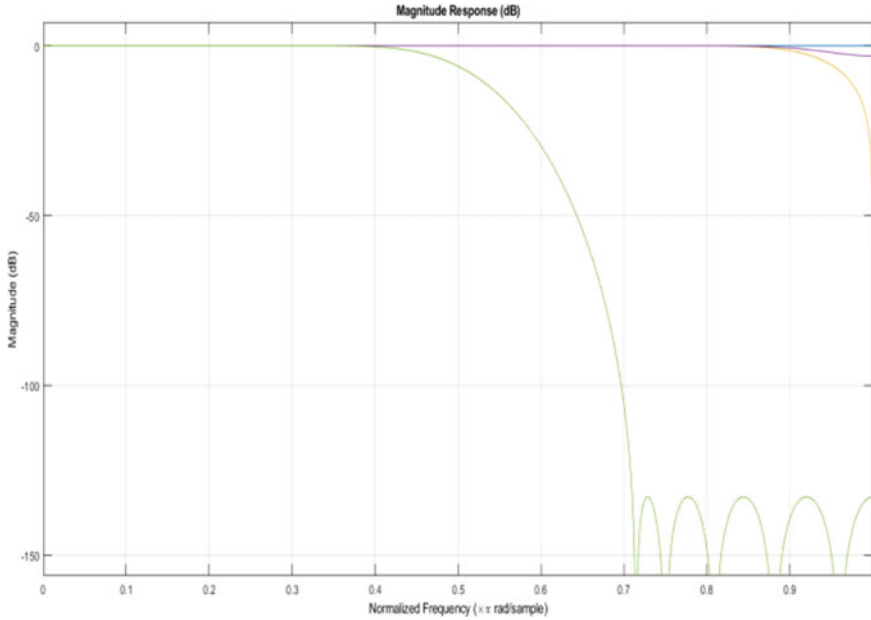


Fig. 18 Magnitude response in normalized frequency(-13 dB) by Kaiser window filter, Nyquist filter, raised cosine filter, and multi filter

3.14 Computation Cost

In the computational costs of polyphase FIR interpolation and polyphase FIR decimation filters are compared.

4 Using Multistage Filter, Nyquist Filter, Kaiser Window Filter and SRRC Filter Techniques of Achieve Efficient Designs in Pole and Zero

The incoming signal from receiver side filter order uses 40 number of symbols which uses Multistage filter, Nyquist filter, Kaiser window filter, and SRRC filter techniques. As a result, pole-zero shown in Fig. 19 and it centered shown 39 is the best performance is SRRC filter.

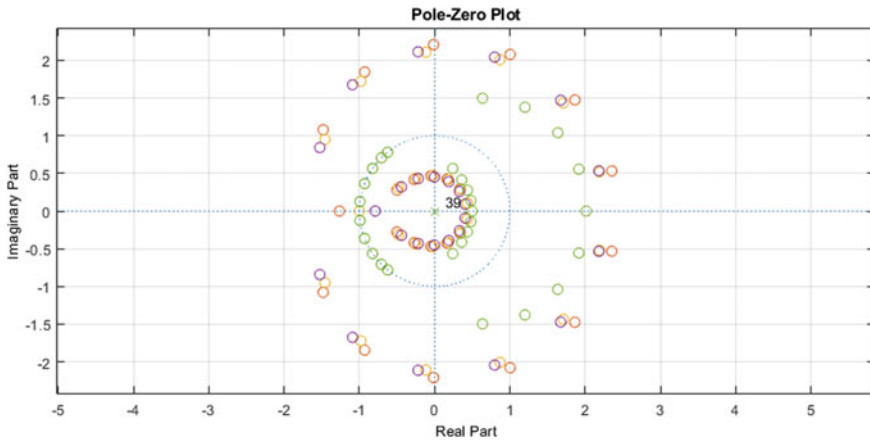


Fig. 19 Pole and zero plot

5 Error Rate Calculation

By comparing received data to the delayed form of transmitted data, this block aids in the computation of the error rate. The block's output is divided into four sections, each of which contains the following components: first, the error rate; second, the error rate; third, the error rate, and fourth error rate. The number of symbols that are compared in total. Table 1 shows C4 Number of the coefficient is 97, Number of State is 96, Multiplication Per 97, and Additions per input. Table 2 shows 256-QAM with Binary $4.03e-02$ and error detect 9638.

6 Conclusion

Transmission and receiver side quadrature amplitude modulation (QAM) with square root raise cosine (SRRC) filter. In the transmission system, four signals travel in at the same time in a multiplication and addition system in one bandwidth, while the incoming signal in the receiver side has detected in simulation in MATLAB 2019a system at a lower cost per time, a lower bit error rate (BER), and a lower signal-to-noise ratio (SNR), and uses less power with high data rate. On the receiver side, we pass through the multistage filter, Nyquist filter, and SRRC filter. As a result, best filter which is QAM with SRRC filter shown in this paper using "ESTIMATING THE LOW COST PROBABILITY ERROR IN QAM USING THE SRRC FILTER WITH OTHER FILTER".

References

1. Preesat B, Shanti R, Khan MR, Kumar SP (2020) A novel approach of digital communication using 256QAM and raised cosine filter. In: 2020 international conference on communication and signal processing (ICCSP)
2. Preesat B, Shanti R, Khan MR (2021) A novel approach of various QAM with roll off factor variation using raised cosine filter and SRRC filter for analysis of BER and SNR. Mater Today Proc
3. Brune S, Popov AA, Sobolev SV (2012) Modeling suggests that oblique extension facilitates rifting and continental break-up. J Geophys Res (2012 Publication)
4. Preesat B, Chanki P, Kumar TA, Khan MR, Shanti R (2020) Algorithm design simulation performance analysis of MIMO GMSK system for radio communication on AWGN channel. In: 2020 international conference on communication and signal processing (ICCSP)
5. Gharaibeh KM (2011) Nonlinear distortion in wireless systems. Wiley
6. Alagha NS, Kabal P (1999) Generalized raised cosine filters. IEEE Trans Commun
7. Shaheen Imad Ahmed A, Abdelhalim Z, Fatma N, Reem I (2017) Absolute exponential companding to reduced PAPR for FBMC/OQAM. In: 2017 Palestinian international conference on information and communication technology (PICICT)
8. Ersoy O, Sahin AB (2020) Investigation of harmonic frequency multiplication on transmitted data through pulse shaping for 6G communication. In: 2020 7th international conference on electrical and electronics engineering (ICEEE)

Designing a Secure Physically Unclonable Function Using Light-weight LFSR



B. V. D. N. Srilakshmi, Kiran Mannem, K. Jamal,
and Manchalla O. V. P. Kumar

Abstract In this concise, the objective is to design a brand new lightweight strong PUF style that will dynamically enlarge the CRP area. In conventional designs of PUFs, there is a drawback related to challenge–response pairs (CRPs) space and large hardware overhead. To overcome this drawback, we can take weak PUF and realize it as strong PUF and implement the linear feedback shift register (LFSR) logic for random number generation which in turn provides good security for authentication. Physical unclonable function (PUF) is an authentic physical safety primitive that is often implemented in FPGAs and ASICs. Strong PUF is a vital PUF classification that gives an oversized challenge–response pairs (CRPs) area for device security.

Keywords Low power LFSR (Linear feedback shift register) · PUF (Physically unclonable function) · CRP (Challenge–response pair) · Power consumption

1 Introduction

FPGAs have the broad spectrum of implementations in the development of embedded systems because of its adaptability adjustments and kind of less designing price in application-specific integrated circuits. In recent past, cloud technology, AI Technology, big data have evolved quickly [1]. In those approaches cases, the central processing units are more adaptable but do not have computing energy. Accelerators work mathematically well but are rigid in this applications. To maintain the stability between efficiency and adjustability, hardware components and CPU structures have become very popular. Like hardware reconstruction, FPGA has strong computing power and adequate flexibility. As the most widely accelerated form of scrutiny in branch of deep learning (DL), field programmable gate array have become a modern field of study and functionality hotspot. Microsoft has been using FPGAs rather than CPUs at their data networks [2]. The Tencent cloud straightly supplies field programmable gate array cloud networks, decreasing the expensive price on

B. V. D. N. Srilakshmi (✉) · K. Mannem · K. Jamal · M. O. V. P. Kumar
Department of ECE, GRIET, Hyderabad, India
e-mail: srilakshmi.bvdn@gmail.com

purchasing engineer equipment [3]. Inside iPhone, there are FPGA chips, which are manufactured by semiconductor lattice, following to chip works [4].

The extensive use of FPGA poses new security challenges, such as complex design, disruption, integration, and deferred engineering [5]. The bitstream used by the user to implement on FPGA is studied and puzzled out by these assault, leads in contention of the designed circuit, sensitive data, and configuration characteristics. FPGA manufacturers provide designers a wide range of solutions for security problems in order to protect their patents and sensitive information, for instance converting of data and secure bitstreams. Encryption keys and verification algorithms stored in non-volatile memory. These techniques will not assure the safety of keys and important data. The keys are readily available on NVM for a physical attack. On the other hand, in some FPGA applications, resources for hardware are very low and including the security of the modules in it will rise the hardware further, which leads to further challenges. Therefore, the first safety feature of lightweight hardware as a fundamental of guarantee, giving safety services like generation of key and validation of FPGA applications, has led to very sensuous in the field of research.

During fabrication process, because of other ungovernable reasons, limitations which includes size, V_{th} (Threshold-voltage) and oxide-thickness of individual device which is not same, also there would be some random deviations, that is also called process deviations. This deviation does not affect device performance nor does it affect circuit integrity. However, these random deviations can be extricated with the help of special design methods to create unique “fingerprints” for the circuit, accurately identify each chip and prevent the chip from being fabricated again and again or disrupting. This activity which is physical is called physically unclonable function (PUF). The arising part of device security primeval, physically unclonable function is extremely delicate to disturbances that are in physical that has an intrinsic physical disruption. PUF has incomparable benefits and wide functionality views in the branch of hardware security. Physically unclonable function produces particularly a consistent result if any challenge specified. Therefore, this approach is known as the challenge–response (CR) approach; also, its every pair of CR for single physically unclonable function is known as challenge–response pair space. The challenge–response safety method provides security keys and confidential information generated physically without storage for easy access to a local location, which reduces the chance that the key will be liable to enemies.

According to the liaison between the number of CRP's and the size of the visible structures, there are two types of PUF's: weak PUF and solid PUF [6, 7]. PUFs having a finite number of CRPs, known as weak PUFs, that are often used to produce the key to cryptographic operations. Alternatively, solid PUFs should have a rapid CRP number; hence, they are worth verifying [8]. These two types of PUFs require high diversity and solidity to protect its resources. At that point, a well-designed PUF should have a little device overhead and be easy to use. Linear feedback shift register (LFSR) produces pseudo-random number sequence (PRNS), mostly utilized in communication and secret-key study. It is a top geared, clear, and customizable circuit that provides an magnificent result of random sequences of less hardware

setup. This work shows that, LFSR is applied to an FPGA-based weak PUF that is lightweight and easy to accoutered solid PUF. It present related activities to PUFs as well LFSR in the beginning. Then, composition is described and application of lightweight PUF for LFSR and conclusion.

In our daily life, the most commonly used word is “Security.” The term security specifies the position or standard of living safe. It points to a particular structure, software, or entity which is unbound to any threat. It should be kept safe from being exposed to aggressor who creates damage either willingly or unwillingly. Subjected to system security, the term “Security” defines safety of our system and gives permission to empowered agents to ingress the system. There are certain layers of security in order to provide safety to companies. They are as follows:

1. PSL (Physical-Security-Layer)
 2. PS (Private-Security)
 3. PJS (Project-Security)
1. **PSL (Physical-Layer-Security):** This is the surface layer which gives safety to real objects. Here, an empowered agent is given ingress to real tools such as DVD, pen drive, and hard disk.
 2. **Private-Security (PS):** This surface layer gives security to discrete or a category.
 3. **Project-Security (PJS):** This surface layer describes the security given to features of any project such as code and design.

Now a days, technology is growing quickly. As the technology is growing, issues related to security are also increasing day by day. Many software tools are readily accessible to aggressor; due to this without having much knowledge on systems, the aggressor can easily attack the devices. Hence, data security is an attractive field in today’s life. Data security helps to secure the data from attackers.

The unauthorized person cannot able to access the system and cannot able to steal the data present in the system. This kind of security can be achieved through data security. Most of the time, the aggressor creates the situation that the systems will be made so busy, so the official people will not be able to access the service. At that point of time, the aggressor will try to attack and stole the information. This type of assault is known as denial of service (DOS).

Features of data security:

The features of data security include:

1. Privacy
2. Probity
3. Accessibility

Privacy: Privacy is the crucial feature in data security. It helps in such a way that it gives access only to the official user and not to any 3rd party or unofficial user. Privacy can be described as providing safety to the information from unofficial declaration.

Probity: Probity is other essential feature of data security. It helps to verify the effectiveness of the information and also verifies whether there is any interchange in

the information or not. Its gives guarantee that while transferring the data from the official agent to receiver there will be no change in the information.

Accessibility: The 3rd important feature is accessibility. It helps the official user to make the information handy at any instance. Accessibility means working state of the network at any specific point of time.

System Security

Cryptography

The term cryptography includes encryption and decryption of information. There are different types of methods involved in cryptography, by which the user can utilize them in order to protect their information.

Encryption

It is a process of converting plain message to a coded format message in order to provide security. Due to this, no 3rd party person will be able to crack the original message. This process of encryption can be achieved by using keys. There are two types of methods involved in encryption process; they are as follows:

1. Symmetric encryption
2. Asymmetric encryption

Symmetric-Encryption

In this method, only, a single key is required for both encryption and decryption process. Symmetric encryption consists of different types of algorithms. Advanced encryption system (AES), data encryption standard (DES), improved proposed encryption standard (IPES) are some types of algorithms in symmetric encryption.

Asymmetric Encryption

This method consists of two types of keys. The key which is exposed publicly is called "Public-Key," and the key which is well-known only to the key holder is called as "Private-key." Rivest, Shamir, Adleman (RSA), Elliptic Curve Cryptography (ECC), Diffie Hellman are some of the algorithms related to asymmetric encryption.

Decryption

It is a process of converting coded message into original message. This process is carried out by making use of keys.

2 Literature Survey

A. G. Schmidt, G. Weisz and M. French proposed a new Python development known as "PYNQ," for creating application development on Xilinx "ZYNQ." PYNQ

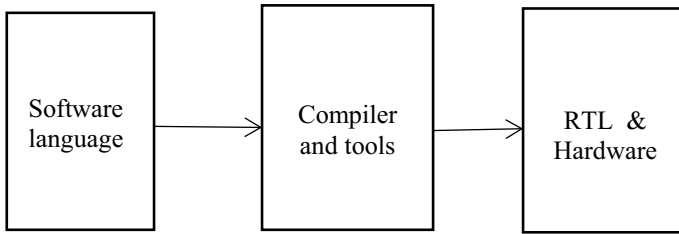


Fig. 1 3 phases in FPGA for application acceleration

consists of various libraries, and its performance is highly efficient when compared with conventional languages such as C and C++. By using Python, time required to develop an application is very less. It is the best way to support software developers to access FPGA using Python programming language].

A. Putnam proposed the concept of introducing FPGA's in data centers (dc), instead of using traditional CPU's. As there are certain issues related to data centers (dc) such as trouble shooting, constraints related to security features, and major issues related to power efficiency, computing power [10]. In order to solve these issues, Microsoft introduced FPGA's in data centers. FPGAs in data centers are used as accelerators for increasing the computing power and solve the issues related to power efficiency (Fig. 1), [2].

S. MC Neil, proposed the solutions for different threats regarding FPGA design security. There are many major issues related to design security. It plays a major role in terms of protecting intellectual property (IP), providing safety to the data, used in many applications such as military. There are solutions for protecting the data during transmission and also for storage, but less attention is paid to FPGA design in terms of security. Hashed message authentication code (HMAC) algorithm is introduced for the means of authentication.

Jorge Guajardo, Sandeep S. Kumar, Geert-Jan Schrijen and Pim Tnyls have proposed advanced set of rules in order to provide solution for patent safety problems on field-programmable gate array (FPGA).The properties of static random access memory-based (SRAM) physically unclonable function are examined while executing mathematical logic's trade off and inspected.

Y. Gao, D. C. Ranasinghe, S. F. Al-Aarawi, O. Kavehei, and D. Abbott have discussed about up-coming physically unclonable function (PUF) styles of designs with nanoelectronics. They have spotted out certain chances provided through micro-devices that can possibly utilized by the engineers. They have discussed important constraints of presently suggested PUF.

K. Jamal, Dr. P. Srihari the role of test vectors (TVs) with minimum power for built-in-self-test (BIST) applications. This method signifies test-per-clock-based (TPC) test vectors using multiple single input change (MSIC) [13, 18, 23].

J. Zhang, X. Tan, X. Wang, A. Yan, and Z. Qin have proposed translucent 2-factor authentication-based physically unclonable function (PUF) and identity verification (biometric). The 2nd authentication uses to verify the cell phone of the owner by means of PUF [6].

R. Pappu, B. Recht, J. Taylor, and N. Gershenfeld proposed a set of rules for authentication which depends upon huge space of address, i.e., the main attribute of physical one-way function. The physical one-way function is less expensive to manufacture, hard to clone, inherently, and is resistive toward tempering. These one-way functions are used mostly in cryptography because they are simple to solve and hard to transpose.

P. Bulens, F.-X. Standaert, and J.-J. Quisquater proposed inexpensive solution helps to organize connection by merging fuzzy extractors, digital signatures, and PUFs. The suggested set of rules supplies 2 stages of safety which can be utilized as per the clock time which is ready for checking the sign and the belief on the copy holder.

Jamal, K., Chari, K. M., and Srihari, P have proposed a new test pattern generation (TPG) with TPC technique (Test-per-clock) for BIST applications and also introduced test vector generation (TVG) that produces multiple-single-input-change (MSIC) vectors [9].

K. Lofstrom, W.R. Daasch, and D. Taylor have proposed integrated circuit identity (ICID) that brings out definite and reproducible mathematical analysis from the uncertainty which is built in during manufacturing process. There is no requirement of programming and additional steps and the process allows any modern methods of CMOS technology.

P. Tuyls, G.-J. Schrijen, B. Skoric, J. van Geloven, N. Verhaegh, and R. Wolters have proposed an implementation of proof-reader hardware which is immune toward incursive attacks. The production is primarily based totally on a hardware and a cryptographic component. The hardware comprises of a shielded coating which is random in nature.

E. Yin, G. Qu, and Q. Zhou have describe advanced framework to generate steady PUF confidentiality from ring oscillator (RO) PUF with advanced hardware performance. The task depends upon recently suggested group-based ring oscillator PUF with the subsequent novel ideas.

G. Hammouri, A. Dana, and B. Sunar initiated an advanced method to bring out fingerprints which are not identical in nature from that of same type of CDs. It shows many benefits of fabricating changeabilities which are seen in CD recessed area.

K. Jamal, P. Srihari, K. Manjunatha Chari, B. Sabitha proposed the task of test instances with minimum power for built-in-self-test (BIST) application. This approaches plan test per scan (TPS) depending on the tests by utilizing multiple single input change (MSIC) design [26].

J. Zhang, X. Tan, X. Wang, A. Yan, and Z. Qin, have proposed translucent 2-factor authentication-based physically unclonable function (PUF) and identity verification (biometric). The 2nd authentication uses to verify the cell phone of the owner by means of PUF [6].

3 Background and Related Works

This section gives some brief about background and previous design and implementations.

3.1 Conventional PUF Designs

The concept of physically unclonable function (PUF) was proposed by Pappu in the year 2002. Later, optical PUF and many other PUFs were also implemented. As per the different types of PUFs, they are mainly segregated into 3 types; they are analog PUF, digital PUF, non-electronic PUF [15–17].

For digital PUF, there is no need of A/D conversion; it straightly produces the digital signal. When we correlate with other types of PUFs, digital PUFs circuits stick to customized chip design, fabrication process and can be completely merged with chips. Thus, it has wide range of applications and used in research perspectives [19]. Digital PUF is again segregated into 2 types delay-based PUF and memory-based PUF.

Figure 2 represents a clear and simple structure of the memory-based PUF. Memory-based PUF is defined as a weak PUF. It simply represents the structure of SRAM PUF, where the inverters are connected back to back.

For suppose, when an input 0 is applied to SRAM PUF, it first passes through the first inverter and gives the output as 1. The output 1 is fed to the 2nd inverter as input, and it gives the output as 0. This means that the whole PUF system is stabilized. But, it is rarely used in field-programmable gate array. The reason behind this is that it instantiates the storage units when switched on.

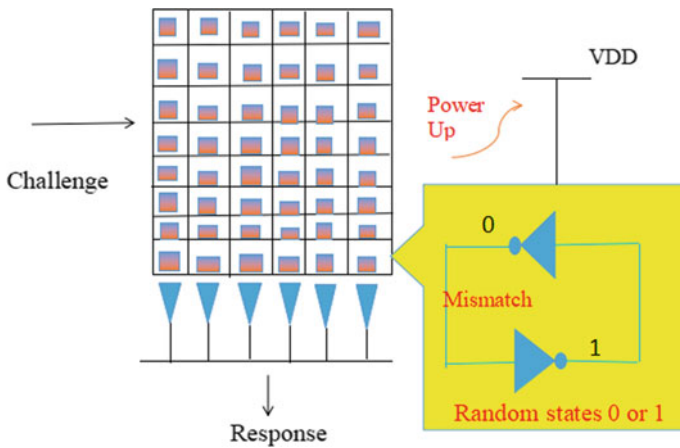


Fig. 2 Memory-based PUF

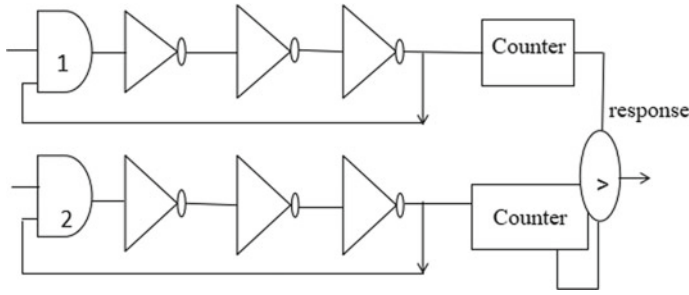


Fig. 3 Ring oscillator PUF

These both PUFs are represented as strong PUFs. The ring oscillator PUF is proposed by Devadas and Suh [20–22]. In delay-based PUFs, we have 2 types of PUFs, they are given as follows:

1. Ring oscillator PUF (RO PUF)
2. Arbiter PUF

Figure 3 represents the ring oscillator PUF. From Fig. 3, we can observe that it uses two AND gates, 6 inverters, and two counters.

When the inputs are primarily applied to the two AND gates, the second input for AND gates will be the previous feedback output of the 3 inverters. Then, the output of the AND gate passes through the 3 inverters and is fed to the counters.

The counters count the responses, i.e., highest count of 0's and 1's and gives the response of the highest count from both the set of inverters and AND gates.

Figure 4 represents the structure of arbiter PUF. It consists of 2 sets of multiplexers. Each set consists of 3 multiplexers and a D flip-flop at the end. As it is known that the functionality of D flip-flop that is when clock is high, the output represents the same at input D, and when clock is low, the output represents the previous value of input D.

Considered two input lines, one line representing 0 and other line represents 1. For example, in Fig. 4, the challenge is considered as 001, so the two input lines are switched by the multiplexers accordingly. When observed carefully, the two outputs which are coming out from the multiplexers are 1's. These 1's are first counted by the counters to evaluate that which output of the multiplexer is faster and has more number of counts to 1 and is fed to D flip-flop. The D flip-flop checks the value with its corresponding truth table and produces the output.

4 Proposed Method

The existed PUF structure is designed by taking a weak PUF and realizing it as a strong PUF [22, 24, 25]. As the strong PUF is occupying more space on the

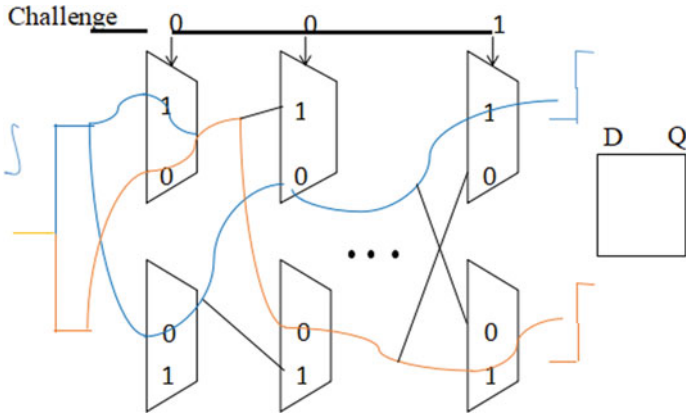


Fig. 4 Arbiter PUF

field-programmable gate array (FPGA), which is creating more hardware overhead, whereas considering the weak PUF which won't occupy much space on FPGA. The LFSR acts as a pseudorandom number generator at background, and the PUF is authenticating devices, i.e., providing security. The architecture defines the total structure of the PUF design that is, combining both the parts LFSR and strong PUF.

Figure 5 represents the architecture of LFSR-based strong PUF. The blocks present in the architecture are weak PUF, bit extractor, sequential bits obtained from array of PUF ($P_i(x)$) and LFSR. The weak PUF is realized as strong PUF, and its output is fed to the bit extractor.

The bit extractor is a 1 bit shift register; it extracts bits one by one from the weak PUF and fed to the array of PUF's. The values present in the array of PUF's are given

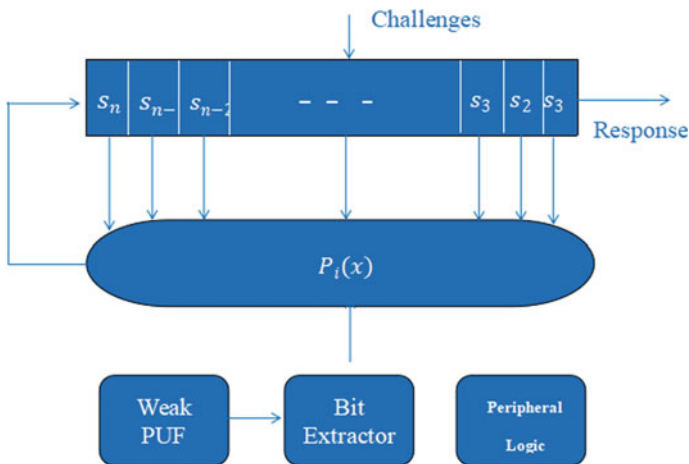


Fig. 5 Architecture of LFSR-based strong PUF

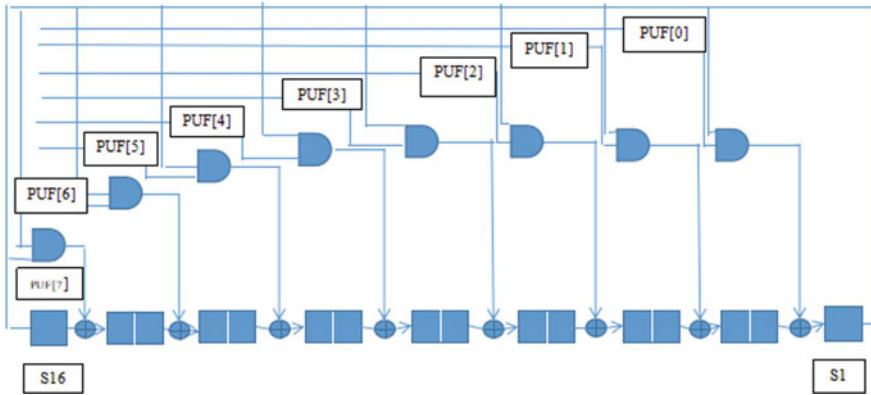


Fig. 6 Existing 16-bit LFSR-based PUF circuit

as inputs to the LFSR so that it produces the output response of random numbers as a sequence.

Existing Design:

Figure 6 represents the 16-bit PUF circuit. If correlated this structure with the architecture given in Fig. 5, from PUF [0] to PUF [7], it represents the array of PUF, i.e., $(P_i(x))$. Here, the array of PUF response bits are connected to LFSR through XOR gate by implementing AND logic. In the design, S1 to S16 represents the D flip-flops. Here, in order to reduce the hardware overhead, the design was implemented in such a way that two D flip-flops are connected as a pair.

Proposed Design:

Figure 7 represents the 32-bit PUF circuit. If correlated this structure with the architecture given in Fig. 5, from PUF [0] to PUF [7], it represents the array of PUF, i.e., $(P_i(x))$. Here, the array of PUF response bits are connected to LFSR through XOR gate by implementing AND logic. In the design, S1 to S32 represents the D flip-flops. Here, in order to increase the random bit response, the design was implemented in such a way that two D flip-flops are connected as a pair at both the ends, and set of four D flip-flops are connected in between both the ends.

5 Simulation Results

In this section, the simulation results of existing and proposed are explained with the help of RTL schematic and timing wave forms.

Figure 8 represents the RTL schematic of existing 16-bit PUF. It uses 8 XOR gates, 16 D flip-flops, bit extractor of 8 bit, where the outputs of each PUF are implemented with AND logic.

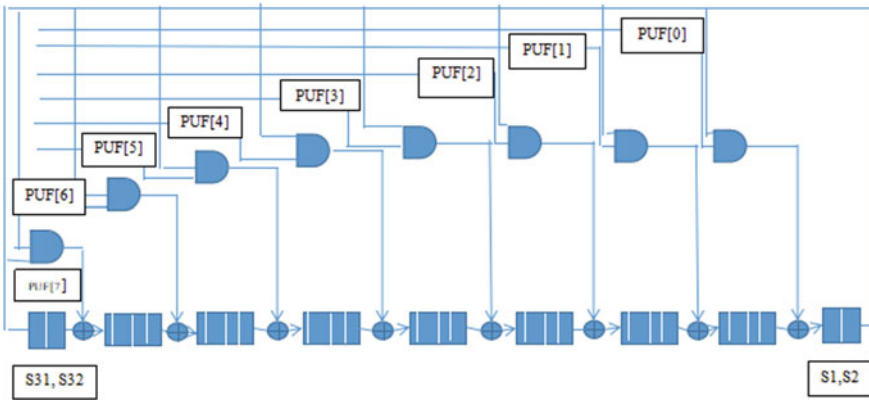


Fig. 7 Proposed 32-bit LFSR-based PUF circuit

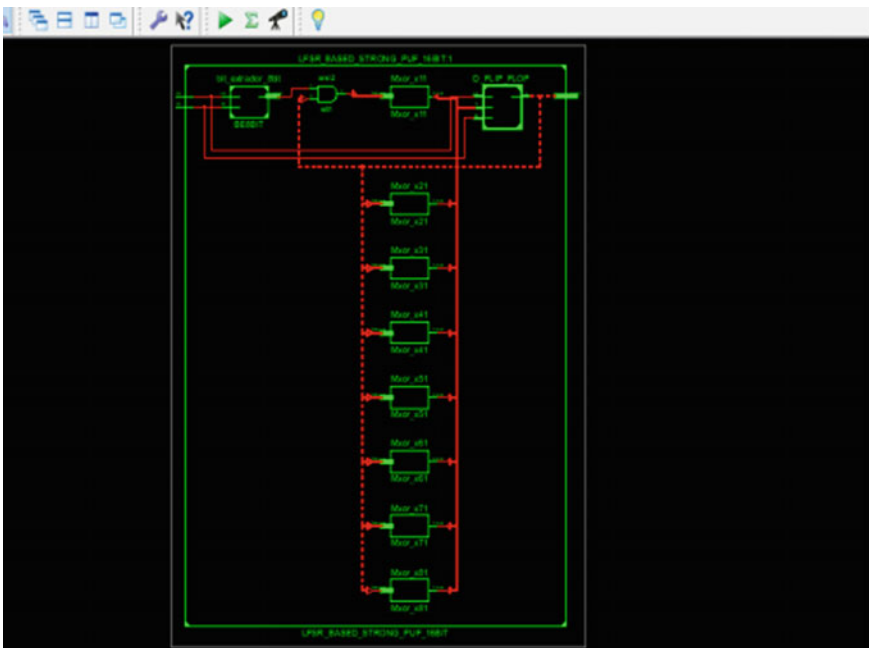


Fig. 8 RTL schematic of existing 16-bit PUF

Figure 9 represents the simulation results of 16-bit PUF. It shows that for every 50 nanoseconds of clock, the randomness in the output increases. For better understanding of simulation results, it is shown in Fig. 10.

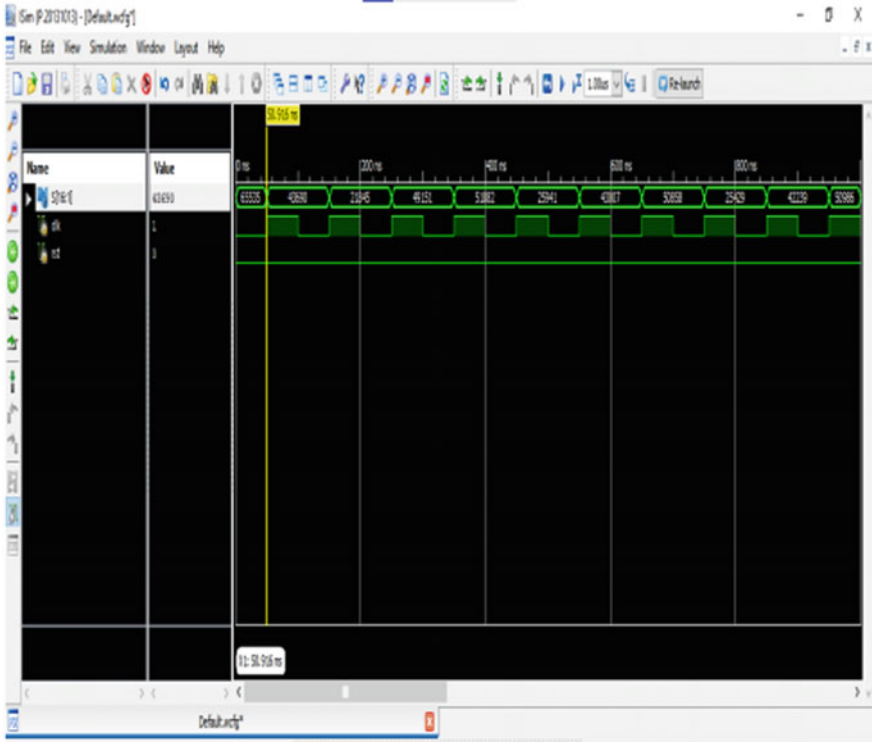


Fig. 9 Simulation results of existing 16-bit PUF

Fig. 10 Simulation waveform of existing 16-bit PUF

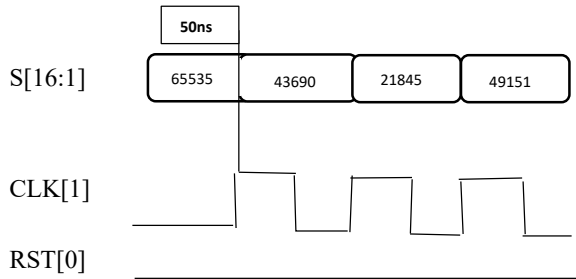


Figure 11 represents the RTL schematic of existing 32-bit PUF. It uses 8 XOR gates, 32 D flip-flops, bit extractor of 8 bit, where the outputs of each PUF are implemented with AND logic.

Figure 12 represents the simulation results of 32-bit PUF. It shows that for every 50 nanoseconds of clock, the randomness in the output increases when compared to 16-bit PUF. For better understanding of simulation results, it is shown in Fig. 13.

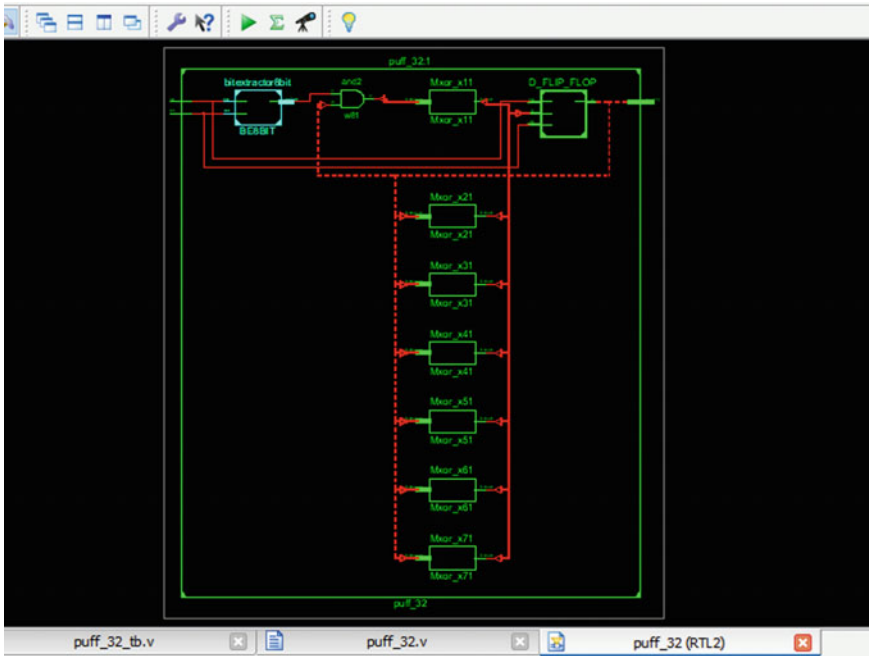


Fig. 11 RTL schematic of proposed 32-bit PUF

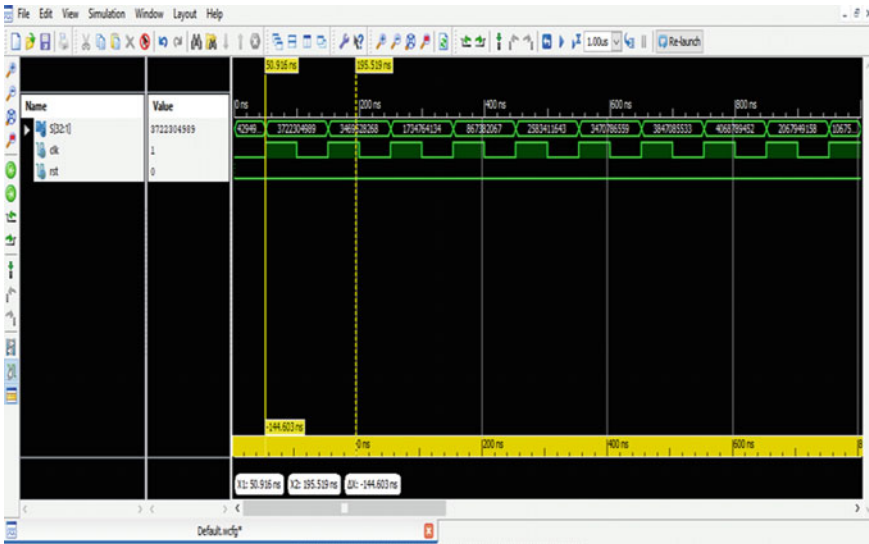


Fig. 12 Simulation results of proposed 32-bit PUF

Fig. 13 Simulation waveform of proposed 32-bit PUF

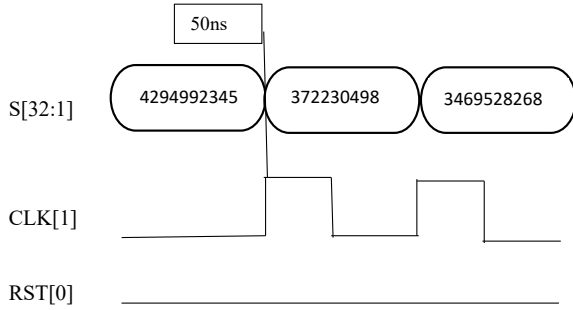


Table 1 Table of 16 and 32-bit PUF

Existing 16 bit PUF	Randomness for every (50 ns)		
S[16:1]	50 ns	100 ns	150 ns
Clk[1]	65535	43690	21845
Rst[0]			
Proposed 32 bit PUF	Randomness for every (50 ns)		
S[32:1]	50 ns	100 ns	150 ns
Clk[1]	4294992345	372230498	3469428268
Rst[0]			

6 Comparison Table

In this section, the comparison between 16 and 32 bit PUF is analyzed in accordance with random number of bits for a specific time period. The comparison table is shown Table 1.

Table 1 represents the comparison between 16 and 32-bit PUF. Here, as per observations, for every 50 ns, there is an increase in random numbers. The proposed 32 bit has produced more random number of bits than 16-bit PUF.

7 Conclusion

Therefore, the proposed 32-bit LFSR-based strong PUF produces more number of random bits in less period of time when compared to existing 16-bit LFSR-based strong PUF. The proposed LFSR-based strong PUF is implemented by Verilog code using the software tool XILINX ISE DESIGN SUITE 14.7 version.

References

1. Schmidt AG, Weisz G, French M (2017) Evaluating rapid application development with Python for heterogeneous processor-based FPGAs. In: Proceedings of IEEE 25th annual international symposium on field-programmable custom computing machines (FCCM), April 2017, pp 121–124
2. Putnam A (2014) Large-scale reconfigurable computing in a Microsoft data center. In: Proceedings of IEEE Hot Chips 26 symposium (HCS), Cupertino, CA, USA, August 2014, pp 1–38
3. McNeil S (2012) Solving today's design security concerns. Xilinx, San Jose, CA, USA, White Paper WP365 (v1.2), p 14
4. Tencent Cloud. Accessed: 8 March 2019. [Online]. Available <https://intl.cloud.tencent.com/>
5. Apple iPhone 7 Teardown. Accessed: 21 May 2019. [Online]. Available <https://www.techinsights.com/blog/apple-iphone-7-teardown>
6. Pappu R, Recht B, Taylor J, Gershenfeld N (2002) Physical one-way functions. *Science* 297(5589):2026–2030
7. Bulens P, Standaert F-X, Quisquater J-J (2010) How to strongly link data and its medium: the paper case. *IET Inf Secur* 4(3):125–136
8. Hou S, Guo Y, Li S (2019) A light weight LFSR-based strong physical unclonable function design on FPGA. Received 8 April 2019, accepted 29 April 2019, date of publication 16 May 2019, date of current version 31 May 2019. <https://doi.org/10.1109/ACCESS.2019.2917259>
9. Jamal K, Chari KM, Srihari P (2019) Test pattern generation using thermometer code counter in TPC technique for BIST implementation. *Microprocess Microsyst* 102890
10. Pavan Kumar OV, Kiran M (2013) Design of optimal fast adder. In: 2013 international conference on advanced computing and communication systems, pp 1–4. <https://doi.org/10.1109/ICACCS.2013.6938692>
11. Gao Y, Ranasinghe DC, Al-Sarawi SF, Kavehei O, Abbott D (2016) Emerging physical unclonable functions with nanotechnology. *IEEE Access* 4:61–80
12. Zhang J, Tan X, Wang X, Yan A, Qin Z (2018) T2FA: transparent twofactor authentication. *IEEE Access* 6:32677–32686
13. Jamal K, Srihari P, Kanakasri G (2016) Test vector generation using genetic algorithm for fault tolerant systems. *Int J Control Theor Appl (IJCTA)* 9(12):5591–5598
14. Hammouri G, Dana A, Sunar B (2009) CDs have fingerprints too. In: *Cryptographic hardware and embedded systems—CHES*. Springer, Berlin, Germany, pp 348–362
15. Lofstrom K, Daasch WR, Taylor D (2000) IC identification circuit using device mismatch. In: *IEEE International solid-state circuits conference (ISSCC) digest of technical papers*, San Francisco, CA, USA, February 2000, pp 372–373
16. Guajardo J et al (2009) Anti-counterfeiting, key distribution, and key storage in an ambient world via physical unclonable functions. *Inf Syst Frontiers* 11(1):19–41
17. Tuyls P, Schrijen G-J, Škorić B, van Geloven J, Verhaegh N, Wolters R (2006) Read-proof hardware from protective coatings. In: Goubin L, Matsui M (eds) *Cryptographic hardware and embedded systems*, vol 4249. Springer, Berlin, Germany, pp 369–383
18. Jamal K, Srihari P (2016) Low power TPC using BSLFSR. *Int J Eng Technol (IJET)* 8(2):759. e-ISSN 0975-4024
19. Yin C-E, Qu G, Zhou Q (2013) Design and implementation of a groupbased RO PUF. In: *Proceedings of design, automation and test in Europe conference and exhibition (DATE)*, Grenoble, France, pp 416–421
20. Suh GE, Devadas S (2007) Physical unclonable functions for device authentication and secret key generation. In: *Proceedings of 44th ACM/IEEE annual design automation conference*, June 2007, pp 9–14
21. Lim D, Lee JW, Gassend B, Suh GE, van Dijk M, Devadas S (2005) Extracting secret keys from integrated circuits. *IEEE Trans Very Large Scale Integr (VLSI) Syst* 13(10):1200–1205

22. Hori Y, Kang H, Katashita T, Satoh A, Kawamura S, Kobara K (2014) Evaluation of physical unclonable functions for 28-nm process fieldprogrammable gate arrays. *J Inf Process* 22(2):344–356
23. Jamal K, Srihari P (2015, January) Analysis of test sequence generators for built-in self-test implementation. In: 2015 international conference on advanced computing and communication systems. IEEE, pp 1–4
24. Bhargava M, Mai K (2014) An efficient reliable PUF-based cryptographic key generator in 65 nm CMOS. In: Proceedings of design, automation and test in Europe conference and exhibition (DATE), pp 1–6
25. Santiago L et al (2017) Realizing strong PUF from weak PUF via neural computing. In: Proceedings of IEEE international symposium on defect and fault tolerance in VLSI and nanotechnology systems (DFT), Cambridge, MA, USA, October 2017, pp 1–6
26. Jamal K, Srihari P, Manjunatha K, Chari, Sabitha B (2018) Low power test pattern generation using test-per-scan technique for BIST implementation. *ARPN J Eng Appl Sci* 13(8)

Empirical Evaluation of Local Model for Just in Time Defect Prediction



Kavya Goel, Sonam Gupta, and Lipika Goel

Abstract Just in time defect prediction abbreviated as JITDP refers to a software that helps to detect instantaneously whether any change made to that software leads to defect or not and that too in no time. It helps us to develop a defect-free software helping both developers and testers to reduce their efforts. We have built a local model for predicting defects just in time for improved performance. A local model makes clusters of the available training data based on their homogeneity, and then each cluster is trained individually, while global models refer to all those models which use all the available training data as a whole and are used to predict a test instance. In this study, we are focusing on (i) the implementation and (ii) execution performance of local models followed by (iii) the comparison of local and global models in three scenarios such as cross-validation, cross-project validation and time-based chronological scenario. Some of the observations made in this study from the comparison are as follows: Local model performs significantly low in classification. However, local models perform better in effort aware prediction in both cross-validation and cross-project validation scenarios. Also, local models have optimum performance when the value of k is set to 2 in k -medoids. Thus, for effort aware prediction in any software, using local models can be a good choice.

Keywords Defect prediction · Local model · Evaluation · Performance

1 Introduction

With the evolution of new technologies in this digital world, the demand of high-tech software is increasing with each passing day. And since the database is quite heavy and the data is growing at quick rate, it requires efficient software to deal in order to keep the data safe and secured. So in any case if the software comes

K. Goel (✉) · S. Gupta
Ajay Kumar Garg Engineering College, Ghaziabad, India
e-mail: Kavya2010004m@akgec.ac.in

L. Goel
Gokaraju Rangaraju Institute of Engineering and Technology, Hyderabad, India

out to be faulty, then the whole purpose fails with losses including time, resources and efforts. So we need to develop robust and failure-free software. Developing software requires not just one but a couple of developers which makes it difficult to rectify the mistake, and for testers, testing all the possible test cases is neither feasible nor economical. So researchers have come up with a solution named JITDP which would alert the developer immediately when some defect inducing change is made to the code and also alerts them with the amount of risk associated with them. This helps the developers to rectify the mistake as it is fresh in their minds. The idea of JITDP was induced in the 90 s but came into use from the last decade. Some multinational companies like Blackberry and Cisco started using the concept of JITDP in years 2012 and 2015, respectively. Many models have been proposed with varying methodologies like ML, DL, neural networks and fusion models, and all these models are referred to as global models. But in this study, we will be focusing on the local models. We will be discussing the benefits and shortcomings of local model and in which scenarios would it be efficient enough to choose local models over global ones. The performance of local models will be evaluated in three possible scenarios which are x fold cross-validation scenario, cross-project validation scenario, and time-based chronological scenario. Some of the advantages of JITDP also referred to as change level prediction include fine granularity at change level because the induced impact of the change made only affects a smaller region of the source code and each change has an assigned author who can easily perform the inspection as the design decisions are still present in their minds. JITDP is performed every time a change is submitted, and this is how it fulfills its objective of continuous activity of quality control. Since every model has its limitations, this model too has some like in order to train a model for making predictions, we need a huge amount of data, but it is not guaranteed that we will definitely be having some historical data for that project and that too in their initial phases itself. Cross-project defect prediction models are developed as a solution to this problem. Cross-project defect prediction model is trained from the available dataset from the previously made projects or models. But another problem which arises with cross-project model is that it is not necessary that we are able to get the historical data for every possible project, for some there might be a possibility that we get ample amount of data, but for some projects, there would not be sufficient training data. We will also try to answer to the following research question in our study.

RQ1: Which model has better classification and effort aware prediction in all the three scenarios?

Paper Organization: The rest of the paper is structured as follows. Section 2 presents the research gaps in this field of study. Section 3 consists of background and related work. The following section describes the study setup, and Sect. 5 includes the results and discussion. The next section, i.e., Section 6, presents the conclusion and future scope.

2 Research Gaps

The major drawback is the availability of proper datasets in this field of study which has been faced by many researchers. Also JIT models require huge amount of data for prediction, and it is not necessary that we have appropriate models for every requirement in order to provide the historical data. So the size of data also matters while evaluation, i.e., if we have small dataset, then the local model will make small clusters which will degrade the performance of the model.

3 Background and Related Work

Many researchers proposed their models like CC2Vec, DeepJIT, JITLine, fusion models, applied random forest algorithm and many other machine learning algorithms for predicting the defects in software to showcase their accuracy and prediction performance for defect inducing changes made to the source code. Basically, the procedure of JITDP consists of the following steps. First of all, it is important to note that to train a model for prediction, it requires huge amount of historical data as discussed above and from which program modules are extracted from them based on their granularity and the requirements of the user. Then software metrics are designed to examine the modules based on the code and software development life cycle. Then defect prediction models are made by using various algorithms like LR, SVM, Naïve Bayes, etc., and defect datasets. Later, these models are evaluated on the basis of their F1-score, precision and other performance indicators. This same metrics is used to detect in the new modules whether the change is defect inducing or not. In this study, we will be evaluating local and global models.

This paper is in continuation to our previous paper which presented the comparison of all the above-mentioned projects, and it was observed that the highest accuracy is observed in case of random forest. TLEL, i.e., two-layered ensemble learning, was also proposed by Yang et al. [1] which involves ensemble learning and decision trees. Researchers claim that it may improve the efficiency of performance indicators as compared to the other models. Earlier the researchers worked on coarse granularity like files, packages, etc., but today in the modern world, the researchers have started working on the fine granularity modules. Coarse granularity prediction technique does have their own advantages, but because of the following reasons, it is advantageous to opt for fine granularity modules. First, it becomes very tedious for developers to inspect huge lines of code in order to find the defect. Also it is easy to locate bugs for the developers when the code is fresh in their minds, but since the code is written by several experts and the prediction of defects is performed in the later stages of the program, it becomes difficult even for the experts to detect them. The fine-grained JITDP focuses on code changes instead of modules, files or packages. Some benefits of this approach are as follows:

- (i) The main advantage is it reduces the human effort of inspecting the code.
- (ii) Since the above-mentioned approach is done at change level, so as soon the code is modified by the developer, it instantly indicates whether the change is defect inducing or not.
- (iii) So it is time efficient.

4 Study Setup

The datasets which we have used for the implementation of our model are the same as that shared by Kamei et al. [3]. The dataset is obtained from six open sources which are, namely Bugzilla which acts as a system for detecting defects, Eclipse JDT is a JDE plugin, Postgres SQL is used as the database, Mozilla web browser, Columbus and PLA. The study setup or we can say the implementation of this model is performed on an Intel Core i5 8th generation hardware with Windows 10 as the operating system and Python as the programming language. This section consists of the workflow of the local model, modeling methods, data analyzing methods and performance indicators which are considered in our study.

4.1 Workflow of Local Models

Figure 1 describes the working of local models. Firstly, the model is a train test split model with 0.2 which means the data is divided into two parts: testing data and training data with 20% and 80%, respectively. The second step in our model is to divide the training data into homogenous regions known as clusters. This clustering of data is done with the help of k-medoids (PAM) algorithm. Each test instance is allocated a cluster ID based on their cluster models. The next step is building a classifier for each and every cluster present in the model. We have used logistic regression for building the classifier. Afterward, the test instance from testing data is predicted from the classifier. The objective of classifier is to calculate the value of defect proneness. Then after setting the threshold value, we can predict whether the particular change made is buggy or not. So this is how we are able to predict the behavior of changes made to the software instantaneously.

4.2 Modeling Methods

Modeling is basically the process of training the model to predict the useful or desirable labels from the extracted features using machine learning algorithms. So the output of modeling is a trained model which can make predictions for new inferences. In our study, we are considering three modeling methods. First to cluster

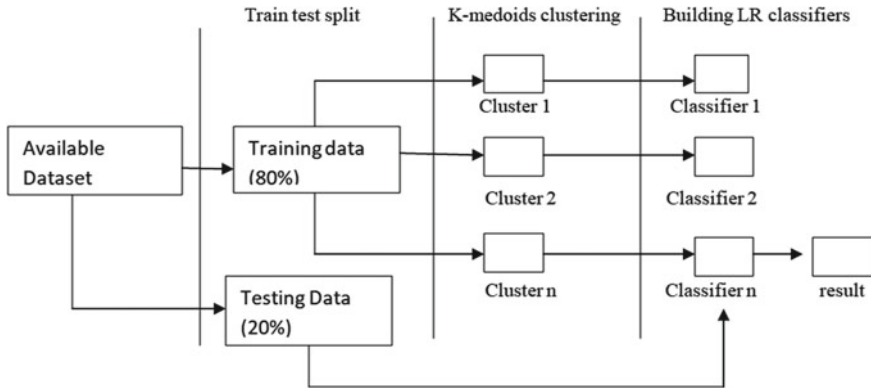


Fig. 1 Workflow in local model

Fig. 2 Formula for k-medoids

$$E = \sum_{j=1}^k \sum_{p \in C_i} |p - O_i|^2.$$

the dataset, we are using k-medoids. Next we are using LR and EALR methods for the purpose of classification and effort aware prediction of the model.

4.2.1 k-medoids

K-medoids also known as the Partitioning Around Medoid (PAM) serve the most crucial and basic functionality of the local models which is dividing the data into homogenous clusters. So the task of clustering into homogenous regions is performed with the help of k-medoids. It is an unsupervised clustering algorithm that clusters the objects of the unlabelled data, and it takes medoid/datacenters/exemplars as the reference point instead of the centroid. PAM reduces the sum of dissimilarities between the points in the clusters and the center of the cluster. This algorithm is not only fast but also is less sensitive to outliers as compared to other portioning algorithms. It also converges in a fixed number of steps. The formula for k-medoids is defined in Fig. 2.

Here p indicates a sample of the cluster which is denoted by C_i . O_i represents medoid in that particular cluster.

4.2.2 Logistic Regression

It is used when we model the probability of a discrete variable or we can say when categorical prediction is to be done. The LR equation helps us to find the relationship of the dependent variable with that of independent variables so that we can be able to

Fig. 3 Formula (1) for LR

$$y(c) = \frac{1}{1 + e^{-(w_0 + w_1 m_1 + \dots + w_n m_n)}}$$

Fig. 4 Formula (2) for LR

$$Y(c) = \begin{cases} 1, & \text{if } y(c) > 0.5, \\ 0, & \text{if } y(c) \leq 0.5. \end{cases}$$

analyze the likelihood of the choice made by the model. For example in our model, a change made to the source code can either be buggy or not. So it can only be either one of them. But the output $y(c)$ coming in our model is a continuous value which ranges between 0 and 1. So in order to determine whether the change is buggy or not, we have taken the threshold value $Y(c)$ as 0.5 in our case. The formula for logistic regression algorithm is denoted by Figs. 3 and 4.

Here in Fig. 3, w represents the coefficient of LR and m depicts the independent variables. The output is denoted by $y(c)$. So $Y(c)$ in Fig. 4 expresses the defect proneness of the change. So if the value of $y(c)$ is more than 0.5, then the change made is known as defect inducing, else for value equals to 0.5 or less than 0.5 will be considered as non-defect inducing change.

4.2.3 EALR

EALR is an abbreviation for effort aware linear regression. Researchers suggest that it is necessary to focus on the cost-effectiveness of the code inspection as well. Cost reduction is a crucial factor in the making of any model. The benefit cost ratio is calculated as depicted in Fig. 5.

4.3 Scenarios for Analyzing Data

In this paper, we are considering three scenarios for data analyzing which are, namely cross-project validation, time-based chronological validation and 10×10 fold cross-validation. We will be discussing them in brief which are as follows.

Fig. 5 Formula for BCR

$$BCR(c) = \frac{P(c)}{Effort(c)}$$

4.3.1 Cross Project Validation

This scenario has gained much popularity from several years. In this approach, we use the historical data of several other projects and use that data to train our model to predict the defects. However, it requires huge dataset, and it is not necessary to have similar models to train the new required model. For evaluating the performance of cross-project model, each within-project model is tested with the help of other projects. We use all the data of each project to build the within-project model. We can calculate the number of test results with the help of the number of projects we are using with the help of the following formula, i.e., $x \times (x - 1)$, where x represents the number of projects. So, in our study, we are using open-source projects so the number of test results come out to be $6 \times 5 = 30$.

4.3.2 10 × 10 fold Cross-Validation

Unlike cross-project validation scenario, in this case cross-validation is performed within the same project. Here we refer to it as 10 × 10 fold cross-validation. For this scenario, we firstly divide the dataset into equal parts with equal size of the data. Then in each iteration, we train nine parts of the available data for the training purpose, and the remaining part is used for testing process. In each iteration the testing dataset as well as the training dataset are treated equally for analyzing data. This process helps to reduce the random deviation of results. We have divided the data into ten equal parts and then iteratively change the testing dataset that is why it is referred to as 10 × 10 fold cross-validation scenario. So it yields 10 × 10 results, i.e., 100 results.

4.3.3 Time-Based Chronological Validation

Like cross-validation scenario, this scenario also deals within the same project rather than using the historical data of several other projects. But what it makes different from cross-validation is that it maintains a chronological or successive order of changes made in the data. For the prediction of defects present later in the code. We use the early committed changes in the datasets. In this scenario, all the changes of the same month come under the same group. The formula for calculating the number of results is $x - 5$, where x refers to the number of projects.

4.4 Performance Indicators

Performance indicators are those parameters which are used to equate or indicate the execution of the model built. We are considering F1-score, accuracy, AUC and Popt. For classification process, F1-score and AUC are evaluated, and for effort aware prediction, accuracy and Popt are evaluated.

4.4.1 F1-Score

Precision and recall are two performance indicators which usually have contradictory results. So F1-score is used to have the combined result of precision and recall. It is the harmonic mean of the precision and recall. The formula for F1-score is twice the product of precision and recall divided by their sum.

4.4.2 Accuracy

Accuracy refers to the ratio of correctly predicted outcomes to total predictions. The best accuracy, i.e., 1, means no error, whereas the worst is 0. Another way to calculate accuracy is $1 - \text{ERR}$.

4.4.3 AUC

It is used to evaluate the classification performance and is represented by the area under the ROC curve. AUC is used to convert the curve into a number for its binary classification. The value ranges between 0 and 1. Higher the value of AUC means higher the performance of the model.

4.4.4 Popt

Popt is calculated with the help of three curves of the ROC curve which are optimal, prediction, and worst model curve.

5 Result and Discussion

In this section, we have the results of our implemented model for all the three scenarios discussed above and will answer RQ 1. Table 1 shows the evaluation and comparison of both the models in cross-validation scenario. We tested our model on nine different values of k which is the number of clusters. The value of k ranges between 2 and 10. After analyzing the results, we observed that local models have optimum AUC at $k = 2$. So in Table 1, we have compared the best obtained values of both local and global models.

From Table 1, we can observe that global models have better scores in F1-score and AUC, while local models at $k = 2$ have better ACC and Popt values. Table 2 shows the comparison between both the models in cross-project validation scenario.

From Table 2, we can observe that global models have better scores in F1-score and AUC, while local models at $k = 2$ have better ACC and Popt values. Table 3 shows the comparison between both the models in time-based chronological cross-scenario.

Table 1 Evaluation in cross-validation approach

Parameter	Dataset	Local model	Global model
AUC	BUGZILLA	0.70	0.73
	COLUMBUS	0.72	0.74
	JDT	0.72	0.73
	MOZILLA	0.54	0.77
	PLA	0.73	0.74
	Postgres SQL	0.76	0.78
F1	BUGZILLA	0.64	0.66
	COLUMBUS	0.67	0.70
	JDT	0.71	0.72
	MOZILLA	0.37	0.83
	PLA	0.68	0.70
	Postgres SQL	0.70	0.76
ACC	BUGZILLA	0.45	0.42
	COLUMBUS	0.46	0.55
	JDT	0.53	0.35
	MOZILLA	0.39	0.19
	PLA	0.47	0.37
	Postgres SQL	0.49	0.34
Popt	BUGZILLA	0.75	0.74
	COLUMBUS	0.66	0.73
	JDT	0.78	0.66
	MOZILLA	0.68	0.55
	PLA	0.72	0.66
	Postgres SQL	0.73	0.77

Table 2 Evaluation in cross-project scenario

Parameter	Local model	Global model
AUC	0.68	0.71
F1-score	0.63	0.68
ACC	0.49	0.31
Popt	0.76	0.66

RQ 1: Which model has better classification and effort aware prediction in all the three scenarios?

Cross-validation: We observe that cross-validation scenario has low F1 and AUC which proves that global model outperforms the local models. So the local models have low classification performance. But ACC and Popt are greater in local models, so we can conclude that they have better effort aware prediction.

Table 3 Evaluation in time-based chronological scenario

Parameter	Dataset	Local model	Global model
AUC	BUGZILLA	0.66	0.79
	COLUMBUS	0.76	0.78
	JDT	0.71	0.74
	MOZILLA	0.76	0.77
	PLA	0.71	0.75
	Postgres SQL	0.79	0.81
F1	BUGZILLA	0.63	0.68
	COLUMBUS	0.71	0.71
	JDT	0.78	0.76
	MOZILLA	0.88	0.85
	PLA	0.77	0.75
	Postgres SQL	0.77	0.77
ACC	BUGZILLA	0.45	0.56
	COLUMBUS	0.50	0.58
	JDT	0.50	0.49
	MOZILLA	0.36	0.34
	PLA	0.56	0.53
	Postgres SQL	0.50	0.49
Popt	BUGZILLA	0.63	0.81
	COLUMBUS	0.75	0.81
	Eclipse JDT	0.76	0.66
	MOZILLA	0.65	0.64
	PLA	0.79	0.74
	Postgres SQL	0.74	0.74

Cross-project validation scenario: We observe that cross-validation scenario has low F1 and AUC which proves that global model outperforms the local models in classification performance. But ACC and Popt are greater in local models, so we can conclude that they have better effort aware prediction.

Timewise cross-validation scenario: We observe that cross-validation scenario has low F1, AUC, ACC and Popt which proves that global model outperforms the local models in both classification and in EALR.

The comparison of local and global models can be easily understood with the help of Table 4 in all the three scenarios.

Table 4 Evaluation of models in three scenarios

Evaluation	Cross-validation	Cross-project validation	Timewise cross-validation
Classification	Global > Local	Global > Local	Global > Local
EALR	Local > Global	Local > Global	Global > Local

6 Conclusion and Future Work

This paper aims at comparing the performance of local and global model for JITDP under three scenarios. For this, we have built a local model using k-medoids, LR and EALR so that we can compare the classification and effort aware prediction performance of both the models. So on comparing, we conclude that local model performs significantly low in classification when compared to global model. However, local models perform better than global model in effort aware prediction in both cross-validation and cross-project validation scenarios. We also analyzed on how varying the number of clusters can affect the performance of the model. The optimum performance is noted when the value of k is set to 2.

In future scope, we would suggest that the performance of both the models in predicting the defects is highly affected by the modeling methods that are chosen by the researchers. We would also like to add some more baselines to these models to verify the results and conclusions in a generalized manner. Also in future, we can evaluate the result of our proposed methodology on closed source real-time software projects as well.

References

1. Yang X, Lo D, Xia X, Sun J (2017) TLEL: a two-layer ensemble learning approach for just-in-time defect prediction. *Inform Softw Technol* 87:206–220
2. Yan M, Fang Y, Lo D, Xia X, Zhang X (2017) File-level defect prediction: unsupervised vs. supervised models, pp 344–353. <https://doi.org/10.1109/ESEM.2017.48>
3. Kamei Y, Fukushima T, McIntosh S, Yamashita K, Ubayashi N, Hassan AE (2016) Studying just-in-time defect prediction using cross-project models. *Empir Softw Eng* 21:2072–2106. <https://doi.org/10.1007/s10664-015-9400-x>
4. Xu Z, Liu J, Luo X, Yang Z, Zhang Y, Yuan P, Tang Y, Zhang T (2019) Software defect prediction based on kernel PCA and weighted extreme learning machine. *Inf Softw Technol* 106:182–200
5. Mockus A, Weiss DM (2000) Predicting risk of software changes. *Bell Labs Tech. J.* 5:169–180
6. Kamei Y, Shihab E, Adams B, Hassan AE, Mockus A, Sinha A, Ubayashi N (2012) A large-scale empirical study of just-in-time quality assurance. *IEEE Trans Softw Eng* 39:757–773
7. Hata H, Mizuno O, Kikuno (2012) Bug prediction based on fine-grained module histories. In: *Proceedings of the 34th international conference on software engineering, Zurich, Switzerland, 2–9 June 2012*, pp 200–210
8. Liu C, Yang D, Xia X, Yan M, Zhang X (2018) Cross-project change-proneness prediction. In: *Proceedings of the 2018 IEEE 42nd annual computer software and applications conference (COMPSAC), Tokyo, Japan, 23–27 July 2018, vol 1*, pp 64–73

9. Yu T, Wen W, Han X, Hayes J (2018) Conpredictor: concurrency defect prediction in real-world applications. *IEEE Trans Softw Eng* 45:558–575
10. Tian Y, Li N, Tian J, Zheng W (2020) How well just-in-time defect prediction techniques enhance software reliability? In: *Proceedings of the IEEE international conference on software quality, reliability and security (QRS)*
11. Albahli S (2019) A deep ensemble learning method for effort-aware just-in-time defect prediction
12. Kim S, Whitehead EJ, Zhang Y (2008) Classifying software changes: clean or buggy? *IEEE Trans Softw Eng* 34(2):181–196
13. Yang X, Lo D, Xia X, Zhang Y, Sun J (2015) Deep learning for just-in-time defect prediction. In: *Proceedings of the IEEE international conference on software quality, reliability and security (QRS)*, pp 17–26, Vancouver, BC, Canada, August 2015
14. Madhuri R, Ramakrishna Murty M, Murthy JVR, Prasad Reddy PVGD et al (2014) Cluster analysis on different data sets using K-modes and K-prototype algorithms. In: *International conference and published the proceeding in AISC and computing*, Springer, vol 249, pp 137–144
15. Praneel ASV, Srinivasa Rao T, Ramakrishna Murty M (2019) A survey on accelerating the classifier training using various boosting schemes within cascades of boosted ensembles. In: *International conference with Springer SIST series*, vol 169, pp 809–825

Secured Messaging Using Image and Video Steganography



Trupthi Mandhula, Blessy Kotrika, and Aditi Rayaprolu

Abstract Protection and security of data is an increasing concern among individuals and organizations. Secure data transmission has a vital application in today's world. Security has become a priority for every user who uses the Internet. Sensitive data transmission is always a risky task. In-order to address this concern, image and video steganography is quite useful in hiding the secret data inside of an image or a video which makes it harder for the outside world to notice the transmission. Steganography focuses more on high security and capacity. Steganography masks the sensitive data inside any cover media like images, videos, etc. The hidden information will not be perceived by the human eye as the cover looks the same as the encoded one. Thus, only the target user will be able to read the message hidden. This application proposes a secure way for transmitting messages using algorithms like least significant bits, K-least significant bits and key-frame selection for image and video steganography.

Keywords Image steganography · Video steganography · Stego object · Cover object · Least significant bit algorithm (LSB) · K-least significant bits algorithm (K-LSB) · Key-frame selection algorithm

1 Introduction

Steganography is a technique of hiding or embedding the secret message inside a cover object to hide the data transmission process. The intruder cannot notice any data being transmitted as the data is in the hidden form inside the cover object (Fig. 1).

T. Mandhula (✉) · B. Kotrika · A. Rayaprolu
Department of Information Technology, Chaitanya Bharathi Institute of Technology (CBIT-A),
Gandipet, Hyderabad, Telangana State 500075, India
e-mail: trupthijan@gmail.com

B. Kotrika
e-mail: blessykotrika@gmail.com

A. Rayaprolu
e-mail: aditirayaprolu5@gmail.com

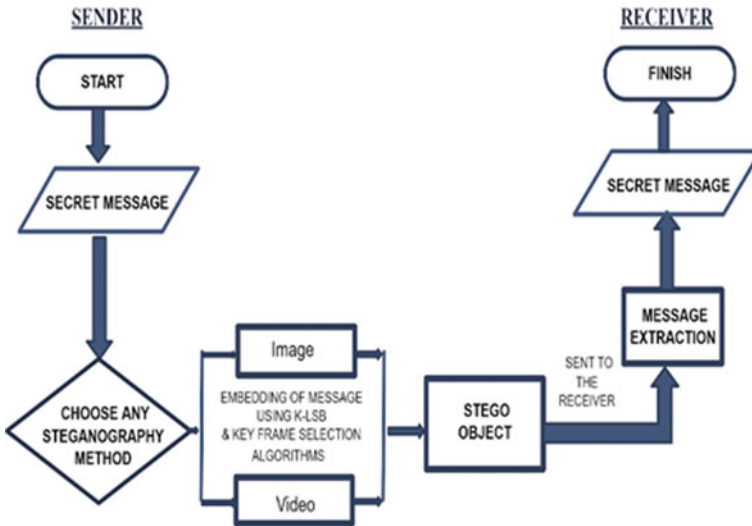


Fig. 1 Message transmission using steganography

2 Related Works

Emad et al. [1], “A secure image steganography algorithm based on least significant bit and integer wavelet transform,” in *Journal of Systems Engineering and Electronics*, June 2018. The algorithms being used are least significant bit algorithm (LSB) and integer wavelet transform algorithm. The drawback is that LSB algorithm which is used here is less secure when compared to K-least significant bits algorithm (K-LSB) as it is easy for the intruder to check and decode the hidden message inside the least significant bits of the image pixels stream of the cover image.

Kiruba and Sharmila [2] “Hiding Data in Videos Using Optimal Selection of Key-Frames,” 2018 International Conference on Computer, Communication, and Signal Processing (ICCCSP), Chennai, 2018. They mainly focused on Video steganography. The techniques used in this are optimal key selection algorithm and least significant bit (LSB) algorithm for the embedding of secret data. Video is a continuous set of frames which are displayed at a faster rate. The data or the secret information is stored in one of the frames of the video in this technique. Video steganography is comparatively secure because the existence of secret data in the video is not visible to the intruders since it is available only for a few seconds of time during the display of the video. The main drawback is that the algorithm used here is LSB algorithm which is less secure when compared to K-LSB algorithm.

3 Methodology

3.1 Image Steganography

Message transmission using steganography generally has two phases. One to embed the secret and another to extract it.

- (a) **Embedding phase:** This process happens at the sender's side. It mainly focuses on hiding the secret message inside the cover object. In image steganography, the cover object is an image and the embedding algorithm K-LSB is used to embed the secret text into the cover object. The binary representation of the secret text to be hidden is taken and replaced with the least significant bits of pixels of the cover image. This results in Stego image. In this way, Stego images contain the hidden secret message inside the pixels.
- (b) **Extracting phase:** This happens at the receiver's side. Only the intended receiver will be able to recognize or identify that there is secret message hidden or embedded inside the cover object which is sent by the sender to the receiver. It performs a reverse operation to extract the message from the cover without any loss of information (Fig. 2).

3.2 Video Steganography

When the human eye looks at something, the perception of an object exists for a little more time (in milliseconds) even after the object is removed. This principle is called "Persistence of Vision". Videos work on the same principle. When a group of images are shown at a faster rate in front of human eyes, the brain perceives it to be in motion. The process of video steganography is complex when compared to image steganography.

In-order to perform video steganography, the video must be processed first by extracting the individual images after splitting the video. The secret message is hidden in one or more of these images. So, in-order to enclose the data inside these frames, the algorithm selects a few frames known as key images based on the key-frame selection algorithm. The data is present in only these key-frames. In-order to identify the key images, the dissimilarity, or the variation between two successive



Fig. 2 **a** Encryption of data inside an image and **b** extraction of message from Stego image

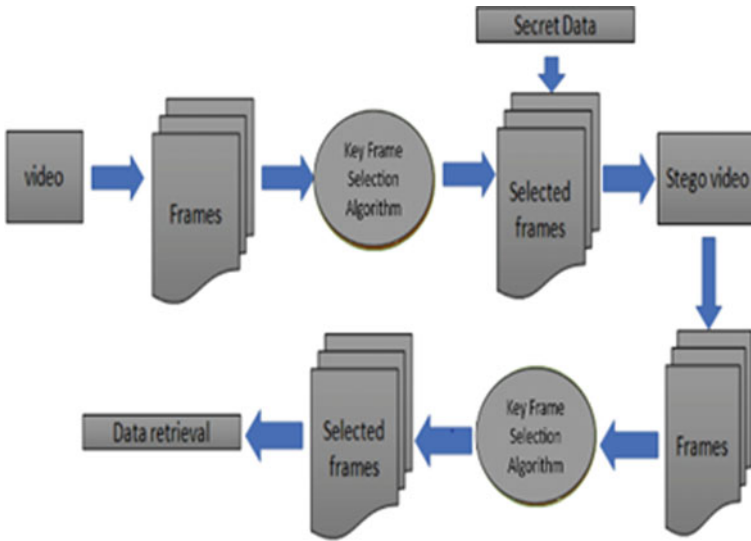


Fig. 3 Message transmission using video steganography

images is calculated. The variation between any two successive frames is denoted by a value. If that value is greater than a threshold, then it is considered as a key-frame. Video steganography also has an embedding and extracting phase (Fig. 3).

4 Implementation

4.1 Algorithms

The important algorithms being used in this model are as follows:

- Least significant bit algorithm
- K-least significant bits algorithm
- Key-frame selection algorithm

Least Significant Bit Algorithm (LSB)

The least significant bit algorithm is very famous in steganography for hiding or embedding the secret message inside the cover object. It works by substituting the least significant bits of the pixels of the cover image by the binary bit representation of the secret text to be hidden inside this cover image. This algorithm is a comparatively less secure for secret data transmission. The Stego image looks like the cover image as the changes in the LSBs of image pixels do not introduce too much difference between the two images.

K-Least Significant Bit Algorithm (K-LSB)

The K-LSB embedding algorithm is an advancement of the LSB algorithm to increase security. It works by replacing or substituting the k-least significant bits of the pixels of the cover image by the binary bit stream of the secret message to be hidden. For addressing the security concern, it becomes better when compared to the LSB Algorithm. The Stego image formed by using this algorithm is almost similar to the cover image as the changes are made to the least significant bits. But the Stego image formed using LSB is more similar than that of K-LSB algorithm.

K-LSB Algorithm Steps:

Input: Cover image and secret data/message to be embedded

Output: Stego image will be generated

Process:

- The input image is used as an envelope to conceal the secret input message.
- The secret message is transformed into its binary form of representation.
- The image is represented in binary matrix format of the pixels.
- The binary 0 and 1 s of the secret data is embedded inside the 0 and 1 s of the image representation.
- An XOR operation is done between the binary bit of message and binary bit of cover.
- The value of the above operation is added to the image pixel.
- Thus, the image pixel is altered.

Key-Frame Selection Algorithm

A video is a group of images which are played successively in order at a rapid pace. The secret data which is input by the user is put inside a few of these images. So, in-order to embed the data in these frames, it is required to perform selection of a few images known as key-frames to put the data inside. By using the key-frame selection algorithm, few images are chosen to embed the data. For the detection of key-frames, the difference between two consecutive images is calculated. This difference value or dissimilarity value that is calculated is denoted by a value. If this value is greater than that of a previously set threshold value, then it is considered as a key-frame.

Key-Frame Selection Algorithm Steps:

Input: Cover Video, secret data/message to be embedded

Output: Stego Video will be generated

Process:

- The input video is used to envelop the secret data which is input by the user.
- The video is split into individual images.
- The dissimilarity value between the successive images is calculated.
- If this value is greater than a prior set threshold value, then that frame is selected as key-frame.

- Else the image is skipped.
- Once all the key-frames are selected, the secret data is embedded inside it using LSB/K-LSB algorithm.

4.2 Evaluation Metrics

Peak Signal to Noise Ratio (PSNR)

PSNR is a similar metric as Signal to Noise Ratio (SNR). The Peak Signal to Noise Ratio is the ratio between the maximum possible quality of an image, and the power of noise that affects the quality of the image representation. Hence, PSNR is calculated by comparing the Stego image to the original cover image. Peak error is represented by PSNR. High PSNR is required for a high quality.

$$\text{PSNR} = 10 \log\left(\frac{(L-1)^2}{\text{MSE}}\right) = 20 \log\left(\frac{L-1}{\text{RMSE}}\right) \quad (1)$$

Equation for calculating the Peak Signal to Noise Ratio (PSNR)

'L' represents the number of maximum possible quality level in an image where minimum value is zero and 'RMSE' represents root of mean squared error.

Mean Squared Error (MSE)

The MSE and the PSNR are metrics used for evaluating the power of an image. The MSE is the average of the sums of the squared errors between the Stego image and the original cover. To ensure low error, it's essential to have a low MSE.

$$\text{MSE} = \frac{1}{mn} \sum_{i=0}^{m-1} \cdot \sum_{j=0}^{n-1} \cdot (O(i, j) - D(i, j))^2 \quad (2)$$

Equation for calculating the Mean Squared Error (MSE)

O—indicates the matrix data of original image

D—indicates the matrix data of degraded image

m—indicates the numbers of rows of pixels

i—indicates the index of that row of the image

n—indicates the number of columns of pixels

j—indicates the index of that column of the image.



Fig. 6 PSNR and MSE values in LSB Algorithm



Fig. 7 PSNR and MSE values in MSB algorithm

5.2 *LSB Versus MSB Manipulation*

In Fig. 6, the obtained PSNR is 80.29 dB. The PSNR is considered high when the value obtained is 60 dB or higher. The value of MSE obtained is very less which lies in the acceptable range.

In Fig. 7, the obtained PSNR is 57.53 dB which is lower than 60 dB. By comparing this with the above, it is observed that when the MSBs of image pixels are altered, we find significant differences that are noticeable by the human eye in the Stego image when compared to the original image. Moreover, the value of PSNR obtained is below the acceptable range. Hence, LSB is preferred over MSB.

5.3 *Video Steganography Results*

See Fig. 8.

6 Conclusion

Steganographic techniques such as image steganography and video steganography together were not supported in the existing model. Most of the models which were proposed earlier were based on implementation of a single steganographic technique. Hence, this model aims to integrate both image and video steganographic techniques.

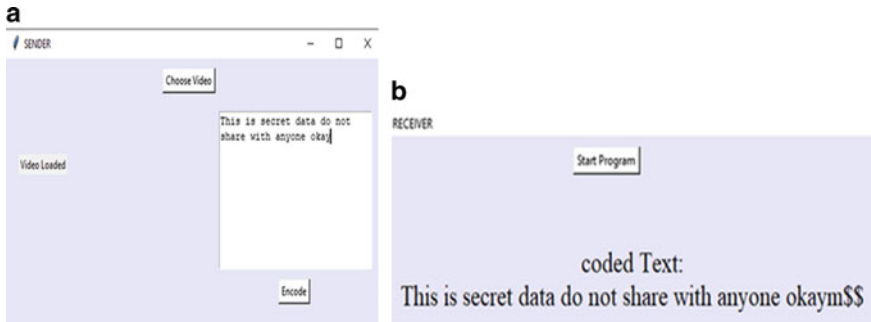


Fig. 8 **a** Embedding of secret message in video steganography using K-LSB and key-frame selection algorithms and **b** extraction of secret message in video steganography

The model successfully implements the secret message transmission between sender and receiver through image and video steganographic techniques. After validation, the sender sends secret data using any of the above steganographic techniques and is decoded at the receiver’s end. The GUI for the model is designed using the ‘tkinter’ module in python. Secure data transmission plays a vital role in today’s world. Hence security has become top priority for every user who is connected to the net. Sensitive data transmission is always a risky task. In-order to address this concern, image and video steganography is quite useful.

In the future, this model can be extended by integrating audio steganography, as well as maintaining multiple databases for storing the user credentials, images, frames of video, audio, etc. This will be helpful for implementing multiple database connectivity for building Web and mobile applications.

References

1. Emad E, Safey A, Refaat A, Osama Z, Sayed E, Mohamed E (2018) A secure image steganography algorithm based on least significant bit and integer wavelet transform. J Syst Eng Electron
2. Roselin Kiruba R, Sharmila TS (2018) Hiding data in videos using optimal selection of key-frames. In: 2018 international conference on computer, communication, and signal processing (ICCCSP), Chennai
3. Patel R, Patel M (2014) Steganography over video file by hiding video in another video file, random byte hiding and LSB technique. In: 2014 IEEE international conference on computational intelligence and computing research, Coimbatore
4. Kaur S, Bansal S, Bansal RK (2014) Steganography and classification of image steganography techniques. In: 2014 international conference on computing for sustainable global development (INDIACom)
5. Pabbi A, Malhotra R, Manikandan K (2021) Implementation of least significant bit image steganography with advanced encryption standard. In: 2021 international conference on emerging smart computing and informatics (ESCI)

6. Priyanka BG, Sathyanarayana SV (2014) A steganographic system for embedding image and encrypted text. In: 2014 international conference on contemporary computing and informatics (IC3I)
7. Yadav P, Mishra N, Sharma S (2013) A secure video steganography with encryption based on LSB technique. In: 2013 IEEE international conference on computational intelligence and computing research
8. Bhole AT, Patel R (2012) Steganography over video file using Random Byte Hiding and LSB technique. In: 2012 IEEE international conference on computational intelligence and computing research
9. Zhang T, Li W, Zhang Y, Ping X (2010) Detection of LSB matching steganography based on distribution of pixel differences in natural images. In: 2010 international conference on image analysis and signal processing
10. Singh A, Singh H (2015) An improved LSB based image steganography technique for RGB images. In: 2015 IEEE international conference on electrical, computer and communication technologies (ICECCT)
11. Manohar N, Kumar PV (2020) Data encryption and decryption using steganography. In: 2020 4th international conference on intelligent computing and control systems (ICICCS)
12. Patel N, Meena S (2016) LSB based image steganography using dynamic key cryptography. In: 2016 international conference on emerging trends in communication technologies (ETCT)

OMSST Approach for Unit Selection from Speech Corpus for Telugu TTS



K. V. N. Sunitha and P. Sunitha Devi

Abstract Design of a text-to-speech system requires fine-tuning to achieve human-like utterance. For Dravidian languages like Telugu that are morphologically rich, this problem can be addressed by minimizing the number of concatenations. In order to reduce the number of concatenations, this research proposes an approach named OMSST to select speech units which minimize the concatenation cost and thus results in more naturally sounding speech. In this approach, most frequent speech units of different length syllables and frequently co-occurring bi-, tri-, and quad-syllables are identified and stored in the corpus. The OMSST algorithm generates the state space tree using the available speech units in corpus for the given word and explores the state space to select the units that result in optimum concatenations. The performance of the algorithm is evaluated by giving the generated utterance to a Telugu speech recognition system, and precision of 97% and recall of 81% are achieved.

Keywords Syllable · State space tree · Speech synthesis

1 Introduction

Rapid increase in growth of computer technology has laid path to design and develop many applications for use to human kind. Computer technology spanned itself in development of applications useful to human beings in their daily life. Text to speech is a natural language modeling process that changes units of text into units of speech. Spoken language-based interfaces provide a convenient mode for a majority of information exchange purposes. TTS systems are useful to build interfaces for the disabled, such as assistance tools for the vision-impaired and reading-based educational tools. The development of text-to-speech systems that

K. V. N. Sunitha

BVRIT Hyderabad College of Engineering for Women, Bachupally, Hyderabad, Telangana, India

P. Sunitha Devi (✉)

G.Narayanamma Institute of Technology and Science, Shaikpet, Hyderabad, Telangana, India

e-mail: sunithareddy.katta@gmail.com

can produce natural-sounding speech segments in several Indian languages is a difficult and ongoing task. Because of the enormous number of possible pronunciations in Indian languages, a significant number of speech segments must be maintained in the speech database, and a concatenative speech synthesis approach is implemented to generate human-like speech [1].

A text-to-speech (TTS) system converts normal language text into speech; this can be achieved by concatenating recorded speech units stored in a database [2]. TTS systems differ in the size of the stored speech units; a system that stores phones or diphones gives the largest output range, but the output speech may not be natural. For natural-sounding speech synthesis, it is essential that the text processing component produces an appropriate sequence of orthographic units corresponding to an arbitrary input text [3]. The difficulty of conversion is highly language depended and includes many problems. The conversion of English and most other languages is substantially more difficult. To achieve correct pronunciation and prosody for synthetic speech, a huge number of different rules and exceptions are required. The majority of Indian languages are phonetic [4]; the conversion of such languages is simple because the written word almost exactly matches the pronunciation. Text preparation, the generation of linguistic data for right pronunciation, and the analysis of prosodic aspects for correct intonation, stress, and duration are the three primary phases of conversion.

To build a text processing component of a TTS system, current state-of-the-art TTS systems in English and other well-researched languages use a rich set of linguistic resources such as word-sense disambiguation, morphological analyzer, part-of-speech tagging, letter-to-sound rules, syllabification, and stress patterns in one form or another. However, for minority languages (which are understudied or lack sufficient linguistic resources), it entails a number of complications, beginning with the collection of text corpora in a digital and processable format. Linguistic components for all languages of the world are not available in such a comprehensive way. Minority languages, particularly several Indian languages, do not have the luxury of assuming some or all of the linguistic components in the real world.

2 Features of Telugu Language

India is the world's seventh-largest country and second-most populous, with 1.2 billion people. India's culture is influenced by a diverse range of societies, religions, and ethnicities. There is also a lot of linguistic diversity, with diverse languages spoken and written natively in the majority of Indian states. There are 22 constitutionally recognized languages spoken and written in different states of India, in addition to English, out of 122 live languages in India [5]. Furthermore, all literate people of various linguistic zones communicate using their regional script [6]. Telugu is a Dravidian language spoken mostly in the Indian states of Andhra Pradesh and Telangana, where it is the official language. Except for English and Urdu, all of India's official languages share a common phonetic foundation, or a set of speech

sounds. While all of these languages share a common phonetic basis, some of them, such as Hindi, Marathi, and Nepali, also use the Devanagari alphabet. The phonotactics in each of these languages, rather than the scripts and speech sounds, is the trait that distinguishes these languages. The allowed combinations of phones that can co-occur in a language are known as phonotactics.

2.1 Text Corpus

It is essential that the text data chosen includes all of a language's common words, phrases, and syllables. The DoE-CIIL Text Corpora is employed, which is a collection of phonetically rich phrases and newspaper articles totaling over 5 million words in Telugu. The text corpus includes sentences from publications in sociology, history, poetry, and a variety of other fields. All of these words have been phonetized in order to examine the distribution of basic speech units such as phones, biphones, and triphones. The basic Telugu language has 48 phonemes: 10 vowels, 2 diphthongs, 33 consonants, and three varieties of anuswaras. The number of phonemes in Telugu, both vowels and consonants, is a divisive subject. Telugu has several phonemic systems that distinguish between social dialects such as standard and non-standard, educated and uneducated, formal and informal, and native and non-native. For digital representation of Telugu text, many notations such as WX, IT3, and ROMAN are used. The disadvantages of transliteration schemes include the following:

- (i) The use of many notations to indicate the same sound. For example, we can express the long form of 'a' with either 'aa' or 'A'.
- (ii) Unpredictable notation, such as w for 't' and 'x' for 'd'.

To prevent the disadvantages described in the preceding notations, distinct codes are used wherever there is a chance of mistake. To avoid this challenge, the text transcribed using these notations may not be easy to read; hence, KNS notation is adopted [7].

3 Syllabification of Corpus

When the number of concatenation points necessary to create a waveform is limited, the naturalness of synthetic speech generated through concatenative voice synthesis improves. Concatenation with syllable like units produces a waveform with the fewest junctures and discontinuity effects. Because Indian languages already have a well-defined syllable structure, using this unit improves synthesis quality [8].

3.1 Syllabification Rules

In Indian languages, there is practically a 1:1 match between what is written and what is said. Each character in the Indian language script corresponds to one of the language's sounds. A consonant letter in Indian languages is inherently linked with a vowel sound /a/ and is always pronounced with this vowel [9]. This vowel is not always pronounced, which is referred to as Inherent Vowel Suppression (IVS). This happens in both the final and middle positions of a word. While the letter-to-phone rules in Indian languages are simple, the syllabification rules are not. To split the word into syllables, some rules must be devised. Single phone (just vowels—V), biphone (CV or VC), triphone (CVC or CCV), and quadphone (CCVC) syllables can be broadly categorized into four types based on the number of phones they include [10].

Based on a heuristic examination of many Telugu words, we have generated some simple rules for syllabification, i.e., rules for grouping clusters of (C + V) *. The rules used for GNITS text corpus syllabification are listed as follows:

1. V: a single vowel can exist as a syllable.
2. VV: two consecutive vowels are split into V–V; however, in Telugu language two consecutive vowels never occur.
3. VCV: is split into V–CV.
4. VCCV: is split into VC–CV.
5. VCCCCV: is split into VC–CCV, the first vowel is associated with the left consonant and the remaining consonants are associated with the right vowel.

The syllabification process is explained in the following example word: గట్టుపైన

gaTTupaina
 CVCCVCVCV Rule 4 is applied
 CVC-CVCVCV Rule 3 is applied
 CVC-CV-CVCV Rule 3 is applied
 CVC-CV-CV-CV
 gaT-Tu-pai-na గట్టు-పై-న

4 Optimal Minimum State Space Tree (OMSST) Approach for Minimum Concatenations

The selection of speech units from a speech corpus plays an important role toward naturalness of a text-to-speech system. In the speech unit database, if we store units like mono-syllable, bi-syllable, tri-syllable, and so on up to n-syllable combinations which co-occur frequently in Telugu language minimizes the number of concatenations. When speech units for a word are to be selected from a speech database, first the longest matching syllable combination is searched, and then for the remaining syllables, also the same method is applied. For example if a word consists of syllables

$S_1, S_2, S_3, S_4, S_5,$ and $S_6,$ the speech units selected for synthesis can be of syllable combinations like $\{(S_1, S_2, S_3), (S_4, S_5), (S_6)\}$ or like $\{(S_1), (S_2, S_3, S_4), (S_5, S_6)\}$. An algorithm is proposed to select the speech units from the corpus with minimum concatenation cost.

4.1 Algorithm

To calculate the cost, a function $\Phi(S_i)$ is used which is the relative probability within its corresponding length type units.

The mono-, bi-, tri-, and quad-syllables identified during text analysis are stored in hash table along with $\Phi(S_i)$ where S_i is a unit identified in corpus.

1. Given a word for synthesis
 - a. Extract the syllable sequence and count.
 - b. Generate state space tree with all possible co-occurrence.
2. Initialize the actual cost function A to 1.
3. Compute cost C of root node as $(A \times E)$ where

$$E = \prod_{1 \leq i \leq n} \Phi(S_i) \tag{1}$$

4. Initialize the node 'N' with root of state space tree.
5. While (N is not an answer node)
 - Repeat
 - (a) for all adjacent nodes i of N
 - compute cost

$$C = \min_{1 \leq i \leq n} \{A_i \times E_i\} \tag{2}$$

where A_i is the actual cost from root node to node i and is given as

$$A_i = \prod_1^i \Phi(S_i) \tag{3}$$

and E_i is the estimated cost from node i to answer node and is given as

$$E_i = \prod_{i+1}^n \Phi(S_i) \tag{4}$$

- (b) Set N with the node which is having least cost.

- 6. If N is the answer node, the units that lie in the path from root to answer node are the actual units which lead to minimum number of concatenations giving more naturalness.

For instance, consider an example word:

swa - tan~ - tra - mu - gA
స్వ - తం - త్ర - ము - గా

Table 1 shows the hash table entries corresponding to the example word as per availability of the speech unit in the corpus. The values in the hash table indicate the frequency at which the unit is available and for the units not available it is marked N/A (not available). State space tree is generated dynamically while exploring the possible units to be concatenated for the given word. At each node i , the successor node j is generated with possible unit selection. If the selected unit is available in hash table, the node generated is retained; otherwise, the node generated is killed immediately. For each successor node, the total cost is computed and node with minimum cost is selected for exploring in the subsequent steps. For the given example, Fig. 1 shows the possible nodes that are likely to be generated while exploring the path from root to leaf. The nodes that are colored in yellow are the nodes that are killed immediately after generation. The nodes that are colored in green are the possible answer nodes. The node colored in blue is the answer node with optimal path which indicates the minimum number of concatenations and gives more natural speech utterance. To explore the path, least cost using BFS technique is applied.

Table 1 Hash table entries for the word swatan~tramugA

S. No	Unit S_i	Frequency of unit S_i	$\Phi(S_i) = \log(\text{freq of } S_i / \sum S_i)$
1	swa	1159	3.607876165
2	swa - tan~	132	4.243040117
3	swa - tan~ - tra	N/A	N/A
4	swa - tan~ - tra - mu	N/A	N/A
5	tan~	1020	3.663359429
6	tan~ - tra	212	4.037278187
7	tan~ - tra - mu	N/A	N/A
8	tan~ - tra - mu - gA	N/A	N/A
9	tra	826	3.754979554
10	tra - mu	174	4.1230648
11	tra - mu - gA	N/A	N/A
12	mu	37,050	2.103171389
13	mu - gA	N/A	N/A
14	gA	27,023	2.24022604

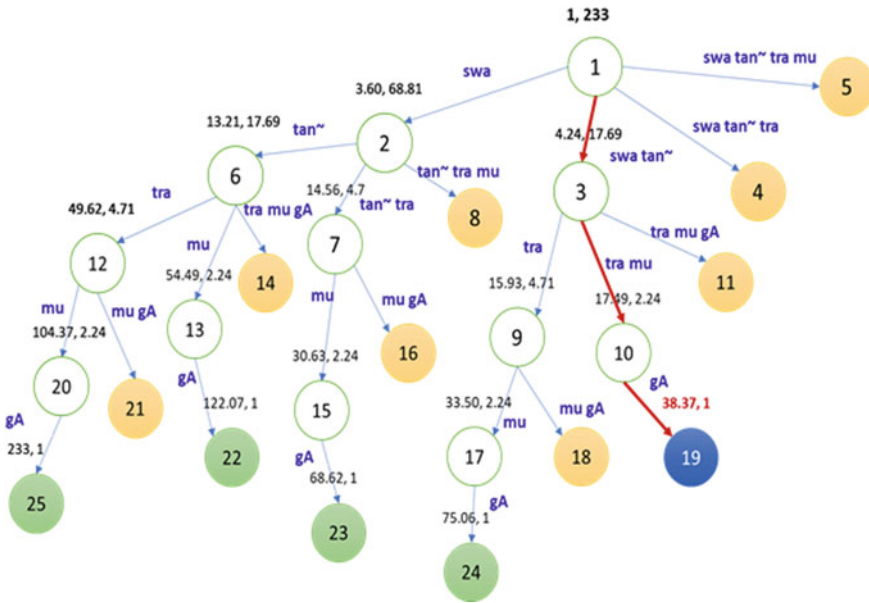


Fig. 1 State space tree construction for the word swatan~tramuga

The state space tree generated for the word is given in Fig. 1, and explanation of finding the path is as follows:

Node 1 is the root node. Nodes 2, 3, 4, and 5 are the nodes generated with possible mono-syllable, bi-syllable, tri-syllable, and quad-syllables. Since the hash table has no entry corresponding to tri- and quad-syllables, the node 3 and 4 are generated and killed immediately. For node 2 and 3, the total cost is computed as shown below:

$$\Phi(\text{swa}) = A(1, 2) + E(2, 25) = 3.60 + 68.81 = 72.41$$

$$\Phi(\text{swa tan } \sim) = A(1, 3) + E(3, 24) = 4.24 + 17.69 = 21.93$$

The next node to be explored is node 3 since it has minimum cost. The successor nodes for node 3 are nodes 9, 10, and 11. Node 11 is generated and killed immediately as the tri-syllable 'tra mu gA' is not available. The cost of nodes 9 and 10 is computed as

$$\Phi((\text{swa tan } \sim)\text{tra}) = A(1, 9) + E(9, 24) = 15.93 + 4.71 = 20.64$$

$$\Phi((\text{swa tan } \sim)(\text{tra mu})) = A(1, 10) + E(10, 24) = 17.49 + 2.24 = 19.73$$

The next node to be explored is node 10 as it has minimum cost. The successor node is node 19 and is the goal state.

$$\Phi((\text{swa tan } \sim)(\text{tra mu})\text{gA}) = 38.37 + 0 = 38.37$$

From the state space tree, we can see that if the units like $\{(\text{swatan}\sim)(\text{tramu})(\text{gA})\}$ are selected as the cost is less and given for synthesis will produce speech with naturalness.

5 Performance Measure

The output of TTS system depends on the type and length of speech units stored in the corpus. Syllabic nature of Telugu language is exploited, and the most promising syllables and the words that cover these syllables are achieved. The quality of speech generated by the system is measured in terms of naturalness, which is directly proportional to the number of units stored. Efforts are made to attain maximum naturalness in the speech produced with minimum speech units stored. Decrease in the number of units stored results in increasing the number of concatenations required which affects the naturalness of output speech. The naturalness in the speech generated was tested by giving to a speech recognizer application.

The test was conducted by taking 120 words which were generated using 2, 3 and 4 concatenations. Few words were generated correctly with the required utterance, but the app could not recognize them properly. Confusion matrix for 120 words with 2, 3, and 4 concatenations is given in Tables 2, 3 and 4.

Table 2 Confusion matrix for 120 words with two concatenations

	Positive	Negative
True	90	7
False	21	2

$$\text{Precision} = 90/111 = 0.81$$

$$\text{Recall} = 90/92 = 0.98$$

Table 3 Confusion matrix for 120 words with three concatenations

	Positive	Negative
True	88	7
False	22	3

$$\text{Precision} = 88/110 = 0.80$$

$$\text{Recall} = 88/91 = 0.97$$

Table 4 Confusion matrix for 120 words with four concatenations

	Positive	Negative
True	83	9
False	25	3

Precision = $83/108 = 0.77$

Recall = $83/86 = 0.96$

6 Conclusions

In this work, we proposed an algorithm OMSST method to minimize the number of concatenations by selection of speech units which produce less cost and natural speech. Naturalness in concatenative TTS systems depends on the type of speech unit stored and the length of each unit. Concatenation using syllables as unit has low discontinuity, and the more the length of each speech unit minimizes the number of concatenation points. To analyze the performance of the method, speech units of different length like mono-, bi-, tri-, and quad-syllables are stored in the corpus and words formed with 2, 3, and 4 concatenations are given to a speech recognizer. It is observed that accuracy is more in two concatenation words than in three and four concatenation words, as the number of concatenations is decreased, the cost is decreased and naturalness in generated speech increases.

References

1. Panda SP, Nayak AK (2017) A waveform concatenation technique for text-to-speech synthesis. *Int J Speech Technol.* <https://doi.org/10.1007/s10772-017-9463-8>
2. Khan RA, Chitode JS (2016) Concatenative speech synthesis: a review. *Int J Comput Appl* 136(3). ISSN 0975-8887
3. Sunitha KVN, Sunitha Devi P (2020) Statistical analysis of text corpus to determine appropriate syllable length for TTS. In: *Proceedings of the 2nd international conference on data science, machine learning and applications ICDSMLA 2020, LNEE*, pp 867–876. https://doi.org/10.1007/978-981-16-3690-5_80
4. Rao PB (2011) Salient phonetic features of Indian languages in speech technology. *Sadhana* 36: 587–599, part 5, October 2011. © Indian Academy of Sciences
5. Retrieved from <http://tdil.mit.gov.in/>
6. Reddy VR, Rao KS (2013) Two-stage intonation modeling using feed forward neural networks for syllable based text-to-speech synthesis. *Comput Speech Lang* 27(5):1105–1126
7. Sunitha KVN, Sharada A (2013) KNS phoneme set—a new Telugu phoneme set for Telugu speech processing technology. In: *ICRTC 2013, 4–5 Oct 2013, SRM University, NCR Campus*. ISBN 978-93-80965065-9
8. Nageshwara Rao M, Thomas S, Nagarajan T, Murthy HA (2005) Text-to-speech synthesis using syllable like units. In: *Proceedings of national conference on communication (NCC)*, pp 227–280, IIT Kharagpur, India, January 2005
9. Sunitha KVN, Sunitha Devi P (2013) Text normalization for Telugu text to speech synthesis. *Int J Comput Technol* 2241–2249
10. Sunitha KVN, Kalyani N, Sreekanth N (2013) Minimum data set based on syllable position for Telugu speech systems. *Int J Adv Res Comput Sci Softw Eng IJARCSSE* 3(10)

An IoT-Based Health Monitoring System for Elderly Patients



Angelin Varghese and Senthil A. Muthukumaraswamy

Abstract Internet of Things in health care significantly improves the requirement of medical facilities to patients and assists healthcare professionals. Since many elderly people require to be checked up on frequently due to high risk of life-threatening diseases, a health monitoring system using a cloud platform becomes effective in real-time observation. This paper focuses on a remote health monitoring system that tracks and updates the patient's caretaker with the data collected from the patient. This enables the patient's overseer to analyze the data being fed to them and subsequently provide treatment for the patient. Any sudden changes in the patient's vitals will ensure that quick assistance be provided to the patient. The data stored in the cloud platform allows the process rate to be even quicker, thus reducing the time required to go to a hospital or waiting for treatment.

Keywords Internet of Things · Arduino UNO · Cloud storage · Remote patient monitoring

1 Introduction

At present all over the world, the elderly community is on the rise. Due to the increasing population issue, a lot of care needs to be given toward elderly citizens as they are more prone to various diseases. In addition to this, seniors are also frail and require special attention throughout the day. Health care for the older generation is rapidly becoming a problem as many of them are not able to make hospital visits on their own [1].

However, remote health monitoring (RPM) has made it possible for elderly patients to sit in the comfort of their own home and has their vitals drawn and

A. Varghese (✉) · S. A. Muthukumaraswamy
School of Engineering and Physical Sciences, Heriot-Watt University, Dubai, United Arab Emirates
e-mail: av44@hw.ac.uk

S. A. Muthukumaraswamy
e-mail: m.senthilarumugam@hw.ac.uk

sent to their doctor, who can properly analyze the data and ergo provide adequate treatment. Smart health monitoring involves the combination of using Internet of Things (IoT) and RPM simultaneously. In fact, this is a rapidly growing industry as smart health monitoring is seen as one of the leading application areas of ubiquitous computing [2].

To effectively monitor the patient, the process needs to be as noninvasive as possible so that the system being used does not disturb the patient's life [3]. For an unobtrusive, effectual procedure, the system will be a wearable device that can be strapped on and taken off.

Before sending information to the IoT platform, the primary data needs to be collected and this is typically done in the form of sensors. Multiple sensors are connected to an Arduino, and the data gathered is prepared to be linked to the Internet. Then, the processed data is stored in a cloud-based platform. In this project, it will be stored on *ThingSpeak*, an open-source analytic platform.

Therefore, the objectives of this project are as follows:

1. To monitor a patient's health
2. To provide an alternative form of health care
3. To collect accurate health parameters of the patient
4. To quicken the assessment and treatment of the patient.

2 Literature Study

RPM is growing in popularity due to its usefulness and its ability to improve the quality of life. IoT is the act of using technology to achieve this. Combining health monitoring and IoT together gives a smart device, capable of managing and storing information [4]. The main aim of this project is to design and implement a fully functioning RPM device that fetches data and updates the patient's caregiver in real time. Using IoT allows for fewer hospital visits, for the patient to get treatment no matter where they are and for keeping the patient's information safe in the cloud platform.

Without the availability of this technology, it can be difficult for doctors to supervise their patients or for the patients to keep track of their health [5]. Patients who especially live far away from hospitals or other healthcare facilities will greatly benefit from this. The combination of a heart rate sensor, temperature sensor, and oxygen sensor will provide the doctor with an adequate amount of information that they can use to check up on the patient.

Almotiri et al. [6] proposed a system where the mobile health (m-health) system is used along with IoT to collect data from patients using wearable devices. The data is stored on a cloud platform, through which it can be accessed by certain users.

Tham et al. [7] proposed a system that would remotely monitor oxygen saturation and heart rate level through IoT. In this system, MAX30100 sensor was incorporated as it could provide data for both oxygen saturation and heart rate. By connecting it with NodeMCU ESP8266, the information could be passed to the Wi-Fi module

and entered into the cloud database. To calculate SpO₂ conditions, two constrains are put down: normal and abnormal. When SpO₂ is 95% and above, the situation is considered as normal. Else, it is abnormal.

Nduka et al. implemented [8] a design that integrated an Arduino board with sensors, GPS, and other components to combine multiple vital sign monitoring sensors into one system. The data gathered from these sensors would be viewed by the patient’s physician in real time. An alarm would sound if any abnormal readings were noted, which would alert the user as well as healthcare professionals. The GPS technology would enable the emergency team to locate and care for the patient.

Kodali et al. proposed a health monitoring system by employing the use of sensors, microcontrollers, and transceivers to send and receive information by using IoT [9]. ZigBee, a low-cost, wireless mesh network, works by using high-level communication protocols to generate personal area networks (PAN). By using ZigBee, the temperature of the patient was constantly monitored and fed to the cloud, where it could be accessed from any part of the world, thereby making it a cheap and effective method.

3 Methodology

The architecture of the proposed model is shown in Fig. 1, where the sensors’ parameters are gathered and processed and sent to the both the Wi-Fi module and LCD display. The LCD display allows the patient to scan their own data, while the data directed to the Wi-Fi module passes to the IoT platform, *ThingSpeak*, from where the patient’s doctor can scan it.

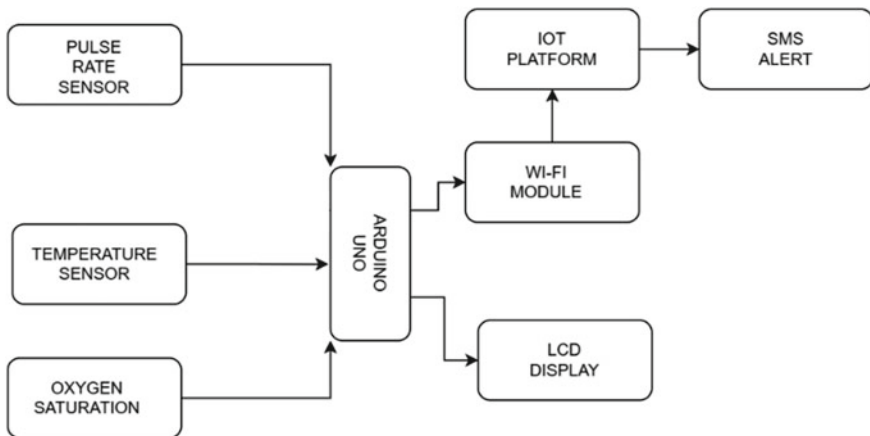


Fig. 1 Complete architecture of the system

Since this project heavily relies on the device continuously monitoring its patient, in order to provide the doctor with the most up-to-date data, the information gathered will need to be passed to an IoT platform, through which it can be clearly analyzed. However, before it is sent to the IoT platform, the data is first gathered from sensors which are coupled to an Arduino microcontroller. An Arduino UNO was chosen for this project as it is a low-cost and effective form of controller.

The parts of the system are described in Sects. 3.1, 3.2, and 3.3.

3.1 Sensors

The sensors are an imperative part of this model as they record the patient's vitals. In Fig. 1, the system architecture presents four sensors. These sensors are as follows:

- Pulse rate sensor
- Temperature sensor
- Oxygen saturation.

The pulse rate sensor is used to monitor the elderly patient's heartbeat. This can help detect signs of heart diseases or heart attacks before they happen, therefore enabling the patient to keep their health in check. Indications of low heart rate could lead to chest pain, dizziness, or fatigue and early detection can prevent this. Alternatively, high pulse rates could cause light-headedness or shortness of breath, which can also be caught ahead of time.

The temperature sensor is used to find the patient's body temperature and ensure it is at normal body temperature. The temperature sensor's parameters were calculated using

$$\text{Temperature}(\text{°C}) = [(\text{ADC value}/1024)5000]/10. \quad (1)$$

The ADC value in (1) is first converted into digital values in Celsius by dividing the number collected by 1024 since the Arduino makes use of a 10-bit analog to digital converter. The value is then multiplied by 5000 and divided by 10 to account for the 10 mv/°.

The oxygen saturation sensor has become more important in modern times due to the spread of the novel coronavirus (COVID-19). The pulse oximeter sensor is used to observe whether the patient's oxygen saturation is between the ranges of 95 and 100%. Anything below 90%, which is also known as hypoxemia, is considered to be low and can cause problems such as headaches, obstruct the functions of the heart and brain, or shortness of breath.

Fig. 2 Output displayed on LCD for patient to view



3.2 Liquid Crystal Display (LCD)

While it is important for the data fetched by the sensors to be delivered to the online medium, it is also essential that the patient be able to read their vitals. For this reason, a liquid crystal display (LCD) is coupled to the Arduino. This allows the data to be output onto the LCD, as depicted in Fig. 2, for the patient to read the information that was collected. This enables the patient to also keep track of their health.

3.3 Wi-Fi Module

To pass on the data to *ThingSpeak*, a Wi-Fi module needs to be used. ESP8266 is a low-cost Wi-Fi microchip which is used to allow microcontrollers to obtain access to any given Wi-Fi network. In this project, ESP8266 was chosen as it is inexpensive, very compatible, and has high integration properties. This component was coupled with the Arduino board, thereby connecting the IoT platform and the sensors together to allow for easy transferring of the information.

With the sensors attached to the Arduino board and the Arduino connected to the ESP8266 Wi-Fi module, the module can send the data it has collected to *ThingSpeak* so that the platform can continuously update itself with the latest figures. The device also sends an alert to its receiver to inform the recipient of any wayward data. Since the sensors have a maximum and minimum threshold value, by which a too-low or too-high reading is deduced, the doctor can be informed of the problem and quickly produce a solution.

The connections of the sensors to the Arduino Uno, as depicted in Fig. 3, show the input to the board, with the output being displayed on *ThingSpeak*. The processed information collected from the components is also output on the LCD for the patient to check the data.

4 Results and Analysis

The data that was collected from the Arduino was sent to the IoT platform via the ESP8266 component. This is done through sending an “HTTP” request from the chosen device to *ThingSpeak*, and *ThingSpeak* adds the data to the fields in the set channel. The information collected by the sensors is output in the form of numerical values. These values are then represented in graphical format using MATLAB

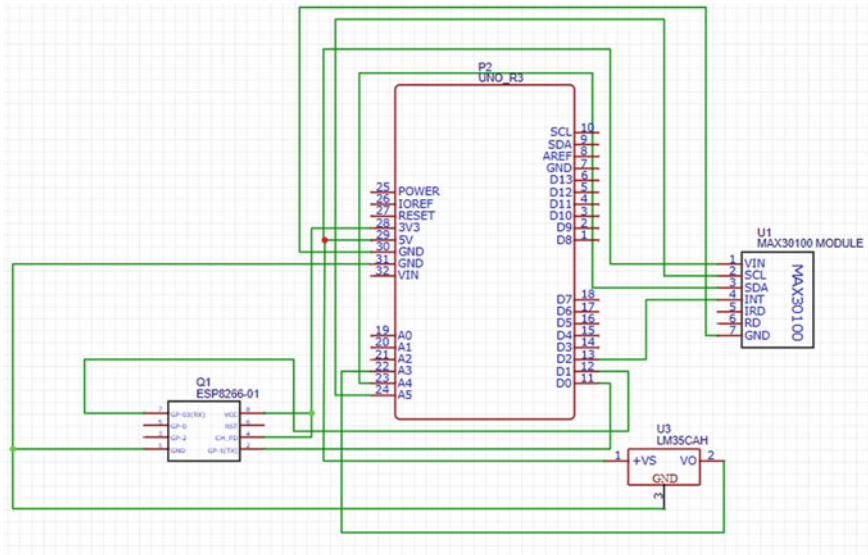


Fig. 3 Connections of sensors to Arduino

analytics. By putting the values in a graph with the y-axis depicting the vital sign recorded and the x-axis as the time, the patient can be closely monitored continuously.

The graphs shown in Fig. 4 depict a person’s heartbeat and body temperature taken in real time. The constant monitoring helps the graph keep a constant legend. This will allow anyone surveying the patient’s vitals to be able to keep track of any abnormal activities and thereby help the patient.

This method of relaying information is clear and easy to follow. The perpetual monitoring ensures that the doctor can keep track of the vital information that is passed through and process the data. The alert message sent to the doctor in case of any reading that passes the maximum and minimum threshold value will ensure that the patient receives help as soon as possible.

5 Conclusion

In conclusion, the system proposed in this paper is not only easily accessible but is also beneficial for seniors and other people who want to check up on their health. With the elderly population on the rise, the provision of this device will enable them to take care of themselves as they will receive real-time parameters of their vitals.

RPM is a concept that is quickly spreading due to its ability to produce fast results with higher patient happiness. Diagnosing patients is also made easier; thus, less time is wasted in this aspect. The use of IoT is imperative as technology is rapidly advancing, and with it being the main distributor of healthcare systems, there can

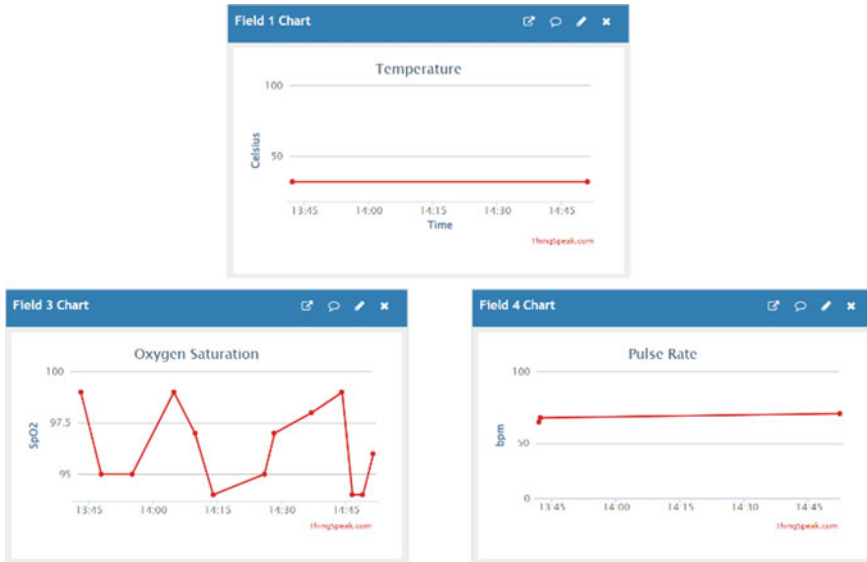


Fig. 4 Analytical graphs from *ThingSpeak*

be much progress in this field. By using IoT, many people will have the benefit of getting access to high-quality health care that they, otherwise, would not be able to get. Any concerning information that is conveyed to the recipient through IoT is further stressed upon through an alert message, which calls for immediate action.

In the future, this system can be developed even further by adding artificial intelligence (AI) aspects. This can be in the form of using AI to calculate vital parameters, having AI robots analyze and treat the patients, or using AI to diagnose patients. This can be explored through finding consistent patterns and training the AI to recognize these patterns and find a solution for it.

References

1. Kai G (2017) A remote health monitoring system for the elderly based on smart home gateway. *J Healthcare Eng* 2017:1–9
2. Park SJ (2017) Development of the elderly healthcare monitoring system with IoT. In: *Advances in human factors and ergonomics in healthcare*, pp 309–315
3. Ohta S (2002) A health monitoring system for elderly people living alone. *J Telemed Telecare* 8
4. Mohammed ZKA, Ahmed ESA (2017) Internet of Things applications, challenges, and related future technologies. *World Sci News* 67(2):132–133
5. Khan NA, Hai M (2016) Real time monitoring of human body vital signs using Bluetooth and WLAN. *Int J Adv Comput Sci Appl* 7(10)

6. Almotiri SH, Khan MA, Alghamdi MA (2016) Mobile health (m-health) system in the context of IoT. In: 2016 IEEE 4th international conference on future Internet of Things and cloud workshops (FiCloudW), pp 39–42
7. Tham OY, Markom MA (2020) IoT health monitoring device of oxygen saturation (SpO₂) and heart rate level. In: 1st international conference on information technology, pp 128–133
8. Nduka A, Samuel J (2019) Internet of Things based remote health monitoring system using Arduino. In: Third international conference on I-SMAC
9. Kodali RR, Swamy G (2015) An implementation of IoT for healthcare. *IEEE Rec Adv Intell Comput Syst*
10. Baker T, Chalmers C (2019) Remote health monitoring of elderly through wearable sensors. *Multimedia Tools Appl* 78:24681–24706
11. Wan J, Li M (2018) Wearable IoT enabled real-time health monitoring system. *EURASIP J Wirel Commun Netw* (298)

Blockchain-Based Solution for Trusted Charity Donations



A. N. Shwetha and C. P. Prabodh

Abstract Nowadays, many people show interest to do social services. It is common that people running charity asks for a help from public people. People who help the charity does not have a way to check proper utilization of the help. Even though many people organizations and industries are extending their help for charities, the people staying in charities are not getting even the basic needs. Recently, we can observe decrease in number of people helping charities due to lack of transparency in the working of charities. Because of lack of transparency in donations, the donors are not able to track the proper utilization of their donated funds. Blockchain technology gives solution to all the above-mentioned problems. Blockchain is a platform which has inherent characteristics like transparency, immutability and security. In blockchain, all transactions will be stored in an immutable ledger and can be accessed transparently by each user. It helps charity organizations to work transparently which builds trust among donors, and it helps donors to monitor their fund utilization with transparent donation route.

Keywords Blockchain · Charity · Immutability · Transparency

1 Introduction

Lack of transparency is involved in the transactions with respect to donations and funds provided by Government for charity organizations. Currently, all transactions with respect to donations and their utilization is monitored by centralized system where data can be manipulated easily. So, the donor or the government is not able to track correct utilization of allotted funds and donations to charities. India has second highest population in the country, many Indians show interest to do donations as per the survey conducted in 2015. India received an overall score of 29% in world giving

A. N. Shwetha (✉) · C. P. Prabodh
Siddaganga Institute of Technology, Tumkur, Karnataka, India
e-mail: shwethaan@sit.ac.in

C. P. Prabodh
e-mail: prabodh@sit.ac.in

index, where most of the donations are informal and they are not recorded anywhere. There is no proper organization and accountability of fund raising to the needy. Even though funds are donated using any digital platforms like Internet banking, mobile banking, or through UPI, funds utilization tracking is very difficult. So there is a need for donors to have proper channel to track their funds and to provide transparency in social funding.

Blockchain is a promising technology and becoming dominant enough to solve many problems related to security in both private and public sectors. Blockchain technology makes the donations transparent. All transactions with respect to donations and fund usage will be recorded in blockchain. This will help charity organizations to work transparently by avoiding third parties involvement and which will also increase the public trust on charities. When a transaction happens in a blockchain network, it will be evaluated by each and every node present in the network. If at least 51% of nodes present in blockchain network approves the transaction, then it is considered as valid, and it can be added to blockchain. The blockchain application can be implemented either by using ethereum platform or hyperledger fabric platform. In ethereum platform, the average time required to create new block is 10 min.

Figure 1 depicts the block diagram of blockchain where the data stored in blockchain will be in the form of blocks. The hash value of previous block will be stored in next block. So when the contents of block are modified, the hash value will also be modified. So modifications can be easily identified. The modification will also be recorded as a transaction. Thus the blockchain has a property called immutability. The data present in blockchain can be viewed by each user, and thus it is transparent.

Once a couple of transactions are completed, one of the node in the network is selected as a miner based on proof of work or proof of stake methods. In proof of work, the node which solves the mathematical puzzle first is considered as a miner. To solve the puzzle, the node should have high computational power. In proof of stake, miner will be selected based on some criteria like oldest node in network or in round robin fashion. The miner will create a new block which comprises all current valid transactions, and a block will be added to blockchain. The complete blockchain will be replicated to all nodes present in a network. So each user can access and track all the transactions happening in the blockchain network.

Objectives:

1. To make the working of charity organizations a convenient one. Because all the transactions are available in single place, report generation becomes easy.

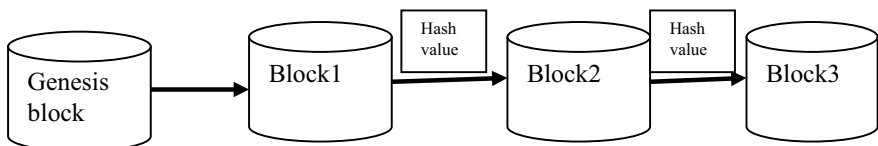


Fig. 1 Block diagram of blockchain

2. To provide transparency in charities action.
3. To explore possibility of integrating multiple charities to one platform.
4. To provide accountability of donated funds to donors.

2 Literature Survey

Zheng et al. [1] presented an overview of blockchain and its architecture, different consensus algorithms used in blockchain, technical challenges and recent trends in the field of blockchain. Alexopoulos et al. [2] investigated the advantages of using open distributed ledgers in secure authentication of systems. Also explored the possible ways in which blockchain mitigates the security attacks. Authors had proposed a model and analysed how exactly blockchain provides security when blockchain is applied to proposed model. Mukhopadhyay et al. [3] evaluated various mining techniques available in cryptocurrencies. Also compared the strengths, weaknesses and threats in various mining techniques. Authors have concluded that each mining techniques has some level threats and weaknesses.

Suma [4] presented privacy and security mechanism offered by blockchain to prevent misuse of voluminous data created by commercial activities, judiciaries, etc. Anjum et al. [5] evaluated that blockchain does not restrict only to finance and banking but it has various merits in different domains like healthcare, supply chain management, education, personal identification and validation of records. Hou [6] evaluated the various benefits brought by blockchain technology in e-government of China like improvement in quality and quantity of government services, transparency in accessing government data, sharing of information across various sectors and building individual credit system. Mudliar et al. [7] evaluated the merits of implementing blockchain technology in national identification records, where the individual will be authorized using his/her personal details and biometrics.

The proposed system is simulated using java. Taş [8] presented the experience, user friendliness and advantages in implementing decentralized application using ethereum platform on blockchain. Sai Sirisha et al. [9] proposed a decentralized blockchain-based solution called charity chain to improve the trust of users on charities. The corruption makes the donors lose trust on charity foundations. The proposed ethereum blockchain solution can provide transparency in charity functions and improve the trust.

Khanolkar et al. [10] explored the merits of implementing blockchain in charity organizations to track the funds from donors to end users in charity. A web-based application is developed using ethereum blockchain to track transactions in charities. Wu [11] evaluates the reliability of charity donation system based on blockchain with respect to COVID-19 pandemic. Authors also discussed the operational mechanism of charity sectors with the donors and the overall system design. Authors evaluated the advantage of blockchain technology in the functioning of charity organizations. Jeong et al. [12] implemented a blockchain network to enhance transparency in donations and to preserve privacy of donors using hyperledger fabric platform. Saleh

[13] discussed about implementing suitable platform for tracking donations of charity organizations using suitable technology called blockchain technology. The system will offer accountability of donors, their donations and the recipients and also used to track and monitor where the resources are utilized.

3 Design

Figure 2 depicts the architecture diagram of blockchain-based solution for trusted charity donation system. The web application is developed to initiate the transactions of trusted charity funding. Donor is a person who wants to donate funds to the needy. The donors will donate their funds through a web application. The total amount of donation will be processed and stored in a blockchain. A manager, who is a trusted third party will initiates the charity campaign for the particular charity organization. When any transaction is initiated either by donor or by manager, all nodes of blockchain network will validate transaction. If more than 51% of users have validated the transaction, then the transaction is considered as authentic, and it is eligible to be stored in blockchain.

Once the campaign is initiated, if any donor want to help can donate the funds to a particular needy. When the donations are done, manager will initiate the withdraw request to withdraw the money which is accumulated in charity campaign. The approvers need to approve the withdraw request. To become approver, the donor should donate at least minimum amount specified. All the approved transactions will be stored in blockchain in form of blocks and they can be viewed by any user. So that it provides transparency to end users and donors. To spend the money withdrawn from charity campaign, the manager has to initiate the transaction and if it is

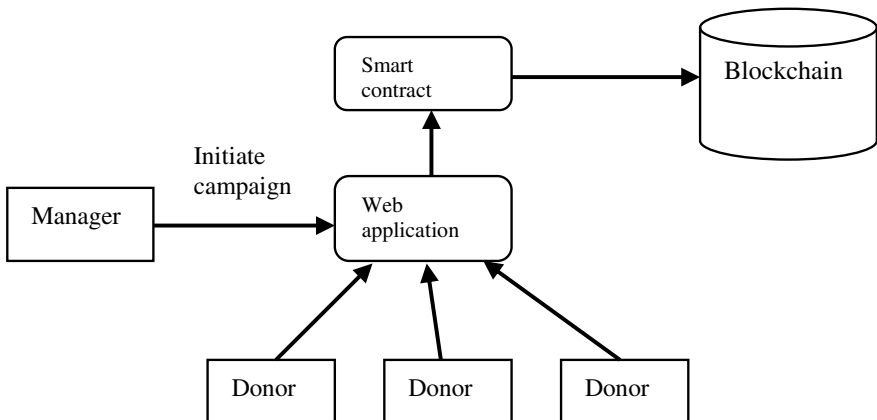


Fig. 2 System architecture

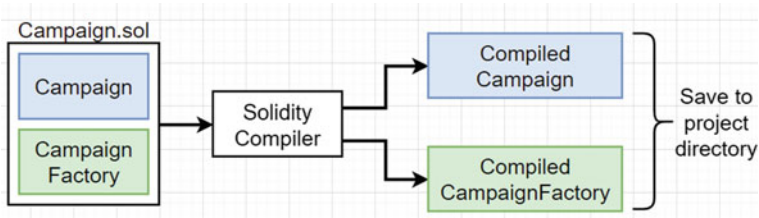


Fig. 3 Block diagram of campaign creation

approved, it will be stored in blockchain. So donor will have accountability of spent funds.

Figure 3 shows the block diagram of campaign creation. In this system, we will create two campaigns, one is campaign and the other is campaign factory. Campaign is created for individual charity organization by a manager to get the donations for the needy. If any donor want to give donations, they can do that by using ID of created campaign. Campaign factory is created to get one stop information about all campaigns created so far in this blockchain network. So here we can get detailed information regarding each campaign created, the number of donations received and details regarding the collected and withdrawn funds.

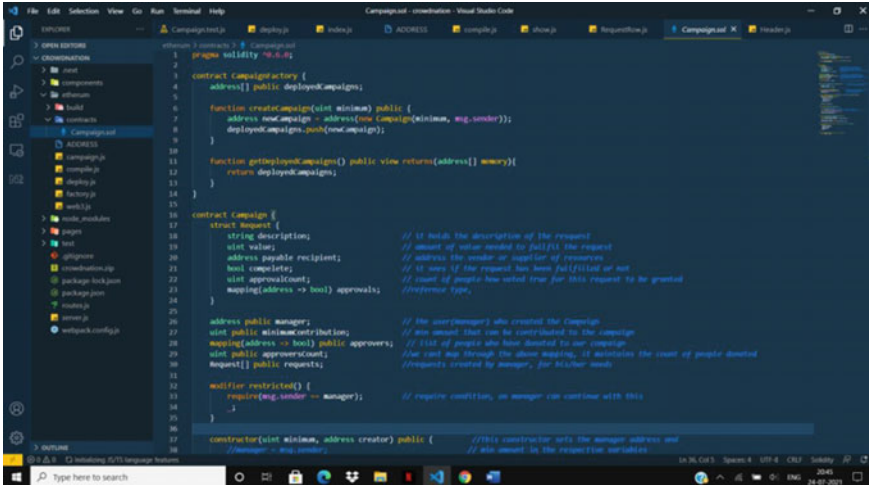
4 Implementation

Blockchain-based solution for trusted charity donations is implemented on ethereum platform by considering a test network. Figure 4 shows the solidity code to create campaign and campaign factory contracts. These are two contracts which will run in this blockchain network. The campaign contract contains information like description of contract indicates who will the needy and amount of funds required, status of campaign and number of approvers had approved this contract.

Figure 5 shows the code of campaign dashboard. Here a code is written to list all active campaigns and when we click on particular campaign, we will be redirected to a page contains detailed information regarding particular campaign. We also have an option to create new campaign.

5 Results

The number of campaigns and campaign factory is created using solidity, number of donors and manager nodes are created to check validity of system. Approvers can verify the validity of each transaction using smart contract and later all the transaction are stored in blockchain for later access.



```
pragma solidity ^0.4.0;

contract CampaignFactory {
    address[] public deployedCampaigns;

    function createCampaign(uint minimum) public {
        address newCampaign = address(new Campaign(minimum, msg.sender));
        deployedCampaigns.push(newCampaign);
    }

    function getDeployedCampaigns() public view returns(address[] memory) {
        return deployedCampaigns;
    }
}

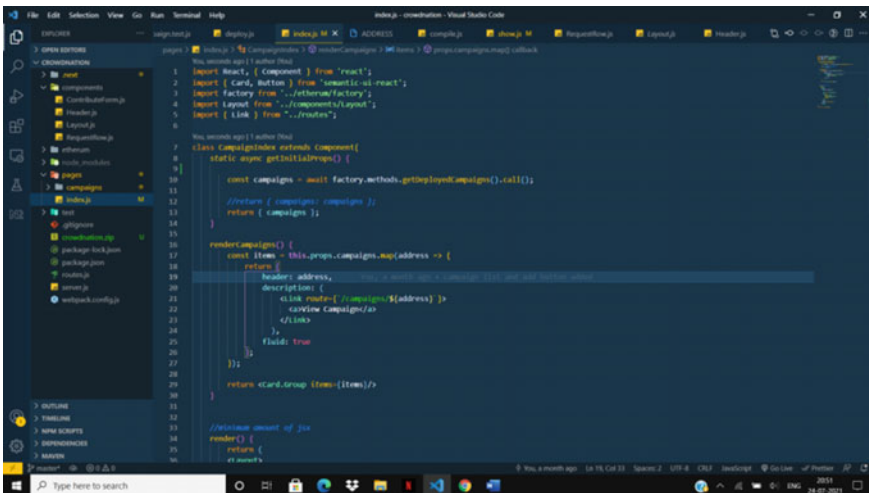
contract Campaign {
    struct Request {
        string description; // to hold the description of the request
        uint value; // amount of ether needed to fulfill the request
        address payable recipient; // address the ether of recipient
        bool completed; // to check if the request has been fulfilled or not
        uint approvalCount; // count of people who voted true for this request to be granted
        mapping(address => bool) approvals; //reference type,
    }

    address public manager; // the user(manager) who created the Campaign
    uint public minimumContribution; // the amount that can be contributed to the campaign
    mapping(address => bool) public approvals; // list of people who have donated to our campaign
    uint public approvalCount; // the total map through the above mapping, it calculates the count of people donated
    Request[] public requests; //the total map through the above mapping, it calculates the count of people donated
    //requests created by manager, for his/her needs

    modifier restricted() {
        require(msg.sender == manager); // require condition, so manager role continue with this
    }

    constructor(uint minimum, address creator) public { //this constructor only the manager address and
        //also amount by the requester, variables
        manager = creator;
    }
}
```

Fig. 4 Contract creation



```
import React, { Component } from 'react';
import { Card, Button } from 'semantic-ui-react';
import factory from './factory';
import Layout from './components/Layout';
import { Link } from './routes';

class CampaignIndex extends Component {
    state = { campaigns: [] };

    componentDidMount() {
        const campaigns = await factory.methods.getDeployedCampaigns().call();
        this.setState({ campaigns });
    }

    renderCampaigns() {
        const items = this.props.campaigns.map(address => {
            header: address,
            description: {
                link: router.push(`/campaigns/${address}`)
            },
            fluid: true
        });

        return <Card.Group>{items}</Card.Group>;
    }

    //display amount of ether
    render() {
        return (
            <Layout>
                <div>
                    <h2>Campaigns</h2>
                    <div>
                        <Link to="/create-campaign">Create Campaign</Link>
                    
```

Fig. 5 Implementation of campaign dashboard

Figure 6 depicts the landing page of web application which will list all the active campaigns. And also there is an option to create new campaign for the needy. Figure 7 depicts the web page and required fields to create a new campaign. For each created campaign, an ID will be generated, and it will be used by donors for donation of funds. A campaign creation requires a description where a detailed information regarding purpose of campaign creation, and the corresponding needy has to be mentioned. Figure 8 shows the list of campaigns created and awaits for approval by

the approvers. Here only one campaign is pending for approval. An approver can look at the description and by taking knowledge of previous transactions, he can either approves the transaction or it can be rejected.

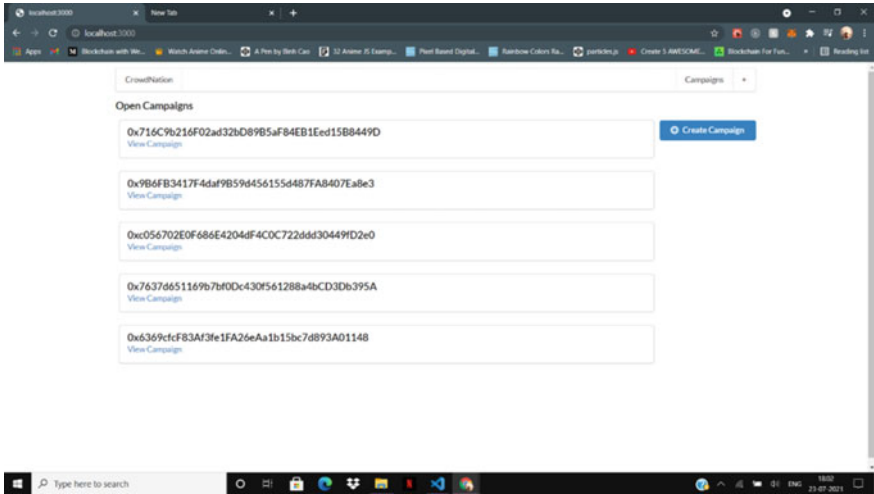


Fig. 6 Web application dashboard

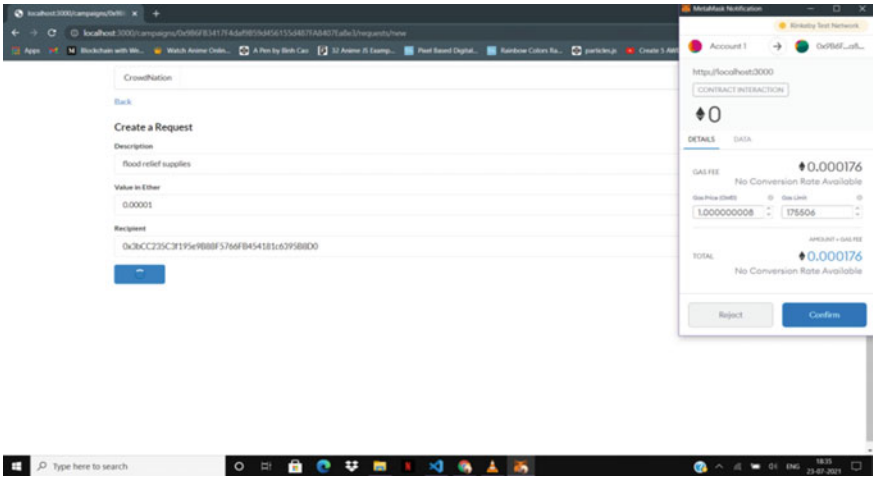


Fig. 7 Campaign creation

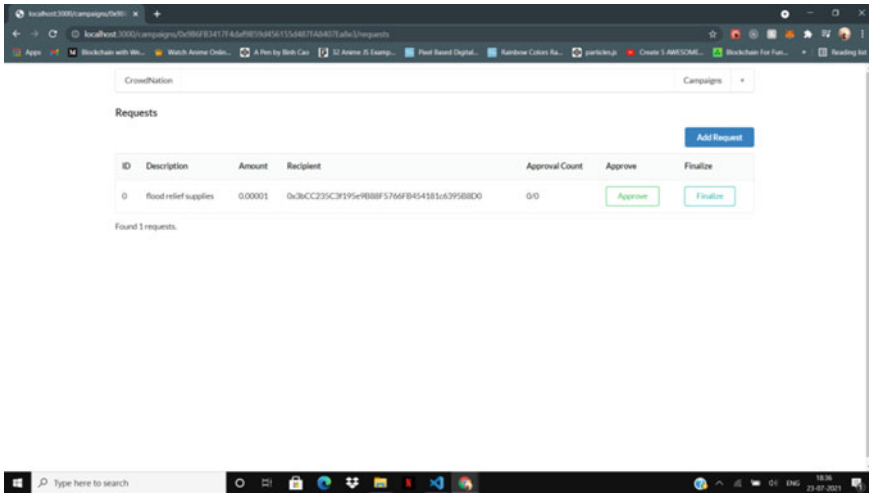


Fig. 8 List of campaigns for approval

6 Conclusion

The current system used to track the donations is a centralized system. Here the manipulations and corruptions are very common which will reduce the trust of people on charities and donations. So that the number of people showing interest towards social service is getting reduced. Because of the corruptions of the third party, the needy are suffering even from basic needs. Even though people are doing donations they are not reaching the needy through proper channel. So a blockchain-based solution for trusted charity donations is proposed.

In the proposed system, each transaction with respect to donations and fund utilization will be stored in blockchain. Each user of a blockchain network can view all the transactions stored in blockchain. As the blockchain data is immutable, there is no provision for anyone to modify the transactions stored in blockchain ledger. So there is a proper accountability of utilization of donated funds to each user which will also increase the trust. Using this system, even the charity organizations can work transparently which will help them to receive more donations by increasing the trust in society.

References

1. Zheng Z, Xie S, Dai H, Chen X, Wang H (2017) An overview of blockchain technology, architecture, consensus, and future trends. In: IEEE international congress on big data
2. Alexopoulos N, Daubert J, Muhlhauer M, Habib SM (2017) Beyond the hype, on using blockchains in trust management for authentication. In: IEEE Trustcom/BigdataSE/ICSS

3. Mukhopadhyay U, Skjellum A, Hambolu O, Oakley J, Yu L, Brooks R (2016) A brief survey of cryptocurrency systems. In: 14th annual conference on privacy, security and trust
4. Suma V (2019) Security and privacy mechanism using blockchain. *J Ubiquitous Comput Commun Technol*
5. Anjum A, Sporny M, Sill A (2017) Blockchain standards for compliance and trust. In: *IEEE cloud computing*
6. Hou H (2017) The application of blockchain technology in E-government in China. In: 26th international conference on computer communications and networks
7. Mudliar K, Parekh H, Bhavathankar P (2018) A comprehensive integration of national identity with blockchain technology. In: International conference on communication information and computing technology
8. Tas R, Tanrıover ÖÖ (2019) Building a decentralized application on the ethereum blockchain. In: 3rd international symposium on multidisciplinary studies and innovative technologies
9. Sai Sirisha N, Agarwal T, Monde R, Yadav R, Hande R (2019) Proposed solution for trackable donations using blockchain. In: International conference on nascent technologies in engineering
10. Khanolkar AA, Gokhale AR, Tembe AS, Bharadi VA (2020) Blockchain based trusted charity fund-raising. *Int J Soft Comput Eng*
11. Wu H, Zhu X (2020) Developing a reliable service system of charity donation during the Covid-19 outbreak. *IEEE Access*
12. Jeong J, Kim D, Lee Y, Jung J-W, Son Y (2020) A study of private donation system based on blockchain for transparency and privacy. In: International conference on electronics, information, and communication
13. Saleh H, Avdoshin S, Dzhonov A (2019) Platform for tracking donations of charitable foundations based on blockchain technology. In: Actual problems of systems and software engineering

Vedic Multiplier for High-Speed Applications



J. V. R. Sudhamsu Preetham, Perli Nethra, D. Chandrasekhar,
Mathangi Akhila, N. Arun Vignesh, and Asisa Kumar Panigrahy

Abstract We live in a technologically advanced society. The use of diverse electronic gadgets is interwoven with even the most fundamental aspects of our daily lives. They increase and smoothen the pace of our life. The multiplier component controls the speed of most electronic systems. The multiplier module is a significant component of high-speed applications that employ the IEEE 754–2008 standard for single precision FPUs. Several existing methods have been included to enhance the multiplier’s speed of operation. They have, however, not demonstrated a substantial difference in speed, raising it by a maximum of 1.182 times. As a result, we presented “Vedic Design,” a novel algorithm with a distinctive architecture. When this was simulated in Vivado, it improved the multiplier’s speed by 3.4478 times, resulting in a multiplier that is nearly 3.5 times more efficient. The gadget is better equipped to function as a result of the reduced computational path latency.

Keywords Computational path delay · Latency · Vedic multiplier · Vivado · Speed

1 Introduction

The world we currently reside in is driven by many gadgets, devices, and several technological advancements made by the human mind since the dawn of time. It is these developments that have equipped us humans to face any challenge thrown at us however daunting they may seem. We have found the innermost constituents of an atom which was considered indivisible. The human mind has always been curious to find ways to make life simpler, to make existing solutions to various problems even more flexible and universally applicable. The most important thing that we users look for in any device or system is the speed at which it works, as no one would want to use a device that would delay the work.

J. V. R. Sudhamsu Preetham · P. Nethra (✉) · D. Chandrasekhar · M. Akhila · N. Arun Vignesh · A. K. Panigrahy
Department of ECE, Gokaraju Rangaraju Institute of Engineering and Technology, Hyderabad, Telangana 500090, India
e-mail: nethra.perli1207@gmail.com

A similar problem of overcoming the speed of the device is dealt with in this paper using our proposed method. Every electronic device irrespective of its usage and purpose has a multiplier as one of its many essential components. Many high-performance systems, such as microprocessors and digital signal processors, require multipliers. The multiplier is the slowest component of the system, hence its performance influences the system's total performance.

The IEEE 754 standard outlines how computers should represent binary floating-point numbers. Binary floating-point numbers are represented in single and double precision forms. In such applications, multiplication is one of the most significant arithmetic operations, hence a fast multiplier circuit is required. Time delay and power usage are crucial in many applications. Along with the IEEE 754–2008 FPU, traditional multipliers such as Booth recoding, Vedic multiplier, and add-sub multipliers are described.

The existing multiplier algorithms are presented using flow charts, followed by the proposed modified Vedic Design Algorithm. The paper concludes with the results of an efficient multiplier as well as potential future work.

2 Literature Survey

In the last few years, there are many methods that tried to implement such proposed algorithms with the sole purpose of decreasing the latency of an electronic device. One of the most renowned is mentioned below.

Novel Vedic and Shift Add design for Single Precision IEEE 754–2008 FPU in High Speed Applications by Anshuman Mohapatra and Abhyarthana Bisoyi [2].

Anshuman Mohapatra and Abhyarthana Bisoyi had introduced 3 different algorithms in order to decrease the latency of an electronic device and increase the overall performance of the device. While all the three methods are minute changes of the existing Shift add and Vedic algorithms, all three of them are proven to be efficient in different categories.

Proposals:

- (1) Modified Shift Add Multiplier
- (2) Proposed Vedic Multiplier—1
- (3) Proposed Vedic Multiplier—2.

The existing multiplier algorithms are presented using flow charts, followed by the Vedic multiplier and shift add algorithms suggested in [2]. In Sect. 5, the proposed Vedic design algorithm is discussed. The algorithms provided are not only fast but also efficient for area considerations. This provided a gateway for a number of applications considering the efficiency of a multiplier. During the process of calculations, there might be few errors which effect the result of the multiplier. To avoid that we can use concurrent error detection and self-repairable adders [3]. The logic design of a computer can be made with the help of few general considerations [4].

3 Identification of the Problem

A multiplier should be fast in order to support any high speed applications as the execution of any process depends on the latency of the electronic device. Multiplier is usually the unit that takes up the greatest space and time. As a consequence, optimizing the multiplier's area and performance is a crucial design consideration for any digital signal processor. This section describes the different types of multiplier algorithms that are widely used in DSP devices for faster applications. Booth's algorithm is presented for demonstrating its relevance with Booth's original algorithm for multiplication processes. [5] In this part, the paper will focus on the remaining traditional multipliers and also a novel multiplier algorithm.

3.1 Vedic Multiplication

The process of Vedic Multiplication [6] was discovered that it had a parallel production of incomplete products that consumed less space [7]. Rai used Vedic mathematics to build a 32-bit floating-point multiplier for the IEEE 754 standard [8]. In 2016, a solution for reducing power consumption by 53% from capabilities and limitations was explored [9]. In DSP processors, MAC unit will be benefited to a great extent [10, 11].

3.2 Booth Recoding

The concept of shifting instead of adding is the basic principle used by the booth recoding algorithm. This approach proved faster execution and smaller area consumption compared to other multipliers. It reduces the number of individual product values that must be combined for the output [12–14].

3.3 IEEE 754–2008 Floating-Point Unit (FPU)

The paper uses single precision floating-point binary numbers. It consists of 32 bits, out of which, 23 belong to mantissa, 8 are for exponent and the remaining 1 is marked for sign bit. Based on the above mentioned literature survey, this paper consists of implementations of the existing multiplier algorithms. From the simulations obtained, novel techniques are obtained by making few small yet significant changes that supports in optimized design of the MAC units of the electronic device.

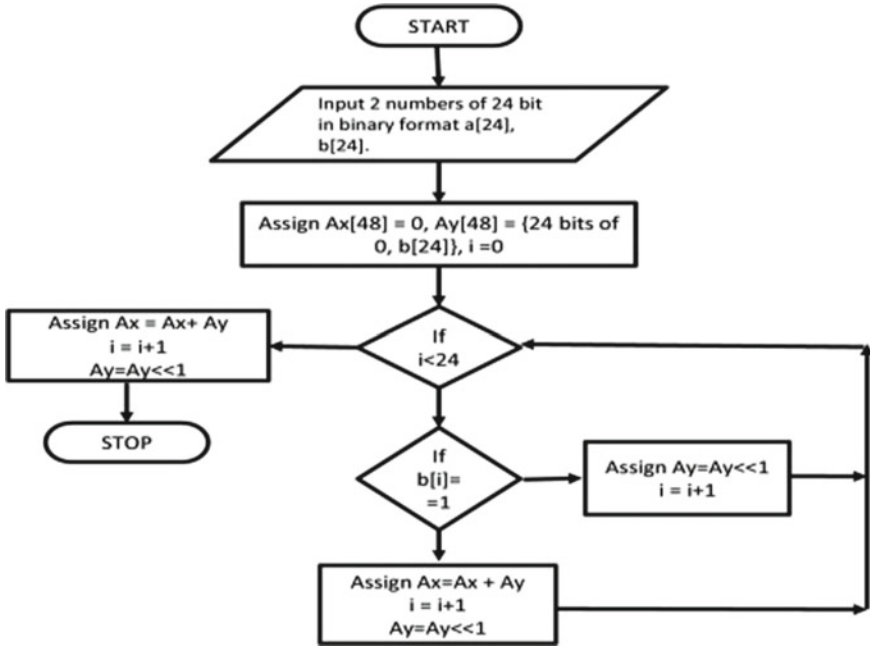


Fig. 1 Existing shift add algorithm flowchart

4 Algorithms

4.1 Shift Add

See Fig. 1.

4.2 Vedic Design

See Fig. 2.

5 Proposed Algorithm

A significant change is made: The final output of a 32×32 bit multiplication is broken down to 2×2 bit multiplication and the gate level implementation is shifted to 2×2 bit inputs. Mantissa multiplication is done with 32 bits here. As a result, we split 32-bit multiplication into its first portion, i.e., 16 bits. Decomposing the $32 \times$

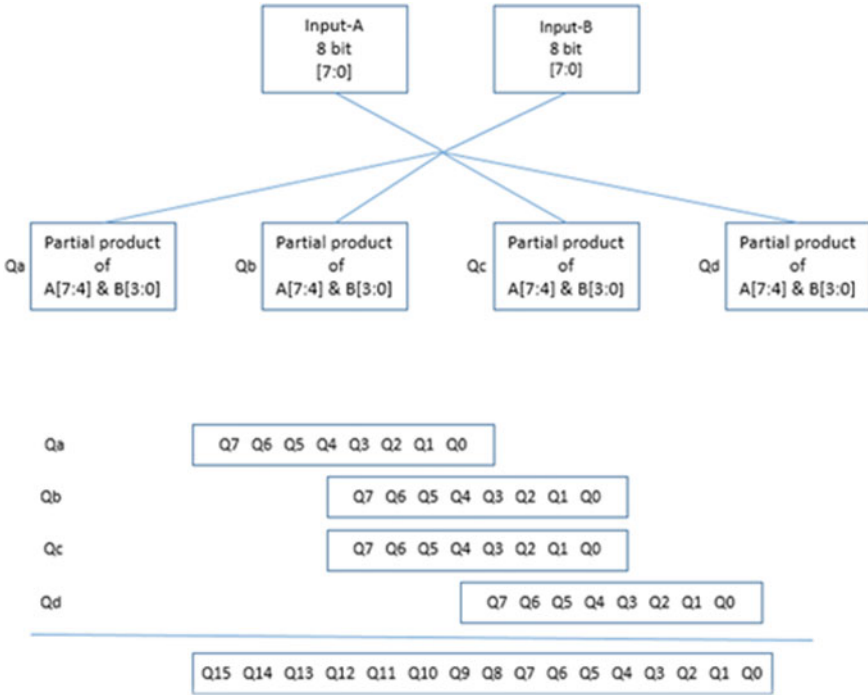


Fig. 2 Flowchart of a basic Vedic multiplication operation

32-bit multiplication into four numbers of 16×16 subunits is done here. Following the Vedic technique of 3-bit multiplication, this is further broken into 8×8 modules, then to 4×4 , followed by gate level implementation at 2×2 bit level multiplication. The gate level implementation of the 2×2 module is used in the proposed algorithm.

The flowchart of the process of implementation for the proposed algorithm is shown in Fig. 3.

6 Result Analysis

The proposed Vedic Multiplier is used to multiply the inputs in the Vivado software.

Considering the inputs,

Input-A: 111,111,101,111,110,110,010,110.

Input-B: 100,110,001,001,101,100,101,111.

- (1) Simulation of 32×32 result using conventional Vedic multiplier [7] (Fig. 4).
- (2) Simulation of 32×32 result using proposed Vedic multiplier (Fig 5).

By comparing multiple algorithms for the same inputs and tabulating the computational path delays, the values are as shown in the Table 1.

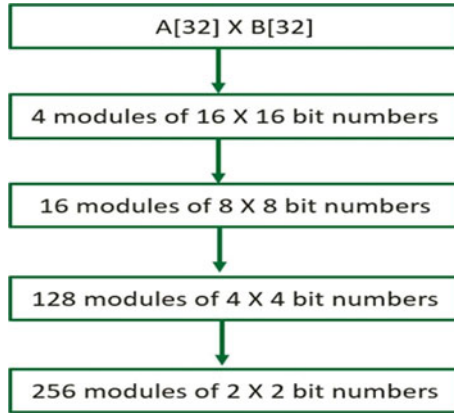


Fig. 3 Flow chart for the proposed Vedic algorithm

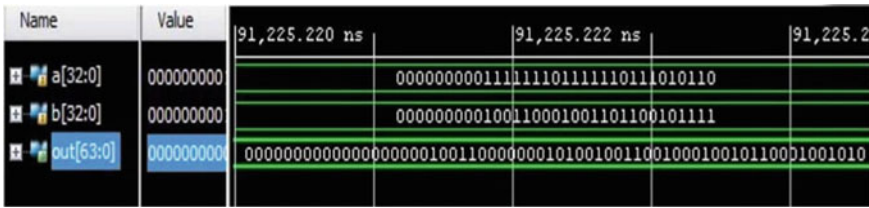


Fig. 4 Simulation result of a standard 32 bit Vedic algorithm

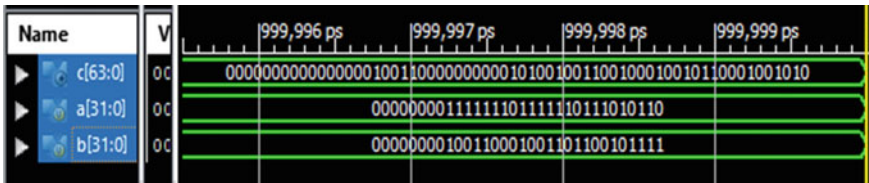


Fig. 5 Simulation result for the proposed 32 bit Vedic algorithm

Table 1 Comparison of maximum path delays in different algorithms

Available algorithms	Maximum expected latency (in ns)
Existing Vedic algorithm [7]	47.10
Standard shift and add algorithm	43.91
Modified Vedic multiplier	13.602

```

Minimum period: No path found
Minimum input arrival time before clock: No path found
Maximum output required time after clock: No path found
Maximum combinational path delay: 13.602ns

```

Fig. 6 Latency proof for modified algorithm

```

-----
Total                13.602ns (6.579ns logic, 7.023ns route)
                    (48.4% logic, 51.6% route)

```

Fig. 7 Detailed usage of time while execution

7 Conclusion

As shown in the above simulation results, the simulation for a 32-bit multiplier by using the conventional Vedic algorithm is using 47.10 ns of time to execute a 32-bit multiplication. This is the computational path delay. Whereas the proposed Vedic algorithm is using only 13.602 ns (mentioned in Fig. 6) which is approximated to 3.5 times better than the conventional one. This simulation has proven to be effective in case of time. This reduces a lot of pressure on the hardware while solving huge and complex calculations. In order to obtain an efficient arithmetic FPU, we can design a fused Add/Sub unit [15] (Fig. 7).

We are currently using hardware co-simulation to implement the aforementioned methods in Vivado system generator. Though developing the block diagram is comparatively simpler, configuring hardware parameters such as gateways in co-simulation necessitates changes. Due to presence of multipliers in every architectural design of a DSP device, creating energy efficient design is important. Future works will include improving the multiplier algorithms to achieve even shorter propagation delays, as well as developing it in python and other developing platforms.

References

1. Kishore P, Sravanthi P, Deepthi G, Rashmitha A (2021) Chapter 41 a review on comparative analysis of add-shift multiplier and array multiplier performance parameters. Springer Science and Business Media LLC
2. Mohapatra A, Bisoyi A (2008) Design of novel Vedic and shift-add multipliers for single precision IEEE 754–2008 floating-point unit applications. In: High speed applications
3. Musala S, Neelam AK, Bharath Sreenivasulu V, Vijaya Vardhan K (2021) Concurrent error detectable and self-repairable carry select adder. Int J Electron
4. Booth AD, Britten KHV (1947) General considerations in the design of an electronic computer
5. Booth AD (1951) A signed binary multiplication technique. Q J Mech Appl Mech 4(pt. 2):236–240

6. Bisoyi A, Baral M, Senapati MK (2014) Comparison of a 32-bit Vedic multiplier with a conventional binary multiplier. In: IEEE international conference on advanced communication control and computing technologies (ICACCCT)
7. Haripriya TK, Sajesh KU (2017) VHDL implementation of novel squaring circuit based on Vedic mathematics. In: 2nd IEEE international conference on recent trends in electronics, information and communication technology (RTEICT), pp 1549–1552
8. Rai P, Kumar S (2014) Design of floating-point multiplier using vedic aphorisms. *Int J Eng Trends Technol* 11(3):123–126
9. Camus V, Schlachter J, Enz C, Gautschi M, Gurkaynak FK (2016) Approximate 32-bit floating-point unit design with 53% power-area product reduction. In: ESSCIRC conference 2016: 42nd european solidstate circuits conference, pp 465–468
10. Kahar DK, Mehta H (2017) High speed vedic multiplier used international vedic Conference mathematics. In: Intelligent computing and control systems (ICICCS), Madurai, pp 356–359
11. Itawadiya AK, Mahle R, Patel V, Kumar D (2013) Design a DSP operations using Vedic mathematics. In: International conference on communication and signal processing, Melmaruvathur, pp 897–902
12. Prabhu AS, Elakya V (2012) Design of modified low power booth multiplier. In: 2012 International conference on computing, communication and applications, pp 1–6
13. Tsoumanis K, Xydis S, Efstathiou C, Moschopoulos N, Pekmestzi K (2014) An optimized modified booth recoder for efficient design of the add-multiply operator. *IEEE Trans Circuits Syst I Regul Pap* 61(4):1133–1143
14. Antelo E, Montuschi P, Nannarelli A (2017) Improved 64-bit Radix-16 booth multiplier based on partial product array height reduction. *IEEE Trans Circuits Syst I Regul Pap* 64(2):409–418
15. Saleh H, Swartzlander EE (2008) A floating point fused add subtract unit. In: Proceedings IEEE midwest symposium circuits and systems (MWSCAS)

Resolving Lexical Level Ambiguity: Word Sense Disambiguation for Telugu Language by Exploiting IndicBERT Embeddings



Palanati Durgaprasad, K. V. N. Sunitha, and B. Padmajarani

Abstract Generally, acquiring proper interpretation of a word or a sentence in a particular context is very important in many natural language applications like machine translation, information retrieval, sentiment analysis, and many others. Performing semantic analysis aims to resolve the misinterpretation of a word or a sentence. Word sense disambiguation (WSD) helps to improve the performance of semantic analysis. In this paper, we have proposed a novel algorithm to solve WSD for the TELUGU language that works based on IndicBERT word embeddings. Our algorithm calculates Cosine similarity between sense and context vectors to assign correct sense. The performance of our algorithm also depends on context window size. In the case of resolving lexical level ambiguity our algorithm has reported an average accuracy of 64.7 and 71.7% for window sizes of 3 and 4, respectively.

Keywords Lexical ambiguity · Machine learning · Word embeddings · Word sense disambiguation

1 Introduction

There are many difficulties while interpreting a natural language. These include ambiguity of language, acquiring common sense, discourse identification, and language being dynamic. The semantic analysis correctly interprets the meaning of words and expressions [1]. Semantic analysis is essential in many applications like concept similarities [2], document summarization [3], semantic hashing in

P. Durgaprasad (✉)

Department of Computer Science and Engineering, UCET, MGU, Nalgonda, Telangana, India
e-mail: dp.cse5@gmail.com

K. V. N. Sunitha

Department of Computer Science and Engineering, BVRIT Hyderabad College of Engineering for Women, Hyderabad, Telangana, India
e-mail: k.v.n.sunitha@gmail.com

B. Padmajarani

Department of Computer Science and Engineering, JNTUCEH, Hyderabad, Telangana, India
e-mail: padmaja_jntuh@jntuh.ac.in

information retrieval [4], Internet of Things [5], Keyword Extraction [6], Sentiment Analysis [7], predicting the helpfulness of product review text [8], Automated essay evaluation [9], and Natural Language Processing (NLP) [1]. Both speech and text require semantic analysis. In this paper, we confine our discussion to semantic analysis of the text only. Semantic analysis needs the concepts to discriminate the words or sentences. Latent Semantic Analysis (LSA) and Explicit Semantic Analysis (ESA) are essential models. LSA [10] depends on the statistics of the corpus to design concepts, whereas ESA [11] depends on the unambiguous concepts (like Wikipedia articles or sense labeled corpora) defined explicitly. The semantic analysis takes the support of Word Sense Disambiguation (WSD) [12] to assign a proper semantic tag (word sense) for a word. Knowledge-based and corpus-based approaches solve the WSD problem [13]. The word ‘*address*’ in the sentence, ‘The captain is responsible to **address** any issue’ means *direct one’s efforts towards something*, and in the sentence, ‘He doesn’t know the correct **address** of new office’ means *a place where a person or organization can be found or communicated with* (senses from WordNet 3.1¹). Let us see an example from the Telugu language. The word ‘అడుగు’ in the sentence ‘పది ఇంచుల పొడవుతో ఉండే ఈ జీవులు సముద్రంలోని అడుగు భాగంలో జీవిస్తాయి’, refers to *the lower side of anything* and in the sentence ‘దేవాలయానికి దారి ఎటో అడుగు’ means asking about something (senses from IndoWordNet²). The goal of WSD is to pick the correct sense of the ambiguous words ‘*address*’ and ‘అడుగు’ in the particular context, which leads to complete semantic analysis at the word level. Our contribution is three-fold towards Telugu WSD, (1) We have prepared sense annotated TELUGU corpus for the WSD task, (2) To our knowledge, we are the first to exploit IndicBERT embeddings for the TELUGU WSD task, and (3) We have tested our algorithm for different parameter values and reported statistically significant results. We have divided this paper into five sections. The second section presents a literature review on semantic analysis and WSD approaches. The third section describes the proposed methodology, followed by the fourth section describes the evaluation and results analysis. The fifth section includes the conclusion and provides recommendations for further work.

2 Related Work

Semantic analysis is fundamental in the NLP pipeline. NLP applications rely on semantics rather than just syntax, which results better. Therefore, it is essential to study the semantic representation in natural language, and computational semantics does this. The computational semantics for NLP has three main components [14] that are (1) Conceptual representation, (2) Link between natural language expressions and conceptual representation, and (3) Link between expressions and objects in the real world. Researchers have put in many efforts [2, 3, 15] to make computers understand

¹ <https://wordnet.princeton.edu/>.

² <https://www.cfilt.iitb.ac.in/indowordnet/>.

text semantics. There are many ways to measure the semantic relatedness between two words. One such way is Wikipedia link-based measure [16]. Latent Semantic Analysis (LSA) [17], which is a corpus-based approach and word thesaurus-based approach [18] to measure semantic relatedness. A methodology to evaluate semantic relatedness measures is required [19]. Contextual information is crucial to show the correlation between different semantics because words can have different meanings in other contexts. As semantics is nothing but the meaning of a word (or sentence), WSD algorithms are required to assign the correct sense/meaning to a particular word in the given context. Knowledge-based and corpus-based (supervised, unsupervised, and semi-supervised) approaches are available for WSD [13]. The most crucial step during the WSD process is representing the context. The context is nothing but a set of words, and features of these words have to be collected to define the word sense in that context. POS tags of Surrounding Words, Surrounding Words, and Local Collocations extracted by the supervised WSD system [20]. This system has reported an accuracy of 65.3 and 72.6% on SensEval-2 and SensEval-3 English lexical-sample tasks, respectively. Context expansion technique [21] considered synonyms as a feature to provide more information for WSD. In this technique, replacing context words with synonyms provides more training knowledge—local and topical features [22] used for sense representation. The local features include the ambiguous word itself, its POS tag, and POS tag of surrounding words, the verb, and noun before and after the ambiguous word. Apart from the features (synonyms and POS tags) which depend on external resources (knowledge sources and feature extractors), the word vector is another feature used to represent the word sense. The word embeddings define a word in a low-dimensional semantic space. The WSD system developed [23] by adding the word embedding as a new feature for the IMS WSD system [21] performs well. This system uses four different methods (Concatenation, Average, Fractional decay, and Exponential decay) to combine pre-trained word embeddings. The Word2vec [24], C&W [25], and Retrofitting [26] features were used [23]. BERT (Bidirectional Encoder Representations from Transformers) [27] pre-trained word embeddings have gained more popularity. It creates contextual dependent word vectors (different word vectors for the same word in other contexts), which are different from a contextual-independent word vector by Word2vec [24] and Glove [28]. Cosine similarity between context (various context window sizes ex. 2, 6, 10 and 14) and sense vectors [29] calculated. The label of sense vector with the highest cosine similarity is the correct sense for the ambiguous word. Considering cosine similarity in our work is inspired by this. Compared to English WSD, the Telugu³ language WSD is in the naïve phase. A decision list WSD algorithm for Telugu [30] used log-likelihood ratio is computed for each sense. Some statistical techniques were applied in [31] for WSD to measure the similarity between the sense bag and context bag of words. Graph-based approach [32] used a modified page rank algorithm for Telugu WSD. IndicNLP Suite [33] provides pre-trained context-dependent word embeddings for 11 Indian languages, and we have used these embeddings in our work to generate sentence embeddings. To this end, our

³ https://en.wikipedia.org/wiki/Telugu_language.

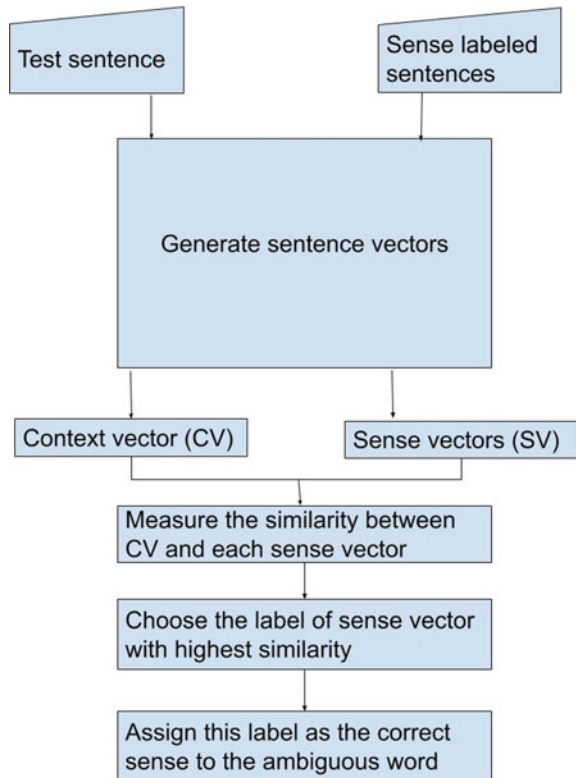
contribution to WSD for the Telugu language is applying IndicBERT embeddings for Telugu WSD.

3 Proposed Methodology

Figure 1 depicts the system flow diagram of the proposed word sense disambiguation. Our proposed system consists of the following steps:

- (1) Input a sentence (contains one ambiguous word).
- (2) Select the sense labeled sentences from the trained data set (containing target ambiguous word).
- (3) Generate sentence vector using Indic BERT embeddings [33] based on the words obtained in step 5.
- (4) Context Vector (CV) obtained from the input sentence.
- (5) Sentence vectors Obtained from sense labeled sentences are called Sense vectors (SV_k for $k = 1, 2, \dots, n$ where ‘ n ’ is the number of sense labeled sentences)

Fig. 1 Steps in proposed methodology



- (6) Measure the similarity (cosine similarity) between the Context Vector (CV) and each sense vectors using Eq. 1.

$$\text{Similarity}(A, B) = \frac{A \cdot B}{|A||B|} = \frac{\sum_{i=1}^n A_i \cdot B_i}{\sqrt{\sum_{i=1}^n A_i^2} \cdot \sqrt{\sum_{i=1}^n B_i^2}} \quad (1)$$

A is CV and B is SV_k for $k = 1, 2, \dots, n$.

- (7) Select the sense vector with the highest similarity.
 (8) Gets the sentence's sense label corresponding to the sense vector selected in step 2.
 (9) Assign this sense to the target ambiguous word.

3.1 Sentence Embedding

We have used pre-trained IndicBERT word embeddings [33]. The configuration settings of IndicBERT is: {"model_type": "albert", "attention_probs_dropout_prob": 0, "hidden_act": "gelu", "hidden_dropout_prob": 0, "embedding_size": 128, "hidden_size": 768, "initializer_range": 0.02, "intermediate_size": 3072, "max_position_embeddings": 512, "num_attention_heads": 12, "num_hidden_layers": 12, "num_hidden_groups": 1, "net_structure_type": 0, "gap_size": 0, "num_memory_blocks": 0, "inner_group_num": 1, "down_scale_factor": 1, "type_vocab_size": 2, "vocab_size": 200,000}.

Example: Sentence1— 'ఉదయం వేళ తూర్పు దిక్కు ఎరుపెక్కుతున్నది.'. Sentence2— 'ఊరి ప్రజలకు పెద్ద దిక్కు జమీందారు వంశం.'. Sentence3— 'పిల్లలంతా తలా ఓ దిక్కు దాక్కోవడానికి పరుగెడుతున్నారు.'. The word 'దిక్కు' means a *direction* in sentences 1 and 3, whereas in sentence2 it means a *person who helps*. Figure 2a shows the word vector of 'దిక్కు' is more similar in sentences 1 and 3 (with similarity = 83%). Figure 2b shows the word vector of 'దిక్కు' is not much similar in sentence1 and 2 (with similarity = 58%).

```

ఉదయం వెళ్ తూర్పు దిక్కు ఎరుపెక్కుతున్నది.
పిల్లలంతా తలా ఓ దిక్కు దాక్కోవడానికి పరుగెడుతున్నారు .
Vector similarity for meaning of the word దిక్కు: 0.83
Vector similarity for sentences: 0.88
>>> |

```

(a)

```

ఉదయం వెళ్ తూర్పు దిక్కు ఎరుపెక్కుతున్నది.
ఊరి ప్రజలకు పెద్ద దిక్కు జమిందారు వంశం.
Vector similarity for meaning of the word దిక్కు: 0.58
Vector similarity for sentences: 0.81
>>> |

```

(b)

Fig. 2 Cosine similarity between the same words in different contexts

3.2 Algorithm

WSD Indic BERT Algorithm

Input: Test sentence with one ambiguous word

Parameters: Context window size CW

Output: Sense label of the ambiguous word

1. Let S be the input sentence
 2. Let p is the position of ambiguous word AW in S
 3. Store the output after the Tokenization step of IndicBERT, tokens in T , where T is an array of words
 4. With all tokens in $T[p-CW:p+CW]$, form a sentence
 5. Generate sentence vector V_c , i.e., the context vector
 6. Let the word AW has ' n ' number of senses
 7. for each sense of n senses
 8. Get *sentences* formed with the word AW from the training data set.
 9. for each *sentence*
 10. repeat steps from 3 to 4
 11. Generate sentence vector V_s , i.e., the sense vector
 12. Calculate cosine similarity between V_c and V_s
 13. **return** the *sense label* associated with the sense vector with the highest cosine similarity
-

3.3 Illustrative Example

- Target ambiguous word: దిక్కు
- Possible senses are 1. దిశ 2. శరణము
- Test sentence: 'పిల్లలంతా తలా ఓ దిక్కు దాక్కోవడానికి పరుగెడుతున్నారు .'.

- Context window size: 3
- Context Words after Preprocessing: పిల్ల, అంతా, తలా, దాక్కో, పరుగెట్టు
- Context vector: V_{c_test}
- Table 1 shows context vectors in the training data set.
- Table 1 contains the similarity between the test context vector (V_{c_test}) and each sense vector (V_1 to V_6) mentioned in Table 1.

By referring to Table 1, the similarity between test context vector (V_{c_test}) and context vector (V_1, V_2, V_3) is more similar than the other context vectors, so the sense label corresponding to it, i.e., 'దిశ'(direction) will be assigned to the ambiguous word 'దిక్కు' in the given test sentence: 'పిల్లలంతా తలా ఒ దిక్కు దాక్కోవడానికి పరుగెడుతున్నారు.' (The children are running in different directions to hide.). Figure 3 shows context vector and sense vectors. This figure shows how similar this context vector V_{c_test} is to the sense vectors V_1, V_2, V_3 , which are associated with sense 'దిశ'.

4 Evaluation and Result Analysis

We have selected a set of 9000 ambiguous words to test our algorithm. The ambiguous words and their senses are collected from various dictionaries.⁴ We have prepared a sense annotated corpus. Our test dataset contains 50 sentences for each of the 9000 ambiguous words. We have evaluated our algorithm on this dataset using this sense annotated corpus. Table 2 shows the algorithm's accuracy compared with Most Frequent Sense (MFS) baseline. In most cases, the algorithm's accuracy is more when the context window is larger (window size = 4). The ROC (Receiver Operating Characteristic) curve for word specific model of ambiguous word 'క్రియ' with 12 senses is shown in Fig. 4.

But whether the classification can be done with the default parameter (context window size $CW = 4$) setting or with changed parameters (context window size $CW = 2$ and 3) has to be decided based on the statistical significance test. The hypothesis testing is conducted with a defined Null hypothesis (H_0) and alternative hypothesis (H_1).

H_0 : Classifier achieves the best accuracy with changed values of parameters.

H_1 : Classifier achieves the best accuracy with default values of parameters.

The change of accuracies of different word-specific classifiers is shown in Fig. 5, and the hypothesis test using t-test is carried out with significance level 0.05 produced p-value $\cong 0.24940078566390272$, T-value $\cong -1.15214382359384$. The observed p-value suggests that the Null hypothesis is not valid, so classification with default parameter values is recommended.

⁴ **Shabdaratnakaram** by Bahujanapalli Sitha Rama Acharyulu, **Telugu-Telugu Dictionary** by Telugu Academy, Hyderabad.

Table 1 Context vectors for various instances of an ambiguous word for different senses

Ambiguous word	Context	Context vector	Sense label	Similarity between V_{c_test}
దిక్కు	ఉదయం వేళ తూర్పు దిక్కు ఎరుపెక్కుతున్నది.	V1	దిశ	0.86
దిక్కు	సూర్యాదేవి ఉత్తరం దిక్కు కనపడటట్లు కుర్చీ తిప్పుకుని కూర్చుంది.	V2	దిశ	0.89
దిక్కు	ఆ ప్రవాహం ఒక దిక్కు నుండి ప్రవహిస్తూంది.	V3	దిశ	0.80
దిక్కు	ఊరి ప్రజలకు పెద్ద దిక్కు జమీందారు వంశం.	V4	శరణము	0.79
దిక్కు	ఆ కులాడిని ఓదార్చే దిక్కు అంతకంటే లేదు.	V5	శరణము	0.78
దిక్కు	ఈ అడవిలో పిల్లిస్త పరిక దిక్కు కూడా కరువైపోయింది.	V6	శరణము	0.75

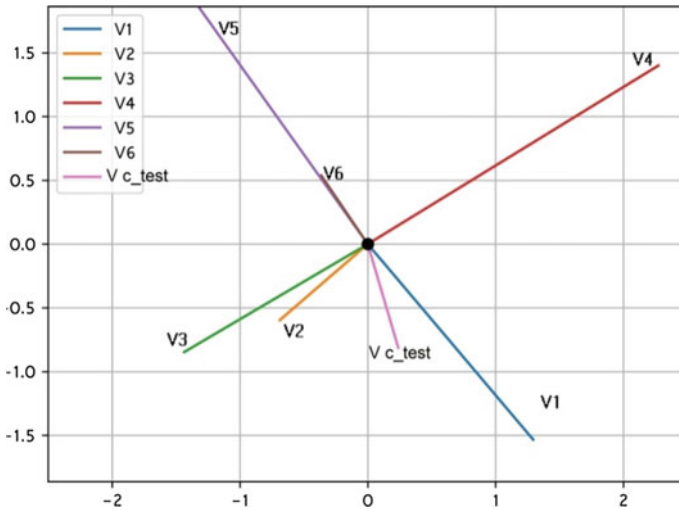


Fig. 3 Context vector and sense vectors in 2-D

Table 2 Comparison of the accuracy of the algorithm with MFS baseline for some ambiguous words

Ambiguous word	Accuracy %			
	Window size = 3		Window size = 4	
	Our algorithm	MFS	Our algorithm	MFS
"ఇల"	55	52	65	68
"గం"	72	74	81	76

5 Conclusion and Future Work

In this digital era, getting semantics from the digitally available massive amount of text is very important and results in better user queries. In this process of getting semantics, analyzing the meaning of a word is very important in NLP. The presence of ambiguous words in any natural language leads to WSD. A lot of work done concerning the English language, but it's in the naive phase for Telugu. So we have attempted to solve WSD in the TELUGU language. The ambiguous word which appears in the same context gets the same meaning. So it is essential to represent the context that Indic BERT embeddings can do correctly. Words in the specific window size have been used for context preparation. The accuracy of our algorithm improves as the size of sense annotated corpus increases, and more efficient context representation techniques are in need.

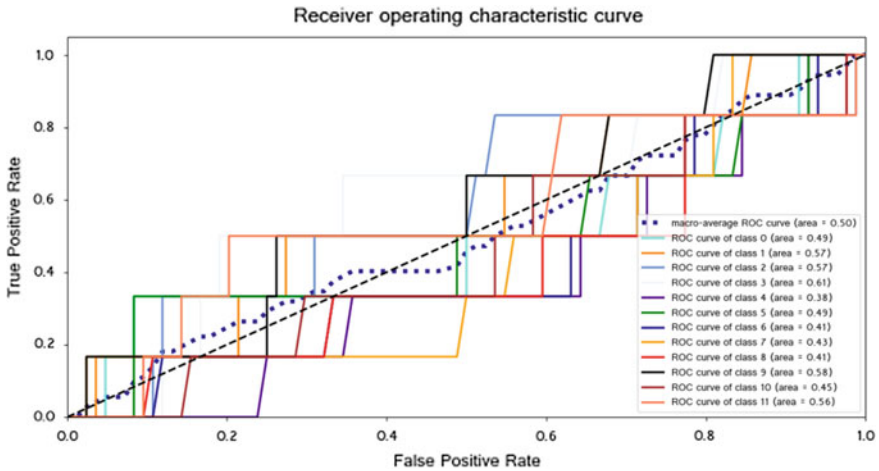


Fig. 4 ROC curve of one for the ambiguous word 'క్రియ' with 12 senses

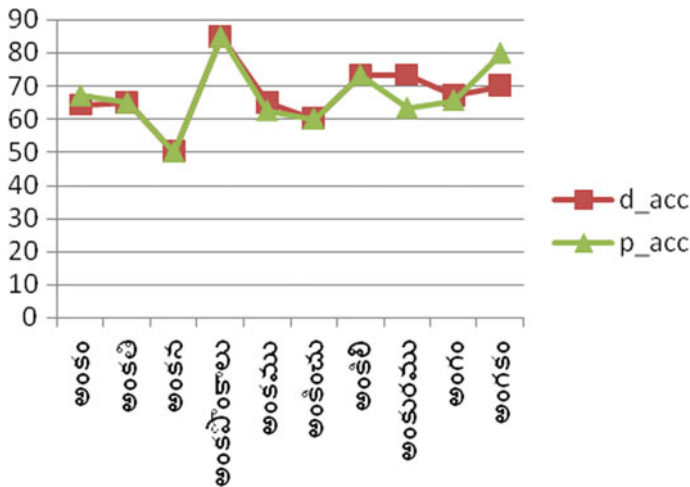


Fig. 5 X-axis shows ambiguous words, and the y-axis shows accuracy where d_acc and p_acc are accuracies with default and changed parameter values, respectively

References

1. Indurkha N, Damerou FJ (Eds.) (2010) In: Handbook of natural language processing, vol 2. CRC Press
2. Koskela M, Smeaton AF, Laaksonen J (2007) Measuring concept similarities in multimedia ontologies: analysis and evaluations. IEEE Trans Multimedia 9(5):912–922
3. Wang D, Li T, Zhu S, Ding C (2008) Multi-document summarization via sentence-level

- semantic analysis and symmetric matrix factorization. In: Proceedings of the 31st annual international ACM SIGIR conference on Research and development in information retrieval, July, pp 307–314
4. Salakhutdinov R, Hinton G (2009) Semantic hashing. *Int J Approximate Reasoning* 50(7):969–978
 5. Huang Y, Li G (2010) A semantic analysis for internet of things. In: 2010 international conference on intelligent computation technology and automation, May, vol 1. IEEE, pp 336–339
 6. Haggag MH (2013) Keyword extraction using semantic analysis. *Int J Comput Appl* 61(1):1–6
 7. Gautam G, Yadav D (2014) Sentiment analysis of Twitter data using machine learning approaches and semantic analysis. In: 2014 seventh international conference on contemporary computing (IC3), August, IEEE, pp 437–442
 8. Yang Y, Yan Y, Qiu M, Bao F (2015) Semantic analysis and helpfulness prediction of text for online product reviews. In: Proceedings of the 53rd annual meeting of the association for computational linguistics and the 7th international joint conference on natural language processing, July, (Volume 2: Short Papers), pp 38–44
 9. Zupanc K, Bosnić Z (2017) Automated essay evaluation with semantic analysis. *Knowl-Based Syst* 120:118–132
 10. Dumais ST, Furnas GW, Landauer TK, Deerwester S, Harshman R (1988) Using latent semantic analysis to improve access to textual information. In: Proceedings of the SIGCHI conference on Human factors in computing systems, May, pp 281–285
 11. Gabrilovich E, Markovitch S (2007) Computing semantic relatedness using Wikipedia-based explicit semantic analysis. In: *IJCAI*, January, vol 7. pp 1606–1611
 12. Ide N, Véronis J (1998) Word sense disambiguation: the state of the art. *Comput Linguist* 24(1):1–40
 13. Navigli R (2009) Word sense disambiguation: a survey. *ACM Comput Surveys (CSUR)* 41(2):1–69
 14. Creary LG, Pollard C (1985) A computational semantics for natural language. In: 23rd annual meeting of the association for computational linguistics, July, pp 172–179
 15. Aiello M, Monz C, Todoran L, Worring M (2002) Document understanding for a broad class of documents. *Int J Doc Anal Recogn* 5(1):1–16
 16. Witten IH, Milne DN (2008) An effective, low-cost measure of semantic relatedness obtained from Wikipedia links
 17. Landauer TK, Foltz PW, Laham D (1998) An introduction to latent semantic analysis. *Discourse Process* 25(2–3):259–284
 18. Tsatsaronis G, Varlamis I, Vazirgiannis M (2010) Text relatedness based on a word thesaurus. *J Artif Intell Res* 37:1–39
 19. Taieb MAH, Zesch T, Aouicha MB (2020) A survey of semantic relatedness evaluation datasets and procedures. *Artif Intell Rev* 53(6):4407–4448
 20. Zhong Z, Ng HT (2010) It makes sense: a wide-coverage word sense disambiguation system for free text. In: Proceedings of the ACL 2010 system demonstrations, July, pp 78–83
 21. Yang Z, Huang HY (2012) Chinese word sense disambiguation based on context expansion. In: Proceedings of COLING 2012: Posters, December, pp 1401–1408
 22. Dandala B, Mihalcea R, Bunescu R (2013) Word sense disambiguation using Wikipedia. In: *The people’s web meets NLP*, Springer, Berlin, Heidelberg, pp 241–262
 23. Iacobacci I, Pilehvar MT, Navigli R (2016) Embeddings for word sense disambiguation: An evaluation study. In: Proceedings of the 54th annual meeting of the association for computational linguistics (Volume 1: Long Papers), August, pp 897–907
 24. Mikolov T, Le QV, Sutskever I (2013) Exploiting similarities among languages for machine translation. arXiv preprint [arXiv:1309.4168](https://arxiv.org/abs/1309.4168)
 25. Collobert R, Weston J (2008) A unified architecture for natural language processing: Deep neural networks with multitask learning. In: Proceedings of the 25th international conference on Machine learning, July, pp 160–167

26. Faruqui M, Dodge J, Jauhar SK, Dyer C, Hovy E, Smith NA (2014) Retrofitting word vectors to semantic lexicons. arXiv preprint [arXiv:1411.4166](https://arxiv.org/abs/1411.4166)
27. Devlin J, Chang MW, Lee K, Toutanova K (2018) Bert: pre-training of deep bidirectional transformers for language understanding. arXiv preprint [arXiv:1810.04805](https://arxiv.org/abs/1810.04805)
28. Pennington J, Socher R, Manning CD (2014) Glove: global vectors for word representation. In: Proceedings of the 2014 conference on empirical methods in natural language processing (EMNLP), October, pp 1532–1543
29. Orkphol K, Yang W (2019) Word sense disambiguation using cosine similarity collaborates with Word2vec and WordNet. *Future Internet* 11(5):114
30. Palanati DP, Kolikipogu R (2013) Decision list algorithm for word sense disambiguation for TELUGU natural language processing. *Int J Electron Commun Comput Eng* 4(6):176–180
31. Durga Prasad P, Sunitha KVN, Rani BP (2018) Context-based word sense disambiguation in Telugu using the statistical techniques. In: Proceedings of the second international conference on computational intelligence and informatics, Springer, Singapore, pp 271–280
32. Koppula N, Rani BP, Srinivas Rao K (2019) Graph-based word sense disambiguation in Telugu language. *Int J Knowled-based Intell Eng Syst* 23(1):55–60
33. Kakwani D, Kunchukuttan A, Golla S, Gokul NC, Bhattacharyya A, Khapra MM, Kumar P (2020) iNLPSuite: monolingual corpora, evaluation benchmarks and pre-trained multilingual language models for indian languages. In: Proceedings of the 2020 conference on empirical methods in natural language processing: findings, November, pp 4948–4961

Location-Based Bus Tracking Application Using Android



Sourav Kumar, Shreyash Moundekar, Mansing Rathod,
and Rupesh Parmar

Abstract In this twenty-first century, as there is a big increase in population, there is also a necessity for a well-organized public transportation application. Due to which, a huge load falls on public transportation like buses, etc. But if you see the facts, many people prefer to take their own vehicles. There is no real time information about the bus and location along the bus route as well as there is no prior knowledge in case the bus is canceled or delayed due to traffic jams. As a result, the precious time of commuters is lost which is not good. The number of buses running daily is huge which makes it very difficult to track all the buses due to which it poses a big challenge before the bus authorities. Hence the smart bus application is essential. So a new application which conquers the limitations of the public transportation system has been put forward by us. Our application takes the required details and by using this information tracing of the bus is done and passenger can get this details in real time any minute.

Keywords Tracking · Bus system · Android · Location tracker

1 Introduction

Many buses are made accessible for people traveling long distances, but issue is that public do not have knowledge about it, i.e., the frequency of buses which visit the said destination, numbers and timings of the bus, ways via the bus could go, time consumed by the bus to cover some particular distance, a good map that will help

S. Kumar (✉) · S. Moundekar · M. Rathod · R. Parmar
K.J. Somaiya Institute of Engineering and Information Technology, Mumbai, India
e-mail: sourav.kumar@somaiya.edu

S. Moundekar
e-mail: s.moundekar@somaiya.edu

M. Rathod
e-mail: rathodm@somaiya.edu

R. Parmar
e-mail: rupesh.parmar@somaiya.edu

user with the way and before anything else, live tracking of the vehicle [1]. So, in our proposed application we have used an Android system that gives required details about all the buses traveling in a particular city. The reason we have used Android Operating System is because it has come up on a big scale and is almost, used by many people. Also, Android is an easy to use Operating System, thereby reducing difficulty for all the users. Motivation of our system is to rectify the Bus application by including the required characteristics into the system, like accuracy, timings of buses, bus indications, etc. This application takes the input from the user, and asks for the preferable output as destination and retrieve the data from dataset and displays map for the same. Based on our research and comparison between various similar approaches, we found none of the systems were fully functioning in desired motive. This diagram shows the working of the Database Administrator with client and Server Application to extract location, bus information and to update the information on the user's side (Fig. 1).

This diagram shows the working of the Database Administrator with client and Server Application to extract location bus information and to update the information on the user's side.

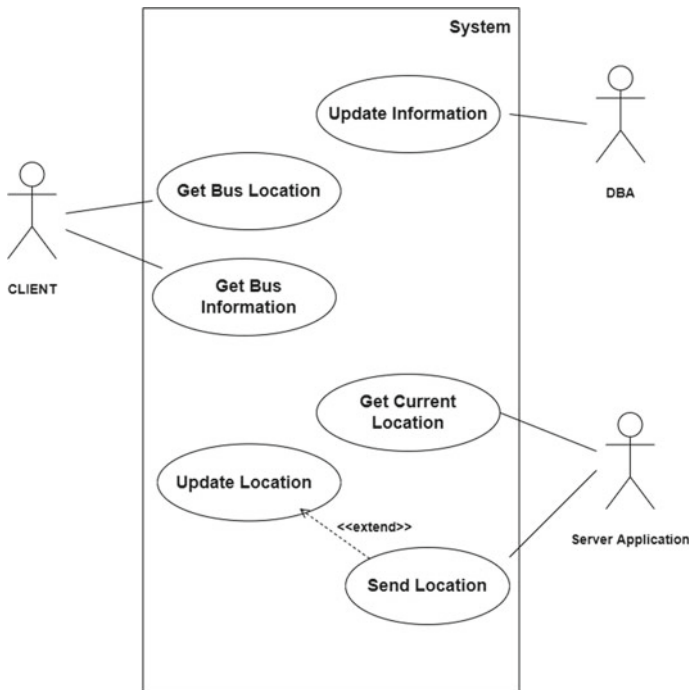


Fig. 1 Use case diagram for bus tracking application

2 Literature Review

Sneha et al. [2] this paper gives a brief summary of the app made for the passengers for locating the bus and then notifying them [3]. Arrival time of buses and various vehicles especially in smart cars Artificial Neural network (ANN) is used to (ETA) to the commuter by means of an application. Use of mobile data for the connectivity and communication and GPS system for the location in real time are embedded in existing system. ITS helps overcome the issue faced while waiting time. And saves time and also solves the issue regarding the choice of the route of same destination [1]. In this paper, a novel approach for location estimation called Bus Tracking Application is presented based on flexible location approximation concept and GPS approach. First novel GPS-based location approximation method is done. The experimental assessment of proposed approach is done using java simulation tool by considering both simulation and real time research. Both results claimed that proposed Advanced Bus Tracking Application has accomplished better accuracy and performance as differentiated to existing Bus Tracking System [4]. Application was proposed for the ease of the parents so they do not have to worry about the children all the time worrying, as the application was able to notify the parent regarding the current location of their children using messaging system [5]. This system was mostly based on these three common factors of bus tracking, cloud computing, and Internet of Things (IOT). Proposed system was able to estimate the nearest stoppage and the time with real time tracking of bus, making user aware of the conditions and timing of the buses along with the checking of availability of the tickets and booking tickets for the same along with the payment method integrated with it and booking for the same. The Google traffic API was used to track the obstacles and variation in the timing for reaching the destination [6]. Proposed system mainly deals with the API, Kalman Filter, web-server, Google maps. This application was focused on helping the students for saving time while reaching colleges by giving them the brief knowledge about various buses, those who already missed any particular bus [7]. An application in Pune, named “Pune Local Bus Guide”—It is an app made for the local residents of Pune but it is pathetic as it keeps on searching endlessly without any results displayed. A passenger enters source and destination and then find routes and add is displayed and the app gets closed automatically [8]. Considering about M- Indicator app—It is not a user-friendly app as it is really confusing for the first time user as many people do not know which bus to take for their destination [9]. Another app known as Delhi Bus Routes has drawbacks like: It has incomplete data and is unable to find all the routes [10]. Bangalore City Bus app has drawbacks like: It does not provide right details and most of the time, it crashes [11]. The bus app Chennai Bus has issues like its performance is poor. Also, a major improvement is required [12]. In this paper, the proposed application tells us about the GPS System used for tracking the bus. The smart ticketing controlling and monitoring device will also contain the dynamic routes which range as per the bus depot [13]. Here, on this paper efforts have been taken by Mane et al. to boom the pleasure and clarifications of modern public transportation for users. Also, it could assist present riders and encourage

new riders through improving the usability of public transportation via top transit tourist statistics systems. A beneficial function of a current cellular tool is that it could function itself. For each use of the tool and for the application that requires monitoring of the tool. Furthermore, monitoring has to supply function updates while confronted with converting situations and instances including delays because of positioning and conversation and converting positioning [14]. In this paper, the application has two units installed in the bus, i.e., one unit at the entry gate and the other unit at the exit gate. Each unit is used to scan the entry and exit instances of the users who will carry a Radio Frequency Identification (RFID) tag that will be inspected by RFID as every unit has GPS module which would update the bus location at specific small periods which will be helpful in capturing user's real time venue at both the situations. The application will interpret the price and the cost for the distance traveled and decreases the fare amount from the passenger's online wallet. Apart from this, the system is also efficient of tracking live bus location, so that the user can plan the desire location as per that. As all the transactions are documented in the database they are initialized and computed for planning the bus schedules and computing the frequency of buses needed on a route. Daily, weekly and monthly passengers traveling details will be computed through graphs and data through real time data reception. Hence, smart bus is a very useful and highly dependable application [15]. Here, the application has WiLocator(p) which uses the historical details of bus locations to analyze dominated road sub-segments of Wi-Fi APs, such that do not take the stress to locate a bus from start, and the suggested structure can be used for searching undisclosed Wi-Fi APs surrounding the bus streets, and indoor localization as well. Also, implementation of the paradigms of WiLocator and WiLocator(p) is done and then conduction of the real time experiments to show their capability in bus tracking.

3 Smart Bus System Overview

Mainly there are two sides of this system—(1) Driver/Conductor side and (2) User's side. Basically, all the functionalities will be performed by Driver/ Conductor according to the pre-decided routes and timings and all these performed tasks and data will be shown to the users. Our application will offer the users the following benefits (1) This system will help the people know if a bus is not on schedule or has been canceled due to technical or weather problems and other natural reasons. (2) Also, system will tell people whether they have just missed the bus so they do not have to wait for the bus and it will also tell them how long it is going to be until the next bus arrives. (3) It would be helpful for the bus drivers as they need not maintain the time log but instead of that system will monitor the accurate log for them. (4) For the users, app will show their current venue and the stop they have reached and what are the next stops, what time it will take and how much distance it is yet to be covered (Fig. 2).

Functionalities of the Driver's/Conductor side –(1) As soon as driver starts the bus according to the pre-defined routes, he will be traced through the app (as he is

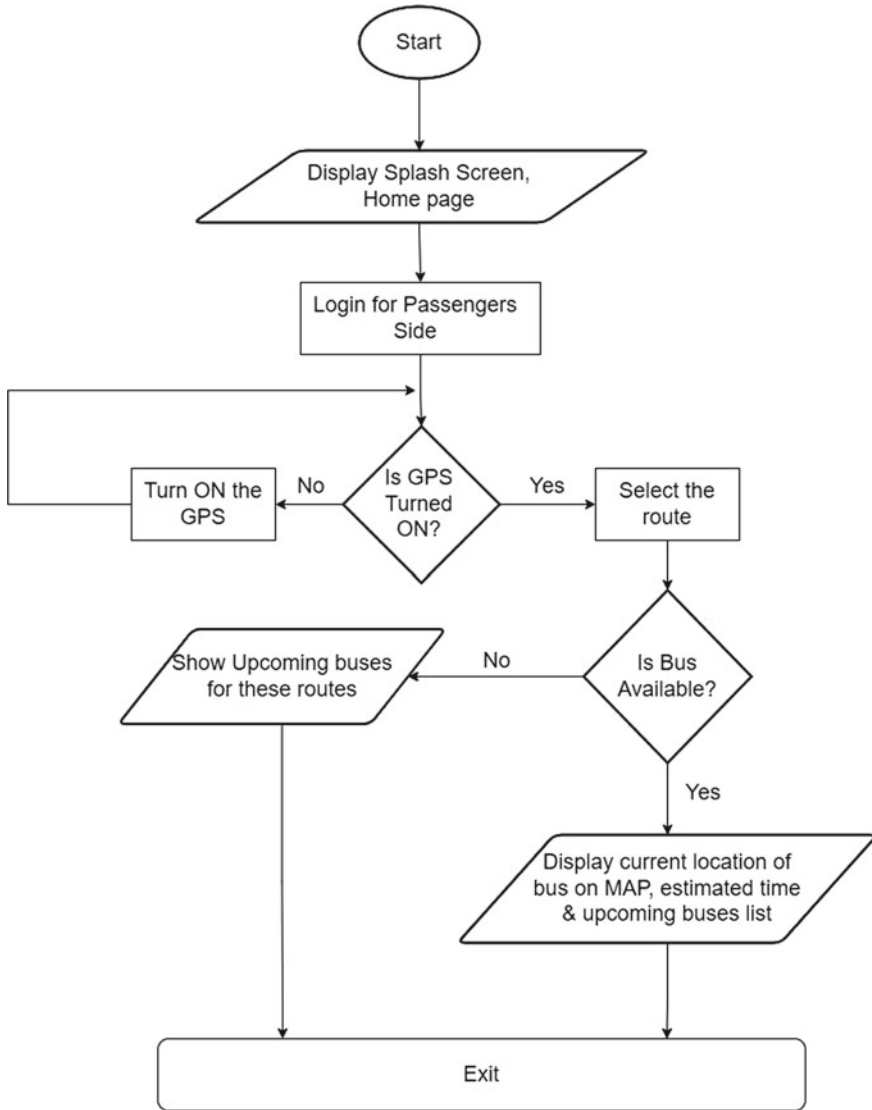
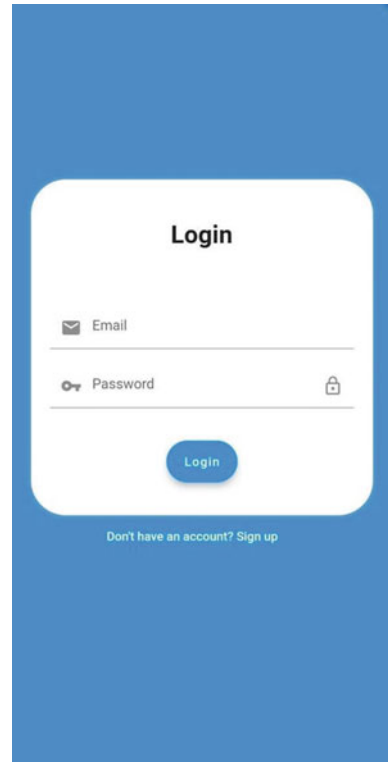


Fig. 2 Flowchart of bus tracking application

the one who represents the bus) and this data will be shown to the users. (2) We will be using drivers/conductor’s phone to know the exact location and show this location data on map which will be refreshed time to time. (3) For other users, those who want to know about the upcoming buses will get to know by selecting starting point and destination, and the application will show the arrival of upcoming buses. Also, it will show the data related to the bus like bus number, frequency of the buses, etc.

Fig. 3 Login page for drivers and passengers



(4) Users will also know whether the bus is canceled or not, as this task is performed on the Driver/Conductor side (Figs. 3 and 4).

4 System Specifications and Requirements

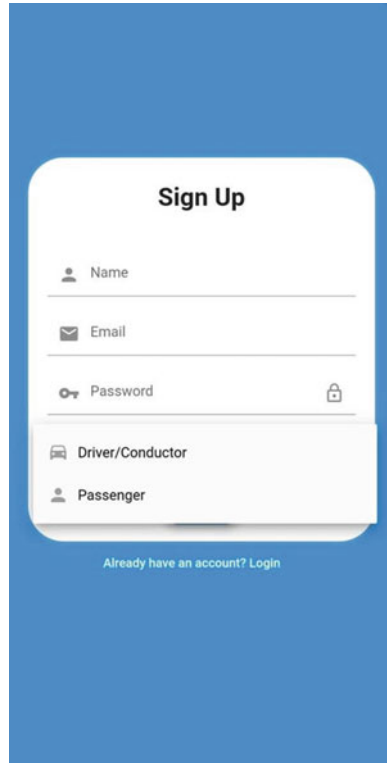
Android Studio and Android SDK

A most basic requirement for android application development is android SDK along with a flutter tool kit. In contrast to the other android platform, Android Studio has a large feature list and is easy to use to increase productivity.

GPS embedded mobiles

In this part regulations encouraging mobile phone tracking, includes E911 and most GPS receiving units are built into mobile android devices and cells, with varying range of coverage and user-friendly. Commercial navigating software program is availability from maximum twenty-first century smart phones in addition to a few Java-enabled mobiles that enables them to apply an inner or outside GPS receiver.

Fig. 4 Sign up page for driver/conductor and passengers



Some mobiles uses assisted GPS (A-GPS) characteristic poorly while out of variety in their carrier’s towers. Considering different consumer can navigate internationally with satellite GPS in addition to a committed transportable GPS receiving unit which upgrades their operation to A-GPS online tracking mode in some predicted area. Still, others occupy a hybrid and awesome tracking device which can use different alerts while GPS alerts are inadequate.

Mobile Messaging

Mobile messaging performs a critical position in Location-Based Service. Messaging, especially Short Message Service, has been utilized in mixture with numerous LBS packages, along with location-primarily-based totally cell marketing and marketing. Most simple and one of the mom generation SMS remains the main generation in marketing. A simple instance of LBS packages the usage of SMS is the transport of cell coupons and reductions to cell subscribers who are close to marketing and marketing business restaurants, cafes, film theaters, etc. Following is the graphical display of the flow of data in a Bus information system. It shows incoming data and outgoing data, and stores data from Server, User and Database. And this flow of data connects the System with the Server and User (Fig. 5).

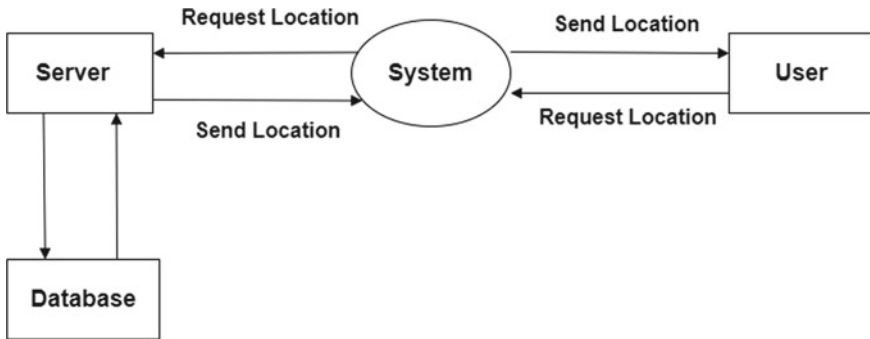


Fig. 5 Data flow diagram (DFD)

5 Results and Discussion

This architecture shows the proper working of Mobile GPS with the server, Google Maps, Driver, and Passenger. It also shows how the system validates the request and provides the required response (Figs. 6 and 7).

This is the exact location tracked by the system using Mobile GPS tracking and all the functionalities are performed by the system keeping this location in mind. Essential area details are provided to the person in addition to bus number so that the passenger identifies his/her bus properly. This software may be placed up at the cloud platform with the intention to be on hand with the aid of each Android user and also, the server will not be burden. We will add a database which is firebase so that the records are not easily exploited by any third-party source. The software will be beneficial for each bus traveler, or maybe site visitors and tourist. Not simply buses, however this software may be beneficial for anybody visiting and non-visiting individual by any method of transport. Also, Location Tracer tells the precise venue of the vehicle that would make it appropriate for the people to navigate. Basically, the system works on the concept that bus drivers/conductors are the carrier, once they log in to their account, the location API (GSM) gets activated and the system comes into the role. Receivers are none other than the passengers, they get notified regarding if the bus has been scheduled or canceled or even late, as it is real time application any change in the driver/conductor (carrier) side will be automatically reflected to the passenger (receiver) side. Flutter was the main source of the software kit used in the system as all the pre-installed libraries are in one software kit. Comparisons were made between Kotlin and Flutter to decide for making a user—friendly application so the person of any age group may be child, adult or aged person can use it easily. Basically, it is a user-friendly application. Further our Flutter code was integrated with the Firebase database. All the confidential dataset were introduced in the Firebase database so that the application can fetch the data. Once the bus gets started, i.e., the bus/conductor have logged in to the application data is retrieved from the database which has already been added regarding the timing of the buses, bus number, starting

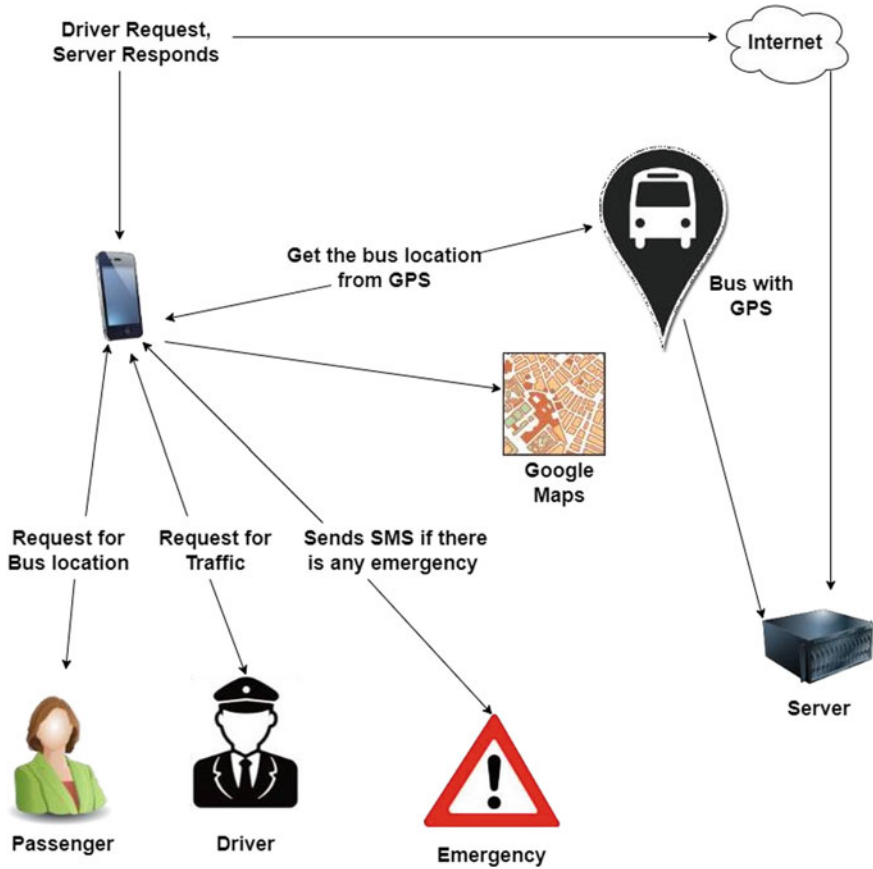
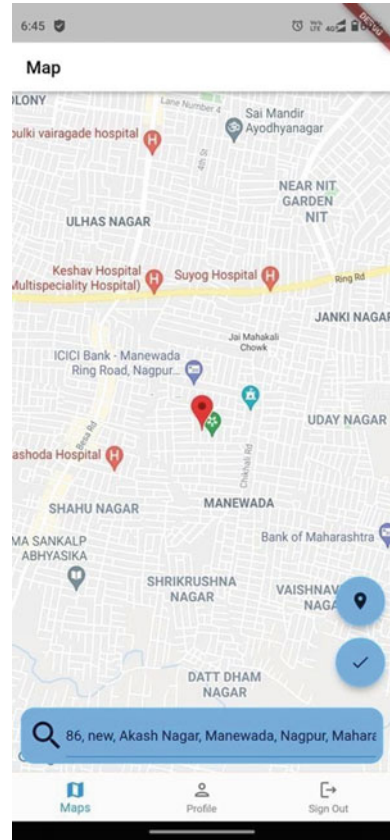


Fig. 6 Design and architecture of bus tracking

location of the bus, the destination, the route that has to be followed on the way. If the conductor side fails to login, then data retrieval gets broken, it notifies the user side that the bus has not been scheduled, or maybe canceled depending on the circumstances. Data is continuously being retrieved by the application from the database to check the time whether the bus is being late or on time. As due to pre-defined data set user or the passenger will be able to see the only readable information like bus number, and detailed route and information like bus conductor or bus driver name that have been allocated to the specific buses and already logged in for the initiation of the bus, however bus driver/conductor side has the rights of readability and any change in log in times, i.e., bus being scheduled late or the path being with more constraints causing bus getting late driver/conductor can add their feedbacks. Later after this main part of the application, Google GSM API has been integrated for the real location-based scenarios; users can fetch the data about their current location, and the location of the buses. Passengers will be able to see the route through which

Fig. 7 Live interactive map



their current bus is traveling and from this they will be able to estimate their time of reaching. As time has been recorded of the destination and starting of the buses, the app will keep the record about the time of being late. Live tracking has been done in this application so estimation of the time and the disregard of the bus being late and the most probable reason for the same can be retrieved by the bus/conductor side through their feedback. Early on all the drawbacks and the functionalities of different kinds of similar applications were studied and compared. All are discussed below (Table 1).

6 Conclusion

This App was put forward on android platform with the use of android SDK and flutter. Also, different functionalities and uses have been added. The necessary parameters have been mentioned above. With the help of GPS, the system will inevitably

Table 1 Comparison table of all major cities bus application

Pune bus guide	M-Indicator	Delhi bus indicator	Bangalore BMTC information
PMPML Bus Routes	BEST, NMMT, TMT, KDMT, MBMT, VVMT, KM T	DTC Buses of red, green, and orange colors	BMTC
Search buses by route number, view the route details and give way to the destination correctly	Route info & the number of buses by the route are available	Shows the routes, transit times, and comparison between two trip options	It has the source and destination added. Users can search bus by choosing Source to Destination
Current location is Disabled in GPS location	The field for the operation remains blank whenever the field of option is selected (no bus routes are displayed)	The application works smoothly when not connected to the broadband but works very badly (lags) when connected to the internet	This application crashes almost always. It has complicated user interface

present the map and ways to the divergent venues and trace down the bus area through client—data processor mechanization and then, give it to the client device. It does analysis of the range between two areas and lay down required information of each and every way so that people pick up buses comfortably or any other convenient way possible on their final destination.

References

1. Darshan I, Bhagwan, A.B (2018) Real-time analysis and simulation of efficient bus monitoring system. In: 2nd international conference on electronics, communication and aerospace technology (ICECA 2018)
2. Sneha M, Urs CN, Chatterji S, Srivatsa MS, Pareekshith JK, Kashyap HA (2014) Darideepa—a mobile application for bus notification system. In: International conference on contemporary computing and informatics
3. Sharad S, Sivakumar PB, Narayanan VA (2016) The smart bus for a smart city. A real-time implementation. In: IEEE international conference on advanced networks and telecommunications systems
4. Majd G, Athar G, Hawraa H, Ali B, Samih A-N (2017) Smart bus- a tracking system for school buses. In: Sensors networks smart and emerging technologies
5. Sharmin A, Thouhedul I, Olanrewaju RF, Binyamin AA (2019) A cloud-based bus tracking system based on internet-of-things technology. In: 7th international conference on mechatronics engineering
6. Shubham J, Adarsh T, Shweta S (2019) Application based bus tracking system. In: International conference on machine learning (2019) Pune Guide
7. <https://play.google.com/store/apps/details?id=com.pune.busticketprice> M-Indicator, <https://play.google.com/store/apps/details?id=com.mobond.mindicator> Delhi, BusInfo
8. <https://play.google.com/store/apps/details?id=com.uwemo.delhibusroutesangalore>

9. <https://play.google.com/store/apps/details?id=com.wmdev.bus.bangalorecitybusChennaiBusRoute>
10. <https://play.google.com/store/apps/details?id=io.ionic.starter67676>
11. Shingare A, Ankita P, Nikita C, Parikshit D, Sonavane S (2015) GPS supported city bus tracking & smart ticketing system. In: 2015 International Conference on Green Computing and Internet of Things (ICGCIoT)
12. Sonavane, Samadhan (2015) GPS supported city bus tracking and smart ticketing system. In: International conference on green computing and internet of things
13. Mane K, Suresh P, Vaishali (2014) Analysis of bus tracking system using GPS on smartphones, March-April
14. Shah MJ, Prasad RP, Singh AS (2020) IOT based smart bus system. In: 3rd international conference on communication system, computing and IT applications
15. Zhang R, Wenping L, Yufu J, Guoyin J, Jing X, Hongbo J (2018) WiFi sensing-based real-time bus tracking and arrival time prediction in urban environments. *IEEE Sensors J* 18(11)

Extended Informative Local Binary Patterns (EILBP): A Model for Image Feature Extraction



Sallauddin Mohmmad and B. Rama

Abstract In the area of Image Processing extraction of feature from an image done by most preferred model of many researches named Local Binary Patterns (LBP) which is widely used local texture descriptors. In the context of feature extraction the global invariant features also applicable for texture classification. Classical LBP has a major drawback which is unable to process the global spatial information in context of little local texture information more global features preserve. In this paper we proposed a model to match the global rotation invariant to local texture information to preserve the more information to classify in better way named as Extended Informative Local Binary patterns (EILBP). The Proposed method will reduce the loss of global special information. In this process instead of computing the joint histogram globally the EILBP evaluate the VAR from local regions accurate them with LBP bins. This process greatly reduced the large training data sets. In our model the classification have done with SVM and normalized feature forwarded as input to the SVM to provide accurate result for match. The experimental results of proposed model achieved significantly improved compared to classical LBP.

Keywords LBP · EILBP · SVM

1 Introduction

Image processing and recognition of objects become most analytical process have played important role in past decade and present due to its importance in current challenges with huge application needs. The current research on image processing reached certain level of technological needs and still to need of more research to expected value in this era. Image processing presently adopted to many areas such

S. Mohmmad (✉)

Department of Computer Science and Artificial Intelligence, SR University, Warangal, Telangana 506371, India
e-mail: sallauddin.md@gmail.com

B. Rama

Department of Computer Science, Kakatiya University, Warangal, Telangana 506009, India
e-mail: rama.abbidi@gmail.com

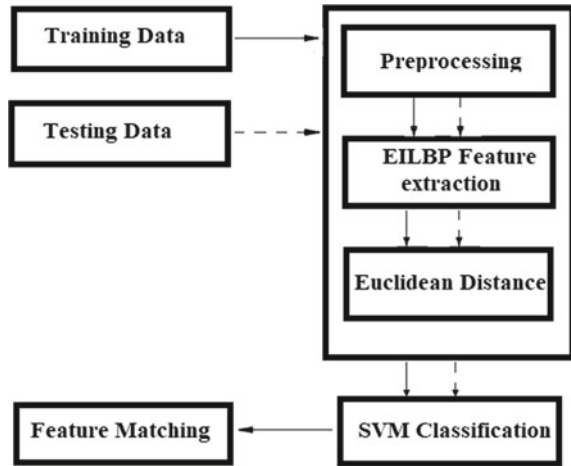
as IoT, ML, Security Data analytical and to act as part of human vision transparency [1, 2]. The major key evaluation processes to the image process are preprocessing of image, feature extraction and classification. Basically preprocessing extracts the accurate features from input image. The most effective preprocessing technique is histogram equalization which is best approach to betterment of image processing. The object detection in an image can follow the basic two approaches to extract the feature they holistic features or local features. In the holistic approach the entire object region formed into subspace representing only object [6]. There are several algorithms are initiated for holistic approach to process the image identification in a better way. The research has done for Neural Networks, linear models, analysis models and, etc. Here some of them are Principle Component Analysis (PCA) [2, 3], Linear Discriminate Analysis (LDA) [4], Locally Linear Embedding (LLE) [5, 6] and Locally Preserving Projections (LPP) [7, 9]. But the holistic feature extraction approach will not find the local differentiation like movements in the object such as appearance, expressions and, etc. According to the image processing local space of image identification need to find each part of the movement to find the expression. On the other hand the local feature extraction process first extracts the local region space feature from the subspace then all local features classify by combining with local statistics [7, 12].

Local Binary Patterns (LBP) one approach to identify and extract the sub regions based on the local feature extraction in a code pattern format. LBP has become more recommended because of their underlying benefits such as ease of implementation [8, 9], invariance to monotonic illumination change [10, 11] and low computational complexity [12, 13]. LBP consisting of some limitations also in extracting of feature in an image they are (1) record the very local textures but not long range information (2) Produce the long histograms (3) limited discriminative capability based purely on local binary differences and (4) Limited noise robustness. On bases of LBP many researchers have done to provide best variant in LBP to improve the performance. In general the feature extraction has done based on the shape, texture, edges and, etc. In this paper we proposed a new model of approach for feature extraction of image which is Extended Informative Local Binary patterns (EILBP). Initially the model start from the pre-processing then EILBP base feature extraction, Euclidean Distance, EILBP coding normalization. Finally to find the feature mating we have implemented the SVM classifier. Figure 1 shows the steps of process in the proposed model.

2 Related Work

Zhang et al. [1] introduced a new concept for secure authentication by using sound and face recognition. They followed a approach that consisting of image preprocessing, histograms identification, feature extraction using LBP and finally classification to find the authorized face. They proved that the gray code variation identified clearly with LBP pattern recognition.

Fig. 1 Flow chart of model execution



Fourati et al. [2] have introduced main feature extractions by using Image Quality measures (IQM) as a key element of their research. In a video initially they extracted the most relevant frames then IQM has applied to find aliveness of motion frames. In their research authors adopted the Replay attack database, Replay mobile database and 3D MAD database dataset to verify the accuracy in the system. The classification process evaluated and results compared with Linear Discriminate Analysis (LDA) and SVM. Vaijyanthimala et al. [3] have proposed a new model to identify the face and signature from the large dataset. The preprocessing of the image has done based on the adaptive median filter (AMF). Consequently the feature extraction from the pre-processed image evaluate by histogram-based for the face vector normalization process for the signature. In their research they have introduced a method to verify the sign and face by using a neural network approach Legion Feature Neural network (LFNN). Ammour et al. [4] introduced a new model for Face and Iris Multi model Biometric Identification using image processing. In this model the feature extracted to find the iris identification separately with normal face identification. The system become more complex than single module identification in a single system. To extract the feature of face they have implemented singular spectrum analysis (SSA) and to extract the features of Iris they have implemented 2D Log-Gabor filter. Beham et al. [5] introduced a new approach for feature extraction of image which is Entropy-based Local Binary Patterns (ELBP). From this model the base for the ELBP will be Local Binary Patterns recognition lonely. To maintain the more information in the extracted feature in this research they also derived a complementary process for ELBP which is Rotation invariant entropy measures (ENTRI). Zhao et al. [8] have experimentally explained the concept of color-based LBP extraction from color image. They proposed the Linear Binary Patterns Histograms (LBPH) to extract the texture features in the colored images. Guo et al. [9] have proposed a hybrid scheme to match the global rotation invariant to local variant LBP named as LBP variance. Proposed method will reduce the loss of global special information. In this process

instead of computing the joint histograms globally the LBPV evaluate the VAR from local regions accurate them with LBP bins. This process greatly reduced the large training data sets. Ojala et al. [10] have introduced a new approach on Multi resolution Gray-Scale and Rotation Invariant Texture Classification used to identify the uniform LBP patterns in any quantization of angles and any resolution. They evaluated the occurrence of histograms and combined the structural and statistical approaches. The research has done based on the texture feature extraction. Cai et al. [11] have proposed a model improved LBP to find the vibration signals of a diesel engine. In this ILBP evaluated the global and local texture information of image by finding of difference among center pixel to all adjacent pixels and adjacent pixels in diagonal also to get better result in image processing. In the result analysis authors applied circular LBP, rotation invariant LBP, uniform LBP, and ILBP separately to generate the codes then implemented nearest neighbor classifier (NNC) and SVM to classification. They proved that ILBP operator perform better than the existing approaches. Liu et al. [13] have done their research on all possible existing procedures related to LBP such as Traditional LBP, The classic, fundamental LBP approach Threshold value Quantization approach and, etc. As per their analysis they proved that Median Robust Extended Local Binary Pattern (MRELBP) is the best approach in feature extraction. They confirmed Fisher vector pooling of deep Convolution Neural Networks are also best approaches but cost effective and need more computational process. Zhao et al. [14] have proposed a new approach to detect the face image recognition which is Extended Local Binary Pattern. ELBP method is underlying with an Angular and Radial differences. Authors proved that the pattern generation with angular and radial difference provided best result.

On the area of image processing to detection of the face several researches have done for better results in different approaches. Still there is a lot of scope to improve the current research. In this work EILBP has proposed to provide high information then classical LBP. In this approach the computation has done for local regions of image instead of complete total histograms. Table 1 shows the comparative study of several researches on image processing.

3 Problem Statement

In this research we introduced a secure face recognition based authentication system with new model of approach. Figure 1 illustrated the steps process in image recognition. Here we introduced the new approach for feature extraction from pre-processed image based on classical LBP called Extended Informative Local Binary Patten (EILBP) which provided better results than classical LBP model. In this research after extraction of feature the system implanted with Euclidean Distance to evaluate the difference between the registered image and authenticated image. Chinese Academy of Science, Institute of Automation (CASIA) has taken into our research dataset where it consisting of 1000 classes for face detection and each class consisting of 4 images. According to this analysis in our research we have included 4000 images

Table 1 Comparison of several research elements on image processing

References	Features	Classifiers	Dataset	Num of images	Result (%)
[2]	IQMs	LDA classifier	Replay attack database and MAD	300	80.0
[3]	HFE	ANN	LHC	256	92.0
[4]	SSA, NIG	FK-NN	CASIA V3 and FERET	2655	97.33
[6]	ELBP	MSVM	CASIA	756	90.0
[7]	color-based LBP	SVM, Naive Bayesian classifier	CORLE,CIFAR	6000	80.0
[9]	LBPV	–	CUReT	205	97.63
[15]	Texture GLCM	KNN	MIAS	265	65.00
[16]	SGLD	ANN	DDSM	377	71.40
[17]	Gray level histogram	PCA + KNN	MIAS	312	71.5
[18]	Morphological features	KNN	MIAS	270	67.0
[18]	Morphological Features	Decision tree	DDSM	300	73.0
[19]	texture	KNN + SFS	DDSM	831	77.0
[20]	Statistical features	SVM	MIAS	43	95.55
[21]	GLCM	KNN + Naïve Bayesian	KBD-FER,	144	79.30
[22]	M-ELBP LBP	Bayesian	MIAS	321	74.0

as our trained dataset. Consequently we should reduce the difference among large number trained samples for EILBP coding vectors. So that EILBP coding vector should be normalize before train. Hear normalization means data fall to small specific interval. In this research we have implemented the min–max normalization method and presented below.

3.1 Pre-Processing

According to proposed method initially the input image pre-processed to extract the accurate features. The most effective preprocessing technique is histogram equalization which is best approach to betterment of image processing. The equalization process transforms the image into histograms where constant for all the brightness

values. Here the brightness distribution applied in a equal probability among all pixels of image. According to the principle procedure the pixel transformation function given for N number of pixel in a image and evaluated for each pixel n .

$$P(i) = \frac{n_i}{N} \quad (1)$$

Here $i \in 0, 1, \dots, k - 1$ gray color level of each pixel n out of N pixels in a image. Histogram equalization complete image transformation function for N pixel image of k number of gray codes given as:

$$I_{\text{out}} = \sum_{j=0}^N \left(\sum_{i=0}^{k-1} P(i) \right) \quad (2)$$

3.2 Feature Extraction

The Feature extraction is a process to map the high dimensional space to lower dimensional space of image by applying different approaches on the original image. The extracted smaller dimensional images aid in better classification. In general the feature extraction has done based on the shape, texture, edges and etc. In this research we followed the texture based extraction which is more efficient approach. More popular texture based feature extraction method is Local Binary Pattern (LBP). In this method the captured image after pre-processing will divided into small portions from this the feature will be extracted. Initially the center or selected pixel threshold the neighborhood pixel and the result will be in a binary coded format. Figure 2 illustrate the central pixel g_c circularly and evenly spaced neighbors on a circle of radius R and Circular symmetric neighbor sets for different (P, R) . The LBP equations have given below:

$$g_c = L(x_c, y_c). \quad (3)$$

$$g_p = L(x_p, y_p). \quad (4)$$

$$R = \sqrt{(x_p - x_c)^2 + (y_p - y_c)^2}. \quad (5)$$

$$x_p = x_c + R \cos\left(\frac{2\pi p}{P}\right). \quad (6)$$

$$y_p = y_c - R \sin\left(\frac{2\pi p}{P}\right). \quad (7)$$

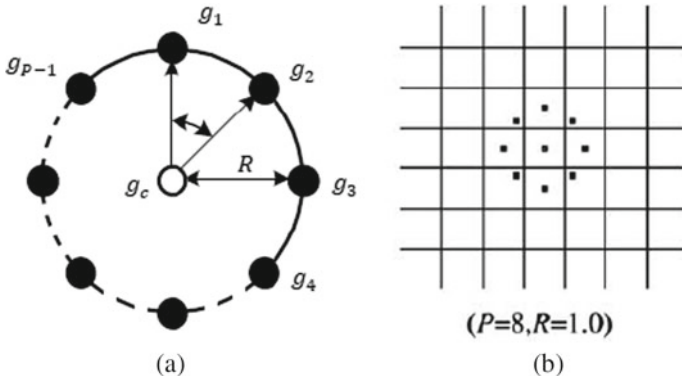


Fig. 2 **a** A central pixel g_c and neighbors on a circle of radius. **b** Neighbor sets for different (P, R)

$$LBP_P^R(x_c, y_c) = \sum_{p=0}^{P-1} 2^p s(g_p - g_c). \tag{8}$$

In the above principles P referred to the number of neighbors from the selected pixel which is depended on the radius R values. Similarly g_p, g_c are the gray code intensity and x_c, y_c are the coordinate points of center pixel. Here x_p, y_p is the coordinate point of selected neighbor point. The function $s(g)$ provided the difference between sampling point to neighbor point. If the difference is greater or equals to the threshold value then that cell coded with 1 otherwise coded with 0

$$s(g) = \begin{cases} 0, & x < 0 \\ 1, & x \geq 0 \end{cases} \tag{9}$$

Finally the patterns generated by sampling in a circular fashion around the central pixel.

The LBP_P^R produces 2^P number of different binary output values, with respect to 2^P different pattern created by the P number of neighbor pixels. As P is increased accordingly the pattern generation will become difficult. The dimensionality of LBP histogram reduced when it need to generate a uniform pattern. Basically the uniform patterns indicate there are two bit transformation between 0 to 1 and 1 to 0 when the bit pattern is considered circularly. There are $p(p - 1) + 2$ uniform patterns except that rest are non-uniform patterns accumulated into a single bin. The uniformity of a pattern $U_p(i, j)$ defined as:

$$LBP_{P,R}^U(x, y) = \begin{cases} U_p(i, j), & \text{if } U(LBP_P^R) \leq 2 \\ P \times (P - 1) + 3, & \text{otherwise} \end{cases}. \tag{10}$$

$$U_p(i, j) = \begin{cases} 1, & i = j = 0, \\ (i - 1) \times P + j + 2, & 1 \leq i \leq P, 0 \leq j \leq P - 1, \\ P \times (P - 1) + 3, & i = P, j = 0. \end{cases} \quad (11)$$

Consider the $U_p(i, j)$ as the label for uniformity of pattern, i denotes the number of 1's in the binary pattern and j denoted the rotation degree.

3.2.1 Rotation Invariant Variance Measures (VAR)

VAR is the complementary information used to maintain the robust information which contains the continuous values used for quantization process. Here the Quantization has done by using all images of to evaluate the feature distribution. By using this evaluation the threshold values of pixels evaluate to get N bins. Here each bin contains equal number of values. The measurement of VAR given as:

$$\text{VAR}_p^R = \frac{1}{P} \sum_{p=0}^{P-1} \left(g_p - \frac{1}{P} \sum_{p=0}^{P-1} g_p \right)^2. \quad (12)$$

3.2.2 Proposed Methodology—Extended Informative Local Binary Pattern

EILBP method proposed to improve the performance compared to previous methods in feature extraction techniques. In the proposed framework not only classify the uniform patterns but also non-uniform patterns. Here we introduced new approach for rotation invariant method that is extraction for conventional models. With this proposal EILBP model on the images where the images are comparatively small which decrease the complexity of computing the non-uniform patterns. Occurrence of one pixel from image of their probability and information are inversely proportional. Lower the probability leads to provide more information vice versa. Based on this approach let consider a pixel X_i and probability p_i accordingly whose probability of occurrence less provided more information about pixel. There is a function $I(g_{pi})$ represents the probability of sampling pixel given as:

$$I(g_{pi}) = \sum_{i=1}^n \log_2 \frac{1}{P(g_{pi})}. \quad (13)$$

The value of $P(g_{pi})$ between 0 to 1 which represents the lower the probability provides the higher the information based on the above function the Extended Informative Rotation Invariant Variance Measures (EIVAR) defined as:

$$\text{EIVAR}_p^R = \frac{1}{P} \sum_{p=0}^{P-1} (g_p - I(g_{pi}))^2 \tag{14}$$

3.2.3 Euclidean Distance

Generally Euclidean Distance used to evaluate the difference between the registered image and authenticated image. Euclidean Distance implemented in this model after extracted the feature of the image. Let consider the feature vectors are $X = (x_1, x_2, x_3, \dots, x_n)^T$ and $Y = (y_1, y_2, y_3, \dots, y_n)^T$. Based on this the Euclidean Distance given as:

$$\text{ed}(X, Y) = \left(\sum_{i=1}^n (x_i - y_i)^2 \right)^{1/2} \tag{15}$$

3.2.4 EILBP Coding Normalization

Chinese Academy of Science, Institute of Automation (CASIA) has taken into our research dataset where it consisting of 1000 classes for face detection and each class consisting of 4 images. According to this analysis in our research we have included 4000 images as our trained dataset. Consequently we should reduce the difference among large number trained samples for EILBP coding vectors. So that EILBP coding vector should be normalize before train. Hear normalization means data fall to small specific interval. In this research we have implemented the min–max normalization method and presented below:

$$x_i = \frac{x_i - \min(X)}{\max(X) - \min(X)} \tag{16}$$

In the above method X denoted the LBP coding vector and $x_i \in X$.

4 Result Analysis

Best way to classify the feature extracted data based on the learned data set is Support Vector Machine which is supervised leaning approach. According to the process SVM classify the or separate the set of EILBP coding vectors of images belongs to two separate classes denoted as (a_i, b_i) . Here in a one image N number of code will generate within radios of R . Each code belongs to the same image represented as $a_i \in R^N$. In this approach the a_i denotes the set of training data EILBP coding and

$b_i \in (-1, 1)$ which represents the class label. The hyper planes to separate the two classes with margin value between positive and negative values. Here the many hyper planes represented as $w \cdot a + e = 0$. The coding vectors of EILBP are usually linear and non-separated. Here the EILBP coding are mapping to the higher dimensional image space with linearly separated two vectors. This approach is complicated evaluate the inner product of high dimensional space. EILBP coding vectors are non-linearly separate and to solve the non-linear problems here we have kernel function K given as:

$$(a_i, a_j) = \Phi(a_i)^T \Phi(a_j) \quad (17)$$

In this research supposed to follow a formula for SVM with considering of non-linear coding data as given below:

$$f(x) = \sum_{i=1}^m \alpha_i b_i K(a_i \cdot a) + e \quad (18)$$

In the above formula α_i values are called the support vectors whose values most probably 0 and a_i are non-zero based on the output formula the result of coding vector a will be positive or negative based on the multi classification function SVM can also used for multi class pattern recognition. Let consider there is N number of classes then process need to be done N number of classifier. Each class from N number classes as set the same as per $N-1$ other classes to overcome the problem of multi class. We have taken CIFAR-10 data set which consisting of ten number of classes and SVM implemented on all sets. Initially one of the classes N th selected and labeled as 1 then remaining classes randomly selected are labeled as 0. Finally, ten sets of different training sets and corresponding testing sets are used to train and test ten different SVMs. In this process different classification results gained for the single data with different SVM parameters. In this model of research the threshold value effects on the classification. The value of threshold increases leads to higher the classification. With the implementation of the EILBP when threshold value equals to 5 and 25 then the performance of the EILBP will be better but at the value of 25 the performance not increased. Because the resolution of the image is small and big value of the threshold leads to reduce the information. Even though the performance of the model not reduced. Bellow results show the threshold value at 5 and 25 with respected to the number of classes value $N = 3$ and $N = 6$. In this research the result analysis showed as given blow. Figure 3 shows the above description and result comparison between LBP and EILBP. Table 2 has information about accuracy result of various models where EILBP comparatively provided better results than some existing approaches.

Fig. 3 Result analysis with comparison of classical LBP and EILBP

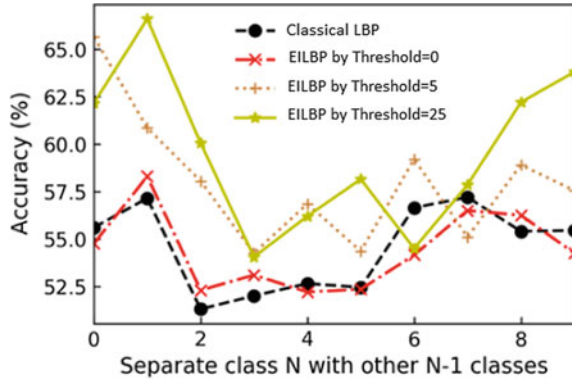


Table 2 Accuracy based on the different classifiers

Classifier	Feature extraction	Accuracy
SVM	LBP	67.07 ± 0.75
MSVM classifier	ELBP	73.11 ± 0.76
KNN	M-ELBP	75.46 ± 0.78
Bayesian network	Uniform ELBP	72.86 ± 1.06
Random forest	LBP	69.19 ± 1.31
SVM	EILBP	74.42 ± 0.92

5 Conclusion

In this paper we majorly concentrated on feature extraction in a better way to reduce the complexity also include the information to match the global rotation invariant to local texture information to preserve the more information to classify in the better way. Our proposed model EILBP also has given good experimental results compared to classical LBP. In the feature our research will continues to find optimal approach to extract the features for color images.

References

1. Zhang X, Cheng D, Jia P, Dai Y, Xu X (2020) An efficient android-based multimodal biometric authentication system with face and voice. *IEEE Access* 1(8):102757–102772
2. Fourati E, Eloumi W, Chetouani A (2020) Anti-spoofing in face recognition-based biometric authentication using image quality assessment. *Multimedia Tools and Appl* 79(1):865–889
3. Vaijyanthimala J, Padma T (2020) Multi-modal biometric authentication system based on face and signature using legion feature estimation technique. *Multimedia Tools and Appl* 79(5):4149–4168
4. Ammour B, Boubchir L, Bouden T, Ramdani M (2020) Face–iris multimodal biometric identification system. *Electronics* 9(1):85

5. Beham MP, Roomi SM (2013) A review of face recognition methods. *Int J Pattern Recognit Artif Intell* 27(04):1356005
6. Sallauddin M, Sheshikala M (2018) Software defined security (SDSec): reliable centralized security system to decentralized applications in SDN and their challenges. *J Adv Res Dynam Control Syst* 10(10 Special Issue):147–52
7. Sheshikala M, Mohammad S (2018) Survey on multi level security for IoT network in cloud and data centers. *J Adv Res Dynam Control Syst* 10(10):134–146
8. Zhao Q (2021) Research on the application of local binary patterns based on color distance in image classification. *Multimedia Tools and Appl* 80(18):27279–27298
9. Guo Z, Zhang L, Zhang D (2010) Rotation invariant texture classification using LBP variance (LBPV) with global matching. *Pattern Recogn* 43(3):706–719
10. Zhao Y, Huang DS, Jia W (2012) Completed local binary count for rotation invariant texture classification. *IEEE Trans Image Process* 21(10):4492–4497
11. Cai Y, Xu G, Li A, Wang X (2020) A novel improved local binary pattern and its application to the fault diagnosis of diesel engine. *Shock Vib* 21:2020
12. Mohammad S, Dadi R, Pasha SN, Mendu M, Harshavardhan A (2020) Cost function for delay (CFD) in software defined network with fog computing and associated IoT application. In: *IOP conference series: materials science and engineering 2020 Dec 1, vol 981. No. 3*, IOP Publishing, pp 032097
13. Liu L, Fieguth P, Guo Y, Wang X, Pietikäinen M (2017) Local binary features for texture classification: Taxonomy and experimental study. *Pattern Recogn* 1(62):135–160
14. Liu L, Fieguth P, Zhao G, Pietikäinen M, Hu D (2016) Extended local binary patterns for face recognition. *Inf Sci* 1(358):56–72
15. Blot L, Zwiggelaar R (2001) Background texture extraction for the classification of mammographic parenchymal patterns. In: *Medical image understanding and analysis 2001 July 16*, pp 145–148
16. Bovis K, Singh S (2002) Classification of mammographic breast density using a combined classifier paradigm. In: *4th international workshop on digital mammography 2002 July 22*, pp 177–180
17. Zwiggelaar R, Muhimmah I, Denton ERE (2005) Mammographic density classification based on statistical gray-level histogram modelling. In: *Proceedings medical image understanding and analysis, July*, pp 183–186
18. George M, Zwiggelaar R (2019) Comparative study on local binary patterns for mammographic density and risk scoring. *J Imaging* 5(2):24
19. Oliver A, Freixenet J, Marti R, Pont J, Pérez E, Denton ER, Zwiggelaar R (2008) A novel breast tissue density classification methodology. *IEEE Trans Inf Technol Biomed* 12(1):55–65
20. Subashini TS, Ramalingam V, Palanivel S (2010) Automated assessment of breast tissue density in digital mammograms. *Comput Vis Image Underst* 114(1):33–43
21. Muštra M, Grgić M, Delač K (2012) Breast density classification using multiple feature selection. *automatika*. 53(4):362–72
22. Yoo Y, Baek JG (2018) A novel image feature for the remaining useful lifetime prediction of bearings based on continuous wavelet transform and convolutional neural network. *Appl Sci* 8(7):1102

Performance Analysis of 5G Micro-Cell Coverage with 3D Ray Tracing



Viswanadham Ravuri, M. Venkata Subbarao, Sudheer Kumar Terlapu,
and T. Sairam Vamsi

Abstract This paper presents the performance analysis of cell coverage and channel characteristics of millimeter-wave (mmWave) band outdoors with 3D ray-tracing simulation. The study is done by deploying the 3D building data into the site viewer and analyzing the link performance in non-line-of-sight (NLOS) conditions by varying the transmitter power and channel conditions. The shooting and bouncing rays (SBR) technique is used to analyze the performance such as path loss and received power under fading conditions. In addition to it, the study visualizes the coverage is under a different number of reflections. Investigations will help the service provider to identify the proper location of the transmitter, transmitter power to provide better services to the user.

Keywords mmWave · NLOS · Long-term evolution (LTE) · 5G · SBR

1 Introduction

The main objective of future wireless systems is to enhance the capabilities of existing systems. They may include reliable, flexible, fast, and more efficient when providing services to the end-users. According to International Mobile Telecommunications (IMT) latest 2020 Standards, the next generation systems must have the capabilities of higher user experience and peak data rates, lower latency, supports massive connections, good quality of service, enhanced spectral efficiency, enhanced energy efficiency, large capacity, and frequency and bandwidth flexible [1].

Revolution in mobile technology changes dramatically for every decade. There is a great improvement in the services offered with new technology. In [2], 5G deployment challenges, standardization trials, and research overview are presented. Ge [3] presented a new orbital angular momentum (OAM) technique in mmWave communications to provide a novel approach for information transmission. Table 1 presents the different frequency bands used in mmWave technology in 5G [4]. In [5],

V. Ravuri (✉) · M. Venkata Subbarao · S. K. Terlapu · T. Sairam Vamsi
Department of ECE, Shri Vishnu Engineering College for Women, Bhimavaram, A.P, India
e-mail: ravuri.viswanadh@gmail.com

Table 1 Frequency bands for 5G

Freq. Band	Uplink freq. (GHz)		Down link freq. (GHz)	
	Min	Max	Min	Max
n257	26.50	29.50	26.50	29.50
n258	24.25	27.50	24.25	27.50
n260	37.00	40.00	37.00	40.00
n261	27.50	28.35	27.50	28.35

experimental setup for analysis of multipath characteristics of 28-GHz channel is presented. Wideband mmWave propagation measurements in an indoor office environment are analyzed at 28 and 73 GHz in [6]. The analysis is carried out under ultra-dense 5G networks. In [7], for PHY layer design, mmWave channel measurements are analyzed and their implications are derived. In [6, 8–10], 5G channel characteristics and modeling are analyzed in indoor environments such as building coverage with mmWave technology. Most of the research is measured the channel characteristics under the indoor dense environment. The proposed paper is done the channel characteristics measurement under outdoor with 3D ray tracing with NLOS communication.

The rest of the paper is organized as follows. Section 2 describes the ray tracing and its mathematical modeling. Section 3 presents the experimental modeling for the simulation. The measurement of channel characteristics under different environments is presented in Sect. 4. Section 5 concludes the paper.

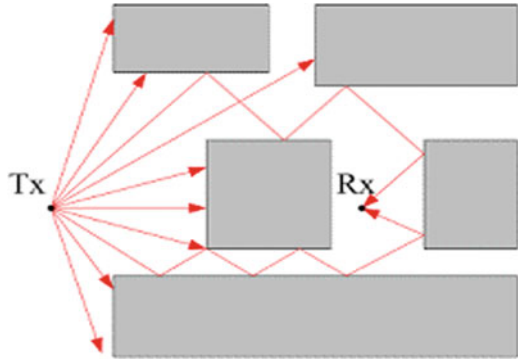
2 Shooting and Bouncing Rays

Ray tracing is a method for interpretation of 3D visuals with complex light interactions. It generates pictures with transparent surfaces, full of mirrors, and shadows. For indoor and outdoor 5G dense environments, ray tracing is the best technique to the mmWave band. It gives the prediction of channel characteristics instantly so that it is cheap and quick technique when compared to other techniques.

The generation of rays is classified in to SBR and method of images. Figure 1 illustrates the SBR method. In SBR approach, huge number of rays are launching in arbitrary directions and then, the rays are traced until the stopping criteria is met. As the number of interactions is increased, the complexity is also increase linearly.

A large number of scatters such as buildings with perfect reflector glasses, concrete buildings, trees, vehicles, and other pedestrians are present in a distinctive outdoor 5G radio propagation environment. The ray signals interact these scatters and arrive at the receiver with different path gains and losses. In 5G, dense environment most of the cases a line-of-sight communication is not possible either in indoor environment or outdoor environment. The mobile environment is stationary or mobile. Several channel characteristics are defined for a radio channel is as follows.

Fig. 1 Illustration of SBR method



Path loss is defined as

$$PL(\text{dB}) = 10 \log_{10} \left(\frac{P_{\text{transmitted}}}{P_{\text{received}}} \right) = P_{\text{transmitted}}(\text{dB}) - P_{\text{received}}(\text{dB})$$

The free-space path loss is

$$PL(\text{dB}) = 10 \log_{10} \left(\frac{P_{\text{transmitted}}}{P_{\text{received}}} \right) = -10 \log_{10} \left[\frac{\lambda^2}{(4\pi^2)d^2} \right]$$

Assumed that the antenna gain is unity and the d is the distance between Tx and Rx .

Total received power at the receiver is given by

$$P_{\text{received}} = \sum_i P_i$$

where P_i is the power of i th ray and can be given as

$$P_i(W) = \frac{\lambda^2}{480\pi^2} |E|^2$$

3 Simulation Setup

To analyze the performance of 3D ray tracing, we consider Shri Vishnu Engineering College for Women (SVECW) as the urban environment it may have dense concrete buildings where direct path between transmitter and receiver is impossible. Figure 2 shows the layout of the area which is considered for simulation.



Fig. 2 Site viewer of the SVECW

Figure 3 shows the transmitter location and its characteristics. The antenna height is considered as 10 mts, surface elevation of 9 mts, and latitude and longitude are 16.57° and 81.52 , respectively. Similarly, Fig. 4 shows the location and characteristics of the receiver. The antenna height is 1mt, surface elevation is 9 mts, and the latitude and longitude of the receiver are 16.59° and 81.52 , respectively.

The distance between transmitter and receiver is 130 mts. The above setup is simulated with 4G environment and in 3D ray-tracing environment. The complete analysis of simulations is discussed in Sect. 4.



Fig. 3 Site viewer of transmitter

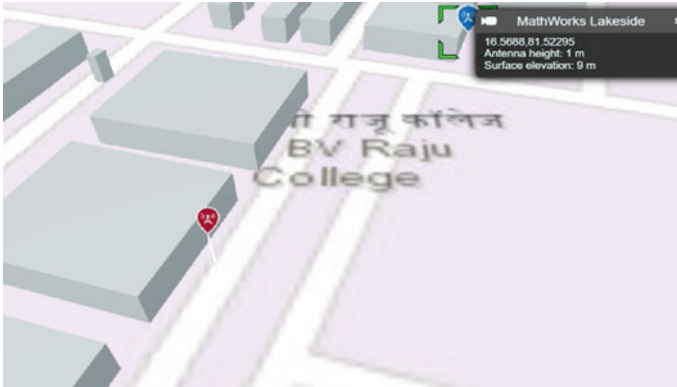


Fig. 4 Characteristics of receiver

4 Results and Discussions

The analysis is carried out in both 4G RF and 3D ray-tracing outdoor NLOS environment. The SVECW, Bhimavaram is considered as dense 5G mmWave environment to carry out the simulations. The frequency band is considered to carry out the simulations is centered at 28 GHz. The performance analysis is carried out with fixed transmitter antenna height with 10 mts and the receiver height with 1mt. To analyze, the path loss and received power different transmitter powers are considered between 5 and 25 W with a step size of 5 W. The analysis is also carried with three different scatter scenarios such as the perfect reflector like glasses, pure concrete walls, and with and without raining conditions. Figure 5a and b shows the received power and coverage maps with 4G RF environment.

Figure 6 shows the coverage of 3D ray tracing with no reflection, single, double, and four reflections paths, and it is clear that as the number of reflections in more

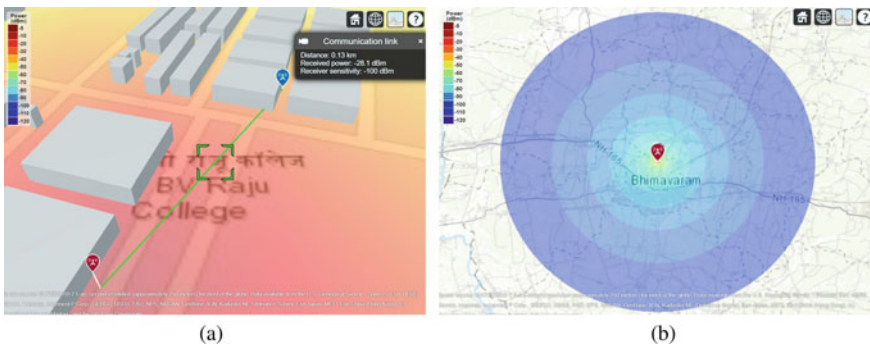


Fig. 5 Received power at receiver in 4G environment and the coverage map in 4G

the coverage area is increasing. So, in order to cover 250 mts from the transmitter location, four to six reflections are sufficient.

Tables 2, 3 and 4 represent received power with single, double, and four reflections, respectively. As the number of reflections is increasing, the received power is increasing because of the greater number of paths to the receiver.

Figures 7, 8 and 9 represent the estimation of channel characteristics under perfect reflector, pure concrete building, and raining conditions, respectively.

From these simulations, it is clear that even in 5G the received power is directly proportional to received power. The received power is more in case perfect reflector and is less in concrete buildings as reflectors. Similarly, the path loss is indirectly proportional to transmitted power and the losses are more in concrete building than that of reflector. The building material places an important role in 5G mmWave small cell deployment with 3D ray tracing.

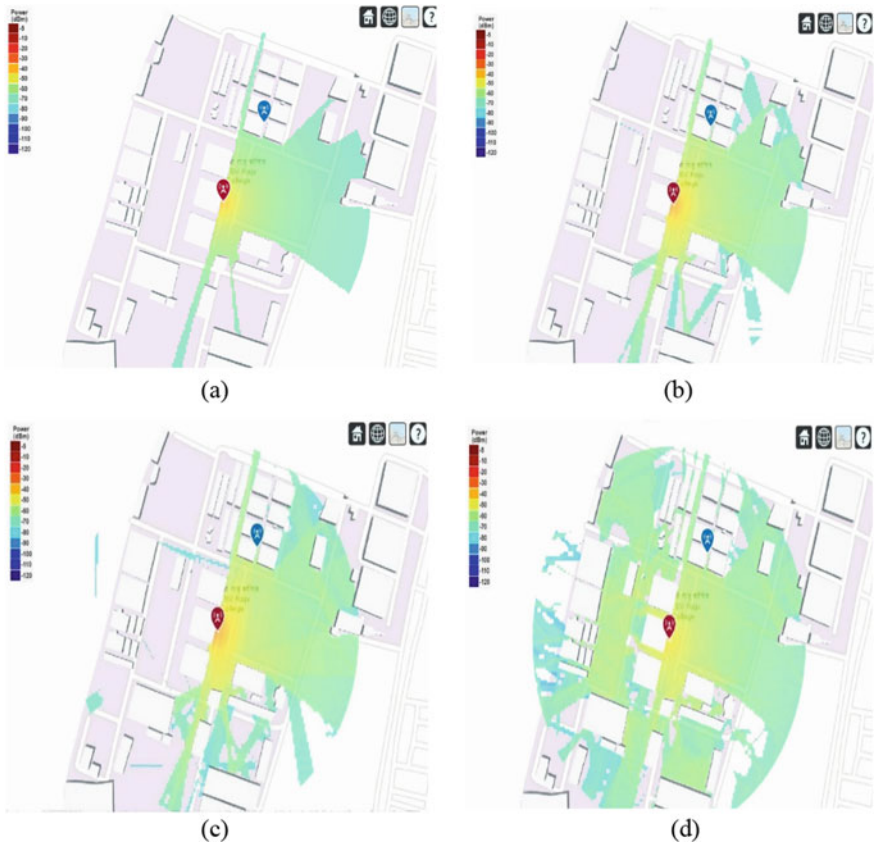


Fig. 6 Coverage area using ray tracing with **a** no reflection, **b** single reflection, **c** double reflection, and **d** four reflections

Table 2 Received power with single reflection (dBm)

Transmitted power (W)	Building material/environment		
	Perfect	Concrete	Weather
5	-66.018	-73.4873	-74.6516
10	-63.006	-70.477	-71.641
15	-61.2455	-68.7161	-69.8804
20	-59.9962	-67.4667	-68.631
25	-59.0271	-66.4976	-67.6619

Table 3 Received power with double reflections (dBm)

Transmitted power (W)	Building material/environment		
	Perfect	Concrete	Weather
5	-63.011	-70.963	-72.128
10	-60.003	-67.962	-69.117
15	-58.229	-66.192	-67.357
20	-56.99	-66.942	-66.1
25	-56.0291	-63.973	-65.138

Table 4 Received power with four reflections (dBm)

Transmitted power (W)	Building material/environment		
	Perfect	Concrete	Perfect
5	-59.07	-69.46	-60.124
10	-56.06	-66.45	-57.114
15	-54.3	-64.693	-55.35
20	-53.05	-63.44	-54.104
25	-52.083	-62.474	-53.13

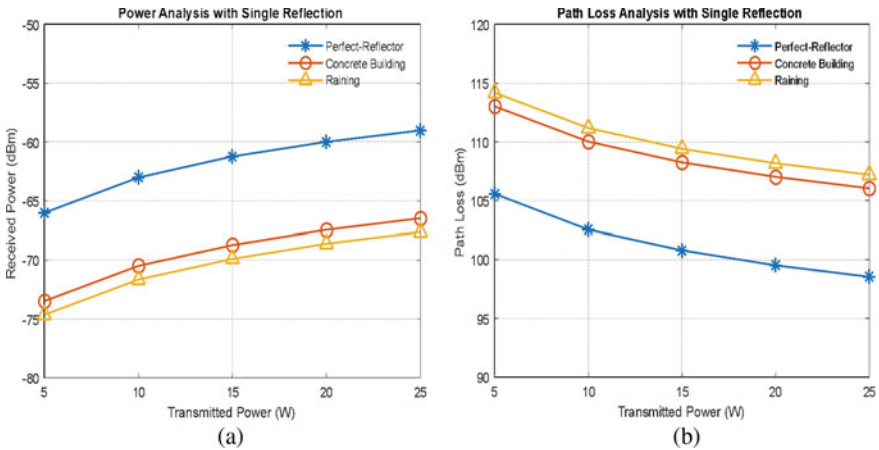


Fig. 7 Analysis with single reflection **a** received power and **b** path loss analysis

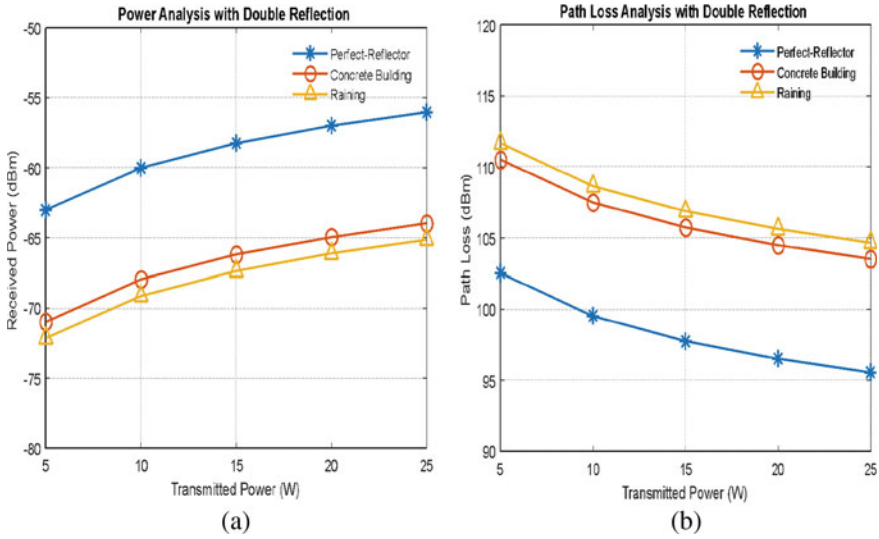


Fig. 8 Analysis with double reflections **a** received power and **b** path loss

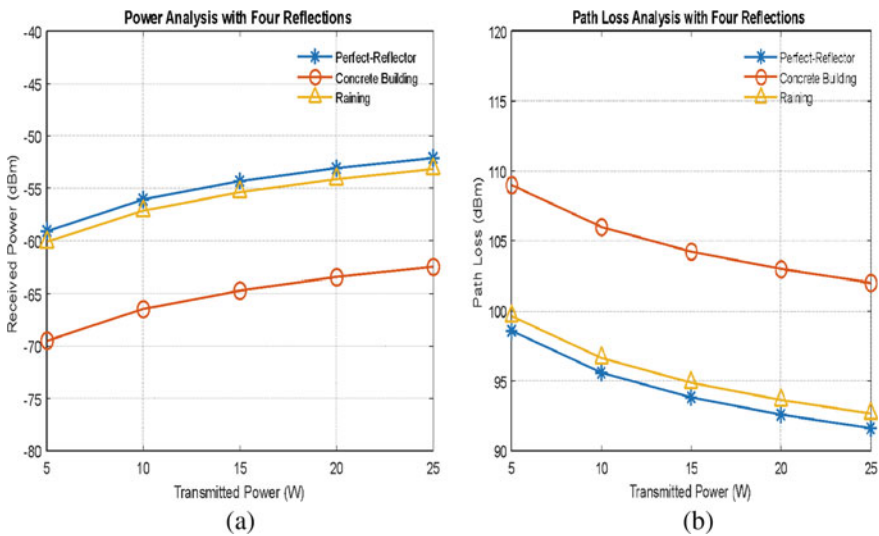


Fig. 9 Analysis with four reflections **a** received power and **b** path loss

5 Conclusion

This paper presents the performance analysis of cell coverage and channel characteristics of millimeter-wave (mmWave) band outdoors with 3D ray-tracing simulation. The entire simulations are carried out at constant transmitter and receiver antenna

heights. It is observed from simulations there is a 10 dB degrade in the path loss in the concrete building as scatter than that of the perfect reflector. Further, it is observed that there is around 8 dB degradation is observed in received power if the scatter environment is a concrete building. Due to raining conditions, it is observed that there is a 2 dB loss in received power, and 2 dB more path loss is observed regarding the concrete building.

References

1. Rappaport TS et al (2013) Millimeter wave mobile communications for 5G cellular: it will work! *IEEE Access* 1:335–349
2. Shafi M et al (2017) 5G: a tutorial overview of standards, trials, challenges, deployment, and practice. *IEEE J Sel Areas Commun* 35(6):1201–1221
3. Xiao M et al (2017) Millimeter wave communications for future mobile networks. *IEEE J Sel Areas Commun* 35(9):1909–1935
4. 3GPP TS 38.101–2 (2020) NR User Equipment (UE) radio transmission and reception; Part 2: Range 2 Standalone V16.4.0, June 2020
5. Yin X, Ling C, Kim M (2015) Experimental multipath-cluster characteristics of 28-GHz propagation channel. *IEEE Access* 3:3138–3150
6. Maccartney GR, Rappaport TS, Sun S, Deng S (2015) Indoor office wideband millimeter-wave propagation measurements and channel models at 28 and 73 GHz for ultra-dense 5G wireless networks. *IEEE Access* 3:2388–2424
7. Raghavan V, Partyka A, Akhoondzadeh-Asl L, Tassoudji MA, Koymen OH, Sanelli J (2017) Millimeter wave channel measurements and implications for PHY layer design. *IEEE Trans Antennas Propag* 65(12):6521–6533
8. Zhang P, Yi C, Yang B, Wang C-X, Wang H, You X (2020) In building coverage of millimeter-wave wireless networks from channel measurement and modeling perspectives. *Sci China Inf Sci* 63(8):180301
9. Zhang P, Li J, Wang H, Wang H, Hong W (2018) Indoor small-scale spatiotemporal propagation characteristics at multiple millimeter-wave bands. *IEEE Antennas Wireless Propag Lett* 17(12):2250–2254
10. Wang H, Zhang P, Li J, You X (2019) Radio propagation and wireless coverage of LSAA-based 5G millimeter-wave mobile communication systems. *China Commun* 16(5):1–18
11. <https://www.ei.tum.de/hft/forschung/advanced-electromagnetic-ray-tracing-methods/advanced-electromagnetic-ray-tracing-methods/>

A Novel Asymmetric Group Key Encryption Mechanism in MANETs



R. Rekha, M. Sandhya Rani, and K. V. N. Sunitha

Abstract The mobile ad-hoc network (MANET) comprises a collection of wireless components which communicate within radio frequency ranges. Due to the frequent mobility of nodes and the lack of fixed infrastructure, providing security in multicast communication of MANETs is a big challenge. The group key agreement (GKA) protocol is one of the essential cryptographic primitives for providing a secure channel among multicast group members. We proposed a novel asymmetric group key management protocol, in which a group encryption key is calculated based on CRT technique which uses the individual user's secret share and distributed to all users, and the decryption key is kept private by each user. The main advantage of our protocol is that it not only ensures security but also provides better quality of service metrics like key delivery ratio, end-to-end delay, and energy consumption than the existing key management mechanisms.

Keywords MANET · Secret key · Encryption · Decryption · Group key

1 Introduction

Secure communication system involves transmission of messages in a secret mode. That means except sender and receiver, no one should know the content of the message. In peer to peer or multicast communication, two types of encryption extensively used are symmetric encryption and asymmetric encryption. In either of the

R. Rekha

University College of Engineering and Technology, MGU, Nalgonda, Telangana, India
e-mail: rekhareddy@yahoo.com

M. Sandhya Rani (✉)

Bhoj Reddy Engineering College for Women, Hyderabad, Telangana, India
e-mail: sandhya_medi@yahoo.com

K. V. N. Sunitha

BVRIT Hyderabad College of Engineering for Women, Hyderabad, Telangana, India
e-mail: k.v.n.sunitha@gmail.com

encryption mechanisms, key management plays a vital role. Secure communications involve a key distribution method between communication entities presented in Zamani et al. [1], in which the key might be transmitted through unreliable channels. In our proposed work, we employed asymmetric encryption for multicast communication in MANETS. The public key encryption overcomes the problem of key generation and distribution. Secure group key is calculated that is used as a group encryption key, and each individual user's private key is used as a decryption key for group communication. Group key management schemes can be classified into centralized, decentralized, and distributed. In centralized mechanisms, a single entity called trusted third party generates and distributes the key. But this scheme has the single point of failure limitation. Decentralized mechanisms usually have sub groups or clusters to avoid the above drawback. Each cluster has cluster head which locally distributes the keys. In distributed key management mechanism, all users equally participate in secret key calculation.

We used distributed key management mechanism in which each user contributes its share to prepare the group encryption key (GEK). This calculation is based on Chinese remainder theorem which uses secret shares and public keys of individual users. Each user who wishes to send message in multicast group uses this key for encrypting the message. Only the group members can decrypt the message with the decryption keys and secret share to obtain the original message. Moreover, GEK is transmitted to individual users in a secure way.

Our "Asymmetric Group Key Encryption Mechanism (AGKEM)" gives better security and quality of service (QoS) parameters like key delivery ratio, end-to-end delay, and energy consumption. We compared our results with two existing approaches: optimized cluster-based multicast tree (OCBMT) and enhanced cluster-based multicast tree (ECBMT). The rest of the paper is organized in four sections. Section 2 describes about related work, Sect. 3 focuses methodology and process flow of "Asymmetric Group Key Encryption Mechanism", Sect. 4 illustrates the simulation parameters and experimental results, and Sect. 5 presents the conclusion of this research work.

2 Related Work

Much research work has been done in multicast group key management protocols for MANETs. Burmester and Desmedt [2] developed a method to provide a group key management protocol based on the two-party Diffie-Hellman protocol, in which the group key is computed in two rounds using broadcast method. But it failed to provide the authentication. Boneh and Silverberg [3] demonstrated that a one-round multi-party group key agreement protocol is implemented from n -linear pairings. Choi et al. [4] and Du et al. [5] enhanced the above mentioned schemes using the bilinear pairings, which made it to be authenticated. Zhang and Cheng [6] demonstrated a solution to impersonation attack in group communication. In this model,

an attacker can masquerade an entity with the known keying material to compromise some session keys which are provided during initialization phase of multicast communication.

Zheng et al. [7] developed a two-round GKA mechanism based on Elgamal signature that provides information security and authentication. It avoids replay attacks but it suffers from network overload problem, as it broadcast many messages for key computation. Zhang et al. [8], which also confronts the same issue. Shi et al. [9] and Zhong et al. [10] both presented a one-round identity-based GKA method, in which, the public key of the members is not considered as identification strings. Yao et al. [11] come up with ID-based provable secure GKA protocol with three rounds, first round is focused on identity authentication, key conformity is implemented in second round, and the key distribution is done in final round.

From the perspective of identity-based encryption, Huang et al. [12] proposed a hybrid encryption method, which provides higher computational effectiveness than Boneh's method. Sandhya Rani et al. [13] developed a symmetric group key management scheme, in which a common group key is calculated for all members to provide secure communication. But the authors focused only on QOS parameters not on reducing computation time.

An asymmetric group key management protocol proposed by Sandhya Rani et al. [14] illustrated the computational complexities for various operations in key management. But the authors not provided QOS metrics of multicast communication. To solve all these limitations, we extended asymmetric key management scheme known as Asymmetric Group Key Encryption Mechanism (AGKEM) which provides secure communication through asymmetric encryption and decryption. And it also provides QOS like better key delivery ratio, less delay, and moderate energy consumption.

3 The Proposed Methodology

In this section, we describe the process flow of our proposed distributed asymmetric group key encryption methodology, which is explained in detail by Sandhya Rani et al. [14]. As in Fig. 1, the first step is public parameter generation and distribution to all users in the multicast group. Based on the received value range, each user generates a secret share value and sends it to the group head. In the next step, each user generates public and private key pairs using the RSA algorithm. Then, based on the Chinese remainder theorem, the group head prepares and distributes a group encryption key using secret values and public keys of all users. After receiving the group encryption key, the sender encrypts a message and transmits it to the multicast group. Upon receiving the cipher text, only the group members can decrypt the message with their private keys and secret values. Thus, it provides secure communication in the group by avoiding external attacks. It also provides better quality of service metrics.

Illustration example:

- (1) Let us consider number of users in the multicast group = 3

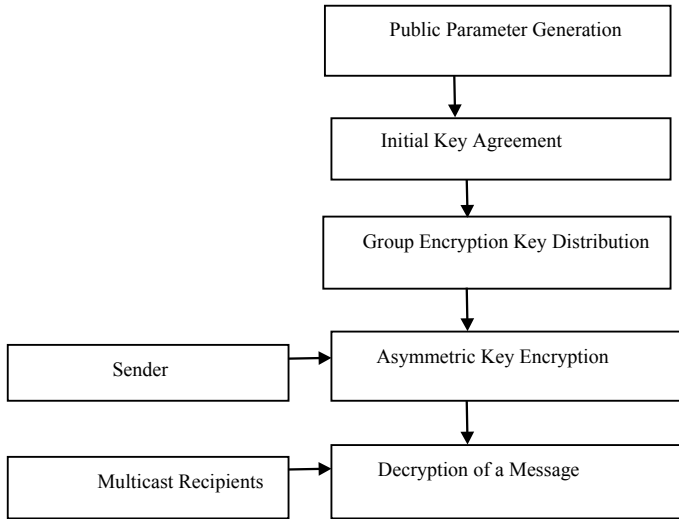


Fig. 1 Process flow of the AGKEM

- (2) Let us assume secret shares of three users 13, 17 and 19, respectively.
- (3) Three users (e, d) pairs—(7103), (3267), and (5269) based on chosen p, q values.
- (4) Based on CRT theorem group encryption key (GEK) = 2893
- (5) Suppose user 2 wants to send the message to the group members, cipher text is calculated for message m (assumed8)
- (6) Calculated $C = 2149$
- (7) User 1 and user 3 decrypt the message with their own private keys and secret shares.
- (8) User 1 computes plain text m by its public value 103 and secret value 13.
- (9) User 1 obtains the original content as 8.

4 Simulation Evaluations

The experimental studies were conducted in the Linux environment, as it provides enormous programming tools for analyzing the workflow between communication devices. The experiments were done in the NS2 Simulator. NS2 is an open source event triggered simulator. It is used to simulate, analyze, and demonstrate the data transmission and performance metrics of any kind of network. The network animator (NAM) is used to analyze the experimental results. AWK scripts are used to process the data from the logs (trace files) which are generated by the NS2 tool command language (tcl) scripts. The graphs have been plotted based on the recorded output data of our proposed algorithm. We compared our results with two existing protocols optimized cluster-based multicast tree (OCBMT) and enhanced cluster-based

Table 1 Simulation parameters

Parameters	Value
Simulator	NS-2(Version 0.35)
Channel type	Channel/wireless channel
Routing protocol	MAODV
Traffic type	CBR
Simulation duration	50 ms
MAC layer protocol	802.11
Transmission range	800 × 1000 m
Packet size	512 bytes
Number of nodes	20, 40, 60, 80, 100

multicast tree (ECBMT). We have used MAODV as underlying routing algorithm for distribution of keys where as OCBMT and ECBMT used MDSRV routing algorithm.

4.1 Simulation Environment

In Table 1, we explained various simulation parameters and corresponding values used in our simulation to implement our proposed algorithm.

4.2 Performance Metrics

The performance of the proposed model is analyzed using three metrics:

- (1) **Key Delivery Ratio (KDR):** The keys delivery ratio (KDR) metric refers to the ratio between number of keys received and sent keys.

$$\text{KDR} = \text{Keys delivered} / \text{Keys sent} \times \text{Number of multicast receivers}$$

This metric is used to calculate the reliability rate of transmission of keys during multicast communication.

- (2) **Delay in Key transmission:** This metric represents the average key transmission delay between sender and receiver. It computes the required time to transmit the group keys.

$$\text{Avg. EED} = \text{Total EED} / \text{No. of keys sent}$$

where EED = end-to-end delay.

(3) **Energy Consumption:** The total energy consumed is the difference between initial energy of all nodes and the remaining energy of the nodes.

$$\text{Energy consumption} = (\text{No. of nodes} \times \text{IE}) - \text{RE}$$

where IE = initial energy and RE = remaining energy

Key delivery ratio, delay in key transmission, and energy consumption values of various distributive key management schemes are shown in Figs. 2, 3 and 4, respectively.

Key delivery ratio of AGKEM is on an average 6% more than ECBMT and 11% more than OCBMT approaches. This increase of KDR in our proposed work is due to its distributive nature and underlying MAODV routing algorithm.

End-to-end delay (ms) of AGKEM is on an average 50% less than OCBMT and 40% less than ECBMT approaches. In OCBMT and ECBMT methods, due to local controllers, there is no direct transmission of keys to recipients and takes some delay to reach the keys to all users.

As shown in Fig. 4, it is proved that energy consumption is moderately decreased for nodes 20, 40, 60, 80 and 100 nodes. OCBMT and ECBMT secure key management

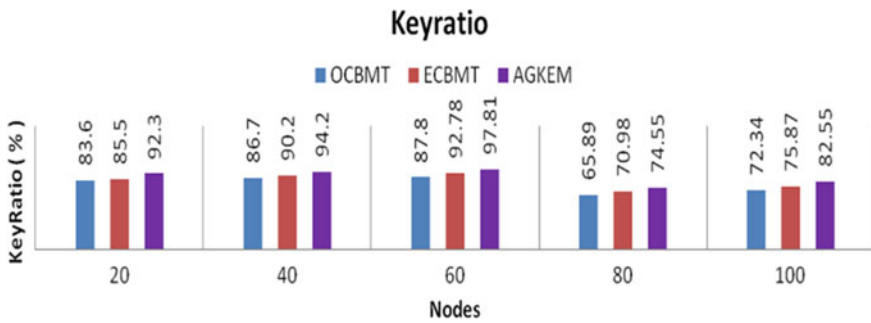


Fig. 2 Key delivery ratios of OCBMT, ECBMT and AGKEM

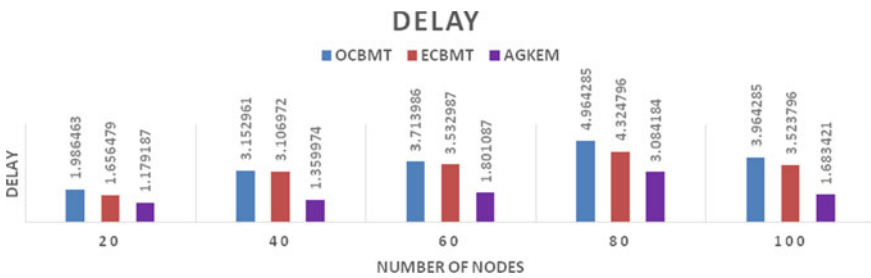


Fig. 3 End-to-end delays of OCBMT, ECBMT, and AGKEM

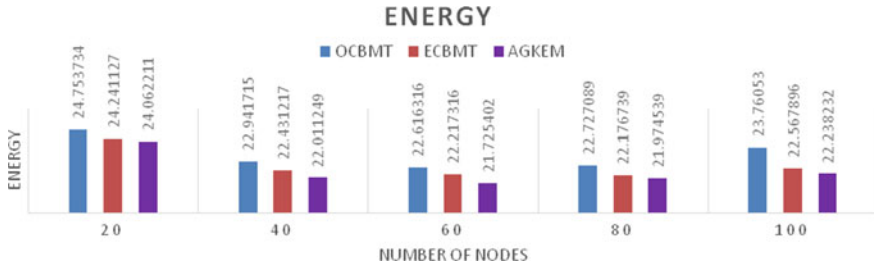


Fig. 4 Energy consumptions of OCBMT, ECBMT, and AGKEM

methods deliver the keys to all users through local controllers which consumes more energy where as our proposed protocol AGKEM uses distributive approach to deliver the keys. So, from Figs. 2, 3 and 4, it is proved that our proposed protocol have better key delivery ratio, less delay, and with little minimized energy consumption than OCBMT and ECBMT protocols.

5 Conclusion

Group key generation and distribution are the core of secure multicast communication in MANETs. We developed a secure asymmetric distributed group key management scheme for multicast communication. This solution is based on the idea of a CRT and a secret share mechanism. The sender who wishes to send a message encrypts the content with the calculated group key, which is calculated by our method. The group members can obtain the message by decrypting the cipher text with the individual’s private keys. Thus, no other entity other than group members can decrypt the message. We showed illustrations of the same. AGKEM uses the multicast version of the AODV routing protocol and provides better key delivery ratio, less delay, and moderate energy consumption than OCBMT and ECBMT. We can conclude that our proposed protocol provides more security and performance in terms of better QOS values.

References

1. Zamani AT, Zubair S (2014) Secure and efficient key management scheme in MANET. IOSR J Comput Eng 16:146–158
2. Burmester M, Desmedt Y (1995) A secure and efficient conference key distribution system. In: Advances in cryptology—EUROCRYPT’94, Springer, Berlin, Heidelberg, pp 275–286
3. Boneh D, Silverberg A (2003) Applications of multi linear forms to cryptography, In: Contemporary mathematics, vol 324. pp 71–90
4. Choi K, Hwang JY, Lee DH (2004) Efficient ID based group key agreement with bilinear maps. In: Public key cryptography—PKC 2004, Springer, Berlin, Heidelberg, pp 130–144

5. Du XJ, Wang Y, Ge JH (2003) ID-based authenticated two round multiparty key agreement. Iacr Cryptology Eprint Archive
6. Zhang F, Chen X (2003) Attacks on two ID-based authenticated group key agreement schemes. In: Iacr Cryptology Eprint Archive
7. Zheng S, Wang S, Zhang G (2007) A dynamic, secure and efficient group key agreement protocol. In: Frontiers of electrical and electronic engineering in China, pp 182–185
8. Zhang Q, Wang R, Tan Y (2014) Identity-based authenticated asymmetric group key agreement. J Comput Res Developm
9. Shi Y, Chen G, Li J (2005) ID-based one round authenticated group key agreement protocol with bilinear pairings. In: Information technology: coding and computing-ITCC 2005, International conference on IEEE, pp 757–761
10. Zhong Y-T, Jian-feng M (2011) Identity based group key management scheme for LEO/MEO double-Layer space information network. J Astronautics 32:1551–1556
11. Yao G, Wang H, Jiang Q (2008) An authenticated 3-round identity-based group key agreement protocol. In: Availability, reliability and security-ARES 08. third international conference on IEEE, pp 538–543
12. Huang Y, Jianzhu LU (2007) A new identity-based authenticated encryption scheme. J Comput Eng 33:149–152
13. Sandhya Rani M, Rekha R, Sunitha KVN (2020) Multicast symmetric secret key management scheme in mobile adhoc networks. In: ICETE-2020 Springer conference, pp 182–189. https://doi.org/10.1007/978-3-030-24322-7_24
14. Sandhya Rani M, Rekha R, Sunitha KVN (2021) An efficient and secure ID based asymmetric key management scheme for dynamic groups. Int J Scientif Res Netw Secur Commun 9(2):1–4

EEG—Brainwaves Signal Based BCI Control Wheel Chair System



B. Ramesh and Phanikumar Polasi

Abstract The movement with man-less support for a physically disabled or challenged people is a challenging task. Many techniques had been established such as joystick-based wheel chair movement, eyeball movement-based wheel chair movement control. But, these methods were executed and resulted with drawbacks and constraints. This made to enhance the working model by utilizing the brain signals for controlling the wheel chair. The most significant part of the human body to control wholesome is the brain whose cognitive behavior makes the researchers to perform various tests on it for identifying and studying the functionalities. Though various methods are available for studying the brain functionality, study through the electroencephalography (EEG) signals was preferred in designing the working model such as the wheel chair system with man-less control drive for the physically challenged people or patients. The human brain controls the entire body through the interconnected neurons by generating waves or signals which support in controlling the wheel chair. In the proposed work, EEG signals are considered for activating the wheel chair movement. The wave patterns differ based on the patient thoughts and emotions in turn the generated electrical signals. The proposed work has been carried over by pre-processing where Notch filter is used, followed by feature extraction where FFT is used. The extracted signals are then used for training the machine language (ML) model. The classified signals are compared, and an optimistic approach has been identified to derive the physical model. The metrics evaluated for comparison are accuracy, sensitivity, precision and specificity. The optimistic signals are utilized for controlling the 360° movement of the wheel chair. The acquired EEG signals are communicated through wireless to the model after converting the waves into mental commands through appropriate software for a human-less support.

Keywords ML · EEG · Brainwaves signal · BCI

B. Ramesh (✉)
SKR Engineering College, Chennai, India
e-mail: <mailto:ramesh.ece@skrengcollege.org>

P. Polasi
SRM Institute of Science and Technology, Chennai, India
e-mail: <mailto:phanikup@srmist.edu.in>

1 Introduction

The quantity of physically challenged people is increasing continuously across the world. The considerable care on these people is a challenging task which instantiated the thought of developing a wheel chair for their comfort mobility aid. But, the medical officers suggested as statistics that more than 50% patients including paralysis patients could not control the wheel chair by conventional methods. Specifically, the people getting MND can use only their eyes and brain to exercise their willpower which drastically increases the stress and strain on the parts leading to additional medical issues. So, to avoid and reduce these difficulties, to suit the paralysis patients in their mobility as an aid, EEG-controlled wheel chair has been proposed, as an application of brain computer interface (BCI).

The patients affected by paralysis will be checked for the specific parts of the body having symptoms, and the medical officers diagnose the category of the disease such as localized or generalized. The localized paralysis affects only the specific parts in the human body, rather multiple body gets affected due to general paralysis. Considering the lateral cause as a much serious issue, the patient status can be categorized into four main conditions such as:

1. The effect of paralysis on one arm or one leg is said to be monoplegia.
2. The effect on both the legs is called as paraplegia.
3. When one arm and one leg on the same side if it gets affected, then it is said to be called as hemiplegia.
4. The other type of paralysis which affects all the four limbs of the human is said to be quadriplegia or tetraplegia.

The electroencephalographic (EEG) signals detect the brain activities, and the signals are transferred for controlling the wheel chair through BCI without any human interruption. The generated EEG signals are enhanced in its amplitude, and their features are also extracted through spectral and spatial filters. The EEG signals which are acquired from the brain depend on human gesture and thoughts with various frequencies and magnitude. The variations in values were observed between instant to instant. For instants, the change in frequency happens when there were movements and thoughts which were volunteered. The μ rhythm magnitude varies based on the brain activities which are either synchronized or asynchronized to suit the BCI for different applications.

The EEG signal acquired is generally classified based on the amplitude, frequency, shape of the acquitted signals along with the positioning of the electrodes with frequency band such as up to 4 Hz from 0.1, it is called as delta, 4 Hz, 8 Hz the waves are called as theta, the alpha waves frequency ranges 8 Hz, 12 Hz, for beta and gamma, the frequency ranges are 13 Hz, 30 Hz, 30 Hz and 100 Hz, respectively. Apart from the above-stated types, the signals are also classified based on the head distribution and symmetry property [1]. Since the waves are all categorized for its abnormality with reference to frequencies, the continuous rhythms suspected to be based on the behavior and mental status of the brain [2–4].

2 Related Works

In the recent years, various techniques were suggested by different authors. It was also meticulously tried to show that the proposal on BCI system was optimistic. In the year 2020, an effective survey was made [6] on BCI interfacing with neuro-feedback by introducing various haptic technologies and their applications. This survey resulted that the historically visual stimuli are unsuitable for engaging the transmission and reception between the patient and BCI system. It was also proved that though the hearable or recognizable feedback sensory had been explored, multiple sensational testing is expected for improving the interaction loop fineness. Ziebell et al. [7] progressed a low workload approach for the patients struggling due to locked in syndrome (LIS) to communicate the BCI systems. The process was made by P300 BCI by preventing inefficient BCI potentials. The study was carried over on two different strategies such as auditory and tactile BCIs through training effects and cross-stimulus modality transfer effects.

It was identified strongly that the training effect results in transition of cross-stimulus modality to tactile version and not the vice versa. It was also suggested that modality stimulus considerations are to be made based on individual patient preferences too. The disabilities in nerves system have been evaluated by analyzing the EEG signals through brain computer interface (BCI) implementation [8]. This sort of system supports in diagnosing nerves system disorders in the human body. The BCI channel transfers the generated signals as commands for controlling patients movement disability such as brain-controlled arm or wheel chair. The author made comparison on the acquired EEG signals when the patient was under normal condition and also while in drowsiness condition. The testing was done for the identical mentality condition of the patient and made the BCI implementation perfectly. Extending the test on classification, for the acquired EEG signals on different status of the patient, the fast Fourier transform (FFT) and power spectral density (PSD) are manipulated. This manipulation of FFT and PSD comparison differentiates the mental status of the patient or difference between two mental conditions.

It was stated that [9] the renaissance of the physically disabled people was uplifted through wheel chair facility to the patient by creating wireless communication between the wheels and patient seat gloves in an unidirectional way. It was observed that the designers had a challenging task [10] in creating and implementing a two-wheeled wheel chair which was comparable to the four-wheeled wheel chair. The data collected were used undergo eight imagery tasks [11] after classification and analysis. Also based on the absolute band power spectral density (PSD), the feature extraction was performed. It was also studied that [12] the modified version of ML classifier called OS-ELM found to result in an optimistic manner. Through ten-fold cross-validation, around 97.62% of accuracy was obtained using the specified OS-ELM classifier.

Phenomenally, accuracy of the EEG signal features decides the efficiency of BCI success in realizing the control. The difficulty in extracting the brain signals accurately increases when the patient is medicated with more alcoholic medicine which

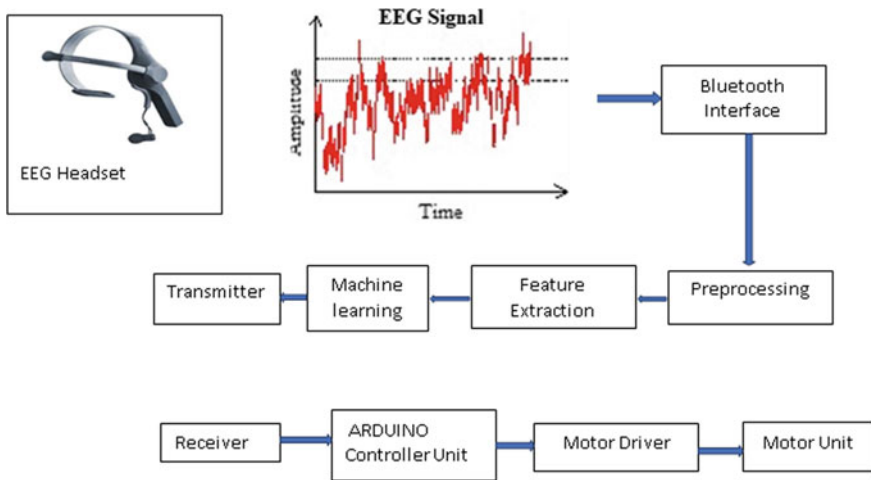


Fig. 1 Proposed model of EEG signal-based BCI Interfacing wheel chair control

leads more drowsiness. Using PCA, based on t-statistics feature selection, the EEG signals dimensions were reduced [13]. Based on the assessment [14] of deep learning made, it was concluded that an accurate result has been obtained through adaptive classifier. But, SVM, LDA, ANN and KNN algorithms may be utilized to obtain considerable accuracy when the classifiers were trained for it. Through the combination of PCA and WPT [15], EMD and wavelet transform (WT) [16], the authors extracted hybrid feature attained more than 74% of accuracy by performing two-stage classifications. While performing classification to obtain 80.09% of accuracy, SVM, KNN, Naïve Bayes, decision tree and LR algorithms were utilized.

Though there were different techniques in connecting the brain and external devices directly such as BCI or mind machine interface (MMI), it was studied that people confirmed with amyotrophic lateral sclerosis (ALS) or stokes may be affected by paralysis enormously. The motivation of the proposed work supports the physically challenged ones to move from place to place by means of controlling the wheel chair through the brainwaves by BCI. The BCI also supports the wheel chair control in all four directions such as front, back, right and left of the patient. The objective of the proposal was to merge the basic imagery tasks such as hungry, food, water and sleep with motor imagery tasks. The design was tested and simulated; later, it was also implemented Fig. 1.

3 Methodology

The proposed model comprises of Neurosky [17] headset for EEG data acquisition which was preprocessed to filter the unwanted signals and by ML algorithm; the featured data were given as input. The net outcome of the process was to transmit the required data as decision through the arduino board to control the wheel chair.

A. Data collection The experiment has been carried over by considering a quantity of subjects (healthy patients) comprising mixed gender. The subjects were permitted to participate in EEG data collection on their interest after communicating the instructions to be followed while data acquisition. Wearing the EEG device as head band, the EEG data were recorded from the subjects keeping their eyes closed and think on the imaginary task suggested in a noise-free atmosphere ensuring them to be under pressure-less mindset. The EEG signals were recorded by conducting several trials on all subjects for the suggested imagery tasks such as forward, backward, left, right, emergency.

B. Preprocessing The quality of acquired signals is verified for lossless information, and the signals were permitted to under filtration for removing noise data. The EEG signals has been protected from other appliances to avoid data corruption. The signals were converted to frequency domain by following FFT technique. By studying the frequency of the signal, the undesired signals are removed using notch Filter. Sampling the signal at set frequency 256 Hz, digitization has been performed followed by noise reduction using the filter resulting a range of frequency between 0.3 Hz 30 Hz. Signals less than 0.3 Hz and 30 Hz was neglected considering to be feasible and noise signals say gamma signals, respectively.

C. Feature extraction The desired signals were extracted from the raw EEG signal by filtering the noise available in the background. The EEG signals are characterized based on the frequency range such as gamma, beta, alpha, theta and delta. It has been inferred that the imagery frequencies between alpha or beta ranges. While performing FFT process, the imagery signals were compared with the sine wave, and the matching scores were also deduced which were progressed based on the similarities between the comparing signals. To improve the computational efficiency, linear discriminant analysis (LDA) has been applied to FFT for dataset reduction in dimension. Thus, an optimized subspace [18] has been obtained by performing the class separability and overfitting reduction. The proposed work has been carried over by applying FFT on the input matrix which results a matrix where the frequency components of input signals gets discrete for computation purpose. Statistical features such as mean, entropy and standard deviations are as shown in Eqs. (1), (2) and (3) [19], respectively, which support to study the status of the signals before classification.

$$\text{Mean} = \frac{\sum_{i=1}^M x_i}{M} \tag{1}$$

$$\text{Standard Deviation (SD)} = \sqrt{\frac{\sum_{i=1}^M (x_i - x)^2}{M - 1}} \tag{2}$$

$$\text{Entropy} = - \sum_{x=1} (P_x)(\log P_x) \tag{3}$$

where, x represents data value, M —total number of values and P_x —entropy calculation.

D. Classification Generally, researchers suggest for effective signal classification through neural networks—deep learning. There are several algorithms and methods had been suggested for classification such as ELM [20, 21] and OS-ELM [22] for multi-class classification. It was also identified that a modified version of OS-ELM called OR-ELM algorithm for classification which is capable of leaning RNN through a normalization method called as layer normalization (LN) by applying ELM auto-encoder. For getting zero-mean error approximation, the following equation has been defined for a single-layer feedforward neural network which comprises of M different sample (v_i, t_i) , N_h number of hidden layer, $f(x)$ activation function. Assuming the weight vectors between input layer and hidden layer, hidden layer and output layer as $w_i = [w_{11}, w_{12}, w_{13}, \dots w_{1n}]T$ and $\beta_i = [\beta_1 \beta_2 \beta_3 \dots \beta_n]$, the below Eqs. 4 and 5 quantify for zero error.

$$\sum_{i=1}^{M_h} \beta_i f(w_i.v_j + b_i) = t_j \tag{4}$$

where, $j = 1$ to M

$$H\beta = T \tag{5}$$

The matrix H was observed to be over determined matrix as the training example is greater than the hidden neurons. Equation (5) ensures that the H matrix has an unique solution. During the weights and bias, the hidden neurons may be left free without adjustment [22, 23]. The random values have been assigned, and considering the pseudo-inverse concept, the weight of the output β was obtained as shown in Eqs. (6) and (7).

$$\beta_1 = H^+ T \tag{6}$$

where H^+ is the psuedo-inverse which can be calculated by various methods.

$$H^+ = (H^+ H)^{-1} H^T \tag{7}$$

Hence, the least square solution:

$$\beta_1 = H^+ = (H^+ H)^{-1} H^T \tag{8}$$

Using the new approaches for RNN structure such as auto-encoding with normalization and feedback input on the conventional OS-ELM, it was proved that OR-ELM results better than the OS-ELM [24]. The networks RNN and a pair of SLFN considered to be an auxiliary ELM-AE networks for learning RNN’s input and hidden weight were considered to explain the configuration of OR-ELM. The RNN consists of n -dimensional input layer with a weight of as $W \in R_L \times n$ connected to L -dimensional hidden layer and the output layer, and the hidden layer weights were inferred to be $\beta \in R_m \times L$ and $V \in R_L \times L$, respectively.

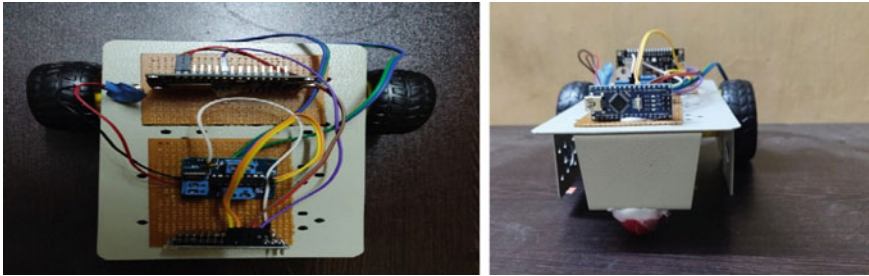


Fig. 2 Top and front views of the wheel chair

4 Working Model

It has been progressed that the developed model works for the automatic navigation and control of wheel chair to support the physically impaired due to paralysis or any other disease. Since the model works on EEG signals of brainwaves, the control of navigation has been realized for the mindset of the patient or user. The acquired brainwaves through electrodes are generally analog in nature. So, for processing and manipulation, the signal has been converted and conditioned to digital through an analog to digital converter. The EEG waves are acquired through NeuroSky, an EEG sensor.

The obtained digital signal of EEG waves for processing is transmitted through in-built Bluetooth transmitter for brainwave interfacing. A Bluetooth receiver was connected to the personal computer where the acquired raw brain signals were extracted and processed. The processed output is sent control unit through wireless transmitter. Generally, wireless transmitter and receiver work with our 434 MHz. Wireless receiver was connected to the Arduino controller unit. In the developed hardware model, the selected Arduino controller is a powerful single-board computer that gains a considerable traction professional market. The features and specification of the Arduino type are 1 Kb EEPROM storing space, 32 Kb flash for program space with 5 V operating volts and the vendor com version are ATMEL—Atmega327 microcontroller.

The controller outputs were given to the wheel chair module. The wheel chair module consists of relay drivers, relays and DC motor which makes the movement in different directions such as forward, reverse, left and right according to the acquired brain signals Fig. 2.

5 Results and Discussion

The input to the OS-ELM and OR-ELM was the feature extracted signals, and the datasets were partitioned as 88% and 12% for training and testing, respectively. The experiment results of different gestures acquired signals are shown in

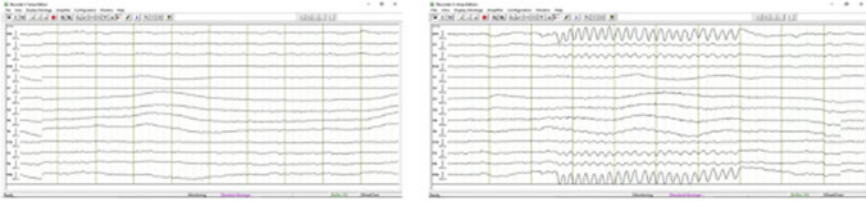


Fig. 3 Neutral mode and Forward movement mode

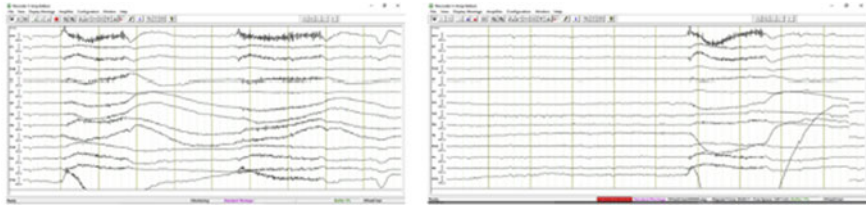


Fig. 4 Left side movement mode and Reverse movement mode

Figs. 3 and 4. By performing several iterations, it was observed that by cross-validation, the accuracy was 97.9%, sensitivity was 98.1%, and specificity was 99% for OS-ELM, and the accuracy was 98.2%, sensitivity was 98.8%, and specificity was 99% for OR-ELM. The parameters were compiled using the below-stated equations such as (9), (10), (11) and (12), respectively. The dataset responses of several other techniques such as random forest, SVM and OR-LEM were also computed as shown in Table 1. The OR-ELM has the highest accuracy and sensitivity compared with other classifiers.

$$\text{Accuracy} = \frac{TP + TN}{TP + TN + FP + FN} \tag{9}$$

$$\text{Precision} = \frac{TP}{TP + FP} \tag{10}$$

$$\text{Sensitivity} = \frac{TP}{TP + FN} \tag{11}$$

$$\text{Specificity} = \frac{TN}{TN + FP} \tag{12}$$

Table 1 Comparison of performance measures in different classifiers

Classifier	Specificity	Sensitivity	Accuracy
Random forest	77.28	84.12	79.15
SVM	88.01	84.98	89.98
ELM	98.01	95.02	94.32
OS-ELM	99.00	98.1	97.9
OR-ELM	99.00	98.8	98.2

6 Conclusion

The main aim of the work was to support the physically disabled and patients affected by paralysis. Objective of the paper was for the real-time support for disabled and paralyzed patients. It has been confirmed that the doctors and patients are more benefited for their references and utilization, respectively. The migration of wheel chair depends on the brainwaves of the patient, and the frequency ranges of the brainwaves are lower. Progressively, the wheel chair and brainwaves communication need to be done with lesser distance in the executed work. The medication values will vary from person to person and so the attention required also changes based on the requirements. Henceforth, the requirement for disabled people is lower, and thus, the threshold value can be assigned lower. The patient’s information will be received quickly by the doctors through brainwaves using the executed model of ours. After studying the various classification techniques, it was observed that OR-ELM and OS-ELM result better output comparatively such as in terms of accuracy, sensitivity and specificity. To improvise and enhance the working of the model developed, the sensor acceleration may be considered along with implementing the model through artificial intelligence and increasing the direction of movement across the land space in spite of staircase also.

References

1. Salmelin R, Hari R (1994) Spatiotemporal characteristics of sensorimotor neuromagnetic rhythms related to thumb movement. *Neuroscience* 60(2):537–550
2. Birbaumer N, Elbert T, Canavan AG and Rockstroh B (1990) Slow potentials of the cerebral cortex and behavior. *Phys Rev* 70
3. Kaufman MJ (2010) *Brain imaging in substance abuse: research, clinical, and forensic application* 1st edn, Totowa
4. Fell J, Axmacher N, Haupt S (2010) From alpha to gamma: electrophysiological correlates of meditation-related states of consciousness. *Med Hypotheses* 75(2):218–24. <https://doi.org/10.1016/j.mehy.2010.02.025>
5. Sathesh Kumar J, Bhuvaneshwari P (2012) Analysis of EEG signals and its characterisation—a study. Elsevier. <https://doi.org/10.1016/j.proeng.2012.06.298>

6. Fleury M, Lio G, Barillot C, Lecuyer A (2020) A survey on the use of haptic feedback for brain computer interfaces and neurofeedback. <https://doi.org/10.3389/fnins.2020.00528>
7. Ziebell P, Stümpfig J, Eidel M, Kleih SC, Kübler A, Latoschik ME, Halder S (2020) Stimulus modality influences session-to-session transfer of training effects in auditory and tactile streaming-based P300 brain-computer interfaces <https://doi.org/10.1038/s41598-020-67887-6>
8. Upadhyay R, Kankar PK, Prabinkumkarpadhy (2012) Classification of drowsy and controlled EEG signals. <https://doi.org/10.1109/NUICONE.2012.6493289>
9. Padmapriya S (2014) Design and development of a hand-glove controlled wheel chair 1(2). ISSN No: 2347–7210
10. Ahmad S, Tokhi MO (2008) Forward and backward motion control of wheelchair on two wheels. <https://doi.org/10.1109/ICIEA.2008.4582558>
11. Tiwari S, Goel S, Bhardwaj A (2020) Machine learning approach for the classification of EEG signals of multiple imagery tasks. In: IEEE, 11th international conference on computing, communication and networking technologies
12. Fahim MA, Damodar Reddy E, Dodia S, Kuppili V (2019) Brain-computer interface for wheelchair control operations: an approach based on fast fourier transform and on-line sequential extreme learning machine, vol 7 Elsevier, Clinical Epidemiology and Global. Health, pp 274–278
13. Rahman MA, Hossain MF, Hossain M, Ahmmed R (2020) Employing PCA and t-statistical approach for feature extraction and classification of emotion from multichannel EEG signal. Egyptian Inf J 21(1):23–35
14. Mansoor A, Usman MW (2020) Deep learning algorithm for brain-computer interface. Hindawi Scientific Programming Volume 2020, Article ID 5762149
15. Rahman MA, Hossain MK, Khanam F, Alam MK, Ahmad M (2019) Four-class motor imagery EEG signal classification using PCA, wavelet, and two-stage neural network. Int J Adv Comput Sci Appl
16. Gupta A, Agrawal RK, Kaur B (2015) Performance enhancement of mental task classification using EEG signal: a study of multivariate feature selection methods. Soft Comput 19(10):2799–2812
17. NeuroSky (2014) MindWave mobile: myndPlay bundle. In: EEG biosensor solutions. <http://neurosky.com/products-markets/eeg-biosensors>
18. Raschka S (2016) Python machine learning
19. Dixon WJ, Massey Jr FJ (1951) Introduction to statistical analysis
20. Tan P, Sa W, Yu L (2016) Applying extreme learning machine to classification of EEG BCI. In: 2016 IEEE international conference IEEE on cyber technology in automation, control, and intelligent systems (CYBER), pp 228–232
21. Ding S, Zhang N, Xu X, Guo L, Zhang J (2015) Deep extreme learning machine and its application in eeg classification. Math Probl Eng 2015:129021 11 pages. 8. Duan L, Bao M, Miao J, Xu Y, Chen J. Classification based on multi-layer extreme
22. Huang G-B, Liang N-Y, Rong H-J, Saratchandran P, Sundararajan N (2005) On-line sequential extreme learning machine. Comput Intell 2005:232–237
23. Guang-Bin H, Lei C, Siew CK (2006) Universal approximation using in cemental constructive feedforward networks with random hidden nodes. IEEE Trans Neural Network 17(4):879–892
24. Park J-M, Kim J-H (2017) Online recurrent extreme learning machine and its application to time-series prediction. In: 2017 International joint conference on neural networks (IJCNN). IEEE ISSN: 2161-4407

Web Book Recommendation System Based on Collaborative Filtering and Association Mining



S. Prasanth Vaidya and G. Naga Satish

Abstract Recommendation systems are used to make suggestions for products to buy or view. They steer consumers to the things that will meet their demands by sifting through a big database of information. For recommending items, several techniques such as content filtering, collaborative filtering, and association mining techniques have been employed. This improves performance by integrating collaborative-based filtering with association rule mining to overcome the problem of data sparsity. The results show that the suggested recommendation algorithms outperform the competition and address issues like data sparsity and scalability. To overcome the issue of no similarity, the proposed recommending system is based on similar items by computing similarity between user chosen items and available database items.

Keywords Recommendation systems · Collaborative filtering · Association mining

1 Introduction

Recommendation system (RS) is that the sort of info filtering that involves prediction of rating and user preferences, which might facilitate user to shop for things according to their desires and interest [1, 6, 13]. RS directs the thanks to end products, information in line with their interest [12, 15]. RS uses following technologies to suggest products: content filtering, cooperative filtering, and association mining (AM).

Content filtering recommends item, which is predicated on users profile, which he has likable in past [12, 15].

S. Prasanth Vaidya (✉)
Aditya Engineering College, Surampalem, India
e-mail: vaidya269@gmail.com

Jawaharlal Nehru Technological University Kakinada, East Godavari, Andhra Pradesh, India

G. Naga Satish
BVRIT Hyderabad College of Engineering for Women, Hyderabad, Telangana, India
e-mail: nagasatish.g@bvrithyderabad.edu.in

© The Author(s), under exclusive license to Springer Nature Singapore Pte Ltd. 2023
V. Bhateja et al. (eds.), *Communication, Software and Networks*, Lecture Notes in Networks and Systems 493, https://doi.org/10.1007/978-981-19-4990-6_38

421

Cooperative-dependent filtering is technique to investigate the user' behavior by predicting the users style to it of comparable to a different user [8, 9].

AM is detecting relations/correlation among things during a massive database. Associate in nursing association rule may be a condition of the shape $X \rightarrow Y$ wherever X and Y are 2 sets of items. It means that it finds correlation between X and Y , i.e., if we have a tendency to buy X item, then it finds possibilities to shop for Y items [10, 11].

All existing systems are based on content filtering (recommend items based on users previous history and this system will not work if user don't have any previous history) and collaborative filtering which are based on similar users, and if current user has no similarity, then this system will not work. To overcome from this issue, we proposed recommending items to users based on similar items by computing similarity between user chosen items and available database items.

Collaborative filtering faces following drawbacks: (a) Sparsity: The person who is very lively can provide score to few gadgets to be had in database. Popular object can be rate, through just a few numbers of customers that's referred to as facts sparsity problem. (b) Cold start: It is likewise referred to as new person problem, think if a person is new, then it is far hard to signify any object, due to the fact no person object is rated through the person. So, it is far hard to advice object to new person.

2 Modules

Collaborative filtering is to expect the person's opinion thru the usage of other person's opinion. It makes use of an method referred to as: Association rule prediction [4, 14]:

- common patterns, institutions, correlations, or causal structures among units of gadgets in transaction databases [3].
- client shopping for behavior through locating institutions and correlations among the extraordinary gadgets that clients vicinity of their cart [7].

Collaborative Filtering is of two types: user-based CF, item-based CF [2, 5].

User-based CF: In this algorithm, similarity among, as proven in Fig, extraordinary customers are calculated through the use of similarity measures, and then, those similarity measures are used to expect ratings. The underneath figure represents the actual time example. Figure 1 it is shown as the standing person buys three products, and the cycling person buys the two products which are similar to the standing person so, the cycling person will get a suggestion of a new product from the standing person. Because the users similarity is same.

Item based CF: In this algorithm, similarity among extraordinary gadgets, as proven in Fig.2, is calculated through the use of similarity measures after which those similarity measures are used to expect ratings.

If third person likes watermelon, then system can recommend him grapes as first person also likes watermelon, grapes. So, both users have similar likes for water-

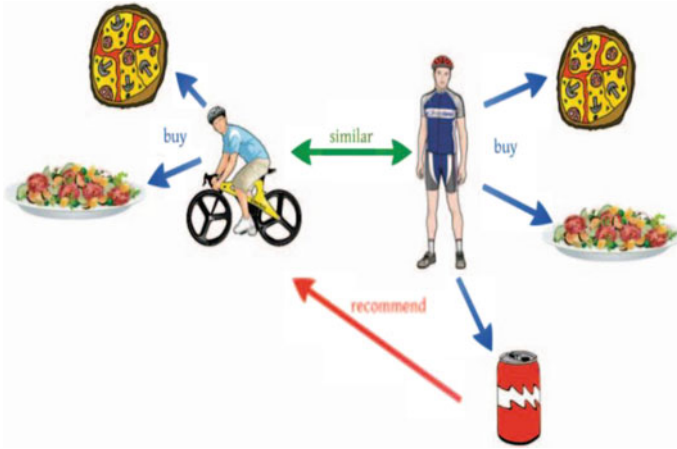


Fig. 1 User-based collaborative mining

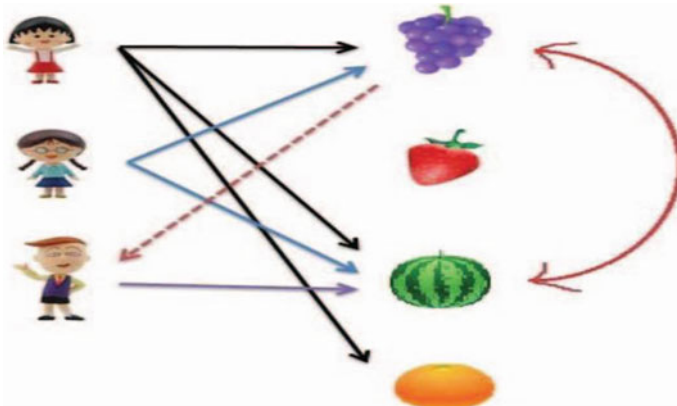


Fig. 2 User-based collaborative mining

melon. To implement this concept, the proposed scheme applied collaborative filtering by taking two user's data and use associating mining for comparing similar items. If User A, User C like watermelon, then User C may like grapes. User A \rightarrow User C = watermelon, grapes. In the above dataset data, the proposed scheme used mainly five columns ISBN, Book-Title, Book-Author, Year-Of-Publication, Publisher.

3 Proposed System

The proposed device makes use of mixture of collaborative filtering and affiliation mining. Collaborative filtering is used for locating similarity among objects which could assist the device to advise objects, and affiliation mining is used for filling the vacant scores wherein necessary. Then, it makes use of prediction of goal person to the goal object the usage of object primarily based totally collaborative filtering. Thus, the usage of both techniques can assist to manipulate information sparsity hassle and bloodless begin hassle in recommender device.

Advantage of Proposing System

The combination of both CF and AM methods can in assisting DSP and CSP in RS.

The recommendation system became a major use in present generation, not only foods or online gadgets recommendations, book recommendation is also necessary for the society and useful, therefore creating interest in reading and learning in day to day life, to upskill and survive in tech world, and this recommendation implements accuracy and best time complexity. The growing power of generation progressed has intensely progressed the records storage, collection, and manipulation ability. As the records are developing very fast along with its complexity, information mining has emerged as greater important. The goal of the proposed device is to advise books to the person that are much more likely to be associated with their input. The device first describes approximately exclusive strategies for advice and the studies concerning advice device, then shows a higher method for an amazing advice device and explains the outcomes of that method. Here, a mixture of collaborative filtering and affiliation mining strategies are completed in order that a higher advice listing can be obtained (Fig. 3).

The options in the proposed system are as follows:

- Upload book dataset is used to upload a dataset into the software.
- Filter dataset is used to convert the text into vector format.
- Get suggestion is used to enter the input and by clicking ok then it will give the recommendations based on the given input.
- Recommendation graph is used to show the graph of recommended books compared to total books data in the dataset.

All the steps of the proposed scheme are given in figures below.

1. Graphical user interface(GUI) consisting of all options.
2. Upload Book Dataset Button Function: Click on 'Upload Book Dataset' button to upload dataset directly to the software. By clicking the Upload Book Dataset button, it will open an file dialog box, in that we want to select the Excel file to load the data in the GUI.
3. Loaded Dataset.
4. Filtered Dataset: to generate vector with each work count. This vector helps us to get similarity between items. Wait for some time till it processes complete dataset.

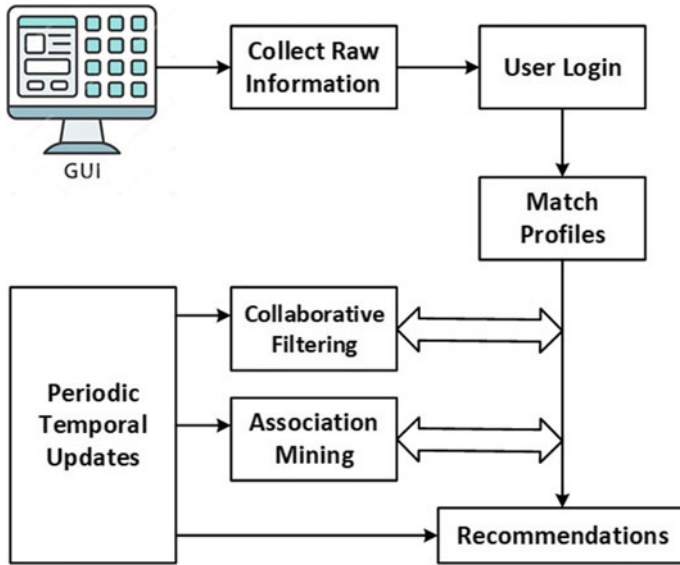


Fig. 3 Workflow of book recommendation systems

5. Get Suggestion: enter your desired book details to get recommended items list with similarity scores.
6. Output: recommended list for input ‘C Programming’. In each line at last column, we can see similarity score. And in the middle, it shows the Number of Books Count, Recommended Books Count, Similarity Percent. In the bottom, it shows the ‘You may also like’ which are related to the given input.
7. Recommendation Graph: get the graphical representation of dataset si for given input.
8. Get Suggestion search with Author Name ‘Reema Thareja’.
9. The recommended list for input ‘Reema Thareja’. In each line at last column we can see similarity score. And in the middle, it shows the Number of Books Count, Recommended Books Count, Similarity Percent. In the bottom it shows the ‘You may also like’ which are related to the given input.
10. Get suggestion search with input a Publisher name as ‘Cengage Learning’.
11. The recommended list for input ‘Cengage Learning’. In each line at last column, we can see similarity score. And in the middle, it shows the Number of Books Count, Recommended Books Count, Similarity Percent. In the bottom, it shows the ‘You may also like’ which are related to the given input (Figs. 4, 5, 6 and 7).

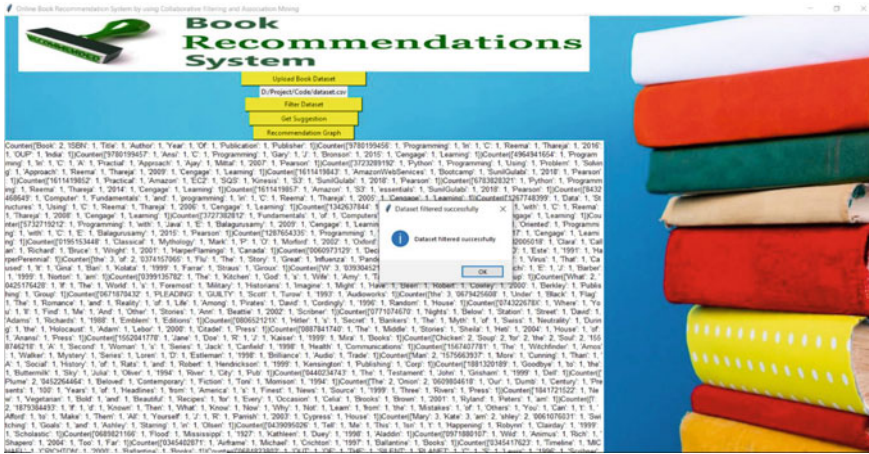


Fig. 4 Filtered dataset

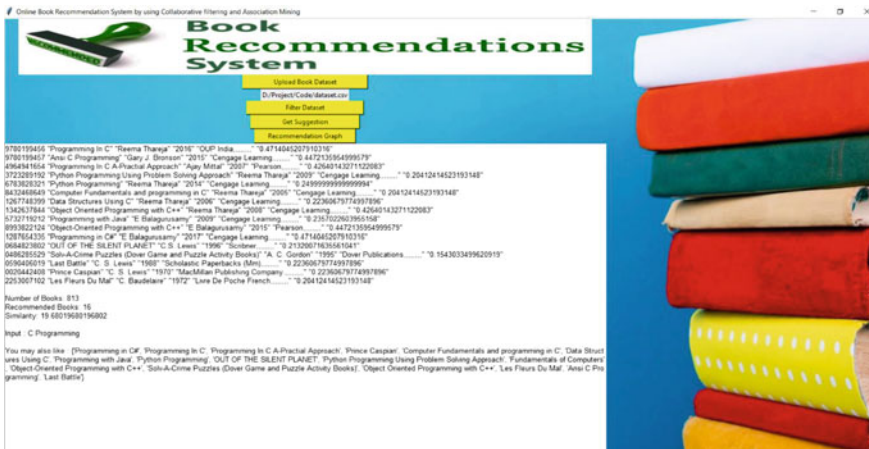


Fig. 5 Recommended books based on 'c Programming'

4 Conclusion

The growing needs of online information have result in invent new strategies for prioritizing and providing gadgets of users interests. This paper uses item primarily based totally collaborative filtering to produce ratings. The item primarily based totally collaborative filtering can put off the records sparsity trouble and might offer right recommendation. Finally, the consequences of similarity calculation supply right overall performance at accuracy.

The recommendation system became a major use in present generation, not only foods or online gadgets recommendations, book recommendation is also necessary



Fig. 6 Get suggestion search with author name 'Reema Thareja'

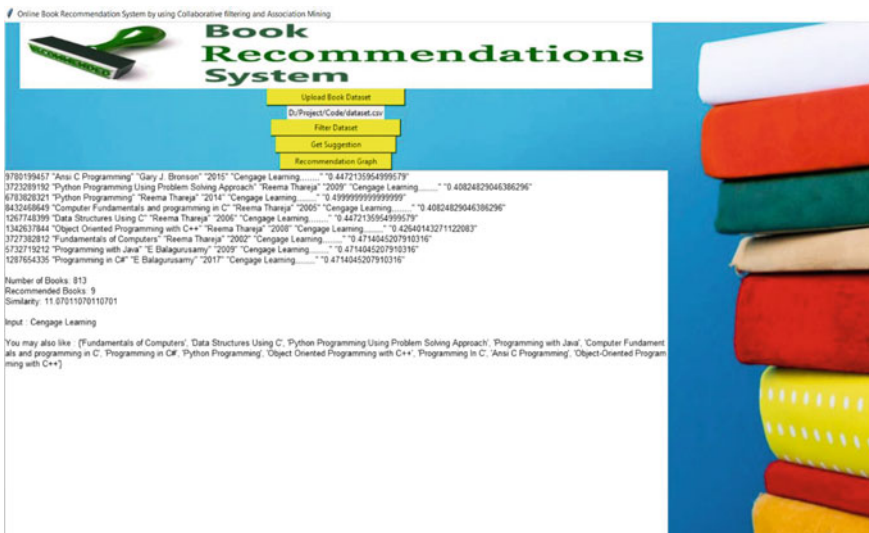


Fig. 7 Get suggestion search with input a publisher name as 'Cengage Learning'

for the society and useful, therefore creating interest in reading and learning in day to day life, to upskill and survive in tech world and this recommendation implements accuracy and best time complexity. We can develop an application for the book recommendation system for the easy access when we want to know the recommendations of the particular book.

References

1. Bogers T, Koolen M (2017) Defining and supporting narrative-driven recommendation. In: Proceedings of the eleventh ACM conference on recommender systems, pp 238–242
2. Cai X, Hu Z, Zhao P, Zhang W, Chen J (2020) A hybrid recommendation system with many-objective evolutionary algorithm. *Expert Syst Appl* 159:113648
3. Chen YC, Hui L, Thaipisutikul T (2021) A collaborative filtering recommendation system with dynamic time decay. *J Supercomput* 77(1):244–262
4. Cui Z, Xu X, Fei X, Cai X, Cao Y, Zhang W, Chen J (2020) Personalized recommendation system based on collaborative filtering for IoT scenarios. *IEEE Trans Serv Comput* 13(4):685–695
5. Gondaliya S, Amin K (2021) A framework based on latent neighbourhood and tensor based method for recommender system. In: Applications of artificial intelligence in engineering. Springer, Berlin, pp 883–892
6. Ma X, Lu H, Gan Z, Zeng J (2017) An explicit trust and distrust clustering based collaborative filtering recommendation approach. *Electron Commer Res Appl* 25:29–39
7. Nassar N, Jafar A, Rahhal Y (2020) A novel deep multi-criteria collaborative filtering model for recommendation system. *Knowl-Based Syst* 187:104811
8. Raghuvanshi SK, Pateriya R (2019) Recommendation systems: techniques, challenges, application, and evaluation. In: Soft computing for problem solving. Springer, Berlin, pp 151–164
9. Si M, Li Q (2020) Shilling attacks against collaborative recommender systems: a review. *Artif Intelli Rev* 53(1):291–319
10. Singh SP, Solanki S (2019) A movie recommender system using modified cuckoo search. In: Emerging research in electronics, computer science and technology. Springer, Berlin, pp 471–482
11. Srivastava A, Bala PK, Kumar B (2020) New perspectives on gray sheep behavior in e-commerce recommendations. *J Retail Consum Serv* 53:101764
12. Thakkar P, Varma K, Ukani V, Mankad S, Tanwar S (2019) Combining user-based and item-based collaborative filtering using machine learning. In: Information and communication technology for intelligent systems. Springer, Berlin, pp 173–180
13. Xiong R, Wang J, Zhang N, Ma Y (2018) Deep hybrid collaborative filtering for web service recommendation. *Expert Syst Appl* 110:191–205
14. Zarzour H, Al-Sharif Z, Al-Ayyoub M, Jararweh Y (2018) A new collaborative filtering recommendation algorithm based on dimensionality reduction and clustering techniques. In: 9th International conference on information and communication systems (ICICS). IEEE, pp 102–106
15. Zhang L, Luo T, Zhang F, Wu Y (2018) A recommendation model based on deep neural network. *IEEE Access* 6:9454–9463

IOT-Based Smart Trash Collection with Swachh Survekshan



Nalla Siva Kumar, N. Akhila, S. Prasanth Vaidya, and G. Naga Satish

Abstract In the current era examining, detection and management of garbage are one of the major problems. The conventional policy of physically supervising wastes in dust bins is a burdensome practice and requires extra human power, day, and expenditures can be bypassed with the proposed technologies. To conquer the complications produced by the dust bins, the proposed approach utilizes smart dust bins with the help of sensors, IoT.

Keywords IoT · Smart Trash Collection · Swachh Surveskhan

1 Introduction

In the present world, managing the waste generated by human beings is a great burden to the municipality workers. The maintenance of the trash bins is not up to the mark which is causing a major effect to the environment and life cycle [8]. The waste generated by the humans should be well managed by collecting them in regular intervals and providing more number of workers in maintaining clean and green environment. In addition to this, our government started a survey on cleanliness to rank the cities by “Swachh Survekshan” where the results will not be exactly correct because it is

N. S. Kumar · N. Akhila · S. Prasanth Vaidya (✉)
Aditya Engineering College, Surampalem, India
e-mail: vaidya269@gmail.com

N. S. Kumar
e-mail: sivakumar.nalla@aec.edu.in

N. Akhila
e-mail: akhila.nalla@aec.edu.in

Jawaharlal Nehru Technological University, EG District, Kakinada, Andhra Pradesh, India

G. Naga Satish
BVRIT Hyderabad College of Engineering for Women, Hyderabad, Telangana, India
e-mail: nagasatish.g@bvrithyderabad.edu.in

© The Author(s), under exclusive license to Springer Nature Singapore Pte Ltd. 2023
V. Bhateja et al. (eds.), *Communication, Software and Networks*, Lecture Notes
in Networks and Systems 493, https://doi.org/10.1007/978-981-19-4990-6_39

a survey that depends on municipality bodies and the citizens feedback [11]. Tran et al. [1] considered waste management as a serious issue and proposed an optimal waste management by calculating the level of waste in the trash bin. Sohail et al. [14] proposed an intelligent trash bin and efficient optimization for trash collection. The proposed method utilizes Internet of Things (IoT) in implementing Swatchh Survekshan with real-time utilization.

2 Existing Recognition Systems

In the present scenario, most of the municipality workers are not working affectively due to multiple reasons like less salary, more workload, and more waste generated by humans. Due to this, the waste generated by humans is increasing which can be observed in many areas with foul smell, full of mosquitoes, house flies. The spread through these waste is leading to health problems to humans, especially to kids with different kinds of diseases like tuberculosis, pneumonia, diarrhea, tetanus, whooping cough, and so on [12–14, 17].

3 Proposed Systems

The proposed scheme utilizes smart trash bins in managing the waste generated by human beings. The smart trash bins act as micro-controller system with the help of ultra-sonic wireless sensors placed with in the dustbin. This helps in monitoring the status of the smart trash bin with waste. The ultra-sonic sensors help in knowing the quantity of the waste place on the top of the bin. The smart bin is monitored and managed through the Web site by updating the level of the bin, status of waste with Wi-Fi. The proposed system architecture is shown in Fig. 2. The system uses MSP430 micro-controller which is connected to two different ultra-sonic sensors and Wi-Fi mobule with 3.3 V power supply. The LCD which displays 16×2 character is also connected with 5V power supply. With the help of Internet, the server collects data from the trash bins with Wi-Fi router and sends them to the destination devices of PC or mobile.

4 Components of Proposed System

4.1 Trash Bin

A container for demonstration is being kept to store waste or scrap usually made up of metal or plastic [4, 9] as shown in the Fig. 1.

Fig. 1 Trash bin

4.1.1 Ultrasonic Sensor

Ultrasonic sensors are used to emit and receive sonic waves with the help of transducer. Sonic waves will be reflected back when they hit an object or opaque substances [5, 6, 16]. This methodology helps us to find the empty space in the trash bin.

4.2 *Wi-Fi Component(ESP8266)*

The Wi-Fi component is unified with TCP/Ip protocol. It provides permission for the micro-controller to connect to the smart trash bin through Wi-Fi network [10, 15]. The Wi-Fi component has the advantages of presenting or showing the application with different network functionalities.

4.3 *Micro Controller MSP430 G2553*

The MSP430 series of micro-controllers consumes very low power as ultra-low power. It has five low-power modes to keep safe of battery life [3, 7]. It contains powerful 16-bit RISC CPU, 16-bit registers. To contribute maximum code efficiency, constant generators were used.

5 Design and Implementation

Initially, the sensor detects the level of the trash bin, and it sends to the micro-controller where the process is done and the bin status data are sent to the server by using Wi-Fi, and then, the data are retrieved to the Web page and can be cats as monitoring screen requires users to attain a token before they are granted network entry as shown in the Fig. 2.

The proposed system uses MSP 430 micro-controller consisting of LCD screen and Wi-Fi component in providing the status of the smart trash bin. The quantity of waste present in the trash bin is displayed in the LCD screen in terms of level. The Web page displays the status of the different trash bins with their level of waste collected in the smart bins. The Web page can be monitored by municipality authority or supervisor. The Web page also provides the waste collection and their status in terms of graphical representation to easily know the status of different smart bins with their level of waste collection. The supervisor can observe and analyze from which areas the waste is generated more and which areas are facing waste pollution.

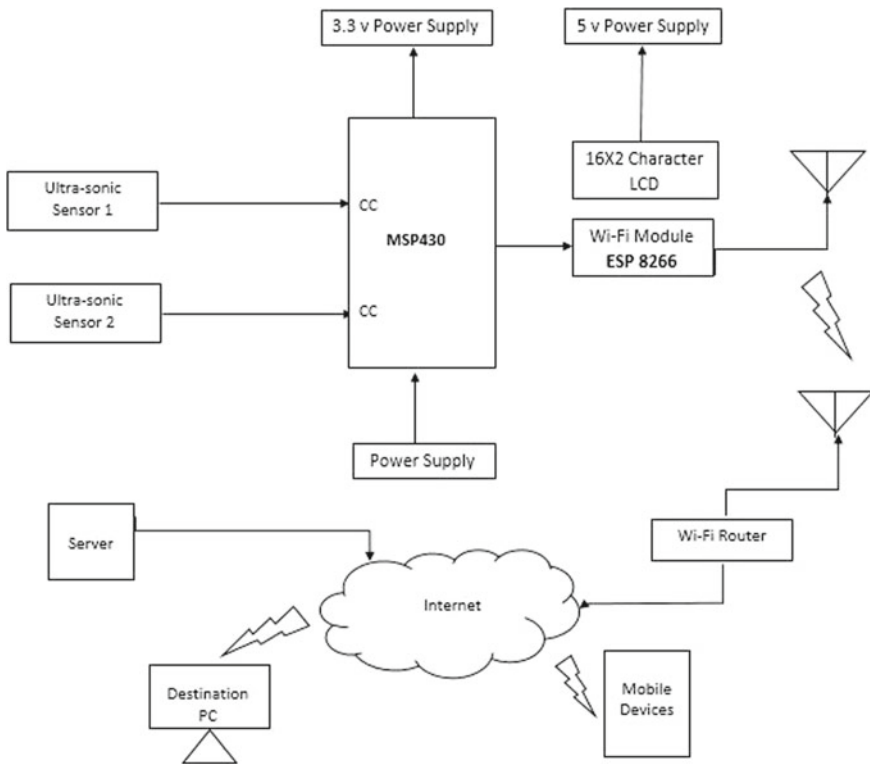
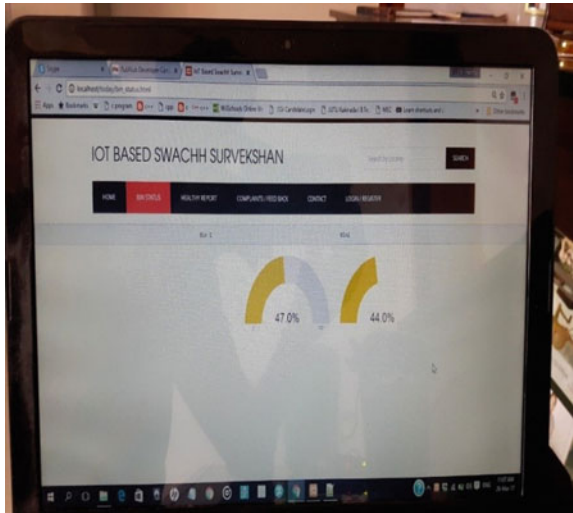


Fig. 2 Block diagram for IoT-based Smart Trash Collection and Swachh Survekshan

Fig. 3 Bin status



Fig. 4 Bin Status of Swachh Survekshan monitoring system



The bin status with the level of waste in it is displayed on the LCD is shown in Fig. 3. The proposed Swachh Survekshan monitoring system is shown in Fig. 4.

5.1 Pubnub Cloud Server

In real time, data transfer and connection to the device is possible with Pubnub cloud server. This helps in establishing a connection to devices, i.e., smart trash bins in getting the status to the system with less than 1/4 s [2]. The server transfers data from

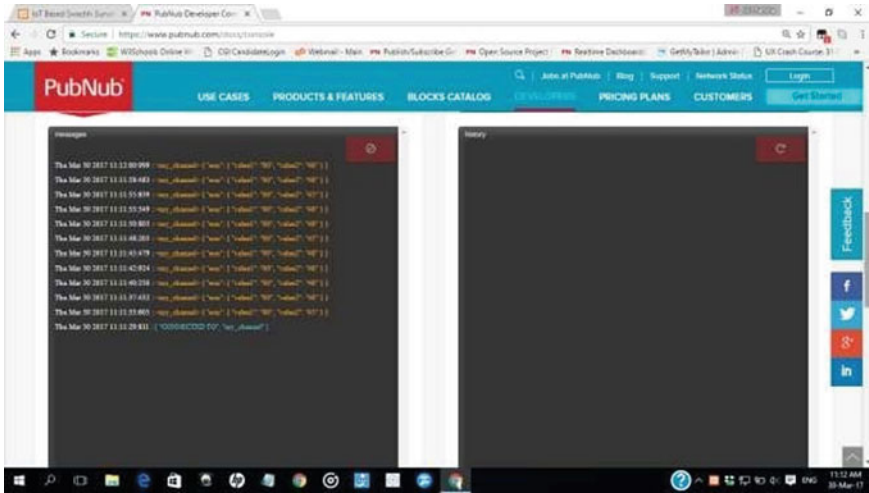


Fig. 5 Data streaming of Pubnub cloud server

sender to the receiver through multiple channels. Data streaming of Pubnub cloud server is shown in Fig. 5.

6 Testing and Deployment

Initially Citizen should sign up with the user name and password in order to access the Web site. After that registered user can login and upon verification, can initiate the subsequent actions like he/she can posts complaints as shown in the Fig. 6.

If garbage reaches the threshold, bin status data collected from the sensor is stored in the database. Municipal department can view the healthy reports by seeing the complaints in Table 1.

7 Conclusion

The idea of IoT-based smart trash collection and Swachh Survekshan is to provide exact data to the authorities. The proposed method collects data directly from the smart trash bin where sensors collect the data from the trash bin and send it to the cloud server, and then, it will be retrieved by the local monitoring system for better waste disposal and management practices. The propose method helps in monitoring the trash bins and analyzing the trash quantity and maintenance of cleanliness.

Table 1 Feedback results of Swachh Survekshan monitoring system

Name	Ram Muthy	Karuna	Lakshmi	Kalyan	Murali	Kirammai	Mehar
Contact No	98719*****	867876*****	67345*****	90009*****	67655*****	89123*****	98739*****
Gender	M	F	F	M	M	F	M
City	Hyd	Rjy	Rjy	Hyd	Rjy	Hyd	Hyd
Pincode	5600101	533254	533254	5600101	533254	5600101	5600101
How did you get to know about Swachh Survekshan?	News Paper	Social Media	Social Media	News Paper	FM Radio	Man Ki Baat	News Paper
Are you aware that your city is participating in Swachh Survekshan?	Yes	Yes	Yes	Yes	Yes	Yes	Yes
Do you find your area cleaner than last year	Yes	No	No	Yes	No	Yes	Yes
Do you think the availability of dust or litter bins have improved in market area this year?	Yes	Yes	Yes	Yes	Yes	Yes	Yes
Are you satisfied with the door to door waste collection from your house this year?	Yes	No	No	Yes	No	Yes	Yes
Do you think the number of toilets has increased in comparison to the last year?	Yes	Yes	Yes	Yes	Yes	Yes	Yes
Has the maintenance of public/community toilets improved?	Yes	No	No	Yes	No	Yes	Yes
Want to rate with us for customer service?	4	3	3	4	3	5	4
Any Complaints?	NA	NA	NA	NA	NA	NA	NA

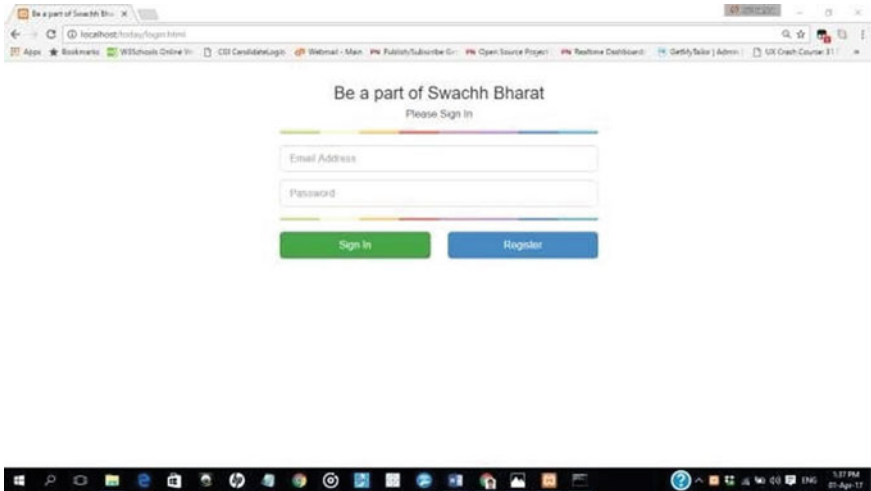


Fig. 6 Login page

References

1. Anh Khoa T, Phuc CH, Lam PD, Nhu LMB, Trong NM, Phuong NTH, Dung NV, Tan-Y N, Nguyen HN, Duc DNM (2020) Waste management system using iot-based machine learning in university. In: Wireless communications and mobile computing
2. Anthi E, Ahmad S, Rana O, Theodorakopoulos G, Burnap P (2018) Eclipseiot: a secure and adaptive hub for the internet of things. *Comput Security* 78:477–490
3. Garbhapu VV, Gopalan S (2017) Iot based low cost single sensor node remote health monitoring system. *Proc Comput Sci* 113:408–415
4. Haribabu P, Kassa SR, Nagaraju J, Karthik R, Shirisha N, Anila M (2017) Implementation of a smart waste management system using iot. In: 2017 International Conference on Intelligent Sustainable Systems (ICISS). IEEE, pp 1155–1156
5. Kumar NS, Vuayalakshmi B, Prarthana RJ, Shankar A (2016) Iot based smart garbage alert system using arduino uno. In: 2016 IEEE region 10 conference (TENCON). IEEE, pp 1028–1034
6. Lee C, Han Y, Jeon S, Seo D, Jung I (2016) Smart parking system using ultrasonic sensor and bluetooth communication in internet of things. *KIISE Trans Comput Pract* 22(6):268–277
7. Mischie S, Pazsitka R (2019) Designing a msp430 bootloader. In: 2019 international conference on Applied Electronics (AE). IEEE, pp 1–4
8. Nirde K, Mulay PS, Chaskar UM (2017) Iot based solid waste management system for smart city. In: 2017 International Conference on Intelligent Computing and Control Systems (ICICCS). IEEE, pp 666–669
9. Ramson SJ, Moni DJ, Vishnu S, Anagnostopoulos T, Kirubaraj AA, Fan X (2021) An iot-based bin level monitoring system for solid waste management. *J Mater Cycles Waste Manage* 23(2):516–525
10. Rezwan S, Ahmed W, Mahia MA, Islam MR (2018) Iot based smart inventory management system for kitchen using weight sensors, ldr, led, arduino mega and nodemcu (esp8266) wi-fi module with website and app. In: 2018 Fourth International Conference on Advances in Computing, Communication and Automation (ICACCA). IEEE, pp 1–6

11. Saha HN, Auddy S, Pal S, Kumar S, Pandey S, Singh R, Singh AK, Banerjee S, Ghosh D, Saha S (2017) Waste management using internet of things (iot). In: 2017 8th annual industrial automation and electromechanical engineering conference (IEMECON). IEEE, pp 359–363
12. Sanivarapu PV (2021) Multi-face recognition using cnn for attendance system. In: Machine learning for predictive analysis. Springer, Heidelberg, pp 313–320
13. Singh A, Vaidya SP (2019) Automated parking management system for identifying vehicle number plate. *Indonesian J Electrical Eng Comput Sci* 13(1):77–84
14. Sohail H, Ullah S, Khan A, Samin OB, Omar M (2019) Intelligent trash bin (itb) with trash collection efficiency optimization using iot sensing. In: 2019 8th International Conference on Information and Communication Technologies (ICICT). IEEE, pp 48–53
15. Srivastava P, Bajaj M, Rana AS (2018) Overview of esp8266 wi-fi module based smart irrigation system using iot. In: 2018 fourth international conference on Advances in Electrical, Electronics, Information, Communication and Bio-Informatics (AEEICB). IEEE, pp 1–5
16. Suryawanshi S, Bhuse R, Gite M, Hande D (2018) Waste management system based on iot. *Waste Manage* 5(03):1–3
17. Wilson ST, Sebastine T, Daniel M, Martin V, Neenu R (2019) Smart trash bin for waste management using odor sensor based on iot technology. *Int J Adv Res Ideas Innov Technol (IJARIIT)* 5(2):2048–2051

Particle Swarm Optimization-Based Energy-Aware Task Scheduling Algorithm in Heterogeneous Cloud



Roshni Pradhan and Suresh Chandra Satapathy

Abstract Task scheduling in a cloud computing environment is one of the important aspects in the field of information technology. An efficient schedule is required to enhance the performance of the whole system which results a good quality of services (QoS). It is an NP-complete problem and attracts many researchers to use various meta-heuristics algorithms to develop task scheduling methods in the cloud environment. In most of the evolutionary methods, search space is large and initialized randomly which is one of the key components. In this paper, using the working mechanism of particle swarm optimization (PSO) algorithm, a set of solutions or schedules is created. Solution with efficient QoS parameters like makespan, cloud utilization, and energy consumption is chosen for allocation of the task into the heterogeneous multi-cloud environment. The algorithm undergoes a simulation process and is tested upon benchmark datasets which shows a better result in comparison to some existing cloud scheduling algorithms like min-min, max-min, cloud min-min scheduling (CMMS), cloud max-min scheduling (CMAXMS), and cloud normalized min-min max-min (CNXM) algorithms, genetic algorithm, etc.

Keywords Cloud · NP-complete · Makespan · Cloud utilization · Meta-heuristics

1 Introduction

The huge requirement of internet-based technology and application heads toward the rapid development of the cloud computing environment. It offers numerous services over the internet. Users of cloud computing avail facilities like computing resources, storage for data, system resources, etc. with an illusion of infinite computing facilities. All these are handled by data centers that are geographically distributed and situated in many regions. Cloud computing provides mainly three types of services

R. Pradhan (✉) · S. C. Satapathy
School of Computer Engineering, KIIT Deemed to be University, Bhubaneswar, India
e-mail: roshni.pradhanfcs@kiit.ac.in

S. C. Satapathy
e-mail: suresh.satapathyfcs@kiit.ac.in

infrastructure as a service (IaaS), platform as a service (PaaS), and software as a service (SaaS) [1]. Resource provision along with elastic computing is provided by the IaaS cloud. In PaaS, clients are given authority to use the cloud environment to build their software in the platform provided by cloud service providers (CSP). Users can avail of PaaS to use the software directly from the CSP. Virtualization is an important aspect of cloud computing, which enables a required number of virtual machines (VM) to the users [2]. It plays a vital role in task scheduling in a cloud computing environment. Different users submit their requests to the cloud environment in the form of a set of tasks that are allocated to machines or VMs in the cloud. Cloud computing follows the technique behind a combination of parallel and distributed computing. In a cloud system, the user aims to achieve efficient scheduling parameters after allocating all the tasks to the available resources [3, 4]. To provide an efficient and optimal schedule, it is required to analyze different optimization parameters which can be implemented in cloud task scheduling. In most of the research studies, evaluation parameters like makespan, cloud utilization, deadline time, energy consumption, etc. are considered [5–7].

Nowadays, energy consumption has become the crucial factor in cloud data-centers. To reduce it, cloud engineers are approaching nature-inspired optimized scheduling techniques which focus on less energy consumption in data centers.

Energy estimation and cloud resources usage are profoundly coupled [8, 9]. Low cloud resource usage is hollering an unsuitable measure of energy when they are completely used or adequately stacked. A new review on energy utilization and carbon emission of huge data centers is exceptionally high in the year of 2005, in the USA. Data centers in European locale have been assessed to devoured 1% sum of carbon emission, while in the USA, it is 2.8% around the same time [9–13]. In distributed computing, the basic equipment framework is hidden from the end client. Even though application solicitation can be thought about for low utilization of energy and high usage of cloud resources, cloud resources ought not to be over-burden or underloaded by the undertakings, rather ought to be utilized ideally [14].

In cloud task scheduling, different types of techniques are like heuristics scheduling, workflow scheduling, static scheduling, and dynamic scheduling [15]. According to the complexity of an algorithm, task scheduling can be described as heuristic, meta-heuristic, and hybrid task scheduling approaches [16]. Heuristics algorithms are mainly used to evaluate task scheduling algorithms like minimum execution time (MET), minimum completion time (MCT), shortest job to fastest processor (SJFP), min-min, max-min. In a cloud environment, generating a task schedule using a meta-heuristic algorithm is becoming the most approachable area of research. It deals with a multi-modal optimization problem. Task scheduling in the cloud is an NP-complete problem using meta-heuristics methods. Traditional meta-heuristics algorithms are particle swarm optimization (PSO), ant colony optimization (ACO), genetic algorithm (GA). In the recent study, a variety of approaches are found like Jaya algorithm, social-group optimization (SGO), teaching learning-based optimization (TLBO), etc. All these algorithms focus on a set of populations. In PSO, these populations are considered as particles. Scheduling is applied on this

set of solutions to generate an efficient schedule. Using popular cloud scheduling parameters like makespan, it is evaluated [17].

In PSO, a set of particles is considered and initialized randomly. Each particle is assumed to be a task and is allocated to the available VM. Random initialization of particles is an important key factor in PSO. It leads to providing a wide range of search space for the particles which is a boost to an optimal solution [18]. It improves the performance of the PSO algorithm. The working mechanism of PSO is given through a flowchart in Fig. 1.

In this paper, the proposed method is to utilize heuristic scheduling algorithms to initialize the PSO search process. Makespan, cloud utilization, and energy consumption are also considered as optimization parameters [19]. The rest of the paper is listed as follows. Section 2 overviews the related works. Section 3 describes the system model of our scheduling approach. The scheduling algorithm is presented in

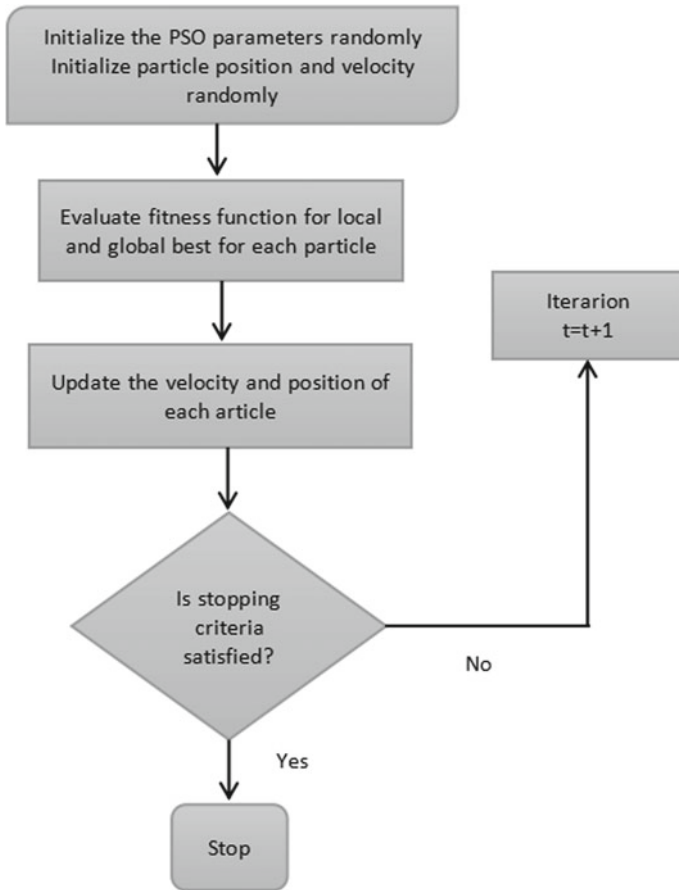


Fig. 1 PSO working mechanism

Sect. 4. Experimental evaluations and importance of dataset are described in Sect. 5. Section 6 concludes our work and highlights the future works.

2 Background and Related Work

In the current research area of interest, optimizing the scheduling parameters using an efficient schedule is gaining popularity. Besides this, resource allocation, cloud load balancing, security aspects in the cloud, energy efficiency are also major issues that attract attention. Clients or users, data centers, task managers are the components of this model. Data centers are responsible for the provision of an ample number of virtual machines required for the processing of requests. A task manager and scheduler are implemented to track the tasks before and after submitting into the resources and to prepare a schedule for upcoming tasks. Client requests in the form of tasks are updated in the task queue and later allowed for submission into resources.

In recent years of the survey, it has been noticed that many task scheduling algorithms are generated. These algorithms are either heuristics or meta-heuristics. Some of the algorithms focus on reducing makespan, whereas some algorithm designs a schedule that maximizes the cloud utilization values. There are some static traditional cloud scheduling algorithms proposed among which min-min, max-min, suffrage heuristics are included. The most important aspect is energy consumption in the cloud environment. In cloud computing, virtualization plays an important role, where data centers are engaged to create VMs. Data centers are globally distributed, and the number of data centers is growing rapidly to fulfill the client requests. In a recent study, it has been observed that 16% of data centers have been added. This results in a high increase in carbon emission, and the computation rate raised to 76%. To neutralize this impact, the USA has taken initiatives like the European code of conduct, the Energy Star program, and the 80 PLUS. The cloud environment has an architecture of two types, i.e., hardware and software. It is a tedious task to manage this architecture. The hardware environment can be manipulated by modifying the circuits to reduce energy consumption. In cloud data centers, the resource and energy consumption using an efficient task scheduling method is applied as suggested by [14]. But, the performance evaluation is not conducted in this paper. Energy-aware task consolidation is proposed by Refs. [19, 20] which aims to restrict CPU utilization. Hierarchical scheduling method is proposed to optimize the energy parameters in many research articles.

3 Models Used in the Proposed Algorithm

3.1 Cloud Task Scheduling Model

A cloud computing scenario is an architecture that incorporates several servers inside a data center. Servers are nothing but high-end processors and are treated as the resources for the client's requests. Requests are submitted in the form of a task queue. Tasks follow a specific algorithm, pass through a queue and task manager, and result the output. These algorithms are judged or analyzed in terms of their efficiency. Data transfer cost is also one among the quality of service (QoS) parameters which are treated as a vital factor. However, in most of the research papers, it is considered negligible. Using PSO, an efficient schedule is prepared, and along with that, QoS parameters like makespan, completion time, cloud utilization, and energy consumption are tracked.

3.2 Application Model

A group of tasks is taken in the form of application model. These are prepared to form a schedule, and a queue is generated. All the tasks are treated as independent and have their individual properties like execution time, completion time, etc. In this application model, execution time is used and previously estimated. It is stored in a task to machine/cloud matrix popularly known as the expected time to compute (ETC) matrix [2]. This application model preferably runs on a static multi-cloud environment. It is assumed to be no interference between the tasks and other I/O requests, cloud storage, and cloud resources.

3.3 Energy Model

A new energy model [21] is referred to estimate the total amount of energy consumption using the PSO scheduling method in a heterogeneous multi-cloud environment. To calculate this estimation, makespan and cloud utilization are formulated. It is found that average cloud utilization and energy consumption are linearly proportional according to a few research propositions. The execution time of the task on each cloud is referred to from the ETC matrix. Makespan is calculated as the completion time of the last task. Alternatively, it refers to the overall completion time required to execute all tasks in a multi-cloud environment. It is mathematically defined as given by Eq. (1).

$$M = \max \left(\sum_{i=1}^n \text{ETC}(i, 1) \times F(i, 1), \sum_{i=1}^n \text{ETC}(i, 2) \times F(i, 2), \dots, p \sum_{i=1}^n \text{ETC}(i, m) \times F(i, m) \right) \tag{1}$$

Energy consumption can be overly calculated as per Eq. (2). It is also seen that energy consumption is using overall cloud utilization for the calculation of energy used in a particular algorithm.

$$E_i = (P_{\max} - P_{\min}) \times U_i + P_{\min} \tag{2}$$

where

U_i = denotes the utilization of cloud i .

P_{\max} = power use at the maximum load (or 100% cloud utilization).

P_{\min} = minimum power consumption in the active mode (or as low as 1% utilization).

Here for idle resources, overhead to turnoff time is negligible. Hence, it is not considered.

Average energy consumption is denoted as in Eq. (3).

$$E = \frac{\left(\sum_{i=0}^m E_i \right)}{m} \tag{3}$$

where $1 \leq i \leq n$ and $1 \leq j \leq m$.

3.4 Scheduling Model in Cloud

In this scheduling model, a set of tasks and a set of machines are taken to compile the overall energy consumption using PSO algorithms. $T = \{T_1, T_2, T_3, \dots, T_n\}$ is a set of independent tasks, and $C = \{C_1, C_2, C_3, \dots, C_m\}$ is a set of machines or clouds. Each task has some execution time on each machine. This mapping is represented in the expected time to compute (ETC) matrix. ETC matrix is given in Eq. (4), where T th task execution time on C th cloud is denoted.

$$\text{ETC} = \begin{matrix} & \text{ETC}_{11} & \text{ETC}_{12} & \dots & \text{ETC}_{1m} \\ & \text{ETC}_{21} & \text{ETC}_{22} & \dots & \text{ETC}_{2m} \\ \dots & \dots & \dots & \dots & \dots \\ & \text{ETC}_{n1} & \text{ETC}_{n2} & \dots & \text{ETC}_{nm} \end{matrix} \tag{4}$$

4 Proposed PSO-Based Task Scheduling Algorithm

PSO is one of the traditional meta-heuristics scheduling algorithms, which provides the optimal solution for a group of particles. In task scheduling, PSO also outperforms to generate an efficient method. It is inspired by the social behavior of particles which later follows an evolutionary computational method. In this proposed task scheduling model, a group of swarm or particles is considered as a set of scheduled tasks. Each schedule has its behavior as the particles have. A predefined searched space is introduced to enhance the efficiency of the algorithm. Each particle represents a solution to the optimization problem, which is optimizing some cloud QoS parameters. Each particle is associated with position and velocity which helps them to move forward to the next step or position. Here, fitness function is evaluated at each step or position to identify the best solution or best particle. It will optimize the overall makespan, and the corresponding energy consumption will be calculated using the proposed algorithm. Velocity at the next position is defined by Eq. (5).

$$v_l^{t+1} = \omega v_l^t + c_1 r_1 (p_l^{\text{best}} - p_l^t) + c_2 r_2 (p^{\text{gbest}} - p_l^t) \quad (5)$$

where

p_l^t is the l th particle at iteration t .

v_l^t is the velocity of the l th particle at iteration t .

p^{best} is the best position found.

p^{gbest} is the best global position among all p^{best}

$1 < l < L$, where L is the population size.

Parameters c_1 and c_2 are the acceleration constants, r_1 and r_2 are random numbers between 0 and 1, and ω is the inertia factor.

In the proposed cloud task scheduling algorithm using PSO, solution (particle) which is denoted as $S_1, S_2, S_3 \dots S_n$ is given in Fig. 1. For an instance, solution S_1 is a schedule where T_1 is allocated to C_2 , T_2 is allocated to C_2 , etc. Optimization function ($F(x)$) is calculated for each solution after the end of each iteration, and p^{best} and p^{gbest} are chosen.

The parameters p^{best} and p^{gbest} are the velocities of the current particle and best particle. The best particle is one with less $F(x)$ value (in of case minimization function). Here, schedule which gives less makespan is chosen. Hence, optimization parameter is a minimization function. A newly updated position of the particle can be calculated using Eq. (6).

$$p_{t+1} = (|v_{t+1}| + \text{mod}m) + 1 \quad (6)$$

where p_{t+1} = next position of particle (here, it is cloud/machine).

v_{t+1} = velocity at next position.

m = number of cloud or machine.

For each solution, the updated position for each machine is calculated. Here, it is assumed that the number of iteration is the same as the number of solutions or particles. An algorithm is given in the following table.

Algorithm: PSO based task scheduling

Input:

1. A set of n independent tasks
2. A set of m cloud
3. An ETC matrix

Output:

1. Makespan
 2. Energy consumption
-

1. Particle or solution = m^n is randomly initialized and a set of solutions is randomly chosen(40% of solution size). $iter = 40\%$ of m^n

2. $F(x)$ = makespan of selected solution is calculated .

3. for $l = 1$ to $iter$ and $t = 1$ to $iter$ (where $iter = 40\%$ of m^n)

$$v_l^{t+1} = \omega v_l^t + c_1 r_1 (p_l^{best} - p_l^t) + c_2 r_2 (p^{gbest} - p_l^t)$$

For, m = number of cloud

$$p_{l+1} = (|v_{l+1}| + \text{mod}m) + 1$$

4. Repeat step 3 until the termination condition is fulfilled.

5. Update fitness function value, choose the best schedule and calculate average energy consumption (Eqs. 2, 3)

4.1 Illustration

In Fig. 2, a set of solutions or particles is there which will undergo a series of steps to generate an optimized result. Best $F(x)$ value is treated as $gbest$, and the makespan of each solution is $pbest$. In the first iteration, the new velocity and position of the particle are calculated using Eqs. 5 and 6. Here, the position of the particle indicates, to which cloud the task will be assigned. For each solution, this process will be repeated, and simultaneously value of $F(x)$ is also calculated. After reaching the termination condition, the solution with the best $F(x)$ (minimization function) value is chosen. An example is illustrated in Fig. 3a–d.

In this example, the proposed algorithm is running for only one iteration. After a desired number of iteration, an updated solution will be obtained with a task to cloud allocation sequence. Makespan, cloud utilization, and energy consumption are

Fig. 2 Representation of a particle

Solution/ tasks	T_1	T_2	T_3	T_n	$F(x)$
S_1	C_2	C_2	C_4	C_1	V_1
S_2	C_5	C_2	C_3	C_2	V_2
S_3	C_7	C_1	C_6	C_6	V_3
					
S_n	C_1	C_7	C_3	C_4	V_n

Task\cloud	C_1	C_2
T_1	150	18
T_2	32	7
T_3	20	3
T_4	50	15

(a) ETC matrix

Solution\Task	T_1	T_2	T_3	T_4	F(x)
S_1	2	1	1	1	102 (Pbest)
S_2	2	2	2	2	43
S_3	2	2	1	2	40 (Gbest)
S_4	2	2	1	1	70

(b) Initial solution set

Solution\Task	T_1	T_2	T_3	T_4	F(x)
S_1	1	1	1	1	252
S_2	2	1	1	2	52
S_3	1	2	2	2	150
S_4	1	2	2	1	200

(c) Updated position of cloud

Solution\Task	T_1	T_2	T_3	T_4	F(x)
S_2	2	1	1	2	52

(d) Optimized schedule after first iteration

Fig. 3 a ETC matrix. b Initial solution set. c Updated position of cloud. d Optimized schedule after first iteration

estimated for the solution. For the example given above, cloud utilization and the energy consumption are found to be 81% and 0.563 units, respectively.

5 Experimental Evaluation and Results

To evaluate the performance of different cloud scheduling parameters, both synthesized and benchmark datasets are taken. It is implemented using an Intel processor (2.6 GHz) using. Benchmark datasets are heterogeneous. The 1024×32 and 512×16 datasets are represented in exam format for input to the proposed algorithm [22]. A geographical comparison of makespan, cloud utilization, and energy consumption for various cloud task algorithms like min-min, max-min, GA, etc. is given in Fig. 3 (1024×32) and Fig. 4 (512×16). Average cloud utilization and energy consumption are given in Table 1. In Table 1, instances of datasets are given in u_x_yyzz format, where

- u = uniform distribution to generate these instances.
- x = type of consistency (i.e., consistent (\underline{C}), inconsistent (I), or semi-consistent (S)).
- yy = task heterogeneity (i.e., high (Hi) or low (Lw)).
- zz = machine or cloud heterogeneity (i.e., high (Hi) or low (Lw)).

Note that these instances are especially used in cloud scheduling.

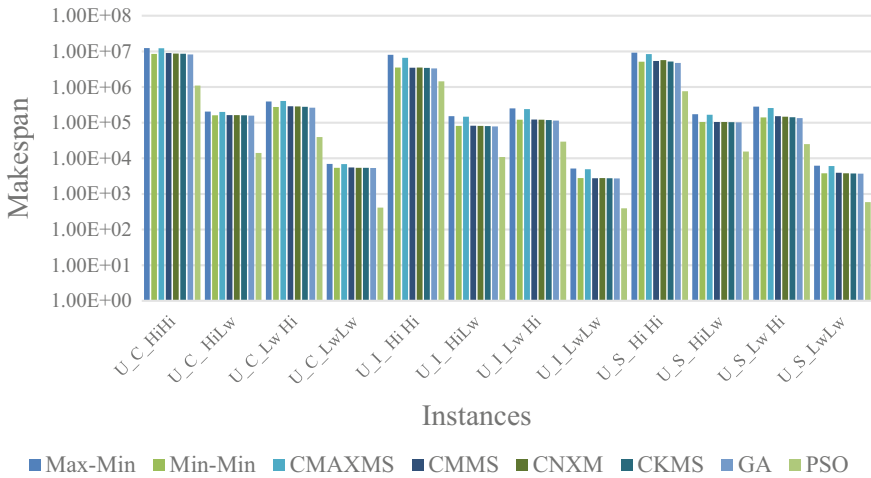


Fig. 4 Makespan comparison of 1024 × 32 benchmark dataset

Table 1 Cloud utilization and energy consumption for benchmark dataset

Instance	512 × 16 dataset		1024 × 32 dataset	
	Cloud utilization	Energy consumption	Cloud utilization	Energy consumption
<i>U_C_HiHi</i>	23.644943	22.36449	34.618919	23.461892
<i>U_C_HiLw</i>	49.596478	24.959648	45.784740	24.578474
<i>U_C_LwHi</i>	39.804482	23.980448	49.978962	24.997896
<i>U_C_LwLw</i>	42.455082	24.245508	58.015507	25.801551
<i>U_I_HiHi</i>	22.282265	22.228227	46.481632	24.648163
<i>U_I_HiLw</i>	31.728653	23.172865	43.350269	24.335027
<i>U_I_LwHi</i>	45.031673	24.503167	48.920189	24.892019
<i>U_I_LwLw</i>	48.759373	24.875937	51.085800	25.108580
<i>U_S_HiHi</i>	20.487280	22.048728	47.697536	24.769754
<i>U_S_HiLw</i>	53.183056	25.318306	59.066074	25.906608
<i>U_S_LwHi</i>	49.785385	24.978538	41.195431	24.119543
<i>U_S_LwLw</i>	53.189140	25.318914	52.242702	25.224270

6 Conclusion

In this paper, the working of the PSO algorithm in a heterogeneous multi-cloud environment has been portrayed. It is resulting from an efficient scheduling mechanism by taking a large search space. Hence, it is improving the overall makespan and generates cloud utilization and average energy consumption in cloud systems. These

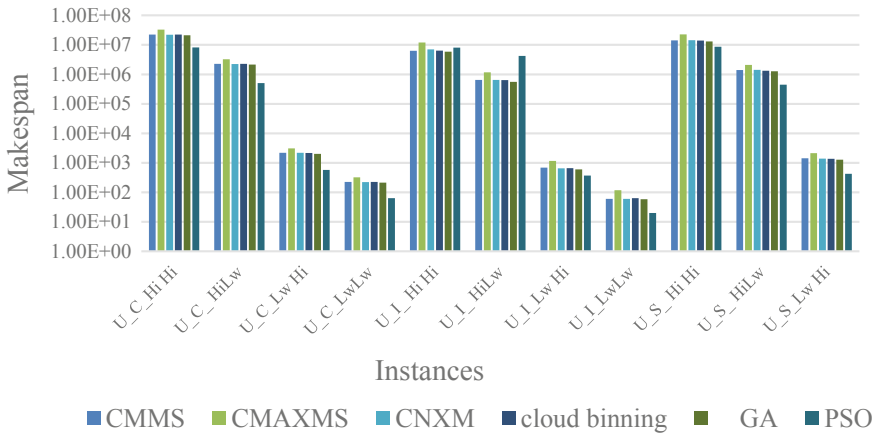


Fig. 5 Makespan comparison of 512 × 16 benchmark dataset

are cloud parameters required to evaluate the performance of the scheduling algorithm. PSO is one of the traditional evolutionary algorithms which performs better in a large search space. In the proposed algorithm, it is evaluating the overall energy consumption after completion of the scheduling method. It outperforms the existing algorithms in a distributed environment and evolutionary task scheduling. Synthesized and benchmark datasets are tested upon the proposed algorithm. The future work will be the implementation of the proposed algorithm in a real cloud environment and analysis of the proposed algorithm with advanced evolutionary scheduling strategies.

References

1. Buyya R, Yeo CS, Venugopal S, Broberg J, Brandic I (2009) Cloud computing and emerging IT platforms: vision, hype, and reality for delivering computing as the 5th utility. *Futur Gener Comput Syst* 25(6):599–616. <https://doi.org/10.1016/j.future.2008.12.001>
2. Li J, Qiu M, Ming Z, Quan G, Qin X, Gu Z (2012) Online optimization for scheduling preemptable tasks on IaaS cloud systems. *J Parallel Distrib Comput* 72(5):666–677. <https://doi.org/10.1016/j.jpdc.2012.02.002>
3. Panda SK, Pradhan R, Neha B, Sathua SK (2015) Fairness-aware task allocation for heterogeneous multi-cloud systems
4. Pradhan R, Dash AK (2019) A novel task scheduling algorithm in heterogeneous cloud environment using equi-depth binning method. *Adv Wireless Technol Telecommun*
5. Ibarra OH, Kim CE (1977) Heuristic algorithms for scheduling independent tasks on nonidentical processors. *J ACM* 24(2):280–289. <https://doi.org/10.1145/322003.322011>
6. Pradhan R, Panda SK, Sathua SK (2015) K-means min-min scheduling algorithm for heterogeneous grids or clouds. *Int J Inf Process* 9(4):89–99
7. Zhou X, Zhang G, Sun J, Zhou J, Wei T, Hu S (2019) Minimizing cost and makespan for workflow scheduling in cloud using fuzzy dominance sort based HEFT. *Futur Gener Comput Syst* 93:278–289. <https://doi.org/10.1016/j.future.2018.10.046>

8. Kaabouch N, Hu W (2012). Energy-Aware Syst Netw Sustainab Initiatives. <https://doi.org/10.4018/978-1-4666-1842-8>
9. Koomey JG (2007) Estimating total power consumption by servers in the US and the world. Stanford University, Lawrence Berkeley National Laboratory
10. Barroso L, Hölzle U (2007) The case for energy-proportional computing. *Computer* 40(12):33–37
11. Bohrer PN, Elnozahy E, Keller T, Kistler M, Lefurgy C, McDowell C et al. (2002) The case for power management in web servers. *Power-Aware Comput* 261–289
12. Fan X, Weber W, Barroso L (2007) Power provisioning for a warehouse-sized computer. *ACM SIGARCH Comput Archit News* 35(2):13–23
13. Koomey J (2008) Worldwide electricity used in data centers. *Environ Res Lett* 3(3):034008
14. Meisner D, Gold B, Wenisch T (2009) PowerNap. *ACM SIGARCH Comput Archit News* 37(1):205–216
15. Pradhan R, Satapathy SC (2020) Task scheduling in heterogeneous cloud environment—A ICICC 2019. In: *Advances in intelligent systems and computing*, vol 1034. Springer, Singapore. https://doi.org/10.1007/978-981-15-1084-7_1
16. Mahmood A (2000) A hybrid genetic algorithm for task scheduling in multiprocessor real-time systems. <http://www.ici.ro/ici/revista/sic2000-3/art05.html>
17. Alsaidy SA, Abbood AD, Sahib MA (2020) Heuristic initialization of PSO task scheduling algorithm in cloud computing. *J King Saud Univer—Comput Inf Sci*. <https://doi.org/10.1016/j.jksuci.2020.11.002>
18. Agarwal M, Srivastava GMS (2019) A PSO algorithm-based task scheduling in cloud computing. In: Ray K, Sharma T, Rawat S, Saini R, Bandyopadhyay A (eds) *Soft computing: theories and applications. Advances in intelligent systems and computing*, vol 742. Springer, Singapore. https://doi.org/10.1007/978-981-13-0589-4_27
19. Hsu CH, Chen SC, Lee CC, Chang HY, Lai KC, Li KC, Rong C (2011) Energy-aware task consolidation technique for cloud computing. In: *2011 IEEE third international conference on cloud computing technology and science*. <https://doi.org/10.1109/cloudcom.2011.25>
20. Rizvandi NB, Taheri J, Zomaya AY, Lee YC (2010) Linear combinations of DVFS-enabled processor frequencies to modify the energy-aware scheduling algorithms. In: *2010 10th IEEE/ACM international conference on cluster, cloud and grid computing*. <https://doi.org/10.1109/ccgrid.2010.38>
21. Lee Y, Zomaya A (2010) Energy efficient utilization of resources in cloud computing systems. *J Supercomput* 60(2):268–280
22. Braun et al (2015) [https://code.google.com/p/hcsp-chc/source/browse/trunk/AE/ProblemInstances/HCSP/Braun et al/uchihi.0?r=93](https://code.google.com/p/hcsp-chc/source/browse/trunk/AE/ProblemInstances/HCSP/Braun+et+al/uchihi.0?r=93). Accessed on 2 Feb 2015

Deviation and Cluster Analysis Using Inductive Alpha Miner in Process Mining



M. Shanmuga Sundari  and Rudra Kalyan Nayak 

Abstract Process mining is an effective method to discover information about the sequence of event execution in the business. Process mining helps interconnect event logs data and find any patterns in the process flows. Process mining (PM) provides a simple visualization to identify and organize data available in the healthcare system. We collected information from the hospital and applied PM methods. We processed structured and unstructured data and models using PM algorithms. Hospitals generate events logs that are considered complex and inconsistent. We found deviations and inconsistencies by comparing an existing process model with the event logs. In this paper, we created the design of Petri nets and analyzed the abnormality of the process flow. We propose an effective model to detect deviations using the event logs. Then, the abnormal activities are identified and displayed on the Petri nets. The Petri nets create clusters of dependent activities. The healthcare information from the hospital is used in the research process to convey our work. Experimental results show improvement in the effectiveness and efficiency of the proposed hospital information system.

Keywords Cluster analysis · Event log · Petri net · Process mining

1 Introduction

Healthcare processes always depict a dynamic approach in various departments and activities that significantly increase the performance of the healthcare domain. Healthcare processes have many divisions like cardiology, oncology, radiology, and

M. Shanmuga Sundari (✉)

Department of Computer Science and Engineering, Koneru Lakshmaiah Education Foundation, Vaddeswaram, Andhra Pradesh, India

e-mail: mshanmugasundari@gmail.com

Computer Science and Engineering, BVRIT Hyderabad College of Engineering for Women, Hyderabad, India

R. K. Nayak

School of CSE, VIT Bhopal University, Madhya Pradesh, Sehore, India

other specializations. Each department executes its process flow and significantly improves the performance of its department in health care. In general, hospitals are considering patients and outpatients as activities. The various departments have their patient records and execute based on their diagnostic cycle consisting of clinical observations and actions. Procedures are changed and modified by the new technology, resource person's experience, and the invention of new drugs. The deviation of the process will demand changes in environments which leads to repair of the process model. We propose a method to correct the deviations and produce a new process flow in this paper.

Process mining [1] identifies the proper sequence belonging to the business process. In these activities, conformance checking is most crucial by checking the actual data and finding the differences between the behavior observed in the event log and its captured attribute values. The first input of the data finds the conformance by checking the business model and tracing the event log. On the whole, a business process model specifies the path to find the execution of tasks in the process. In this point, Petri nets represent a diagrammatical form showing the business model. Petri net implies the event log as traces, each consisting of a sequence of events that execute the process flow or case. Petri net will work based on the timestamp of the events happening in the process with the reference of a task in the business process.

Nowadays, many technical models can describe process models and their different control logic, such as business process models, Petri nets, and event-based causal nets. The business process model will define the entire process flow and educate the activities with their proper channel.

2 Literature Survey

Process mining is an emerging technique nowadays. In literature [2], authors discover the healthcare process with the static process flow. It can find the performance analysis in the most significant process flow. In literature [3], authors experimented with the clinical process in the general checkup criteria. It may have many dynamic processes flow in the day-to-day life cycle. In literature [4], authors proposed a system for out-patient diagnostic flow to complete a patient diagnosis and treatment. It depends on the time taken for the patient based on their medical problem. Doctors can swing between multiple activities and capture them as event logs. In literature [5], authors explored the event log data and process deviations in a particular department.

In literature [6], authors proposed a graphical representation of the causal nets and Petri nets. The diagrammatic representation describes the process flow invariantly to predict the entire activities. The Petri net gives the source to destination process activities connectivity and displays each patient's dynamic flow. In literature [7], authors discovered the event log traces and showed the different simulation models to predict the deviation. In literature [8], authors explained algorithmic derivation for the process and found the deviation accuracy in various algorithms. In literature [9],

authors projected the critical care complex analysis using graphical representation in healthcare systems.

In literature [10], authors proposed the connectivity of the interrelated events and found the cluster analysis using the Petri net. In literature [11], authors mentioned deviation discovery and conformance checking in the process. The enhancement technique is enlightened to reach the proper output. In literature [12], authors experimented with process mining in different domains to enhance the performance of the process. In literature [13], authors implemented process flow enhancement using various event log traces and found cluster creation of the process activities. Conformance checking is the technique to find the root cause of process deviation in process mining. Many classification methods [14] are used to find the accuracy in the medical field.

3 Proposed System

3.1 Dataset

In this research, we used Dutch academic hospital data gathered from web resources [15]. This dataset contains 1000 traces which are dynamic process flow in different departments in the hospital. The dataset contains 17 attributes or features. We need the timestamp of each activity. Each activity has a different timestamp. Eventually, the process depends on the timestamp.

3.2 Data Preprocessing

The dataset should have attributes suitable to apply in process mining. The timestamp attribute is an important criterion to find deviation in the event log. The event log lists the required data features.

The event log contains:

- Patients registration ID.
- Treatment activity for patients.
- Activities traces from start to end of the process.
- Time taken for activities.

Fig. 1 Framework of process mining in the healthcare industry

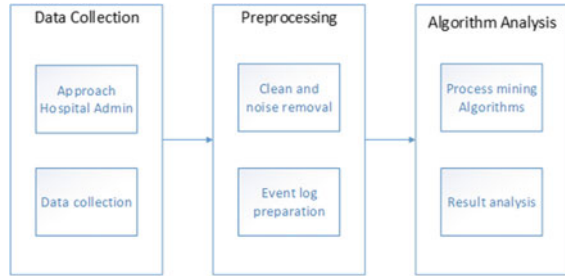
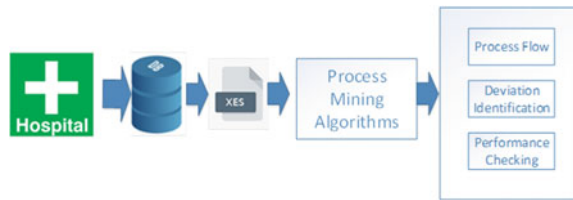


Fig. 2 Architecture of process mining



4 Architecture

Figure 1 shows the overall framework of mining in the healthcare industry. Initially, the event log collection is followed by preprocessing the data according to the tool perspective.

Figure 2 explains that data mining is an enormous field to enable people with machines to extract the work in many ways that minimize the overhead of the resource and business. The business process is data driven from the activities. Based on the model accuracy, we can rerun the model next time. But, process mining is the mining technique that solves the processing overhead in the early stage. It helps to produce the result with better accuracy in the overall process. We can exploit the process using process mining techniques to find the pattern and insights of the processes in the business domain.

5 Implementation

The alpha algorithm shows the pseudocode for the next activity prediction. The algorithm shows the T_i (*trace of the event*) and trained model. The tokenizer is used to encode T_i . The tokenized node will be padded on the left side, and the remaining sequence will be added with zeros to manage full length. The final vector–matrix will be embedded with the model. The probability distribution can happen with the next traces. The next trace will be built with a high probability value. A new trace is designed to concatenate T_i with the new framed activity. This procedure is repeated until the model m is found at the end of the activity named *END*.

5.1 Alpha Algorithm

```

Input: Ti: prefix, Model: m
Output: Trace: T
n = 0
T = Ti
while(  $\alpha < \text{END}$  ) and ( n < Event log_End ) do

    Ti = Tokenize(Ti)
    Ti = pad(Ti)
    Ti = embed(Ti)
    i = predict(.,Ti)

    if  $\alpha = \text{highest\_probability}$  then
        T = Ti
        n = n + 1

return T
end

end
    
```

5.2 Trace

The hospital management system has the traces as shown in Fig. 3. In our dataset, three traces are similar, and the remaining are individual traces. In the event log, activities (A, B, C, D, E, F, G, H) happen three times in the hospital treatment flow. The fourth trace (A, B, C, D, A) happened once in the event log. The remaining traces in the event log also happened only once.

Process mining is an efficient approach for analyzing the activity trace in an activity flow manner. In Fig. 4, we can visualize the start and end activity process flow. Activity C is following Activity G or Activity H in most cases. Figure 3 highlights the

Fig. 3 Traces in hospital event log

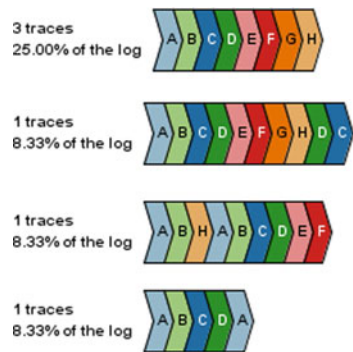


Fig. 4 Activity Petri net

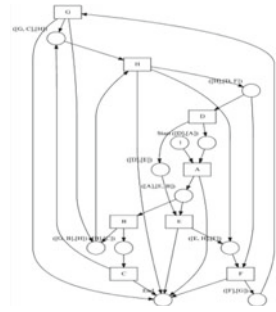
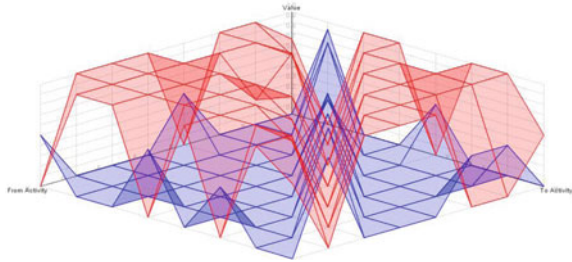


Fig. 5 Event log cluster connectivity



most significant root path. Flow always starts with Activity A. The Petri net shows the complete activity with start and end flow in the following diagram.

Figure 5 shows the graphical representation of the process flow movement from starting activity to ending activity. The highest value in the graph displays the dependencies between the activities.

6 Results

Figure 6 shows the resultant cluster formation of the activity event log after the deviation reduction. The activities are clustered based on the maximum dependent connectivity. The mining algorithm can find the most connective nodes and trace formally to maintain the process on a proper track. Each cluster is created based on the dependency of the nodes and analyzing the path. The management can find the deviation with ease and rectify the deviation in the event activity. Process deviation is the resultant metric for this research. Activities of the trace are considered as the metrics and formed as clusters.

Fig. 6 Cluster creation after resolving deviation

	A	B	C	D	E	F	G	H
Cluster 1	X	X	X	X		X	X	X
Cluster 2		X	X	X				X
Cluster 3				X	X	X		
Cluster 4	X		X	X	X			X
Cluster 5	X	X		X	X			X
Cluster 6					X	X	X	
Cluster 7					X	X	X	X
Cluster 8	X	X	X					X

7 Conclusion and Future Scope

The proposed models show the performance analysis and correlate patterns. In real-time applications, process mining is effective in improving the process. Based on the pattern analysis, we can find the instance of the events with deviations. The matrix shows the interdependent activities in the process. The Petri net displays the process flow of each activity and finds the bottleneck in the process. The management can find bottleneck resources to resolve the issues and improve process performance. The Petri net shows cluster of activities that happened for each instance. This research shows that registration, payment, and laboratory are high bottleneck activities. The hospital management takes action to improve the process flow in these areas. In the future, we can extend the work into more activities and find the accuracy difference after tuning the process mining activities. The main challenges are finding the process deficiency that leads to the proper performance improvement in data analytics. It can be added in the future work and enhance the process in the healthcare industry.

References

1. Van der Aalst W (2016) Process mining: data science in action
2. Sundari MS, Nayak RK (2020) Process mining in healthcare systems: a critical review and its future. *Int J Emerg Trends Eng Res* 8(9):5197–5208. <https://doi.org/10.30534/ijeter/2020/50892020>
3. Shinde SA, Rajeswari PR (2018) Intelligent health risk prediction systems using machine learning: a review. *Int J Eng Technol*. <https://doi.org/10.14419/ijet.v7i3.12654>
4. Tripathy R et al (2021) Spectral clustering based fuzzy C-means algorithm for prediction of membrane cholesterol from ATP-binding cassette transporters. In: *Intelligent and cloud computing*. Springer, pp 439–448
5. Akhila G, Madhubhavana N, Ramareddy NV, Hurshitha M, Ravinder N (2018) A survey on health prediction using human activity patterns through smart devices. *Int J Eng Technol*. <https://doi.org/10.14419/ijet.v7i1.1.9472>
6. Mans RS, Schonenberg MH, Song M, Van Der Aalst WMP, Bakker PJM (2008) Application of process mining in healthcare—a case study in a Dutch hospital. https://doi.org/10.1007/978-3-540-92219-3_32
7. Sundari MS, Nayak RK (2021) Efficient tracing and detection of activity deviation in event log using prom in health care industry. In: *2021 fifth international conference on I-SMAC (IoT in social, mobile, analytics and cloud) (I-SMAC)*, pp 1238–1245

8. Kukreja G, Batra S (2017) Analogize process mining techniques in healthcare: sepsis case study. <https://doi.org/10.1109/ISPPC.2017.8269727>
9. Sekaran SC, Saravanan V, Rudra Kalyan Nayak R, Shankar SS, Human health and velocity aware network selection scheme for WLAN/WiMAX integrated networks with QoS. *Int J Innov Technol Explor Eng (IJITEE)*, ISSN, 2278–3075
10. Reddy RR, Ramadevi Y, Sunitha KVN (2017) Enhanced anomaly detection using ensemble support vector machine. In: 2017 International conference on big data analytics and computational intelligence (ICBDAC). IEEE, pp 107–111
11. Jin J, Sun W, Al-Turjman F, Khan MB, Yang X (2020) Activity pattern mining for healthcare. IEEE Access. <https://doi.org/10.1109/ACCESS.2020.2981670>
12. Rebuge Á, Ferreira DR (2012) Business process analysis in healthcare environments: a methodology based on process mining. *Inf Syst*. <https://doi.org/10.1016/j.is.2011.01.003>
13. Van Dongen BF, De Medeiros AKA, Verbeek HMW, Weijters AJMM, Van Der Aalst WMP (2005) The ProM framework: a new era in process mining tool support
14. Padmaja B, Prasad VR, Sunitha KVN (2016) TreeNet analysis of human stress behavior using socio-mobile data. *J Big Data* 3(1):1–15
15. <https://www.tue.nl/en/research/researchers/boudewijn-van-dongen/>

Image and Video Processing-Based Traffic Analysis Using OpenCV



Devineni Pooja Sri and K. Kiran Kumar

Abstract Traffic a significant problem in a lot of cities at different places due to increase in number of vehicles. For traffic related problems, computer vision approaches are preferable. System during any installation will not trouble traffic and are easily changed. We proposed an advance vehicle detection, vehicle classification and vehicle counting system for traffic analysis. Input either image or a video. First detection and classification of vehicles takes place followed by vehicle count. In this project, we detect and classify heavy motor and light motor vehicles like car, motor-bike, truck, bus on the roads and also count the number of vehicles travel through the roads. YOLOv4 model, Configuration file and Weight file of YOLOv4, COCO dataset, Non Max Suppression and OpenCV are used to implement the system. Counted data is stored in file to analyze different vehicles that are traveling through the roads which is used for analysis and diversion.

Keywords Vehicle detection · Vehicle classification · Vehicle counting · YOLOv4 · COCO dataset · Non max suppression · OpenCV

1 Introduction

In this world, development has given many gifts but not without the bane. Moving too far locations become more easy and quick due to the success in the automotive industry. Traffic management defines planning, monitoring and control or influencing of traffic on roads. Roadways are the most common paths are selected to moving short distances, traveling and also for daily activity. Over the past times the number of vehicles has tremendously increased. There are approximately one billion vehicles present all over the world and only in India actively Sixty to Seventy million of

D. Pooja Sri (✉) · K. Kiran Kumar
Koneru Lakshmaiah Education Foundation, Vaddeswaram, India
e-mail: devinenipoojasri1999@gmail.com

K. Kiran Kumar
e-mail: kiran5434@kluniversity.in

vehicles. Handling such moments of traffic and providing the ample parking lots is not a simple task.

Object detection an interesting field in computer vision, which moves to a new level when we deals with supervised and unsupervised data. Object detection algorithms can do different task like management of traffic, ball tracking in sports and also perform sub tasks like object count. Vehicle detection is one in all applications of object detection, thereby focuses on the multiple vehicles detection in image and video. Classification of Vehicles is the process of categorization of vehicles according to their predefined name of classes. Vehicle counting means provides information like flow of traffic, occurrences of vehicle crash and traffic at peak times in roadways.

By integrating the proposed system to traffic light camera, one can simply track more things like In a day how many vehicles are there at junction?, At what time does the traffic is more?, What kind of vehicles are passing at junction?, and Is there any way to optimize and distribute the traffic through a different places? Simultaneously.

A person can simply detect and identify the objects in complex flash scene. Forthcoming to the thinking process of machine, computer vision algorithms are used to train machines on the object detection art to detect the different types of vehicles via camera or in real-time or a video.

Finding and Categorizing, Counting of various vehicles on roads and highways that are helpful to the authorities get to know the traffic flow statistics, understand and learn the traffic patterns. So, that they are able to analyze and handle the traffic in a better way.

2 Related Works

In this, the author's proposed an end-to-end approach for vehicle detection using a lightweight Tiny-YOLOv3 in which will identify, locate and also classify different vehicles and its types in an image. In this method, the Tiny-YOLOv3 which is a pre-trained model took as referral and then next trimmed, simplifies at train of dataset and named as BIT-vehicle and a few unneeded layers of networks are cutout. This proposed network can able to find and divide 6 differ vehicles with the precision of 95.05%, and speed of 17 frames per second. The advantages are low power systems can deploy this method, faster that real Tiny-YOLOv3, accuracy and speed are high [1].

In this, the author's presented a method to detect, classify and count different vehicles using image processing approach. The tasks of vehicles detection and vehicles counting are cut into six phases which can be done using different algorithms. These six steps are Acquisition, Analysis, Object identification, Count, Classification and results display. Classification is done by using any one of the following type. They are buses trailers, trucks, Bicycles and motorcycles, minibus and pickup vans, motor cars. This system is used for traffic monitoring, to design patterns for traffic and number of road users [2].

In this, the author's proposes a system which is used for vehicle detection and vehicle classification method using deep learning for intelligent transport. An existing Convolutional Neural Network (CNN) architecture is made adjustments and improvements for this application. This system can classify three different vehicles. The proposed system gives an accuracy of 90%, miss rate which is around 10% when the FPPI is 0.1, realize on the NVIDIA Titan-X GPU and the design can reach out the performance about 720×480 video under various weather conditions like day, night, raining at a speed of 25 frames per second (fps) [3].

In this, the author's designed a system named video-based traffic analysis using the techniques of computer vision. This system gathers all the main stats for making policies and regulations in automatic fashion. Faster RCNN and MoG with SVM are used for vehicle finding. The system mainly developed for find and divides the vehicles in the videos related to traffic and also for vehicle speed estimation. The experiment results show that the vehicle detection using Faster RCNN are better than the MoG algorithm and also the vehicle classification using Faster RCNN are better than the SVM algorithm [4].

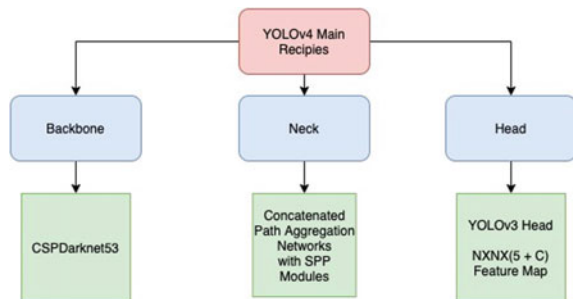
3 YOLOv4 Model

YOLO means You Only Look Once which is a real-time object recognition system that recognizes the multiple objects in a single frame. YOLO recognizes the objects more accurately and faster than others.

YOLOv4 means You Only Look Once version 4 which is an evolution of the previous model YOLOv3. YOLOv4 architecture has four different blocks namely the backbone, the neck, the dense prediction, and the sparse prediction. YOLOv4 network develops a CSPDarknet53 which splits the present layer into two parts. By using CSPDarknet53 the Backbone Network forms Features layers (Fig. 1).

In Neck, feature aggregation is done by using PANet and SPP. At different levels, shortening of the path connecting low-level and high-level information and converging parameters Path-Aggregation Network plays a major role. Addition of

Fig. 1 Main blocks of YOLOv4 architecture



Spatial Pyramid Pooling module after CSPDarknet53 in order to increase the receptive field and help out to separate the contextual features. It also used for improve accuracy. The head is prediction part. It is used to locate bounding boxes and classification. Detection of an object takes place at head which deploys the YOLOv3 head for anchor based detection steps and granularity the detection of three levels. There are two types of predictions takes place in head part. They are One is the Dense Prediction also called as One-stage detector and the another one is the Sparse Prediction also called as Two stage detector [5].

YOLOv4 is two times fast as EfficientDet. In comparison with YOLOv3 the mean average Precision is improved by 10% and also the number of frames per second is improved by 12%.

4 Proposed System

Figure 2 represents the implementation work of developed system. The necessary inputs are COCO.names file, Configuration file and Weights file of YOLOv4, confidence and non max suppression threshold values, and image or video as user input. The full form of COCO is Common Objects In Context. It is a dataset with eighty non-identical image classes. The main aim of the COCO dataset is to identify different classes in an image. YOLOv4 configuration file is needed to construct the neural network architecture. This configuration files carries CNN Architecture along with layers, activations, input size, batch sizes, Learning Rate, probability score threshold, etc. YOLOv4 weights file have different weights for a node in layers. The confidence and non max suppression threshold values are need for detection.

An object is created to take input. If the input is a video then cross lines namely middle, up and down line position are drawn in frame for counting the number of

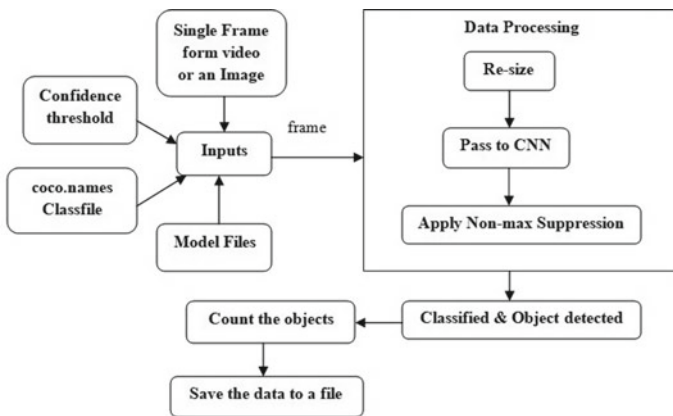


Fig. 2 Workflow diagram

vehicles. Based on the input size of YOLOv4 network the frame is resized and then normalized and send back to the created object to feed in to the network. Now detection action activates and then store all detected classes and its class id, confidence score. We check the obtained confidence score with pre-defined confidence score if obtained confidence score is more that original confidence score then we go for non max suppression with inputs namely, box coordinate points, class id's and confidence score. Automatically we can get a best class with a box detection is chosen using non max suppression technique.

Now for counting vehicles, if the input is a video then we use middle, up and down line positions and also a fixed threshold distance value. Based on the requirements we can change all line position and threshold distance. For this purpose we use Euclidean distance method. A vehicle is counted when it crosses the down line position only. When it comes to present and previous frames count if Euclidean distance value is less than threshold distance the system consider it as same object. If the input is an image then we count text method. The count text method means it counts the repeated words in an image.

Finally the count of vehicles is stored in a file. That is the system itself simple creates a file along with write only permissions. In the file the first line or a row contains the class names of vehicles and the next contains count of each vehicle exactly down to the class name.

5 Results

Table 1 presents the examined results of three types of inputs of road images and as well as the videos. For the first test we took basic count and later on increased it. The vehicles Car count is almost near to the actual count. Next position is taken by the vehicle Motorbike and last others namely Bus and Truck. YOLOv4 performs one go at the detection of vehicles in comparison with other version of YOLO and other object identification algorithms.

Figure 3 represents the output for an image taken as an input from the user by the system. Now the proposed system processes and gives the output as below. The output would contains the bounding boxes around the vehicles along with vehicle name and confidence score on top of the box and the count of each vehicle type is presented on top left side as shown in the Fig. 3 and at last the data is saved into a required file type.

Figure 3 is the output for video taken as an input from the user. The system processes and produces the output like Fig. 4. The output has up and down count of vehicles on the road at top left, position lines and bounding boxes throughout each vehicle. The pink color is middle line, red color is up and down line positions in figure.

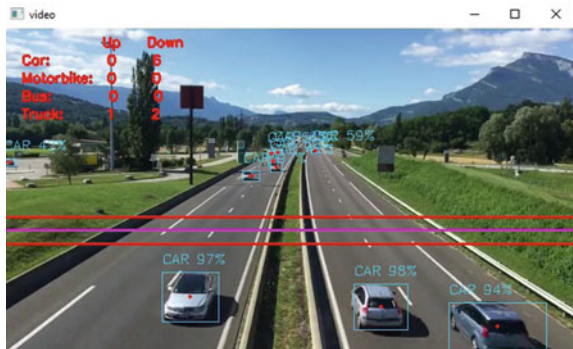
Table 1 Results of three testing for both inputs

Names of vehicles	Image as input	System count	Original count	Video as input	System count	Original count
Car	Image1	30	32	Video1	67	67
Motorbike		21	28		46	54
Bus		3	5		2	2
Truck		4	7		2	2
Car	Image2	45	51	Video2	117	129
Motorbike		0	0		72	78
Bus		1	1		3	5
Truck		3	3		1	3
Car	Image3	66	72	Video3	146	152
Motorbike		33	37		96	98
Bus		5	7		1	3
Truck		2	2		2	2

Fig. 3 Image as input



Fig. 4 Video as input



6 Conclusion

We have implemented an advance system using the YOLOv4 model for the three different activities like the detection, the classification and the counting of four different vehicles namely they are bus, car, motorbike and truck. The input is either the video or an image. Classification and finding is same for both the inputs but only change is in count method that is when the input is an image the counting is done by using a word count method whereas the video using line position. It is automated for each process just one need to provide input only. It is used to examine traffic and helpful for divert it.

Acknowledgements I thank my guide Dr. Kothamasu Kiran Kumar for supporting and helping me with successful completion of this project.

References

1. Taheri Tajar A, Ramazani A, Mansoorizadeh M (2021) A lightweight Tiny-YOLOv3 vehicle detection approach. *J Real-Time Image Proc* 18:2389–2401
2. Chandrika RR, Ganesh NSG, Mummooorthy A, Raghunath KMK (2019) Vehicle detection and classification using image processing. In: 2019 international conference on emerging trends in science and engineering (ICESE). IEEE, pp 1–6
3. Tsai C-C, Tseng C-K, Tang H-C, Guo J-I (2018) Vehicle detection and classification based on deep neural network for intelligent transportation applications. In: 2018 Asia-Pacific signal and information processing association annual summit and conference (APSIPA ASC). IEEE, pp 1605–1608
4. Arinaldi A, Pradana JA, Gusinga AA (2018) Detection and classification of vehicles for traffic video analytics. *Procedia Comput Sci* 144:259–268
5. Bochkovskiy A, Wang CY, Liao HYM (2020) Yolov4: optimal speed and accuracy of object detection. [arXiv:2004.10934](https://arxiv.org/abs/2004.10934)
6. Mahto P, Garg P, Seth P, Panda J (2020) Refining yolov4 for vehicle detection. *Int J Adv Res Eng Technol (IJARET)* 11(5):409–419
7. Zhnag F, Li C, Yang F (2019) Vehicle detection in urban traffic surveillance images based on convolutional neural network with feature concatenation. *Sensors* 19(30):594
8. Song H, Liang H, Li H et al (2019) Vision-based vehicle detection and counting system using deep learning in highway scenes. *Eur Transp Res Rev* 11:51
9. Wang X, Cheng P, Liu X, Uzochukwu B (2018) Focal loss dense detector for vehicle surveillance. In: 2018 international conference on intelligent systems and computer vision (ISCV). IEEE, pp 1–5
10. Huang R, Pedoem J, Chen C (2018) Yolo-lite: a real-time object detection algorithm optimized for non-gpu computers. In: 2018 IEEE international conference on big data (big data). IEEE, pp 2503–2510
11. Ma J, Chen L, Gao Z (2017) Hardware implementation and optimization of tiny-yolo network. In: International forum on digital TV and wireless multimedia communications. Springer, pp 224–234
12. Qu T, Zhang Q, Sun S (2017) Vehicle detection from high-resolution aerial images using spatial pyramid pooling-based deep convolutional neural network. *Multimed Tools Appl* 76(20):21651–21663

Energy Usage Data Extraction Methodology in Smart Building Using Micro Controller



K. Sai Himaja Chowdary, M. Neelakantappa, Ch. Ramsai Reddy,
and M. Prameela

Abstract Smart buildings are prevailing in the real world due to technology innovations such as cloud computing, sensors and Internet of Things (IoT). With such reliable ecosystem, it is made possible to extract data, which is accumulated in large scale, and provide opportunities to mine it in order to extract business intelligence for expert decision making. One area, which needs continuous improvement, is the energy usage in smart buildings. Extracting such data and preserving for mining and decision making is an indispensable research area. From the literature, it is understood that energy usage data extraction in smart buildings is a complex process that needs further investigation. Toward this end, we proposed a system that has required components and laboratory setup comprising Raspberry Pi as main controller, communication bus, RS485 device, USB, server and cloud infrastructure. The smart building is equipped with smart metering containing main meter and many sub meters. The system extracts data from the meters and saves it to the cloud. An algorithm named Energy Data Extraction and Persistence (EDEP) is proposed to achieve this. An empirical study made has revealed the importance of the proposed system in energy usage data extraction that further, in future, leads to big data analytics and optimization of power usage in smart buildings.

Keywords Smart building · Smart metering · Data extraction · Cloud · Data dissemination · Energy usage statistics

K. Sai Himaja Chowdary
Amazon Development Center India Private Ltd, Bangalore, India

M. Neelakantappa (✉)
Associate Professor in IT, Vasavi College of Engineering, Hyderabad, India
e-mail: neelakantappa.m@bvrit.ac.in

Ch. R. Reddy
Technology Leaders Program, Plaksha University, Punjab, India

M. Prameela
Department of Electrical and Electronics Engineering, B V Raju Institute of Technology,
Narsapur, India

1 Introduction

Smart buildings are prevailing in the real world due to technology innovations such as cloud computing, sensors and Internet of Things (IoT). With such reliable ecosystem, it is made possible to extract data which is accumulated in large scale and provide opportunities to mine it in order to extract business intelligence for expert decision making. One area which needs continuous improvement is the energy usage in smart buildings. Extracting such data and preserving for mining and decision making is an indispensable research area. In the contemporary era, there has been considerable growth in the usage of smart buildings and smart homes and smart city use cases in the real world. There are many contributions in the area of smart buildings for energy efficiency as explored in [1–7]. Stamatescu et al. [1] on the other hand focus on data driven control in smart cities and buildings besides sensing phenomena. Pesic et al. [2] investigated on data dissemination in smart building. They also built a tool to collect data from sensor and perform data analytics to arrive at utility of information for decision making. Madani et al. [3] investigated on smart building related patent information on several aspects of the buildings. Ma et al. [4] focused on energy awareness approaches used in smart buildings. They proposed a framework known as smart meter re-deployment where the fingerprint of energy appliances is tracked and analyzed. Bashir and Gill [5] proposed an IoT data analytics framework for analyzing data of a smart building use case. Their framework is evaluated with Cloud Era platform. Qolomany et al. [6] explored the role of deep learning using Long Short-Term Memory (LSTM) for analyzing data of smart building. Moreno et al. [7] focused on big data usage and data analytics and found that big data technology is indispensable for energy efficiency in smart buildings. From the literature, it is understood that energy usage data extraction in smart buildings is a complex process that needs further investigation. Our contributions in this paper are as follows.

1. We proposed a system which includes required components including Raspberry Pi controller, RS 485 device, server, smart meters and cloud infrastructure.
2. An algorithm known as Energy Data Extraction and Persistence (EDEP) is proposed and implemented for efficient data extraction.
3. A prototype application is built using Python language in order to evaluate the utility of the proposed system.

2 Different Methods Used for Energy Data Extraction in Smart Buildings

This section reviews prior works on smart buildings and energy data extraction. Dong et al. [8] focused on smart buildings and key information related to data dissemination and intelligent operations. Stamatescu et al. [1] on the other hand focus on data driven control in smart cities and buildings besides sensing phenomena. Pesic et al. [2] investigated on data dissemination in smart building. They also built a tool to collect

data from sensor and perform data analytics to arrive at utility of information for decision making. Waterworth et al. [9] explored neural languages in order to extract data from smart buildings. Automated meta data extraction is made in order to have better monitoring of the system. They also analyzed on the energy productivity in the system. Le et al. [10] studied the process of multiple electric energy consumption and its forecasting for better decision making with regard to energy distribution. They used cluster based approach and transfer learning to achieve this. Madani et al. [3] investigated on smart building related patent information on several aspects of the buildings. Ma et al. [4] focused on energy awareness approaches used in smart buildings. They proposed a framework known as smart meter re-deployment where the fingerprint of energy appliances is tracked and analyzed. Almalaq et al. [11] investigated on energy management systems in smart buildings. Their approach toward it includes energy system, artificial system, management and control, learning and training besides environment and evaluation. Xu et al. [12] focused on smart building ecosystem based on Artificial Intelligence (AI) models and platform-based business models. Their analysis includes ecosystem platform, value chain platform and organization's internal platform. Amin et al. [13] studied on the performance analysis of smart buildings in various aspects including energy efficiency.

Bashir and Gill [5] proposed an IoT data analytics framework for analyzing data of a smart building use case. Their framework is evaluated with Cloud Era platform. Qolomany et al. [6] explored the role of deep learning using Long Short-Term Memory (LSTM) for analyzing data of smart building. Moreno et al. [7] focused on big data usage and data analytics and found that big data technology is indispensable for energy efficiency in smart buildings. Bolchini et al. [14] proposed methodology to monitor energy information collected from smart building. It could analyze different aspects of the data and provide optimization strategies. Terroso-Saenz et al. [15] proposed a framework based on IoT technology to monitor and evaluate the energy usage data collected from smart building application. Manic et al. [14] discussed about different energy management systems for smart buildings use cases. Plageras et al. [16] explored big data technology for collection and analysis of energy data from smart building. Sensors in the use case are used to gather data. Zeng et al. [17] discussed many data driven approaches used to predict energy usage in smart buildings for performance optimization. Aguilar et al. [18] discussed on various methods used to have self-management of energy in smart buildings using AI. From the literature, it is understood that energy usage data extraction in smart buildings is a complex process that needs further investigation.

3 Methodology

The methodology described here is encapsulated in the block diagram shown in Fig. 1.

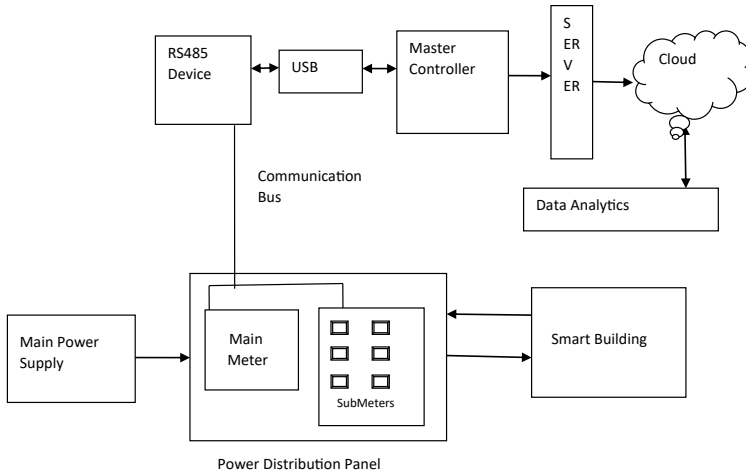


Fig. 1 Block diagram of the system

3.1 The Block Diagram

The block diagram is provided to reflect the connectivity and structure of various components involved in the proposed system. The master controller, RS485 device and different meters provide required communication network and the data is sent to cloud storage and thus it can be used and processed later.

As presented in the block diagram, the proposed system is cloud-assisted and has provision for data analytics as well. However, the main focus of the paper is on efficient data extraction. The main power supply that is associated with smart building is linked to main meter and in turn many sub meters are maintained. The smart metering system helps in data gathering and saving to public cloud. The meter and sub meters provide valuable information about the power usage patterns as part of Building Monitoring System (BMS). There is a data communication bus that links the meters with RS485 device. In turn the device is linked to USB through which master controller is connected. The master controller connects to server and the server in turn usages gateway to connect to cloud platform.

3.2 Smart Meters

In the proposed system, smart meters play crucial role in data gathering and saving the same to cloud platform. The main meter and sub meters are able to produce statistics that are useful data analytics.

As presented in Fig. 2, the bus is used to connect all meters. Each meter is identified with unique identification number. There is master and slave phenomenon used in

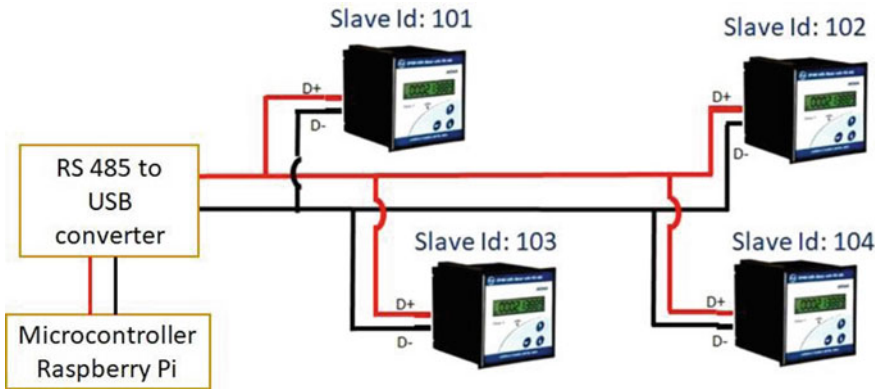


Fig. 2 Meters connected to bus

order to have proper arrangements of meters that are lined to RS485 device. The device is then connected to Raspberry Pi which is the micro controller or master controller in the smart building setup.

3.3 The Algorithm

We proposed an algorithm known as Energy Data Extraction and Persistence (EDEP) for efficient energy usage data extraction.

Algorithm 1: Energy Data Extraction and Persistence algorithm.

Algorithm: Energy Data Extraction and Persistence (EDEP).

Inputs: Meters in distribution panel M .

Output: Energy usage data D .

1. Start
2. Initialize energy usage data map D
3. For each meter m in M
4. $id \leftarrow getId(m)$
5. $reading \leftarrow getReading(m)$
6. $D.append(id, reading)$
7. End For
8. File $f \leftarrow D$
9. Connect to cloud server
10. Identify location on server
11. Boolean $b \leftarrow Save\ f\ to\ server\ location$
12. IF $b = True$ Then
13. Display “data saved to cloud server successfully”

14. Else
15. Display “Error in saving data to cloud server”
16. End
17. Return D

As presented in Algorithm 1, it takes all the meters involved in the system and generate energy usage data which is saved to cloud. There is an iterative process to collect energy usage data from different sub meters. Then the data is bundled into a file format prior to sending it to cloud. It ensures that the data is successfully saved to cloud. If there is any discrepancy in saving data, it alerts the user about the same.

3.4 Implementation Details

The implementation of the proposed system includes a lab setup and meters that have required equipment to have smart metering.

As presented in Fig. 3, the lab setup contains all the components needed in order to gather data from meters. It has the main controller and equipment needed to have data collection and saving to cloud storage. Different connection of loads is exercised in order to have empirical study. Different phases are considered such as R, Y and B with PR watts in P phase, PY watts in Y phase, PB watts in B phase in different timestamps.

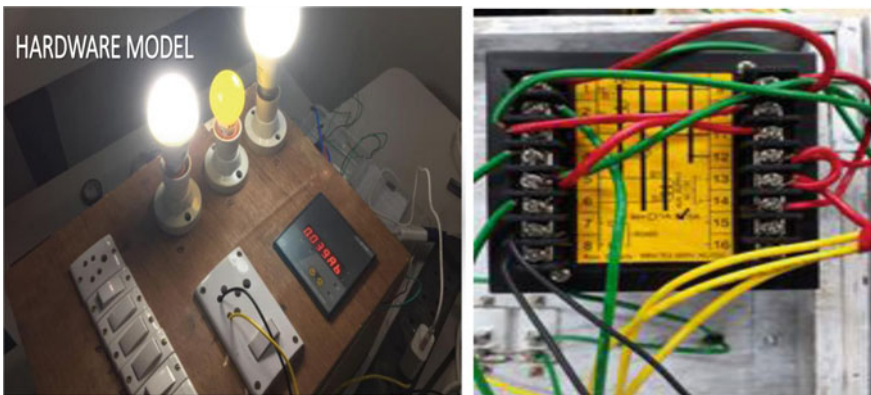


Fig. 3 Shows lab setup and meter backside

4 Experimental Results

The observations are made in terms of power usage in each phase and power factor analysis. Power in each phase is monitored continuously. The graphical representation for power consumption in each phase for a particular day is shown. This continuous data extraction is used for further analysis (Table 1).

4.1 Power Factor Analysis

The power factor of the main incoming feeder of the campus was measured for duration of eight days on 24 h basis (Mention which date to date). The data chart for power factor data at location incoming feeder 1 (ID 1) as shown in Fig. 4.

The above presented data gives the information regarding the. The campus will start at 9:30PM and closes around 17:00PM. The campus loaded with light load condition before the 9:30PM, hence the power factor of the load is almost unity power factor. The load condition of campus, the power factor of the campus is fluctuating,

Table 1 Power consumption in each phase

Time	PR	PY	PB
00:00:00	38.227	41.086	37.243
01:00:00	37.606	43.777	35.911
02:00:00	36.128	42.584	32.68
03:00:00	36.521	38.328	33.734
04:00:00	35.27	43.334	36.292
05:00:00	34.044	38.894	32.68
06:00:00	46.152	40.752	38.892
07:00:00	37.845	52.822	42.901
08:00:00	31.454	28.907	35.347
09:00:00	58.092	48.255	34.744
10:00:00	22.376	35.808	12.169
11:00:00	24.377	23.625	9.565
12:00:00	10.962	11.502	3.279
13:00:00	12.361	8.401	21.623
14:00:00	6.502	1.533	16.74
15:00:00	11.13	21.52	10.486
16:00:00	23.452	23.161	17.989
17:00:00	34.852	44.345	30.751
18:00:00	47.679	55.306	43.391

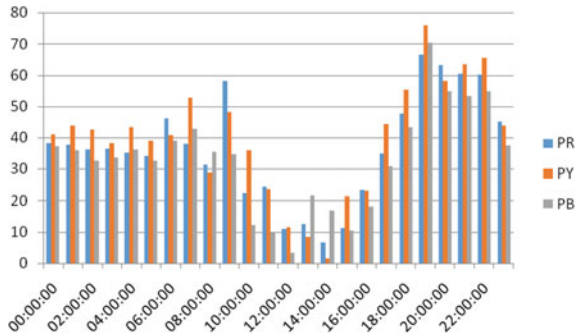


Fig. 4 Different phases and corresponding power in watts

and which is poor power factor. The power factor will lead to unnecessary increasing energy billing due to inductive load (Fig. 5).

The power factor shall be improved of electrical network in the campus working hours by placing the suitable capacitor bank for power factor improvement. There are various power factor improvement methods available.

1. Connecting the suitable value static capacitor in parallel to equipment.
2. Using phase shifters.
3. Using synchronous motors.
4. Using synchronous condensers.
5. Using high power factor motors.

Among the above-mentioned methods, the using static capacitor is economical methods compared with other methods. These static capacitors will supply the leading current during the low power factor condition to improve the power factor. In this

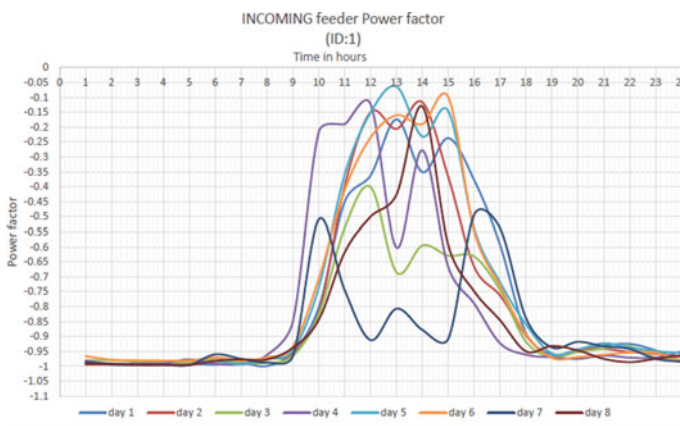


Fig. 5 Incoming feeder 1 power factor analysis

Fig. 6 Power demand and tariff graph



case, the lowest power factor recorded around 11:00 h. to 15 h. is 0.05 lagging. To increase the power factor of 0.98 lagging. The suitable values of shunt capacitors shall be included in the distribution system.

4.2 Recommendation for Savings on Electricity Bill for BVRITN

Electricity Bill to be paid only for meter 1 toward consumption on 16th Feb 2021 = 17,557 Rs. Total energy consumed by meter 1 on 16-Feb = 2477 Kwh—Patten is shown below. If 250 units are shifted from 8 to 6rs tariff, savings will be 500 Rs per day = 182,000 Rs/Year (Fig. 6).

5 Conclusion and Future Work

Due to the emergence of smart applications like smart buildings, it is made possible to have control over the energy usage and optimization of the same. From the literature, it is understood that energy usage data extraction in smart buildings is a complex process that needs further investigation. Toward this end, we have proposed a methodology and implemented it for empirical study. It is observed that the proposed system is capable of gathering the energy usage data from the smart building case study. However, the research in this paper is limited to data extraction and saving to cloud only. The big data analytics and optimization of power usage is left to future work.

References

1. Stamatescu G, Făgărășan I, Sachenko A (2019) Sensing and data-driven control for smart building and smart city systems. *J Sens* 2019:1–3
2. ŠasaPješić M, OgnjenIkočić M, Ivanović M, Bōšković D (2019) BLEMAT: data analytics and machine learning for smart building occupancy detection and prediction. *Int J Artif Intell Tools* 28(6):1–29

3. Madani F, Daim T, Weng C (2015) ‘Smart building’ technology network analysis: applying core–periphery structure analysis. *Int J Manag Sci Eng Manag* 1–11
4. Ma M, Lin W, Zhang J, Wang P, Zhou Y, Liang X (2017) Towards energy-awareness smart building: discover the fingerprint of your electrical appliances. *IEEE Trans Ind Inf* 1–11
5. Bashir MR, Gill AQ (2016) [IEEE 2016 IEEE 18th international conference on high performance computing and communications; IEEE 14th international conference on smart city; IEEE 2nd international conference on data science and systems (HPCC/SmartCity/DSS)—Sydney, Australia (2016.12.12–2016.12.14)]
6. Qolomany B, Al-Fuqaha A, Benhaddou D, Gupta A (2017) [IEEE 2017 IEEE 19th international conference on high performance computing and communications; neural networks and Wi-Fi networks in support of occupancy prediction in smart buildings, pp 50–57
7. Moreno MV, Dufour L, Skarmeta AF, Jara AJ, Genoud D, Ladevie B, Bezian J-J (2016) Big data: the key to energy efficiency in smart buildings. *Soft Comput* 20(5):1749–1762
8. Dong B, Prakash V, Feng F, O’Neill Z (2019) A review of smart building sensing system for better indoor environment control. *Energy Build* pp 1–43
9. Waterworth D, Sethuvenkatraman S, Sheng QZ (2021) Advancing smart building readiness: automated metadata extraction using neural language processing methods. *Adv Appl Energy* 3:1–10
10. Le T, Vo MT, Kieu T, Hwang E, Rho S, Baik SW (2020) Multiple electric energy consumption forecasting using a cluster-based strategy for transfer learning in smart building. *Sensors* 20(9):1–17
11. Almalaq A, Hao J, Wang J-Y (2019) Parallel building: a complex system approach for smart building energy management. *IEEE/CAA J Automatica Sinica* 6(6):1–10
12. Xu, Ahokangas, Turunen, Mäntymäki, Heikkilä (2019) Platform-based business models: insights from an emerging Ai-enabled smart building ecosystem. *Electronics* 8(10):1–19
13. Amin U, Hossain MJ, Lu J, Fernandez E (2017) Performance analysis of an experimental smart building: expectations and outcomes. *Energy* 1–23
14. Bolchini C, Geronazzo A, Quintarelli E (2017) Smart buildings: a monitoring and data analysis methodological framework. *Build Environ* 1–17
15. Terroso-Saenz F, González-Vidal A, Ramallo-González AP, Skarmeta AF (2017) An open IoT platform for the management and analysis of energy data. *Future Gen Comput Syst* 1–45
16. Plageras AP, Psannis KE, Stergiou C, Wang H, Gupta BB (2017) Efficient IoT-based sensor BIG Data collection-processing and analysis in smart buildings. *Future Gen Comput Syst* 1–18
17. Zeng A, Liu S, Yu Y (2019) Comparative study of data driven methods in building electricity use prediction. *Energy Build* 1–42
18. Bashir MR, Gill AQ (2017) [IEEE 2017 intelligent systems conference (IntelliSys)—United Kingdom (2017.9.7–2017.9.8)] 2017 intelligent systems conference (IntelliSys)—IoT enabled smart buildings: a systematic review, pp 151–159

Designing a Secure Wide Area Network for Multiple Office Connectivity



Shaik Rehna Sulthana and Pasupuleti Sai Kiran

Abstract In today world, wide area network is the most necessary computer network for communication and administration in most of the companies and organization. In today's epidemic situation all home-based IT professionals need to go in from a distance to access their company's network. In this paper, designing a secure wide area network to connect multiple offices using the CISCO package tracker simulation tool. The paper is divided into two parts, one for the network design and the other for the protection provided by that network. The paper Provides detailed information about routers and servers such as domain name server, telnet server, network time protocol and system logging protocol. The main purpose of the organization is to share information through network and specially, it is far essential to make sure the change of data; as a result, no person can spoil or harm it. For comfy and dependable transfers among customers, integrity and trustworthiness are vital questions for all statistics transfer troubles. Therefore, created a complete secure wide area network (SWAN) for sending and receiving facts among exceedingly comfortable quit customers and also added the maximum crucial protection settings to the community used in our construction. We used huge variety of protocols to shield and host users of the SWAN machine.

Keywords Router · Switch · HTTP · DNS · DHCP · Telnet · SMTP

1 Introduction

In any formal and effective communication system, there must be a way to control the information in order to trade between the negotiating parties. On computer network, router and switches go across Internet. "Routers have a fixed policies that they use to perform path work, those policies are known as protocols based

S. R. Sulthana (✉) · P. S. Kiran
Koneru Lakshmaiah Education Foundation, Vaddeswaram, India
e-mail: rehna26198@gmail.com

P. S. Kiran
e-mail: psaikiran@kluniversity.in

on computers networks” [2]. Routers use these processes to make decisions about which methods to use to send a message from a network source to your destination. The computer network connects devices via a variety of communication media such as fiber, strong cable, twisted pairs and other types of unregulated media. The end devices are connected to the network using low-level devices such as switches and hubs. The paper provides detailed explanations about dynamic routing algorithm. It also includes login protocol, network time protocol and Telnet.

“A network can be fall underneath multiple threats and the reason at the back of that is the development of Internet technologies and services. Such attacks can arise in many methods that can be damage in your physical devices or maybe in your code” [1]. That kind of access motive lot of problems because of inaccuracies. Therefore, security has a significant impact on network. Network protection is one of the key issues for many firms as organizations. As an end result, we have developed a complete secure wide area network (SWAN) that integrates more than one networks. Those networks are supported through a protection machine that blocks get right of entry to without authentication. Additionally, it protects the privateness of every person, so no one can assault his or her non-public information.

2 Related Works

In this writer proposed a “secure Campus Network” (SCN) is a state of design and simulation using cisco packet tracer system. It exhibits a topology consisting of four systems, with distinctive networks devices. They divide end devices into separate VLANs for protection problems. Additionally, they implemented safety devices that join networks and switches that be part of end devices with another to save you external or unauthorized access. Moreover, this creator shows the genuine weight of different protocols in coordinating and defensive the whole campus machine [1].

In this the author’s proposed two routing protocols, RIPv1 and OSPF by using Cisco Packet Tracker. RIP can be configured the usage of a well-known IP address subnetting scheme. The rate is declining of this subnetting machine, it does no longer provide flexibility and moreover causes IP address harm. OSPF, alternatively, it enables classless subnetting and CIDR, this OSPF feature gives network administrators the ability to apply and save IP addresses by assigning the right variety of IP addresses to every subnet [2].

In this author proposed designing the state of the Wide Area Network provides sub-element of all other system exposure, similar to a network security and provides the basis for security, organization efficient, electronic learning environments and secure transaction. This paper tells us about the design of the network made by Cisco tool, and we can get started these conditions in different parts of the region. Wide area network, we may provide email security and more improve its security during message transmission [3].

3 Methodology

The Cisco packet tracer (CPT) is a major generation that relied on the design and implementation of a comprehensive secure wide area network. This Packet Tracer is an advanced with the aid of the Cisco for digital design of different networks inclusive of LAN and WAN which assist corporation to design, configure and troubleshoot all form of networks. It consists modes specifically physical mode and logical mode. This software allows all users to use the command line interface to build devices also it allows with protection problems via safety agreements.

3.1 Implementation

To design a secure wide area network for multiple office connectivity we used different devices such as routers, switches, servers, pc and laptops. Ethernet cable is a communication media for connecting devices. We also implemented many important configurations as DNS sever, HTTP server, syslog server, Telnet server, Mail server and dynamic host configuration. In addition, we have implemented security and management strategies on key network equipment; to make the wide area network more secure and to defend it from internal and external attackers. Therefore, it protect information and provide privacy to the users in the organization.

3.2 Required Resources

The following networking devices used to set up the topology:

- 5 Router (Cisco 1841)
- 5 Switch (2950–24)
- 8 server (server-PT)
- Laptops (laptop –PT)
- PCs (pc-PT)
- Serial DCE
- Straight-Through Cable.

3.3 WAN Topology

The topology is designed to connect multiple offices which are located in different geographical areas. In the paper different geographical areas are India, UK, USA, Germany and Singapore which are connected through wide area network. “All

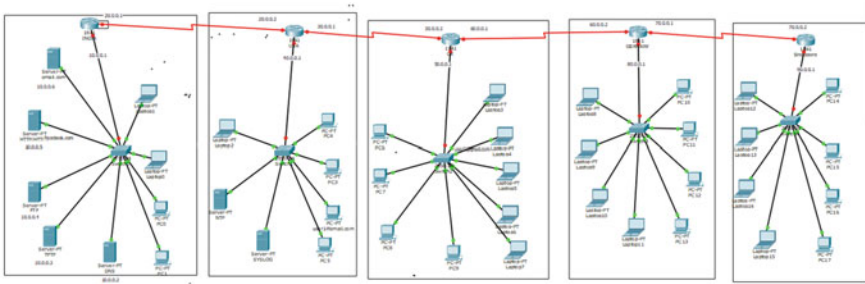


Fig. 1 Secure wide area network

devices are connected to a switch that connects them immediately to a router through serial cable”. Assign IP addresses and hostnames for all the devices as shown in Fig. 1.

4 Router Configuration

The router is important networking device and it perform its functions on the network click on Indian router and go to CLI mode. It contain two interfaces fa0/0 and se0/0/0 assign IP address to that network and for routing below are the commands.

```

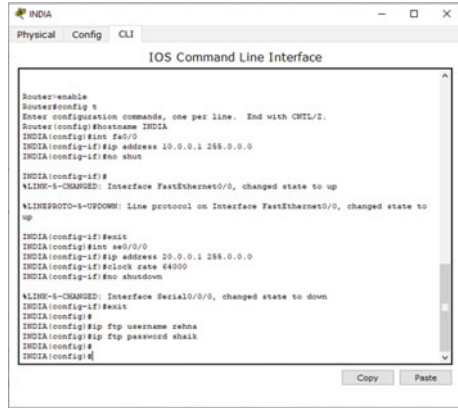
Router > enable
Router # config t
Router (config)#host name INDIA
INDIA(config)#int fa0/0
INDIA(config-if)#ip address 10.0.0.1 255.0.0.0
INDIA(config-if)#no shut
INDIA(config-if)#exit
INDIA(config)#int se0/0/0
INDIA(config-if)#clock rate 64000
INDIA(config-if)#no shut
INDIA(config-if)#exit
    
```

Router configuration for UK, USA, Germany and Singapore follow above process and command by defining respective IP addresses and hostnames (Fig. 2).

5 IP Address and Service Configuration

The IP Configuration, configures the Internet Protocol parameters, allowing the tool to receive and send IP packets and Service configuration is the method of setting a network’s controls of an organization.

Fig. 2 Indian router routing configuration



DNS Server IP configuration:

The following steps were followed to configure DNS server:

1. Click on DNS Server
2. In top desktop option is available click on it
3. Go to IP configuration and provide corresponding details
 - IP address—10.0.0.2
 - Default Gateway—10.0.0.1
 - DNS server—10.0.0.2
4. Close it

DNS Service Configuration:

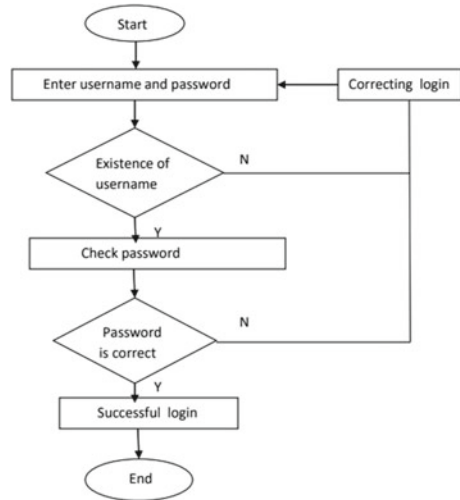
1. Click on DNS server.
2. In top services option is available click on it.
3. On left side list of service options are available click on DNS.
4. Add domain name and IP address and make sure that DNS is in ON state.

For TFTP, FTP, HTTP/HTTPS, Mail, Syslog and NTP server follow above steps to provide IP and Service configuration (Fig. 3).

6 Network Security

To protect network from internal and outside attacker there are numerous distinct ways. Attack can be physical vandalism or hacking the system to get admission to without authorization. For that we required a robust security policies to protect the network from those sort of attacks. Network rules and procedures monitor whole network system constantly to prevent and guard it from unauthorized get entry to. Therefore we applied SWAN used for excessive high class security on large devices and it additionally guard all ports in a network.

Fig. 3 Flow chart of remote login access



Security Router configuration:

- First step is to prevent remote access for that we provide security measures by setting console password.
- We set the password to the VTY 0 4 line to limit unauthorized access.
- MD5 algorithm is used to encrypt passwords.
- Finally, implemented some more limitations on creating passwords such as number of attempts and length of passwords.

6.1 Router and Switches Password Set up

This can be completed by turning on the CLI s router by entering the following instructions:

```

USA#en
USA#config t
USA(config)#enable secret password usa123
USA(config)#exit
  
```

“Enable secret password” is the command that enable password encryption and it is stored in memory.

6.2 Telnet Password Setup

This can be completed by turning on the CLI router by entering the following instructions:

```

USA>en
USA#config t
USA(config)username rehna password sulthana
USA(config)#user name password linux 12345
USA(config)#line vty 0 4
USA(config line)#login local
USA(config)#exit

```

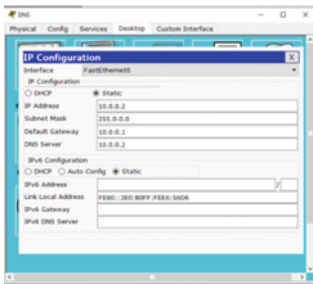
The password set for telnet (vty) port communication.

7 Results

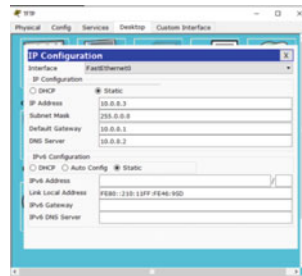
The design and implementation of secure wide area network results are as follows:

IP Address and Service configuration Results:

See Fig. 4 and 5.



DNS Server(10.0.0.2)



TFTP(10.0.0.3)

Fig. 4 IP address configuration

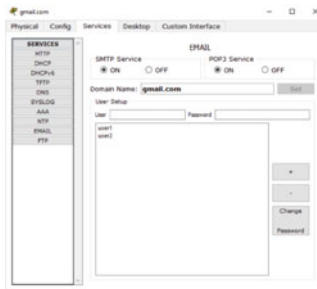
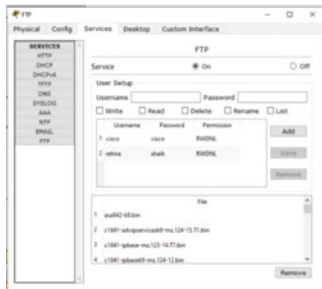
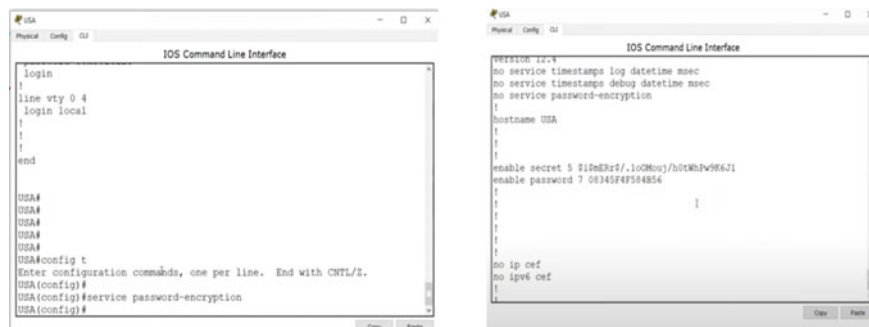


Fig. 5 Service configuration

Network Security Results



```

IOS Command Line Interface
login
!
line vty 0 4
login local
!
!
!
end
USA#
USA#
USA#
USA#
USA#
USA#config t
Enter configuration commands, one per line. End with CNTL/Z.
USA(config)#
USA(config)#service password-encryption
USA(config)#

IOS Command Line Interface
#VERSION 12.1
no service timestamps log datetime msec
no service timestamps debug datetime msec
no service password-encryption
!
hostname USA
!
!
!
!
enable secret 5 $1$mERrF/.1oCMouj/h01MhPw9K6Z1
enable password 7 08345f4F584854
!
!
!
!
no ip cef
no ipv6 cef
!
!
!
!

```

8 Conclusion

The implementation of the WAN using the packet Switching Technology is flexible enough to meet the requirements of the organization. This project will help to improve knowledge and reduce skills in the field of communication by joining hands in a similar experience for anyone. This project not only enhances operational efficiency but also meets the high demands of users by providing them with the right service. The most important factor in any organization is how quickly one can get the latest information in one place. The level of security in the network system, especially in planning, has raised a secure wide area network (SWAN) network. This paper introduces a topology comprising WAN and also implemented security measures for network connectors and switches that connect storage devices to prevent external or unauthorized access.

References

1. Ahmed AH, Mokhaled N, Al-Hamadani A (2021) Designing a secure campus network and simulating it using Cisco packet tracker. Indonesian J Electric Eng Comput Sci 23(1). ISSN: 2502-4752. 10.11591
2. Balarabe AT, Hassan ZL, Rufa A (2019) Implementation of RIPv1 and OSPF routing protocol, DHCP, DNS, and HTTP configurations in CISCO Packet Tracer. Int J Innov Res Electric Electron Instrum Control Eng 7(4)
3. Sanam N, Sai Anil P, Pavan EVS, Amarendra V (2019) Performance evaluation of wide area network using cisco packet tracer. Int J Adv Trends Comput Sci Eng 8(6)
4. Yousif MK, Al-Saffar SK (2018) Project scenario of communication network using cisco packet tracer. Int J Comput Appl (0975-8887) 181(29)
5. Massner et al (2011) A dynamic host configuration protocol based service discovery mechanism. In: Computer software and applications conference workshop, 2011 IEEE 35th annual, pp. 62-67

6. Lin CR et al (1997) Adaptive clustering for mobile wireless networks. *IEEE J Selected Areas Commun* 15(7):1265–1275
7. Mohammad Zunnun Khan, Prof. (Dr.) Mohd. Rizwan Beg and Mohd. Shahid Husain , “Designing of Wide Area Network with the use of Frame Relay Concept in Real Time Environment: a Proposal” , *IJRITCC* | MAR 2013, Available @ <http://www.ijritcc.org>.
8. Kadry S, Network security for an enterprise with worldwide branches. *Appl Inf Technol* 2005–2008 JATI

Polarity Identification from Micro Blogs Using Multimodal Sentiment Analysis



Haritha Akkineni, Myneni Madhubala, Madhuri Nallamothu,
and Venkata Suneetha Takellapati

Abstract Now-a-days, people are freely expressing their opinions in multiple ways through micro blogs usage like Twitter and Facebook in the Web. These channels are rich social media repositories, which provide an emerging channel for web users to express their sentiments in multimodal way, which is composed of image, video, short text, and emoticons. Such multimodal social media has significant application ranging from event monitoring, social network analytics, to commercial recommendations, etc. The existing unimodal sentiment analysis is purely on textual modality or emoticon based alone. Predicting sentiment of multimodal micro blogs in the current scenario by incorporating two types of data for analysis like texts and images. To analyze the images, Haar feature classifier was used which uses the rectangle integral to calculate the value of a feature and for the text analysis the Artificial neural networks algorithm was used which is trained with a large set of data consisting of different texts and their emotion. A few sample images and texts are used to test this work and sentiment was correctly predicted.

Keywords Sentiment prediction · Unimodal · Multimodal

H. Akkineni (✉)

PVP Siddhartha Institute of Technology, Vijayawada, Andhra Pradesh 520007, India

e-mail: aharitha@pvpsiddhartha.ac.in

M. Madhubala

Institute of Aeronautical Engineering, Hyderabad, Telangana 500043, India

M. Nallamothu

Dhanekula Institute of Technology, Vijayawada, Andhra Pradesh 521139, India

V. S. Takellapati

Gokaraju Rangaraju Institute of Engineering and Technology, Hyderabad, Telangana 500090, India

1 Introduction

Sentiment analysis is an important tool that categorizes data as having a positive or negative opinion, and as being subjective or objective as a whole. In this case, the definition of emotions and opinions is based, the opinions are evaluated in detail to assess the strength of opinions closely linked to the intensity of emotions such as joy, anxiety, disappointment, rage, surprise and soon. It is believed that the feelings of the people can be defined by analyzing their language expressions, and can be graded according to their strength level. It is often used in advertising placement, product benchmarking and market intelligence, as well as in detecting business credibility or brand recognition and recognizing false or misinforming comments. Multimodal sentiment analysis is computational study of mood, emotions, opinions, affective state, etc. from the text and audio, video data Opinion mining is used to evaluate a speaker's or a writer's attitude toward some subject Opinion mining is a form of NLP to monitor the mood of the public toward a specific product [1]. Collect and review feedback on the product from the message forum, review pages, forums, Multimodal Sentiment Analysis on Big Data, etc. We also have seen a rapid proliferation of microblogs such as Twitter and Sina Weibo on the web today. For example, by March 2016S in a Weibo hits remarkable 261million active monthly users. Such a vast repository of social media provides the web users with a new platform to share their feelings. More importantly, such communication appears to be more and more multimodal, consisting of image, video, short text, and emoticons. Nevertheless, for the analysis of emotions, most current works still retain an examination of the textual modality alone, whereas the examination of feelings from visual and other modalities retains an open question [2].

2 Literature Survey

In this paper, we research the challenging issue of predicting multimodal feelings for tweets on social media. Our principal contribution is to train a discriminative model for multimodal prediction from readily accessible emoticon labels. A new, weakly-supervised multimodal deep learning architecture (WS-DML) achieves this. In particular, from the pre-trained CNN and DCNN models, we measure first of all the sensation likelihood distributions and the multimodal emotion consistency. Then we train a probabilistic graphic model to discern the contribution weights of the noisy mark, which are sent back to update the CNN and DCNN models parameters, respectively. Experimental comparisons to state-of-the-art methods show that our method has achieved state-of-the-art performance on the task of multimodal prediction of sentiment. For example, if accessible from the social media website, the noisy mark may be the online actions of the user, or logs. In addition, we must further examine the order of the emoticon labels in our future research, which may be incorporated as a constraint in the WS-MDL model [3].

We call the question of identifying reports not by content, but by general opinion, for example, deciding whether a summary is true or false. Using film reviews as evidence, traditional deep learning strategies were considered. Though, the triple algorithms approach we used (Naive Bayes, maximum likelihood identification, and matrix support systems) do not do too well on the identification of feelings as on standard topic-based criteria. We end by analyzing variables that render the question of classifying feelings more difficult [4]. We investigate the effectiveness of expression and syntactic features in software-human verbal tutoring dialogs to forecast participant emotions [5]. We first preprocess changes for bad, moderate, optimistic and confused emotions among the students. Electric guitar-prosodic elements were derived from pulse of expression, and semantic elements from the transposed or remembered voice. Using such functions or in addition, we analyze the outcomes of deep learning tests to forecast different classifications of the participant feelings noted. The strongest tests show a cumulative gain of 19–36% over a benchmark of failure elimination. At last, in living creature-tutoring conversations we equate the findings with emotion forecast [6].

Emotional tests can adequately describe the essence of such an emotional event, which should assess if it is common or special to a subset or society. We explored the importance of measuring emotion by skin capacitance (a physiological indicator that is simple to define) and wedge (frequently utilized and precise indicators of subjective anger). The paper summarizes observations from two tests. The first tested different combinations of sliders and noticed that emotions assessed effectively described the subjective essence of short films. The second study gathered the emotional measurements of multiplier and skin capacitance, while one group of Japanese researchers and then another group of Canadian researchers observed longer recordings. The interventions were adequately adaptive to recognize cultural variations in accordance with current research, but were able to distinguish areas of the interaction where participants from various cultures responded appropriately, recognizing material that produced a common experience. To obtain further visibility into the latent and overt emotion results, we give a framework of data analysis techniques: Elegance and consensus analyzes that can suggest conditions like dedication and exhaustion. In a diagram, we outline the facets of our measuring method and toolkit: the capacity to determine the subjective essence of objects, persons, and affective experience [7]. Although conventional statistical analysis requires months or even years to finish, the framework seen here evaluates opinion as to the vote in just the entire blog stream [8], producing results instantaneously and continuously. It provides a fresh and relevant view on the complexities of the democratic cycle and popular sentiment to the electorate, the media, policymakers and educators [2, 9]. In this specific segment the papers concentrate on artificial intelligence for either the study of large social data. Though, distilling intelligence from such a vast volume of unorganized material is an exceedingly challenging job, since the components of today's network are ideally designed for human use, yet are barely comprehensible to equipment. Large social web research stems from this want and integrates various fields, including web monitoring, digital production, social networking research, pattern identification and view digging [4, 10].

3 Methodology

The proposed model displays the information in the sequential order of the undergoing operations. The inputs are mainly of two modals (types), i.e., text and images. The text inputs from the user are passed through a model which is trained to identify the sentiments of the text. For the image inputs the first process which is done is face extraction and it can be done by using the HAAR cascade. Now, for the extracted image we analyze the sentiment using face detection model which gives us the sentiment of the image, by combining both the text and image outputs we display the detailed statistics output of number of negative, positive and neutral comments are presented in content. The overall procedure is shown in Fig. 1.

3.1 Inputs from Social Sites

To train our model we need a huge dataset and we took the dataset from the Kaggle. Identify the text sentiment using NN model.

The text-based sentiment detection is performed in two step process using NN model is shown in Fig. 2.

3.1.1 TF-IDF Vectorizer

TF-IDF stands for Term frequency-inverse document frequency and TF-IDF vectorizer transforms the text into vectors that can be used as an estimator input, it uses vocabulary as a dictionary that translates each term into a matrix function index, each single word gets an index function.



Fig. 1 Step wise process of multimodal sentiment analysis



Fig. 2 NN model for text-based sentiment detection

3.1.2 MLP Classifier

The MLP stands for Multilayer perceptron, i.e., there can be more than one linear layer. When we take the simple example of the three-layer network, the first layer will be the layer of input and the last layer of output will be called the hidden layer and the middle layer. We fill in the input layer with our input data and take feedback from the feedback layer. It takes the input from the TF-IDF and classifies the input and predict the sentiment.

3.2 Face Extraction Using HAAR Cascade

For the given image input we have used HAAR cascade which is able to detect the faces from the given image.

3.2.1 HAAR Cascade

The Haar Cascade classifier is based on the Haar Wavelet methodology, which divides pixels in an image into squares by line. It computes the identified “functions” using “integral image” concepts. To identify the face in an image, Haar Cascades employ the Ada-boost learning algorithm, which chooses a limited number of significant characteristics from a huge collection to generate an effective performance for the classifiers, and then uses cascading techniques.

3.2.2 Sentiment Extraction Using Face Detection Model

In this model the input is the detected face which is done by the HAAR cascade and now FER2013 is used to detect the sentiment of the image by analyzing the face expression of the image.

Figure 3 represents the process of how the sentiments of the image inputs are predicted. It starts with training the model using fer2013, then detecting the face from the image and then finding the expressions using the HAAR cascade and each of this is explained clearly below.



Fig. 3 Face sentiment detection model

3.2.3 FER2013

Fer2013 is an open-source dataset, which consists of 35,887 grayscale, 48×48 scaled face portraits of various emotions. The dataset contains the following emotion labels: 4593 images of Angry 547 images of Disgust, 5121 images of Fear, 8989 Images of Happiness, 6077 images that are depressing, 4002 images of surprise and 6198 images that are indifferent. The input for fer2013 is the detected face from the image input. Now, the fer2013 compares the face expression with the dataset present in it to identify the sentiment of the image and show as an output.

3.2.4 OPEN CV Cascade Classifier

Several hundred “positive” sample views of a single object are trained as cascading classifiers, and random “negative” images of the same size. After training you can apply the classifier to a region of an image and classify the object in question. The search window can be rotated around the image to look for the object in the whole picture, and to scan for the classifier at each location. This method is most widely used for object detection and tracking purposes in image processing, especially facial detection and recognition.

3.3 Combined Sentiment

In combined sentiment the text sentiment output and image sentiment output are stored and the overall output is displayed which is of a detailed statistics report.

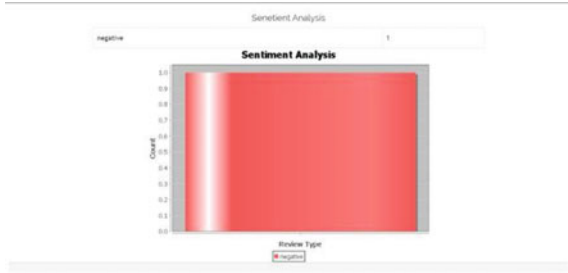
4 Results and Discussion

This section presents results of the proposed application that reflects the functionalities of different modules integrated together. It provides the proposed system in detail with figures. When taking only image as an input with no text data to check for the unimodality of our system. The image is send as input to check for the unimodality of the system, the image is analyzed using the HAAR cascade and then the expressions are detected which is compared with the trained dataset to identify the sentiment of the image.

Figure 4 shows the analyzed report for the unimodality system, and the displayed output is Accurate, and it is represented as a bar graph for better comprehension of the report.

Then two text inputs are taken to check for the sentiment analysis of only text data. Now, checking unimodality of the system for text data type is being done. The

Fig. 4 Result of image input



input texts are analyzed by using the trained model and depicted sentiments of the inputs are shown in the form of a bar graph as in Fig. 5.

Now, the main functionality of the research work, i.e., multimodality will be checked. Then both the image and text inputs together are checked and their sentiments are analyzed. The sample inputs are shown in Fig. 6.

For the multimodality, the text inputs and image inputs are taken, they are analyzed separately by passing the text inputs through the NN Model and the images through the Face sentiment detection model. The detailed analyzed statistics report output of the above inputs are shown in Fig. 7.

Fig. 5 Output of text input

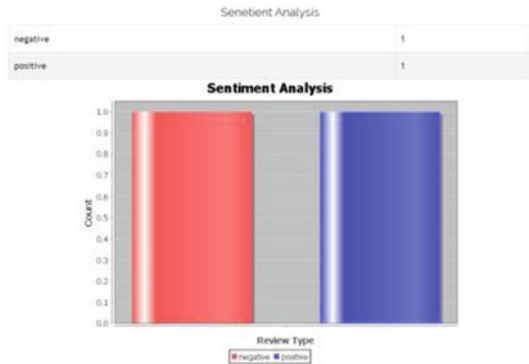
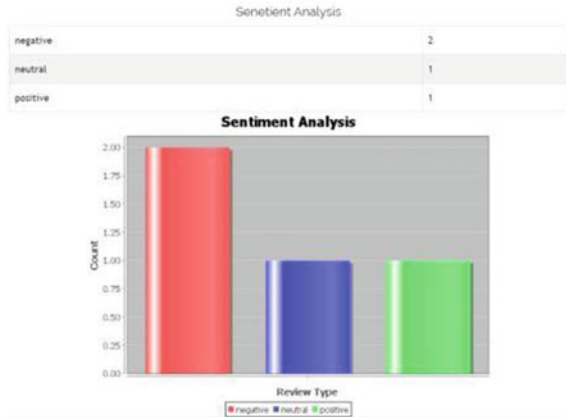


Fig. 6 Text and image as input



Fig. 7 Output for text and image input



From this experiment sentiments of a multimodal system are analyzed which typically consists of texts and images as inputs.

5 Conclusion

Sentiment analysis is primarily concerned with the automatic recognition of the polarity of opinions, whether positive or negative. Multimodality is defined as the examination of more than one modality. The combination of multiple input modes to improve analytical efficiency is referred to as multimodal sentiment analysis. From our research work paper, we conclude that we use two algorithms, i.e., artificial neural networks for text analysis and the Haar feature classifier for image analysis, and we can predict the feeling of the texts and images that are taken as inputs and can display the statistics as a bar graph.

In the future, the work can be extended to predict the sentiment using short videos, GIFs or audio for the development of recommender system in different fields by analyzing all the different types of data that could exist. In future, we can improve it by using different algorithms for the better accuracy.

References

1. Soleymani M, Garcia D, Jou B, Schuller B, Chang SF, Pantic M (2017) A survey of multimodal sentiment analysis. *Image Vision Comp* 65:3–14
2. Scott B, Nass C (2007) Emotion in human computer interaction. Retrieved from <http://ircm.com.umontreal.ca/dufresne/COM7162/EmotionHumanInteraction.pdf>

3. Chen F, Ji R, Su J, Caoand D, Gao Y (2018) Predicting microblog sentiments via weakly supervised multimodal deep learning. *IEEE Trans Multimedia* 20(4):997–1007
4. Pang B, Lee L, Vaithyanathan S (2002) Thumbs up? Sentiment classification using machine learning techniques. In: Proceedings of the conference on empirical methods in natural language processing (EMNLP), ACL, pp 79–86
5. Lee CM, Narayanan SS (2005) Toward detecting emotions in spoken dialogs. *IEEE Tran Speech Audio Proc* 13(2)
6. Litman DJ, Forbes-Riley K (2004) Predicting student emotions in computer-human tutoring dialogues. In: Proc. of the 42nd annual meeting of the association for computational linguistics (ACL)
7. Lottridge D, Chignell M, Yasumura M (2012) Identifying emotion through implicit and explicit measures: cultural differences, cognitive load, and immersion. *IEEE Trans Affec Comp* 3(2)
8. Singh PK, Husain MS (2014) Methodological study of opinion mining and sentiment analysis techniques. *Int J Soft Comp (IJSC)* 5(1)
9. Wang H, Can D, Kazemzadeh A, Bar F, Narayanan S (2012) A system for real-time twitter sentiment analysis of 2012 us presidential election cycle. In: ACL system demonstrations, pp 115–120
10. Cambria E, Howard N, Xia Y, Chua T (2016) Computational intelligence for big social data analysis[guest editorial]. *IEEE Comput Intell Magazine* 11(3):8–9

Software Defect Prediction: An ML Approach-Based Comprehensive Study



Kunal Anand and Ajay Kumar Jena

Abstract Software testing is a vital phase in the software development life cycle. Testing validates a developed software against the input test cases by identifying the defects present in the system. The phenomenon of testing is not only time-consuming but also a costly affair. Although there are automated tools available that reduce the effort of testing up to some extent, the high maintenance cost of these tools only increases the cost. Earlier defect prediction in software significantly reduces the effort and cost without affecting the constraints. It identifies the defect-prone modules that require more rigorous testing. A practical and effective defect prediction mechanism is the need of the hour due to the challenges, namely dimensionality reduction and class imbalance, present in software defect prediction. Lately, machine learning (ML) has emerged as a powerful decision-making approach in this regard. This research work aims to do an extensive study on the implementation of ML techniques in software defect prediction. This comprehensive report is based on two different aspects named feature selection/reduction techniques and ensemble learning methods that have been used in software defect prediction. This study has also discussed the widely used software and performance measure metrics used in software defect prediction. This concise work would guide future researchers in this emerging research area. Further, this paper also emphasizes the need to identify a suitable feature selection approach that could enhance the model's predictive performance when applied with ensemble learning.

Keywords Software testing · Software defect prediction · Feature selection · Machine learning · Ensemble modelling

K. Anand (✉) · A. K. Jena
Kalinga Institute of Industrial Technology, Bhubaneswar, Odisha 751024, India
e-mail: kunal.anandfcs@kiit.ac.in

A. K. Jena
e-mail: ajay.jenafcs@kiit.ac.in

1 Introduction

Nowadays, software has become an essential and integral part of our lives. The industry and society are immensely reliant on software-backed surroundings as it significantly reduces human endeavour and time [1]. Any electronic device or system, modern household product or spacecraft revolves around the software. Due to the high demand for good-quality software products across different walks of life, it is crucial to develop a software product free from defects. However, good quality and reliable software products come with complexities and challenges. In software development, a defect is an outcome of some programming mistakes due to which the software system does not show the expected results. Software testing enables the developers to develop a quality and reliable software product by identifying and fixing the defects. Defects present in a software module increase the development and maintenance costs and, at times, are the prime reason for the failure of the software product. At present, a significant part of the software development and maintenance budget goes into identifying and fixing defects [2]. This high maintenance cost can come down significantly by identifying the defects in the earlier stage of the development. Mantyla et al. [3], in 2008, described two types of defects named functional defects and evolvability defects. Functional defects affect the system's behaviour, whereas evolvability defects improve the evolvability of the software by making it easy to understand and modify.

Software defect prediction (SDP) focuses on defect-prone modules that require extensive testing. This way it facilitates the efficient utilization of the available resources without affecting the testing constraints. For a software product, the timely defect prediction boosts the quality of the software besides giving the flexibility to the project managers to manage the resources optimally [4]. Additionally, it also helps increase the quality of the developed software, leading to higher customer satisfaction and subsequently to the product's success. A practical and powerful defect prediction mechanism is vital due to the challenges, namely dimensionality reduction and class imbalance. The class imbalance problem is an extreme imbalance between the defect-prone (DP) and non-defect-prone (NDP) modules. Hence, the data set is highly skewed towards DP or NDP modules. Usually, the DP modules are fewer than NDP modules, and initially, the learners mainly focus on NDP modules. Hence, data balancing is required to resolve the skewness in the data set [5]. Another major challenge most defect prediction models face is irrelevant features present in the data set. These features do not possess any significant information and are hence considered noise. Like the class imbalance problem, irrelevant features also reduce the model's predictive performance.

Organization of the paper: Sect. 1 discusses the formal requirement of a software defect prediction model and its challenges. Section 2 describes the basic concepts that might help understand this work. Section 3 discusses the methodology that has been followed in this work. The literature review has been discussed in Sect. 4. It also raises three research questions. Section 5 consists of the discussion on our findings.

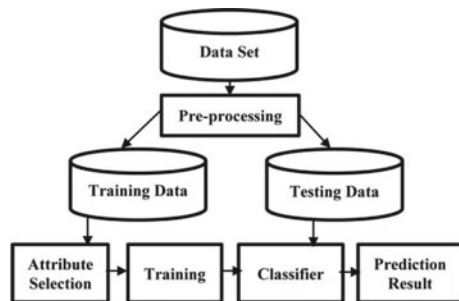
The answer to the research questions also follows here. Finally, the paper concludes with the summary and future action in Sect. 6.

2 Software Defect Prediction

Here, we discuss the fundamental concepts of defect prediction in software modules and the applicability of machine learning. First, Fig. 1 depicts the block diagram of software defect prediction [7]. Next, the data set, taken from publicly available repositories like NASA, PROMISE, ECLIPSE, AEEEM, or a real-life project, undergoes some pre-processing to remove any noise or missing values. After pre-processing, the dis-aggregation of the data set is done into training and testing data. Unfortunately, the training set may contain irrelevant attributes that do not contribute significantly to the defect prediction but can lower the model's performance. A suitable feature selection technique can significantly solve this issue. Then, a suitable machine learning classifier uses this reduced training data to build the model. Further, the built model measures the performance using the test data.

Machine learning (ML) enables computers to learn automatically without human intervention and adjust their actions accordingly. Lately, ML has emerged as a powerful decision-making approach in software defect prediction. It helps in identifying the defective modules more effectively and reduces maintenance costs. Several defect prediction models have been proposed using the classifiers such as Naïve Bayes (NB), logistic regression (LR), random forest (RF), support vector machine (SVM), K-NN, decision tree (DT). However, the performance of these machines was not that satisfactory as these models suffer from challenges like class imbalance and irrelevant features [6].

Fig. 1 Software defect prediction: An overview



3 Methodology

This study intends to review and assess the experimental evidence gained from the existing work done in software defect prediction using machine learning techniques. The overall methodology followed in this review is as below:

3.1 Research Questions

The following research questions have been framed to assist us in the assessments as mentioned earlier.

RQ1: Does the feature selection/reduction techniques impact the model's predictive performance? What are the increasingly used feature selection/reduction techniques for defect prediction?

RQ2: Do Ensemble Learning methods give a better predictive performance in defect prediction models than the individual classifiers?

RQ3: What are the frequently used software and performance measure metrics in software defect prediction?

3.2 Review Protocol

The general process of identifying relevant works includes selecting appropriate digital repositories, determining search keywords and finding a list of existing works that match the search keywords. This survey includes research papers since 2010 from several databases/publishers such as Google Scholar, IEEE, Science Direct, and Springer Link. Further, we defined the search keyword "Defect Prediction in software modules using Machine Learning", intending to include relevant studies for our study. We identified 117 papers from the repositories mentioned above in the initial list. We did a preliminary study based on the title, abstract, and conclusion of those papers and reduced the number to 79 in our second list. The statistical distribution of the publisher-wise studies and the methods followed has been shown in Figs. 2 and 3.

We went through these papers thoroughly and selected 15 final papers based on the inclusion criteria as mentioned below:

- **Inclusion Criteria:**
 - Papers that used ML techniques in software defect prediction.
 - Papers that compared the performance of different defect prediction models.
 - Empirical papers.

Fig. 2 Statistical distribution of publisher-wise studies

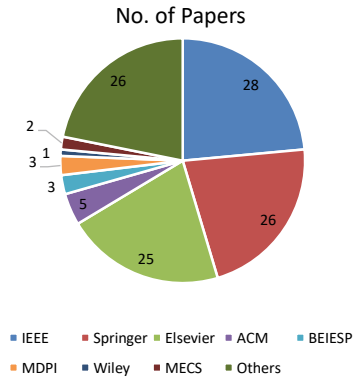
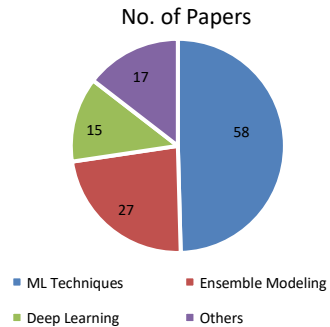


Fig. 3 Statistical distribution of studies on the methods followed



We examined the final list of papers based on characteristics like feature selection/reduction techniques, ensemble learning methods, software metrics, and performance measurement metrics to check if they covered the above-defined research questions or not. The results are represented in Table 1.

4 Literature Review

In this section, we present the findings of our literature survey. We divided our survey into two categories. The first category included studying the conventional ML approach using feature selection/reduction techniques. In Table 3, we summarize the findings of the study (Table 2).

Though the defect prediction models based on individual classifiers using the conventional machine learning approach showed good performance, they still faced challenges like class imbalance. This challenge paved the way for further research to strengthen the achievement of defect prediction models. As a result, ensemble learning methods came into existence that combined several individual classifiers

Table 1 Data extraction results

Sl. No	Reference	RQ1	RQ2	RQ3
1	Afzal et al. [14]	Y		Y
2	Ghotra et al. [15]	Y		Y
3	Sabharwal et al. [18]	Y		Y
4	Huda et al. [19]	Y		Y
5	Balogun et al. [20]	Y		Y
6	Kondo et al. [21]	Y		Y
7	Amit et al. [22]	Y		Y
8	Balogun et al. [23]	Y		Y
9	Laradji et al. [13]	Y	Y	Y
10	Saifan et al. [4]	Y	Y	Y
11	Zuber Khan [24]		Y	Y
12	Alsawalqah et al. [25]		Y	Y
13	Malhotra et al. [26]		Y	Y
14	Mangla et al. [5]		Y	Y
15	Mehta et al. [27]		Y	Y

and built the prediction models using the ensemble classifiers. Table 3 represents the findings of defect prediction using the ensemble learning methods.

5 Discussion on Our Findings

5.1 Answer to the Research Questions

Through a detailed study of the selected papers, we observed that though software defect prediction system has made significant progress in recent times, it still faces challenges like irrelevant features and data imbalance. While feature selection and reduction techniques have helped to an extent in removing the irrelevant features, ensemble learning techniques have significantly improved the model's performance compared to individual classifiers. The above study's findings answered the research questions raised in this paper.

RQ1: Does the feature selection/reduction techniques impact the model's predictive performance? What are the increasingly used feature selection/reduction techniques for defect prediction?

Answer: The above survey found that the feature selection/reduction techniques significantly improved the model's performance [4, 13–15, 18–23, 26, 27]. The widely used feature selection techniques are filter-based, wrapper-based, correlation-based, and consistency-based. Similarly, the widely used feature reduction techniques

Table 2 Conventional ML approach using the feature selection/reduction techniques

Author	Objectives	Conclusion	Limitations
Afzal et al. [14]	To assess the consequence of feature subset selection methods on the model’s accomplishment	The studied feature subset selection methods significantly improved the model’s accomplishment	The authors did not interpret the features retained using FSS methods
Ghotra et al. [15]	To study different feature selection techniques spread across different families on different classifiers	Correlation-based filter subset feature selection outperformed other given feature selection techniques	Variation in performance if used with some other datasets classifiers
Huda et al. [19]	A novel defect prediction approach combined the metric selection using wrapper and filter techniques and a training process as a single process	Hybrid models obtained more accurate predictions than a conventional wrapper or filter approaches	High in complexity, time-consuming
Sabharwal et al. [18]	A hybrid feature selection approach to portray the usage of feature ranking along with the feature subset selection	After eliminating the irrelevant features, the model’s performance was either the same or better	The study did not explore the Wrapper-based feature selection technique
Balogun et al. [20]	To compare the impact of filter feature ranking and the feature subset selection methods	Feature selection (FS) approaches improved the performance of the classifiers	Varied performance when used among a variety of datasets and classifiers
Kondo et al. [21]	To investigate and liken the outcome of feature selection/reduction techniques on the model’s implementation	Feature selection/reduction techniques positively affected the model’s performance	Did not explore the performance with other feature selection methods, different datasets and classifiers
Amit et al. [22]	To compare the performance of several defect prediction models using feature selection	Feature selection methods improved the performance of the model	Performance analysis of models based on cognitive techniques and other feature selection methods is missing
Balogun et al. [23]	To propose an enhanced wrapper feature selection technique that selects the feature dynamically and iteratively	The proposed EWFS technique outclassed existing sequential search-based WFS techniques	The impact of the proposed methods remained unexplored in ensemble classifiers

Table 3 Defect prediction employing an ensemble learning approach

Author	Objectives	Conclusion	Limitations
Laradji et al. [13]	An ensemble learning algorithm based on two variants to gain a more robust data imbalance and feature redundancy system	Greedy forward feature selection gave the best results compared to other correlation-based feature selection techniques	Lack of generalization due to varied performance across feature selection methods classifiers
Saifan et al. [4]	The authors proposed a prediction model using feature subset selection approaches and ensemble classifiers	The model's outcome was bettered when applied with feature subset selection methods	Variation in performance if used with some other datasets classifiers
Zuber Khan [24]	To compare the performance of well-known ML classifiers with hybrid ensemble learning techniques (HELT)	HELTS gave a better performance as compared to individual classifiers. AdaBoost-SVM and bagging-SVM gave the best performance	High in complexity, time-consuming
Alsawalqah et al. [25]	To propose a proficient and sturdy heterogeneous grouping model based on identical patterns	The proposed approach boosted the performance of the ensemble techniques and single classifiers	Automatic determination of the best clusters for each data set remains a challenge
Malhotra et al. [26]	This work explored boosting-based ensemble methods to compare various defect prediction models	The resampling method improved the model's performance. In addition, the RUSBoost ensemble method outperformed all other studied boosting-based ensemble models	There was no comparison with other ensemble methods like bagging and cost-sensitive ensembles
Mangla et al. [5]	To predict the defects in a software system using a sequential ensemble model and further compare the proposed model's performance with existing models	The proposed performed better than the existing ensemble learning techniques like the random forest, bagging, stacking, and XGBoost	This work did not apply Feature selection techniques to mitigate the possible impact of irrelevant features
Mehta et al. [27]	To propose an ensemble prototype to forecast the defects in software modules To reduce the impact of data imbalance and high dimensionality	Ensemble model based on XGBoost and stacking improved the performance from accuracy	Did not explore other performance measures such as AUC, recall, precision. The study used only small size datasets

are principal component analysis, FastMap, feature agglomeration, transfer component analysis and TCA+ , random projection, restricted Boltzmann machine, and autoencoder. The study also found that the selection techniques exceeded the reduction techniques in supervised learning. Similarly, reduction techniques based on neural networks were better in unsupervised learning [27].

RQ2: Do ensemble learning methods give a better predictive performance in defect prediction models than the individual classifiers?

Answer: Several core models are combined to produce one optimal predictive model in the ensemble method. It improves the model's predictive performance compared to the individual classifiers [5, 13, 23, 24]. When applied with ensemble learning methods, the feature selection methods mostly gave a better performance than the scenario when the feature selection was not used [4, 13, 26, 27]. However, in some cases, the performance was decreased when ensemble learning methods used specific feature selection methods [4]. Some widely used ensemble methods are bagging, boosting, and stacking.

RQ3: What are the frequently used software and performance measure metrics in software defect prediction?

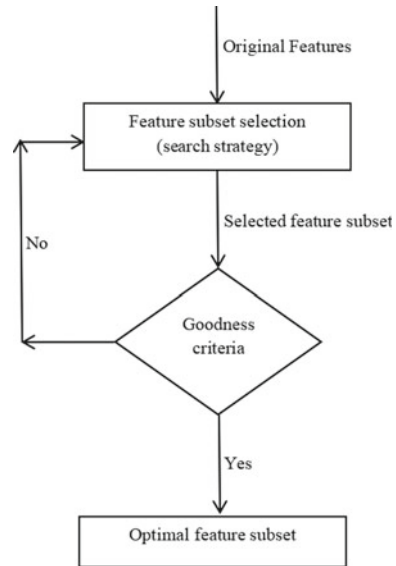
Answer: In this review, we extensively studied the different software metrics used in software defect prediction. From our analysis, we found that majority of the studied works have used McCabe metrics, Halstead base and derived metrics. In terms of performance measurement metrics. Our study observed that the area under the receiver operating characteristic curve (AUC) is the most widely used performance measure as the skewness of defect data does not affect AUC. AUC is followed by accuracy as the second most widely used performance measure metric. Some other popular performance measures are precision, accuracy, specificity, *G*-mean, *F*-measure, performance variance, and error rate.

5.2 Filter-Based Feature Subset Selection Technique

The feature subset selection techniques examine the importance of each feature and produce a subset of relevant features. Filter-based and wrapper-based feature subset selection techniques are prevalent in defect prediction. The past research works have extensively used filter-based feature subset selection techniques, which were found very effective [15–17]. An overview of subset-based feature selection has been depicted in Fig. 4.

Correlation subset-based techniques do not evaluate individual features. Instead, they result in subsets of features. The best feature subset is low on intercorrelation but high correlation with the class label [17]. Consistency subset-based techniques focus on consistency to estimate the relevance of a feature subset. This approach provides a nominal feature subset with consistency equivalent to all the features [16]. Ghotra et al. [15] did an extensive study and assessed the influence of feature selection techniques on the defect forecast model. Through their trial outcome, the authors established that correlation-based subset feature selection techniques,

Fig. 4 Feature subset selection technique



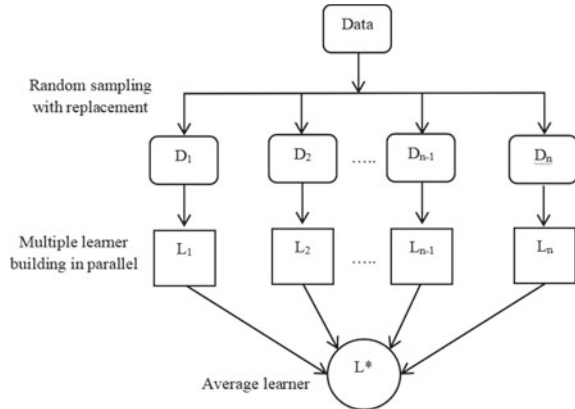
coupled with best-first search, outperformed other feature selection approaches over different datasets used in this study. Balogun et al. [20] scrutinize the effect of diverse feature selection approaches on the predictive accomplishment of the models. They also compared the effect of filter-based feature selection methods with filter-based feature ranking methods on fault forecast models. The authors concluded that although the filter-based feature selection methods, in addition to the best-first search technique, enhanced the achievement of the fault forecast model, the filter feature ranking approach-based models gave a more stable predictive performance. Kondo et al. [21] applied different filter-based feature subset selection techniques and filter-based feature ranking techniques and observed the outcome of the fault forecast model in both supervised and unsupervised learning. They observed that filter-based feature subset selection procedures gave the best performance for the supervised defect prediction model. Similarly, neural network-based feature reduction approaches (RBM and AE) provided better-unsupervised patterns.

Balogun et al. [23] proposed an enhanced wrapper feature selection technique that selects features dynamically and iteratively and found that the proposed technique not only selected the subsets in less time but also returned an improved prediction rate.

5.3 Bagging Ensemble Learning

Bagging, an acronym of bootstrap aggregation, is one widely used ensemble learning method. It is a parallel method that fits several weak learners independently, making it

Fig. 5 Bagging ensemble learning



possible to train them simultaneously. Bagging uses random sampling with replacement to generate additional data for training from the data set. Multiple models are trained in parallel using these multidata sets. Finally, the average predictions from different ensemble models are calculated. Bagging not only reduces the variance but also attunes the forecast to an anticipated outcome. Figure 5 depicts an overview of the bagging ensemble learning method.

5.4 Boosting Ensemble Learning

Boosting is another type of ensemble method where the weak learners learn in sequence and enhance the performance of a model adaptively—boosting increases the weight of a wrongly predicted data point. Each resulting model is allocated with weight during training. Figure 6 shows the boosting ensemble method.

Khan et al. [24] explored the idea of a hybrid ensemble learning technique using AdaBoost and bagging ensemble approaches using Naive Bayes, support vector machine, and random forest classifiers using PROMISE datasets. They equated the outcome of the studied models and concluded that AdaBoost-SVM and bagging SVM gave the best performance compared to the other methods.

From our study, we observed that most of the studied papers used bagging and boosting as an ensemble learning method in software defect prediction [4, 13, 24–27]. Mangla et al. [5] used a sequential ensemble model based on a neural network and compared the performance of their proposed model with other ensemble methods such as bagging, boosting, stacking. Laradji et al. [13] used the average probability ensemble (APE) method on two variants to gain a more robust data imbalance and feature redundancy system. Figure 7 shows the distribution of selected ensemble method-based papers.

Fig. 6 Boosting ensemble learning

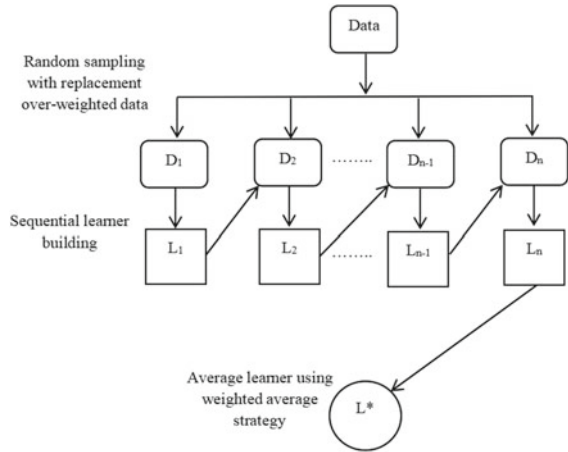
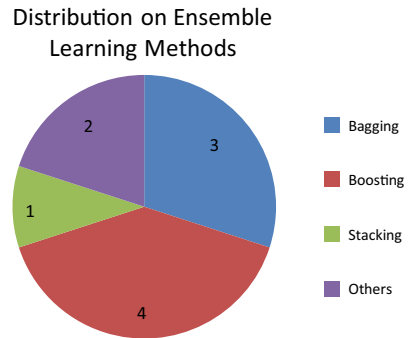


Fig. 7 Distribution on ensemble learning method



5.5 Metrics Used in Software Defect Prediction

5.5.1 Software Metrics

The static source code consists of some features known as software metrics. These features are helpful, user-friendly, and extensively used. The data are module-based, and mainly it includes McCabe and Halstead features extractors of source code. For example, a practical defect prediction model only considers the best metrics and discards the metrics that may hurt the model’s predictive performance. McCabe [8] argued that the code containing a complex pathway is more prone to errors. Hence, the metrics reflect the pathways within a code module. Some commonly used McCabe metrics are (LOC, cyclomatic complexity, essential complexity, design complexity). Halstead [9] argued that a hard to read code is more error-prone. So, the metrics estimate the various concepts in a module and determine the complexity—Table 4 lists the software metrics.

Table 4 Software metrics in software defect prediction

Metrics Type	Metrics	Description
McCabe metrics	Cyclomatic complexity, $v(G)$ Essential complexity, $ev(G)$ Design complexity, $iv(G)$ Lines of Code	Maximum count of linearly independent paths Reduced flowgraph by decomposing the D-structured primes sub flowgraphs The complexity of the module's reduced flowgraph lines of code in a source code
Halstead base metrics	Number of unique operators, μ_1 Number of unique operands, μ_2 Total number of operators, N_1 Total number of operands, N_2 Length, N Vocabulary, μ	Count of unique operators in the code Count of unique operands in the code Total count of operators in the code Total count of operands in the code The sum of N_1 and N_2 the sum of μ_1 and μ_2
Halstead derived metrics	Volume, P Potential minimum volume, V^* Program level, L Difficulty, D Effort, E Time, T	Count of mental resemblances to write a programme of length N Minimum source code used to solve the problem The ratio of potential minimum volume with program volume Difficulty level in the code The effort to write a program Time to write a program

The widely used Halstead metrics are base Halstead metrics (number of unique operators, number of unique operands, total number of operators, total number of operands, length, vocabulary), derived Halstead metrics (volume, potential minimum volume, program level, difficulty, effort, and time) [10]. Our study noted that all the selected papers used the software as mentioned above metrics in their defect prediction model.

5.5.2 Performance Measure Metrics

Performance measure metrics measure the model's predictive performance. Table 5 furnishes some performance measure metrics used in software defect prediction.

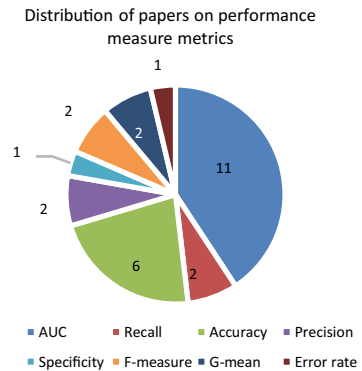
Our study observed that the area under the receiver operating characteristic curve (AUC) is the most widely used performance measure as the skewness of defect data does not affect AUC. AUC is followed by accuracy as the second most widely used performance measure metric. Some other popular performance measures are precision, accuracy, specificity, G -mean, F -measure, performance variance, and error

Table 5 Performance measure metrics in software defect prediction

Metrics	Description	Formula
Accuracy	Accurate forecast made over the total number of points estimated	$\frac{tp+tn}{tp+tn+fp+fn}$
Precision	The fraction of rightly classified instances to the overall positive classified instances	$\frac{tp}{tp+fp}$
Recall or sensitivity	Accurately categorized instances from the total categorized instances	$\frac{tp}{tp+fn}$
Specificity	The ratio of negative instances that are rightly grouped	$\frac{tn}{tp+fp}$
F-measure	Harmonic average of Precision and sensitivity	$\frac{2 * p * r}{p+r}$
Geometric mean	This metric maximizes the tp and tn rates	$\sqrt{tn * tp}$
Error rate	The ratio of false estimates over the total estimates	$\frac{fp+fn}{tp+fp+tn+fn}$
Area under Curve (AUC)	The plot of the True Positive against the False Positive at different thresholds	By plotting the cumulative distribution function of the True Positive on the y-axis against the cumulative distribution function of the False Positive on the x-axis

rate. Figure 8 represents the distribution of studied works on the usage of performance measure metrics.

Fig. 8 Distribution on performance measure metrics



5.6 Limitations of Existing Research

The research gap in the existing works lies in the lack of universally acceptable techniques across different datasets and classifiers, though past research used several feature selection techniques. Therefore, an approach is needed to find the right balance of the features using a suitable feature selection technique to enhance the model's performance across different datasets and classifiers. In addition, high complexity in ensemble-based defect prediction models remains an unaddressed challenge that is crucial in bringing down the maintenance cost.

6 Conclusion

This literature survey aimed to comprehensively study different machine learning techniques used in software defect prediction. The study found that though defect prediction has come a long way, it still lacks a suitable approach in selecting appropriate features while discarding the irrelevant ones as there is no universally accepted feature selection technique available. This research work discussed different feature selection/reduction techniques accustomed to enhancing the accomplishment of the fault forecast system. The study has given a good emphasis on ensemble learning methods and observed that forecast model based on ensemble learning approaches give enhanced performance than individual classifier-based models. This work has also discussed the widely used software and performance measurement metrics in defect prediction. This concise work would guide future researchers in this emerging research area. In future, we aim to introduce a hybrid feature selection technique using the filter and wrapper approaches to an ensemble learning-based defect prediction model to enhance its predictive performance.

References

1. Jena AK, Das H, Mohapatra DP (eds) (2020) Automated software testing: foundations, applications and challenges. Springer Nature
2. Tassef G (2002) The economic impacts of inadequate infrastructure for software testing. National Institute of Standards and Technology. RTI Project, 7007(11):1–309
3. Mäntylä MV, Lassenius C (2008) What types of defects are discovered in code reviews? IEEE Trans Softw Eng 35(3):430–448
4. Saifan AA, Abu-wardih L (2020) Software defect prediction based on feature subset selection and ensemble classification. ECTI Trans Comput Inform Technol (ECTI-CIT) 14(2):213–228. <https://doi.org/10.37936/ecti-cit.2020142.224489>
5. Mangla M, Sharma N, Mohanty SN (2021) A sequential ensemble model for software fault prediction. Innov Syst Softw Eng 1–8
6. Zhou T, Sun X, Xia X, Li B, Chen X (2019) Improving defect prediction with deep forest. Inf Softw Technol 114:204–216

7. Sharmin S, Arefin MR, Abdullah-Al Wadud M, Nower N, Shoyaib M (2015) SAL: an effective method for software defect prediction. In: 2015 18th International conference on computer and information technology (ICCIIT). IEEE, Dec 2015, pp 184–189
8. McCabe TJ (1976) A complexity measure. *IEEE Trans Softw Eng* 4:308–320
9. Halstead MH (1977) Elements of software science (operating and programming systems series). Elsevier Science Inc.
10. Mall R (2018). Fundamentals of software engineering. PHI Learning Pvt. Ltd.
11. Zhang F, Zheng Q, Zou Y, Hassan AE (2016) Cross-project defect prediction using a connectivity-based unsupervised classifier. In: 2016 IEEE/ACM 38th international conference on software engineering (ICSE). IEEE, May 2016, pp 309–320
12. Tantithamthavorn C, Hassan AE (2018) An experience report on defect modelling in practice: Pitfalls and challenges. In: Proceedings of the 40th international conference on software engineering: software engineering in practice, May 2018, pp 286–295
13. Laradji IH, Alshayeb M, Ghouti L (2015) Software defect prediction using ensemble learning on selected features. *Inf Softw Technol* 58:388–402
14. Afzal W, Torkar R (2016) Towards benchmarking feature subset selection methods for software fault prediction. In: Computational intelligence and quantitative software engineering. Springer, Cham, pp 33–58
15. Ghotra B, McIntosh S, Hassan AE (2017) A large-scale study of the impact of feature selection techniques on defect classification models. In: 2017 IEEE/ACM 14th international conference on mining software repositories (MSR). IEEE, May 2017, pp 146–157
16. Dash M, Liu H (2003) Consistency-based search in feature selection. *Artif Intell* 151(1–2):155–176
17. Hall MA (1999) Correlation-based feature selection for machine learning
18. Sabharwal S, Nagpal S, Malhotra N, Singh P, Seth K (2018) Analysis of feature ranking techniques for defect prediction in software systems. In: Quality, IT and business operations. Springer, Singapore, pp 45–56
19. Huda S, Alyahya S, Ali MM, Ahmad S, Abawajy J, Al-Dossari H, Yearwood J (2017) A framework for software defect prediction and metric selection. *IEEE Access* 6:2844–2858
20. Balogun AO, Basri S, Abdulkadir SJ, Hashim AS (2019) Performance analysis of feature selection methods in software defect prediction: a search method approach. *Appl Sci* 9(13):2764
21. Kondo M, Bezemer CP, Kamei Y, Hassan AE, Mizuno O (2019) The impact of feature reduction techniques on defect prediction models. *Empir Softw Eng* 24(4):1925–1963
22. Balogun AO, Basri S, Capretz LF, Mahamad S, Imam AA, Almomani MA, Adeyemo VE, Alazzawi AK, Bajeh AO, Kumar G (2021) Software defect prediction using wrapper feature selection based on dynamic re-ranking strategy. *Symmetry* 13(11):2166
23. Kumar A, Kumar Y, Kukkar A (2020) A feature selection model for prediction of software defects. *Int J Embedded Syst* 13(1):28–39
24. Khan MZ (2020) Hybrid ensemble learning technique for software defect prediction. *Int J Modern Educ Comput Sci* 12(1)
25. Alsawalqah H, Hijazi N, Eshstay M, Faris H, Radaideh AA, Aljarah I, Alshamaileh Y (2020) Software defect prediction using heterogeneous ensemble classification based on segmented patterns. *Appl Sci* 10(5):1745
26. Malhotra R, Jain J (2020) Handling imbalanced data using ensemble learning in software defect prediction. In: 2020 10th International conference on cloud computing, data science & engineering (confluence). IEEE, Jan 2020, pp 300–304
27. Mehta S, Patnaik KS (2021) Improved prediction of software defects using ensemble machine learning techniques. *Neural Comput Appl* 1–12

Stock Price Prediction Using Data Analysis and Visualization



K. Yashwanth Raj, B. S. Devpriyadharsan, and B. Sowmiya

Abstract A large amount of investment is done in the stock market which plays a bridge role in the financial system of different countries. With the evolution of technology and more advanced and accurate prediction methods, stock market analysis has gained the attention of businessmen and traders to invest at a low-risk rate. Machine learning techniques are used to predict the end results from huge data sets. In this paper Long Short-Term memory model has been implemented and high accuracy results have been obtained. Time series prediction technique has been implemented using LSTM model. On the premise of effects obtained, LSTM fashions are proposed which give much full-size mistake reduction. Results received a display that by utilizing an LSTM model, destiny inventory marketplace conduct may be predicted accurately.

Keywords Stock market analysis · Prediction · Long short-term memory · Visualization

1 Introduction

The stock market can be described as a very volatile entity, with great sensitivity to different types of parameters. The inventory market can be defined as a remarkably volatile entity that has excellent sensitivity to many kinds of parameters.

With the provision of legacy and current inventory market data, researchers have attempted to anticipate the target area of the inventory market through models that can examine the facts of the inventory market. Typically, these ancient facts include

K. Yashwanth Raj · B. S. Devpriyadharsan (✉) · B. Sowmiya
Department of Computing Technologies, SRM Institute of Science and Technology, Chennai,
India
e-mail: dp7450@srmist.edu.in

K. Yashwanth Raj
e-mail: kr8196@srmist.edu.in

B. Sowmiya
e-mail: sowmiyab@srmist.edu.in

opening, closing, maximum, minimum, and volume. With the help of time recording evaluation modes, daily events can be analyzed and the target area of the warehouse market can be expected.

In this project, all predictions are made with the Long-Term Memory Network Model. We check the expected price with the facts in real-time. The version implemented the use of Python programming. It is a type of RNN that has found recognition in the collection of temporal/sequential evaluation. They include an input layer, a hidden layer, and an output layer. The hidden layer of an LSTM community contains memory cells, which in turn contain three gates that are responsible for updating their molecular realm. These three doors are an entrance door, an exit door and an observation door. Our goal is to acquire the best possible precision stage and get the greatest sales from a given inventory.

2 Related Work

Ojo et al. [1] use Long Short-Term Memory (LSTM) model to predict the stock market action. The author uses the time series analysis for this process. The author also states about the previous predictions done using other models that use Autoregressive Integrated Moving Average (ARIMA), Support Vector Machine (SVM), Multilayer perception ANN, Convolutional Neural network (CNN), and Recurrent Neural Network (RNN). By using LSTM author was able to reach a Mean square error value of 0.0022 and a Mean absolute divination value of 0.0495 which was better when compared with other models and produced accurate output. The dataset used for this model was drawn from NASDAQ Composite.

Shah et al. [2] use Artificial Intelligence for the prediction of stock market behavior. The author uses traditional Artificial Neural networks (ANN), adaptive neuro-fuzzy inference (ANFIS) and improved artificial neural networks for this study. At the end of the study, the improved ANN had an *R*-square value of 0.99, an RMSE value of 0.87, and a prediction time of 2.948 s, which was better than other models. Compared to other conventional methods, ANN's accurate prediction gave an *R*-square value of 0.98, an RMSE value of 1.881, and ANFIS gave an *R*-square value of 0.98116, an RMSE value of 1.86.

Pathak et al. [3] combines machine learning and sentimental analysis technique for Indian stock market prediction. The author describes the traditional and modern-day approaches to stock market analysis. The experiment combines machine learning and sentiment analysis into a fuzzy logic module to get accurate and robust output. Sentiment analysis consists of sequential steps that includes data collection, tokenizing, lemmatizing, finding most informative features, classifying features into positive and negative, training and testing module. The results of the experiment show that if the news were positive, the stock faith increased and vice versa if the news was negative. This study was conducted on stocks under the National Stock Exchange (NSE) of India.

Vazirani et al. [4] address the stock market prediction using the single module and hybrid model. The author uses Linear Regression, K-Nearest Neighbor (KNN), Support Vector Machine (SVM), Decision tree, and Random Forest for a single model. And for the hybrid model, a Linear Regression is added as an extra layer with all the single models. In the single model, the result produced by linear regression was accurate with a score mean value of 0.998110 and in the hybrid model, double linear regression had more accuracy when compared with other hybrid models.

Ren et al. [5] uses Support Vector Machine (SVM) and sentiment analysis for the prediction of stock market analysis. The author gives a detailed study on the working of SVM and sentiment analysis. For this experiment SVM and sentimental analysis as-built together as a hybrid model. The author also explains the prediction of the model, and sentiment calculation. Two sets of experiments are conducted and their results are compared, one with fivefold cross-validation and another with a rolling window. The rolling window performed better with an accuracy of 0.7133 where fivefold cross-validation gave an output of 0.7996.

Pahwa et al. [6] use the supervised learning technique in the machine learning domain to predict the stock market behavior. The uses linear regression for prediction and divided the process into three modules. The first module is data collection and analysis, the second is the training and testing stage finally the result stage. The attributes in the data set are adjacent high, adjacent low, adjacent open and adjacent close. The constructed model's prediction is not much accurate due to poor gradient descent. The author also suggests a few other techniques for accurate prediction which includes newton's method, batch learning, stochastic gradient descent, Lagrange duality and constrained methods. After the inclusion of these techniques, the author was able to achieve an accuracy of 97.67.

Idrees et al. [7] address the stock market prediction using the ARIMA model which is a time series forecasting. The author uses the Box-Jenkins methods for accurate prediction. For long-term forecasting, Qualitative methods are used whereas short-term forecasting is done using quantitative methods. The experimental set is divided into sub-modules namely analyze the time series, identity, estimation, ARIMA model, and forecast. The authors extract the stock data from the National Stock Exchange (NSE) and Bombay Stock Exchange (BSE). The experiment is conducted on Sensex and Nifty. The L-Jung Box test results for nifty were 4.7061, the p -value was 0.9099, and for Sensex, it was 5.3276, the p -value was 0.8682, suggesting the model is an accurate output.

Waqar et al. [8] utilized Principal Component Analysis (PCA) to forecast the stock market behavior. Linear regression machine learning algorithm used for this study. The authors compare the results between a single linear regression model and linear regression combined with PCA to produce a result, which performs better prediction. Three stock exchanges were chosen for this experiment namely, London Stock Exchange, New York Stock Exchange, And Karachi Stock Exchange. The single linear regression model gave an RMSE value of 16.43 for the London stock exchange, 36 for the New York stock exchange, and 0.13 for the Karachi stock exchange whereas the hybrid model gave an RMSE value of 1.4 for the London stock exchange, 1.00 for the New York stock exchange, and 1.01 for the Karachi

stock exchange. The above results indicate that the hybrid model which as PCA worked better and gave accurate output.

Nivetha et al. [9] compares different forecasting models for stock market prediction. The author uses Multiple Linear Regression (MLR), Support Vector Machine (SVM), and Artificial Neural Network (ANN). A detailed distribution about the working of all the above-stated models is given with sentimental analysis. Comparing all the results produced by the models the author concludes that the deep learning model (ANN) produces accurate output. The reason behind ANN's accurate output was the hidden layer neuron learning in every prediction step.

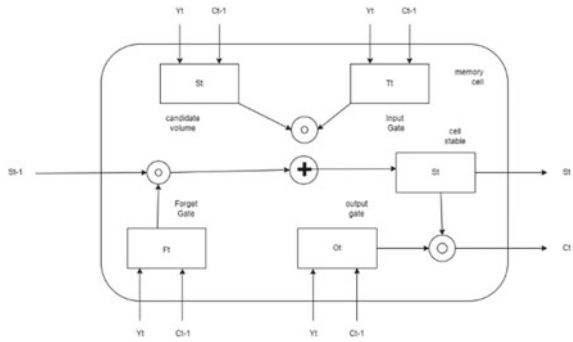
Sharaff et al. [10] compares different stock market prediction techniques. For this experiment, the author chooses the ARIMA model, Holt Winters Model, Artificial Neural Network (ANN), and RNN. The author gives a detailed illustration of the working process for each model. After the training and testing of all models with the same dataset, the ARIMA model had a Mean absolute percentage error (MAPE) of 3.99251, the holt winters had a MAPE of 12.56901, ANN had a MAPE value of 2.83544, and the RNN had a MAPE value of 5.088394. The author concludes the paper by stating the ANN model gave the accurate prediction and robust output.

3 Proposed Work

Stock market price prediction is that the scene of trying to finish the long-run price of organization inventory. By the use of the neural community, we broaden a model. Within the neural community, we use a recurring neural community that reminds each other of any data record. LSTM networks preserve to live contextual records of inputs via way of means of partner a loop that permits records to journey from one step to the following. These loops make recurrent neural networks appear magical. Each x educate has the closing price for y data. This will add extra correct consequences while a degree to current inventory fee prediction algorithms. The community is skilled and evaluated for accuracy with numerous sizes of knowledge, and additionally, the consequences are tabulated.

Long Short-Term Memory (LSTM) method is a kind of RNN has won popularity in time series/sequential analysis. They encompass an enter layer, a hidden layer, and an output layer. In Fig. 1, the hidden layer of an LSTM community contains reminiscence cells which in flip incorporate 3 gates that are chargeable for updates to its molecular state. These three gates are: an enter gate, an output gate, and a neglect about gate. Unlike RNNs, LSTM networks do now no longer be afflicted by the vanishing gradient the hassle that's a crucial component in inventory fee prediction as preceding facts being processed with inside the neural community will have an effect on the future/next facts.

Fig. 1 LSTM memory cell



4 System Architecture

The architecture of LSTM is represented in Fig. 2. The stock data is collected with the tiingo API. It is then pre-processed, i.e., removing unnecessary values. The pre-processed data is the final dataset. This is divided into test and train data. The data is trained with the LSTM model and is available for prediction.

4.1 Parameters Used

List of parameters/Symbols employed is listed in Table 1.

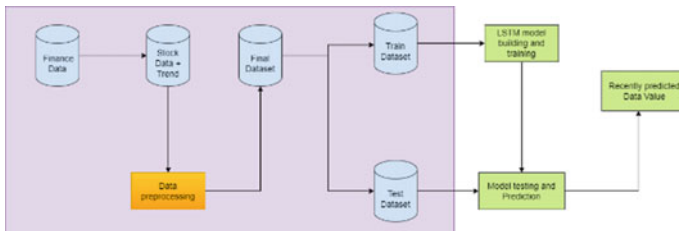


Fig. 2 Architecture of LSTM

Table 1 Parameters used

Parameter	Meaning
High	Highest price of the associated share value for the day
Open	Opening price of a share
Close	Closing price of a share
Adjacent close	Closing price after adjustments/accounting
Volume	Number of shares exchanged
Low	Lowest price of the associated share value for the day

5 Implementation

5.1 Obtaining Dataset

Stock market information is available from major sources: Tiingo API, Yahoo and Google Finance. These websites provide APIs from which you can obtain records of stocks of various companies by simply specifying parameters.

Algorithm 1: Stock prediction using LSTM

Input: Historical stock price data

Output: Prediction of stock prices based on stock price variation

Step 1: Start

Step 2: Stock data is collected

Step 3: Data pre-processing after getting the data

Step 4: Import the dataset

Step 5: Test and Train data are split

Step 6: Feature scaling is done so the values will vary from 0 and 1

Step 7: Compiling it using adam optimizer and the loss as mean_squared_error

Step 8: Making predictions

Step 9: Visualizing the graphs

The range of information is the main step in our planned framework. The dataset to be used within market expectations should be used to separate into completely different perspectives. Our information for the upper half includes share prices from the previous year.

The next step is to pre-process the data. In this step, data preprocessing in data mining is important here. A change in the raw information is required in a basic configuration. The recovered data is inconsistent, fragmented, and contains errors. The preprocessing step cleans the information.

The modeling includes the cross approval, which can be a well-founded, projected model execution with information processing. The aim of the tuning models is to

expressly adapt the training to include information in the calculation itself. The data is rescaled to the real supply costs. The last step is to visualize the data.

6 Results and Discussion

The proposed LSTM model is implemented using Python, which predicts the future price of Tata Motors Limited stock based on its historical data.

The data was obtained from <https://www.nasdaq.com/market-activity/stocks/ttm> [11]. Figures 3 and 4 shows the Tata Motors Limited share’s price prediction. The article describes the implementation of the algorithm for predicting the share price of a stock. Over a period of time, the following graphs (Figs. 3 and 4) of our algorithm was drawn for the adjacent open data set and adjacent close data set along with the test data (orange) and the trained data (green), showing that the algorithm is able to perform with a minimal loss. Predicting the given data of a particular stock and the predictions were made very similar to the stock prices, as seen in Figs. 3 and 4.

The predicted output of adjacent close test data almost matches with the original adjacent close data as seen in Fig. 4.

Figures 5 and 6 shows the predicted value for next 7 days. This model is able to predict the price of the stock with low loss. If the epoch batch size is increased, the model will be more efficient, in this model batch size of 64 and 100 epoch were used.

In Figs. 5 and 6, the prediction for next 7 days were made using adjacent open and adjacent close dataset and denoted by orange color.

Table 2 gives the comparison of the Actual and Predicted Values of Adjacent Open.

Table 3 states the comparison of the Actual and Predicted Values of Adjacent Close.

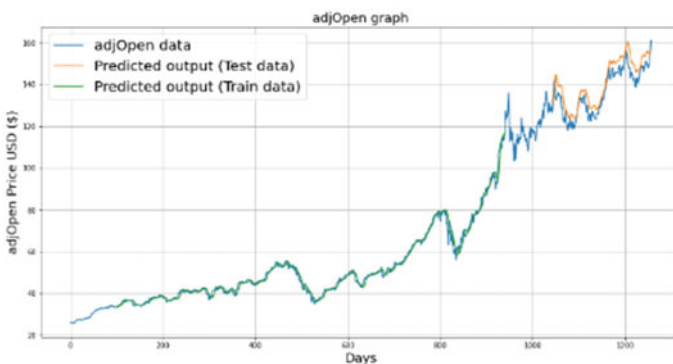


Fig. 3 Training, testing, and actual price value for Tata Motors Limited shares using adjacent open

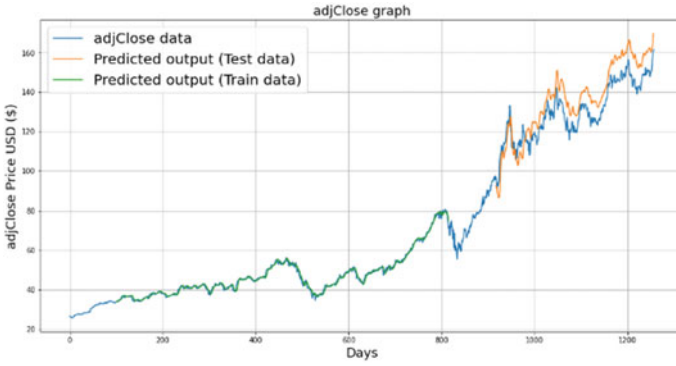


Fig. 4 Training, testing, and actual price value for Tata Motors Limited shares using adjacent close

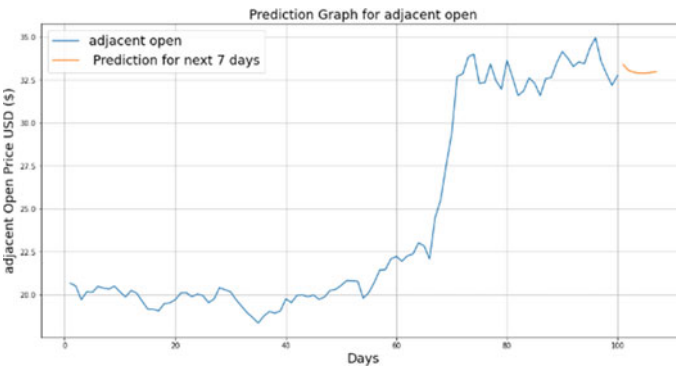


Fig. 5 Prediction graph using adjacent open value

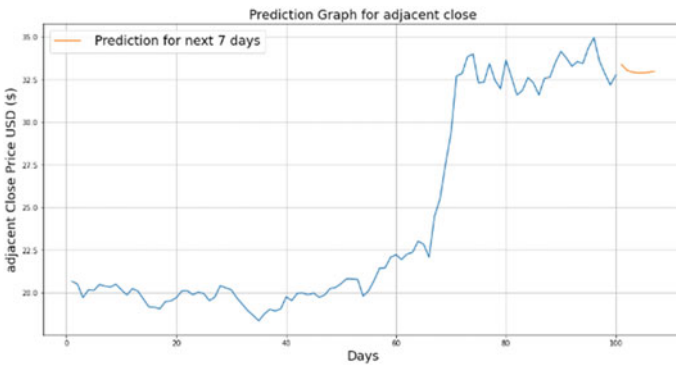


Fig. 6 Prediction graph using adjacent close value

Table 2 Comparative analysis of Adjacent Open Values

Days	Actual values	Predicted values
1	33.70561	34.90051
2	33.34641	33.4283
3	33.06584	33.10531
4	31.95632	33.98106
5	33.91367	33.95622
6	33.94658	33.99349
7	33.07987	33.08046

Table 3 Comparative analysis of Adjacent Close Values

Days	Actual values	Predicted values
1	33.5142	33.70764
2	32.63541	33.28672
3	31.8756	33.95246
4	32.4532	32.66772
5	32.45218	32.76676
6	32.6218	32.7541
7	32.7563	33.89056

Table 4 RMSE values

RMSE value	Adjacent open	Adjacent close
	22.20457342305621	20.3232616215837

The accuracy of the predictive model is estimated using the Root Mean Squared Error (RMSE) metric. Higher accuracy is obtained when the RMSE values are low. Table 4 clearly shows that the Stacked LSTM model created is accurate.

7 Conclusion

The prediction could be more reliable if the model trains a larger number of data sets using larger computing capacities, a larger number of layers, and LSTM modules. More than 75% accuracy has been achieved by using Stacked LSTM method. With greater data, greater styles may be fleshed out via the model, and the weights of the layers may be adjusted. Finding the right resource, incredible speed and volume information, a reactionary market, the bottom line are the reasons not to get higher predictions with modern machine learning techniques. A decent prediction system can facilitate investors with building investments that are additionally correct and more profitable by providing supporting data admire future stock value guidance. Additionally, to historical costs, different connected information may have an effect

on prices such as politics, economic growth, monetary matters and also the atmosphere on social media. Various studies have shown that emotion analysis has a decisive influence on future prices. Therefore, the mix of technical and basic analysis will turn out superb predictions.

In future enhancement, a probable extension of this prediction machine might be reinforced with an information feed evaluation from social media platforms along with Twitter, Facebook where feelings are gauged from the articles. This sentiment evaluation may be related with the LSTM for better weights and in addition enhance accuracy.

References

1. Ojo SO, Owolawi PA, Mphahlele M, Adisa JA (2019) Stock market behaviour prediction using stacked LSTM networks. In: 2019 International multidisciplinary information technology and engineering conference (IMITEC), pp 1–5. <https://doi.org/10.1109/IMITEC45504.2019.9015840>
2. Shah HN (2019) Prediction of stock market using artificial intelligence. In: 2019 IEEE 5th international conference for convergence in technology (I2CT), pp 1–6. <https://doi.org/10.1109/I2CT45611.2019.9033776>
3. Pathak A., Shetty NP (2019) Indian stock market prediction using machine learning and sentiment analysis. In: Behera H, Nayak J, Naik B, Abraham A (eds) Computational intelligence in data mining. Adv Intell Syst Comput 711. Springer, Singapore. https://doi.org/10.1007/978-981-10-8055-5_53
4. Vazirani S, Sharma A, Sharma P (2020) Analysis of various machine learning algorithm and hybrid model for stock market prediction using python. In: 2020 International conference on smart technologies in computing, electrical and electronics (ICSTCEE), pp 203–207. <https://doi.org/10.1109/ICSTCEE49637.2020.9276859>
5. Ren R, Wu DD, Liu T (2019) Forecasting stock market movement direction using sentiment analysis and support vector machine. IEEE Syst J 13(1):760–770. <https://doi.org/10.1109/JSYST.2018.2794462>
6. Pahwa K, Agarwal N (2019) Stock market analysis using supervised machine learning. In: 2019 International conference on machine learning, big data, cloud and parallel computing (COMITCon), pp 197–200. <https://doi.org/10.1109/COMITCon.2019.8862225>
7. Idrees SM, Alam MA, Agarwal P (2019) A prediction approach for stock market volatility based on time series data. IEEE Access 7:17287–17298. <https://doi.org/10.1109/ACCESS.2019.2895252>
8. Waqar M, Dawood H, Guo P, Shahnawaz MB, Ghazanfar MA (2017) Prediction of stock market by principal component analysis. In: 2017 13th International conference on computational intelligence and security (CIS), pp 599–602. <https://doi.org/10.1109/CIS.2017.00139>
9. Nivetha RY, Dhaya C (2017) Developing a prediction model for stock analysis. In: 2017 International conference on technical advancements in computers and communications (ICTACC), pp 1–3. <https://doi.org/10.1109/ICTACC.2017.11>
10. Sharaff A, Choudhary M (2018) Comparative analysis of various stock prediction techniques. In: 2018 2nd International conference on trends in electronics and informatics (ICOEI), pp 735–738. <https://doi.org/10.1109/ICOEI.2018.8553825>
11. <https://www.nasdaq.com/market-activity/stocks/ttm>

A Comparative Study for Determining the Vehicle Routing Optimal Path



R. Aditi, R. Dhinakar, and B. Sowmiya

Abstract The Vehicle Routing Problem requires the determination of the optimum set of routes to be carried out through a fleet of automobiles to assist a given set of customers. It is an important benchmark issue of logistic management and has been widely studied and used in transportation systems, logistics distribution systems, and express delivery systems. It is a subset of the Travelling Salesman Problem and is considered a NP-hard problem. This problem can be solved using meta-heuristic algorithms—Genetic Algorithm and Ant Colony Optimization. In this paper, we will be comparing the above-mentioned optimization techniques for interpreting the vehicle routing problem and arriving at a solution.

Keywords Travelling Salesman Problem (TSP) · Vehicle Routing Problem (VRP) · Swarm Intelligence · Evolutionary algorithms · Ant Colony Optimization (ACO) · Genetic Algorithm (GA)

1 Introduction

The Vehicle Routing Problem (VRP) is among one of the important challenges that logistics businesses are dealing with in the last few years. It is a generalization of the Travelling Salesman Problem (TSP) and it can be observed in supply chain operations, transportation systems, logistics distribution systems, and express delivery systems. The problem of routing vehicles and scheduling of deliveries has been studied by researchers since its first introduction in 1959 when Dantzig and Ramser introduced the Truck Dispatching Problem. The objective of the Vehicle Routing

R. Aditi · R. Dhinakar (✉) · B. Sowmiya
Department of Computing Technologies, SRM Institute of Science and Technology, Chennai,
India
e-mail: dr6543@srmist.edu.in

R. Aditi
e-mail: ar3426@srmist.edu.in

B. Sowmiya
e-mail: sowmiyab@srmist.edu.in

Problem, both in practice and in theory, remains the same and it is the minimization of the total distribution costs, while the services remain at a high level. It is considered the paradigmatic case of the Travelling Salesman Problem and refers to the distribution of goods, from a starting point (Example—central depot) to geographically scattered destination points or customers.

The Vehicle Routing Problem is classified as a NP-hard problem since it is not possible to find its solution in definite polynomial time. In other words, required solution time increases considerably with size. The number of possible solutions to the problem is of the order of $n!$, where n is the number of destination nodes (locations the vehicle must reach). This problem finds its presence in numerous fields which includes social community analysis, array clustering, scheduling, and plenty of problems of the modern age. Since many real-life problems also show this property, the VRP is taken into consideration as a benchmark problem of optimization.

This paper presents a study for determining the optimum vehicle routing path by comparing two different types of optimization techniques—Ant Colony Optimization (ACO) & Genetic Algorithm (GA) from Swarm Intelligence and Evolutionary Algorithms respectively. Benchmark dataset Augerat 1995—Set P will be used to do the comparison since it is widely accepted and has a realistic appearance.

2 Related Work

First, Eggenschwiler et al. [1] compared swarm algorithms and a graph algorithm for solving the traveling salesman problem. It includes four versions of ACO and PSO and four graph algorithms. The author concludes by saying that graph algorithms outperformed both ACO and PSO algorithms. It has to be cited that the author has examined only one parameter setting. The study was then extended by varying parameter settings for both ACO and PSO to test if it improves its accuracy.

Juneja et al. [2] used the optimization ability of Genetic Algorithm to search for an optimum solution for the Travelling Salesman Problem. The author obtained many optimum solutions for the problem by utilizing combinations of selection, crossover and mutation. The author also conveys that the preferred method to solve the TSP is through using heuristic methods and genetic approaches.

Al-Furhud et al. [3] considered Multiple Travelling Salesman Problem through using sequential constructive crossover (SCX) and its types—adaptive, greedy, reverse greedy and comprehensive. The author concluded that in an effort to discover better solutions, constructive local search and immigration techniques can be mixed for the betterment of the simple genetic algorithm.

Li et al. [4] used an improved Ant Colony Optimization Algorithm to solve multi-depot vehicle routing problem. The ACO algorithm used in this study uses an innovative approach in updating the pheromones which results in higher solution quality. The author concludes that meta-heuristics algorithms are desirable for solving complex problems, while producing close-to-optimal solutions for the problem.

Dorigo et al. [5] performed a review on the developments and research trends in ACO Algorithm. The author talks about Construction Algorithms, Local Search Algorithms and compares it with ACO Metaheuristic. The author adds that ACO Algorithms are particularly useful when problems for which it is not clear how to apply local search, or for highly dynamic problem where only local information is available.

Stodola et al. [6] used Hybrid Ant Colony Optimization to solve the vehicle routing problem. The cited algorithm combined probabilistic and exact techniques. The experiments confirmed that the proposed algorithm overcomes different techniques because it has the smallest average error for the complete set of benchmark instances.

Takan et al. [7] proposed a brand new hybrid algorithm that makes use of the precise augmented Lagrangian through considering the zero duality gap condition for the vehicle routing problem. It combines an altered sub gradient algorithm based on attainable values and a Genetic Algorithm. The results produce a computational advantage while using the proposed hybrid algorithm.

Er et al. [8] used Ant Colony Optimization to remove the tour loop for the Open Vehicle Routing Problem. The proposed technique is not only used to plot the open and close routes of vehicles but also to lessen the overall length and operation of the vehicle, which in addition lessens the transportation and operational cost of the vehicle. The study is then extended to implement a navigation system based on ACO Algorithm, to achieve the route together with the timing so that it could be applied in real-life scenarios.

Zhang et al. [9] produced a method which puts forward the two-stage service model of vehicle routing problem. Genetic Algorithm is proposed to find an optimum solution for the problem which is verified by the example data. The author concludes by implementing a solution algorithm for vehicle routing problem and proves its optimal performance by experimental calculation.

Halim et al. [10] performed a comparative analysis of computation, accuracy and convergence of six algorithms for the travelling salesman problem (TSP). Nearest Neighbour, Simulated Annealing, Tabu Search, Ant Colony Optimization, Tree Physiology Optimization and Genetic Algorithm. It is considered an NP-hard problem with a larger number of solutions. The author expressed that GA is able to find solutions better for bigger problems and faster. ACO on the other hand takes much longer to reach an optimum solution.

3 Proposed Work

Vehicle Routing Problem determines a set of vehicle routes that includes a single depot, a fleet of equal vehicles stationed at the depot, and a fixed set of clients who require the delivery of products from the depot. The vehicle routing problem is officially described as a weighted orientated graph $G = (V, B)$ wherein the nodes are represented by,

$$V = \{v_0, v_1, \dots, v_n\}$$

and the arcs are represented by,

$$B = \{(vx, vy) : x = y\}$$

A central depot is a unique node in which each vehicle begins its route. The central depot is denoted by means of v_0 and the rest of the nodes are the customers. The following constraints are to be kept in mind:

- Every customer must be visited only once by a given single vehicle.
- Both the algorithms must start at the same beginning node, v_0 .

The optimum path for the vehicle routing problem must meet the above mentioned constraints for it to be successful.

4 Implementation

To ensure fair comparison between the two algorithms, the following simulation parameters are needed to be set for both the algorithms. The maximum number of iterations for both the algorithms is set to 500 iterations while the number of agents used in the algorithms is set to 44 ants/chromosomes (Table 1).

The architecture diagram of the comparative study can be found in Fig 1. The benchmark dataset is obtained, and data pre-processing is done on it to obtain the final dataset. The final dataset is then implemented with ACO & GA algorithm respectively and the comparative study is performed.

Table 1 Simulation parameter specification of various algorithms of VRP

Parameter	ACO	GA
Maximum iterations	500	500
Number of agents	44 Ants	44 Chromosomes
Initial pheromone on all edges	0.5	NA
Pheromone exponential weight (α)	1	NA
Heuristic exponential weight (β)	5	NA
Evaporation rate (ρ)	0.5	NA
Pheromone quantity constant	3	NA
Selection Strategy	NA	Elitism selection
Mutation Operator	NA	Swap
Mutation rate	NA	0.5

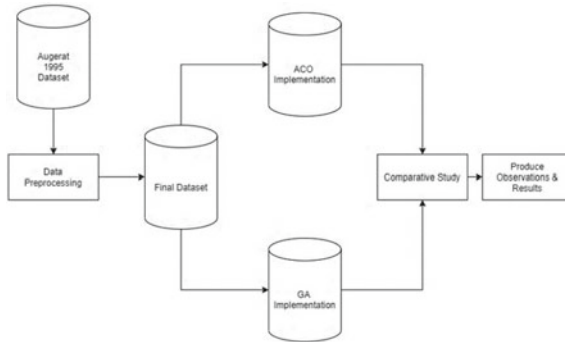


Fig. 1 Architecture diagram

4.1 Ant Colony Optimization

Ant colony optimization (ACO) is a metaheuristic method that is stimulated by the reputedly smart conduct of ant colonies, and it fashions artificial ants to discover answers to optimization problems such as the VRP. Ant colonies have the capacity to resolve complicated problems like locating and amassing food and this is carried out via the use of a chemical substance known as a pheromone.

As an individual ant travels between its nest and a food source, it deposits a trail of pheromone as it moves over the path it travels in. As a trail is traveled more frequently the pheromone trail becomes stronger, and therefore more appealing to following ants. Ants in nature usually follow the trails that have the highest concentration of pheromone, where more of their fellow ants are traveling. Those trails that are traversed (to the food source and back to the nest) most quickly, soon become the trails with the highest level of pheromones, thereby encouraging more ants to choose them for travelling while also further strengthening the trail.

However, ants will occasionally branch out and ignore the current best-known-shortest path and search for food on other paths. If they find a shorter route to a food source more quickly, then pheromone accumulation on the new route would over time cause the present solution to get replaced with the new shorter path. As new short trails are being discovered, older trails' pheromones evaporate, thereby causing the trails to be less desirable to the ants and causing older paths to be abandoned over time. This process of route selection by ants is described as a pseudo-random proportional process and it is considered to be a primary element of ACO.

Pseudocode: Ant Colony Optimization (ACO)

```
1. Compute trail
2. Initialize pheromone level
3. while (maximum no. of iterations is not reached)
4. for each ant
5.   while (not all cities are visited)
      select a not yet visited city
      update tour length and list of not yet visited cities
   end while
6.   update local trail
7. end for
8. perform pheromone update
9. update global trail
10. end while
```

4.2 Genetic Algorithm (GA)

The second approach which will be employed to work out the Vehicle Routing Problem is the Genetic Algorithm. It is a metaheuristic inspired by Darwin's theory of natural selection.

In the recent few years, Genetic Algorithm has found its application in path selection algorithms. It belongs to the family of evolutionary algorithms and mimics natural selection, where only the fittest individuals survive through the method of mutation, selection, and crossover. It includes a populace that represents the feasible answers for the given problem space. With the traits which take place with inside the populace primarily depend on the fitness characteristic evaluation, chromosomes which are considered "fit" are given the chance to breed. This method is repeated for a preferred range of iterations to acquire the optimum solution.

In Genetic Algorithm, different populations are working parallelly to find an optimum solution. This helps in exploring the complete problem space in every directions. GA is favoured for problems wherein the problem area is big and the time taken to search is extensive. It additionally does not require any preceding expertise to achieve the solution.

Pseudocode: Genetic Algorithm (GA)

1. Start
 2. Initialize a random population P
 3. For the given problem, define a fitness function $f(x)$
 4. Calculate the fitness of the population by executing it through the function $f(x)$
 5. *while!* Optimum value not reached or function not converging
do:
 - > Select the fittest from the population as parents for the next generation
 - > Perform crossover operation to create new population for next generation
 - > Mutation operation applied to the existing population
 - > Fitness calculation for the population
 6. *end*
 7. If optimum achieved, display the final result
 8. Stop
-

5 Results Discussion

This section explores the output of the simulations using Python. The output was analysed and the total accumulated length was compared for both the algorithms. For the nature-inspired algorithms, Genetic Algorithms was tested with the population size of 44 chromosomes and Ant Colony Optimization with 44 ants. Table 2 provides information about the length obtained for each instance of the benchmark dataset using both the algorithms.

Genetic Algorithm outperformed ACO Algorithm for the first few instances of the dataset and the length differences between them is negligible. However, ACO Algorithm performs better than Genetic Algorithm as the number of cities in the instances of the dataset keeps increasing and this is shown in Fig 4. There are significant differences in the length analyzed between the two algorithms (Fig. 2, 3, 4).

5.1 Fixed Number of Cities Versus Varying Number of Vehicles

Fixing the number of cities constant and varying the number of vehicles, the ACO Algorithm does not seem to be affected. It still outperforms Genetic Algorithm and produces the optimum length. This is represented in Figs. 5 and 6.

Table 2 Length obtained for each instances of the dataset for both the algorithms

Instance	N	K	ACO length	GA length
P-n16-k8	15	8	461.31	406.63
P-n19-k2	18	2	221.38	203.44
P-n20-k2	19	2	220.18	222.34
P-n21-k2	20	2	220.51	216.87
P-n22-k2	21	2	222.56	217.44
P-n23-k8	22	8	552.55	490.93
P-n40-k5	39	5	520.74	635.9
P-n45-k5	44	5	591.29	715.86
P-n50-k7	49	7	648.72	810.14
P-n50-k8	49	8	709.91	931.65
P-n50-k10	49	10	791.604	1068.73
P-n51-k10	50	10	839.91	1142.52
P-n55-k7	54	7	664.9	839.09
P-n55-k10	54	10	768.06	1102.99
P-n55-k15	54	15	1028.55	1402.21
P-n60-k10	59	10	856.38	1102.05
P-n60-k15	59	15	1076.42	1459.52
P-n65-k10	64	10	953.81	1215.53
P-n70-k10	69	10	1006.24	1259.32
P-n76-k4	75	4	742.15	770.49
P-n76-k5	75	5	795.11	832.91
P-n101-k4	100	4	908.2	1007

N = Number of cities, K = Number of vehicles

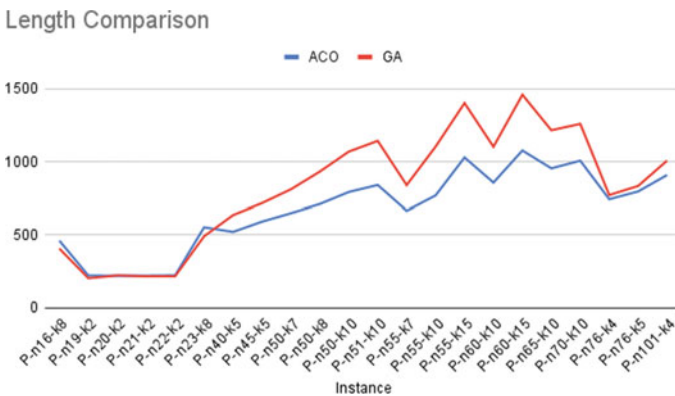


Fig. 2 Length comparison flowchart

Fig. 3 Number of cities = 49

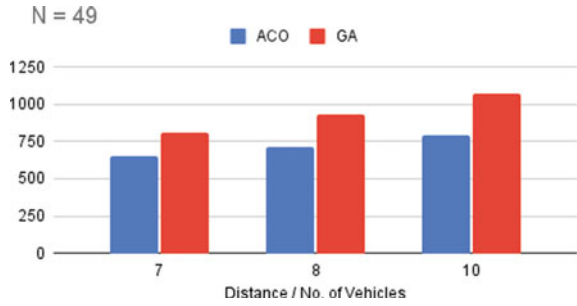


Fig. 4 Number of cities = 54

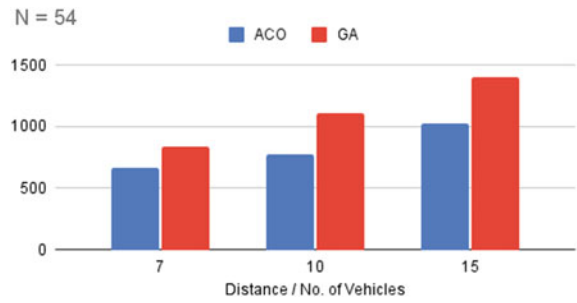


Fig. 5 Number of vehicles = 2

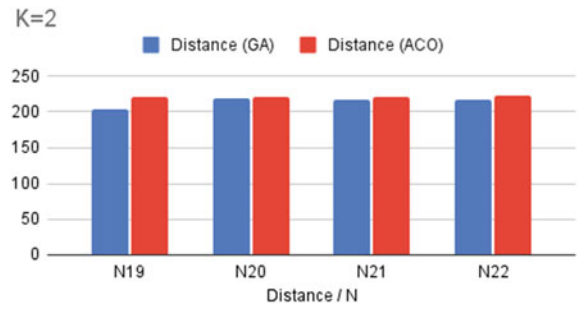
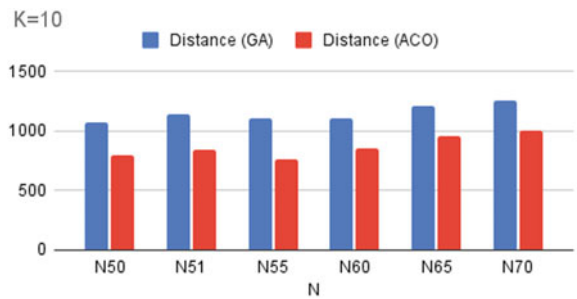


Fig. 6 Number of vehicles = 2



5.2 Fixed Number of Vehicles Versus Varying Number of Cities

There are negligible differences between the length of ACO Algorithm and Genetic Algorithm when the number of vehicles being used for the instance is small i.e They produce similar optimum lengths. However, when the number of vehicles being used is more, ACO Algorithms provides more optimum length.

6 Conclusion

In conclusion, our comparative study shows that ACO Algorithm outperformed Genetic Algorithm for solving the vehicle routing problem. Although there was negligible difference in the beginning, Genetic Algorithm performed rather poorly as the number of cities kept increasing with each instance of the dataset.

The ACO algorithm also provides optimum solutions while varying constraints such as the number of cities and vehicles. In an extension of this project, it will be interesting to check alternative optimization techniques used to solve the vehicle routing problem and examine it with the ACO Algorithm.

References

1. Eggenschwiler S, Spahic-Bogdanovic M, Hanne T, Dornberger R (2020) Comparison of swarm and graph algorithms for solving travelling salesman problems. In: 2020 7th International conference on soft computing & machine intelligence (ISCMI), pp 1–7. <https://doi.org/10.1109/ISCMI51676.2020.9311558>
2. Juneja SS, Saraswat P, Singh K, Sharma J, Majumdar R, Chowdhary S (2019) Travelling salesman problem optimization using genetic algorithm. In: 2019 Amity international conference on artificial intelligence (AICAI), pp 264–268. <https://doi.org/10.1109/AICAI.2019.8701246>
3. Al-Furhud MA, Ahmed ZH (2020) Genetic algorithms for the multiple travelling salesman problem. *Int J Adv Comput Sci Appl* 11:553–560. <https://doi.org/10.14569/IJACSA.2020.0110768>
4. Li Y, Soleimani H, Zohal M (2019) An improved ant colony optimization algorithm for the multi-depot green vehicle routing problem with multiple objectives. *J Cleaner Prod* 227. <https://doi.org/10.1016/j.jclepro.2019.03.185>
5. Dorigo M, Stützle T (2019) Ant colony optimization: overview and recent advances. In: Gendreau M, Potvin JY (eds) *Handbook of Metaheuristics*. International Series in Operations Research & Management Science, vol 272. Springer, Cham. https://doi.org/10.1007/978-3-319-91086-4_10
6. Stodola P (2020) Hybrid ant colony optimization algorithm applied to the multi-depot vehicle routing problem. *Nat Comput* 19:463–475. <https://doi.org/10.1007/s11047-020-09783-6>
7. Takan MA, Kasimbeyli R (2019) Hybrid algorithm for solving the heterogeneous fixed fleet vehicle routing problem. In: 2019 3rd International Symposium on multidisciplinary studies and innovative technologies (ISMSIT), pp 1–4. <https://doi.org/10.1109/ISMSIT.2019.8932935>

8. Er GS, Dhir V (2014) Open vehicle routing problem by ant colony optimization. *Int J Adv Comput Sci Appl (IJACSA)*. <https://doi.org/10.14569/IJACSA.2014.050308>
9. Zhang R, Song Z, Zhu W (2019) Research on vehicle routing problem based on improved genetic algorithm. *Chinese Autom Congress (CAC) 2019*:1452–1455. <https://doi.org/10.1109/CAC48633.2019.8996964>
10. Halim AH, Ismail I (2019) Combinatorial optimization: comparison of heuristic algorithms in travelling salesman problem. *Arch Computat Methods Eng* 26:367–380

Tool-Based Prediction of SQL Injection Vulnerabilities and Attacks on Web Applications



B. Padmaja , G. Chandra Sekhar , Ch. V. Rama Padmaja ,
P. Chandana , and E. Krishna Rao Patro 

Abstract In today's present time, SQL injection has become a significant security threat over the web for diverse dynamic web applications and websites. SQL Injection may be a sort of associate injection attack that produces it doable to execute malicious SQL statements into an online application consisting of SQL information. Attackers use these SQL Injection Queries or Statements specified if an Internet site or an application hosted on web contain SQL vulnerabilities to bypass application security measures. The Attacker will even go around authentication associated with authorization of an online page or Internet application and might bypass these methods and retrieve the content of the whole SQL information of an online application. The purpose of the proposed system is to predict the occurrence of a SQL injection attack on a particular server where an application is deployed from a given supply at a particular point in time. This predictive experiment is managed using the JMeter tool. From network logs, you can now pre-measure, exclude choices, analyze, and feed machine learning models to predict SQLIA.

Keywords SQL injection · Web application · Classification · Prediction · JMeter

1 Introduction

As the world is developing with the exponential development of Internet technology and therefore the development of recent Internet Products like Web 3.0, SNS, Apache Axis, the net-based web applications are being widely employed by all the people. At the same time evolving and rapid use of Internet-based Web applications and Web business attracted many hackers toward it which resulted in various Web security issues. Among all the online Security issues, one of the most notable and

B. Padmaja (✉) · Ch. V. Rama Padmaja · P. Chandana
Department of Computer Science and Engineering (AI & ML), Institute of Aeronautical Engineering, Hyderabad, India
e-mail: b.padmaja@gmail.com

G. C. Sekhar · E. Krishna Rao Patro
Department of Computer Science and Engineering, Institute of Aeronautical Engineering, Hyderabad, India

dangerous ones is SQL Injection. SQL Injection ranks 6th in today's top 10 Security issues that are more dangerous, universal in Web application programs consistent with OPEN WEB APPLICATION SECURITY PROJECT (OWASP). Basically, the hackers tamper the Webpage contents and even steal the important internal information which is stored in the database by using SQL injection flaws. Even hackers install some malicious code into the database such that they can take over the entire system administration. For instance, in August 2009—Eleven Breach—a bunch of programmers (hackers) utilized SQL Injection to Penetrate corporate Systems at some organizations, principally the 7-Eleven corporate store, taking 130 million Mastercard numbers and their information. These SQL injection attacks have continued arising and therefore the SQL injection is presently till proceeding. In early 2021, 70 gigabytes of information were taken from the acute right website GAB by an SQL Injection attack. Therefore, it is very significant and important to review the prediction and prevention technology targeting SQL Injection attack to enhance the online security and to stop that attack before it is happening on a web Server. In this paper, the goal is to predict SQLIA in a web application. We used the open source software Apache JMeter to generate the log data. The log data is then preprocessed to perform a feature extraction and compare it to the available SQLIA search commands. This logistic regression model is used to predict the SQLIA in web Applications.

2 Procedure of SQL Injection

SQL Injection is especially done on Dynamic sites not on Static web content because dynamic websites load the data from an information base instead of stored on a system like Static website. SQL Injections are old, dangerous, powerful and versatile to attack on an online site database. The Procedure of SQL Injection is principally done in six steps mentioned in Fig. 1.

2.1 Seeking Injection Points

Injection point is the websites which contain injection flaws. There is no Injection flaw in Static websites of URL which are ending with HTML, etc. The Injection may only occur in Dynamic websites ending with '?'. This is often because the page information is loaded with different input queries from the users and so the net page is loaded by obtaining information from the database. It should be users' information or another site information. The SQL Injection is determined by the data given to the browser by inputting some special characters like $1 = 1$ or) within the address bar of the browser or the page table like login page. The SQL injections are performed through the Internet or mainly we will say Network. These attacks are versatile so much so that they will be performed from anywhere on Earth. Since the HTTP or HTTPS has two request methods GET and POST methods, SQL Injection

Fig. 1 Procedure of SQL injection



also has two methods GET INJECTION and POST INJECTION. The requests are very similar to Normal requests specified firewalls allow them as Normal HTTP or HTTPS requests hence no alarm is raised.

2.2 Obtaining Information from Database

Obtaining database Information is the main target in performing SQL Injection. The database type is judged by performing SQL false statements with special structures. As an example, there's URL LINK: <http://www.amazon.com/show.asp?id=6>. If we are going to add single quotation mark (') at the end of web link, i.e., is <https://www.aamzon.com/show.asp?id=6'>, the type database will be judged to the result we get if the Microsoft server returns it an error, then the access may be judged as backend database login. When a user enters their valid username and password will pass authentication and the user will login.

SQL QUERY: `SELECT * FROM USER_TABLE WHERE Username='user1' and Password='pass1'`.

However, some users enter some malicious code in the Username and Password fields of the website where Username—usr1, Password—'or '1'='1'.

The SQL QUERY now it will be constructed as.

SQL QUERY—`SELECT * FROM USER_TABLE WHERE Username='user1' and Password=' 'or '1'='1'`.

Since $1 = 1$ will always be true, this user will always login to the website. Now the user gets unauthorized access to someone else's Account details and this information is resulted within the serious consequences for the person whose account information had been stolen. This is a very Simple example SQL Injection attack for understanding, and most of the websites can easily prevent this type of attack. This is often a case of theft of data privacy. This will let an unauthorized user get access to a database system and may end up in various unauthorized actions on the information base like deleting, modifying, retrieving important information and many more dangerous things and an SQL Injection makes all this Possible.

Since $1 = 1$ will always be true, this user will always login to the website. Now the user gets unauthorized access to someone else's Account details and this information can result in serious consequences for the person whose account information had been stolen. This is a very Simple example SQL Injection attack for understanding, and most of the websites can easily prevent this kind of attack. This is a case of theft and violation of data privacy. This will let an unauthorized user get access to a database system can result in various unauthorized actions on the database like deleting, modifying, retrieving important information and many more dangerous things and an SQL Injection makes all of this Possible.

3 Related Work

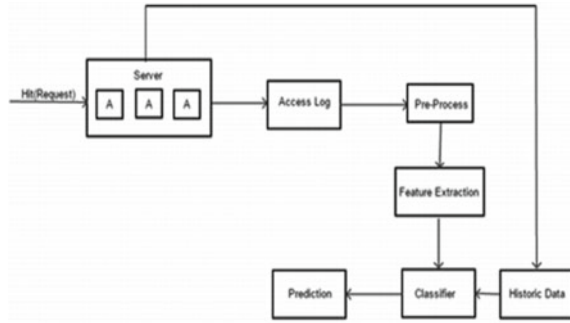
SQL injection attacks are difficult to get detected using the firewalls. These detections of those attacks are usually possible through IIS log, checking databases and user inputs. First, the IIS log file contains the pages accessed by users, their IP addresses and files they have accessed. With careful observation of log files, its size and content, one can detect the SQL injection attacks. Second in databases, if SQL injection attack is there, then it will generate a variety of temporary tables. A user can check those tables, its structure and content to determine whether an attack went on or not. Third, the user's input data are often checked by testing its format, type, length and range [1]. Kamtuo et al. [2] focuses on the relationship between each programming language and the normal delivery of web applications, as well as frequently reported vulnerabilities, and almost all SQLIA and XSS vulnerabilities are prevented by a simple mechanism [2]. Singh et al. [3] Described different types of SQL injection attacks: Fast Flux Sql injection, Compounded SQL injection, and Deep Blind SQL injection. The author also described various techniques for analyzing, detecting, and preventing these attacks [3]. Saqlain Hussain Shah (2018) [4], the author has summarized all known vulnerabilities and attacks. They outlined current technologies and approaches to server-side security for web applications. Devietal [5] conducted a survey on the tautology of SQL injection attacks, a technique widely used by banks on the Internet. In [6], the author predicted a method for validating input values in Java-based Internet applications that validate code instrumentation and run-time input validation for static computer storage devices. This approach looks for the target path or object constructor in the compiled Java category file and statically

inserts the memory unit code module. Xiaowei et al. [6, 7] worked to protect online applications from various server-side attacks. The author described three commonly used approaches to check for vulnerabilities along with attacks, such as input validation, session management, and application logic. Current methods have been dealt with in two mechanisms: attacks and vulnerabilities on the one hand, and design goals and the Internet application phase on the other. Komiya et al. [8] discussed various varieties of vulnerabilities in input functions of web applications. The author used a variety of machine learning techniques like SVM, Naïve Bayes, KNN, etc. to detect vulnerabilities in web applications. Ross et al. [9] used two datasets one from the online application host and another from Datiphy appliance node associated with MySQL server to spot attacks. The author used rule-based learning algorithms, decision trees and neural network algorithms to spot the attacks with reasonable accuracy. Jemal et al. [10] discussed various SQL injection attacks, detection and its prevention. The author experimented on different attack sources and its types using machine learning and ontology. Das et al. [11] proposed multiple approaches for classifying a dynamic SQL query as safe or malicious. One is predicated on distance and therefore the other one is web profile-based. The author observed the supervised classification algorithms to be more efficient for identifying attacks and providing security. Som et al. [12] identified SQL injection attack (SQLIA) to be the most hazardous among all for web applications and therefore the author experimented on stored procedures to stop SQLIA. The author's work is to produce protection and prevent attacks on web pages from SQLIA. Medeiros et al. [7, 13] proposed a mechanism called SEPTIC for preventing attacks on a database. This method also assists in identifying vulnerabilities in many applications using MySQL. The author proved his technique to be more efficient than the prevailing solutions up to now. Lwin Khin et al. (2012) [14, 15] proposed a collection of static code attributes for predicting vulnerabilities in web applications like SQL injection and cross site scripting. The proposed vulnerability predictor attributes were more efficient and proven to detect quite 80% of the vulnerabilities compared to other techniques of that time. Padmaja et al. [16] proposed anomaly-based intrusion detection techniques using supervised machine learning models to detect malicious users in real time network traffic. The authors proved Artificial Neural Networks (ANN) to be more superior than Support Vector Machine (SVM) on NSL-KDD dataset [17].

4 Proposed Method

The SQL injection prediction of a particular system that the system is considered as a server and application system, and forecasting of SQL injection and predicting where SQL injection can be performed can be collected. From the IP address, clock, time and requests from requests requested by the user, requests from requests, requests and dates from the same IP address. Because the server is increasingly done in request, log data will increase with the information about confirmation of SQL injection prediction. The proposed system shown in Fig. 2 consists of system A, which can be

Fig. 2 Proposed method for predicting SQL injection attacks



provided from different servers or servers to another source to another source, and system A that can be provided at different times and different times It consists of To overcome this problem, the proposed system is all logistics from both servers, and data for predicting SQL injections is composed of all logistics from both servers.

5 Implementation

SQL Injection is a dangerous and old methodology which targets databases of web applications which also comprises the server as a normal request. The assault exploits weak input validation in code and site administration. The attacker can profit from the Database of web application when an SQL query is passed consisting of some characters which might comprise fire wall and http or https as Normal Query and may gain access to the administration user.

Http or https as Normal Query and may gain access to the administration user. As an example, observe the below PHP-1 code. If the user enters ‘OR 1 OR username=’ rather than \$_GET [‘username’] now it is an SQL Injection which might get access to the database. Hence the user can enter this query and can manipulate the database.

PHP-1

```

$result=MySQL query (“SELECT * FROM users WHERE username=“ ‘. $_GET [‘username’].’”);
    
```

If the user manipulates the get username the PHP-2 code is that the resultant which might be employed in login or search bar.

PHP-2

```

SELECT * FROM users WHERE username=“ OR 1 OR username=”.
    
```

Any requests sent to a web server are found in log data. This log data can contain may fields like IP address, date, Time, Request parameter etc. At first, we need to create a raw data which is then went to feed to the logistic regression model. To make Log Data, we used a PHP login form. Here in order to create a huge data set we

6 Results and Discussion

This work is used to predict SQL Injection which occurs on a web server or a web application from a given place at any particular time through the network. Here we use logistic regression for prediction, Logistic regression is basically a supervised classification algorithm. It is utilized for predicting the dependent variable by utilizing a given set of independent variables. Logistic regression can be worked with either yes or no 0 or 1, true or false etc. But instead of giving exact values it gives the probability value which lies between 0 and 1. Logistic regression is used to solve classification problems. Here we used the norm for normal queries and the anomaly for abnormal queries. You can use norm 0 and anomaly 1. Click Train Model to train your model using the uploaded dataset. Once the training model is generated, click Generate Predictive Model. The predictive output is now classified as a normal or abnormal query in all queries. The confusion matrix is a table that is used regularly to show the performance of the classification model. From the confusion matrix, the ROC score and the predicted percentage are calculated. This model is designed to anticipate SQL injection queries such as union, select everything, select where or as from like, and so on. Our models are trained on large datasets, 70% of which are used for training and 30% of which are used for testing. Confusion matrices and model predictions are based on considering only SQL queries that are classified as normal or abnormal. The model is deployed to a local server, where there is a SQL query that looks up the web address and predicts it as SQLIA or NOT. For logistic regression models, the dataset accuracy is 90%.

7 Conclusion and Future Scope

The main purpose of this research is to focus on a technique called SQL injection that allows hackers to execute malicious SQL queries on a database server. This is the most common technique used by hackers to retrieve information and data about what is stored in the database of online web-based applications. Here, the model proposed for predicting SQL injection attacks in web applications using JMeter can detect up to 90% of vulnerabilities. For future work, you can run the module to trigger an alert when a SQL injection attack occurs. Similarly, you can backtrack from the source IP to identify the actual area of the attack. You can also distinguish the actual client at the same time. You can run deep learning techniques and tree regressors for better results.

References

1. Qian L et al (2015) Research of SQL injection attack and prevention technology. In: 2015 IEEE International conference on estimation, detection and information fusion (ICEDIF 2015). <https://doi.org/10.1109/ICEDIF.2015.7280212>
2. Kamtuo K, Soomlek C (2016) Machine learning for SQL injection prevention on server-side scripting. In: 2016 IEEE international computer science and engineering conference (ICSEC), pp.1–6, Chiang Mai, Thailand
3. Singh JP (2016) Analysis of SQL injection detection techniques. *Cryptography and Security*, Cornell University. <https://doi.org/10.20904/281-2037>
4. <https://github.com/SaqlainHussainShah/SQLi-Detection-using-Machine-Learning>
5. Rubidha Devi D et al (2016) A study on SQL injection techniques. *Int J Pharm Technol* 8(4):22405–22415, ISSN: 0975-766X
6. Li X, Xue Y (2014) A survey on server-side approaches to securing web applications. *ACM Comput Surveys* 46(4), article no: 54, pp 1–29. <https://dl.acm.org/doi/10.1145/2541315>
7. Medeiros I, Neves NF, Correia M (2014) Automatic detection and correction of web application vulnerabilities using data mining to predict false positives. In: ACM 23rd International conference on world wide web, pp 63–73
8. Komiya R, Paik I, Hisada M (2011) Classification of malicious web code by machine learning. In: 2011 IEEE 3rd international conference on awareness science and technology (iCAST), China. <https://doi.org/10.1109/ICAwST.2011.6163109>
9. Ross K (2018) SQL injection detection using machine learning techniques and multiple data sources. Master's Thesis and Graduates Research, San Joe State University. <https://doi.org/10.31979/etd.zknb-4z36>
10. Jemal I, Cheikhrouhou O, Hamam H, Mahfoudhi A (2020) SQL injection attack detection and prevention techniques using machine learning. *Int J Appl Eng Res* 15(6):569–580, ISSN 0973-4562
11. Das D, Sharma U, Bhattacharyya DK (2019) Defeating SQL injection attack in authentication security: an experimental study. *Int J Inform Security* 18(3):1–22. <https://doi.org/10.1007/s10207-017-0393-x>
12. Som S, Sinha S, Kataria R (2016) Study on SQL injection attacks: mode, detection and prevention. *Int J Eng Appl Sci Technol* 1(8):23–29, ISSN No. 2455-2143
13. Padmaja B, Sai Sravan K, Krishna Rao Patro E, Chandra Sekhar G (2021) A system to automate the development of anomaly-based network intrusion detection model. In: 1st International conference on applied mathematics, modeling and simulation, journal of physics: conference series, vol 2089(1)
14. Padmaja B, Naga Shyam Bhargav P, Ganga Sagar H, Diwakar Nayak B, Bhushan Rao M (2021) Indian currency denomination recognition and fake currency identification. In: Journal of physics: conference series, vol 2089
15. Padmaja B, Srinidhi C, Sindhu K, Vanaja K, Deepika NM, Patro EK (2021) Early and accurate prediction of heart disease using machine learning model. *Turkish J Comput Mathe Educ* 12(6):4516–4528
16. Padmaja B, Reddy BR, Sagar RV, Pradhan HK, Chandra Sekhar G, Krishna Rao Patro E (2021) Prognosis of Vitamin D deficiency severity using SMOTE optimized machine learning models. *Turkish J Comput Mathe Educ* 12(6):4553–4567
17. Kishor Kumar Reddy C, Anisha PR, Shastry R, Ramana Murthy BV (2021) Comparative study on internet of things: enablers and constraints. *Adv Intell Syst Comput*

Review on Load Balancing Techniques, Resource Scheduling, Sidechannel Attacks in Cloud Environment



C. Lakshminathreddy and Subbiah Swaminathan

Abstract Cloud computing is an inventive innovation that has acquired a progressive changes in computing administrations. It has empowered to drive the concentration from neighborhood/individual calculation to datacenter-driven algorithm by giving resources powerfully in a virtualized way by means of Internet. The aim of load adjusting is to clearly comprehend the client prerequisites, the information and data which can be sent and obtained without taking additional time. In this paper, we have focused on cloud computing, load balancing techniques, cloud resource scheduling process. Review on load balancing techniques and resource scheduling, sidechannel attack is also presented in this paper.

Keywords Cloud computing · Load balancing · Sidechannel attacks · Resource scheduling

1 Introduction

The cloud computing organization can be partitioned into three cloud service models, such IaaS, PaaS, SaaS [1]. Every worker has different capacity and processing power [2]. Different measurements are taken in cloud computing [2] and provide scalability, resource utilization techniques.

In any case, cloud computing uphold virtual machine framework is more perplexing while at the same time dispatching assortment of undertakings to worker's applications at the same time. The enormous number of assignments, a suitable and effective planning calculation to distribute these errands to fitting workers inside the base finishing time, and to accomplish the load adjusting of execution remaining task at hand of the cloud framework. The primary idea of the IES calculation is to allot errands to worker have by contrasting all estimation of makespan season of

C. Lakshminathreddy (✉) · S. Swaminathan
Computer Science and Engineering, Saveetha School of Engineering, Chennai, India
e-mail: laxminathreddy842@gmail.com

S. Swaminathan
e-mail: subbaiah.sse@saveetha.com

the worker hubs between each assignment. Essentially, the IES calculation can get preferable errand consummation time over past works and can accomplish dynamic load adjusting in cloud computing climate. Proficient dynamical framework asset the executive's strategy in cloud computing [3]. Mell et al. [1] focused on cloud computing. Chana et al. [2] describe the "Cloud Load Balancing Techniques". Raja rajeswari et al. describe various cloud concepts [4].

Paper organization is as follows: The related work is presented in Sect. 2. Section 3 gives cloud computing concept. Section 4 describes the load balancing concept. Section 5 presents cloud resource scheduling problem. Section. 6 presents resource scheduling and sidechannel attacks, e-healthcare in cloud and conclusion are given in remaining sections.

2 Related Work

In cloud computing resources for various clients in an organization with versatility and dependability of the data center [1]. Virtualization innovation permits us to work with ground-breaking and various virtual machines change-based setups and acquire the resources with center, RAM, and capacity to run on a similar actuators. Rajarajeswari et al. have been focused on cloud computing concepts [5–7]. Kishorekumar et al. focused on innovation methods in computer science [8–10]

(i) Paper Title: Issues and Challenges of Load Balancing Algorithm in Cloud Computing Environment

Authors: Tianshu Wu; Shuai Wang; Xiaoyu Shi. [11]

Virtualization framework is a center issue in the field of cloud computing. For accomplishing the objective of proficient oversee framework asset without execution misfortune in blurring climate, the creators propose an ideal load adjusting regulator to dole out the asset to various virtual machines, which run on a solitary actual worker. Here, the creators center on dynamical web remaining loads that the framework asset the board issue can be formed as a dynamical streamlining issue. Despite dynamical and remaining loads, the creators present an elective methodology dependent on the obliged limit straight quadratic control strategy, the ideal resources assignment conspire is tackled by limiting the quadratic expense work with compels on the framework information and yield.

(ii) Paper title: Stochastic Load Balancing for Virtual Resource Management in Datacenters

Authors: Yu et al. [12]

Cloud computing offers a practical and flexible registering worldview that encourages enormous scope information stockpiling and examination. By sending virtualization innovations in the datacenter, cloud empowers effective resource the board and confinement for different huge information applications. Notwithstanding, the

past burden adjusting plans settle on movement choices dependent on deterministic asset request assessment and remaining task at hand portrayal, without thinking about their stochastic properties. By concentrating true follows, we show that the asset interest and remaining task at the hand of virtual machines are exceptionally powerful and bursty, which can make these plans make wasteful relocations for load adjusting.

- (iii) Paper title: New approach for load rebalance, scheduler in large information with security system in cloud climate [13]

Authors: Dhande, Priyanka A.; Kadam, A. J

In cloud applications, dispersed document framework is very center innovation. Numerous functionalities of registering applications can be performed with the assistance of document framework; such applications depend on the dispersed programming and having various disseminated pieces are dole out to every hubs; hub get each different lump that acts in equal.

- (iv) Paper title: Experimental Setup for Investigating the Efficient Load Balancing Algorithms on Virtual Cloud.

Authors: Alankar et al. [14]

The cloud computing is a quickly arising appropriated framework worldview that offers a gigantic measure of IT assets as utility administrations at a decreased expense and adaptable plans. The key of such adaptability is a productive burden balancer that offers better administration and usage of virtualized fundamental cloud.

3 Cloud Computing

Cloud computing gives PC framework and administrations “on-need” premise [4]. The figuring framework could incorporate worker, hard circle, CPU cycles, information base and advancement stage or complete programming applications, etc. Clients (associations and people) don’t have to pay any huge scope capital consumptions to get to these resources from the cloud clients [15]. These clients need to “pay-per-use”, for example, they need to pay just, however, much they utilize the figuring foundation. The charging model of distributed computing is pay-per-utilize, for example, the power or water installment that we do based on utilization. Along these lines it diminishes equipment and programming speculation cost. In the middle of 2008 and 2009, as indicated by an overview embraced by the International Data Corporation (IDC) gathering, most of results highlight use cloud processing as a minimal effort doable alternative to clients [3]. Seller of distributed cloud computing offers the types of assistance over the web, so these administrations are accessible from any area. The purchaser doesn’t have to know anything about the product, interface administrations, and stage (Fig. 1).

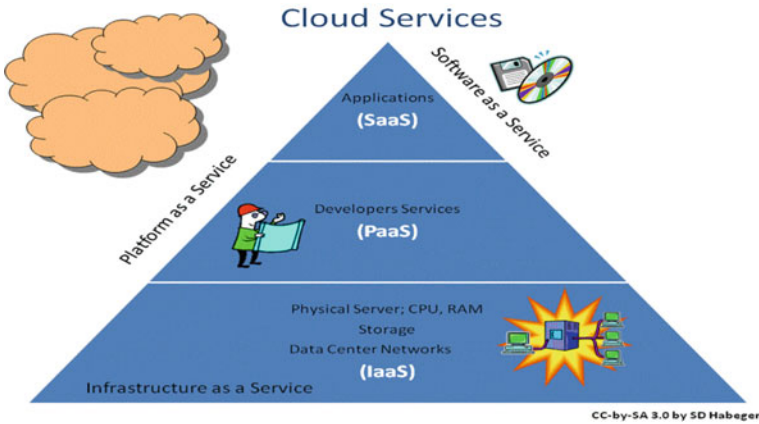


Fig. 1 Cloud service models

4 Load Balancing Concept

All in all terms, the load adjusting is a method to appropriate the remaining work of the framework across various workers to guarantee that no worker is caught up with taking care of a weighty outstanding task at hand while another worker is inactive. Hence, a load balancer can be considered as an opposite intermediary that disseminates organization or application traffic across various workers. Load balancers [11,12] advance accomplishing three principle destinations. To start with, improving generally framework execution by arriving at high asset use proportion. Second, evading framework bottleneck that happens because of burden awkwardness [16]. At last, accomplishing high suppliers' and clients' fulfillment by endeavoring to expand the framework throughput and decline the work handling time [2, 17]. This engineering has the known bit of leeway of powerful administration conspire however experiences helpless adaptability and comprises a solitary purpose of disappointment. The decentralized load adjusting engineering has no focal load balancer to disperse remaining task at hand among accessible assets; all things considered, work demands are separated on appearance, similarly among many load balancers where every one of them may run an alternate calculation to apportion occupations to assets. This design offers extraordinary adaptability and versatility. Then again, it yields helpless load balance among hidden assets [4].

5 Cloud Resource Scheduling Problem

On the off chance that is consistent asset (e.g., working framework, energy, throughput, transmission capacity and so forth). The executives of these assets include both productive provisioning and planning (Fig. 2).

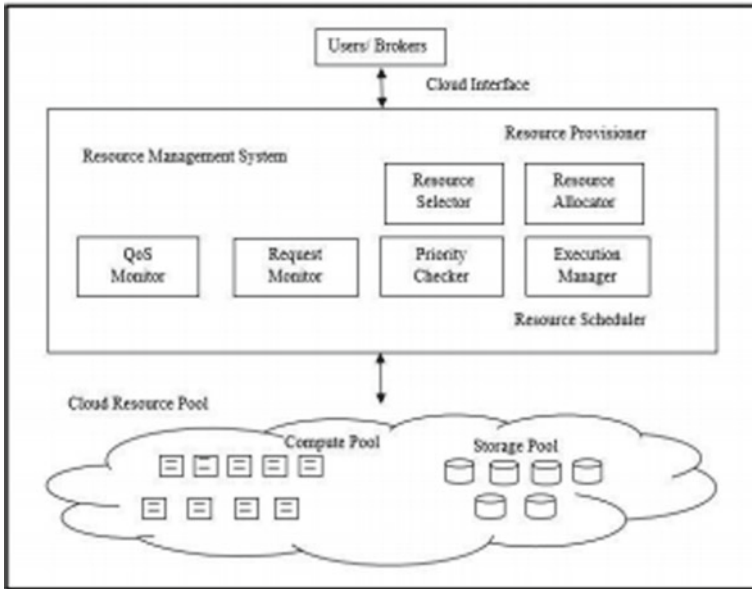


Fig. 2 Resource scheduling process

We have focused on asset planning stage and on methodologies that are intended to create viable timetables. The resource scheduling [18] marvel is portrayed. Presently, the duty lies on the Resource Management System (RMS) to monitor the status of undertakings presented, the quantity of assets required, keeping up the SLAs and fruitful finish of the errands. Asset Provisioner cautiously chooses the assets for the assignments. At the point when these assets are effectively accommodated the execution, RMS calls asset scheduler. Different intelligent parts of asset scheduler incorporate QoS screen, execution. Administrator, demand screen and need checker which they work, they can be grouped into free assignment booking and work process planning. Here, work process alludes to a bunch of reliant undertakings where the effective fruition of the multitude of errands cause the work process to finish. Contingent upon the sort of techniques utilized, the planning calculations are characterized into deterministic and stochastic calculations [19].

Ant Colony Optimization acquires a superior arrangement with a superior speed of combination. We initially portray different straight procedures. At that point, we proceed onward for explaining the nature enlivened and metaheuristic calculations that will in general handle RSP. Asset SCHEDULING ALGORITHMS: In prior days, when cloud computing was another worldview, planning systems accessible for network and bunch booking were utilized for cloud too.

While these calculations performed well, they didn't consider cloud boundaries just as different other QoS boundaries. SCFP, as the name proposes, organizes assignments according to their length and orchestrates the processors according to their

handling capacities. It at that point, map the undertakings from the arranged assignment rundown to the arranged processor list. Devipriya et al. [16] pointed toward changing the Max–Min calculation by choosing the asset that limits by and large fulfillment time [20].

6 Resource Scheduling Process

As referenced prior, scheduling issue is a NP-difficult problem, subsequently accomplishing ideal arrangement utilizing direct techniques isn't a lot of attainable. Hence, scientists have demonstrated a lot of revenue toward nature enlivened calculation [21–23]. The algorithmic intricacy of developmental methodologies has polynomial relationship with the issue scale [20, 24] and BAT calculation alongside the works did utilizing such methodologies in cloud computing climate [24]. Each developmental methodology has three fundamental stages specifically [14], introduction of populace, wellness assessment, and updation and finding the ideal arrangement iteratively [25]. In the subsequent stage, these chromosomes structure new offsprings by performing hybrid and change activities [21] (Fig. 3).

7 Sidechannel Attacks

Different attacks are generated by using sidechannel attacks. Every attack has detection techniques, attack generation and defense mechanisms. Due to user demand services, profits are gained in cloud environment. The users should know about the cloud computing issues to utilize the cloud services in a secured manner (Table 1).

8 E-healthcare in Cloud

Cloud computing technology can be applied to healthcare application for producing models in industry. This new model has many benefits like flexibility, cost and energy savings, resource sharing, and fast deployment [20]. Privacy and security are provided with the help of data centralization on the cloud for individuals and healthcare providers. Data is moving from data ownership to the cloud service providers [5].

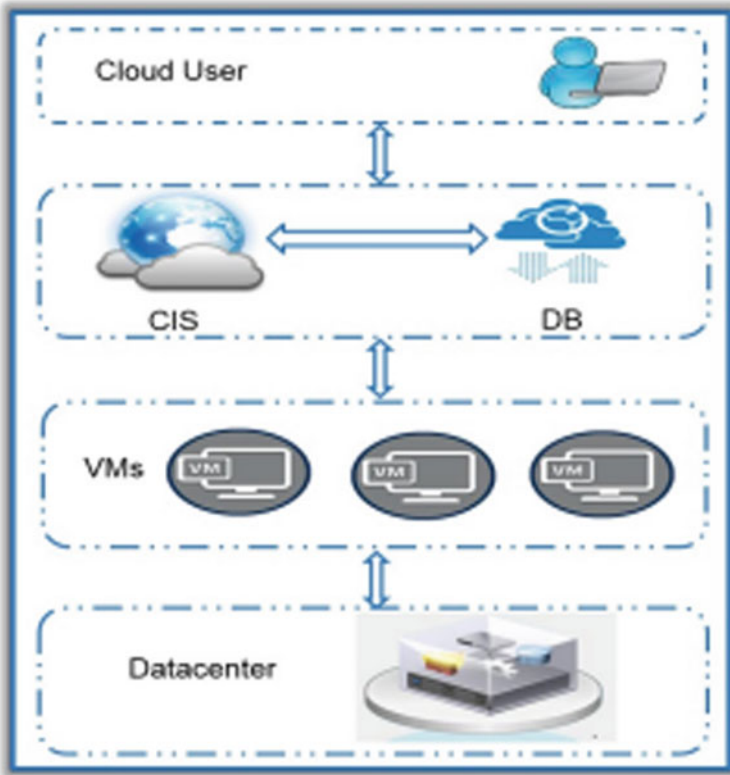


Fig. 3 Resource scheduling process in cloud [22]

9 Conclusion

Cloud computing provides resources based on user needs. In this paper cloud computing, load balancing concepts are clearly described. Cloud resource scheduling problem is explained clearly. Systematic literature survey on resource scheduling, load balancing techniques in cloud computing is presented. This paper presents various authors views on load balancing, scheduling algorithms for resource allocation in cloud environment. Sidechannel attacks and e-healthcare benefits are also described.

Table 1 Comparison table on sidechannel attacks [23]

Attack type	Behaviour	Physical security attack
Cache attack	Shared cache memory will be monitored by the attacker to steal the sensitive information	Non-invasive, Passive
Timing attack	Keep track, of computation time to detect the strength of the algorithm	Non-invasive, Passive
Power-monitoring attack	Examines the power consumption by the hardware devices	Non-invasive, Passive
Electromagnetic attack	Monitoring the electromagnetic radiations. Leaked to steal the sensitive information Like decryption key	Non-invasive, Passive
Acoustic cryptanalysis	Examines the sound produced by the hardware device including the key press	Non-invasive, Passive
Differential fault analysis	Faults or errors will be introduced in the system to monitor the original sensitive data	Non-invasive, Passive
Data reminisce	Sensitive data will be revoked even after deleting it from primary memory,	Invasive, Passive
Optical attack	Through visual recording the sensitive data will be hacked	Non-invasive, Passive

References

1. Mell P, Grance T (2012) The NIST definition of cloud computing. National Institute of Standards and Technology, Internet: <http://csrc.nist.gov/publications/nistpubs/800-145/SP800-145.pdf>. 11 Dec 2012
2. Kansal N, Chana I (2012) Cloud load balancing techniques: a step towards green computing. *IJCSI Int J Comput Sci Issues* 9(1):238–246
3. Stanojevic R, Shorten R (2009) Load balancing versus distributed rate limiting: a unifying framework for cloud control. In: *Proceedings of IEEE international conference on communication (ICC)*. Dresden, Germany, Aug 2009, pp 1–6
4. Rajarajeswari P, Pradeepkumar J, Vasumathi D (2018) Design and implementation of weather forecasting system based on cloud computing and data mining techniques. *Int J Eng Technol* 7
5. Al-Issa Y, Ottom MA, Tamrawi A (2019) E-health cloud security challenges: a survey. *J E-Healthcare Eng*
6. Rajarajeswari P, Sreevani M, Suryakumari PL (2021) Secure cloud risk architecture analysis for mobile banking system and its performance analysis based on machine learning approaches. *J Phys: Conf Ser* 2089(1):012007
7. Rajarajeswari P, Pradeep Kumar J, Vasumathi D Design and Implementation of Weather forecasting System based on Cloud computing and Data mining Techniques. *Int J Eng Technol*
8. Kishor Kumar Reddy C, VijayaBabu B (2015) ISPM: improved snow prediction model to Nowcast the presence of snow/no-snow. *Int Rev Comput Softw*
9. Anisha PR, Kishor Kumar Reddy C, Nguyen NG (2022) Blockchain technology: a boon at the pandemic times—a solution for global economy upliftment with AI and IoT. *EAI/Springer Innovations in Communication and Computing*
10. Kishor Kumar Reddy C, Anisha PR, Shastry R, Ramana Murthy BV (2021) Comparative study on internet of things: enablers and constraints. *Adv Intell Syst Comput*

11. Alam M, Khan ZA (2017) Issues and challenges of load balancing algorithm in cloud computing environment. *Indian J Sci Technol* 10(25). <https://doi.org/10.17485/ijst/2017/v10i25/105688>
12. Yu L, Chen L, Cai Z, Shen H, Liang Y (2014) Stochastic load balancing for virtual resource management in datacenters. *IEEE Trans Cloud Comput* Nov 2014
13. Dhande PA, Kadam AJ (2016) New approach for load rebalancer, scheduler in big data with security mechanism in cloud environment 2016. In: *IEEE International conference on advances in electronics, communication and computer technology*
14. Alankar B, Sharma G, Kaur H, Valverde R, Chang V (2020) Experimental setup for investigating the efficient load balancing algorithms on virtual cloud. *Sensors* 20(24):7342
15. Rajagopal TKP, Venkatesan M, Rajivkannan A (2020) Under heterogeneous networks in hybrid cloud environment ,wireless personal communications (2020) 111:1837–1851 <https://doi.org/10.1007/s11277-019-06960-4>
16. Devipriya S, Ramesh C (2013) Improved max-min heuristic model for task scheduling in cloud. In: *Green computing, communication and conservation of energy (ICGCE), 2013 international conference on*. IEEE, pp 883–888
17. Gaurav R et al (2012) Comparative analysis of load balancing algorithms in cloud computing. *Int J Adv Res Comput Eng Technol* 1(3):120–124
18. Salot P (2013) A survey of various scheduling algorithm in cloud computing environment. *Int J Res Eng Technol* 2(2):131–135
19. Singh S, Chana I (2016) A survey on resource scheduling in cloud computing: issues and challenges. *J Grid Comput* 14(2):217–264
20. Rajarajeswari P (2018) Design and Implementation of municipal services for human welfare by using smart phones. *Int J Sci Res Sci Technol*
21. Wen X, Huang M, Shi J (2012) Study on resources scheduling based on ACO algorithm and PSO algorithm in cloud computing. In: *Distributed computing and applications to business, engineering & science (DCABES), 2012 11th International Symposium on*. IEEE, pp 219–222
22. Al-Arasi RA, Saif A, Yemen S (2020) Task scheduling in cloud computing based on metaheuristic techniques: a review paper. *EAI Endrosed Trans*
23. Vanathi R, Chokkalingam SP (2019) Side channel attacks in IaaS and its defense mechanisms. *IJEAT*
24. Zhan S, Huo H (2012) Improved PSO-based task scheduling algorithm in cloud computing. *J Inform Comput Sci* 9(13):3821–3829
25. Rodriguez MA, Buyya R (2014) Deadline based resource provisioning and scheduling algorithm for scientific workflows on clouds. *IEEE Trans Cloud Comput* 2(2): 222–235.1
26. Sarood O, Gupta A, Kalé LV *Cloud friendly load balancing for HPC applications: preliminary work*, Publisher: IEEE
27. Al-Rayis E, Kurdi H (2013) Performance analysis of load balancing architectures in cloud computing. In: *2013 European modelling symposium computer modeling and simulation. UKSIM European Symposium on Modelling Symposium (EMS)*, IEEE Language: English, Database: IEEE Xplore Digital Library
28. Addis B, Ardagna D, Panicucci B, Squillante MS, Zhang L (2013) A hierarchical approach for the resource management of very large cloud platforms. *IEEE Trans Dependable Secure Comput* 10(5):253–272
29. Buyya R, Yeo CS, Venugopal S, Broberg J, Brandic I (2009) Cloud computing and emerging IT platforms: vision, hype, and reality for delivering computing as the 5th utility. *Futur Gener Comput Syst* 25(6):599–616
30. Wadhonkar A, Theng D (2016) A survey on different scheduling algorithms in cloud computing. In: *Advances in electrical, electronics, information, communication and bio-informatics (AEEICB), 2016 2nd international conference on*. IEEE, pp 665–669
31. Cao Q, Wei ZB, Gong WM (2009) An optimized algorithm for task scheduling based on activity based costing in cloud computing. In: *Bioinformatics and Biomedical Engineering, 2009. ICBBE 2009. 3rd International Conference on*. IEEE, pp. 1–3
32. Wu X, Deng M, Zhang R, Zeng B, Zhou S (2013) A task scheduling algorithm based on QoSdriven in cloud computing. *Procedia Comput Sci* 17:1162–1169

33. Abdullah M, Othman M (2013) Cost-based multi-QoS job scheduling using divisible load theory in cloud computing. *Procedia Comput Sci* 18:928–935
34. Pandey S, Wu L, Guru SM, Buyya R (2010) A particle swarm optimization-based heuristic for scheduling workflow applications in cloud computing environments. In: *Advanced information networking and applications (AINA)*, 2010 24th IEEE international conference on. IEEE, pp 400–407
36. Varshney S, Singh Madan Mohan Malaviya A Survey on Resource Scheduling Algorithms in Cloud Computing University of Technology, Gorakhpur, Uttar Pradesh- 273010, India. *Int J Appl Eng Res* ISSN 0973–4562 Volume 13, Number 9 (2018) pp. 6839–6845 © Research India Publications. <http://www.ripublication.com>
37. Al-Rayis E (2013) Performance analysis of load balancing architectures in cloud computing. Computer Science Department Imam Muhammad Ibn Saud Islamic University Riyadh, Saudi Arabia Ektemal.a.r@gmail.com Heba Kurdi, 2013 European Modelling Symposium 978-1-4799-2578-0/13 \$31.00 © 2013 IEEE DOI 486 DOI <https://doi.org/10.1109/EMS.2013.10520> 2013 European Modelling Symposium
38. Rajarajeswari P (2017) E learning system in mobile using cloud computing. In: *National conference on innovative technologies in Big Data, Cloud, Mobile Applications 2017*

Visual Heart Rate—A Key Biomarker to Diagnose Depressive Disorder



Purude Vaishali and P. Lalitha Surya Kumari

Abstract Depression is a disorder impacting people of all ages globally. If depression is detected at early stage, then it can be diagnosed. According to research, depression affects heart rate of an individual. By observing heart rate, depression can be predicted. In this paper, heart rate is calculated using facial videos as input. To calculate heart rate from facial video, algorithm used is Eulerian video magnification. Heart rate of person suffering from depression is not in normal range. Hence, estimated heart rate is used to train the model using algorithms of machine learning and proved that visual heart rate is key biomarker to diagnose depressive disorder. Performance of three machine learning algorithms is compared by varying test-train ratio.

Keywords Depression · Eulerian video magnification · Heart rate · Machine learning

1 Introduction

In medical science, definition of depression is given as drastic changes in mood (mood swings) that causing continuous sad feeling. It causes loss of interest in daily routine works, example eating, sleeping, talking, discussing, gossiping, office work, outing, or any work that brings pleasure in person life. When talked about depression, sometimes, people take lightly and ignore it. And sometimes, it causes life threat like suicide attempt. Depression do not has specific properties. Person should be under observation to take the decision of prediction and treatment. The subfield of artificial intelligence which aims for making predictions is predictive modeling. In it, model is learning from inputted dataset and gets trained for predictive analysis [1, 2].

P. Vaishali (✉) · P. Lalitha Surya Kumari
Department of CSE, Koneru Lakshmaiah Education Foundation, Aziznagar, Hyderabad,
Telangana State, India
e-mail: vaishupurude@gmail.com

P. Vaishali
Neil Gogte Institute of Technology, Uppal, Hyderabad, Telangana, India

The Eulerian video magnification (EVM) algorithm makes use of spatial and temporal filtering. It enlarges the color change of skin caused due to the blood circulation in facial vessels [3]. When each pixel is processed independently and treated as a series of time series for applying signal processing to it [3]. The blood is pushed by heart to each part of body. Hence, EVM estimates heart rate using changes in skin color caused by blood flow [4]. Heart rate is key biomarker to diagnose and treat the depression [5]. Monitoring heart rate for 24 h, depression can be predicted with 90% accuracy, if person is suffering with symptoms of depression. Depressed person has heart rate 10–15 beats higher than normal person [6]. Machine learning (ML) algorithms are implemented to get a predictive model in this paper which classifies individuals as healthy or depressed [7].

2 Previous Work

The author in [8] devised classification accuracy for prediction. In this referred paper, algorithms were used to prove improved classification accuracy via predictor variable than neuroimaging. Research developed programmed framework based on outward appearance. It has many applications like understanding human behavior and detecting any mental disorder [9, 10]. It is possible to calculate heart rate from facial expression [11]. Author in [12] introduced a network model for recognizing of facial expressions automatically. Author in [13] proposed CNN model based on collaboration of human and machine. It performs classification of facial expressions for real-time applications with low-cost embedded devices.

Author in [14] examined 40 individual persons having suspected for depressive symptoms and got information using eye tracking. Author in [15] proposed a system based on smart watch to measure the emotions of individual person. Heart rate of person was collected using sensors of smart watch with the goal of usefulness of sensors predict different moods in a person.

Author in [16] used calculated heart rate of videos to identify original videos and fake videos. This helps for controlling the spreading of wrong information in media and also used for facial identity recognition. As emotion becoming trending topic in different fields like health care, medical science, neuroscience, psychology, and biomedical engineering, author in [17] proposed a CNN-based architecture called LeNet for recognition of facial expressions. It serves uses in diagnosis of psychological and brain disorders.

Heart rate can be collected using sensor and used as input to smart healthcare system [18]. Author in [19] cancelled noise from healthcare devices which input cardiac signals, while author in [20] cancelled artifact. Author in [21] used novel sampling approach for healthcare system management.

As per study of all previous authors, videos are used for facial identity or emotion recognition. In this article, experiments calculate heart rate using videos. It serves as a key biomarker to predict depression using Eulerian perspective in videos.

3 Diagnosis of Depressive Disorder

It is possible to predict depression using visual heart rate.

3.1 Introduction of Parametric and Nonparametric Machine Learning Algorithms

Parametric means converting the input data to the output data using mapping function. These methods need less data, operate faster but not powerful. The other category, nonparametric methods use less or maybe zero assumptions for the mapping function. Hence, demand more input data, and training process is slow. These have more complexity but are powerful as compared to parametric [2].

3.2 Heart Rate Estimation

Heart circulates blood to each and every part of body. Heart rate of normal person is 60–85 bits per minute (bpm), whereas depressed person has heart rate 10–15 bpm more than normal person [22].

If person heart rate crosses 85 bpm, which indicates person is suffering from depressive disorder. Due to variation in heart rate, change in facial skin color is observed. When facial videos are inputted, it is magnified using EVM algorithm. It helps to estimate heart rate. Estimated heart rate is key biomarker to classify an individual as healthy or depressed.

3.3 Analysis Using Binary Classifiers

In this research paper, decision tree (DT), random forest (RF), and support vector machine (SVM) classifiers are used to predict depression.

4 Proposed Model

Proposed model used for diagnosis is indicated in Fig. 1.

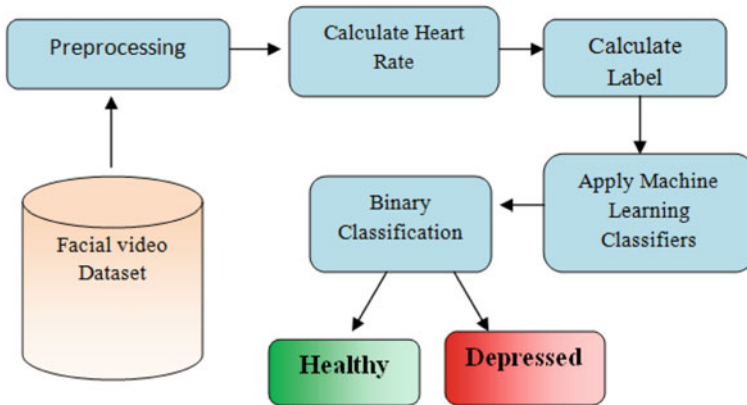


Fig. 1 Proposed model

Algorithm used for experiment is divided into three and mentioned below stepwise.

Algorithm 1:

Input: Facial Video Dataset

Steps:

1. Dataset is read and loaded into dataframe.
2. From dataframe, each video is preprocessed to select ROI on all frames.
3. Laplacian video pyramid is generated to get video pyramids.
4. Using fast Fourier transform, bandpass filtering is performed.
5. From FFT results, heart rate is estimated and stored in dataframe.

Output: Heart rate

Algorithm 2:

Input: Estimated Heart rate from Algorithm 1

Steps:

1. Condition is applied on heart rate to find whether it is in normal range (60–85 bpm).
2. If heart rate is in normal range, then labeled as healthy (0).
3. If heart rate is crossing normal range, then labeled as depressed (1).

Output: Label 0/1 indicating diagnosis

Algorithm 3:

Input: Generated labeled data from Algorithm 2

Steps:

1. Using standard test-train ratio (70–30%), multiple binary classifiers are applied, namely logistic regression, decision tree, SVM, random forest, KNN, LDA, QDA, Naïve Bayes, and only change in fitting time observed.
2. By changing test-train ratio, 3 binary classifiers are applied, namely decision tree, random forest, and SVM.
3. Performance is analyzed through evaluation metrics like accuracy, F1-score, recall, and RMSE.

Output: Evaluation metrics indicating performance

5 Experimental Results

Algorithm is evaluated by performing experiments on real-world dataset which is clinically validated named as BAUM-1 [23]. From this dataset, 27 videos with different emotions are selected to perform experiments. Using EVM algorithm, heart rate of 27 videos is calculated. Results obtained are, three videos got heart rate more than 85 bpm, while remaining 24 videos heart rate is in normal range of 60–85 bpm [22]. Hence, it can be concluded that three persons are predicted as suffering from depressive disorder, while remained are healthy [22]. Results after performing experiment as in proposed model are indicated in Fig. 2.

In Fig. 2, Label 0 indicates diagnosis as healthy, while label 1 indicates depressed person. In the plot, it indicates 24 healthy and 3 depressed individuals from dataset of 27 videos. Dataset of 27 videos is used for classification. Dataset divided into standard train-test ratio (70–30%). Multiple binary classifiers are applied, namely logistic regression, decision tree, SVM, random forest, KNN, LDA, QDA, Naïve

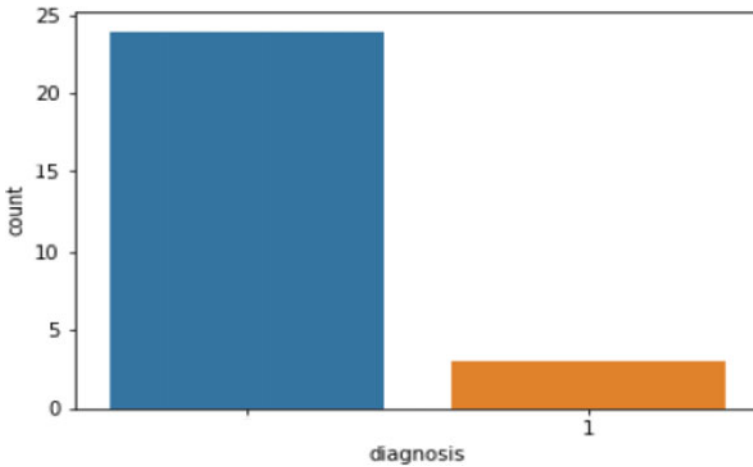


Fig. 2 Plot of healthy and depressed persons

Bayes. Observation is only fitting time is changed as shown in Fig. 3 and its plot in Fig. 4.

In Fig. 4, it is observed that fitting time of decision tree, random forest, and Bayes is good as compared to other binary classifiers.

Model	Fitting time
Logistic Regression	0.0000
Linear Discriminant Analysis	0.0000
Support Vector Machine	0.0025
Quadratic Discriminant Analysis	0.0025
K-Nearest Neighbors	0.0025
Random Forest	0.0050
Bayes	0.0050
Decision Tree	0.0050

Fig. 3 Fitting time for classifiers

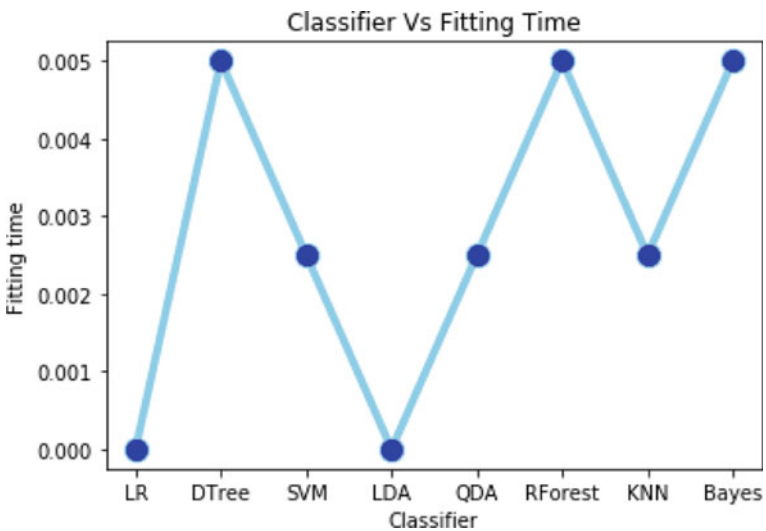


Fig. 4 Plot of fitting time for classifiers

Table 1 Results

Algorithm	Test size	Acc	Prec	Rec	Fitting time	F1	MAE	MSE	RMSE
Decision tree	0.4	0.90	0.0	0.0	0.0055	0.0	0.09	0.09	0.30
Random forest	0.5	0.93	0.67	1.0	0.0010	0.8	0.07	0.07	0.26
SVM	0.7	0.95	0.67	1.0	0.0025	0.8	0.05	0.05	0.22

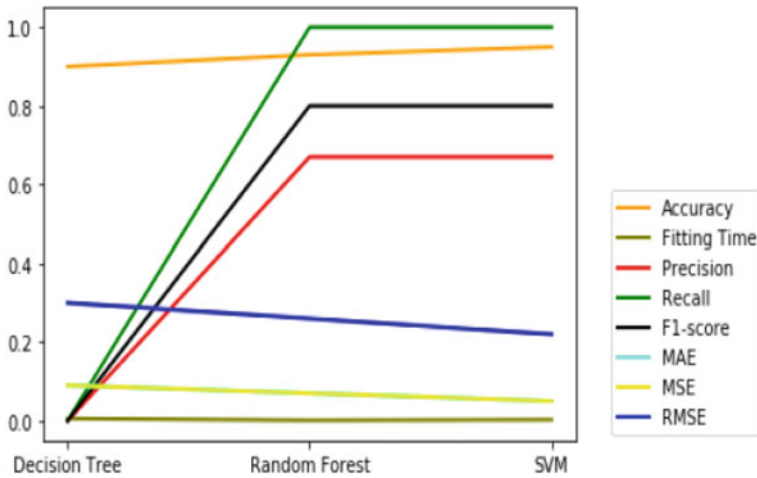


Fig. 5 Metrics for three classifiers

When module is trained using three ML algorithms decision trees, random forest, and SVM, evaluation metrics are accuracy (Acc), precision (Prec), recall (Rec), fitting time (FT), f1-score (F1), mean absolute error (MAE), mean squared error (MSE), root mean square error (RMSE). These metrics are changed according to test-train split ratio. These observations are noted in Table 1.

In addition to that when fitting time is compared for these three algorithms, random forest algorithm is better than SVM and decision tree as shown in Table 1. As per observations in Table 1, accuracy for classifiers for performed experiment ranges from 0.90 to 0.95. Precision ranges from 0.0 to 0.67, and recall ranges from 0.0 to 1.0. Accuracy of SVM is good as compared to DT and RF for test size 70%. Same results plotted using graph in Fig. 5.

6 Conclusion and Future Work

If depression is not detected at an early stage, then it leads to suicide attempt. Hence, to predict depression, heart rate is useful biomarker. As depression increases heart rate of person, in this paper, heart rate is estimated from facial videos using EVM

algorithm. Calculated heart rate is used as training parameter for machine learning algorithms. By changing test-train ratio, three binary classifiers are applied, namely decision tree, random forest, and SVM. After analyzing performance, accuracy of SVM is good as compared to decision tree and random forest for test size 70%.

In this research article, only, three ML algorithms are experimented, and performance is compared. In future, experiments can be repeated for more machine learning algorithms, and performance can be analyzed.

References

1. Kishor Kumar Reddy C, Anisha PR, Apoorva K (2021) Early prediction of pneumonia using convolutional neural network and X-Ray images. In: Satapathy SC, Bhateja V, Favorskaya MN, Adilakshmi T (eds) Smart computing techniques and applications. Smart innovation, systems and technologies, vol 224. Springer, Singapore. https://doi.org/10.1007/978-981-16-1502-3_67
2. Brownlee J Mastering machine learning algorithms
3. Alghoul K (2015) Heart rate variability extraction from video signals. Canada, Ottawa, 2015
4. Upadhyay U (2019) Heart rate detection using camera. Intel-software-innovators, 4 Jun 2019
5. <https://www.medscape.com>
6. [www.medicalnewstoday.com/article/Heart rate could predict depression risk](http://www.medicalnewstoday.com/article/Heart-rate-could-predict-depression-risk)
7. Depression risk detected by measuring heart rate changes. <https://neurosciencenews.com>. 12 Sept 2020
8. Lee Y (2018) Applications of machine learning algorithms to predict therapeutic outcomes in depression: a meta-analysis and systematic review. *J Affect Disord* 241:519–532
9. Durga BK, Rajesh V (2019) In illumination variations facial emotion recognition by using local ternary patterns. *Int J Adv Sci Technol* 28(8):197–205, 2019
10. Videla LS, Rao MRN, Anand D, Vankayalapati HD, Razia S (2019) Deformable facial fitting using active appearance model for emotion recognition. *Smart Innov, Syst Technol*
11. Bhatia M, Goecke H (2017) Heart rate estimation from facial videos for depression analysis. *ACII*, 2017
12. Hasani B, Negi PS, Mahoor M (2020) Facial affect computing using adaptive residual networks with bounded gradient. *IEEE Trans Affect Comput*
13. Hou Lee JR, Wang L, Wong A (2020) EmotionNet Nano: an efficient deep convolutional neural network design for real-time facial expression recognition. June 2020
14. Wu L, Pu J, Allen JJ, Pauli P Recognition of facial expressions in individuals with elevated levels of depressive symptoms: an eye-movement study. *Hindawi Publishing Corporation Depression Research and Treatment Volume 2012, Article ID 249030*
15. Arano KA, Gloor P, Orsenigo C, Vercellis C (2019) Emotions are the great captains of our lives: measuring moods through the power of physiological and environmental sensing. In: *IEEE transactions on affective computing*, vol x, no x, June 2019
16. Fernandes S, Raj S, Ortiz E, Vintila I, Salter M, Urosevic G, Jha S Predicting heart rate variations of deepfake videos using neural ODE. *Workshop on CVF Computer Vision Foundation, IEEE Explore*
17. Ozdemir MA, Elagoz B, Alaybeyoglu A, Sadighzadeh R, Akan A (2019) Real time emotion recognition from facial expressions using CNN architecture. *Izmir Katip Celebi University Izmir, Turkey, IEEE Conference 2019*
18. Rao KRRM, Reddy VA, Shankar CH, Reddy KVG (2019) Smart health care system using IOT. *Int J Innov Technol Exploring Eng*
19. Salman MN, Trinatha Rao P, Ur Rahman MZ (2017) Adaptive noise cancellers for cardiac signal enhancement for IOT based health care systems. *J Theor Appl Inf Technol* 95(10):2206–2213

20. Sulthana A, Ur Rahman MZ (2019) Artifact cancellation from cardiac signals in health care systems using a zoned adaptive algorithm. *Int J Eng Adv Technol* 8(5):988–993
21. Jabber B, Sai Venkat P, Sri Sai Nikhil K, Lakshmi Avinash B (2019) A novel sampling approach for balancing the data and providing health care management system by government. *Int J Adv Trends Comput Sci Eng* 8(6):2753–2761. <https://doi.org/10.30534/ijatcse/2019/12862019>
22. Purude Vaishali N, Lalitha Surya Kumari P (2021) Estimation of visual heart rate to predict depression. *Turkish J Comput Mathe Educ* 12(11):6050- 6055
23. Zhalehpour S, Onder O, Akhtar Z, Erdem CE BAUM-1: A spontaneous audio-visual face database of affective and mental states. *IEEE Trans Affect Comput*. <https://doi.org/10.1109/TAFFC.2016.2553038>

Predictive Analysis for Prognostication of Breast Cancer



Karuppiah Santhi, Kandasamy Thinakaran, J. Jegan,
and Perepi Rajarajeswari

Abstract Nowadays, most of the women affected by one of the type of cancer is Breast Cancer (BC). The main objective is to identify and prognosis of the Breast Cancer at its earlier stages using supervised machine learning (ML) techniques like Naive Bayes (NB) classifier, support vector machine (SVM), random forest classifier (RFC), K-nearest neighbor (KNN) and decision tree classifier (DT). The data are collected from the Wisconsin Diagnostic Breast Cancer dataset then malignant and benign tumors are classified based on the dataset and using various ML techniques to predict the Breast Cancer in advance manner. Various parameters like accuracy, precision, sensitivity (recall), F-measure (specificity), regression score, variance measure, maximum error and balanced accuracy are measured in each algorithms. Using Python experimental tool PyCharm to execute ML algorithms for predicts the Breast Cancer. Our final result indicates that support vector machine is the best one for predictive Breast Cancer efficiently with accuracy of 99%.

Keywords Machine learning (ML) · Breast Cancer (BC) · Support vector machine (SVM) · K-nearest neighbor (KNN) · Random forest classifier (RFC) · Decision tree classifier (DT) · Naive Bayes (NB)

1 Introduction

Breast Cancer (BC) is one of the most typical kinds of cancer in the world and many ladies are died for Breast Cancer. Various test like MRI, mammograms, ultrasound

K. Santhi (✉)

Panimalar Engineering College, Chennai, Tamil Nadu, India
e-mail: santhiglorybai@gmail.com

K. Thinakaran

Saveetha School of Engineering, Chennai, Tamil Nadu, India

J. Jegan

Aditya College of Engineering, Madanapalle, Andhra Pradesh, India

P. Rajarajeswari

Vellore Institute of Technology, Vellore, Tamilnadu, India

and diagnostic tests are used to diagnose the Breast Cancer. Cancer means growth of cells is uncontrolled and Breast Cancer means unstrained growth of cells within the breast tissue. We can distinguish three kinds of breast tumors: benign breast tumors, *in situ* cancers and invasive cancers. In our study, we are specializing in the differentiation between benign and malignant tumors.

The primary objective of the Breast Cancer prediction is to either cluster of malignant means cancerous tumors or cluster of benign means non-cancerous tumors. Using Wisconsin Diagnostic Breast Cancer (WDBC) dataset, ML algorithms are used to predict the Breast Cancer tumors category like benign or malignant via analyzing mixtures of various key attributes. Due to the variations between patients, they have a similar Breast cancer category; the values of various attributes won't be identical. The identical Breast cancer tumor category is divided into different serious situations by physicians based on these values then effective treatments are often given to the patients.

2 Materials and Methods

Amrane et al. [1] using Naive Bayes (NB) classifier and K-nearest neighbor (KNN) classifier for the classification of BC based on the cross-validation to evaluate the accuracy. Based on the results, KNN produces the highest accuracy that is 97.51% among lowest error rate, and accuracy of NB classifier is 96.19%.

Karim et al. [2] using subtypes and survival rates are used to analyze the multi-modal genomics data to classify the Breast Cancer patients. Data are collected as of the cancer Genome Atlas (TCGA). In the BC, diagnosis multiple factors are analyzed that is Estrogen Receptor (ER), Progesterone Receptor (PGR), and Human Epidermal Growth Factor Receptor 2 (HER2). Accuracy of ER is 91% and PGR is 86%. Alghunaim and Al-Baity [3] using two types of data that is Gene Expression (GE) and DNA Methylation (DM) then the datasets are applying separately and jointly in machine learning algorithms, to deal with the problem of BC prediction in the big data context. Finally, support vector machine performance is best one that other classifiers.

Peng et al. [4] to discover the genes related to BC using CapsNetMMD which is a deep learning method. In this work, related BC genes to change the concern gene identification into the concern of supervised classification. Kretz et al. [5] using virtual mammography which is apply to generate a database for training CNN. The trained net is used to efficiently predict the images.

Naveen et al. [6] using cancer features to predict Breast Cancer in high accuracy which collects data from UCI, decision tree produces 100% accuracy, and also K-nearest neighbor algorithm produces 100% accuracy based on 90% of training and 10% of testing data. Bharat et al. [7] used Wisconsin Breast Cancer dataset in the ML algorithms and like support vector machine (SVM), Naive Bayes, KNN and CART to calculate the accuracy and also prediction for each algorithm is also compared with each algorithm performance. Sharma et al. [8] compare the performance of

random forest, KNN and Naïve Bayes with the parameters of accuracy and prediction using Wisconsin Diagnosis Breast Cancer dataset. [Al-Azzam and Shatnawi [9]] Using supervised and semi-supervised algorithms to predict the BC, accuracy of both supervised and semi-supervised is very close to each other. Naji et al. [10] compare five machine learning algorithm to diagnose the BC earlier stages, SVM produces the good result compare than remaining algorithms. Kishore Kumar Reddy et al. focused on machine learning methods [11–13]. Rajarajeswari et al. described various computational methods [14, 15].

3 Results and Discussion

This work classify the machine learning techniques like random forest (RF), support vector machine (SVM), decision tree (DT), Naive Bayes (NB) and K-nearest neighbor (KNN) are used to predict the Breast Cancer. Wisconsin dataset is used in the supervised machine learning algorithms, and the dataset which one is separated into training and testing dataset, and also dataset has 32 real world attributes, 569 instances and no missing value in the dataset. Using Python's PyCharm tool to analyze all the find out which algorithm that gives the best results. The dataset has a diagnosis of malignant or benign of tumors in Breast Cancer.

Various parameters are applied to analyze the performance of supervised ML algorithms similar to decision tree (DT), support vector machine (SVM), random forest (RF), Naive Bayes (NB) and K-nearest neighbors (KNN) for BC prediction. Wisconsin datasets are utilized in this work which has multivariate 32 attributes, 569 instances and no omitted value in the dataset. Compare all the five algorithms and using various parameters to analyze the algorithms. Confusion matrix of all the algorithms is represented in Fig. 1, Performance of SVM, DT, RF, NB and KNN algorithms is represented in Fig. 2.

3.1 Performance Analysis

The performance of supervised ML algorithms like support vector machine (SVM), decision tree (DT), random forest (RF), Naive Bayes (NB) and K-nearest neighbor (KNN) are analyzed for Breast Cancer predictions pedestal on the following metrics like accuracy, precision, sensitivity, F-measure, regression score, max_error, balanced accuracy and variance measure.

Consider our classification task that tumors can be able to predict whether these are benign or malignant. Benign tumors mean non-cancerous tumors and cancerous tumors are malignant tumors. Classified by the system, tumors as malignant means True Positive, incorrectly classifies benign tumors is malignant means False Positive, incorrect prediction of benign tumors means False Negative and correct prediction of tumors as being benign means True Negative. Based on the four outcomes

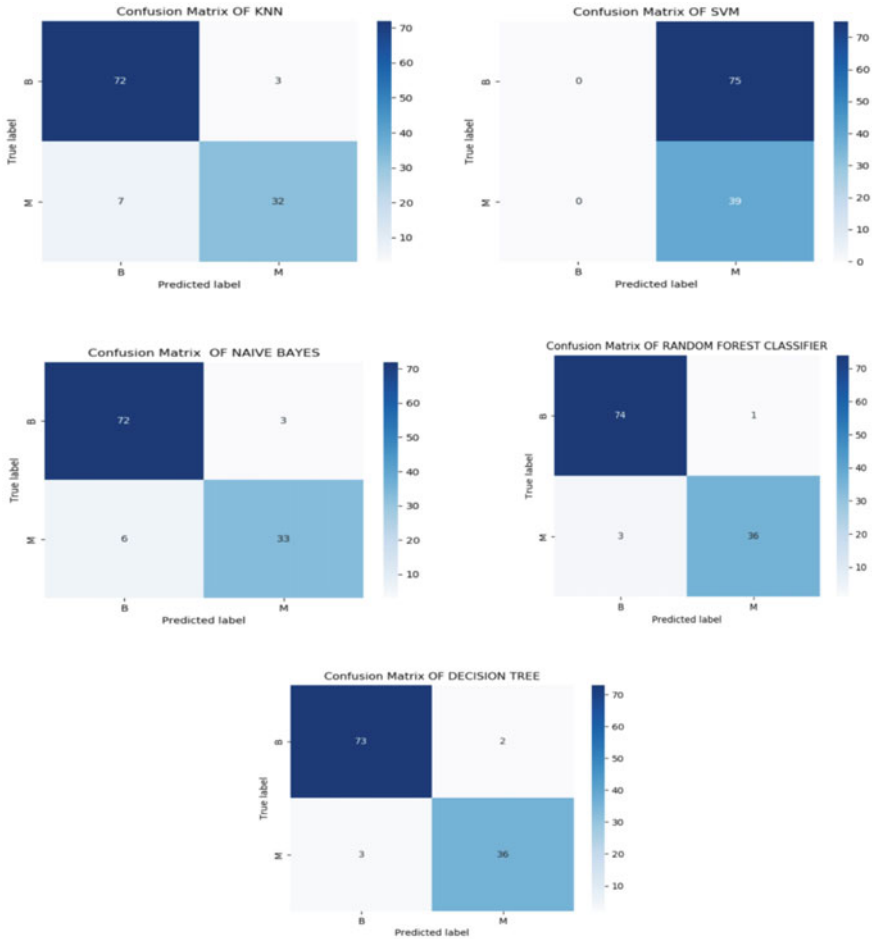


Fig. 1 Confusion matrix

like True Positive, False Negative, False Positive and True Negative are applied in the following parameters like accuracy, precision, sensitivity, F-measure regression score, max_error, balanced accuracy and variance measure to estimate the performance of the supervised ML algorithms for BC prediction.

Accuracy. Accuracy is used to measure the performance of programs and does not make the distinction between malignant tumors and benign tumors.

In Fig. 3, accuracy of KNN algorithm is 91.2, SVM algorithm is 99.1, Naïve Bayes algorithm is 92.1, random forest algorithm is 96.4 and decision tree algorithm is 95.6, support vector machine algorithm’s accuracy is higher than other algorithms.

Precision. Precision measure the tumors that are predicted be malignant.

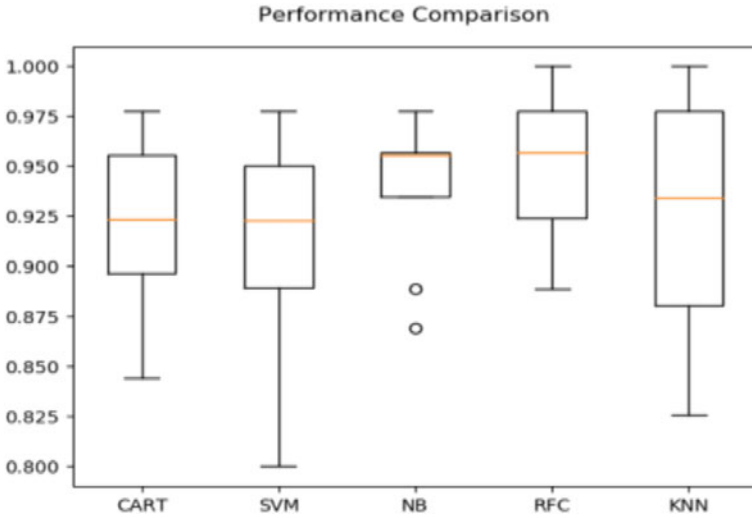
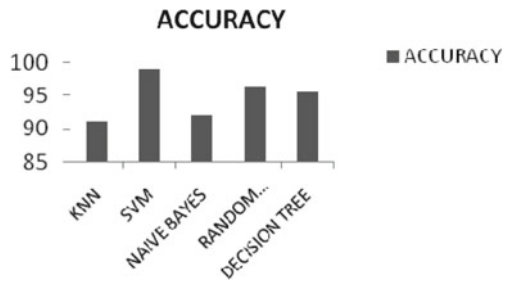


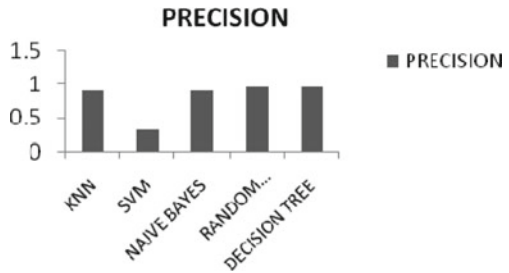
Fig. 2 Performance comparison

Fig. 3 Accuracy calculation



In Fig. 4, precision of KNN algorithm is 0.91, SVM algorithm is 0.34, Naïve Bayes algorithm is 0.91, random forest algorithm is 0.97 and decision tree algorithm is 0.97, evaluate from other algorithms support vector machine algorithm's precision result is very low.

Fig. 4 Precision calculation



Sensitivity. Another name is recall which is the fraction of malignant tumors that the system identified.

In Fig. 5, sensitivity of KNN algorithm is 0.82, SVM algorithm is 1.0, Naïve Bayes algorithm is 0.84, random forest algorithm is 0.92 and decision tree algorithm is 0.89, support vector machine algorithm’s sensitivity result is high with compare to other algorithms.

F-Measure. Another name is balanced F-score which helpful to find balance between precision and sensitivity represented in Fig. 6.

F-Measure of KNN algorithm is 0.86, SVM algorithm is 0.50, Naïve Bayes algorithm is 0.88, random forest algorithm is 0.94 and decision tree algorithm is 0.93.

Regression score and max_error. Regression score of KNN algorithm is 0.61, SVM algorithm is -1.92 , Naïve Bayes algorithm is 0.78, random forest algorithm is 0.84 and decision tree algorithm is 0.80. max_error can be used to calculate the maximum residual error. Maximum error of all the algorithms are 1.0.

Balanced_accuracy and Variance Measure. The balanced_accuracy is used to deal in imbalanced datasets. Balanced_accuracy of KNN algorithm is 0.89, SVM algorithm is 0.50, Naïve Bayes algorithm is 0.90, random forest algorithm is 0.95 and decision tree algorithm is 0.94.

Variance is calculated by how far the observed values vary from the average of predicted values. Variance measure of KNN algorithm is 0.61, SVM algorithm is 0.00, Naïve Bayes algorithm is 0.78, random forest algorithm is 0.84 and decision

Fig. 5 Sensitivity calculation

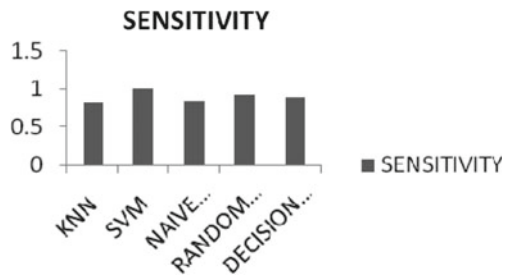


Fig. 6 F-Measure calculation

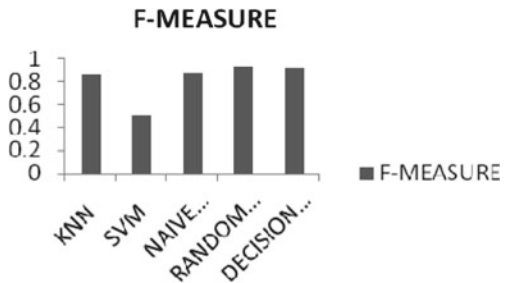


Table 1 Comparison of algorithms based on parameters

Algorithm	Accuracy	Precision	Sensitivity	F-Measure	Regression score	Variance measure	Maximum error	Balanced accuracy
KNN	91.2	0.91	0.82	0.86	0.61	0.61	1.0	0.89
SVM	99.1	0.34	1.0	0.50	-1.92	0.00	1.0	0.50
NB	92.1	0.91	0.84	0.88	0.78	0.78	1.0	0.90
RF	96.4	0.97	0.92	0.94	0.84	0.84	1.0	0.95
DT	95.6	0.97	0.89	0.93	0.80	0.80	1.0	0.94

tree algorithm is 0.80. Table 1 represents the comparison of KNN, SVM, Naïve Bayes, random forest and decision tree algorithms based on various parameters.

4 Conclusion

Our main aim is to expect the BC at its earlier stages, if BC is efficient to find out in the early stages then thousands of human beings lives will save. Using supervised machine learning techniques to identify and prognosis the Breast Cancer at its earlier stages which is used to classify and predict the Breast Cancer is cancerous or non-cancerous. The accuracy measurements are used to select the highly accurate and fast detecting algorithm model which is helpful for doctors to report the patients within few minutes at its earlier stages of Breast Cancer.

Our experimental and final results shows that support vector machine is the best for expect analysis of BC with an accuracy of 99%. In the analysis of supervised ML algorithms, efficient and best one for predict the BC is support vector machine and the next one is random forest.

References

1. Amrane M, Oukid S, Gagaoua I, Ensari T (2018) Breast cancer classification using machine learning. In: IEEE international conference on 2018 electric electronics, computer science, IEEE Press, Turkey
2. Karim MR, Wicaksono G, Costa IG, Decker S, Beyan O (2019) Prognostically relevant subtypes and survival prediction for breast cancer based on multimodal genomics data. *IEEE Access* 7:133850–133864
3. Alghunaim S, Al-Baity HH (2019) On the scalability of machine-learning algorithms for breast cancer prediction in big data context. *IEEE Access* 7:91535–91546
4. Peng C, Zheng Y, Huang DS (2019) Capsule network based modeling of multi-omics data for discovery of breast cancer-related genes. *ACM Trans Comput Biol Bioinform* 7:91535–91546
5. Kretz T, Müller KR, Schaeffter T, Elster C (2020) Mammography image quality assurance using deep learning. *IEEE Trans Biomed Eng* 67:3317–3326
6. Naveen, Sharma RK, Nair AR (2019) Efficient breast cancer prediction using ensemble machine learning models. In: IEEE 4th international conference on recent trends on electronics, information, communication & technology, IEEE Press, India

7. Bharat A, Pooja N, Reddy RA (2018) Using machine learning algorithms for breast cancer risk prediction and diagnosis. In: IEEE 3rd international conference on circuits, control, communication and computing, IEEE Press, India
8. Sharma S, Aggarwal A, Choudhury T (2018) Breast cancer detection using machine learning algorithms. In: IEEE international conference on computational techniques, electronics and mechanical systems, IEEE Press, India
9. Al-Azzam N, Shatnawi I (2021) Comparing supervised and semi-supervised machine learning models on diagnosing breast cancer. *Ann Med Sur* 4128:1148–1158
10. Naji MA, El Filali S, Aarika K, Benlahmar EH, Abdelouhahid RA, Debauche O (2021) Machine learning algorithms for breast cancer prediction and diagnosis. *Procedia Comput Sci* 191:487–492
11. Kishore Kumar Reddy C, Anisha PR, Apoorva K (2021) Early prediction of pneumonia using convolutional neural network and X-ray images. *Smart Innov Syst Technol* 673–681
12. Kishore Kumar Reddy C, Rupa CH, Vijaya Babu B (2015) SLGAS: supervised learning using gain ratio as attribute selection measure to now cast snow/no-snow. *Int Rev Comput Softw* 10:120–128
13. Kishore Kumar Reddy C, Rupa CH, Vijaya Babu B (2014) A pragmatic methodology to predict the presence of snow/no-snow using supervised learning methodologies. *Int J Appl Eng Res* 9:11381–11394
14. Rajarajeswari P, Anwar Beg O (2021) An executable method for an intelligent speech and call recognition system using a machine learning-based approach. *J Mech Med Biol* 21(7)
15. Rajarajeswari P, Hemashri R (2020) Hyperspectral image classification by using K-Nearest Neighbor algorithm. *Int J Psychosoc Rehab* 24(5):5068–5074

Framework of Crop Yield Using pH Soil and Temperature Values



B. V. Ramana Murthy and B. N. S. M. Chandrika

Abstract The agricultural sector needs an agricultural industry and needs a systematic system to predict and improve crop production globally. The complexity of predicting the best plants is high due to the unavailability of relevant information on the basis of crop knowledge that affects the quality of the forecast. In data mining, data segregation is an important step in extracting useful information. Dividing strategies such as decision tree, neural network, SVM, Naive Bayes, and KNN which makes this task difficult due to a problem such as random selection of key parameters. Here we propose a crop prediction system using a decision tree and compare the results of the proposed system with the different class dividers. Decision tree has been shown to be a powerful modeling and predictive tool, which increases its effectiveness. Crop prediction methodology is used to predict the correct yield by sensing different soil parameters and atmospheric-related parameters. Parameters such as soil type, pH, and temperature. For that purpose, we used a cutting tree. Agricultural researchers around the world emphasize the need for an effective way to predict and improve crop growth. The complexity of yield prediction is very high due to various multi-sided metrics, and the lack of modeling, which leads to crop losses. It works in the form of a dynamic collection of a variety of crop data reviewed in history to predict crop yields and improve agricultural decision-making accurately. The proposed system will incorporate measurement data obtained from storage and IoT sensors, pH sensor, weather department, and application of the machine-machine learning algorithm, predicting the most appropriate yield according to current environmental conditions. This gives the farmer a variety of crops that can be grown. Therefore, the project improves the system by combining data from a variety of sources, analyzing data, and analyzing forecasts that can improve crop yields and increases the profit margins of assisted farmers over time.

B. V. Ramana Murthy (✉)

Department of CSE, Stanley College of Engineering and Technology for Women, Hyderabad, India

e-mail: drbvr@gmail.com

B. N. S. M. Chandrika

Department of Math, Stanley College of Engineering and Technology for Women, Hyderabad, India

Keywords Vector support machine (SVM) · K-nearest neighbor (KNN) · IoT sensor · pH sensor · Naïve Bayes

1 Introduction

Internet of Things and gadget studying are latest technologies from previous couple of years. On this task, we proposed a sort of plants and small plant life prediction for clever agriculture primarily based on the key technologies: net of things, sensors, and system learning strategies. Sensor era has been superior and kinds of sensors like environmental sensors (temperature and humidity), soil moisture sensor, and pH degree sensors are utilized in smart agriculture. Uses of these technology in smart agriculture, i.e., crop prediction, are used for development of agriculture.

Device studying is a trending technology, and it could be used in contemporary agriculture industry. The makes use of ML in agriculture which help to create greater healthy seeds and crop. It miles a brand-new era and has been used for studying the soil moisture, temperature, and pH fee to classify them. It is useful for kind of crops and small vegetation predictions based totally on certain parameters like environment situations, moisture of soil, and pH degree in farmland. Machine studying is specially utilized in agriculture area for forms of crops prediction, where they use changed selection tree algorithm.

The Internet of Things is a generation that connects the world's realities to be had online. Apps are developed primarily based on IoT-enabled gadgets to monitor and control a spread of domains along with domestic appliances, clever towns, and clever homes. In the agricultural zone, a few research have pro. The net of factors is a generation that connects the sector's realities available online. Apps are advanced primarily based on IoT-enabled gadgets to monitor and manipulate an expansion of domains including domestic appliances, smart towns, and smart homes. In the agricultural region, a few studies have proposed IoT-based systems for system studying to be expecting plant species and micro-organisms. IoT with system learning is a mature generation, and lots of paintings have been finished in the agricultural quarter. Sensors are to be had to hit upon numerous parameters inclusive of temperature and humidity, soil moisture, and pH degree required within the agricultural zone. IoT with mechanical mastering houses become proposed to be expecting plant species inside the agricultural region. Posed IoT-based structures for machine getting to know to expect plant species and micro-organisms. IoT with system getting to know is a mature era, and a variety of paintings has been achieved in the agricultural zone. Sensors are to be had to discover diverse parameters which include temperature and humidity, soil moisture, and pH level required inside the agricultural quarter. IoT with mechanical mastering residences become proposed to predict plant species within the agricultural zone.

Agriculture is one of the major sources of income for most Indians and is one of the major contributors to the Indian economy. A system that uses real-time data on environmental conditions, soil moisture, and pH levels from farms. Plants are

heavily planted depending on the location of the soil [1] and determines soil level. The pH value of the soil and the quantity of nutrients including nitrate, phosphate, and potassium in the soil are critical factors in determining soil high-quality and form of crop production. Soil moisture evaluation facilitates to add water on every occasion vital to keep away from water harm. Also, environmental situations which includes temperature and humidity additionally affect crop yields inside the agricultural vicinity. The pH sensor to collect soil systems and cutting-edge environmental conditions. This encourages the introduction of an inexpensive and portable sensory kit to detect soil moisture of a spread of vegetation grown on farms. Soil information from farms desires to be amassed through a sensor package and sent to cloud garage for further processing. The facts amassed and then analyzed by using king plant life and small-scale crops grown on farms. One of the backbone of the Indian economy is farming, ensuing in negative soil fertility. The form of crop forecast is a completely difficult assignment in the agricultural zone. The agricultural crop depends on a spread of factors. Boom of agricultural vegetation depends on a variety of things such as weather, soil characteristics, and better temperatures. Diverse different retrospective models such as choice tree, rows, a couple of rows, and aid vet taking flight are examined to decide the powerful type of crop prediction. This activity presents a higher predictor for farmers to plant what form of crops in their discipline primarily based at the above parameters so as to enhance productiveness. If we study the modern-day scenario facing Indian farmers, we have seen a boom in suicide prices over time. Motives for this include weather conditions, debt, circle of relatives issues, and standard changes in Indian government regulations. Farmers from time to time do no longer know approximately the yield that fits their soil great, soil nutrients, and soil composition. Therefore, the gadget specializes in assessing soil great, pH, and an appropriate temperature to predict the crop appropriate for soil type and to boom crop yields.

Promoting and cooling agricultural manufacturing at a speedy rate is one of the key drivers of agricultural development. Any crop and production show the way with the interest in the area or the improvement of the crop or both. In India, there's no wish of growing the place underneath any crop until it is rehabilitated to growth planting power or crop rotation. Consequently, crop production variety keeps to plague the environment and purpose exquisite strain. Therefore, there's a need to strive a higher crop control approach to triumph over the present day hassle. One of the mainstays of the Indian economy is farming, which is because of poor soil fertility. The type of crop forecast is a very hard project in the agricultural area. The rural crop depends on a ramification of factors. The growth of agricultural crops relies upon on a ramification of things including weather, soil characteristics, soil moisture, and higher temperatures. The extra selection tree is used for the effective kind of crop forecast. This hobby offers a higher predictor for farmers to plant what kind of crops in their subject based at the above parameters on the way to enhance productiveness.

2 Literature Survey

In 2013, Fan, “Smart Agriculture Based on Cloud Computing and IoT” [2], Journal of Convergence Information Technology (JCIT), described intelligent agricultural management systems based on IoT and cloud computing.

In 2014, Dahikar and Rode, “Agricultural Crop Yield Prediction Using Artificial Neural Network Approach” [3], an international journal of new research on electricity, electronics, and a proposed neural network-based predictor crop yield, by sensing soil structures and atmospheric boundaries.

In 2014, Sonka, “Big Data and Ag Sector: Multiplication” [1], International Food Management and Agribusiness Management, Big Data Technology in the agricultural sector and how it will affect cost reductions and benefits are explained.

In 2014, Tsai et al., “Data Mining for Internet of Things: A Survey” [4], IEEE COMMUNICATIONS SURVEYS AND TUTORIALS, IoT with data mining is discussed. Data generated by IoT and using various data mining techniques on this data. The authors also discuss the changes needed to data mining in the IoT perspective and issues with future trends.

In 2011, Kumar and Kannathasan, “A Survey on Data Mining and Pattern Recognition Techniques for Soil Data Mining” [5], JCSI International Journal of Computer Science, explored data mining techniques to find the most effective extraction techniques. New information and information from the profile of the soil profile contained in the ground dataset. Explain the data mining techniques that are relevant to different agricultural predictions.

In 2014, Mankar and Burange, “Data Mining—An Evolutionary View of Agriculture” [6], International Journal of Application or Innovation in Engineering and Management (IJAIEEM), Yield measurement using available data using minute data proposed. For this, they used the four elements of the year, rain, sowing, and production.

In 2013, Ramesh and Vardhan, “Data Mining Techniques and Applications to Agricultural Yield Data” [7], International Journal of Advanced Research in Computer and Communication Engineering, analyzed data mining algorithms to predict crop yields with more accuracy and regularity. Using existing data.

In 2011, Rajesh, “Application for Agricultural Area Data Mining” [8], International Journal of Computer Applications, described the use of local data mining in the agricultural area. They used the K-means algorithm and method to improve the continuous development of spatial integration analysis. Temperature and rainfall are provided as primary location data and analyzed to improve crop yields and reduce crop losses.

In 2013, Ananthara et al., “Cry: An improved crop prediction model using beekeeping techniques in agricultural datasets” [9], at the Pattern Recognition, Informatics and Medical Engineering (PRIME), 2013 IEEE International Conference of the ground.

In 2014, Narkhede and Adhiya, “A Study of Clustering Techniques for Crop Prediction—A Survey” [10], American International Journal of Research in Science, Technology, Engineering and Mathematics, February 2014, ISSN no: 2328 -3491, pp. 45–48, predictions made by plant managers to minimize losses where adverse conditions may occur.

In 2014, Dahikar and Rode, “Agricultural Crop Yield Prediction Using Artificial Neural Network Approach” [11], Vol. 2, Issue 1, January 2014, pp-683–685, attempted to develop a different yield prediction model using ANNs. As an illustration, a methodology has been used to model and predict crop yields on the basis of a variety of forecasts, viz. soil type, PH, nitrogen, phosphate, potassium, organic carbon, calcium, magnesium, manganese, copper, iron, depth, temperature, rainfall, and humidity. ANN zero, one, and two hidden layers are noted.

In 2017, Bhangale and Yogesh, “Implementing the Advanced Harvest Prediction using the Neural Network” [12], discussed how ANN could be used to predict yields based on climate.

3 About the Data

First, the data is collected in various fields. PH, soil type, and temperature are collected using a variety of sensors. Collected prices favor the growth of a particular crop. Amassed information is stored within the gadget from sensors used with the Wi-Fi device. Now the data is cleared, i.e., it is checked for incorrect values and incorrect or invalid number. Prices must be completed and after that the cleaning process is completed. Purified data is developed and ready for use with the most appropriate algorithm. The most suitable algorithm has been selected, and in this algorithm, we have selected the decision tree, to give the best result.

pH is described because the decimal logarithm for the duplication of hydrogen ion pastime in answer. The pH range is 0–14. Solutions with low pH values are naturally acidic, solutions with high pH values are naturally basic, and pure water is acidic and non-essential. The acidic and basic elements of the solution in the soil depend on ions such as nitrate, potassium, etc., depending on the type of soil in which the plant is grown [13–16].

Soil can be defined as organic rely and inorganic count number that offers the basis for plant growth. The soil grows slowly over the years and is made from many unique materials. Inanimate items, or the ones inanimate items, consist of inanimate flexible stones, which includes transformed stones and minerals. Soils vary in their composition and shape of their debris, and these factors are carefully taken into consideration by farmers, who want appropriate soil for growing crops.

There are three simple kinds of soil: sand, mud, and clay. But maximum of the soil is made up of an aggregate of various kinds. The sand inside the soil is actually small particles of bendy rock. The sand is difficult and free so the water can effortlessly get

out of it. Dust may be considered pleasant sand, and it will keep water higher than sand. It forms very best soil. Its debris are a good deal smaller than mud, so there may be little space among small particles to circulate air or water.

Temperature also affects the soil which leads to changes in humidity levels. At constant humidity, low temperatures cause water loss and nutrient uptake. At lower temperatures, transport from root to root and vice versa is reduced. Khalif plants are plants that are sown early in the rainy season, e.g., between April and May. Rabin plants are plants that are sown in late monsoon or early winter, e.g., between September and October. There are plants known as monsoon plants. This system is helpful for farmers to choose the right crop at the right time based on the soil properties of the farm. The proposed system uses machine learning and predictive algorithm such as decision tree to identify the pattern between data and process it in terms of input.

The proposed system looks at information related to soil type, temperature, and pH value and proposes the good field of crops that can be grown in the right place and environment. As this system lists all possible crops, it assists the farmer in deciding which crop to grow. There are many crops prediction papers, very few focusing on crop type forecasting, and this proposed system is one such method. There are many factors that affect crop prediction, and good prediction is found when all factors are considered.

4 Architecture

- The project is designed to design the crop prediction framework that continuously collects live data of selected parameters such as pH, temperature, and soil type using IoT sensors that develop a variety of preprocessing methods and ultimately obtain the required common data by database construction, namely numerical values derived from common sensors become ordinal elements [17–20] (Fig. 1).
- The framework is responsible for classifying the processed data into a training database and a set of standardized data analysis (80% -20%), and these sub-databases are included in the decision tree separator to train the accuracy model and predictive results.

5 Algorithm

Program training steps:

1. Collect data with the help of a sensor–pH meter and a DHT sensor kit.
2. Import data from the kit with Arduino software and collect data over a Wi-Fi connection via ThingSpeak cloud computing platform.

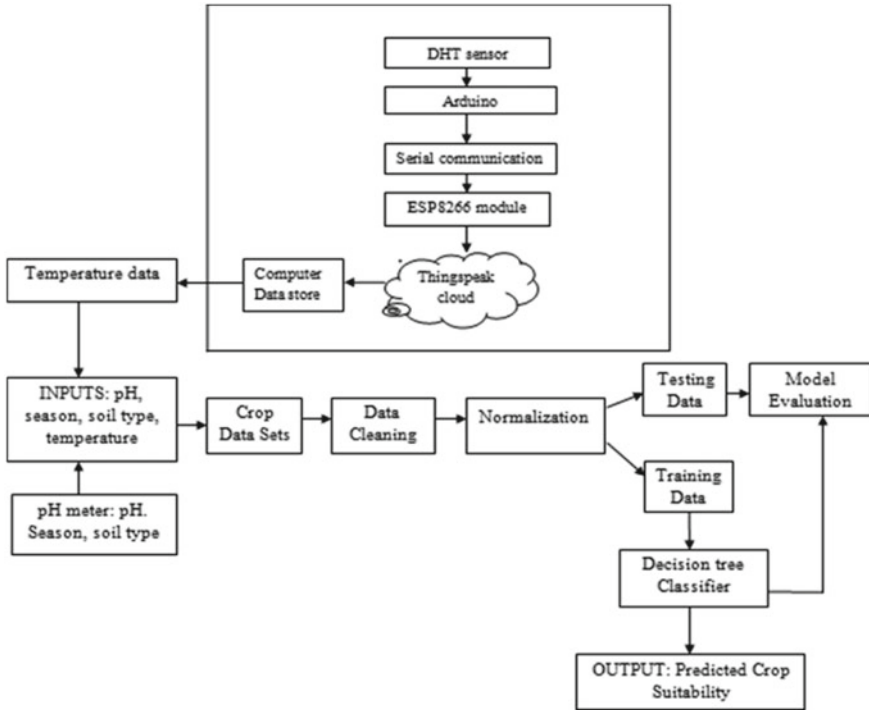


Fig. 1 Architecture diagram

3. Preliminary data processing which includes maintenance of missing data and other required functions.
4. Generalized data encryption which includes coding data categorical or independent variable.
5. Divide the database into a training set and a test set.
6. Feature rating.
7. Fit decision tree classifier in the training set.
8. Display a performance report of the model.
9. Predicting a new outcome.

6 Expected Results and Conclusion

The purpose of this program is to create a model that mimics the crop prediction aspect for the duration of one of a kind sorts of system learning levels contemplating live data for higher accuracy. The model is liable for collecting statistics approximately farmers’ knowledge along with crop sorts, soil kinds, soil cost-PH, and seasonal parameters including califice, rabies, and summer time crops. The understanding base also incorporates place facts on environmental parameters inclusive of high value and

occasional temperature value. Records processing became accrued. It also evaluates machine overall performance the use of a ramification of take a look at techniques. Yield changed into predicted based on installed policies. Crop parameters—soil type, pH, season, and temperature are protected in the forecast model.

References

1. Sonka S (2014) Big data and the ag sector: more than lots of numbers. *Int Food Agribus Manage Rev*
2. Fan T (2013) Smart agriculture based on cloud computing and IOT. *J Convergence Inf Technol (JCIT)*
3. Dahikar SS, Rode SV (2014) Agricultural crop yield prediction using artificial neural network approach. *Int J Innov Res Electr Electron (2)*
4. Tsai CW, Lai CF, Chiang MC, Yang LT (2014) Data mining for internet of things: a survey. *IEEE Commun Surv Amp Tutorials*
5. Kumar DA, Kannathasan N (2011) A survey on data mining and pattern recognition techniques for soil data mining. *IJCSI Int J Comput Sci*
6. Mankar AB, Burange MS (2014) Data mining—an evolutionary view of agriculture. *Int J Appl Innov Eng Manage (IJAIEM)*
7. Ramesh D, Vardhan BV (2013) Data mining techniques and applications to agricultural yield data. *Int J Adv Res Comput Commun Eng*
8. Rajesh D (2011) Application of spatial data mining for agriculture. *Int J Comput Appl*
9. Ananthara M, Arunkumar T, Hemavathy R (2013) Cry: an improved crop yield prediction model using bee hive clustering approach for agricultural data sets. *Pattern Recogn Inform Med Eng (PRIME)*
10. Narkhede U, Adhiya KP (2014) A study of clustering techniques for crop prediction—a survey. *Am Int J Res Sci, Technol, Eng Math* 45–48 ISSN 2328-3491
11. Dahikar SS, Rode SV (2014) Agricultural crop yield prediction using artificial neural network approach. 2(1):683–685
12. Bhangale PP, Patil YS, Patil DD, Implementation of improved crop yield prediction using neural network
13. Padmaja P, Sophia IJ, Hari HS, Kumar SS, Somu K et al (2021) Distribute the message over the network using another frequency and timing technique to circumvent the jammers. *J Nucl Eng Sci Power Gener Technol* 10:9
14. Thirupathi L, Padmanabhuni VN (2020) Protected framework to detect and mitigate attacks. *Int J Anal Exp Modal Anal XII(VI):2335–2337. 18.0002.IJAEMA.2020.V12I6.200001.0156858943*
15. Rekha S, Thirupathi L, Renikunta S, Gangula R (2021) Study of security issues and solutions in Internet of Things (IoT). *Mater Today: Proc* ISSN 2214-7853. <https://doi.org/10.1016/j.matpr.2021.07.295>
16. Gangula R, Thirupathi L, Parupati R, Sreeveda K, Gattoju S (2021) Ensemble machine learning based prediction of dengue disease with performance and accuracy elevation patterns. *Mater Today: Proc* ISSN 2214-7853. <https://doi.org/10.1016/j.matpr.2021.07.270>
17. Thirupathi L, Padmanabhuni VN (2021) Multi-level protection (MLP) policy implementation using graph database. *Int J Adv Comput Sci Appl (IJACSA)* 12(3). <https://doi.org/10.14569/IJACSA.2021.0120350>
18. Thirupathi L, et al (2021) *J Phys: Conf Ser* 2089 012049. <https://doi.org/10.1088/1742-6596/2089/1/012049>

19. Thirupathi L, et al (2021) J Phys: Conf Ser 2089 012050. <https://doi.org/10.1088/1742-6596/2089/1/012050>
20. Pratapagiri S, Gangula R, Ravi G, Srinivasulu B, Sowjanya B, Thirupathi L (2021) Early detection of plant leaf disease using convolutional neural networks. In: 2021 3rd international conference on electronics representation and algorithm (ICERA), pp 77–82. 9.1109/ICERA53111.2021.9538659

A Blockchain-Based and IoT-Powered Smart Parking System for Smart Cities



A. R. Sathya

Abstract Blockchain the decentralized, transparent, and immutable ledger technology is revolutionizing different business domains like FinTech, supply chain, health care, and governance. Automotive industry is one such domain where blockchain can be adopted for a decentralized access and operations. On the contrary, Internet of Things (IoT) also offers numerous opportunities for business that needs smart operations. Therefore, the combination of these promising technologies creates wider opportunities for development of efficient systems. This paper briefs how blockchain driven by smart contracts helps in parking lots powered with IoT helps in creating a smart parking system as there is a huge difficulty in finding parking ports in metro cities. The system can be automated with the help of smart contracts, and the IoT sensors help in easy finding of vacant spots and parking fee and fine.

Keywords Blockchain · Internet of Things · Smart parking · Smart contracts

1 Introduction

In recent days, finding a parking slot in urban cities is a real challenge. Sometimes it even leads to high priced slot bookings. Unavailability of parking space and overpriced reservations result in high traffic congestions and accidents [1]. This real-time problem needs a real-time solution where the users can find all parking-related information in a single platform [2]. Blockchain the radical technology has the potential to unravel various business opportunities and business process for various business domains [3]. Almost all business sectors are trying the possibility to adopt blockchain technology in their business processes for its unique features like security, transparency, distributed, and trust free [4].

IoT is another digital transformation technology which is revolutionizing the world right now. Almost all devices are connected to a sensor nowadays and transmits the data to cloud. Therefore, combining these two technologies can lead to smart and

A. R. Sathya (✉)

Department of Computer Science and Engineering, Faculty of Science and Technology, ICFAI Foundation for Higher Education, Hyderabad, Telangana 501203, India
e-mail: sathya.renu@gmail.com

efficient systems. IoT devices can utilize blockchain in a way to improve the security and transparency in their ecosystems [5]. Combination of these two technologies creates multiple use cases in several areas such as supply chain and logistics, smart homes, health care, automotive industry, agriculture, e-governance, and so on.

2 Convergence of Blockchain and IoT

Based on the benefits that blockchain offers, it is right to say that blockchain is becoming a third-generation security [6]. And in recent days, blockchain is often looked at the context of Internet of Things. It is claimed that the benefits of blockchain may not be solution for all the problems of digital economy, but it definitely plays a major role in the growing Internet of Things. By nature, IoT applications are distributed, and it is evident that blockchain will influence how the devices will interact with each other. It is aware that blockchain supports applications that involves transactions or interactions and that can be achieved with the help of smart contracts [7]. Using smart contracts, the IoT processes can be supported by blockchain. By this, blockchain improves the IoT features, cost, and compliances. As blockchain contributes to much of the digital infrastructure, the fusion of these two promising technologies will bring larger impacts to many areas ranging from data analysis to safety and security system which were of a centralized ecosystem. Some of the use cases of the convergence of blockchain and IoT are IoT infrastructure administration, supply chain, end user/consumer authentication, asset sharing system, smart contract agreement with security, transactions, and authentication as foundations. Figure 1 shows the convergence of technologies with different use cases.

3 Blockchain for IoT

With a safe and trustworthy time-stamped contractual agreement, blockchain technology might enable a simple framework for two or more devices to directly transfer a piece of data or digital assets with each other using smart contracts. Thus, allowing the smart devices to act independently without any central authority. Leveraging blockchain technology with IoT devices can unveil new opportunities to automate business processes without having an expensive yet complicate centralized environment [8]. The key benefits of blockchain and IoT interoperability are:

1. **Trust:** Blockchain reduces the risk of tampering thereby builds trust among the users and between the users and devices (IoT).
2. **Cost:** Blockchain removes the need for intermediaries and enables peer-to-peer communication. This reduces the cost involved to a greater extent.
3. **Speed:** The transactions over blockchain are instantaneous and reduces the delay which usually is the case in traditional systems.

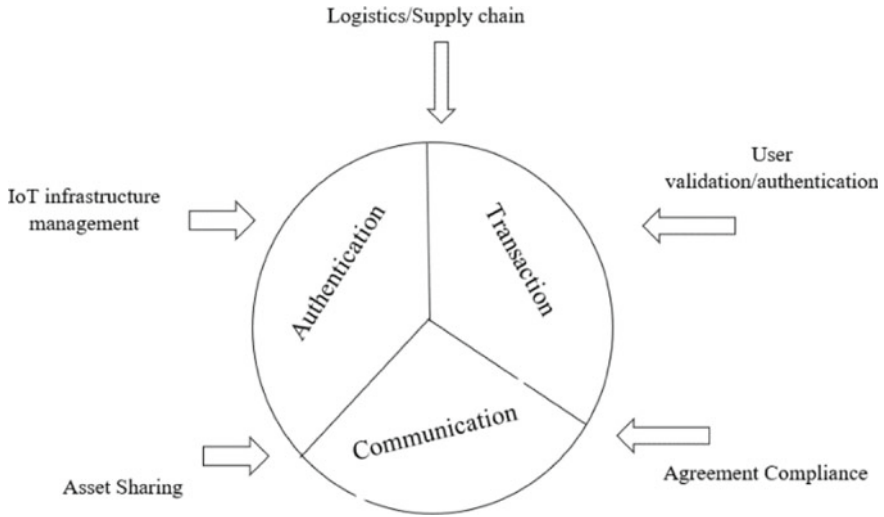


Fig. 1 Use cases of IoT and blockchain

4. **Cross-Communication:** IoT technology is centralized in nature which would be a hindrance for cross-device communications. However, blockchain is the solution for the problem.

Blockchain has the potential to empower IoT devices with enhanced security and transparency in an IoT environment [9]. The integration of blockchain and IoT is already making its mark in popular banks and financial institutions like Deutsche bank and HSBC. Similarly, other business sectors are also leaning towards these integrations and is shown Fig. 2.

4 Blockchain and IoT for Automotive Industry

IoT-enabled sensors are being used by the automobile industry to develop fully automated vehicles. Enabling IoT-based solutions in automobile sector to a distributed network allows many people to share critical information quickly. The automotive sector is an excellent blockchain IoT use case, as it has the potential to revolutionize automatic and smart fuel payments, smart parking, traffic control, and automated cars. The various applications where IoT and Blockchain can be adopted in automotive industry are shown in Fig. 3.

Many smart transport applications have been developed as a result of widespread usage of gadgets in smart cities. Smart parking is one of the developments that uses extensive sensors and flexible payment options to provide easy-to-use parking services to daily commuters. But existing smart parking solutions are inadequate to

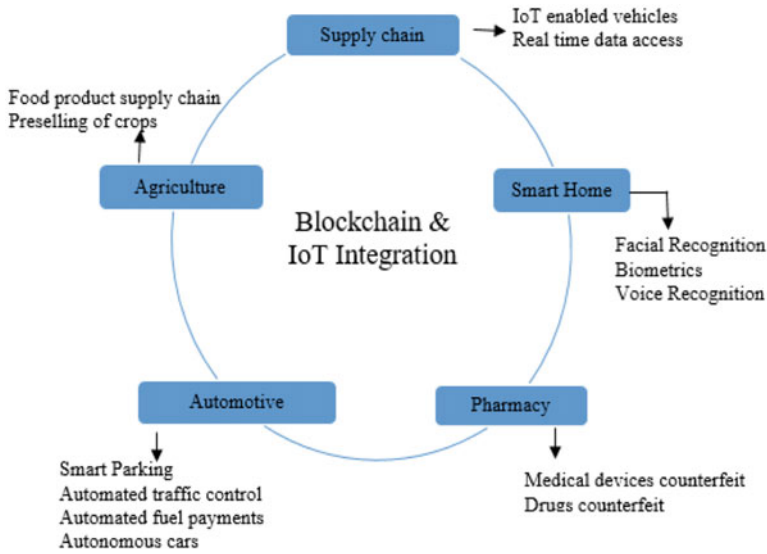
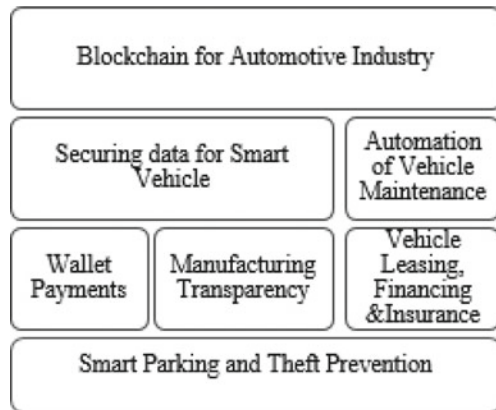


Fig. 2 Integration of blockchain and IoT for various business sector

Fig. 3 Blockchain in automotive industry



fulfil the needs of the commuters. For example, there is no system that can provide specific parking information like available parking spaces, price, and proximity.

One of the major challenges in solving the above-mentioned problem is reliability and integrity of the parking space information. The parking service providers have to reveal their sensitive parking space information onto a system where trust is a major factor. At the same time, the system should provide data which cannot be tampered by any intruder. Therefore, a system with all parking information, integrity, and trust is much needed [10]. This paper intends to propose a blockchain-based system for smart parking using IoT devices. The real-time parking information can be made

available in a decentralized environment and use IoT sensors to monitor the parking space. The IoT devices detect the location of vehicles in real time there by finding the availability of the vacant space in the parking area [2].

5 The Proposed System

In a smart parking system, there can be several stakeholders as a part of the network. From a blockchain context, these stakeholders are considered as nodes of the decentralized network. They can be a land owner, parking service provider, or even a government body. All these stakeholders provide parking-related information like, the fees, location, and other related data over the network. A land owner may be willing to rent or lease out his land for parking or to a parking service provider. This unused land can be created as a digital asset and by deploying smart contract between the land owner and the service provider. The process of renting/lease can be carried out without much complexity. Smart contracts would, therefore, execute the lease, cost, and other terms of the agreement [11].

Most of the existing parking solutions suffers single point operational failures. The system would be impossible to work effectively if there was a disparity in the central server. Thereby leaving the end user stranded as they will not be accessing the server data. However using blockchain technology, a distributed digital ledger will be created where the customers will access the parking data from multiple parking providers using a mobile/web application. And any transaction carried out on the blockchain network is direct and does not require any third-party agreements. This will help the parking providers and government agencies in successfully monetizing parking spaces and developing a transparent revenue model (Fig. 4).

A real-time parking data can be obtained by connecting IoT sensors to the smart parking platforms. This will help in retrieving the most up to date information on vacant parking spots to the user's proximity in a blockchain network. Blockchain networks can also provide data like the best route to take to get to the allotted parking place. If the recommended parking spot or route is unavailable, the network provides alternate parking spots and routes that are less crowded [12]. Smart contracts can be deployed to reserve a parking spot in a blockchain network. Again, IoT sensors can be used to calculate the amount of time a vehicle is parked in the allocated spot based on which the parking fee or fine can be calculated. Payment can be made either through fiat currency or crypto wallets. All parking transaction on the blockchain network will be validated and confirmed using a consensus mechanism [13].

6 IoT and Blockchain Challenges

Not just the benefits these radical technologies have some key challenges which cannot be ignored. Some of the challenges of these technologies are:

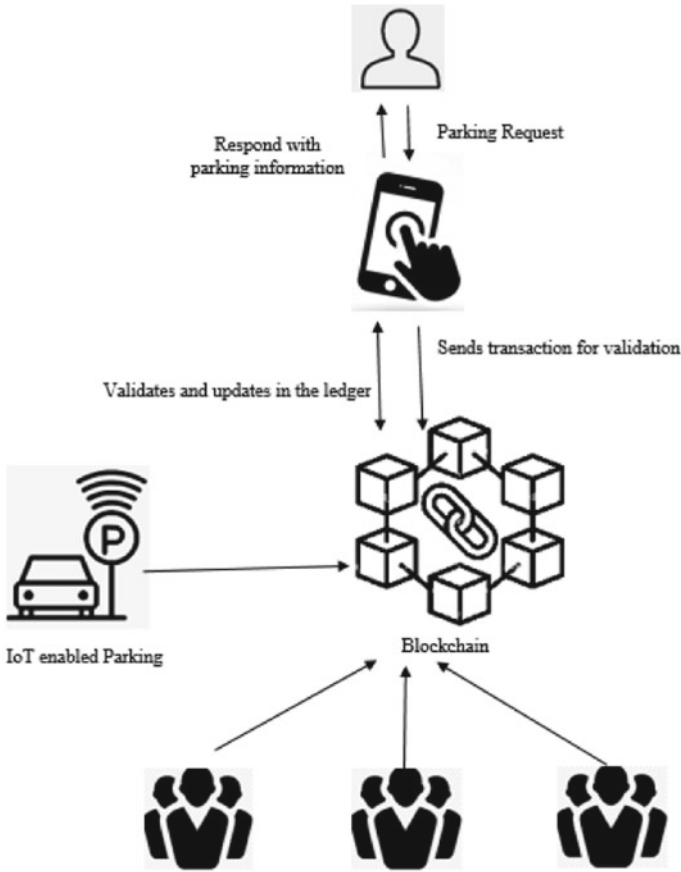


Fig. 4 Proposed blockchain-based parking system

Security: It is a well-known fact that IoT applications suffer security. Even though blockchain seem to solve the security aspects of IoT applications, researchers are still not clear of the efficiency of the blockchain-based IoT systems. Even if blockchain network is robust and hackproof, but if the OS of the IoT device is not updated, then it is possible to hack it at the edge level [14].

Stakeholders: The blockchain-based IoT environment is too broad. And the business and the practical ecosystem of the technologies need many stakeholders to be involved and many contracts to be agreed upon. This develops a complex environment to opens operational challenges [15].

Ownership: Agreements are always complex even outside blockchain context. Similarly, the ownership responsibility to own the legal compliances involved if certain actions are performed automatically by a device executed by a blockchain-based application is a challenge till date.

7 Conclusion

The convergence of blockchain and IoT can be incredible. Intelligent traffic management systems will be a necessity as smart cities emerge as the number of vehicles on the road grows. The search for parking space increases the mobility concerns. This paper suggests an IoT-powered and blockchain-based model for increasing and managed parking spots. Smart contracts manage the revenue systems and create a better business model without much complexities. The parking system is handled and monitored by IoT-powered sensors connected to the network, and the end users can be assisted with location, payment, and reservation via a user application.

References

1. Taherkhani MA, Kawaguchi R, Shirmohammad N, Sato M (2016) Blue parking: An IOT based parking reservation service for smart cities. In: Proceedings of the second international conference on IoT in Urban space. ACM, pp 86–88
2. Zajam A, Dholay S (2018) Detecting efficient parking space using smart parking. In: 2018 9th international conference on computing, communication and networking technologies (ICCCNT). IEEE, pp 1–7
3. Mendling J, Weber I, Aalst WV, Brocke JV, Cabanillas C, Daniel F, Debois S, Ciccio CD, Dumas M, Dustdar S, Gal A, García-Bañuelos L, Governatori G, Hull R, La Rosa M, Leopold H, Leymann F, Recker J, Reichert M, Zhu L (2018) Blockchains for business process management—challenges and opportunities. *ACM Trans Manage Inf Syst* In press, Accepted. <https://doi.org/10.1145/3183367>
4. Panda SK, Elngar AA, Balas VE, Kayed M (eds) (2020) Bitcoin and blockchain: history and current applications. 1st edn. CRC Press. <https://doi.org/10.1201/9781003032588>
5. Yarali A (2022) Digital transformation trends in the automotive industry. In: Intelligent connectivity: AI, IoT, and 5G. IEEE, pp 223–237. <https://doi.org/10.1002/9781119685265.ch12>
6. Sathya AR, Banik BG (2020) A comprehensive study of blockchain services: future of cryptography. *Int J Adv Comput Sci Appl (IJACSA)* 11(10). <https://doi.org/10.14569/IJACSA.2020.0111037>
7. Buterin V (2014) A next-generation smart contract and decentralized application platform. White paper
8. Sadawi AA, Hassan MS, Ndiaye M (2021) A survey on the integration of blockchain with IoT to enhance performance and eliminate challenges. *IEEE Access* 9:54478–54497. <https://doi.org/10.1109/ACCESS.2021.3070555>
9. Panda SK, Rao DC, Satapathy SC (2021) An investigation into the usability of blockchain technology in the Internet of Things. In: Bhateja V, Satapathy SC, Travieso-González CM, Aradhya VNM (eds) Data engineering and intelligent computing. *Advances in Intelligent Systems and Computing*, vol 1. Springer, Singapore. https://doi.org/10.1007/978-981-16-0171-2_53
10. Da Silva Rodrigues CK, Rocha V (2021) Towards blockchain for suitable efficiency and data integrity of IOT ecosystem transactions. *IEEE Lat Am Trans* 19(7):1199–1206. <https://doi.org/10.1109/TLA.2021.9461849>
11. Panda SK, Satapathy SC (2021) An investigation into smart contract deployment on ethereum platform using web3.js and solidity using blockchain. In: Bhateja V, Satapathy SC, Travieso-González CM, Aradhya VNM (eds) Data engineering and intelligent computing. *Advances in Intelligent Systems and Computing*, vol 1. Springer, Singapore. https://doi.org/10.1007/978-981-16-0171-2_52

12. Rahaman MS, Mei Y, Hamilton M, Salim FD (2017) Capra: a contour-based accessible path routing algorithm. *Inf Sci* 385–386:157–173
13. Jennath HS, Adarsh S, Chandran NV, Ananthan R, Sabir A, Asharaf S (2019) Parkchain: a blockchain powered parking solution for smart cities. *Front Blockchain* 2:6. <https://doi.org/10.3389/fbloc.2019.00006>
14. Panda SK, Jena AK, Swain SK, Satapathy SC (eds) (2021) *Blockchain technology: applications and challenges*. Springer, Intelligent Systems Reference Library. <https://doi.org/10.1007/978-3-030-69395-4>
15. Panda SK, Dash SP, Jena AK (2021) Optimization of block query response using evolutionary algorithm. In: Bhateja V, Satapathy SC, Travieso-González CM, Aradhya VNM (eds) *Data engineering and intelligent computing*. *Advances in Intelligent Systems and Computing*, vol 1. Springer, Singapore. https://doi.org/10.1007/978-981-16-0171-2_54

Proximity Coupled Antenna with Stable Performance and High Body Antenna Isolation for IoT-Based Devices



Anupma Gupta, Bhawna Goyal, Ayush Dogra, and Rohit Anand

Abstract A proximity coupled and parallel slot patch is considered for on-body and off-body communication for IoT-based health-monitoring devices. Due to virtue of proximity coupled feed various significant features such as high efficiency, unidirectional radiation pattern, large bandwidth, and low SAR are obtained, which are necessary for WBAN communication. Full ground plane structure with thick substrate covers the radiating patch from the tissue, provides good isolation and avoids frequency detuning when placed directly on tissue. Results show that antenna impedance, resonating frequency bands, and radiation pattern remain stable in biological environment.

Keywords Antenna · IoT · Stable radiation performance · SAR · Proximity coupled

1 Introduction

Over the last decade, realm of wearable smart devices is getting more interest for research and progressions. People are adapting to the fast-living style which has opened the way to the bio-telemetry. Regular check-ups and health monitoring is avoided due to which millions of persons are exposed to fatal ailments. Pro-active health-monitoring devices are making inroads for the premature recognition of the health issues. Antenna is one of the key components for the wearable (on-body) and implantable (in-body) health-monitoring devices to implement the IoT and bio-telemetry [1].

A. Gupta (✉) · B. Goyal
Department of ECE, Chandigarh University, Mohali, India
e-mail: anupmagupta31@gmail.com; anupma.e10352@cumail.in

A. Dogra
Ronin Institute, Montclair, NJ 07043, USA

R. Anand
ECE Department, DSEU, G.B. Pant Okhla-1 Campus, New Delhi, India

Antenna performance degrades significantly when it is deployed on the human body. Electromagnetic (EM) waves interface with heterogeneous multi-layered tissue structure consisting of bone, muscle, fat, and skin and generates internal scattering and reflection. Thus, designing of antenna for biological operating environment is very inspiring and challenging. Scattered and reflected waves interact with the impedance matching and varies the radiation (power) patterns of antenna [2, 3]. Beside this, it is practically impossible to maintain the fixed gap between body and the deployed device due to various postures and movements. A minor change in the body and antenna interface distance may cause a major difference in antenna reflection coefficient and resonance frequency [4]. Therefore, to establish the reliable communication link from the on-body wearable sensor node to the off-body monitoring device, an antenna with robust and stable characteristics, high gain, and efficiency is required.

Various antenna designs with number of isolation methods have been studied including AMC [5] and EBG [6] integrated structures, aperture coupled [7], stacked patch [8], SIW [9, 10], magneto-electrical dipole [11], circular patch antenna [12, 13], proximity coupled [14], and dipole with reflector [15]. In [5], to achieve the finest performance, a constant gap has to be kept between AMC structure and antenna. In addition to this, constant space between antenna and skin is also need to be maintain for avoiding impedance variation and frequency detuning. In [14], wide band proximity coupled antenna is designed on an extremely low-profile textile substrate. To reduce the radiations towards the body surface, front to back ratio of an aperture-coupled antenna is improved in [7]. However, radiation characteristics are sensitive to the bending along various radii. A coplanar waveguide (CPW) fed antenna with an octagonal-shaped radiator has been designed to operate in the close vicinity of a human body, bidirectional radiation pattern, and the high SAR value makes antenna unsuitable for real-time applications. Further, an additional full ground plane is added below the substrate as a reflecting surface to mitigate the consequence of conducting body tissue on antenna performance [8]. Electromagnetic radiations are shielded from the body tissue by the surface integrated waveguide technology [9]. In a dual band wearable antenna structure, magneto-electrical-dipole has been used to achieve the stable on-body radiation characteristics [11]. Multi-layered thick rubber polymer substrate has been added with the meandered dipole structure for reliable on and off-body antenna [14]. In [16], it has been observed that thin substrate causes increase in near E-field that result in higher specific absorption rate.

In this paper, a dual band antenna configuration at 2.45 GHz and 5.8 GHz ISM band has been proposed for on and off-body communication, respectively. Antenna is designed to attain wide bandwidth using proximity coupled patch antenna. Beside this a full ground plane buffers the near field power from the tissue and provides good skin-antenna separation and reduces SAR.

2 Antenna Design

The geometry of proximity coupled; dual band patch antenna is shown in Fig. 1. Antenna is designed using FR-4 as a substrate [17] for both substrate layers with ‘h = 3.2 mm’ each. A rectangular radiating patch with two parallel vertical slots is printed on the upper surface of substrate. Slots are symmetrical about the y-axis. This substrate is placed on the second substrate covered with full ground plane on its bottom side and has a conductive strip on its upper side working as feed line. This feed line is proximity coupled feeding that electromagnetically couples the radiator. Antenna design approach is taken as the characteristic’s impedance Z_f of the feed line and antenna radiator impedance Z_{rad} would be equal to 50Ω . In Fig. 2, flow chart represents the antenna design approach. Table 1 gives the parameters and dimensions for the proposed antenna.

Width ‘wf’ of the strip line is calculated using the design equations given in [18].

$$Z_f = \frac{120 \times \pi}{\sqrt{\epsilon_{reff}}} \left[\frac{w_{eff}}{h} + 1.393 + 0.667 \times \ln\left(\frac{w_{eff}}{h} + 1.444\right) \right]^{-1} \tag{1}$$

$$w_{eff} = wf + 0.398 \times t \left[1 + \ln\left(\frac{2 \times h}{t}\right) \right] \tag{2}$$

$$\epsilon_{reff} = \epsilon_r \left[1 - \exp\left(\frac{-1.55 \times (2 \times h + t)}{h}\right) \right] \tag{3}$$

Considering the electric permittivity ‘ ϵ_r ’ as 4.4 for the substrate used, ‘wf’ is obtained as 5.714 mm from Eqs. (1)–(3) for $Z_f = 50 \Omega$. Figure 3 indicates the return

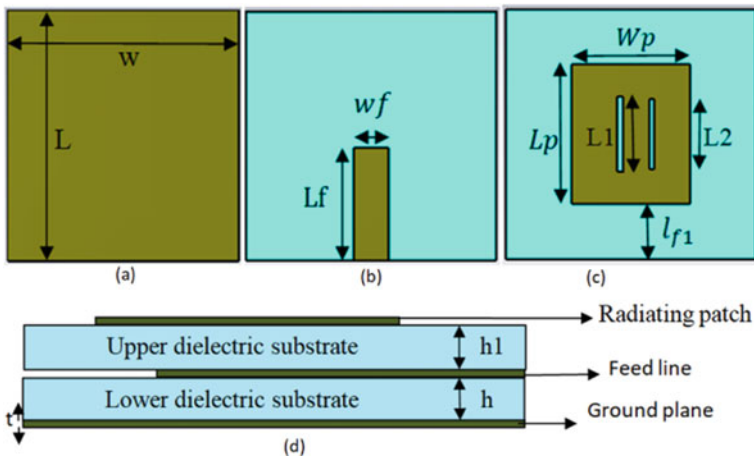


Fig. 1 Geometrical structure, **a** back view of bottom substrate, **b** front view of bottom substrate, **c** top view of upper substrate, and **d** side view

Fig. 2 Flow chart for design procedure of the proposed antenna

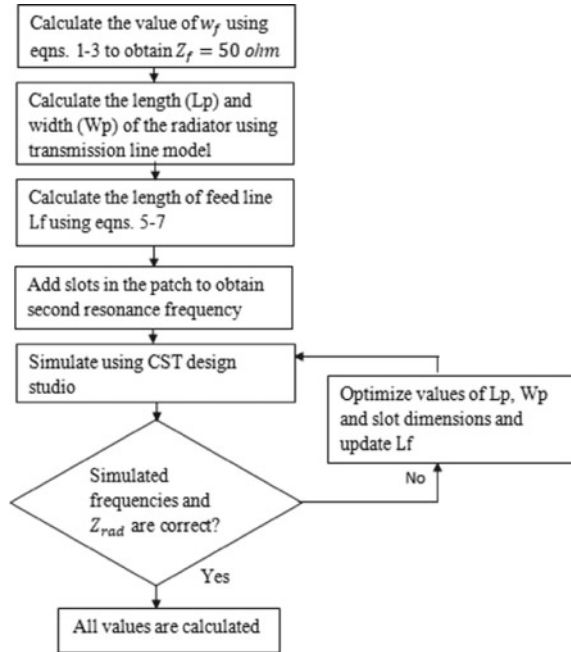


Table 1 Various parameters and their values for the proposed antenna

Dimension parameter	Value in mm	Dimension parameter	Value in mm
W	46	h	3.2
L	46	t	0.035
L2	9.2	Lp	24.3
h1	3.2	L _{fl}	26.22
L1	10	Lf	40
Wf	6.33	wp	22.13

loss for varying feed width from 5 to 7 mm, impedance of antenna deteriorates with decreasing wf at lower resonance. Increasing value of feed width affects the impedance at upper frequency. Thus, to obtain the optimal performance at both the operating bands, value of feed length is imposed as 6.33 mm. Length of the radiating patch Lp defines the resonating frequency. Initially, Lp is calculated as 25.8 mm (0.5λ) for the 2.5 GHz resonating frequency. Parallel slots are designed on the radiator surface to achieve the 2.45 GHz band. Width of the patch Wp, slot length, and gap between the slots are optimized [19, 20] to attain the impedance matching. Maximum coupling is attained if the feed line terminates at the centre of the patch [21–23]. Length of feed line ‘L_f’ is calculated using Eqs. (5)–(7).

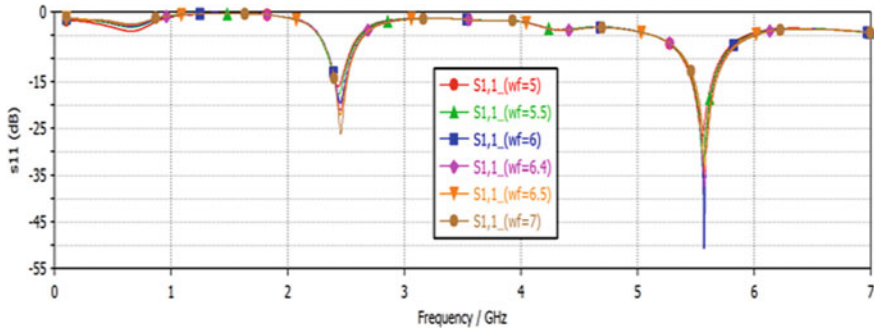


Fig. 3 Return loss of proposed structure with different values of feed width 'wf'

$$Z_{\text{rad}} = \frac{Z_f^2}{Z_{\text{in}}} \quad (4)$$

$$l_{f1} = \frac{c}{4 \times f \times \sqrt{\epsilon_{\text{reff}}}} \quad (5)$$

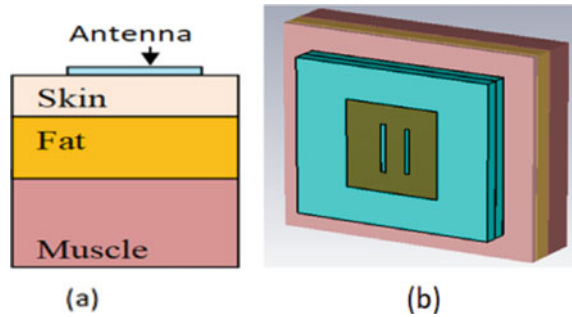
$$l_{f2} = L_p/2 \quad (6)$$

$$L_f = l_{f1} + l_{f2} \quad (7)$$

3 Design of Tissue Model

It is clear from the literature studied that impedance and radiation characteristics of antenna varies significantly when operated in the close approximation of human body. In turn, human tissues are also faces the diverse impact of electromagnetic power. While designing and simulating the antenna, it is required to consider this effect. Thus, a tissue phantom model is considered while simulation. Muscle layer has the maximum water content and electrical permittivity. Planar dimensions of phantom are 80 mm \times 80 mm. Thickness of muscle, fat, and skin is 12 mm, 5 mm, and 2 mm, respectively. Figure 4 shows the simulation environment of antenna and phantom model structure [24]. Fabricated antenna is experimentally measured on a 2/3 muscle equivalent phantom gel. This gel mimics the actual bio-tissue surroundings for the antenna measurement setup. References [12, 24] are considered to fabricate the gel.

Fig. 4 **a** Stacked multi-layered tissue model and **b** prospective view of antenna simulation environment



4 Result Analysis

A fabricated prototype for the measurement of the proposed structure is represented in Fig. 5. Grounded feed line of the proximity coupled antenna is connected to a $50\ \Omega$ SMA connector at the lower substrate.

Antenna behaviour is evaluated for both the on-body and free space operation. Antenna is placed directly on phantom gel to measure the maximum frequency detuning and impedance mismatch. Figures 6 and 7 show the simulated and measured return loss in free space and on the tissue gel.

Measured bandwidth on phantom gel is 330 MHz which is larger than the simulated bandwidth of 260 MHz at the 2.45 GHz resonance. Similarly, for the 5.8 GHz band measured bandwidth on gel is 550 MHz, while simulated bandwidth is 415 MHz. This difference is due to the manual fabrication process and variation in gap between the two substrate layers. Measured free space and on gel return loss are compared in Figure to ensure the robustness of antenna. A very small variation in impedance and resonance frequency is observed when antenna is operated directly on human body.

Simulated and measured radiation patterns of antenna are shown in Fig. 8. It can be analysed that antenna has unidirectional radiation pattern. Antenna has maximum

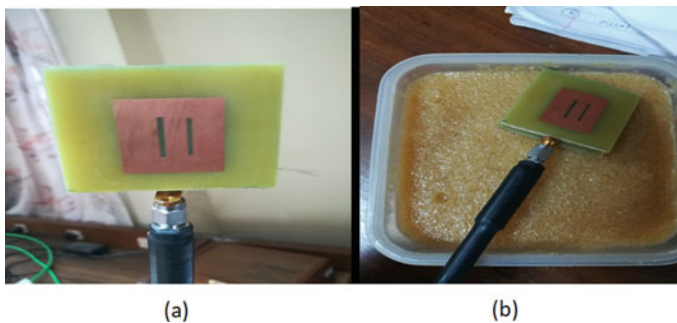


Fig. 5 Fabricated prototype: **a** in free space and **b** on phantom gel

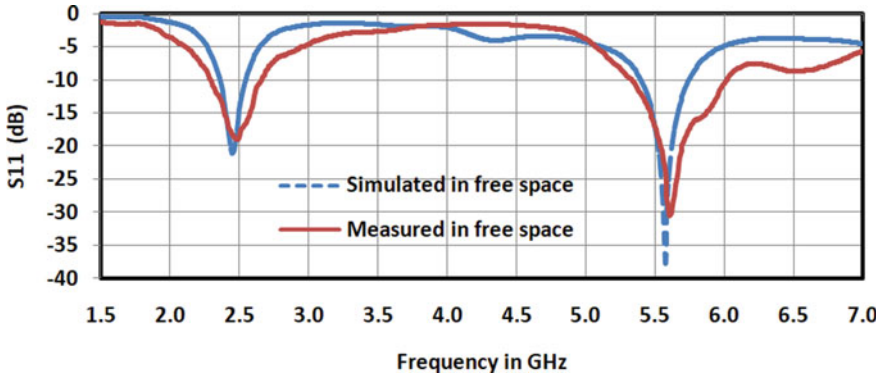


Fig. 6 Return loss of antenna in free space

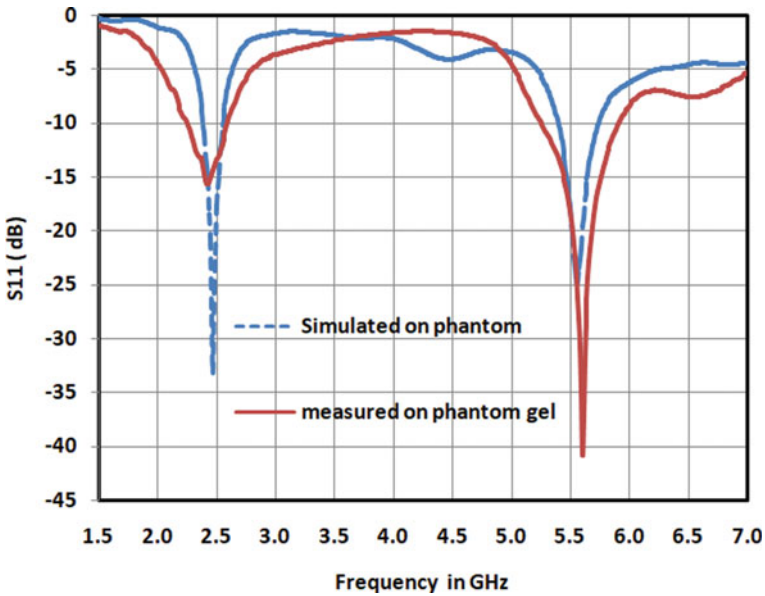


Fig. 7 Return loss of antenna on phantom gel

radiation in $+z$ direction that results in very low backward radiation (towards the body) and also reduces the absorption of electromagnetic radiation by human body. Loading of tissue model has changed the radiation characteristics in $-z$ direction. Directive gain of antenna has been improved from 5.93 dBi (free space) to 6.96 dBi (on body) at 2.45 GHz and from 6.63 dBi (free space) to 9.07 dBi (GHz) at 5.8 GHz. It is due to the reflection of electromagnetic radiations from the multi-layered tissue structure with different dielectric permittivity.

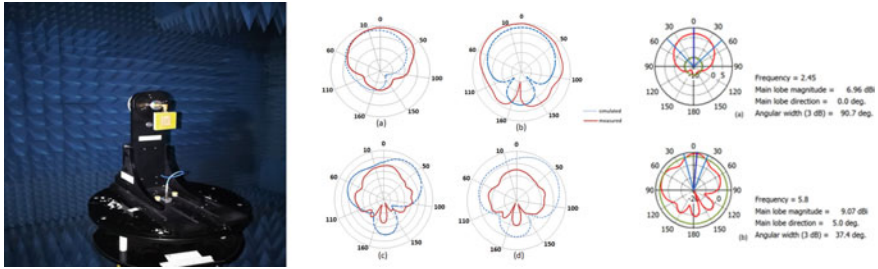


Fig. 8 Radiation pattern of antenna in free space (a and c) E-plane at 2.45/5.8 GHz (b and d) H-plane at 2.45/5.8 GHz (e and f) on tissue model

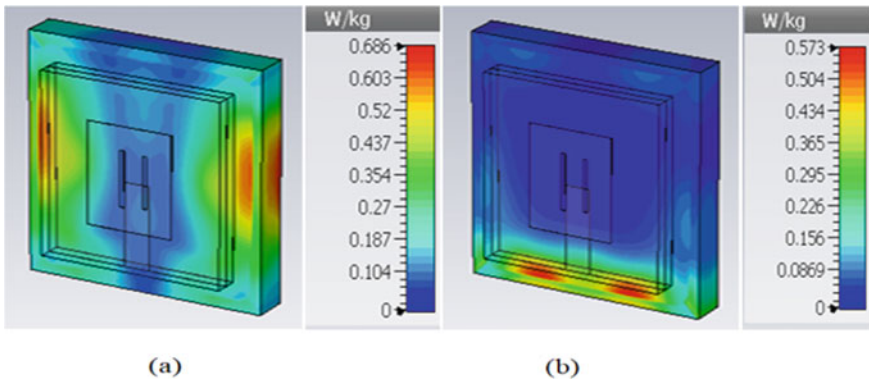


Fig. 9 Simulated SAR value of antenna on stacked tissue model: a at 2.45 GHz and b at 5.8 GHz for 0.1 W of input power

Absorbed electromagnetic radiations by human tissue can be considered by the standard SAR parameter. Simulated SAR of the antenna is represented in Fig. 9. Maximum SAR is 0.686 W/kg for 2.45 GHz frequency and 0.573 W/kg for 5.8 GHz frequency measured for 0.1 W of input power.

5 Conclusion

Proximity coupled antenna topology is used to design a dual band antenna for on/off-body communication. It leads to improve the antenna performance near the human body. A prototype covering 2.45/5.8 GHz ISM bands was designed, fabricated, and measured in free space and on muscle equivalent phantom gel. Antenna’s measured bandwidths are 330/540 MHz for 2.45/5.8 GHz bands. Stable performance was observed when antenna was placed on body model. Unidirectional radiation pattern

and thick dielectric substrate of antenna has reduced the absorption of electromagnetic radiation by tissue. No frequency detuning and impedance mismatch were found when antenna is operated directly on the tissue. Finally, SAR value was simulated for both the operating bands to ensure the safety of user; it is 0.686/0.583 W/kg for 10 g of tissue model. Simulated and measured results show that the proposed antenna is a good candidate for body-worn devices.

References

1. Zhang J, Yan S, Vandenbosch GAE (2017) A miniature feeding network for aperture-coupled wearable antennas. *IEEE Trans Antennas Propag* 65(5):2650–2654
2. Tak J, Woo S, Kwon J, Choi J (2016) Dual-band dual-mode patch antenna for on-/off-body WBAN communications. *IEEE Antennas Wirel Propag Lett* 15:348–351
3. Tsai CL, Chen K, Yang C (2016) Implantable wideband low-specific-absorption-rate antenna on a thin flexible substrate. *IEEE Antennas Wirel Propag Lett* 15:1048–1052
4. Roy BV, Simorangkir B, Yang Y, Matekovits L, Esselle KP (2017) Dual-band dual-mode textile antenna on PDMS substrate for body-centric communications. *IEEE Antennas Wirel Propag Lett* 16:677–680
5. Grilo M, Seko MH, Corraera FS (2016) Wearable textile patch antenna fed by proximity coupling with increased bandwidth. *Microwave Opt Technol Lett* 58(8):1906–1911
6. Poffelie LY, Soh PJ, Yan S, Vandenbosch GAE (2016) A high-fidelity all-textile UWB antenna with low back radiation for off-body WBAN applications. *IEEE Trans Antennas Propag* 64(2):757–760
7. Yan S, Soh PJ, Vandenbosch GAE (2015) Wearable dual-band magneto-electric dipole antenna for WBAN/WLAN applications. *IEEE Trans Antennas Propag* 63(9):4165–4169
8. Kumar V, Gupta B (2016) On-body measurements of SS-UWB patch antenna for WBAN applications. *Int J Electron Commun (AEÜ)* 72:184–191
9. Al-Sehemi A, Al-Ghamdi A, Dishovsky N, Atanasov N, Atanasova G (2017) On-body investigation of a compact planar antenna on multilayer polymer composite for body-centric wireless communication. *Int J Electron Commun (AEU)* 82:20–29
10. IPC Standard IPC-2141A (2004) Design guide for high-speed controlled impedance circuit boards
11. Pozar DM, Kaufman B (1987) Increasing the bandwidth of a microstrip antenna by proximity coupling. *Electron Lett* 23:368–369
12. Balanis CA (2005) *Antenna theory: analysis and design*, 3rd edn. Wiley, Hoboken
13. Mersani A, Lotfi O, Ribero J-M (2018) Design of a textile antenna with artificial magnetic conductor for wearable applications. *Microwave Opt Technol Lett* 60:1343–1349
14. Gao G, Hu B, Wang S, Yang C (2018) Wearable planar inverted-F antenna with stable characteristic and low specific absorption rate. *Microwave Opt Technol Lett* 60:876–882
15. Agneessens S (2018) Coupled eighth-mode substrate integrated waveguide antenna: small and wideband with high body antenna isolation. *IEEE Access* 6:1595–1602
16. Movassaghi S, Abolhasan M, Lipman J, Smith D, Jamalipour A (2014) Wireless body area networks: a survey. *IEEE Commun Tutorials* 16(3):1658–1686
17. Anand R, Chawla P (2020) Optimization of inscribed hexagonal fractal slotted microstrip antenna using modified lightning attachment procedure optimization. *Int J Microwave Wirel Technol* 12(6):519–530
18. Gupta A, Kansal A, Chawla P (2018) A review of antennas for wireless body area network devices. In: *IEEE conference on computing for sustainable global development, India*
19. Anand R, Chawla P (2016) A review on the optimization techniques for bio-inspired antenna design. In: *2016 3rd international conference on computing for sustainable global development (INDIACom)*. IEEE, pp 2228–2233

20. Chawla P, Anand R (2017) Micro-switch design and its optimization using pattern search algorithm for applications in reconfigurable antenna. *Modern Antenna Syst* 10
21. Dahiya A, Anand R, Sindhwani N, Deshwal D (2021) Design and construction of a low loss substrate integrated waveguide (SIW) for S band and C band applications. *Mapan* 36:355–363
22. Agneessens S, Lemey S, Vervust T, Rogier H (2015) Wearable, small, and robust: the circular quarter-mode textile antenna. *Antennas Wirel Propag Lett* 14:1482–1485
23. Dahiya A, Anand R, Sindhwani N, Kumar D (2021) A novel multi-band high-gain slotted fractal antenna using various substrates for X-band and Ku-band applications. *MAPAN* 1–9. <https://doi.org/10.1007/s12647-021-00508-3>
24. Shakib M-N, Moghavvemi M, Mahadi W (2017) Design of a tri-band off-body antenna for WBAN communication. *IEEE Antennas Wirel Propag Lett* 16:210–213

Microscopic and Ultrasonic Super-Resolution for Accurate Diagnosis and Treatment Planning



Shivam Sharma, Ritika Rattan, Bhawna Goyal, Ayush Dogra,
and Rohit Anand

Abstract Super-resolution is a techniques use to increase the resolution of an image. Super-resolution to notice each and every section of lesion image, and it also raise the probability to identify and heal the problem. In this paper, we will observe the microscopic and ultrasonic super-solution for accurate diagnosis and treatment planning like brain surgery, lesion images, and liver cancer. With the advancement in the medical image fusion method and system, this system is successfully bid to detect tumor. Medical imaging may face trouble, due to intense location of the lesion, operation background, and other condition of disease. Image fusion method is successful to mark these types of challenges. By using this method, one can obtain real-time image which is helpful in finding location of the problem.

Keywords Microscopic and ultrasonic super solution · Lesion images · Image fusion method

1 Introduction

In recent years, there is increase of new methods and techniques in the medical field or health care. The new characteristics presentation studying techniques such as deep learning and image fusion has enhanced result [1]. With the advancement of the deep learning method, convolution neural networks (CNN) have been shown a strong tool for digital observation [2–5]. CNN can significantly decrease the number of specification of neural network and at the same time, lower the complication in the neural network [3]. Medical imaging like X-Ray, CT scan, ultrasound, and other

S. Sharma · R. Rattan (✉) · B. Goyal

Department of Electronics and Communication Engineering, Chandigarh University, Mohali,
India

e-mail: ritisharma58@gmail.com

A. Dogra

Ronin Institute, Montclair, NJ 07043, USA

R. Anand

Department of ECE, DSEU, G.B.Pant Okhla-1 Campus, New Delhi, India

are commonly used in the medical field to examine different area in this field [6–8]. Doctors are bounded with low resolution images due to which they will not be able to clearly notice or observe the factor in lesion image, which is not right or truthful diagnosis and treatment of infection and disease.

With the reconstruction of super-resolution images from L.R images help the doctor to notice each and every factor of medical images and will also raise the likelihood of disease to be diagnosis and get cured. Accordingly, super-resolution is very important in the medical image field. There are two important types of medical imaging. First one is anatomical mode that mostly gives anatomical data with H.R, X-Ray imaging, and CT imaging comes under the classification of anatomical imaging. The second is functional imaging that gives functional metabolic data. Single photograph emanation processed tomography and position discharge tomography. SPECT and PET, these two comes under functional imaging. All these accessible imaging techniques have separate durability and flaws. So, an ideal mix of these modes of imaging will help to get the information from different sides of human body in a single medical image. Such type of image can perfectly show the internal structure and function of the human body.

Medical image

1. CT imaging

An X-Ray flash is utilized to scan the internal structure up to fixed depth. In this method, an indicator will accept x-attenuation values of the different organ in separate direction, accompany by acquiring the digital matrix of tissue attenuation coefficient of inspecting thickness besides the information modification.

2. PET

It comes under medicine functional imaging method utilized to notice metabolic procedure in tissue of organ as support to identify the disease. In positron emission tomography (PET), two photons are released in nearly inverse direction are registered at the same time by ring pointer circling the patient, the PET can exactly find and inspect the spread or scattering of radioactive named drug in the human body. After that digital reconstruction of 3D human body image is attained [9]. So, PET is functional imaging method with intense vulnerability and construction support in depicting metabolism of liver cancer, pointing reappearance and analyzing the end result of radio frequency.

3. SPECT

It comes under functional imaging. It is an imaging tool that gives 3D images of the scattering of radioactive molecule injected into the human body which is obtained by different two dimensional images of human body from several point of view or different areas of human body that are need to be examine. The major contrast in SPECT and PET is the decay procedure of radioactive utilized. SPECT calculate photon of gamma decay where as PET can examine the use of 0.511-kew annihilation photons which are created when positron are released from radioactive, slow down, and join with free electrons in the organs in human body.

2 Inoperative Ultrasound (IoUS)

It is a three-dimensional device that provide a real-time image of any shape medical surgical area.

1. Imaging modalities for interoperative ultrasound

The 3D interoperative ultrasound technique utilizes so called pulse-echoed method. But actually they depend upon piezoelectric transducer releasing pulse at a frequency 1–20 MHz, and on the note of respected events created by sound pulse [9, 10] (Fig. 1).

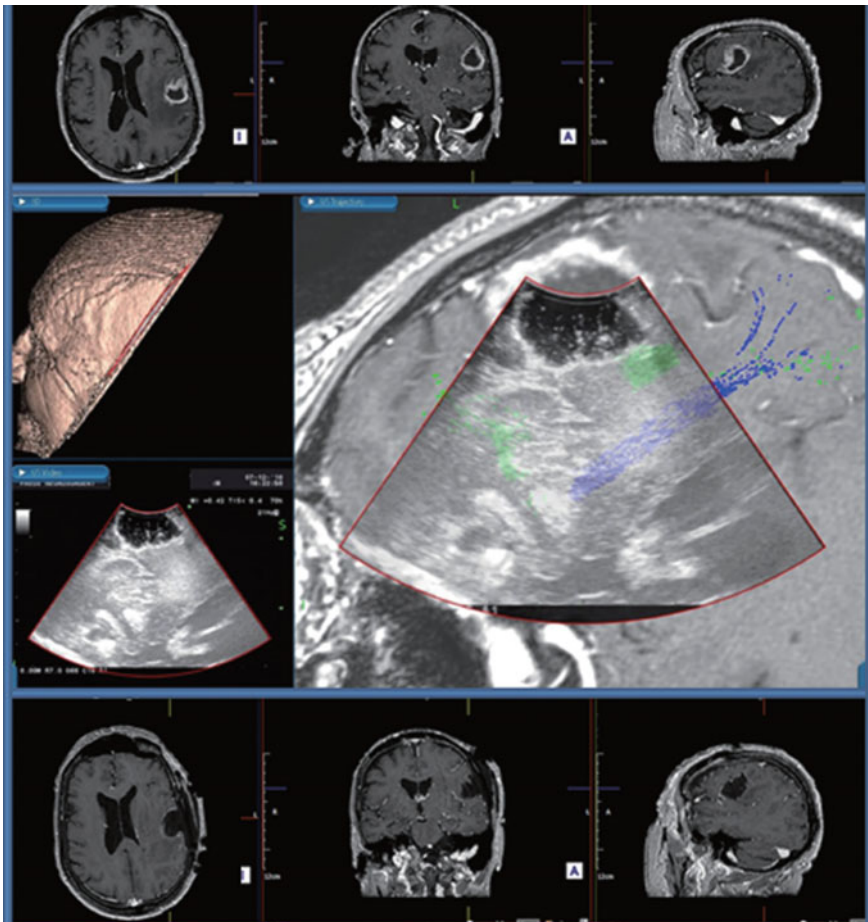


Fig. 1 MRI image [9]

(top line displaying an uneven shape of tissue or lesion, middle line displaying the snapshot made for neuro-navigation motive by combining IoUS with MRI image, and bottom line of the MRI image displaying the full surgical process) [9] (Fig. 2).

Observe, relay on unusual acoustic parameters of tissues interrelated, those pulse can either grasped, diffused or returned, this define the various attenuation coefficient of any specific tissue [11, 12].

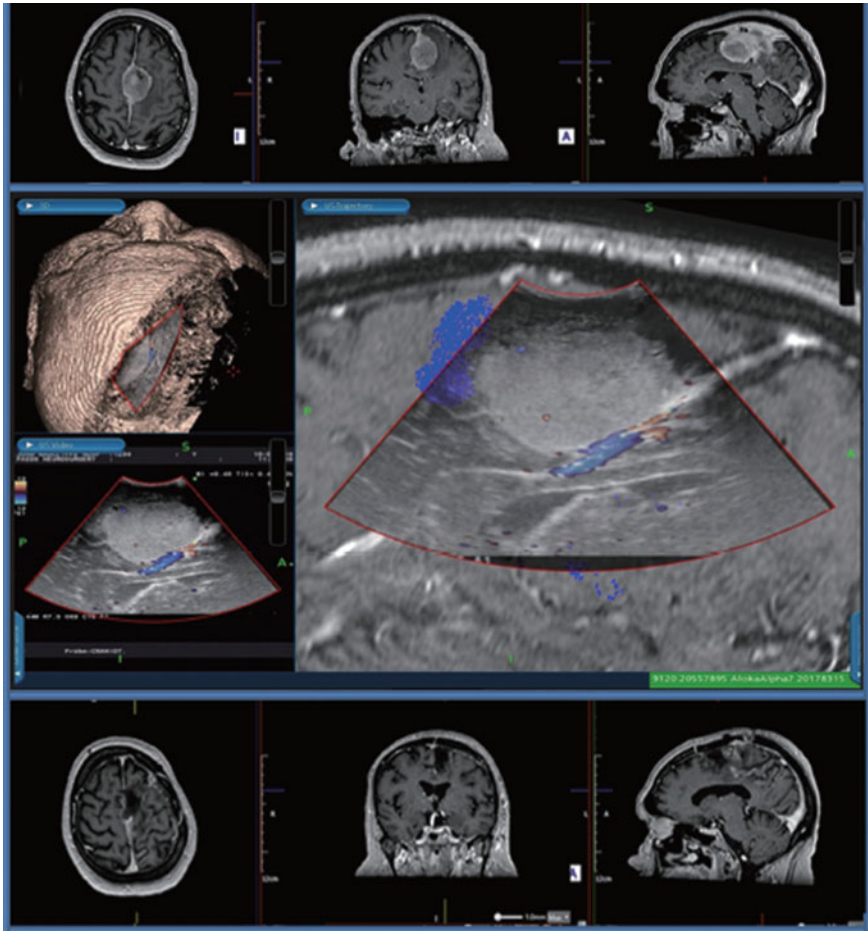


Fig. 2 MRI image displaying the presence of uneven or irregular tissues in the brain [9]

3 Preventing Artifacts

Alongside for better understanding, the material science of IoUS with regards to research white and dim issue, neurosurgeons ought to likewise be very much up-to-date about the assortment of potential antiquities that are not in trained hands could prompt improper confusion [10]. Examined the most well-known explanations behind blemished ultrasound picture, and inferred that they typically result as an infringement of at least one of the principal suspicions for an inactive chronicle. Those suppositions can be summed up as follows:

- (I) The ultrasound shaft ought to be thin with uniform width;
- (II) The ultrasound rays should go in an orderly fashion straightforwardly to the reflecting article and return to the transducer;
- (III) The speed of sound ought to be consistent and known in some random delicate tissue;
- (IV) The constriction of ultrasound ought to be consistent and stable.

Rely upon the careful situation; it is legitimized to get one of the accompanying techniques:

1. A method to deal with address, the constriction of the sound heartbeat is known as time-secure compensation. This framework makes comparatively echogenic tissues looks identical even if they are arranged at various profundities [13, 14].
2. The specialist should think about possible bone-initiated high sign lessening and orientate the shaft beat suitably [6, 15, 16].
3. An ultrasound imaging approach is set up to survey mechanical properties of tissues which ought to be considered to get an all the more sharp perspective on the physical issue edges stood apart from standard B-mode IoUS [17].

4 Perfection of IoUS in Neuro-navigation

The precision of IoUS was from the outset attempted in research place by setting a precision of 1.40 ± 0.45 mm for ultrasound-based neuro-navigational framework, and featured that inappropriate test change was the basic partner of these precision bungles. All things considered, these degrees of precision are thoroughly satisfactory in standard clinical practice for extraction of brain tumors [18, 19]. The reasons lie in the usage of various boundaries that the specialists or specialist's considers refining the signs given by IoUS and addition the level of resection of mind tumors. Taking everything into account, by joining IoUS over preoperative MRI channels, it is attainable to assemble the overall precision of neuro-navigation [15]. Furthermore, by allowing various acquisitions, the standard update of the image course system in all seasons of the development incredibly decline if not totally discards blunder issues [20–22].

5 Benefits and Constraints of IoUS

Generally, IoUS has a monstrous edge across the other intraoperative aides for picture recalling an activity, especially concerning independency, cost, and versatility to different gathered clinical conditions. By relationship with mechanical gatherings utilizing on preoperative neuro-radiology and atomic medication evaluations, IoUS is an insignificant and flexible framework that can openly give ongoing imaging. To be sure, IoUS suites are not massive and can be composed.

The expenses for securing and upkeep of IoUS suites are essentially less expensive when contrasted with some other intraoperative imaging instrument for particular representation of veins or tumor residuals. Furthermore, IoUS appears to be a more adaptable surgical companion since it fills a lot more needs. Then again, IoUS imaging is client subordinate, with a lofty expectation to absorb information, and explicit measurements amiable for the depiction of brain lesion are justified. As of late, [22] gave a critical commitment to this subject by portraying new, dependable measurements, at last having the option to connect their IoUS discoveries with the histological evaluation of the lesion extracted. New ages of IoUS suites with incorporated calculation for image investigation, and by the dispersion of difference improved ultrasound imaging.

6 Differentiation Specialists and the Eventual Fate of IoUS

The above all goal of ultrasonic contrast experts is to redesign picture definition, offering the probability to study the circulation system inside mind wounds through perfusion imaging of minimal thin veins [23, 24]. Numerous makers showed that distinction updated IoUS got together resection control in neurosurgery, even in single ultrasound-guided activities and with B-mode ultrasound improves tumor territory [15, 24–26]. Designs for picture blend and virtual course setting intraoperative reliable IoUS with reconstructive preoperative coplanar MRI are as of now accessible for picture guided resection of critical level gliomas. Those frameworks are these days more easy to use and reasonable in any case, for neurosurgeons that come up short on the skill in ultrasound progression. Wu et al. [27] detailed that image blend of separation overhauled IoUS licenses to see the cerebrum structure and get a predominant affirmation, constant and in multiplane from different focuses, of the tumor/edema interface differentiated and reconstructive preoperative coplanar-redesigned MRI. Fundamental, miniature air pockets, and nano particles contrast experts have been actually proposed as the latest improvement for ultrasound imaging: Following-endogenous association, they are permitted to stream in the flow framework and because of their micrometer or nanometer size and the restricting ligands on their surfaces can avoid vascular endothelial cells and hoard at tissue areas that over-express those nuclear targets [23, 28, 29].

7 General Specialized Parts of Ultrasound Limitation Microscopy

Same as optics, ultrasound also came across a restrict inborn to all wave-based imaging measures, where diffraction of the transferred or accepted waves aim point sources become unclear from each other when near than around a large portion of the transferred frequency. Above this, obstruction of dispersed sound outcomes in acoustic spot. Followed by progressive improvements spotted inside the optical area, similar to approaches were offered to abuse these equivalent standards, yet in the ultrasound field. Here, rather than using particles to give the individual sign sources needed, ultrasound distinct specialists, known as microbubbles, were offered (Fig. 3).

Procedure followed by SR ultrasound imaging.

(1) Acquisition—Securing the ultrasound information after some time out of different improved vascular locale. (2) Detection—Finding signals from microbubble contrast specialist. (3) Isolation—Segregation of single microbubble signals and intersecting and blocking signs are dismissed. (4) Localization—Localizing microbubble to correctness a long ways after the diffraction—restricted goal. (5) Tracking—Following microbubbles from continuous frames. (6) Mapping—Computing the localization collected over the sequence of frames build a picture of vascular shape.

Consequently, the super-goal ultrasound measure needs the presentation of a differentiation specialist into the body. Similar to its optical partner, it additionally needs the procurement of a succession of casings. A vital rule inside restriction microscopy methods is that by restricting the quantity of sources distinguished in each picture, the reactions don't meddle with one another. Under this limitation, the area of the hidden dissipates, for this situation, microbubbles can be assessed to accuracy far higher than the diffraction-restricted goal of the framework. Here, this is abused to aggregate limitation of streaming microbubbles more than a huge number of pictures to reproduce a super-settled picture of vascular designs. Expanded overall consideration inside this space of exploration implies the commitment of numerous worldwide gatherings is working with quick movement, variety, and advancement in this field, which will unavoidably empower and speed up medical exercise [30].

(a) Micro bubble

All current single-bubble limitation techniques for super-goal include infusion of various specialists as a dose or mixture. Being limitation-based techniques; the

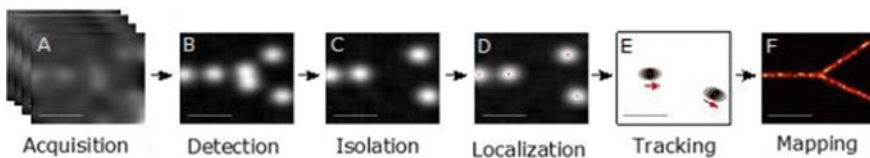


Fig. 3 Procedure followed by SR ultrasound imaging [30]

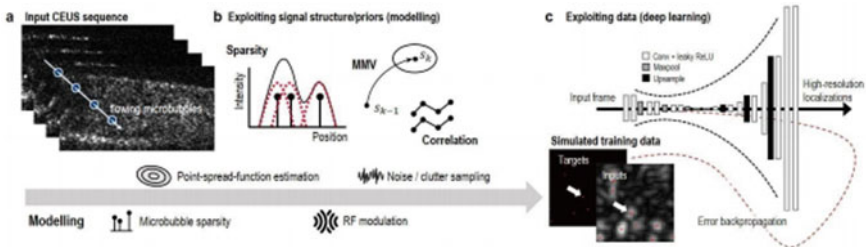


Fig. 4 Outline of various non-localization procedure leverage before signal system [26]

grouping of specialist is needed to be that much small that air pockets can be spatially isolated from the picture framework's radiation-restricted point lay out capacity followed by post-treatment sifting. Current sparsity-formed methodologies and profound learning-based strategies.

8 SR Ultrasound without Localization

Standard localization put together methods for ULM depends upon adequate detachability of microbubbles, putting an upper bound on the reasonable fixation. Contingent upon the ideal picture constancy, this thus puts a considerable lower link on securing time, normally being on the request for small interval of time [31–34]. By presenting other compromises, SR ultrasound can be performed quicker through various techniques misusing organized enlightenment [35] with the signal design. Within this segment, a few non-localization formed procedures are depicted, which mean to press this lower link down altogether by allowing high rise focuses without trading off correctness. These strategies utilize primary signal earlier to beat the limits of restriction formed methods for situations with covering point lay out capacities (PSFs). Such priors are acquired from signal models or verifiably by gaining from information. An outline of these methodologies is provided in Fig. 4.

9 Conclusion

SR ultrasound has disturbed the diffraction control of ultrasound imaging from the procedures, for example, ultrasound limitation microscopy. By noticing straight forwardly, the microvasculature in any organ and in tumors in creatures and, sometimes in people, give another way to consider the physiology along with pathologies of tissue. In detail, microscopy is presently feasible with a medical methodology, which can give an abundance of the recent data [26]. IoUS has absolutely everything necessary to count as an outstanding device for careful arranging and real-time picture directed extraction of intracranial sores. Neurosurgical/anatomical seminars

on the utilization of IoUS are getting much normal and will probably increment in the future, when more specialized improvement will upgrade picture detail and grow the utilization of this system. The significance of the dispersion of those courses is striking, on the grounds that the previous age of neurosurgeons needed to depend entirely on improper use to enhance their authority of mind ultrasound. Moving ahead, it's not difficult to conjecture that official recognitions and certificate will be given by public [36, 37] and global neurosurgical social orders to guarantee similar showing principles, abilities prerequisites, and revalidation rehearses [38, 39].

References

1. Yang W, Wang Z, Zhang B (2016) Recognition using adaptive local ternary patterns method. *Neurocomputing* 213:183–190
2. Tu Y, Lin Y, Wang J, Kim J (2018) Semi-supervised learning with generative adversarial networks on digital signal modulation classification. *Comput Mater Contin* 55(2):243–254
3. Kamalraj R, Neelakandan S, Kumar MR, Rao VCS, Anand R, Singh H (2021) Interpretable filter based convolutional neural network (IF-CNN) for glucose prediction and classification using PD-SS algorithm. *Measurement* 183:109804
4. Sindhwani N, Verma S, Bajaj T, Anand R (2021) Comparative Analysis of intelligent driving and safety assistance systems using YOLO and SSD model of deep learning. *Int J Inf Syst Model Des (IJISMD)* 12(1):131–146
5. Bakshi G, Shukla R, Yadav V, Dahiya A, Anand R, Sindhwani N, Singh H (2021) An optimized approach for feature extraction in multi-relational statistical learning. *J Sci Ind Res* 80:537–542
6. Unsgaard G, Rygh OM, Selbekk T, Müller TB, Kolstad F, Lindseth F, Hernes TA (2006) Intra-operative 3D ultrasound in neurosurgery. *Acta Neurochir (Wien)* 148:235–253
7. Kumar R, Anand R, Kaushik G (2011) Image compression using wavelet method & SPIHT algorithm. *Digital Image Process* 3(2):75–79
8. Vyas G, Anand R, Holê KE, Implementation of advanced image compression using wavelet transform and SPHIT algorithm. *Int J Electron Electr Eng* ISSN 0974-2174
9. Ganau M, Ligarotti GK, Apostolopoulos V (2019) Real-time intraoperative ultrasound in brain surgery: neuronavigation and use of contrast-enhanced image fusion. *Quant Imaging Med Surg* 9(3):350
10. Selbekk T, Jakola AS, Solheim O, Johansen TF, Lindseth F, Reinertsen I, Unsgård G (2013) Ultrasound imaging in neurosurgery: approaches to minimize surgically induced image artefacts for improved resection control. *Acta Neurochir (Wien)* 155:973–980
11. Strowitzki M, Brand S, Jenderka KV (2007) Ultrasonic radiofrequency spectrum analysis of normal brain tissue. *Ultrasound Med Biol* 33:522–529
12. Pichardo S, Sin VW, Hynynen K (2011) Multi-frequency characterization of the speed of sound and attenuation coefficient for longitudinal transmission of freshly excised human skulls. *Phys Med Biol* 56:219–250
13. Pye SD, Wild SR, McDicken WN (1992) Adaptive time gain compensation for ultrasonic imaging. *Ultrasound Med Biol* 18:205–212
14. Ilyina N, Hermans J, Verboven E, Van Den Abeele K, D'Agostino E, D'hooge J (2018) Attenuation estimation by repeatedly solving the forward scattering problem. *Ultrasonics* 84:201–209
15. Unsgaard G, Ommedal S, Muller T, Gronningsaeter A, Nagelhus Hernes TA (2002) Neuronavigation by intraoperative three-dimensional ultrasound: initial experience during brain tumor resection. *Neurosurgery* 50:804–812

16. Unsgaard G, Gronningsaeter A, Ommedal S, Nagelhus Hernes TA (2002) Brain operations guided by real-time two dimensional ultrasound: new possibilities as a result of improved image quality. *Neurosurg Focus* 51:402–412
17. Prada F, Del Bene M, Rampini A, Mattei L, Casali C, Vetrano IG, Gennari AG, Sdao S, Saini M, Sconfienza LM, DiMeco F (2018) Intraoperative strain elastosonography in brain tumor surgery. *Oper Neurosurg (Hagerstown)* [Epub ahead of print]. <https://doi.org/10.1093/ons/opy323>
18. Akeret K, Bellut D, Huppertz HJ, Ramantani G, König K, Serra C, Regli L, Kraysenbühl N (2018) Ultrasonographic features of focal cortical dysplasia and their relevance for epilepsy surgery. *Neurosurg Focus* 45:E5
19. Morin F, Courtecuisse H, Reinertsen I, Le Lann F, Palombi O, Payan Y, Chabanas M (2017) Brain-shift compensation using intraoperative ultrasound and constraint-based biomechanical simulation. *Med Image Anal* 40:133–153
20. Ohue S, Kumon Y, Nagato S, Kohno S, Harada H, Nakagawa K, Kikuchi K, Miki H, Ohnishi T (2010) Evaluation of intraoperative brain shift using an ultrasound-linked navigation system for brain tumor surgery. *Neurol Med Chir (Tokyo)* 50:291–300
21. Drouin S, Kochanowska A, Kersten-Oertel M, Gerard JJ, Zelmann R, De Nigris D, Bériault S, Arbel T, Sirhan D, Sadikot AF, Hall JA, Sinclair DS, Petrecca K, DelMaestro RF, Collins DL (2017) IBIS: an OR ready open-source platform for image-guided neurosurgery. *Int J Comput Assist Radiol Surg* 12:363–378
22. Camp SJ, Apostolopoulos V, Raptopoulos V, Mehta A, O'Neill K, Awad M, Vaqas B, Peterson D, Roncaroli F, Nandi D (2017) Objective image analysis of real-time three dimensional intraoperative ultrasound for intrinsic brain tumour surgery. *J Ther Ultrasound* 5:2
23. Kaneko OF, Willmann JK (2012) Ultrasound for molecular imaging and therapy in cancer. *Quant Imaging Med Surg* 2:87–97
24. Yan F, Song Z, Du M, Klibanov AL (2018) Ultrasound molecular imaging for differentiation of benign and malignant tumors in patients. *Quant Imaging Med Surg* 8:1078–1083
25. Pysz MA, Guracar I, Tian L, Willmann JK (2012) Fast microbubble dwell-time based ultrasonic molecular imaging approach for quantification and monitoring of angiogenesis in cancer. *Quant Imaging Med Surg* 2:68–80
26. Ruan H, Mather ML, Morgan SP (2015) Ultrasound modulated optical tomography contrast enhancement with non-linear oscillation of microbubbles. *Quant Imaging Med Surg* 5:9–16
27. Wu DF, He W, Lin S, Han B, Zee CS (2019) Using real-time fusion imaging constructed from contrast enhancement ultrasonography and magnetic resonance imaging for high grade glioma in neurosurgery. *World Neurosurg* [Epub ahead of print]. <https://doi.org/10.1016/j.wneu.2018.12.215>
28. Ganau M (2014) Tackling gliomas with nanoformulated antineoplastic drugs: suitability of hyaluronic acid nanoparticles. *Clin Transl Oncol* 16:220–223
29. Lee JH, Park G, Hong GH, Choi J, Choi HS (2012) Design considerations for targeted optical contrast agents. *Quant Imaging Med Surg* 2:266–273
30. Christensen-Jeffries K, Couture O, Dayton PA, Eldar YC, Hynynen K, Kiessling F, O'Reilly M (2020) Super-resolution ultrasound imaging. *Ultrasound Med Biol* 46(4):865–891
31. Opacic T, Dencks S, Theek B, Piepenbrock M, Ackermann D, Rix A, Lammers T, Stickeler E, Delorme S, Schmitz G (2018) Motion model ultrasound localization microscopy for preclinical and clinical multiparametric tumor characterization. *Nat Commun* 9:1527
32. Hingot V, Errico C, Heiles B, Rahal L, Tanter M, Couture O (2019) Microvascular flow dictates the compromise between spatial resolution and acquisition time in ultrasound localization microscopy. *Sci Rep* 9:2456
33. Dencks S, Piepenbrock M, Opacic T, Krauspe B, Stickeler E, Kiessling F, Schmitz G (2019) Clinical pilot application of super-resolution US imaging in breast cancer. *IEEE Trans Ultrason Ferroelectr Freq Control* 66:517–526
34. Gupta A, Anand R, Pandey D, Sindhwani N, Wairya S, Pandey BK, Sharma M (2021) Prediction of breast cancer using extremely randomized clustering forests (ERCF) technique: prediction of breast cancer. *Int J Distrib Syst Technol (IJDSST)* 12(4):1–15

35. Ilovitsh T, Ilovitsh A, Foiret J, Fite BZ, Ferrara KW (2018) Acoustical structured illumination for super-resolution ultrasound imaging. *Commun Biol* 1:3
36. Chaudhary R, Jindal A, Aujla GS, Kumar N, Das AK, Saxena N (2018) LSCSH: lattice-based secure cryptosystem for smart healthcare in smart cities environment. *IEEE Commun Mag* 56(4):24–32. <https://doi.org/10.1109/MCOM.2018.1700787>
37. Kaur M, Wasson V (2015) ROI based medical image compression for telemedicine application. *Procedia Comput Sci* 70:579–585. <https://doi.org/10.1016/j.procs.2015.10.037>
38. Mittal N, Singh U, Salgotra R, Sohi BS (2018) A boolean spider monkey optimization based energy efficient clustering approach for WSNs. *Wirel Networks* 24(6):2093–2109. <https://doi.org/10.1007/s11276-017-1459-4>
39. Singh U, Salgotra R, Rattan M (2016) A novel binary spider monkey optimization algorithm for thinning of concentric circular antenna arrays. *IETE J Res* 62(6):736–744. <https://doi.org/10.1080/03772063.2015.1135086>

Breast Cancer Detection Using Machine Learning



Somya Goyal, Mehul Sinha, Shashwat Nath, Sayan Mitra, and Charvi Arora

Abstract Through studies and statistics, it has been found that these days, breast cancer is the most common cancer leading to frequent deaths among women. Early screening and subsequent treatment can raise the chances of survival. Through this paper, we aim to demonstrate the ability to detect breast cancer cases using MRI scan data by analyzing the given data with machine learning algorithms. Using machine learning, we hope to ease the process of cancer detection in the hospitals so the patient can be afforded the right treatment as soon as possible before the situation can become critical. It also opens the door toward new possibilities in cancer detection for other different types of cancers as well as other diseases by use of machine learning in medical science, where detection using conventional means is usually laborious and time-taking.

1 Introduction

During the past years, doctors have classified breast cancer into various subtypes. In 2020, there were 2.3 million women diagnosed with breast cancer and 685,000 deaths globally. At the end of 2020, there were 7.8 million women alive who were diagnosed with breast cancer in the past 5 years. According to GLOBOCAN, breast cancer is the predominant cancer in women, making up to 25.1% of all cancers. There has been a significant decline in the amount of cases of breast cancer because of improvement in the medical sector with the help of advanced technology and software. Over a period of time, machine learning has helped a lot in improving the accuracy of detection of breast cancer in early stages. Breast cancer is more difficult and costly to treat as it reaches upper stages, hence, proper machinery and technology for detection and treatment are called for. This paper lays out a machine learning algorithm that helps to detect breast cancer in women efficiently and with great accuracy.

S. Goyal (✉) · M. Sinha · S. Nath · S. Mitra · C. Arora
Manipal University Jaipur, Jaipur, Rajasthan 303007, India
e-mail: somyagoyal1988@gmail.com

2 Related Works

This section gives the review of literature work in the field of “Breast cancer detection using machine learning.” Multiple sources were reviewed by the authors for the literature which have been referred for the analysis of breast cancer using machine learning. Further, the authors reviewed datasets from reliable sources for testing purposes of the methods reviewed. The most popular methods [1] of breast cancer detection, namely Naive Bayes classifier, K-nearest neighbors (KNN) [2], logistic regression, decision tree classifier, support vector machine (SVM) classifier [3] and random forest classifier [4, 5], which are given in Table 1.

3 Proposed Methodology

The purpose of this work is to analyze the dataset using random forest classifier, logistic regression and decision tree classifier and compare the efficiency of the respective algorithms in terms of accuracy in detecting cancer in the subject.

3.1 Experimental Setup

The program was made using Python programming language on Jupyter Notebook application. We have used the Wisconsin Breast Cancer datasets [14] from the UCI machine learning repository for our analysis regarding the scope of our work.

We imported NumPy library for working with data using arrays. We imported Pandas library to analyze, clean and manipulate the given dataset. We imported Matplotlib and Seaborn libraries for data visualization of the statistics. We made use of Sclearn which is a machine learning library for Python to import and implement logistic regression, random forest classifier and decision tree classifier algorithms on the given data.

Logistic Regression: It uses a logistic function to for modeling data using dependent and independent variable. It is used for binary data and it is efficient to train. Logistic regression algorithm performs efficiently when the given dataset is separable linearly.

Decision Tree Classifier: A decision tree consists of decision nodes and leaf nodes. It begins with the root node and finds the best attribute using attribute selection measure so as to divide it into multiple subsets. From these, a decision tree node is generated. The process repeats recursively until no further classification of nodes is possible. It makes predictions from all types of outcomes.

Random Forest Classifier: It uses the functionality of a group of decision trees. It is an ensemble algorithm. Individual trees are generated by attribute selection indication. Greater number of trees lead to computation of a better average and thus

Table 1 Literature work

S. No	Study	Technique used	Strength	Weakness
1	Tahmooresi et al. [6]	Artificial neural network (ANN) Support vector machine (SVM) K-nearest neighbors (KNN)	SVM is a performant algorithm and produces accurate results	Large datasets not suitable for SVM algorithm
2	Nallamala et al. [7]	NumPy Pandas	Powerful libraries for representation and manipulation of data	None
3	Bazazeh et al. [8]	Random forest (RF) Bayesian networks (BN)	Stable and unbiased algorithm producing accurate results	Heavy use of computational resources
4	Agarap et al [9]	GRU-SVM Linear regression	Used for predictive analysis	Performs poorly in nonlinear relationships between variables
5	Vaka, Soni et al. [10]	R-CNN (convolutional neural networks) classifier Bidirectional recurrent neural networks (HA-BiRNN)	Deep learning models with unsupervised feature extraction	Computationally taxing and big dataset required for training
6	Chaurasia et al. [11]	Sequential minimal optimization (SMO) BF tree	Resolves quadratic programming problem that arises during training of SVM	Necessary to solve QP scaling with number of SVMs
7	Gayathri et al. [12]	Supervised, unsupervised, semi-supervised and reinforcement learning	Optimize performance in case of supervised algorithm and implement real-world problems	Preprocessing required. Computation time is vast for supervised algorithms
8	Ganggayah et al. [13]	Support vector machine neural networks logistic regression	Outperforms most of the machine learning algorithms	Unpredictable output and computationally its very expensive

increases the accuracy of the making predictions on the given dataset. It resolves the overfitting problem that arises with decision trees.

3.2 Feature Analysis

First up, the features are analyzed for their frequency count [15], and then, their pairwise correlation is computed. The code is given below.

```
In [1]: #This program detects breast cancer using data.
```

```
In [2]: #import libraries
import numpy as np
import pandas as pd
import matplotlib.pyplot as plt
import seaborn as sns
```

```
In [3]: #Load the data
df = pd.read_csv('data.csv')
```

```
In [4]: #count the number of rows and columns
df.shape
```

```
Out[4]: (569, 32)
```

The plot for the count of diagnosis for malignant (M) and benign (B) is shown in Fig. 1. The pairwise correlation is shown with the help of a heat map [15–17] as in Fig. 2.

```
In [8]: #get a count of Malignant (M) or Benign(B) cells
df['diagnosis'].value_counts()
```

```
Out[8]: B    357
        M    212
        Name: diagnosis, dtype: int64
```

```
In [9]: #visualize the count
sns.countplot(df['diagnosis'], label = 'count')
```

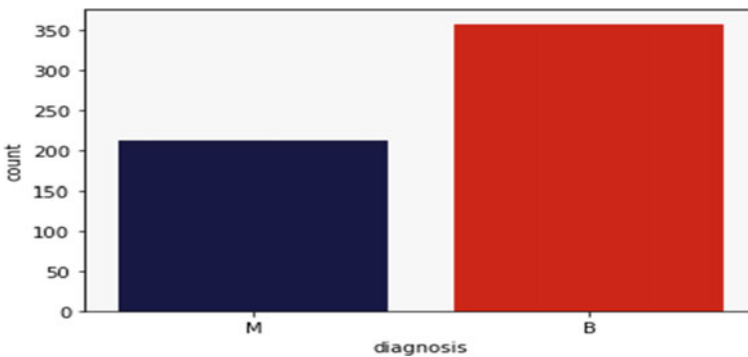


Fig. 1 Frequency plot for two classes-malignant (M) and benign (B)

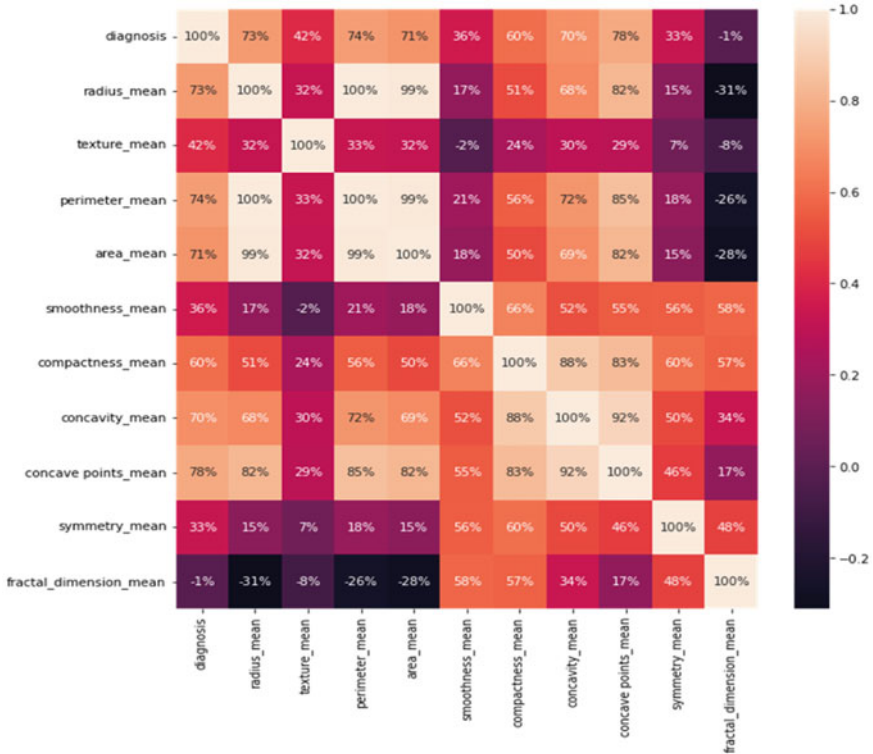


Fig. 2 Heat map plot for pairwise correlation among features

```
In [11]: #Encode the categorical data values
from sklearn.preprocessing import LabelEncoder
labelencoder_Y = LabelEncoder()
df.iloc[:,1] = labelencoder_Y.fit_transform(df.iloc[:,1].values)
```

```
In [12]: #Create a pair plot
sns.pairplot(df.iloc[:,1:8], hue = 'diagnosis')
```

```
In [13]: #get the correlation of the cloumns
df.iloc[:, 1:12].corr()
```

```
Out[39]:
```

	diagnosis	radius_mean	texture_mean	perimeter_mean	area_mean	smoothness_mean	compactness_mean	concavity_mean
diagnosis	1.000000	0.730029	0.415185	0.742636	0.708984	0.358560	0.596534	0.696360
radius_mean	0.730029	1.000000	0.323782	0.997855	0.987357	0.170681	0.506124	0.676764
texture_mean	0.415185	0.323782	1.000000	0.329533	0.321086	-0.023389	0.236702	0.302418
perimeter_mean	0.742636	0.997855	0.329533	1.000000	0.986507	0.207278	0.556936	0.716136
area_mean	0.708984	0.987357	0.321086	0.986507	1.000000	0.177028	0.498502	0.685983
smoothness_mean	0.358560	0.170681	-0.023389	0.207278	0.177028	1.000000	0.659123	0.521984
compactness_mean	0.596534	0.506124	0.236702	0.556936	0.498502	0.659123	1.000000	0.883121
concavity_mean	0.696360	0.676764	0.302418	0.716136	0.685983	0.521984	0.883121	1.000000
concave points_mean	0.776614	0.822529	0.293464	0.850977	0.823269	0.553695	0.831135	0.921391
symmetry_mean	0.330499	0.147741	0.071401	0.183027	0.151293	0.557775	0.602641	0.500687

```
In [14]: #Visualize the correlation
plt.figure(figsize = (10,10))
sns.heatmap(df.iloc[:, 1:12].corr(), annot = True, fmt='.0%' )
```

The classification models are constructed. After training the model with the given algorithms, we computed accuracy and confusion matrix from Sclearn library to ascertain the performance of the algorithms on the constructed model.

```
In [15]: #split the data set into independent (X) and dependent (Y) data sets
X = df.iloc[:, 2:31].values
Y = df.iloc[:, 1].values
```

```
In [16]: #split the data set into 80% training and 20% testing
from sklearn.model_selection import train_test_split
X_train, X_test, Y_train, Y_test = train_test_split(X, Y, test_size = 0.20, random_state=0)
```

```
In [17]: #Scale the data (Feature Scaling)
from sklearn.preprocessing import StandardScaler
sc = StandardScaler()
X_train = sc.fit_transform(X_train)
X_test = sc.fit_transform(X_test)
```

```
In [18]: #Create a function for the models
def models(X_train, Y_train):

    #Logistic Regression
    from sklearn.linear_model import LogisticRegression
    log = LogisticRegression(random_state = 0)
    log.fit(X_train, Y_train)

    #Decision Tree
    from sklearn.tree import DecisionTreeClassifier
    tree = DecisionTreeClassifier(criterion='entropy', random_state = 0)
    tree.fit(X_train, Y_train)

    #Random forest classifier
    from sklearn.ensemble import RandomForestClassifier
    forest = RandomForestClassifier(n_estimators = 10, criterion = 'entropy', random_state = 0)
    forest.fit(X_train, Y_train)

    #Print the models accuracy on the training data
    print('Logistic Regression gives a Training Accuracy ', log.score(X_train, Y_train))
    print('Decision Tree gives a Training Accuracy ', tree.score(X_train, Y_train))
    print('Random Forest Classifier gives a Training Accuracy ', forest.score(X_train, Y_train))

    return log, tree, forest
```

```
In [19]: #Getting all of the models
model = models(X_train, Y_train)
```

We calculated the accuracy of each model using a confusion matrix:

TrPo True Positive
 TrNe True Negative
 FaNe False Negative
 FaPo False positive

$$\text{Accuracy} = (\text{TrPo} + \text{TrNe}) / (\text{TrPo} + \text{TrNe} + \text{FaNe} + \text{FaPo})$$

```
In [20]: #test model accuracy on test data on confusion matrix
from sklearn.metrics import confusion_matrix

for i in range(len(model)):
    print('Model ', i)
    cm = confusion_matrix(Y_test, model[i].predict(X_test))
    TP = cm[0][0]
    TN = cm[1][1]
    FN = cm[1][0]
    FP = cm[0][1]

    print(cm)
    print('testing accuracy =',( TP + TN ) / ( TP + TN + FN + FP ))
    print()
```


Fig. 3 Confusion matrix for logistic regression

TrPo = 66	FaPo = 1
FaNe = 3	TrNe = 44

Fig. 4 Confusion matrix for decision tree

TrPo = 64	FaPo = 3
FaNe = 4	TrNe = 43

Fig. 5 Confusion matrix for random forest classifier

TrPo = 67	FaPo = 0
FaNe = 3	TrNe = 44

4 Results and Discussions

We were successful in detection of breast cancer in patients through the use of machine learning algorithms. To assess the performance of all the algorithms, we used a confusion matrix to provide the best evaluation. We took 80% of the dataset to train each of the model and 20% of the dataset to test the precision of each model.

Logistic regression algorithm has an accuracy of 96.49%, while the decision tree algorithm has an accuracy of only 93.85%. However, the best results were shown by random forest classifier algorithm with an accuracy of 97.36%. Hence, we are able to tell with high accuracy if the cancer is benign or malignant in the subject (Figs. 3, 4 and 5).

5 Conclusions

Breast cancer is one of the most predominant cancers found in women. Detection at an early stage and diagnosis of this disease can save lives and the patient can undergo suitable treatment. Machine learning has vast applications in the modern healthcare system. One such use of machine learning is detection and diagnosis of diseases that has been thoroughly discussed in this paper. Integration of machine learning with medical databases and devices will make healthcare system more efficient and help in better organization of data. Healthcare industries such as tempus are using machine learning on their clinical data to provide personalized treatments for patients. Hence, an increased adoption of machine learning technology is expected in medical fields in the future.

References

1. Goyal S, Bhatia PK (2020) Comparison of machine learning techniques for software quality prediction. *Int J Knowl Syst Sci (IJKSS)* 11(2):21–40. <https://doi.org/10.4018/IJKSS.2020040102>
2. Goyal S (2021) Handling class-imbalance with KNN (Neighbourhood) under-sampling for software defect prediction. *Artif Intell Rev.* <https://doi.org/10.1007/s10462-021-10044-w>
3. Goyal S (2021) Effective software defect prediction using support vector machines (SVMs). *Int J Syst Assur Eng Manag.* <https://doi.org/10.1007/s13198-021-01326-1>
4. Goyal S, Bhatia PK (2021) Heterogeneous stacked ensemble classifier for software defect prediction. *Multimed Tools Appl.* <https://doi.org/10.1007/s11042-021-11488-6>
5. Goyal S (2021) Predicting the defects using stacked ensemble learner with filtered dataset. *Autom Softw Eng* 28:14. <https://doi.org/10.1007/s10515-021-00285-y>
6. Tahmoorei M, Afshar A, Rad BB, Nowshath KB, Bamiah MA (2018) Early detection of breast cancer using machine learning techniques. *J Telecommun Electr Comput Eng (JTEC)* 10(3–2):21–27
7. Nallamala SH, Mishra P, Koneru SV (2019) Breast cancer detection using machine learning way. *Int J Recent Technol Eng* 8:1402–1405
8. Bazazeh D, Shubair R (2016) Comparative study of machine learning algorithms for breast cancer detection and diagnosis. In: 2016 5th international conference on electronic devices, systems and applications (ICEDSA). IEEE, Dec 2016, pp 1–4
9. Agarap AFM (2018) On breast cancer detection: an application of machine learning algorithms on the wisconsin diagnostic dataset. In: Proceedings of the 2nd international conference on machine learning and soft computing, Feb 2018, pp 5–9
10. Vaka AR, Soni B, Reddy S (2020) Breast cancer detection by leveraging machine learning. *ICT Express* 6(4):320–324
11. Chaurasia V, Pal S (2017) A novel approach for breast cancer detection using data mining techniques. *Int J Innov Res Comput Commun Eng* 2 (An ISO 3297: 2007 Certified Organization)
12. Gayathri BM, Sumathi CP, Santhanam T (2013) Breast cancer diagnosis using machine learning algorithms-a survey. *Int J Distrib Parallel Syst* 4(3):105
13. Ganggayah MD, Taib NA, Har YC, Lio P, Dhillon SK (2019) Predicting factors for survival of breast cancer patients using machine learning techniques. *BMC Med Inform Decis Mak* 19(1):1–17
14. <https://www.kaggle.com/uciml/breast-cancer-wisconsin-data/version/2>
15. Goyal S, Bhatia PK (2021) Software fault prediction using lion optimization algorithm. *Int J Inf Technol.* <https://doi.org/10.1007/s41870-021-00804-w>
16. Goyal S, Bhatia PK (2020) Feature selection technique for effective software effort estimation using multi-layer perceptrons. In: Proceedings of ICETIT 2019. Lecture Notes in Electrical Engineering, vol 605. pp 183–194. Springer, Cham. https://doi.org/10.1007/978-3-030-30577-2_15
17. Goyal S (2022) FOFS: firefly optimization for feature selection to predict fault-prone software modules. In: Nanda P, Verma VK, Srivastava S, Gupta RK, Mazumdar AP (eds) Data engineering for smart systems. Lecture Notes in Networks and Systems, vol 238. Springer, Singapore. https://doi.org/10.1007/978-981-16-2641-8_46

Current Trends in Methodology for Software Development Process



Somya Goyal, Ayush Gupta, and Harshit Jha

Abstract Software development processes are heart core to finish a new project successfully. A wide range of software development methodologies is available from literature. This study analyzes the available methodologies for software methodology and finds out the most suitable methodology for a project. A survey-based research is carried out among developers and managers with varying experience in their field. For this study, agile and waterfall methodologies are focused as these are the popular methodologies to find our results. The results from our survey show that there is no “perfect” method to for a project as one needs to consider factors like resources, duration of project, etc., to select methodology to follow. It infers that waterfall-based process is popular among small projects in which requirements are well defined, whereas agile methodology is preferred with all kinds of projects as it provided better flexibility and continuous feedbacks, and delivery was provided to deliver a project with higher satisfaction rate.

Keywords Software development · Waterfall · Agile · Scrum · Kanban

1 Introduction

Software development process follows steps such as initiation, planning, execution and closing the project which are essential for development of a project and are discussed in the section below. There are various number of software development process models that have been created to make the project efficient [1, 2] such as waterfall, Six Sigma Lean, Spiral, V-Shape and agile. Waterfall model is oldest of all and one of the most followed models, it is performed in sequence of stages

S. Goyal (✉) · A. Gupta · H. Jha
Manipal University Jaipur, Jaipur, Rajasthan 303007, India
e-mail: somyagoyal1988@gmail.com

A. Gupta
e-mail: ayush20118@gmail.com

H. Jha
e-mail: harshitjha7777777@gmail.com

and only after completing one stage one can move to second. Six Sigma Lean is one of the newest models, in this both Lean and Sigma are merged to improve the quality of result and taking out the reasons to reduce variability in whole process. Spiral model emphasis risk analysis of project by repeatedly passing project through iteration. The V-Shape model executed in a sequence based on testing after each step. Agile software development model is a group of various methodology such as Scrum, Kanban, Extreme programming (XP), Lean, Crystal, who focused on satisfaction of stakeholders by rapid delivery after every stage which results in a better-quality product, and it is considered as one of the best methods and widely used in organizations presently.

The purpose of this study is to practically analyze the use of methodologies by developers using a survey. We focused more on agile and waterfall method as they are the most used methodologies used by product managers.

In agile model, we will focus on Kanban and Scrum for our study as these are one of the most used methodologies used by developers according to the survey. Kanban method gives visuals of the entire project to whole team and stakeholders which makes it more transparent and develops better coordination between team. Scrum framework developed by Ken Schwaber and Jeff Sutherland Inn 1993 [3], as explained [4] its implementation is done in a cross functional team by ensuring sprint goal is matched.

2 Related Work

In the field of project management, there are many methodologies to deal with software development life cycle (SDLC) after studying and evaluating many theories [5–7], with their advantages and disadvantages, we concluded to get a closer look at waterfall and agile. These methodologies and approach have been studied and are continuously improved like introduction of DevOps by Patrick Debois which helped the agile development by making it more efficient and providing continuous delivers to make improvement in every step of project [16, 24]. This also helped with more flexibility in project and minimizing errors.

There are many other studies on various models of SDLC, as we know, both waterfall and agile [8] are most used SDLC methodology and as agile replacing waterfall in industry is the reason why we selected those as our survey.

All models have their weakness and strengths [9, 10] but depending on time, resources [11], and nature of project, an organization work with the most suitable method to deliver an efficient project.

3 Proposed Approach

The proposed approach to carry out this study is given as Fig. 1. For this study, we took survey from a group of people including entry level developers and project managers, while finding which one is the most preferred methodology in software development life cycle. We will first compare waterfall with agile and then most preferred agile method between Scrum and Kanban.

3.1 Comparison Between Agile and Waterfall

Waterfall is much organized than Agile as it is sequential process, and hence, the project can only go in next phase when previous one is completed, and testing is done after completion of project, whereas in agile, we continuously test the process and improves it if required [12]. On the other hand, agile is more flexible than waterfall [13] as stakeholders can provide their review after each phase and ask for a change if required. From all the study following points were noted:

- In waterfall model, it is difficult to make changes after completion of a process, whereas we can do it in agile.
- In waterfall, we need to define all the requirements and it should not be changed in between project.
- In agile, there is high chance of interaction with stakeholders.

3.2 Comparison Between Kanban and Scrum

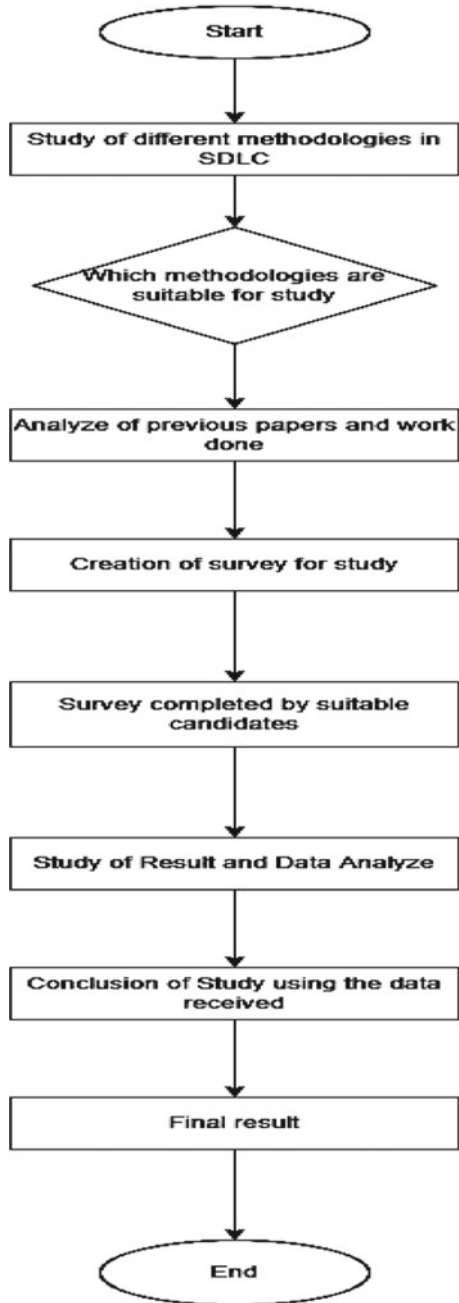
Scrum and Kanban both are agile methods but are different from each other. It is team's decision which methodology they want to follow for their project as Kanban gives more freedom than Scrum, whereas Scrum allows team to work in sprint and teams are not advised to change decision during sprint but in Kanban change at any stage is possible [14]. Here are some points which are useful in our study:

- In Kanban, a team can work without assigning a particular role.
- Meetings are necessary in sprints when Scrum is followed.
- Strict estimation of phase is required in Scrum.

As discussed above, these both are part of agile model, and hence, there are many similarities too, such as:

- Testing of both the processes is required to find which one is more compatible with team.
- Both processes are focused toward delivering project fast.
- In both, the methodologies feedbacks and reviews are taken frequently to deliver a successful product.

Fig. 1 Flowchart of the steps taken to complete the study



- Scrum and Kanban both are transparent.

It should be noted, the final decision of selecting the methodology should be of team as per their work culture and atmosphere [15].

3.3 Study Preferences

To derive the results of this study, we created a survey and distributed it among the developers and managers. The survey helped us with the preference of methodology by a particular individual or team based on their requirements and resources.

We created a section where we asked about the experience of individual as it will help us to determine which methodology is more preferred by an entry level developer and someone more experienced.

In next section, we asked people about the method they preferred and according to the method we asked them different question to get better results. Some important questions which are important for our study like:

- Time project took for completion as it helped with determining which project will be better for long term or short term.
- Satisfaction of the person who took part in research with the methodology their team preferred and what they felt about the project to get better picture of advantages and disadvantages of a particular methodology.
- Success of project was also an important factor for this study as it helped with the efficiency of use of resources in a particular methodology.
- Delivery of project was successful or not as it helped us with determining a particular methodology failed or passed.
- Size of team was also an important factor as it helped us to assess which method is suitable for big team and which works best for a small team.

4 Study Results

We circulated the survey among 64 candidates to get data for the required methodologies. We presented them with some question for waterfall, Scrum and Kanban. In this study, we focused on people with different experiences in their domain, and we categorized them into different categories like less than 2 years, 2–5 years and more than 5 years. We categorized them into these categories to get better idea of methodology preferred by people varying their experiences [16], and hence, we can get a better view at what methodology a person with less experience prefer [17] and what is preferred by someone with more experience. As we can see in Fig. 2, maximum number of people belonged to category with less than 2 years of experience, i.e., entry level developers, we also got a fair number of participants from people with more than 2 years of experience to generalize what method they prefer.

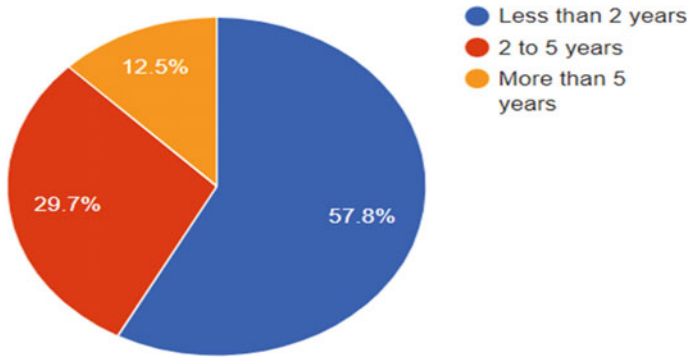


Fig. 2 Experience of candidates

In our study, total 7 number of projects participated with a team of 3–20 people. Teams with members ranging from 3 to 4 preferred waterfall model, teams with 6–8 members used Kanban, while teams with 10–20 people used Scrum for their projects. As we can see in Fig. 3, 28.6% teams who preferred waterfall model were of small size, 28.6% teams who preferred Kanban were of medium size and teams who used scrum were large teams.

Most projects in our study were short-term projects as we can see in Fig. 4, out of 4 short-term projects, 2 followed Kanban, 1 followed waterfall and 1 followed Scrum. From 2 mid-term projects, 1 followed waterfall and the other followed Scrum and 1 long-term project preferred Scrum.

From Fig. 5, we derived 54 candidates prefer Scrum for their projects, 23.6% prefers Kanban and 27.3% prefer waterfall to complete their project. The preference of methodology depends on the size of team and duration of project [18, 19].

Users who preferred Scrum outlined that communication between team was good and nobody felt they are doing any work under burden, but they were not satisfied with the strict routine they followed.

Fig. 3 Methodology used in projects

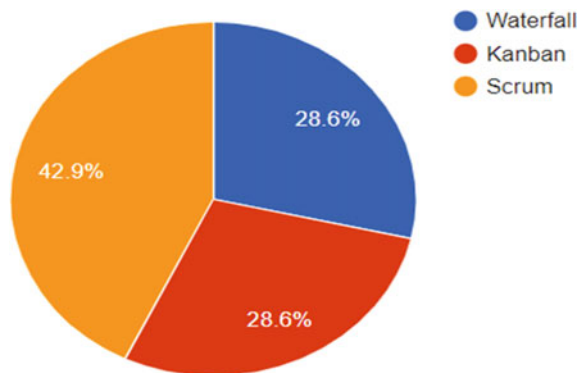


Fig. 4 Duration of project

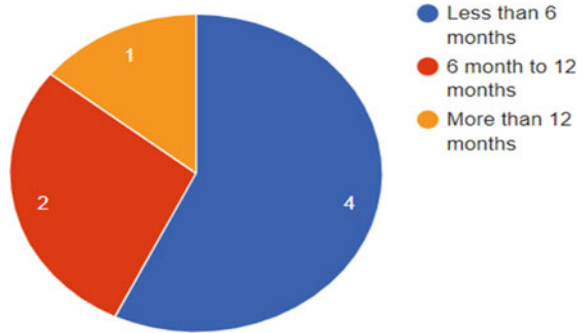
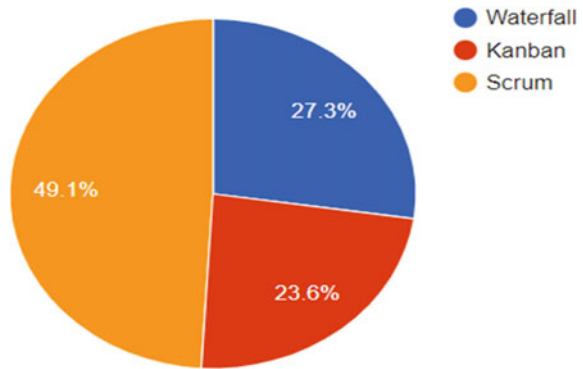


Fig. 5 Candidate satisfaction



Waterfall users responded with satisfaction of the clarity and strictness toward the requirements which were given at start of project, but they faced problems with measurement of progress throughout the project.

Kanban users were happy with the flexibility the methodology offered them but frustrated with updating the cards again and again.

In our study, Scrum provided with the greatest number of successful projects with Scrum which was very close to Kanban. Candidates who participated in the survey preferred agile over waterfall because of the flexibility and synchronization it provided.

5 Conclusions

After the study, we can conclude that every method works different for every project depending on project's requirement, team size and resources. Every methodology has its pros and cons, and hence, everything about the project must be considered while selecting methodology. In Fig. 6, we can see 51 users in our survey preferred agile method and 13 users preferred waterfall method for their project.

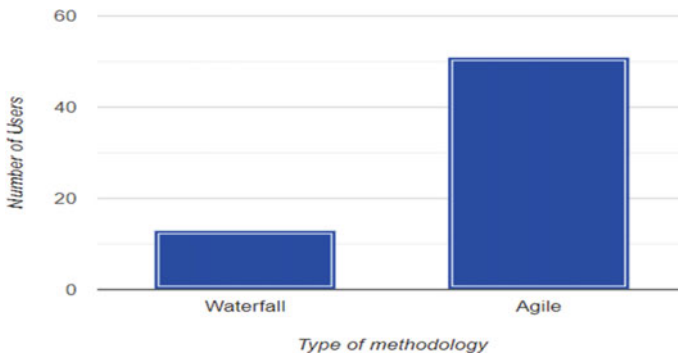


Fig. 6 Preferred methodology by participants

Hence, we found out agile was more popular among users and preferred for projects of all size as it provides more flexibility and synchronization between team, whereas waterfall worked well with short-term projects as and with a small size team having less than 10 members. Therefore, the choice depends on the need of project as there is no perfect method [20]. Waterfall was good with small team and small projects as the requirements were clear before starting of project, while agile worked well with all kinds of team and project as it offered flexibility and continuous review on the process.

References

1. Alshamrani A, Bahattab A (2015) A comparison between three SDLC models Waterfall model, Spiral model, and Incremental/Iterative model. *Int J Comput Sci Issues* 12(1):106–111
2. Goyal S, Bhatia PK (2019) A non-linear technique for effective software effort estimation using multi-layer perceptrons. In: 2019 International conference on machine learning, big data, cloud and parallel computing (COMITCon), Faridabad, India, pp 1–4. <https://doi.org/10.1109/COMITCon.2019.8862256>
3. Thummadi BV, Lyytinen K (2020) How much method-in-use matters? A case study of agile and waterfall software projects and their design routine variation. *J Assoc Inf Syst* 21(4). <https://doi.org/10.17705/1jais.00623>
4. Goyal S (2022) FOFS: firefly optimization for feature selection to predict fault-prone software modules. In: Nanda P, Verma VK, Srivastava S, Gupta RK, Mazumdar AP (eds) *Data engineering for smart systems. Lecture Notes in Networks and Systems*, vol 238. Springer, Singapore. https://doi.org/10.1007/978-981-16-2641-8_46
5. Chowdhury AZM, Bhowmik A, Hasan H, Rahim MS (2018) Analysis of the veracities of industry used software development life cycle methodologies. [arXiv:1805.08631](https://arxiv.org/abs/1805.08631)
6. Matković P, Tumbas P (2010) A comparative overview of the evolution of software development models. *J Ind Eng Manage* 1:163–172
7. Petersen K, Wohlin C, Baca D (2009) The waterfall model in large-scale development. In: Bomarius F, Oivo M, Jaring P, Abrahamsson P (eds) *Product-focused software process improvement. PROFES 2009. Lecture Notes in Business Information Processing*, vol 32. Springer, Berlin, Heidelberg

8. Cocco L, Mannaro K, Concas G, Marchesi M (2011) Simulating kanban and scrum vs. waterfall with system dynamics. In: International conference on agile software development
9. Balaji S, Murugaiyan MS (2012) Waterfall vs v-model vs agile: a comparative study on SDLC. *Int J Inf Technol Bus Manage* 2(1)
10. Gandomani TJ (2016) Agile transition and adoption human-related challenges and issues: a grounded theory approach 62. <https://doi.org/10.1016/j.chb.2016.04.009>
11. Goyal S (2021) Handling class-imbalance with KNN (neighbourhood) under-sampling for software defect prediction. *Artif Intell Rev*. <https://doi.org/10.1007/s10462-021-10044-w>
12. McCormick M (2012) Waterfall vs agile methodology. MPCSC Inc. Revised edn. 8 Sept 2012
13. Petersen K (2010) Doctoral research in Sweden implementing lean and agile software development in industry
14. Mountain Goat Software (2016) Scrum overview: agile software development. Mountain Goat Software. Web. 22 Oct 2016
15. Forsberg K (1991) The relationship of systems engineering to the project cycle. In: First annual symposium of the national council on systems engineering (NCOSE)
16. Goyal S (2021) Effective software defect prediction using support vector machines (SVMs). *Int J Syst Assur Eng Manag*. <https://doi.org/10.1007/s13198-021-01326-1>
17. Goyal S (2022) 3PcGE: 3-parent child-based genetic evolution for software defect prediction. *Innovations Syst Softw Eng*. <https://doi.org/10.1007/s11334-021-00427-1>
18. Goyal S (2021) Predicting the defects using stacked ensemble learner with filtered dataset. *Autom Softw Eng* 28:14. <https://doi.org/10.1007/s10515-021-00285-y>
19. Goyal S (2022) Genetic evolution-based feature selection for software defect prediction using SVMs. *J Circ, Syst Comput* 31(11):2250161. <https://doi.org/10.1142/S0218126622501614>
20. Goyal S, Bhatia PK (2020) Feature selection technique for effective software effort estimation using multi-layer perceptrons. In: Proceedings of ICETIT 2019. Lecture Notes in Electrical Engineering, vol 605. Springer, Cham, pp 183–194. https://doi.org/10.1007/978-3-030-30577-2_15

Author Index

A

Aditi, R., 523
Aditi Rayaprolu, 311
Ajay Kumar Jena, 497
Akanksha Narahari, 247
Akhila, N., 429
Angelin Varghese, 331
Anna Tanuja Safala, B., 191
Anthireddygaru Sushma, 115
Anupma Gupta, 591
Arun Vignesh, N., 349
Asisa Kumar Panigrahy, 349
Ayush Dogra, 591, 601
Ayush Gupta, 621

B

Balaji, N., 137
Battapothula Gurappa, 1
Bhanusree, Y., 247
Bharti Baghel, 259
Bhawna Goyal, 591, 601
Blessy Kotrika, 311

C

Chandana Bai Korra, 181
Chandana, P., 535
Chandrasekhar, D., 349
Chandra Sekhar, G., 535
Chandrika, B. N. S. M., 573
Charan Kumar, 95
Charvi Arora, 613
Chava Sunil Kumar, 1
Chinnaiah, M. C., 235
Chintu Sagar, Y., 43

Cholleti Sriram, 203

D

Devineni Pooja Sri, 459
Devpriyadharsan, B. S., 513
Dhinakar, R., 523
Divija Chinni, 247
Divya Bulusu, 247

G

Gnaneshwara Chary, 95

H

Haritha Akkineni, 487
Harshit Jha, 621
Hindumathi, V., 225

J

Jakka Yeshwanth Reddy, 115
Jamal, K., 283
Janakiram Sunku, 95
Jarupula Somlal, 203
Jayshree Das, 213
Jegan, J., 565
Jugal Kishore Bhandari, 85
Jyoti Chaudhary, 161

K

Kammari Rajesh, 43
Kandasamy Thinakaran, 565
Karthik, R., 61

Karuppiah Santhi, 565
 Kavya Goel, 299
 Khan, M. R., 259
 Kiran Kumar, K., 459
 Kiran Mannem, 283
 Kishore, T. S., 25
 Krishna Rao Patro, E., 535
 Kunal Anand, 497

L

Lakshminathreddy, C., 545
 Lalitha Bhaskari, D., 71
 Lalitha Surya Kumari, P., 555
 Lipika Goel, 299

M

Madhava Rao, K., 225
 Madhavi Vemula, 191
 Madhuri Nallamothe, 487
 Manchalla O. V. P. Kumar, 283
 Manne Praveena, 137
 Mansing Rathod, 369
 Mathangi Akhila, 349
 Meda Lakshmi Hima Bindhu, 181
 Mehul Sinha, 613
 Menaka, R., 61
 Monika Saxena, 161
 Munnavvar Hussain, S., 213
 Myneni Madhubala, 487

N

Naga Satish, G., 149, 421, 429
 Naga Vishnu Vardhan, J., 103
 Naidu, C. D., 137
 Nalini, N. J., 13
 Nalla Siva Kumar, 429
 Neelakantappa, M., 467
 Nilofer Shaik, 33

P

Padmaja, B., 535
 Padmarajani, B., 357
 Palanati Durgaprasad, 357
 Parvathi, M., 235
 Pasha, I. A., 213
 Pasupuleti Sai Kiran, 477
 Perepi Rajarajeswari, 565
 Perli Nethra, 349
 Phani Sridhar Addepalli, 149
 Phanikumar Polasi, 411

Prabodh, C. P., 339
 Prameela, M., 467
 Prasad, J. V. D., 181
 Prasanth Vaidya, S., 421, 429
 Praveen Kumar Malik, 33
 Preesat Biswas, 259
 Puli Sai Sukitha, 115
 Punna Srinivas, 1
 Purude Vaishali, 555

R

Rama, B., 381
 Rama Padmaja, Ch. V., 535
 Rama Sanjeeva Reddy, B., 103, 173
 Ramaiah Konkanchi, 191
 Ramakrishna, T. V., 173
 Ramana Murthy, B. V., 573
 Ramesh, B., 411
 Ramesh Deshpande, 173
 Ramsai Reddy, Ch., 467
 Rekha, R., 403
 Ritika Rattan, 601
 Rohit Anand, 591, 601
 Roshni Pradhan, 439
 Rudra Kalyan Nayak, 451
 Rupesh, M., 1
 Rupesh Parmar, 369

S

Sabavath Sai Kiran, 115
 Sai Himaja Chowdary, K., 467
 Sairam Vamsi, T., 393
 Sallauddin Mohmmad, 381
 Sandhya Rani, M., 403
 Sanjay Dubey, 103
 Santhosh Kumar, V., 225
 Sathya, A. R., 583
 Sayan Mitra, 613
 Senthil A. Muthukumaraswamy, 331
 Sesha Sai Priya, S., 13
 Shaik Rehna Sulthana, 477
 Shanmuga Sundari, M., 451
 Shashwat Nath, 613
 Shesagiri Taminana, 71
 Shirin Khan, 259
 Shivam Sharma, 601
 Shreyash Moundekar, 369
 Shriram Ravindranathan, 95
 Shwetha, A. N., 339
 Siripurapu Sravya, 115
 Somya Goyal, 613, 621

Sonam Gupta, 299
Sourav Kumar, 369
Sowmiya, B., 513, 523
Srilakshmi, B. V. D. N., 283
Subbiah Swaminathan, 545
Sudhamsu Preetham, J. V. R., 349
Sudheer Kumar Terlapu, 393
Suhruith Yambakam, 95
Suma Sree Simhadri, 247
Sunitha Devi, P., 321
Sunitha, K. V. N., 321, 357, 403
Suresh Chandra Satapathy, 439

T

Tejaswi Potluri, 181
Tenneti Krishna Mohana, 149
Trupthi Mandhula, 311

U

Upendra Kumar, P., 25

V

Vaibhav Vyas, 161
Varshitha Bommareddy, 247
Vasudeva Reddy, T., 225
Venkata Subbarao, M., 393
Venkata Suneetha Takellapati, 487
Venkataiah, K. C., 43
Vijay A. Kanade, 127
Vinitha Joshy, P., 61
Viswanadham Ravuri, 393

Y

Yashwanth Raj, K., 513
Yogesh Kumar Verma, 85